Vol. 17. No 1, 2015

ISSN 1507-2711
Cena: 25 zł (w tym 5% VAT)

EKSPLOATACJA I NIEZAWODNOŚĆ
MAINTENANCE AND RELIABILITY

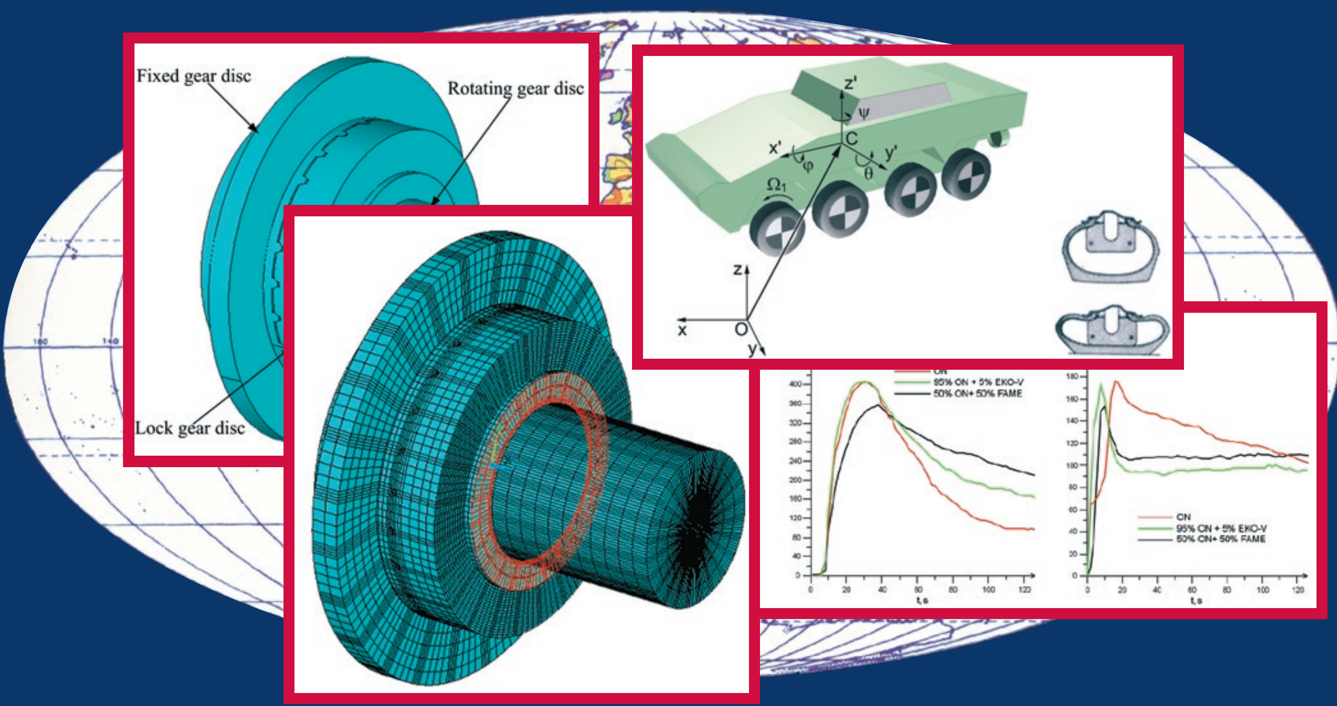

Polskie Naukowo Techniczne Towarzystwo Eksploatacyjne
Warszawa

Polish Maintenance Society
Warsaw

Co-financed by the Minister of Science and Higher Education

The Journal is indexed and abstracted in the Journal Citation Reports (JCR Science Edition), Scopus, Science Citation Index Expanded (SciSearch®) and Index Copernicus International.
The Quarterly appears on the list of journals credited with a high impact factor by the Polish Ministry of Science and Higher Education and is indexed in the Polish Technical Journal Contents database – BAZTECH and the database of the Digital Library Federation.

All the scientific articles have received two positive reviews from independent reviewers.

Our IF is 0.505

Editorial staff:	Dariusz Mazurkiewicz, PhD, DSc (Eng), Associate Professor (Editor-in-Chief, Secretary of the Scientific Board) Tomasz Klepka, PhD, DSc (Eng), Associate Professor (Deputy Editor-in-Chief) Teresa Błachnio-Krolopp, MSc (Eng) (Editorial secretary) Andrzej Koma (Typesetting and text makeup) Krzysztof Olszewski, PhD (Eng) (Webmaster)
Publisher:	Polish Maintenance Society, Warsaw
Scientific patronage:	Polish Academy of Sciences Branch in Lublin
Address for correspondence:	"Eksploatacja i Niezawodność" – Editorial Office ul. Nadbystrzycka 36, 20-618 Lublin, Poland e-mail: office@ein.org.pl http://www.ein.org.pl/
Circulation:	550 copies

Science and Technology

BORAWSKI A. **Modification of a fourth generation LPG installation improving the power supply to a spark ignition engine**. Eksploatacja i Niezawodnosc – Maintenance and Reliability 2015; 17 (1): 1–6.

Fourth generation LPG installations are fuel systems which, apart from their obvious advantages, have numerous disadvantages. One of their weaker elements are the injectors, or rather their improper performance. It was therefore justified to undertake a modification of the alternative fuel system in order to improve its work. The modification itself was preceded by a series of bench and road studies. A mathematical model of the injector was developed, which was later used in simulations. The results of the tests enabled the preparation the fuel system modification project involving the introduction of additional injectors and a system that controls their work. The complete unit was installed in a test vehicle and the modification's effect on the fuel supply process is presented in the results of conducted tests.

BORAWSKI A. **Modyfikacja instalacji LPG IV generacji poprawiająca jakość procesu zasilania silnika o zapłonie iskrowym**. Eksploatacja i Niezawodnosc – Maintenance and Reliability 2015; 17 (1): 1–6.

Instalacje LPG IV generacji są układami paliwowymi, które oprócz oczywistych zalet, mają liczne wady. Jednym ze słabych punktów takiej instalacji są wtryskiwacze, w właściwie ich nieprawidłowa praca. Wobec powyższego podjęto próbę opracowania modyfikacji alternatywnego układu zasilania, usprawniającą jego pracę. Modyfikację poprzedzono szeregiem badań stanowiskowych i drogowych. Opracowano model matematyczny wtryskiwacza, na podstawie którego przeprowadzono badania symulacyjne. Wyniki pozwoliły na wykonanie projektu modyfikacji układu paliwowego. Zmiany polegały na wprowadzeniu dodatkowych wtryskiwaczy oraz układu sterującego ich pracą. Całość zamontowana została w pojeździe testowym, a wpływ wprowadzonej modyfikacji na jakość procesu zasilania pokazują wyniki przeprowadzonych badań.

CHUA SJL, ALI AS, ALIAS AB. **Implementation of Analytic Hierarchy Process (AHP) decision making framework for building maintenance procurement selection: Case study of Malaysian public universities**. Eksploatacja i Niezawodnosc –Maintenance and Reliability 2015; 17 (5): 7–18.

In this paper, the proposed Analytic Hierarchy Process (AHP) based decision making framework was implemented and validated for its capability, applicability and validity in assisting building maintenance personnel to select the most appropriate procurement method. The decision making framework was developed based on AHP technique and principles. Expert Choice Software was employed as the development tool where the shortlisted criteria and alternatives were integrated within the framework. The validation process was carried out through a structured interview with nine public universities selected. The evaluations revealed that majority of the interviewees perceived that the framework developed was good (65%) and excellent (21%) in terms of capability, applicability and validity. The proposed decision making framework introduced expected to be a useful tool for maintenance organization that can assist them in decision making on selecting the most appropriate procurement method.

CHUA SJL, ALI AS, ALIAS AB. **Zastosowanie platformy programistycznej wspomagającej podejmowanie decyzji, opartej na procesie hierarchii analitycznej (AHP) w postępowaniu przetargowym na utrzymanie budynków. Przypadek malezyjskich uczelni publicznych**. Eksploatacja i Niezawodnosc –Maintenance and Reliability 2015; 17 (5): 7–18.

W niniejszej pracy przedstawiono platformę programistyczną wspomagającą podejmowanie decyzji opartą na procesie hierarchii analitycznej (AHP). Po wdrożeniu zaproponowanegoframeworku, weryfikowano jego wydajność, przydatność oraz wiarygodność jako narzędzia wspierającego pracowników utrzymania budynku przy wyborze najodpowiedniejszej metody przetargowej. Platformę opracowano w oparciu o technikę i zasady AHP. Jako narzędzia programistycznego użyto Expert Choice Software, za pomocą którego integrowano z frameworkiem wybrane kryteria i alternatywy. Weryfikację przeprowadzono na podstawie strukturalizowanego wywiadu z wybranymi dziewięcioma uczelniami publicznymi. Otrzymane oceny wykazały, że większość badanych postrzegało opracowaną platformę jako dobrą (65%) lub doskonałą (21%) pod względem wydajności, przydatności i wiarygodności. Przewiduje się, że proponowany framework wspomagający podejmowanie decyzji będzie stanowić użyteczne narzędzie doboru odpowiednich metod przetargowych dla instytucji zajmujących się obsługą techniczną.

FLIZIKOWSKI J, TOPOLIŃSKI T, OPIELAK M, TOMPOROWSKI A, MROZIŃSKI A. **Research and analysis of operating characteristics of energetic biomass micronizer**. Eksploatacja i Niezawodnosc – Maintenance and Reliability 2015; 17 (1): 19–26.

The analysis covers interrelations between the following factors: the machine movement, states and transformations of particles of the micronized biomass, particle shifts, mixing, grinding of energetic straw and its particles. It has been found that these relationships, among other things, depend on friction conditions, impacts, cutting, structural components of the micronizer as the dynamic movement of the machine structural components and biomass (particles) takes place under the conditions of idle movement and workload in order to accomplish an external goal. This paper aims at systematization, calculation and complementary research on micro-grinding performance characteristics (idle and operating), for constant and different rotational speeds (angular and linear).

FLIZIKOWSKI J, TOPOLIŃSKI T, OPIELAK M, TOMPOROWSKI A, MROZIŃSKI A. **Badania i analiza eksploatacyjnych charakterystyk mikronizatora energetycznej biomasy**. Eksploatacja i Niezawodnosc – Maintenance and Reliability 2015; 17 (1): 19–26.

Poddano analizie wzajemne relacje: ruchu użytkowego, stany i przemiany cząstek rozdrabnianej biomasy, ich przemieszczenia, mieszanie, rozdrabnianie słomy energetycznej i jej cząstek. Wykazano, że zależą one m.in. od warunków tarcia, zderzeń, cięcia, cech konstrukcyjnych mikronizatora, przy czym dynamiczne przemieszczanie elementów (części) konstrukcji maszyny i biomasy (cząstek), następuje w warunkach ruchu jałowego i obciążenia roboczego, dynamicznej realizacji celu zewnętrznego. Celem pracy jest systematyzacja, obliczenia i badania uzupełniające charakterystyk użytkowych (jałowych i roboczych) mikro-rozdrabniania, sporządzanych przy stałej i różnej prędkości obrotowej (kątowej lub liniowej).

CHANGYOU L, WEI W, YIMIN Z, SONG G, ZHENYUAN L, CHANGSHUAI Q. **Indexing accuracy reliability sensitivity analysis of power tool turret**. Eksploatacja i Niezawodnosc – Maintenance and Reliability 2015; 17 (1): 27–34.

Power tool turret (PTT) is one of the most key parts of CNC (Computer Numerical Control) turning center and CNC turning and milling machining center. Therefore, it is very important for improving these two types of machine tools' reliability to explore the indexing accuracy reliability of PTT and its sensitivity. To analyze the indexing accuracy reliability sensitivity of PTT, the angular displacement error of the rotating gear disc is discussed based on the measurement uncertainty theory. The tooth thickness wear process of the fixed gear disc, the rotating gear disc and the lock gear disc are modeled using Gamma process of which the parameters are estimated. The indexing error of PTT is formulated by employing the BP neural network and validated by the experiment data. Then, the indexing accuracy reliability equation of PTT is derived and its sensitivity to the mean and the standard deviation of random variables or wear stochastic processes is analyzed. The results show that the presented indexing accuracy reliability and its sensitivity of PTT are effective.

CHANGYOU L, WEI W, YIMIN Z, SONG G, ZHENYUAN L, CHANGSHUAI Q. **Analiza wrażliwości wskaźnika niezawodności w zakresie dokładności indeksowania głowicy narzędziowej z napędzanymi narzędziami**. Eksploatacja i Niezawodnosc – Maintenance and Reliability 2015; 17 (1): 27–34.

Głowica narzędziowa z napędzanymi narzędziami (ang. power tool turret, PTT) stanowi jedną z kluczowych części sterowanych komputerowo tokarskich i tokarsko-frezarskich centrów obróbczych CNC. Dlatego też dla poprawy niezawodności tych dwóch rodzajów obrabiarek istotne jest badanie niezawodności w zakresie dokładności indeksowania głowicy PTT oraz wrażliwości wskaźnika niezawodności. Dla celów analizy wrażliwości wskaźnika niezawodności w zakresie dokładności indeksowania głowicy PTT, omówiono błąd przesunięcia kątowego obrotowej tarczy narzędziowej w oparciu o teorię niepewności pomiaru. Proces zużycia ściernego zębów tarcz narzędziowych: stałej, obrotowej oraz uchwytowej, zamodelowano przy użyciu procesu Gamma o szacunkowych parametrach. Błąd indeksowania PTT obliczono przy zastosowaniu sieci neuronowej BP i zweryfikowano na podstawie danych doświadczalnych. Następnie wyprowadzono równanie niezawodności w zakresie dokładności indeksowania PTT oraz przeprowadzono analizę wrażliwości wskaźnika niezawodności na średnią i odchylenie standardowe zmiennych losowych lub procesów stochastycznych zużycia. Wyniki pokazały skuteczność omawianej analizy niezawodności w zakresie dokładności indeksowania PTT oraz wrażliwości wskaźnika niezawodności.

CHŁOPEK Z, BIEDRZYCKI J, LASOCKI J, WÓJCIK P. **Assessment of the impact of dynamic states of an internal combustion engine on its operational properties**. Eksploatacja i Niezawodnosc – Maintenance and Reliability 2015; 17 (1): 35–41.

CHŁOPEK Z, BIEDRZYCKI J, LASOCKI J, WÓJCIK P. **Ocena wpływu stanów dynamicznych silnika spalinowego na jego właściwości użytkowe**. Eksploatacja i Niezawodnosc – Maintenance and Reliability 2015; 17 (1): 35–41.

Internal combustion engines as systems described by non-linear models do not have any properties that would not depend on their current states. The paper presents results of testing an automotive engine in dynamic states determined by the vehicle acceleration sign in vehicle driving tests simulating the real operation of passenger cars. During the tests, pollutant emission rates and fuel flow rates averaged for specific vehicle states were examined. The processes under investigation were found to be highly sensitive both to the dynamic states and to the types of the vehicle driving tests.

Silniki spalinowe jako układy opisywane modelami nieliniowymi nie mają właściwości niezależnych od stanów, w jakich się znajdują. W pracy przedstawiono wyniki badań silnika samochodowego w stanach dynamicznych zdeterminowanych znakiem przyspieszenia pojazdu w testach jezdnych symulujących rzeczywistą eksploatację samochodów osobowych. Badano uśrednione w tych stanach: natężenie emisji zanieczyszczeń i natężenie przepływu paliwa. Stwierdzono znaczną wrażliwość badanych procesów zarówno na stany dynamiczne, jak i na rodzaje testów jezdnych.

MIKULSKI M, WIERZBICKI S, PIĘTAK A. **Zero-dimensional 2-phase combustion model in a dual-fuel compression ignition engine fed with gaseous fuel and a divided diesel fuel charge**. Eksploatacja i Niezawodnosc – Maintenance and Reliability 2015; 17 (1): 42–48.

The problem of using alternative fueling sources for combustion engines has been growing in importance recently. This is connected not only with the dwindling oil resources, but also with the growing concern for the natural environment and the fight against global warming. This paper proposes the concept for a zero-dimensional model of a multi-fuel engine, enabling the determination of thermodynamic system parameters based on the basic geometric and material object data (complete model). The basic problems in the creation of this model and the modeling of the accompanying subprocesses have been outlined and the methodology of the numerical solution of the obtained mathematical description has been proposed. The basic characteristics of the developed model are: the application of an original model of liquid fraction injection based on normal distribution, a new Assanis correlation for computing the diesel fuel self-ignition delay period in the presence of gas, first-order chemical reaction kinetic equations for describing the course of combustion for combustible components of the gas/air mixture, the implementation of a self-consistency procedure in modeling heat exchange and the effect of exhaust recirculation, the inclusion of both a single liquid fuel injection and the possibility of performing computations for a divided charge.

MIKULSKI M, WIERZBICKI S, PIĘTAK A. **Zero-dimensional 2-phase combustion model in a dual-fuel compression ignition engine fed with gaseous fuel and a divided diesel fuel charge**. Eksploatacja i Niezawodnosc – Maintenance and Reliability 2015; 17 (1): 42–48.

W ostatnim czasie problem wykorzystania alternatywnych źródeł zasilania silników spalinowych zyskuje szczególnie na znaczeniu. Związane jest to nie tylko z kurczącymi się zasobami ropy naftowej, ale również z coraz większą troską o środowisko naturalne oraz walką z globalnym ociepleniem. W niniejszej pracy zaproponowano koncepcję zero-wymiarowego modelu silnika wielopaliwowego, umożliwiającego, wyznaczenie parametrów termodynamicznych układu w oparciu o podstawowe dane geometryczne i materiałowe obiektu (model kompletny). Nakreślono podstawowe problemy w zagadnieniu tworzenia takiego modelu i modelowania podprocesów towarzyszących oraz zaproponowano metodykę numerycznego rozwiązywania uzyskanego opisu matematycznego. Podstawowe wyróżniki opracowanego modelu to: zastosowanie autorskiego modelu procesu wtrysku frakcji ciekłej opartego na rozkładzie normalnym, nowej korelacji Assanisa do obliczenia okresu zwłoki samozapłonu oleju napędowego w obecności gazu, jednostopniowych równań kinetyki reakcji chemicznej do opisu przebiegu spalania składników palnych mieszaniny gaz-powietrze, implementacja procedury samouzgodnienia w modelowaniu procesu wymiany ciepła i wpływu recyrkulacji spalin, uwzględnienie zarówno pojedynczego wtrysku paliwa ciekłego jak i możliwość prowadzenia obliczeń dla dawki dzielonej.

CZECHLOWSKI M, GOLIMOWSKI W, SĘK T, SZYMANOWICZ J. **Exhaust opacity in a diesel engine powered with animal fats**. Eksploatacja i Niezawodnosc – Maintenance and Reliability 2015; 17 (1): 49–53.

The diversification of sources of energy has been recognised as one of the actions preventing the negative effects of human activity on the environment. In order to do so it is necessary to solve the problems related with the replacement of fossil fuels with biofuels, including the increase in the prices of food products caused by the dynamic development of biofuels made from plants. Therefore, the aim of the study was to make an experiment assessing the technical possibilities to replace diesel fuel with rendered animal fats. As results from the initial study, the kinematic viscosity of animal fats at a temperature of 120°C is comparable to that of diesel at 40°C. Apart from that, the diesel engine powered with animal fats emitted 70% less particulates in exhaust than the engine powered with a diesel fuel.

CZECHLOWSKI M, GOLIMOWSKI W, SĘK T, SZYMANOWICZ J. **Zadymienie spalin silnika z zapłonem samoczynnym zasilanego tłuszczami zwierzęcymi**. Eksploatacja i Niezawodnosc – Maintenance and Reliability 2015; 17 (1): 49–53.

Dywersyfikację źródeł energii uznano za jedno z działań zapobiegających negatywnemu oddziaływaniu człowieka na środowisko. W tym celu konieczne jest rozwiązanie problemów związanych z zastępowaniem paliw kopalnych biopaliwami, m. in. wzrost cen produktów spożywczych, wywołany dynamicznym rozwojem biopaliw pochodzenia roślinnego. Dlatego za cel badań przyjęto wykonanie eksperymentu, polegającego na ocenie możliwości technicznych zastąpienia oleju napędowego wytopionymi tłuszczami zwierzęcymi. Z przeprowadzonych badań wstępnych wynika, że tłuszcze w temperaturze 120°C charakteryzują się lepkością kinematyczną porównywalną do oleju napędowego w 40°C, ponadto zasilany nimi silnik ZS emitował o 70% mniej cząstek stałych w spalinach w porównaniu do silnika zasilanego olejem napędowym.

GRĄDZKI R, LINDSTEDT P. **Method of assessment of technical object aptitude in environment of exploitation and service conditions**. Eksploatacja i Niezawodnosc – Maintenance and Reliability 2015; 17 (1): 54–63.

In the article, results of exploitation research of three various technical objects (public transportation bus engines) are presented. Gathered data is presented in three sets (1 – concerning object, 2 – concerning driving conditions, 3 – concerning driver, where sets 2 and 3 are object environment) in form of points (expert number assessments). Relation between point information on object and point information on environment was described using coupled state interaction equations. Such approach allowed to determine the following for each moment of exploitation: technical condition parameter aT and operating condition parameter aR, therefore in each moment of exploitation data regarding operating and technical condition of exploited object (bus) is available. This data allows for identification of object aptitude condition and thus optimally control processes of exploitation and service of particular objects as element of set of objects and set of objects.

GRĄDZKI R, LINDSTEDT P. **Metoda oceny stanu zdatności obiektu technicznego w otoczeniu warunków użytkowania i jakości obsługi**. Eksploatacja i Niezawodnosc – Maintenance and Reliability 2015; 17 (1): 54–63.

W artykule przedstawiono wyniki badań eksploatacyjnych trzech różnych obiektów technicznych (silników autobusów komunikacji miejskiej). Zebrana informacja została przedstawiona w 3 zbiorach (1 – dotyczy obiektu, 2 – dotyczy warunków jazdy, 3 – dotyczy kierowcy; przy czym zbiory 2 i 3 stanowią otoczenie obiektu) w postaci umownych punktów (eksperckich liczbowych ocen). Relację między punktową informacją o obiekcie i punktową informacją o otoczeniu opisano za pomocą sprzężonych równań stanu. Takie podejście pozwoliło wyznaczyć dla każdej chwili eksploatacji: parametr stanu technicznego aT i parametr stanu działania aR, Zatem w każdej chwili eksploatacji może być dostępna informacja o stanie technicznym i stanie działania każdego eksploatowanego obiektu (autobusu). Informacja ta pozwala identyfikować w każdej chwili stan zdatności obiektu, a zatem pozwala optymanie sterować procesami użytkowania i obsługi poszczególnych obiektów jako elementu zbioru obiektów i zbiorem obiektów.

GLOWACZ A, GLOWACZ W, GLOWACZ Z. **Recognition of armature current of DC generator depending on rotor speed using FFT, MSAF-1 and LDA**. Eksploatacja i Niezawodnosc – Maintenance and Reliability 2015; 17 (1): 64–69.

Recognition of states of electrical systems is very important in industrial plants. Article describes a recognition method of early fault detection of DC generator. The proposed approach is based on an analysis of the patterns. These patterns are the armature currents of selected electrical machine. Information contained in signals of armature current is depending on generator state. Researches were carried out for four states of generator with the use of Fast Fourier Transform (FFT), method of selection of amplitudes of frequencies (MSAF-1) and Linear Discriminant Analysis (LDA). The results of analysis show that the method is efficient and can be used to

GLOWACZ A, GLOWACZ W, GLOWACZ Z. **Rozpoznawanie sygnałów prądu twornika generatora prądu stałego w zależności od prędkości obrotowej wirnika z zastosowaniem FFT, MSAF-1 i LDA**. Eksploatacja i Niezawodnosc – Maintenance and Reliability 2015; 17 (1): 64–69.

Rozpoznawanie stanów układów elektrycznych jest bardzo ważne w zakładach przemysłowych. W artykule opisano metodę rozpoznawania stanów przedawaryjnych generatora prądu stałego. Proponowane podejście jest oparte na badaniu wzorców. Wzorce te są prądami twornika wybranej maszyny elektrycznej. Informacja zawarta w sygnałach prądu twornika jest zależna od stanu generatora. Przeprowadzono badania dla czterech stanów generatora z zastosowaniem FFT, metody wyboru amplitud częstotliwości (MSAF-1) i liniowej analizy dyskryminacyjnej (LDA). Wyniki analizy pokazują, że metoda jest protect DC generators. This method was verified with the aid of acoustic signals recognition method.

CHEN X, XIAO L, ZHANG X, XIAO W, LI J. **An integrated model of production scheduling and maintenance planning under imperfect preventive maintenance**. Eksploatacja i Niezawodnosc – Maintenance and Reliability 2015; 17 (1): 70–79.

For a successful company, machines are always required to work continuously to make more profit in a certain period. However, machines can be unavailable due to the scheduled maintenance activities or unexpected failures. Hence, a model connected production scheduling with maintenance planning for a production line which is composed of multiple machines is developed. Suppose preventive maintenance is imperfect and cannot renew all the machines. Age reduction factor and hazard rate increase factor are introduced to illustrate the imperfect character. Aperiodic preventive maintenance policy is adopted. Replacement as perfect maintenance could restore the machine "as good as new". When and whether to perform replacement is based on a cost-time rate function which is defined to judge whether or not the preventive maintenance is economical. The objective of the joint model is to maximize the total profit which is composed of production value, production cost, maintenance cost (including the preventive maintenance cost and replacement cost) and tardiness cost (which is related to the job sequence and maintenance activities). To optimize the objective, immune clonal selection algorithm is utilized. The proposed model is validated by a numerical example.

LOTKO M, LOTKO A. **Cluster analysis of knowledge workers assessment of occupational threats and attitudes to character of work**. Eksploatacja i Niezawodnosc – Maintenance and Reliability 2015; 17 (1): 80–89.

The goal of the paper was to discover, if knowledge workers' occupational threats can be linked to some logical constructs and if knowledge workers can be grouped into some logical items concerning their assessment of these threats and attitudes to character of work. On a basis of literature studies peculiarity of knowledge-based work and specific occupational threats were identified. They were examined as observable variables with the use of a questionnaire method on a sample of 500 knowledge workers. Then, variables were classified using multidimensional exploratory technique - cluster analysis. As a research implication, the structure of perception of knowledge workers' occupational threats and their attitudes to character of work were revealed. As a practical implication, a proposed classification of variables allows to measure perception of occupational threats and use the results e. g. when designing trainings on occupational health and safety and to better fit them to this specific group of employees. Thus, job safety can be effectively improved by raising awareness of certain threats. The paper's contribution is a novel way of measuring and classifying knowledge workers' occupational threats and attitudes to character of work.

BEER-LECH K, SUROWSKA B. **Research on resistance to corrosive wear of dental CoCrMo alloy containing post-production scrap**. Eksploatacja i Niezawodnosc – Maintenance and Reliability 2015; 17 (1): 90–94.

Use of metal base dental prostheses is accompanied by not only wear due to biomechanical loads that occur during the process of chewing, but also by corrosive wear occurring in aggressive oral environment. Corrosive wear of metal elements of prosthesis may result in excluding it from further use by the occurrence of allergic or even carcinogenic reactions in patient, resulting from the release of toxic metal ions into the body. A common practice in prosthetic laboratories used in order to reduce production costs of dental prostheses is using so-called post-production scrap to subsequent castings. This scrap constitute the elements of casting channels, defectively made skeletons of prostheses or metal residues after prosthetic treatment. Use of post-production scrap to manufacture components to fulfill such high performance criteria (presence of complex biomechanical loads), and in particular taking into account the evaluation of biocompatibility, is the subject of discussion not only in the environment of scientists, but also the producers of dental alloys.The aim of the study was to investigate resistance to corrosive wear of dental cobalt alloy containing post-production scrap. The commercial dental alloy Wironit extra-hard with cobalt matrix has been used in this research. The study was based on a conducted polarity by means of potentiodynamic method in a solution of artificial saliva. Tested alloy samples, containing different percentage intake of post-production scrap, were cast by two casting methods - centrifugal and vacuum-pressure. Average values of parameters of Wironit extra – hard alloy resistance to corrosive wear: corrosion potential – E_{cor}, corrosion current I_{cor}, polarisation resistance R_{pol} and pitting potential – E_{pit} were determined. In order to assess alloy surface after corrosion microscopic observation was made. The results of research confirm high resistance of alloy to corrosive wear in environment of artificial saliva. Castings made using centrifugal methods provide lower current density in the passive state than those carried out by vacuum – pressure method, which suggests greater durability of passive layer confirmed by analysis of microstructure of samples after corrosion. Determination of correlation between content of post-production scrap and resistance to corrosion is ambiguous.

skuteczna i metoda może być stosowana do ochrony generatorów prądu stałego. Metoda została zweryfikowana za pomocą metody rozpoznawania sygnałów akustycznych.

CHEN X, XIAO L, ZHANG X, XIAO W, LI J. **Model zintegrowany harmonogramowania produkcji i planowania obsługi technicznej w ramach niepełnej konserwacji zapobiegawczej**. Eksploatacja i Niezawodnosc – Maintenance and Reliability 2015; 17 (1): 70–79.

Aby firma mogła działać z powodzeniem i przynosić większe zyski w danym okresie czasu, zainstalowane w niej maszyny muszą pracować w sposób nieprzerwany. Niestety, z powodu planowych działań obsługowych lub nieoczekiwanych awarii, maszyny są czasami wyłączane z produkcji. Dlatego też w niniejszym artykule opracowano model łączący harmonogramowanie produkcji z planowaniem obsługi technicznej dla linii produkcyjnej złożonej z wielu maszyn. W pracy założono, że konserwacja zapobiegawcza jest niepełna i nie prowadzi do odnowy wszystkich maszyn. Aby zilustrować jej niepełny charakter, wprowadzono pojęcia czynnika redukcji wieku oraz czynnika wzrostu wskaźnika zagrożenia. Przyjęto politykę nieokresowej konserwacji zapobiegawczej. Wymiana jako forma pełnej konserwacji pozwala na przywrócenie maszyny do stanu "fabrycznej nowości". Kiedy i czy należy przeprowadzić wymianę zależy od funkcji wskaźnika kosztu w stosunku do czasu, który pozwala ocenić, czy konserwacja zapobiegawcza jest opłacalna. Model zintegrowany ma na celu maksymalizację całkowitego zysku, który jest wypadkową wartości produkcji, kosztów produkcji, kosztów obsługi (w tym kosztów konserwacji zapobiegawczej oraz kosztów wymiany) i kosztów nieterminowego zakończenia zadania (ang. lateness, związanych z kolejnością wykonywanych zadań i czynności obsługowych). Aby zoptymalizować opisany cel, wykorzystano algorytm odpornościowej selekcji klonalnej Proponowany model zweryfikowano na przykładzie liczbowym.

LOTKO M, LOTKO A. **Zastosowanie analizy skupień do oceny zagrożeń zawodowych pracowników wiedzy i ich postaw wobec charakteru pracy**. Eksploatacja i Niezawodnosc – Maintenance and Reliability 2015; 17 (1): 80–89.

Celem artykułu było zbadanie, czy zagrożenia zawodowe pracowników wiedzy mogą być pogrupowane w logiczne konstrukty i czy pracownicy wiedzy mogą być logicznie pogrupowani biorąc pod uwagę ich ocenę zagrożeń i postawy wobec pracy. Na podstawie studiów literaturowych zdefiniowano szczególny charakter pracy opartej na wiedzy i zagrożeń związanych z jej wykonywaniem. Zbadano je empirycznie jako zmienne obserwowalne z wykorzystaniem metody ankietowej na próbie 500 pracowników wiedzy. Następnie przeprowadzono klasyfikację zmiennych z wykorzystaniem wielowymiarowej techniki eksploracyjnej – analizy skupień. Jako wniosek badawczy odkryto strukturę postrzeganych przez pracowników wiedzy zagrożeń zawodowych. Jako wniosek praktyczny, proponowana klasyfikacja zmiennych pozwala mierzyć postrzeganie zagrożeń zawodowych przez pracowników wiedzy i wykorzystać wyniki np. podczas projektowania szkoleń z zakresu bezpieczeństwa i higieny pracy, aby lepiej dopasować je do tej szczególnej grupy pracowników. Dlatego bezpieczeństwo pracy może być wyraźnie poprawione poprzez podniesienie świadomości określonych zagrożeń. Wkładem artykułu jest nowatorski sposób pomiaru i klasyfikacji zagrożeń zawodowych przez pracowników wiedzy i ich postaw wobec pracy.

BEER-LECH K, SUROWSKA B. **Badanie odporności na zużycie korozyjne stomatologicznego stopu CoCrMo zawierającego złom poprodukcyjny**. Eksploatacja i Niezawodnosc – Maintenance and Reliability 2015; 17 (1): 90–94.

Eksploatacji stomatologicznych protez na podbudowie metalowej towarzyszy nie tylko zużycie wskutek obciążeń biomechanicznych, występujących podczas procesu żucia, ale również zużycie korozyjne mające miejsce w agresywnym środowisku jamy ustnej. Zużycie korozyjne metalowych elementów protezy skutkować może wyłączeniem jej z dalszego użytkowania wskutek wystąpienia u pacjenta reakcji alergicznych lub nawet kancerogennych, będących rezultatem uwalniania do organizmu toksycznych jonów metali. Częstą praktyką w laboratoriach protetycznych stosowaną w celu obniżania kosztów produkcji protez jest stosowanie tzw. złomu poprodukcyjnego do kolejnych odlewów. Złom ten stanowią elementy kanałów odlewniczych, wadliwie wykonane szkielety protez bądź metalowe pozostałości po obróbce protetycznej. Zastosowanie złomu poprodukcyjnego do wytwarzania elementów mających spełniać tak wysokie kryteria eksploatacyjne (występowanie złożonego stanu obciążeń biomechanicznych), a zwłaszcza biorąc pod uwagę ocenę biokompatybilności otrzymanych wyrobów, jest tematem dyskusyjnym nie tylko w środowisku naukowców, ale również i samych producentów stopów stomatologicznych. Celem pracy było zbadanie odporności na zużycie korozyjne stomatologicznego stopu kobaltu zawierającego złom poprodukcyjny. Do badań zastosowano komercyjny stop stomatologiczny Wironit extra-hard na osnowie kobaltu. Badanie polegało na przeprowadzeniu polaryzacji metodą potencjodynamiczną w środowisku roztworu sztucznej śliny. Próbki stopu poddane badaniu, zawierające różny udział procentowy złomu poprodukcyjnego, odlane zostały dwiema metodami odlewniczymi - odśrodkową i próżniowo-ciśnieniową. Wyznaczono średnie parametrów określających odporność stopu Wironit extra–hard na zużycie korozyjne: potencjał korozji – E_{kor}, prąd korozji I_{kor}, opór polaryzacyjny R_{pol} i potencjał przebicia – E_{pit}. W celu oceny powierzchni stopu po korozji dokonano obserwacji mikroskopowych. Wyniki badań potwierdzają dużą odporność stopu na zużycie korozyjne w środowisku sztucznej śliny. Odlewy wykonane za pomocą metody odśrodkowej cechują się niższą gęstością prądu w stanie pasywnym niż te wykonane metodą próżniowo – ciśnieniową, co sugeruje większą trwałość warstwy pasywnej potwierdzoną analizą mikrostruktury próbek po korozji. Wyznaczenie zależności pomiędzy zawartością złomu poprodukcyjnego a odpornością na korozję jest niejednoznaczne.

AMBROZIK A, AMBROZIK T, ŁAGOWSKI P. **Fuel impact on emissions of harmful components of the exhaust gas from the ci engine during cold start-up**. Eksploatacja i Niezawodnosc – Maintenance and Reliability 2015; 17 (1): 95–99.

The paper presents the results of tests on the compression ignition PEUGEOT 2.0 HDI engine. It was fuelled by commercial diesel oil, B50 blend (50 % diesel oil and 50 % rapeseed oil fatty acid methyl esters), and blend of diesel oil and 5% EKO-V fuel additive manufactured by the INWEX company. The tests were conducted for cold and hot engine. When the engine started up from cold, the temperature of the coolant and lubricating oil was equal to the ambient temperature. In hot engine start-up, the temperature of the engine oil and the coolant was 90 ºC. The values of concentrations of the exhaust gas harmful components were measured before the catalytic converter.

AMBROZIK A, AMBROZIK T, ŁAGOWSKI P. **Wpływ paliwa na emisję szkodliwych składników spalin silnika o zapłonie samoczynnym podczas zimnego rozruchu**. Eksploatacja i Niezawodnosc – Maintenance and Reliability 2015; 17 (1): 95–99.

W artykule przedstawiono wyniki badań silnika o zapłonie samoczynnym PEUGEOT 2.0 HDI zasilanego handlowym olejem napędowym, mieszaniną B50 (50 % oleju napędowego i 50 % estrów metylowych kwasów tłuszczowych oleju rzepakowego) i oleju napędowego z dodatkiem 5% preparatu EKO-V firmy INWEX. Badania wykonano dla zimnego i rozgrzanego silnika. Podczas rozruchu zimnego silnika temperatura cieczy chłodzącej i oleju smarnego była równa temperaturze otoczenia, natomiast podczas rozruchu silnika ciepłego temperatura oleju silnikowego i cieczy chłodzącej wynosiła 90ºC. Wartości stężeń szkodliwych składników spalin zmierzono przed katalizatorem utleniającym zainstalowanym w układzie wydechowym silnika.

YANG D, REN Y, WANG Z, LIU L, SUN B. **A novel logic-based approach for Failure Modes Mitigation Control and Quantitative System Reliability Analyses**. Eksploatacja i Niezawodnosc – Maintenance and Reliability 2015; 17 (1): 100–106.

The core idea of reliability design is to mitigate the product's failure modes. However, for the cross-links among potential failure modes of a complex product, it is very difficult to establish the mapping relationship between failure modes mitigation and quantitative values of reliability, and the decision of failure modes mitigation have to be performed by virtue of experience, which always increase design period. In order to solve these problems, a novel logic-based approach for failure modes mitigation control and quantitative system reliability analyses is provided. Firstly, a hybrid of active and passive control process of reliability design is proposed. Secondly, a novel concept of failure modes correlation set (FMCS) and a determination approach based on deductive theory are presented. According to the changes in failure modes probabilities of occurrence, the reliability formulas of the components and assemblies are provided to depict the effects of failure mode mitigation on reliability of components and assemblies. And then the FMCS mitigation sequence is decided to determine reliability design activities. Thirdly, a closed control process of FMCS mitigation is provided integrated with logic decision method. By exposing the design of a helicopter fuel system, the present study demonstrates that all approaches are feasible, and the relationship between reliability parameters and qualitative design exists. Hence the failure modes mitigation could be controlled for the achievement of quantitative reliability requirements.

YANG D, REN Y, WANG Z, LIU L, SUN B. **Oryginalna, oparta na logice metoda kontroli ograniczania przyczyn uszkodzeń i ilościowej analizy niezawodności systemu**. Eksploatacja i Niezawodnosc – Maintenance and Reliability 2015; 17 (1): 100–106.

Podstawowym problemem w procesie projektowania niezawodności jest ograniczenie przyczyn uszkodzeń produktu. Jednakże, w przypadku sieci połączeń pomiędzy możliwymi przyczynami uszkodzeń złożonego produktu, trudno jest ustalić mapę zależności pomiędzy ograniczaniem przyczyn uszkodzeń i ilościowymi wartościami niezawodności, a decyzje względem ograniczania przyczyn uszkodzeń muszą bazować na własnym doświadczeniu, co znacznie wydłuża okres projektowania. W celu rozwiązania powyższych problemów, zaproponowano oryginalną, opartą na logice, metodę kontroli ograniczania przyczyn uszkodzeń i ilościowej analizy niezawodności systemu. Na wstępie, zaproponowano mieszany proces aktywnej i pasywnej kontroli niezawodności projektu. Następnie, zaprezentowano oryginalną koncepcję zbioru korelacji przyczyn uszkodzeń (FMCS) i metodę oznaczania opartą o teorię dedukcji. Na podstawie zmian dotyczących prawdopodobieństwa występowania przyczyn uszkodzeń, określono wzory niezawodności części i układów w celu pokazania wpływu ograniczania przyczyn uszkodzeń na niezawodność części i układów. Określono następnie ograniczającą sekwencję FMCS, ażeby ustalić założenia dla projektowania niezawodności. Na koniec zaprezentowano zamknięty proces kontroli ograniczania FMCS w powiązaniu z logiczną metodą podejmowania decyzji. Analizując pod tym kątem projekt systemu paliwowego helikoptera, wykazano w niniejszej pracy przydatność wszystkich powyższych metod, jak również związek pomiędzy parametrami niezawodności a projektowaniem jakościowym. Dlatego też ograniczanie przyczyn uszkodzeń powinno być kontrolowane w celu osiągnięcia wymaganej niezawodności ilościowej.

ANTOSZ K, STADNICKA D. **Evaluation measures of machine operation effectiveness in large enterprises: study results**. Eksploatacja i Niezawodnosc – Maintenance and Reliability 2015; 17 (1): 107–117.

Maintaining a proper productivity and efficiency level of a technical infrastructure of an enterprise requires, above all, the use of appropriate managing methods and tools as well as an appropriate organization of services responsible for their management. Using a variety of measures is indispensable to evaluate the effectiveness of these practices as well as of the machine performance in any enterprise. The data obtained from measuring particular indicators are a primary source of information on the necessity of taking particular actions. Large companies are particularly willing to implement appropriate indicators of effectiveness evaluation because of a large number of machines and a vast range of their technical maintenance. Different indicators presented in the references are said to be efficient and willingly used by enterprises. The aim of the study, of which the results are presented in this article, was to identify the real actions taken by the surveyed enterprises concerning the use of the machine effectiveness evaluation metrics. Apart from that, the study also intended to obtain the information on which indicators are actually applied by enterprises. The study was carried out in large production enterprises of different industries on a specified area.

ANTOSZ K, STADNICKA D. **Mierniki oceny efektywności funkcjonowania maszyn w dużych przedsiębiorstwach: wyniki badań**. Eksploatacja i Niezawodnosc – Maintenance and Reliability 2015; 17 (1): 107–117.

Utrzymanie infrastruktury technicznej przedsiębiorstwa na odpowiednim poziomie produktywności i wydajności wymaga przede wszystkim stosowania właściwych metod i narzędzi zarządzania oraz właściwej organizacji służb odpowiedzialnych za jego realizację. Nieodłącznym elementem oceny efektywności tych działań oraz funkcjonowania maszyn w przedsiębiorstwie jest stosowanie różnorodnych mierników. Dane uzyskiwane z pomiarów określonych wskaźników są podstawowym źródłem informacji o konieczności podejmowania działań określonego rodzaju. Szczególnie duże firmy są chętne, aby wdrożyć odpowiednie wskaźniki oceny efektywności maszyn ze względu na dużą liczbę maszyn i duży zakres prac związanych z ich obsługą techniczną. W literaturze przedmiotu prezentowane są różne wskaźniki wskazywane, jako skuteczne i chętnie stosowane przez przedsiębiorstwa. Celem badań, których wyniki przedstawiono w niniejszej pracy, było zidentyfikowanie rzeczywistych działań realizowanych przez badane przedsiębiorstwa w zakresie stosowania mierników oceny skuteczności maszyn oraz pozyskanie informacji o tym, jakie wskaźniki są przez firmy stosowane w praktyce. Badania przeprowadzono w dużych przedsiębiorstwach produkcyjnych funkcjonujących w różnych branżach przemysłu na określonym obszarze.

PROCHOWSKI L, WACH W, JACKOWSKI J, PIENIĄŻEK W. **Experimental and model studies on the influence of the run flat tire damage on braking dynamics of the multi-axial special purpose vehicle**. Eksploatacja i Niezawodnosc – Maintenance and Reliability 2015; 17 (1): 118–128.

Tire damage, that occurs quite often during operation of special purpose vehicles (building, forest, military, agricultural heavy-duty vehicles), affects a vehicle motion also during sudden braking. Motion of a four-axial vehicle has been analysed in order to evaluate the influence of tire damage (cracking, tearing) on its behaviour during sudden braking and based on that to evaluate the possibilities of driver's reactions to motion disorders resulting from that emergency condition. Using the PC-Crash software, a vehicle model was designed allowing for simulation of special-purpose vehicle motion. The vehicle model includes a possibility of occurring of sudden tire damage when in motion. In such situation a model of cooperation of a tire and a surface is of crucial significance. A semi-empirical, non-linear TMeasy tire model was used. Its parameters were obtained on the basis of the results of the tests performed on

PROCHOWSKI L, WACH W, JACKOWSKI J, PIENIĄŻEK W. **Eksperymentalne i modelowe badania wpływu uszkodzenia opon run flat na dynamikę hamowania wieloosiowego pojazdu specjalnego**. Eksploatacja i Niezawodnosc – Maintenance and Reliability 2015; 17 (1): 118–128.

Uszkodzenie opony, które dość często pojawia się podczas eksploatacji pojazdów specjalnych (budowlane, leśne, militarne, rolnicze), wpływa na ruch pojazdu, również podczas gwałtownego hamowania. Analizie poddano ruch czteroosiowego pojazdu w celu dokonania oceny wpływu uszkodzenia opon (pęknięcie, rozerwanie) na jego zachowanie się podczas gwałtownego hamowania, a na tej podstawie oceny możliwości reakcji kierowcy na zaburzenia ruchu wynikające z takiego stanu awaryjnego. Korzystając z programu PC-Crash opracowano model pojazdu umożliwiający symulację ruchu pojazdu specjalnego. Model pojazdu uwzględnia możliwość powstania nagłego uszkodzenia opony w czasie jazdy. W takiej sytuacji decydujące znaczenie ma model współpracy opon z nawierzchnią. Zastosowano nieliniowy semi-empiryczny model opony TMeasy, którego parametry uzyskano na podstawie wyników badań opon 14.00R20 z wkładkami run flat. Parametryzacja

14.00R20 tires with run flat inserts. A vehicle model parameterization was based on the results of the vehicle measurements, however the validation was based on the results of experimental road tests of braking with damaged tires. Performed calculations and simulations indicated that when braking is started a process of vehicle deviation and related motion track modification is initialized. The motion track deviation increases as the initial braking speed is increased.

modelu pojazdu została oparta na wynikach pomiarów pojazdu, natomiast walidacja na wynikach eksperymentalnych badań drogowych hamowania z uszkodzonym ogumieniem. Przeprowadzone obliczenia i symulacje pokazały, że po rozpoczęciu hamowania następuje proces odchylania pojazdu i związana z tym zmiana toru jazdy. Odchylenie toru jazdy rośnie wraz ze wzrostem prędkości początkowej hamowania.

KURANC A. **Exhaust emission test performance with the use of the signal from air flow meter**. Eksploatacja i Niezawodnosc – Maintenance and Reliability 2015; 17 (1): 129–134.

The paper presents selected technical solutions in the area of exhaust emissions research conducted in real operational conditions of a vehicle. The author describes his own road emissions research methodology with the use of information about the air flow supplying an engine (OBD II) and the measured volumetric shares of particular fumes components (exhaust gas analyser). Test results confirm the possibility of applying this measurement method, and their analysis shows the inadequacy of the type-approval tests compared to the real operation of the vehicle.

KURANC A. **Eksploatacyjne badania emisji spalin z wykorzystaniem sygnału z przepływomierza powietrza**. Eksploatacja i Niezawodnosc – Maintenance and Reliability 2015; 17 (1): 129–134.

W pracy omawiane są wybrane rozwiązania techniczne w zakresie badań emisji spalin w warunkach rzeczywistej eksploatacji pojazdu. Autor opisuje własną metodykę drogowych badań emisji spalin z wykorzystaniem informacji o wydatku powietrza zasilającego silnik (OBD II) i zmierzonych udziałów objętościowych poszczególnych składników (analizator spalin). Wyniki badań potwierdzają możliwość stosowania opisanej metody pomiarowej, a ich analiza wskazuje ponadto na nieadekwatność testów homologacyjnych w odniesieniu do realnej eksploatacji pojazdu.

KOLAKOWSKI Z, MANIA RJ, GRUDZIECKI J. **Local nonsymmetrical postbuckling equilibrium path of the thin FGM plate**. Eksploatacja i Niezawodnosc – Maintenance and Reliability 2015; 17 (1): 135–142.

The influence of the imperfection sign (sense) on local postbuckling equilibrium path of plates made of functionally graded materials (FGMs) has been analyzed. Koiter's theory has been used to explain this phenomenon. In the case of local buckling, a nonsymmetrical stable equilibrium path has been obtained. The investigations focus on a comparison of the semi-analytical method (SAM) and the finite element method (FEM) applied to the postbuckling nonlinear analysis of thin-walled complex FG plated structures.

KOLAKOWSKI Z, MANIA RJ, GRUDZIECKI J. **Niesymetryczna lokalna ścieżka równowagi pokrytycznej cienkiej płyty z materiału funkcjonalnie gradientowego**. Eksploatacja i Niezawodnosc – Maintenance and Reliability 2015; 17 (1): 135–142.

W pracy przedstawiono analizę wpływu znaku imperfekcji wstępnej na charakterystykę lokalnej pokrytycznej ścieżki równowagi płyty wykonanej z materiału gradientowego. Do wyjaśnienia tego efektu zastosowano teorię Koitera. W przypadku lokalnej utraty stateczności uzyskano niesymetryczne stateczne ścieżki równowagi. Prezentowane badania były skoncentrowane na porównaniu wyników uzyskanych na podstawie własnej metody pół-analitycznej z wynikami uzyskanymi przy zastosowaniu metody elementów skończonych w nieliniowej analizie cienkościennych konstrukcji płytowych wykonanych z materiałów gradientowych.

CAI L, ZHANG Z, CHENG Q, LIU Z, GU P. **A geometric accuracy design method of multi-axis NC machine tool for improving machining accuracy reliability**. Eksploatacja i Niezawodnosc – Maintenance and Reliability 2015; 17 (1): 143–155.

The reliability of machining accuracy is of great significance to performance evaluation and optimization design of the machine tools. Different geometric errors have various influences on the machining accuracy of the machine tools. The main emphasis of this paper is to propose a generalized method to distribute geometric accuracy of component for improving machining accuracy reliability under certain design requirements. By applying MBS theory, a comprehensive volumetric model explaining how individual errors in the components of a machine affect its volumetric accuracy (the coupling relationship) was established. In order to reflect the ability to reach the required machining accuracy, the concept of machining accuracy reliability is proposed in this paper. Based on advanced first order and second moment (AFOSM) theory, reliability and sensitivity with single failure modes were obtained and the model of machining accuracy reliability and the model of machining accuracy sensitivity with multiple failure modes were developed. By taking machining accuracy reliability as a measure of the ability of machine tool and taking machining accuracy sensitivity as a reference of optimizing the basic parameters of machine tools to design a machine tool, an accuracy distribution method of machine tools for improving machining accuracy reliability with multiple failure modes was developed and a case study example for a five-axis NC machine tool was used to demonstrate the effectiveness of this method. It is identified that each improvement of the geometric errors leads to a decrease in the maximum values and mean values of possibility of failure, and the gaps among reliability sensitivity of geometric parameter errors improved also decreased. This study suggests that it is possible to obtain the relationships between geometric errors and specify the accuracy grades of main feeding components of mechanical assemblies for improving machining accuracy reliability.

CAI L, ZHANG Z, CHENG Q, LIU Z, GU P. **Metoda projektowania i poprawy niezawodności dokładności obróbczej wieloosiowej obrabiarki NC wykorzystująca pojęcie dokładności geometrycznej**. Eksploatacja i Niezawodnosc – Maintenance and Reliability 2015; 17 (1): 143–155.

Niezawodność w zakresie dokładności obróbki ma wielkie znaczenie dla oceny funkcjonowania oraz projektowania optymalizacyjnego obrabiarek. Różne błędy geometryczne mają różny wpływ na dokładność obrabiarek. Głównym celem niniejszej pracy jest zaproponowanie uogólnionej metody rozkładu dokładności geometrycznej elementów składowych obrabiarki, pozwalającej na poprawę niezawodności w zakresie dokładności obróbczej przy spełnieniu pewnych wymagań projektowych. Dzięki zastosowaniu teorii układów wielomasowych MBS, opracowano kompleksowy model wolumetryczny, który wyjaśnia, w jaki sposób pojedyncze błędy występujące w elementach składowych obrabiarki wpływają na jej dokładność wolumetryczną (relacja sprzężeń). Zaproponowane w prezentowanym artykule pojęcie niezawodności dokładności obróbki odnosi się do możliwości uzyskania przez urządzenie wymaganej dokładności obróbki W oparciu o zaawansowaną teorię estymacji momentów AFOSM (Advanced First Order and Second Moment theory), obliczono niezawodność i czułość dla przypadku wystąpienia pojedynczej przyczyny uszkodzenia oraz opracowano model niezawodności dokładności obróbki oraz model czułości dokładności obróbki dla przypadku wystąpienia wielu przyczyn uszkodzeń. Przyjmując niezawodność dokładności obróbki za miarę poprawnego działania obrabiarki oraz przyjmując czułość dokładności obróbki za punkt odniesienia dla optymalizacji projektowej podstawowych parametrów obrabiarek, opracowano metodę, opartą na rozkładzie dokładności obrabiarki, mającą na celu poprawę niezawodności dokładności obróbki dla przypadku wystąpienia wielu przyczyn uszkodzeń. Skuteczność metody wykazano na przykładzie pięcio-osiowej obrabiarki NC. Stwierdzono, że każda korekta błędu geometrycznego prowadzi do spadku maksymalnych i średnich wartości możliwości wystąpienia uszkodzenia oraz zmniejsza rozstęp między poszczególnymi czułościami niezawodnościowymi skorygowanych błędów parametrów geometrycznych. Przedstawione badania wskazują, że możliwe jest ustalenie związku pomiędzy błędami geometrycznymi oraz określenie stopni dokładności głównych elementów składowych zespołów mechanicznych odpowiedzialnych za ruch posuwowy obrabiarki w celu poprawy niezawodności dokładności obróbki.

TU J, CHENG R, TAO Q. **Reliability Analysis Method of safety-critical avionics system based on Dynamic Fault Tree under Fuzzy Uncertainty**. Eksploatacja i Niezawodnosc – Maintenance and Reliability 2015; 17 (1): 156–163.

A safety-critical avionics system has to qualify the performance related requirements and the safety-related requirements simultaneously. This paper presents a comprehensive study on the reliability analysis method for safety-critical avionics system by using dynamic fault tree approach based on Markov chain. The reliability models were constructed applying dynamic fault tree (DFT) modeling method according to deeply analysis of the typical failure modes, causes and influence of the safety-critical avionics system by considering the aspect of repairable feature and redundancy. Taking into account the both failure phenomenon of safety-critical avionics system and many uncertainties exist in the fault status and fault reasons, fuzzy sets theory

TU J, CHENG R, TAO Q. **Sposób analizy niezawodności krytycznych dla bezpieczeństwa systemów elektroniki lotniczej oparty na metodzie dynamicznego drzewa błędów w warunkach rozmytej niepewności**. Eksploatacja i Niezawodnosc – Maintenance and Reliability 2015; 17 (1): 156–163.

Krytyczne dla bezpieczeństwa układy elektroniki lotniczej (awioniki) muszą jednocześnie spełniać zarówno wymogi eksploatacyjne jak i wymagania związane z bezpieczeństwem. W niniejszej pracy przedstawiono kompleksowe opracowanie dotyczące metody analizy niezawodności krytycznych dla bezpieczeństwa systemów awioniki wykorzystującej opartą na łańcuchu Markowa metodę dynamicznego drzewa błędów. Modele niezawodności konstruowano z zastosowaniem metody dynamicznego drzewa błędów zgodnie z przeprowadzoną dokładną analizą typowych przyczyn uszkodzeń oraz czynników wpływających na systemy elektroniki lotniczej, z uwzględnieniem aspektu naprawialności i nadmiarowości. Biorąc pod uwagę, że zarówno ze zjawiskiem uszkodzenia krytycznego

is introduced into dynamic fault tree method. Specifically, it adopts expert elicitation and fuzzy set theory to evaluate the failure rates of the basic events for safety-critical avionics system. Furthermore, the fuzzy dynamic fault tree analysis method for safety-critical avionics system based on the consecutive parameter Markov chain is proposed. The modularization design was utilized to divide the dynamic fault trees into static and dynamic sub-trees. The static tree was solved by binary decision diagram (BDD) and the dynamic tree was solved by Markov chain method. The results show that the proposed method is more flexible and adaptive than conventional fault tree analysis for fault diagnosis and reliability estimation of safety-critical avionics system.

dla bezpieczeństwa systemu awioniki jak i ze stanem awarii i przyczynami błędów wiąże się wiele niepewności, metodę dynamicznego drzewa błędów poszerzono o teorię zbiorów rozmytych. W szczególności, zaproponowana metoda wykorzystuje ocenę ekspercką oraz teorię zbiorów rozmytych do oceny intensywności uszkodzeń dla podstawowych zdarzeń zachodzących w krytycznych dla bezpieczeństwa systemach elektroniki lotniczej. Ponadto zaproponowano metodę analizy krytycznych dla bezpieczeństwa systemów awioniki wykorzystującą teorię rozmytych dynamicznych drzew błędów opartą na markowowskim łańcuchu następujących po sobie parametrów. Budowę modułową wykorzystano do podziału dynamicznych drzew błędów na poddrzewa statyczne i dynamiczne. Drzewa statyczne rozwiązywano za pomocą binarnego schematu decyzyjnego (BDD) a drzewa dynamiczne – metodą łańcuchów Markowa. Wyniki pokazują, że proponowana metoda diagnozowania błędów i oceny niezawodności krytycznych dla bezpieczeństwa systemów elektroniki lotniczej jest bardziej elastyczna i łatwiejsza do adaptacji niż konwencjonalna analiza drzewa błędów.

SCIENCE AND TECHNOLOGY

Article citation info:
BORAWSKI A. Modification of a fourth generation LPG installation improving the power supply to a spark ignition engine. Eksploatacja i Niezawodnosc – Maintenance and Reliability 2015; 17 (1): 1–6.

Andrzej BORAWSKI

MODIFICATION OF A FOURTH GENERATION LPG INSTALLATION IMPROVING THE POWER SUPPLY TO A SPARK IGNITION ENGINE

MODYFIKACJA INSTALACJI LPG IV GENERACJI POPRAWIAJĄCA JAKOŚĆ PROCESU ZASILANIA SILNIKA O ZAPŁONIE ISKROWYM*

Fourth generation LPG installations are fuel systems which, apart from their obvious advantages, have numerous disadvantages. One of their weaker elements are the injectors, or rather their improper performance. It was therefore justified to undertake a modification of the alternative fuel system in order to improve its work. The modification itself was preceded by a series of bench and road studies. A mathematical model of the injector was developed, which was later used in simulations. The results of the tests enabled the preparation the fuel system modification project involving the introduction of additional injectors and a system that controls their work. The complete unit was installed in a test vehicle and the modification's effect on the fuel supply process is presented in the results of conducted tests.

Keywords: *LPG injectors, injector modelling, LPG installation modification, gas installation diagnostics, injector performance control.*

Instalacje LPG IV generacji są układami paliwowymi, które oprócz oczywistych zalet, mają liczne wady. Jednym ze słabych punktów takiej instalacji są wtryskiwacze, w właściwie ich nieprawidłowa praca. Wobec powyższego podjęto próbę opracowania modyfikacji alternatywnego układu zasilania, usprawniającą jego pracę. Modyfikację poprzedzono szeregiem badań stanowiskowych i drogowych. Opracowano model matematyczny wtryskiwacza, na podstawie którego przeprowadzono badania symulacyjne. Wyniki pozwoliły na wykonanie projektu modyfikacji układu paliwowego. Zmiany polegały na wprowadzeniu dodatkowych wtryskiwaczy oraz układu sterującego ich pracą. Całość zamontowana została w pojeździe testowym, a wpływ wprowadzonej modyfikacji na jakość procesu zasilania pokazują wyniki przeprowadzonych badań.

Słowa kluczowe: *wtryskiwacze LPG, modelowanie wtryskiwaczy, modyfikacja instalacji LPG, badania instalacji gazowej, sterowanie pracą wtryskiwaczy.*

1. Introduction

An LPG installation, similarly to other fuel supply systems, has its advantages and disadvantages. The primary advantages of this fuels system (mainly, the reduction of operation costs) are well-known among drivers. The disadvantages are not so notable among users, although they are equally or even more important.

It has been observed that recently, the intensity of research on fourth generation gas installations has decreased, mainly due to the technological advances in vehicle design (mass introduction of direct fuel injection). Modern combustion engines required the development of new solutions for gas installations, using the fuel in its liquid state (LPLi) [5].

The installation of an alternative fuel system usually entails a decrease in the engines usefulness factors (power and torque). This, however, can be alleviated with a well-designed intake system. The heat necessary to change the state of LPG can be obtained from inlet air, thanks to which the temperature of the fuel increases while the temperature of the air is decreasing, contradictory to its density. The engine's volumetric efficiency is therefore improved [11] and, consequently, it produces more power and torque.

Injection of any type of fuel (LPG included) entails decreasing its pressure (the pressure of LPG before the injector is higher by approximately 1 bar than the pressure in the engine's inlet line [2]). Expanding fuel draws energy in the form of heat from its nearest surroundings (the outlet nozzle and the air drawn by the engine), which in extreme cases may lead to ice forming on the injector nozzle and cut off the supply of LPG. This situation depends on the geometry of the injector (mainly, the diameter of the outlet nozzle) and the engine's operating parameters. The operating parameters of an engine are determined by the users of the vehicle, its designers may however, through optimization for example, change the geometry of the elements of the fuel supply system, and therefore prevent extensive cooling of injector nozzles [6].

A team of scientists in South Korea has indicated that the composition of the fuel-air mixture has a significant influence on the velocity

(*) Tekst artykułu w polskiej wersji językowej dostępny w elektronicznym wydaniu kwartalnika na stronie ***www.ein.org.pl***

of the flame of the combusted LPG, which in turn has a great impact on the composition of the exhaust gases. Research has shown that the most favourable combustion velocity is observed for a stoichiometric mixtures. The worst results were noted for poor mixtures. Therefore, precision dosage of fuel is essential [7]. Often, in order to obtain a stoichiometric mixture in the full range of engine speeds it is necessary to use an additional controller to supervise the fuel supply in neutral gear, or the engine is controlled using the H-infinity method [4]. In the 1990s, some designs used an additional injector activated at high engine speeds [15].

The appropriate composition of the fuel-air mixture ensures low emission of harmful carbohydrates and carbon oxides. Another significant component of exhaust gases are the nitrogen oxides which are created in consequence with the high temperatures inside the combustion chamber. The use of an exhaust gas recirculation system (EGR) results in a decreased emission of nitrogen oxides. This system is usually controlled by the data encoded in the ECU, which in most cases was devised in-factory for conventional fuel (petrol). The use of alternative fuel systems (such as LPG) entails problems with the proper functioning of the EGR system (the amount of recirculated gasses is too high or too low [3]). Applying an additional, automatically adjustable controller may eliminate this problem. The use of such controller would ensure proper functioning of the exhaust gas recirculation system, even if the conditions in the engine very rapidly [3].

It is also important to dose the fuel uniformly, measured both between particular cylinders as well as between consecutive work cycles of the engine. What is important here is the quality of the LPG injectors, which is often unsatisfactory (considering the criteria used by the manufacturers of combustion engines) [8]. The uniformity of the LPG dosage determines the composition of chemical compounds in the exhaust gasses. The nitrogen oxides content increases in direct proportion, while the amount of carbon oxides and carbohydrates increases in reveres proportion the value differences in the LPG dosages in particular injectors. These differences, in brand new injectors, can be as high as 15% [8].

Numerous analyses of exhaust gasses of combustion engines indicate that LPG fuel systems are more favourable that units fuelled conventionally [12, 14]. Bearing in mind that there is still a vast number of vehicles using fourth generation gas installations (particularly in African countries), the author of this article is convinces that work on improving the design of this fuel system should be continued. The focus here is on the issues with the LPG engine fuel supply, since even the smallest improvement in the engine's performance or fuel consumption may have a significant impact in the global scale.

Preliminary road tests indicated that the gas installation swithes off for some time during acceleration [2]. Similar behaviour was observed in fuel supply systems in other vehicles confirmed the suspicion that this is not an isolated case in special conditions. Preliminary bench tests and numerous consultations helped to determine that one of the reasons for the improper functioning of the fuel supply system are the injectors, or rather their design. However, later experience showed that the injectors are not the only reasons behind the described situation. The situation may also be caused by the reducer, or rather its limited efficiency [9].

The LPG injector is an electric valve that opens and closes the supply of fuel. The design of the gas injector is significantly different from the design of a petrol injector. In its vapour phase, the volume of LPG is higher than the volume of petrol in its liquid state, therefore the overall dimensions of a gas injector are significantly higher. The increase of the dimensions is, however, connected with higher inertial forces of the injector's moving elements [9]. The base components of the studied gas injector are: the needle valve, coil, return spring, sealing-suppressing elements, and a multi-part casing. The main element of the casing (the rail) is also the duct that supplies the fuel to the injector. It also serves as the nest for the needle valve of the injector (Fig. 1).

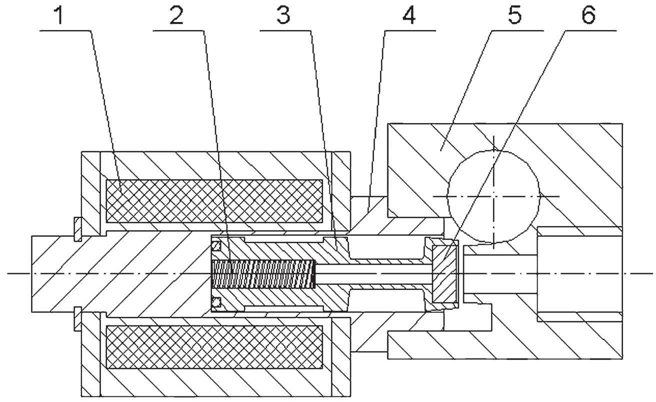

Fig. 1. Fourth generation LPG injector diagram: 1– coil, 2 – return spring, 3 – needle valve, 4 – cylinder, 5 – injector rail, 6 – sealing-suppressing element

The needle valve that moves inside the injector opens or closes the fuel flow. The closing movement is caused by the return spring and the opening movement results from the electromagnetic force generated by the injector's coil. This force is initiated by an electrical impulse from the controlling unit. The LPG controller uses impulses generated by the engine's ECU, dedicated for petrol injectors on the basis obtained from the sensors that monitor the engine's operation (coolant temperature, amount of inlet air, acceleration pedal position, etc.). Based on this data, the gas installation controller selects a proper impulse path from its encoded "map", corrects it against the temperature and the pressure of the LPG, and then sends it to the gas injector.

Most of the LPG injectors manufactured today can be divided into two groups: those of high precision and those of high efficiency. A third group of efficient injectors is a costly alternative, as it is characterised by short interval for both opening and closing.

In the neutral gear and with low fuel supply, it is necessary to measure out precise doses of fuel. The precision of the dosage is significantly influenced by exact measurements of the duration of injection. A precise injector, characterised by low efficiency, must have an appropriately long opening time, in which case the precision of the dosage increases. Problems occur, however, under high stress (with high supply and engine speed) [17]. The low efficiency of the injector results in a too long gas injection period, which exceeds the engine period cycle. The engine is supplied with a poor fuel dosage. Modifying the design of the injector in order to increase its efficiency enables proper dosage under stress, yet it makes the dose imprecise under low stress and in short opening periods.

A properly designed (configured), installed and adjusted gas system, equipped with rapidly opening and closing injectors, guarantees precise composition of the fuel-air mixture in all working conditions. This however entails increased production costs, and consequently increases the price of a gas installation (universal installations are of course less expensive that dedicated installations). It has been observed that for most users, the main criteria of the usefulness of a gas installation are the economical aspects [10]. Therefore, many of such installations are installed and later maintained by incompetent or inexperienced people who charge a low price for their services. An analysis of client behaviour of a car services station showed that approximately 90% of its users service their cars in authorised stations only during the warranty period. After its expiry, the users look for cheaper alternatives.

2. Fuel supply system examination before the modification

The modification of the fuel supply system began with the identification of the problem. As stated in the introduction, the gas installation switches off under certain conditions of work. This occurs when the engine is extensively supplied with fuel (when the duration of the supplying impulse is extended) and the engine speed is high (when the engine cycle is shortened).

In order to confirm these statements, the changes in the controlling signals were measured for both petrol and LPG injectors. The measuring tools consisted in a portable computer and an HD-Scope 9.0 oscilloscope. The voltage on the injectors was measured every 1000 rpm (from 1000 rpm to 5000 rpm). The measurement was based on recording the flow of the signals for approximately 10 seconds, three times for each engine speed. One of the measuring channels of the oscilloscope was connected to the petrol injector's power connector and another measuring channel was connected to the LPG injector's power connector.

The tests were performed on a BMW 520i equipped with a six cylinder M50B25 engine (capacity: 1991 cm^3, power: 110 kW) and an alternative, fourth generation LPG fuel supply (comprised of: a Vector 6 controller, Zavoli Zeta-N reducer, PS-01 pressure sensor, and a Valtek 3Ω injector rail), giving a better look on the conditions of the unfavourable behaviour [2]. At low engine speeds and with small supply, the gas installation works properly. Problems begin to occur with the increase of both the engine sped and the supply level. As shown in Figure 2, at engine speed of approximately 5000 rpm, the voltage on the injector does not drop to zero. The intervals between particular work cycles are short (up to several ms), making it impossible for the injector to close [16]. The engine is therefore supplied constantly. With further increase of the engine speed (up to 6000 rpm, Figure 3), it can be observed that the gas installation switched off (loss of the impulse signal that controls the work of the injectors), while simultaneously starting the conventional, petrol fuel supply (appearance of signals controlling the petrol injectors).

The numerical simulation of the injector needle valve, prepared on the basis of a mathematical model [1], showed that the gas injector begins to not shut properly already at engine speed of 4600 rpm (Fig. 4).

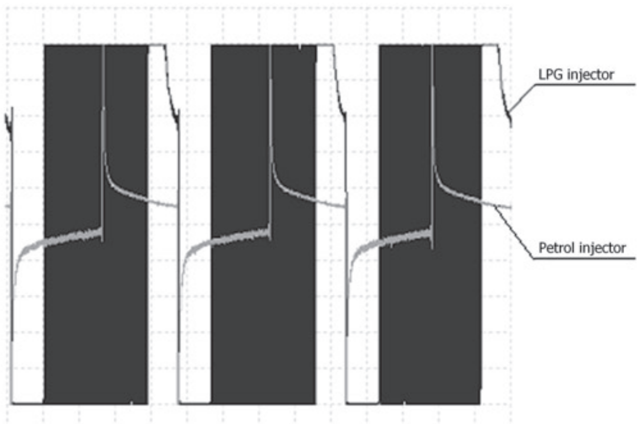

Fig. 2. Voltage changes in the petrol (grey) and LPG (black) injector at maximum engine supply and 5000 rpm engine speed [2]

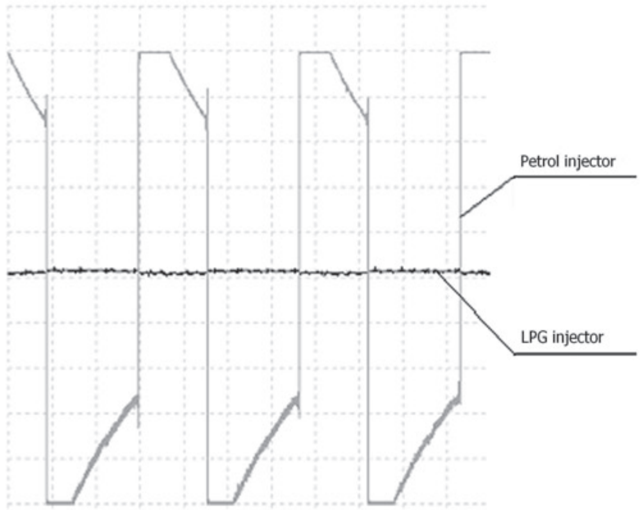

Fig. 3. Voltage changes in the petrol (grey) and LPG (black) injector at maximum engine supply and 6000 rpm engine speed [2]

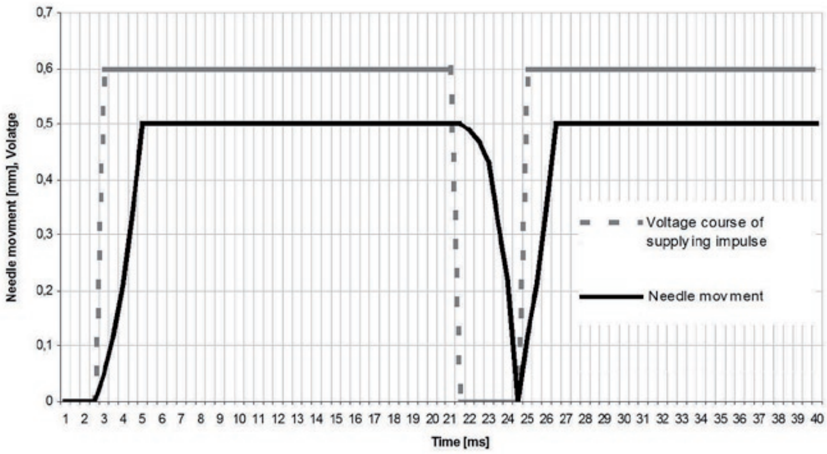

Fig. 4. The simulation of the movement of the needle at engine speed of 4600 rpm

Knowledge of the conditions of the described issue allowed to determine that the occurrence of the disturbance in fuel supply depends strictly on the individual driving style of the driver and, of course, in some cases it may not occur at all.

3. Modification of the fuel supply system

The occurrence of improper closure of injectors has a definite negative influence on the factors used to evaluate the supply system (power and torque, fuel consumption and economic factors). Therefore it was justified to prepare a modification that would allow the engine to be supplied with gas in full range of its work. Among several solution, the final choice was the one that was based on doubling the number of injectors so that each cylinder would ultimately be supplied by two injectors working alternately. The diagram of such supply is presented in Fig. 5.

The proposed solution will cause every injector to open at half of its originally planned frequency (that is, once per every four turns of the crankshaft). The increase of the intervals between work cycles should allow the needle valve to shut freely and cut off the supply of fuel, and it should also allow the supply larger doses of LPG than now. Therefore, after implementing the changes in the design, the alternative fuel system should be able to function properly within the whole range of engine speeds and irrespectively of the level of fuel supply.

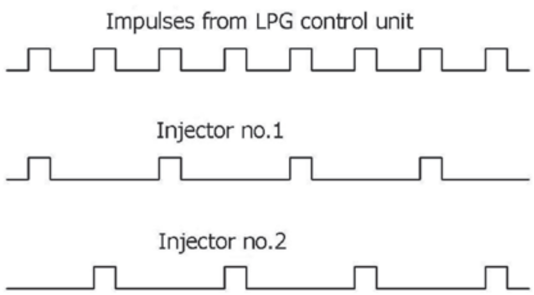

Fig. 5. Modified fourth generation gas installation injector supply diagram

Before moving on to the design phase of the modified fuel system, a simulation was performed to see how the engine would function at 5000 rpm. The simulation was based on the mathematical model discussed above. The results of the simulation are presented in Figure 6.

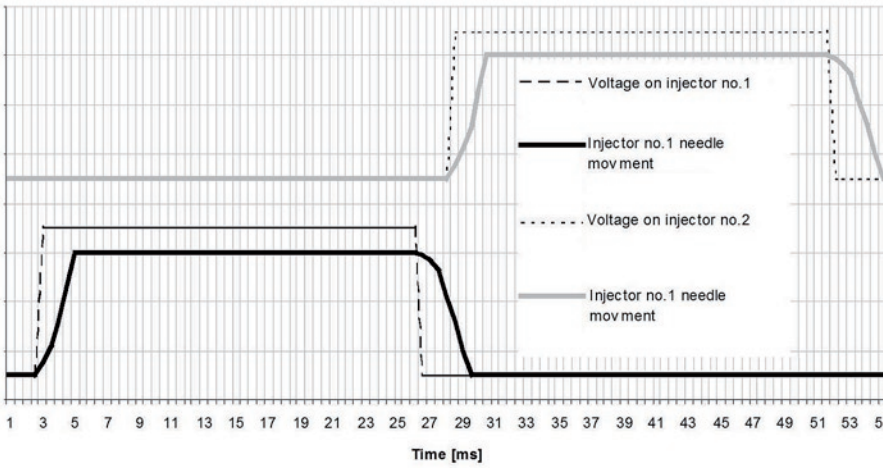

Fig. 6. Simulation of the splitter's function

In order to start the new fuel system, apart from doubling the number of injectors it was also necessary to prepare a controlling system that would split the original signal from the LPG controller into two sub-signals that powered the injectors.

The working principle of such a system should be based on a falling edge. It means that the system should firstly identify the change in voltage from high to low, and based on that information it should switch the path of the original signal, in this case the one generated by the LPG controller. The splitter shouldn't therefore change the form of the signal, but rather send it to appropriate connectors.

Knowing these general assumption, a splitter model was prepared that based on several integrated circuits (2x 7414N, 4013N, 2x TC4422AVPA), two transistors (IRF520 N-FET 100V 8A 40W), as well as resistors, capacitors, and diodes. Everything was then placed on a special circuit board made especially for this system. All incoming and going signals go through precision connectors installed on both ends of the circuit board. The first two are used to connect the 12V power source, the next two are used to intercept the signal generated by the LPG controller. The four remaining connectors are outputs for the signals that control the LPG injectors in the modified fuel system.

This system was build and, along with the injector rail, it was then installed in the test vehicle. The test vehicle was a BMW 316i passenger car equipped with a four cylinder M40 engine (capacity: 1596 cm^3, power: 75 kW) and a sequential gas injection system, whose main elements were: ZENIT JZ controller, Zavili Zeta-S reducer, ZENIT AA-612 pressure sensor and Valterk 3Ω injectors.

The electrical installation of the splitter of the controlling signal was limited to connecting with the wires going from the LPG controller to the injectors. The fuel lines required the installation of additional distributors. The installation method is therefore non-invasive, and allows the original installation to be restored quickly, if the user is not satisfied with the new configuration.

4. Effects of the modification of the alternative fuel system on the process of fuel supply.

After installing, connecting and calibrating the modified elements, the influence of the changes on the supply process was verified. The first test drive showed a significant improvement in terms of high engine speeds. It was noticed that the doubled number of injectors contributed to reducing the loss of power at high engine speeds eliminated the switching back to the conventional, petrol fuel system.

Using an oscilloscope, the voltage was measured on the connectors of the injectors, in order to confirm if the original input is correctly split into two output signals.

The results presented in Figure 7 clearly show that the aim was achieved. The installed electric device split the signal generated by the LPG controller between two injectors that worked alternately. The positive impact of the modifications allowed for further testing: the course of the voltage for higher engine speeds.

The voltage on the injectors was measured every 1000 rpm (from 1000 rpm to 5000 rpm).

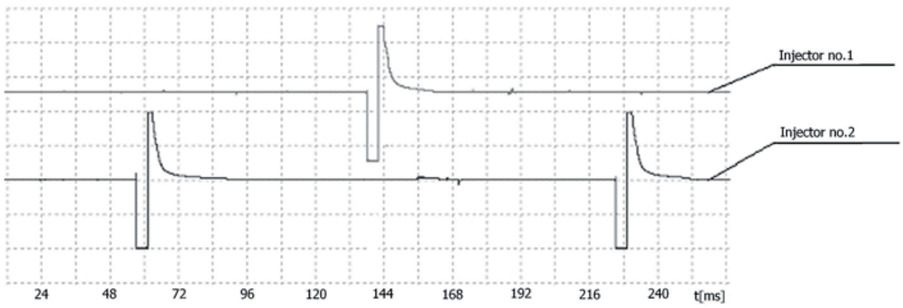

Fig. 7. Course of the impulses in the injectors of one cylinder in the modified installation; engine speed approx. 700 rpm.

The measurement was based on recording the course of the controlling signals for approximately 10 seconds, three times for each engine speed. This again was done using the oscilloscope and computer mentioned above. In each test, the signal was split correctly and the injectors supplying the same cylinder worked alternately. In the modified installation, at 5000 rpm (the speed at which the injector remained open in the non-modified installation) it is clear that the voltage on each injector drops to zero and the interval between each work cycle is sufficient for the needle valve to return to its closed position [16] (for valve 1, the loss of controlling impulse occurs at 70 ms of the measurement, while another signal occurs at 78 ms; this time is therefore sufficient for a total closure of the injector [16]).

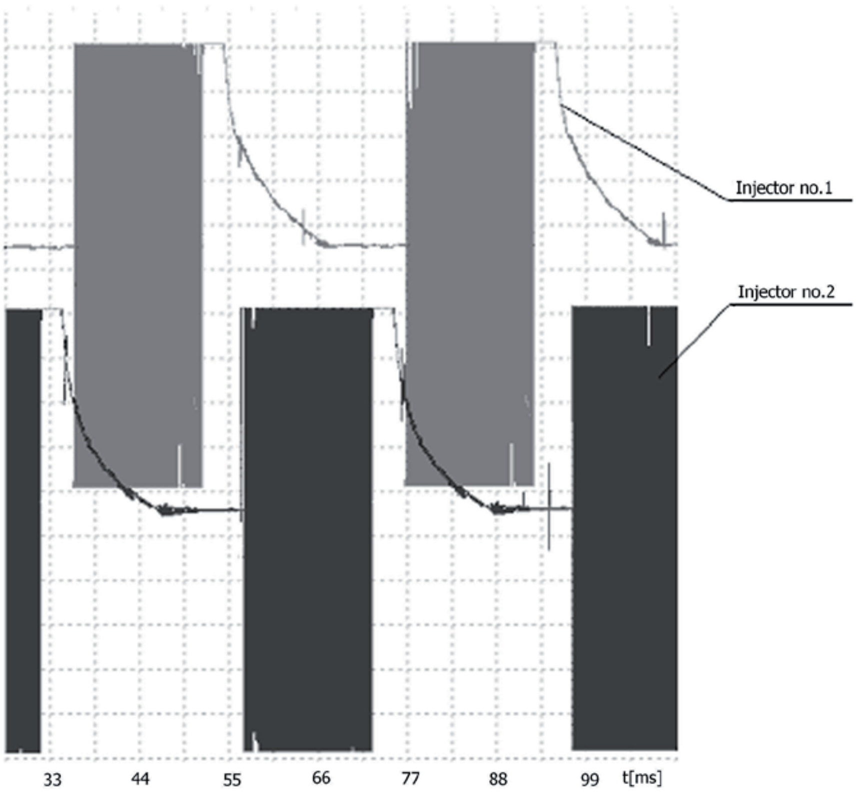

Fig. 8. Course of the impulses in the injectors in the modified installation; engine speed approx. 5000 rpm.

The doubling of the number of injectors also made it possible for the fuel system to supply the required amount of fuel for every engine speed and for each supply level (the maximum capacity was doubled). Therefore, the gas installation stopped to shut down and performed its fuel supply functions in all working conditions.

5. Summary

Poland is one of the top European countries in terms of the popularity of alternative fuels, especially LPG, and the number of vehicles powered by such fuels. Car users install LPG systems mainly due to economical reasons, accepting the numerous disadvantages of gas installations. The constant development of alternative fuel systems designs decreases these disadvantages, although it still is impossible to eliminate them completely. With the mass scale of vehicles used in transport of people and goods, even the slightest improvement of supply systems in combustion engines has a significant importance both to the economy and the natural environment.

The modification of an LPG installation described in this article has a significant impact on the process of the engine's power supply. The developed electronic unit splits the controlling signal generated by the LPG controller into two sub-signals that control the functions of the injectors on a given cylinder. This solution causes provides the engine is powered precisely at low engine speeds and low supply levels, but it also provides adequate power at high engine speeds and supply requirements. Cutting the injector work frequency in half results in lowering the thermal stress on the injectors and decreases the risk of the occurrence of magnetic saturation [13]. Owing to this, the process of dosing the fuel is characterised by a higher level of repetitiveness, and the injectors are characterised by a longer service life.

The implemented modification also eliminated the problem with the shutting down of the alternative fuel system at high engine speed and high supply. The benefits of the changes include:

- reducing the usage costs due to decreased consumption of petrol, which is a more expensive fuel than LPG;
- improving the usefulness factors of the engine, since every change of the power source causes the controlling computer (ECU) to "re-learn" the supply map, with the engine generating less power and torque [16];
- decreasing the level of harmful emissions in exhaust gasses by limiting the emission of carbon monoxide and dioxide, in line with the current trends in the automotive industry (combustion of LPG produces fewer substances that are harmful to the environment that combustion of petrol [12]).

Another advantage of the proposed solution is also the cost of the modification (calculated on the basis of the costs incurred by the author in relation to the construction and installation of the device) which is approximately 10% of the cost of adjusting a vehicle to be powered with an alternative fuel system. The cost is small, considering the advantages stemming from the improved design.

References

1. Borawski A, Siemieniako F. Model matematyczny pracy wtryskiwacza LPG. Pneumatyka 2011; 2: 52-55.
2. Borawski A, Siemieniako F. Wpływ prędkości obrotowej i obciążenia silnika na przebieg impulsu sterującego wtryskiwaczami płynnego gazu ropopochodnego. Acta Mechanica et Automatica 2010; 4(2): 25-28.
3. Cui H. Exhaust Gas Recirculation Control in a Spark-Ignition LPG Engine Using Neural Networks. Intelligent Control and Automation 2006; 2: 6332 - 6335.
4. Cui H. The Fuel Control System and Performance Optimization of a Spark-Ignition LPG Engine. Measuring Technology and Mechatronics Automation 2009; 1: 901-904.
5. Danardono D, Kim K S, Roziboyev E, Kim C U. Design and optimization of an LPG roller vane pump for suppressing cavitation. International Journal of Automotive Technology 2010; 11(3): 323-330.
6. Hosek M, Beroun S, Dittrich A. Pressure in nozzle canal for injection of LPG. XLII International Scientific Conference Of Czech And Slovak University Departments And Institutions Dealing With The Research Of Combustion Engines 2011; 1-31.
7. Lee K, Ryu J. An experimental study of the flame propagation and combustion characteristics of LPG fuel. Fuel 2005; 84: 1116-1127.
8. Majerczyk A, Radzimirski S. Effect of LPG gas fuel injectors on the properties of low emission vehicles. Journal of KONES 2012; 19(4): 401-410.
9. Majerczyk A, Taubet S. Układy zasilania gazem propan-butan. Warszawa: WKŁ, 2006.

10. Merkisz J, Pielacha I. Alternatywne paliwa i układy paliwowe pojazdów. Poznań: Wydawnictwo Politechniki Poznańskiej, 2004.
11. Mohamad T I, Jermy M, Harrison M. Experimental Investigation of a Gasoline-to-LPG Converted Engine Performance at Various Injection and Cylinder Pressures With Respect to Propane Spray Structures. Applied Mechanics and Materials 2013; 315: 20-24.
12. Mustafa KF, Gitano Briggs HW. Liquefied petroleum gas (LPG) as an alternative fuel in spark ignition engine: Performance and emission characteristics. Energy and Environment 2009; 189-194.
13. Rawa H. Elektryczność i magnetyzm w technice. Warszawa: PWN, 2001.
14. Ristovski ZD, Jayaratne ER, Morawska L, Ayoko GA, Lim M. Particle and carbon dioxide emissions from passenger vehicles operating on unleaded petrol and LPG fuel. Science of the Total Environment 2005; 345: 93-98.
15. Sunwoo M, Sim H, Lee K. Design and development of an ECU anti its air-fuel ratio control scheme for an LPG engine with a bypass injector. Vehicle Electronics Conference 1999; 508-513.
16. Szpica D. Analiza możliwości adaptacyjnych silnika spalinowego do zasilania paliwem alternatywnym na przykładzie LPG. Białystok 2013.
17. Wendeker M. Badania algorytmów sterujących samochodowym silnikiem benzynowym. Warszawa: PWN, 2000.

Andrzej BORAWSKI
Faculty of Mechanics and Construction of Machinery
Białystok University of Technology
ul. Wiejska 45C, 15-351 Białystok, Poland
E-mail: a.borawski@pb.edu.pl

Article citation info:
CHUA SJL, ALI AS, ALIAS AB. Implementation of Analytic Hierarchy Process (AHP) decision making framework for building maintenance procurement selection: Case study of Malaysian public universities. Eksploatacja i Niezawodnosc –Maintenance and Reliability 2015; 17 (5): 7–18.

Shirley Jin Lin CHUA
Azlan Shah ALI
Anuar Bin ALIAS

IMPLEMENTATION OF ANALYTIC HIERARCHY PROCESS (AHP) DECISION MAKING FRAMEWORK FOR BUILDING MAINTENANCE PROCUREMENT SELECTION: CASE STUDY OF MALAYSIAN PUBLIC UNIVERSITIES

ZASTOSOWANIE PLATFORMY PROGRAMISTYCZNEJ WSPOMAGAJĄCEJ PODEJMOWANIE DECYZJI, OPARTEJ NA PROCESIE HIERARCHII ANALITYCZNEJ (AHP) W POSTĘPOWANIU PRZETARGOWYM NA UTRZYMANIE BUDYNKÓW. PRZYPADEK MALEZYJSKICH UCZELNI PUBLICZNYCH

In this paper, the proposed Analytic Hierarchy Process (AHP) based decision making framework was implemented and validated for its capability, applicability and validity in assisting building maintenance personnel to select the most appropriate procurement method. The decision making framework was developed based on AHP technique and principles. Expert Choice Software was employed as the development tool where the shortlisted criteria and alternatives were integrated within the framework. The validation process was carried out through a structured interview with nine public universities selected. The evaluations revealed that majority of the interviewees perceived that the framework developed was good (65%) and excellent (21%) in terms of capability, applicability and validity. The proposed decision making framework introduced expected to be a useful tool for maintenance organization that can assist them in decision making on selecting the most appropriate procurement method.

Keywords: *analytic hierarchy process, building maintenance management, procurement strategy alternative, procurement selection criteria, public university.*

W niniejszej pracy przedstawiono platformę programistyczną wspomagającą podejmowanie decyzji opartą na procesie hierarchii analitycznej (AHP). Po wdrożeniu zaproponowanegoframeworku, weryfikowano jego wydajność, przydatność oraz wiarygodność jako narzędzia wspierającego pracowników utrzymania budynku przy wyborze najodpowiedniejszej metody przetargowej. Platformę opracowano w oparciu o technikę i zasady AHP. Jako narzędzia programistycznego użyto Expert Choice Software, za pomocą którego integrowano z frameworkiem wybrane kryteria i alternatywy. Weryfikację przeprowadzono na podstawie strukturalizowanego wywiadu z wybranymi dziewięcioma uczelniami publicznymi. Otrzymane oceny wykazały, że większość badanych postrzegało opracowaną platformę jako dobrą (65%) lub doskonałą (21%) pod względem wydajności, przydatności i wiarygodności. Przewiduje się, że proponowany framework wspomagający podejmowanie decyzji będzie stanowić użyteczne narzędzie doboru odpowiednich metod przetargowych dla instytucji zajmujących się obsługą techniczną.

Słowa kluczowe: *proces hierarchii analitycznej, zarządzanie utrzymaniem budynków, alternatywna strategia przetargowa, kryteria wyboru zamówienia, uczelnia publiczna.*

1. Introduction

Maintenance management to the private and the public sector has been rapidly changing throughout the years due to several factors which include the enhancement of sophisticated technology, globalization and change of economy [13, 48]. The economy of Malaysia has been planned on the basis of five-year strategic plan since independence. Construction industry plays an important role to the economy of Malaysia in generating wealth and improving the quality of life for Malaysians through the translation of government's socio-economic policies into social and economic infrastructure and buildings [10]. The increase in supply of building will lead the increase in the amount invested in building maintenance. Lateef [18]claimed that the allocation for repair and maintenance works in Malaysia is grossly inadequate to meet the ever-growing demand for the maintenance backlog even the government consistently increases allocation to the maintenance sector. The former Prime Minister of Malaysia, Dato' Seri Abdullah Ahmad Badawi stated that Malaysia was losing billions of ringgit due to the poor maintenance of buildings and amenities. He further highlighted that there were weaknesses in the management and maintenance of public facilities [46]. Many academic organizations view building maintenance management as a burden rather than as a value-added strategy[20]. Maintenance management is not regarded as part of the top management function or duties but as an operational function. It only receives management attention when everything has gone wrong.

Public facilities are indeed very essential to a nation. Thus, this research will be mainly focusing on maintenance management of public universities in Malaysia. University buildings are factor of production

[19]. It is essential for education building to plan effective building maintenance management because the facility condition of education building directly impact teaching and learning [22]. Therefore, an improvement in maintenance management processes is very critical for universities in Malaysia. Public universities in Malaysia are categorized into three groups; Research Universities, Focused Universities and Comprehensive Universities. So far, there are 20 public universities in Malaysia, which comprise 5 research universities, 4 comprehensive universities and 11 focused universities.

Selecting an appropriate procurement strategy for building maintenance is a very critical decision in building maintenance management. It is claimed that it is a complex and intimidate task to the client and the client's advisers to select the most appropriate procurement method[12].Procurement is vital since it sets the basis for cooperation between clients and contractors[31]. This statement is true for the local, regional or global project in scope. Procurement method selection becomes a very significant task for clients because employing an inappropriate procurement method may lead to project failure[8, 30].

The adoption of an appropriate sourcing strategy in building maintenance will not only help the good functionality of the building, the mechanical and electrical elements but also in achieving cost savings, higher comfort levels, better economic rent of the building space, elevated corporate image a sustainability of the building[41]. Morledge *et al.* [28]pointed out that their research led them to believe that relatively few professionals fully understood the differences between the various procurement systems and would be unable to make sensible recommendations as to which system would be most appropriate for a specific project. In fact, the amplification of demand on quality services for building or space, changes in business environment and the ever evolving market trend resulting in an emergence of various procurement strategies. Thus, the tasks of decision-makers to select the most appropriate procurement method becoming more challenging.In this respect, a more systematic selection framework is much needed. This paper reports a study conducted among public universities in Malaysia on the development of procurement selection framework based on Analytic Hierarchy Process (AHP) technique and principles. The proposed decision making framework is implemented and validated for its capability, applicability and validity and the results are presented in this paper.

2. Determination of procurement strategy alternative and procurement selection criteria

Procurement is defined as "an organizational system that assigns specific responsibilities and authorities to people and organizations" while maintenance procurement as "the process by which required maintenance works are carried out" [1, 9, 24, 47]. Maintenance work range from very large maintenance projects to a very small maintenance task. Subsequently, many different types of procurement methods have been developed to overcome the weaknesses of the existing procurement method and meet the range of service's requirement. The types of procurement method identified through literature review for building maintenance were listed as below [3, 4, 9, 14, 35, 41, 47]:

I Direct Labour or In-house

In-house is the management process of performing a service by in-house staffdirectly employed by organisationsto run and maintain the building[14, 29].The client organisation usually employ direct labour under the terms of conventional employee relationship to monitor and control the performance of maintenance [5, 29, 45]. Williams [45]highlighted that presentlythere were very less organisations that employ 100% in-house operation but if it really exists, it is not on a large scale.According to Sheng [41], in-house strategy is deemed to be the most fundamental and traditional strategy for the delivery of property management and maintenance services.The operation staffs who are employed directly by the organization are recognized as part of the organization with no existence of service contract tying the relationship together except the ordinary employment contract. Through inhouse strategy, the assigned property manager will need to plan, execute, coordinate and control the team members' work. Internal communication will take place both laterally and vertically.

II Outsourcing

Hui and Tsang [14] explained that outsourcing is a whole package of support function is off-loaded to an external service provider. Sheng [41] stated that outsourcing prepares the organization to engage an external specialist for the provision of certain specialized trade of service under contract basis.Outsourcing can trade of service under several types of contract which include:

1) Outsourcing by Lump Sum Contract.
2) Outsourcing by Measured Term Contract.
3) Outsourcing by Specialist Term Contract.
4) Outsourcing by Day work Term Contract.
5) Outsourcing by Tendered Schedule Term contract.
6) Outsourcing by Repair and Maintenance Contract.
7) Outsourcing by Cost Reimbursement Contract.
8) Outsourcing by Service Level Agreement.

Outsourcing has increasingly become an important approach that can significantly assist organizations to leverage their skills and resources to achieve greater competitiveness [21, 34, 44]. Lau and Zhang [21]stated that outsourcing strategy enable organizations to gain competitive advantage through cost reduction and improved responsiveness to changing business environment and market demand. This is agreed by [3, 42]that outsourcing is a supply strategy often chosen as a means of increasing organizational effectiveness and efficiency.

III Out-tasking

Out-tasking is defined as "a management process whereby specific tasks, as opposed to a whole package of support function in the case of outsourcing, are performed by a contractor"[14, 16]. According to Hui and Tsang [14], the company usually employs a small number of staff to serve as coordinators between internal customers and the external service provider when outsourcing is practised. This is in contrast to out-tasking where the internal staff members play a proactive role of planning and initiating service activities and leading the external service provider for delivery of the needed service. Thus, the internal personnel are fully responsible for the consequences of out-tasking.

IV Public Private Partnership (PPP)

Public Private Partnership (PPP) is "a partnership or strategic alliance has been formed between the organization and service provider based on a sharing of the responsibility for the delivery and performance of the service, including the sharing of the benefits arising from any efficiency gains and cost savings" [3, 4].

V Total Facilities Management (TFM)

An entire scope of services are packaged togetherand externalized to a solitary supplier which gets to be completely in charge of themonitoring, control, delivery and accomplishment of executionobjectives which relate to operational benefit [3, 4].

VI Traditional

Straub [43]stated that maintenance projects mostly adopted traditional procurement method where three to five competitive bids are solicited and the lowest tender price will be selected. Espling and Olsson [11] claimed that traditional procurement produce low productivity, litigation, an adversarial environment and a reduced ability to absorb technological and business process innovations.

VII Partnering
Espling and Olsson [11] defined partnering as "a managerial approach used by two or more organizations to achieve specific business objectives by maximizing the effectiveness of each participant's resources". The approach is based on mutual objectives, an agreed method of problem resolution and active search for continuous measurable improvements [6, 11]. Partnering is becoming increasingly used for procurement of maintenance services [35].Partnering requires changing traditional relationships to a shared culture without regard to organizational boundaries. The relationship is based on dedication to common goals, trust and an understanding of each other's individual expectations and values. Expected benefits include cost effectiveness and improved efficiency, the continuous improvement of quality products and services and increased opportunity for innovation. It should be noted that these types of arrangements do not create a business partnership [35].

As this research mainly focusing in assisting the universities organization that wishes to outsource the services, direct labour which is known as in-house was excluded in this present study.

Masterman [27] claimed that many clients had been selecting procurement systems in a cursory manner simply based upon subjective past experience and the conservative decisions and some client even employ a specific procurement strategy by default without making a deliberated choice. Although past experiences may be an essential factor that influences the selection of procurement strategy, but experiences and solutions to problems retrieved from past projects may not be applicable to the current projects because each building has its own distinct characteristic. In addition, Love *et al.* [25] highlighted that owners who have similar nature do not certainly have similar needs. In fact, the needs rely on many factors and are usually specific to the particular project. Some researches highlighted that it is essential to establish a list of procurement selection criteria before various procurement methods were evaluated. The procurement selection criteria should reflect the requirements and characteristics of the client, project and external environment [2, 17, 26]. There are 26 criteria identified from literature review, which are divided into three main categories that are clients' requirement, project characteristic and external environment or factor which can be referred to Table 1.

In order to derive a particular set of procurement method and procurement selection criteria for public universities in Malaysia, postal questionnaires survey was conducted with all the public universities in Malaysia. The assessment criteria and alternatives for selection are evaluated by the maintenance personnel in public universities in Malaysia. The main purpose of evaluation is to eliminate those criteria and alternatives that are considered less or not important for the development of the decision making framework.

Likert scale and ranking analysis were employed. In order to derive a set procurement selection criteria that were considered essential, only those procurement method and criteria obtained both mean rating and mode equivalent to or above 4, which were considered as important and very important according to likert scales of 5 (from which 1 indicate "least important" to 5 indicate "very important") were included in this study for the proposed decision making framework.

The mean is computed by adding up all the scored and dividing by the number of scores ($M=\sum X/N$) [23]. It is essential to calculate a mean to rank the variables. Mode is known as the most common category whereby the score most frequently exist in a distribution.

There are only 19 criteria will be considered for the development of decision making framework. On the other hand, the procurement methods that are considered as most commonly used (percentage of cases more than 50%) and categorized as important and very important with both mean rating and mode equal or above 4 will be considered for the proposed decision making framework. The procurement selection criteria and procurement option that were selected are provided in Table 2.

3. Analytic Hierarchy Process (AHP)

The Analytic Hierarchy Process (AHP) is "a theory of measurement through pairwise comparisons and relies on the judgments of experts to derive priority scales" [37]. Ibbs and Chih [15]stated that the first steps of AHP are to develop a hierarchy of criteria and to identify all possible alternatives. AHP uses a pairwise comparison procedure whereby a decision maker is required to compare all alternatives with respect to evaluation criteria in turn. The decision maker's preferences are presented in a ratio scale and are combined into an overall rating. The basic steps for conducting study using AHP are as follow [33, 36, 38–40]:

Table 1. Procurement Method Selection Criteria

Criteria			
C 1	**Client Requirement and Characteristics**		
C 1.1	Experience contractor availability	C 1.11	Involvement of owner in the project
C 1.2	Quality level	C 1.12	Working relationship
C 1.3	Knowledge of the strategy	C 1.13	Intuition and past experience
C 1.4	Degree of responsibility	C 1.14	Client in house technical capability
C 1.5	Client's financial capability	C 1.15	Price or cost certainty
C 1.6	Price competition	C 1.16	Risk allocation or avoidance
C 1.7	Time Certainty	C 1.17	Dissatisfaction with previous process
C 1.8	Speed	C 1.18	Degree of complexity
C 1.9	Public accountability	C 1.19	Degree of flexibility
C 1.10	Clarity of scope		
C 2	**Project Characteristic**		
C 2.1	Existing building condition	C 2.2	Project size
C 3	**External environment/ factor**		
C 3.1	Objective or policy of organization	C 3.4	Political issue/constraint
C 3.2	Government policy	C 3.5	Cultural differences
C 3.3	Dispute and arbitration		

Table 2. Selected procurement selection criteria and procurement options for the proposed decision making framework

Procurement Selection Criteria	Mean	Mode	Procurement method used in universities	Mean	Mode	Percent of Cases
Experience contractor availability	4.71	5	Outsourcing by Repair and Maintenance Contract	4.06	4	82.4%
Existing building condition	4.59	5	Outsourcing by Specialist Term Contract	4.18	4	76.5%
Objective or policy of organization	4.53	4	Outsourcing by Tendered Schedule Term Contract	4.12	4	70.6%
Quality level	4.47	5	Outsourcing by Measured Term Contract	3.94	4	64.7%
Government policy	4.41	4				
Knowledge of the strategy	4.41	5				
Degree of responsibility	4.41	5				
Client's financial capability	4.41	5				
Price competition	4.35	4				
Time Certainty	4.35	4				
Speed	4.35	4				
Public accountability	4.29	4				
Clarity of scope	4.29	4				
Involvement of owner in the project	4.24	4				
Working relationship	4.24	5				
Project size	4.18	4				
Intuition and pass experience	4.12	4				
Client in house technical capability	4.06	4				
Price or cost certainty	4.00	4				

(a) Define the problem and determine its goal.
(b) Structure the hierarchy with the decision-maker's objective at the top with the intermediate levels capturing criteria on which subsequent levels depend and the bottom level containing the alternatives.
(c) Construct a set of n × n pair-wise comparison matrices for each of the lower levels with one matrix for each element in the level immediately above. The pairwise comparisons are made using the relative measurement scale. The pair-wise comparisons capture a decision maker's perception of which element dominates the other.
(d) There are n (n−1)/2 judgments required to develop the set of matrices in step (c). Reciprocals are automatically assigned in each pair-wise comparison.
(e) The hierarchy synthesis function is used to weight the eigenvectors by the weights of the criteria and the sum is taken over all weighted eigenvector entries corresponding to those in the next lower level of the hierarchy.
(f) After all the pair-wise comparisons are completed, the consistency of the comparisons is assessed consistency ratio (CR) calculated by the formula below [7, 9, 36]:

Consistency Ratio (CR) = Consistency index (CI)/ Random Index (RI)

Where CI = (λmax – n)/(n−1), with n the number of elements, λmax = the maximum eigenvalue of the comparison matrix and RI = the consistency index of a randomly generated reciprocal matrix within a scale of 1 to 9. The consistency ratio (CR) is acceptable if it does not exceed 0.10. Repeat and review the judgment if the CR is greater than 0.10.

4. Proposed decision making framework

The proposed decision making framework was developed based on Multiple Criteria Decision Making (MCDM) particularly Analytic Hierarchy Process (AHP). The framework employed AHP techniques and principles using Expert Choice 11 software as the development tool. The development of decision making framework using AHP mainly focused on two important components that are the possible assessment criteria and the alternatives available for selection whereby the assessment criteria were used to evaluate the alternatives as shown in Figure 1.

There are three basic principles of the AHP which include the principle of constructing hierarchies where a complex system was structured hierarchically by decomposing the elements into constituent parts according to essential relationships towards a desired goal which can make the whole system well understood, the principle of establishing priorities where priority of elements in a decision problem is established to make pairwise comparison that is to compare the elements in pairs against a given criterion and finally the principle of logical consistency to ensure that elements are grouped logically and ranked consistently according to a logical criterion [36]. Logical consistency ensures that elements are grouped logically and ranked consistently according to a logical criterion.

The AHP implementation steps of the framework will be simplified by using the Expert Choice professional software that is available commercially and designed for implementing AHP. Expert Choice 11 software was employed as a development tool to assist in developing the decision making framework. Expert Choice software offers a model view containing either a tree view or cluster view of the decision hierarchy. Expert Choice allows the decision maker to re-examination and revises the judgments for all level of the hierarchy and shows where inconsistency exists and how to minimize it in order

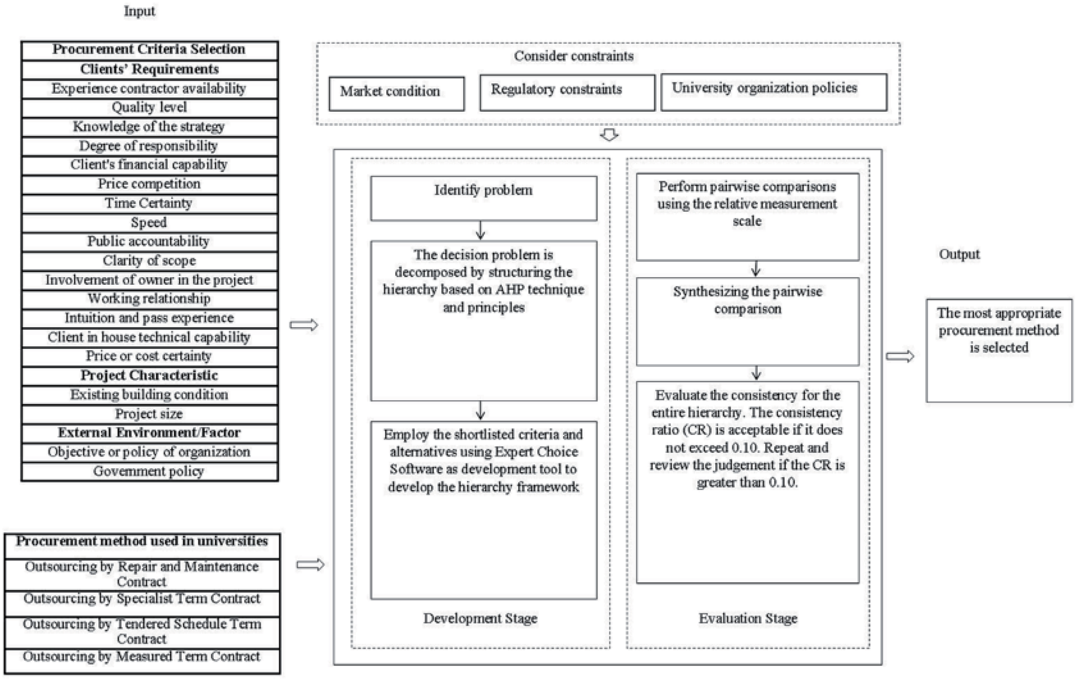

Fig. 1. Decision Making Framework for Procurement Method Selection of Building Maintenance Management for Public Universities

to improve the decision. The inconsistency value will be shown once the judgment is done.

5. Research design and methodology

Structured interview was conducted to validate the framework developed. The framework produced was demonstrated to the interviewees. Then, the interviewees were asked to run the framework and were asked to evaluate the framework in terms of capability, applicability and validity. Structure interview is chosen so that the researcher can explain the framework in detail to the respondents, clarify any doubts arises by the interviewees and at the same time the researcher able to examine the level of understanding of the respondents towards the topic and the framework. All the interviewees were explained and asked the same questions in the same manner to standardize in order to make it easier to repeat the interview and provide a reliable source of qualitative data.

As mentioned previously, the total populations of public universities in Malaysia are 20, comprise of 5 research universities, 4 comprehensive universities and 11 focused universities. However, there are only 17 universities replied in the postal questionnaires survey. The interviewees for the structured interview were selected from the universities that have responded in the postal questionnaires survey. There were 9 universities equivalent to 52.9% selected from 17 uni-

Table 3. Interviewees Profiles

Name of Universities	Nos. of Interviewees	Position	Experience (years)
Research Universities			
University RA	3	Head of Civil Engineering Division	20
		Head of Contract & Quantity Surveying Division	30
		Quantity Surveyor	10
University RB	1	Assistant Head of Quantity Surveying Department	17
University RC	1	Head of Contract Department	31
Comprehensive Universities			
University CA	1	Head of Contract Management And Cost Control Section	12
University CB	1	Acting Senior Facilities Engineer	7
Focussed Universities			
University FA	1	Head of Quantity Surveying Department	10
University FB	1	Deputy Director of Facility and Estate Management Department	25
University FC	1	Head Department of Building Maintenance Section	11
University FD	1	Deputy Director of Development & Facilities Management Department	23

Table 4. All vector of priorities for main criteria, sub criteria and alternative

Level 1: Goal	Select the most appropriate procurement method of building maintenance management services for public university																		
Level 2: Main Criteria	Clients' Requirements (C1)															Project Characteristic (C2)		External Environment or Factor (C3)	
Vector of Priorities	0.300															0.100		0.600	
CR	0.00															0.00		0.00	
Level3: Sub Criteria	**C1.1**	**C1.2**	**C1.3**	**C1.4**	**C1.5**	**C1.6**	**C1.7**	**C1.8**	**C1.9**	**C1.10**	**C1.11**	**C1.12**	**C1.13**	**C1.14**	**C1.15**	**C2.1**	**C2.2**	**C3.1**	**C3.2**
Vector of Priorities	0.071	0.068	0.042	0.023	0.025	0.092	0.070	0.040	0.017	0.168	0.063	0.065	0.078	0.070	0.109	0.875	0.125	0.125	0.875
CR	0.08	0.08	0.08	0.08	0.08	0.08	0.08	0.08	0.08	0.08	0.08	0.08	0.08	0.08	0.08	0.00	0.00	0.00	0.00
Level 4: Alternatives	Vector of Priorities																		
Outsourcing by Repair and Maintenance Contract	0.532	0.053	0.079	0.063	0.216	0.265	0.046	0.06	0.118	0.116	0.091	0.426	0.055	0.250	0.250	0.250	0.250	0.250	0.250
Outsourcing by Specialist Term Contract	0.061	0.585	0.219	0.501	0.112	0.265	0.147	0.619	0.487	0.245	0.266	0.111	0.532	0.250	0.250	0.250	0.250	0.250	0.250
Outsourcing by Tendered Schedule Term Contract	0.095	0.121	0.200	0.120	0.350	0.094	0.296	0.215	0.118	0.073	0.091	0.171	0.213	0.250	0.250	0.250	0.250	0.250	0.250
Outsourcing by Measured Term Contract	0.312	0.242	0.503	0.316	0.322	0.375	0.511	0.107	0.276	0.567	0.552	0.292	0.200	0.250	0.250	0.250	0.250	0.250	0.250
CR	0.02	0.04	0.05	0.04	0.04	0.05	0.05	0.04	0.06	0.07	0.09	0.07	0.02	0.00	0.00	0.00	0.00	0.00	0.00

***CR= Consistency Ratio**

Table 5. Vector of overall priorities with respect to main criteria

Main Criteria	Clients' Requirements (C1)	Project Characteristic (C2)	External Environment/Factor (C3)	Vector of Overall Priorities
Vector of Priorities	0.300	0.100	0.600	
CR	0.00	0.00	0.00	
Alternatives	Vector of Priorities			
Outsourcing by Repair and Maintenance Contract	0.203	0.250	0.250	0.240
Outsourcing by Specialist Term Contract	0.273	0.250	0.250	0.255
Outsourcing by Tendered Schedule Term Contract	0.18	0.250	0.250	0.236
Outsourcing by Measured Term Contract	0.344	0.250	0.250	0.269
CR	0.07	0.00	0.00	0.03

***CR= Consistency Ratio**

versities responded. The 9 universities are selected from the 3 main categories of universities so that this research covers different type and category of university. Piaw [32] highlighted that in qualitative research, the sample size is usually small and 5 subjects are accepted if the demography data are same. Besides, Musa [29] research on determining the best options for Facilities Management (FM) service delivery in UK shopping centers, which also integrated AHP and Expert Choice in developing the framework did 5 interviews on shopping complexes for validation of his research framework. Thus, 9 universities are considered satisfactory and accepted because the evaluation done by the 9 universities were quite equivalent. The interviewees' profiles are tabulated in Table 3 according to the 3 main types of public universities categories.

In the structured interview, the interviewees were first requested to do a pair-wise comparison with the assessment criteria and procurement option which was stored in Expert Choice software as an interview instrument. This Expert Choice software instrument offers a questionnaire with scale of 1 to 9 to perform pair-wise comparison. The judgments can be performed in three ways by numerical, verbal and graphical in Expert Choice software. The interviewees were requested to perform pair-wise comparisons for all levels of hierarchy in the framework produced. This instrument brings a lot of advantages in terms of time saving, simple, easy to be explained and understand as well as well-structured.

Once the interviewee obtained the proposed procurement method from the framework, the interviewee requested to rate the Decision Making Framework for Procurement Method Selection of Building Maintenance Management for Public Universities in terms of capability, applicability and validity. Each evaluation form was labeled with distinctive reference number (UM/FBE/BHA1100007/FBF/0XX) at the right top to identify which university gave what evaluations and comments. The interviewees can also provide comments, cop and sign the form after evaluation done. The example of evaluation form as shown in Appendix A.

6. Results and discussion

The validation process was carried out through structured interviews with 9 universities selected. The interviewees were selected from the maintenance and facilities' maintenance management department of university. The interview commenced on 9th of April 2013 and lasted on 9th of May 2013. The structured interview took exactly one-month time. The interview was scheduled so that two to three universities were interviewed in a week. The interviewees had at least five-year experiences in selecting procurement method for building maintenance work and had been involved in the decision-making process.

In the proposed method, the interviewees are first requested to do a pair-wise comparison with the assessment criteria and procurement

Table 6. Summary results to compare all interviewees' priority vector to select the most appropriate procurement method for different type of building maintenance services

Priority Ranking	Universities, Maintenance Services and Vector of Priorities				
	University RA	University RB	University RC	University CA	University CB
	Maintenance of Water-proofing System	Maintenance of Air-conditioning Services	Housekeeping	General Repair Work	Roof Repair Work
1	EEF (0.600)	PC (0.540)	CR (0.481)	CR=EEF (0.444)	PC (0.667)
2	CR (0.300)	EEF (0.297)	EEF(0.405)	CR=EEF (0.444)	CR (0.222)
3	PC (0.100)	CR (0.163)	PC(0.114)	PC (0.111)	EEF (0.111)

EEF=External Environment or Factor, CR=Clients' Requirement, PC=project characteristic

Table 7. Summary results to compare all interviewees' priority vector to select the most appropriate procurement method for different type of building maintenance services

Priority Ranking	Universities, Maintenance Services and Vector of Priorities			
	University FA	University FB	University FC	University FD
	Building Cleaning	Maintenance of electrical system	Maintenance of road	Maintenance of Lift
1	EEF (0.528)	CR = PC(0.455)	CR (0.427)	EEF (0.600)
2	CR (0.333)	CR = PC(0.455)	EEF (0.318)	PC=CR (0.200)
3	PC (0.140)	EEF (0.091)	PC (0.254)	PC=CR (0.200)

EEF=External Environment or Factor, CR=Clients' Requirement, PC=project characteristic

Table 8. Vector of Overall Priorities for the Four Alternatives and Ranking of the Alternatives

Alternatives	Vector of Overall Priorities	Rank
University RA		
Outsourcing by Repair and Maintenance Contract	0.240	3
Outsourcing by Specialist Term Contract	0.255	2
Outsourcing by Tendered Schedule Term Contract	0.236	4
Outsourcing by Measured Term Contract	**0.269**	**1**

Table 8. Vector of Overall Priorities for the Four Alternatives and Ranking of the Alternatives

University RB		
Outsourcing by Repair and Maintenance Contract	0.300	2
Outsourcing by Specialist Term Contract	**0.432**	**1**
Outsourcing by Tendered Schedule Term Contract	0.108	4
Outsourcing by Measured Term Contract	0.160	3
University RC		
Outsourcing by Repair and Maintenance Contract	0.235	2
Outsourcing by Specialist Term Contract	0.349	1
Outsourcing by Tendered Schedule Term Contract	**0.216**	3
Outsourcing by Measured Term Contract	0.201	4
University CA		
Outsourcing by Repair and Maintenance Contract	**0.289**	**1**
Outsourcing by Specialist Term Contract	0.274	2
Outsourcing by Tendered Schedule Term Contract	0.225	3
Outsourcing by Measured Term Contract	0.213	4
University CB		
Outsourcing by Repair and Maintenance Contract	0.238	3
Outsourcing by Specialist Term Contract	0.164	4
Outsourcing by Tendered Schedule Term Contract	0.251	2
Outsourcing by Measured Term Contract	**0.347**	**1**
University FA		
Outsourcing by Repair and Maintenance Contract	0.266	2
Outsourcing by Specialist Term Contract	0.181	3
Outsourcing by Tendered Schedule Term Contract	0.169	4
Outsourcing by Measured Term Contract	**0.384**	**1**
University FB		
Outsourcing by Repair and Maintenance Contract	0.223	3
Outsourcing by Specialist Term Contract	**0.367**	**1**
Outsourcing by Tendered Schedule Term Contract	0.264	2
Outsourcing by Measured Term Contract	0.146	4
University FC		
Outsourcing by Repair and Maintenance Contract	0.235	3
Outsourcing by Specialist Term Contract	0.227	4
Outsourcing by Tendered Schedule Term Contract	**0.293**	**1**
Outsourcing by Measured Term Contract	0.246	2
University FD		
Outsourcing by Repair and Maintenance Contract	0.245	2
Outsourcing by Specialist Term Contract	**0.295**	**1**
Outsourcing by Tendered Schedule Term Contract	0.222	4
Outsourcing by Measured Term Contract	0.238	3

Table 9. Procurement Methods Comparison (Actual versus Proposed)

No.	University	Type of building maintenance services	Actual Procurement method used	Procurement Method proposed by the Framework	Similarity
1	RA	Maintenance of Waterproofing System	Outsourcing by Measured Term Contract	Outsourcing by Measured Term Contract	√
2	RB	Maintenance of Air-conditioning Services	Outsourcing by Repair and Maintenance Contract	Outsourcing by Specialist Term Contract	X
3	RC	Housekeeping	Facilities Management Condition of Contract	Outsourcing by Specialist Term Contract	X
4	CA	General Repair Work	Outsourcing by Repair and Maintenance Contract	Outsourcing by Repair and Maintenance Contract	√
5	CB	Roof Repair Work	Outsourcing by Measured Term Contract	Outsourcing by Measured Term Contract	√
6	FA	Building Cleaning	Outsourcing by Measured Term Contract	Outsourcing by Measured Term Contract	√
7	FB	Maintenance of Electrical System	Outsourcing by Repair and Maintenance Contract	Outsourcing by Specialist Term Contract	X
8	FC	Maintenance of Road	Outsourcing by Tendered Schedule Term Contract	Outsourcing by Tendered Schedule Term Contract	√
9	FD	Maintenance of Lift	Outsourcing by Specialist Term Contract	Outsourcing by Specialist Term Contract	√

Table 10. Nine universities evaluation towards Decision Making Framework for Procurement Method Selection of Building Maintenance Management for Public Universities

No.	Evaluation Question	Rating				
		Very Poor	**Poor**	**Satisfactory**	**Good**	**Excellent**
1	The capability of the framework			11%	75%	14%
1.1	How well the framework in supporting the decision process?			2 (22%)	7 (78%)	
1.2	How reliable the assessment procurement selection criteria employed in the framework?			1 (11%)	8 (89%)	
1.3	How well the framework reflect the real situation in decision making process for procurement method selection?			1 (11%)	7 (78%)	1 (11%)
1.4	How useful was the Expert Choice software employed in the framework?				5 (56%)	4 (44%)
2	The applicability of the framework			10%	63%	27%
2.1	How relevant the framework in selecting the most appropriate procurement method?				6 (67%)	3 (33%)
2.2	How appropriate was the assessment criteria employed in the selection process?			1 (11%)	7 (78%)	1 (11%)
2.3	How appropriate was the framework to act as an alternative decision making for a supporting system?			1 (11%)	6 (67%)	2 (22%)
2.4	How relevant was the framework in improving the existing decision making process?				7 (78%)	2 (22%)
2.5	How relevant was the framework in term of:-					
2.5.1	Speed			3 (33%)	4 (44%)	2 (22%)
2.5.2	Flexibility			1 (11%)	4 (44%)	4 (44%)
2.5.3	Consistency				6 (67%)	3 (33%)
3	The validity of the result			33%	50%	17%
3.1	How convinced were you with the result produced by this framework?			3 (33%)	4 (44%)	2 (22%)
3.2	How confident were you in using the result as a selection making process in real situation?			3 (33%)	5 (56%)	1 (11%)
Overall score		**0%**	**0%**	**14%**	**65%**	**21%**

option which was stored in Expert Choice software. All the pair-wise comparison judgments made in Expert Choice software were synthesized to obtain vector of priorities. Table 4 showed all the vector of priority for main criteria, sub criteria and alternatives for University RA in selecting procurement method for maintenance of waterproofing. All main criteria judgments consistency ratio (CR) were 0.00 that were less than 0.10 (<0.10) which represent good consistency while Table 5 revealed vectors of priorities for the alternatives with respect to the main factor and alternatives' vector of overall priorities. The vector of overall priorities for the four alternatives as shown in Table 5 indicated that outsourcing by measured term contract (0.269) which obtained the highest of vector of overall priorities is the best procurement method for maintenance of waterproofing in University RA.

Similarly, the assessments were done by other 8 public universities and hence 9 procurement methods were successfully derived. The interviewees' decisions on vector of priorities for main criteria were different in selecting procurement method for different type of building maintenance services. Table 6 and Table 7 showed the summary results to compare all interviewees' priority vector to select the most appropriate procurement method for different type of building maintenance services. It can be seen in Table 6 and Table 7 that owners of a similar nature do not necessarily have similar needs. In fact, the needs are usually specific to the particular project. The vector of overall priorities for the four alternatives and ranking of the alternatives were shown in Table 8.

Table 9 compares the proposed and the actual procurement method used. From Table 9, out of 9 assessments conducted there were 6 matching and 3 non-matching. For all the 6 matching universities' respondents stated that they were satisfied with the result proposed by the framework. While for the non-matching, the University RB interviewee stated that the proposed procurement method was very suitable as the maintenance work for air-conditioning services required specialist to carry out. The University RC interviewee also claimed that the proposed framework was very useful and a new knowledge for him to make a more deliberate decision compared with the decision made previously. On the other hand, the respondent of University FB clarified that she was satisfied with the proposed framework as the maintenance of the electrical system should be done by specialists who are certified. The interviewees admitted that the selection of the procurement process proposed was decided on a judgmental basis which was not simply based on previous experience and perception. Clients may suffer if their selection simply based upon biased past experience and the conservative decisions of their in-house experts[30]. Although past experiences may be an essential factor that influences the selection of procurement strategy, but experiences and solutions to problems retrieved from previous projects may not be applicable to the current projects because each building has its own distinct characteristic. Thus, the proposed decision making framework will be capable to assist the decision-makers to select the most appropriate procurement method as the decision maker able to derive his set of important criteria in the selection according to the characteristics of the building.

Once the judgments completed and obtained the proposed procurement method from the framework, the interviewees were requested to rate the decision making framework in terms of capability, applicability and validity. The summary of the evaluations done by the 9 universities were shown in Table 10. The results revealed that majority of the interviewees perceived that the decision making framework developed was good (65%) and excellent (21%) in terms of capability, applicability and validity in assisting the decision-makers to select the most appropriate procurement method in building maintenance work. In terms of capability, the majority (75%) of the interviewees considered that the framework has the capability to assist them to select the most appropriate procurement method and 89% of the interviewees conceived that the assessment procurement selection criteria employed in the framework were reliable. In addition, majority of the interviewees (78%) also perceived that the framework was well in supporting the decision process and reflect the real situation in the decision-making process for procurement method selection.

In evaluating the applicability of the framework, 63% of the interviewees considered the framework had good applicability and 27% of the interviewees conceived that the framework had excellent applicability in selecting the most appropriate procurement method. Majority thinks that the framework was good (78%) and excellent (22%) in improving the existing decision making process. The results also indicated that the framework was good (67%) and excellent (22%) to act as an alternative decision making for a supporting system.

In terms of evaluating the results obtained from the framework, the interviewees conceived that the results obtained were good (44%) and excellent (22%) in convincing them to employ the result obtained. There were 56% (good) and 11% (excellent) of the interviewees were confident in using the result as a selection making process in real situation.

7. Conclusion

The proposed framework was well received by the interviewees and they admitted that the selection of the procurement process proposed was decided on a judgmental basis which was not simply based upon previous experience and perception. The evaluations done by the 9 universities regarding the proposed decision making framework revealed that majority of the interviewees perceived that the Decision Making Framework for Procurement Method Selection of Building Maintenance Management for Public Universities developed was good (65%) and excellent (21%) in terms of capability, applicability and validity in assisting the decision-makers to select the most appropriate procurement method in building maintenance work. Thus, the proposed decision making framework will be capable to assist the decision-makers to select the most appropriate procurement method.

Acknowledgement:

The authors gratefully acknowledge the financial support of the University of Malaya Research Grant (UMRG), grant no RG183/12SUS established at the University of Malaya, Sustainability Science Research Cluster.

References

1. Adekunle, S.O., D. Michael, M.A.K. Malik, M. Peter, and R. Steve. Construction project procurement routes: an in-depth critique. International Journal of Managing Projects in Business 2009; 2(3): 338-354.
2. Ambrose, M.D. and S.N. Tucker. Matching a Procurement System to Client and Project Needs: A Procurement System Evaluator. in W055/W065 Triennial Symposium on Customer Satisfaction. 1999.

3. Ancarani, A. and G. Capaldo. Supporting decision-making process in facilities management services procurement: A methodological approach. Journal of Purchasing and Supply Management 2005; 11(5–6): 232-241.
4. Atkin, B. and A. Brooks, Total Facilities Management. 2nd ed. 2005, Oxford: Blackwell Publishing Ltd.
5. Barret, P. and D. Baldry, Facilities Management: Towards Best Practice. 2nd ed. 2003, Oxford: Blackwell Publishing Ltd.
6. Bennett, J. and S. Jayes, Trusting the Team: The Best Practice Guide to Partnering in Construction. 1995, Reading: Centre for Strategic Studies in Construction, The University of Reading.
7. Cheung, S.O., T.I. Lam, M.Y. Leung, and Y.W. Wan. An analytical hierarchy process based procurement selection method. Construction Management and Economics 2001; 19(4): 427-437.
8. Chua, D., Y. Kog, and P. Loh. Critical Success Factors for Different Project Objectives. Journal of Construction Engineering and Management 1999; 125(3): 142-150.
9. Chua, S.J.L., A.S. Ali, and A.B. Alias. An Analytic Hierarchy Process (AHP) Decision Making Framework for Procurement Strategy Selection in Building Maintenance Work. Journal of Performance of Constructed Facilities 2013.
10. Construction Industry Development Board (CIDB), Construction Industry Master Plan Malaysia 2006-2015. 2007, Malaysia.
11. Espling, U. and U. Olsson. Part II. Partnering in a railway infrastructure maintenance contract: a case study. Journal of Quality in Maintenance Engineering 2004; 10(4): 248-253.
12. Hashim, M., M.C.Y. Li, N.C. Yin, N.S. Hooi, S.M. Heng, and T.L. Yong, Factors influencing the selection of procurement systems by clients, in International Conference on Construction Industry 2006 2006: Padang, Indonesia: 1-10.
13. Horner, R.M.W., M.A. El-Haram, and A.K. Munns. Building maintenance strategy: a new management approach. Journal of Quality in Maintenance Engineering 1997; 3(4): 273-280.
14. Hui, E.Y.Y. and A.H.C. Tsang. Sourcing strategies of facilities management. Journal of Quality in Maintenance Engineering 2004; 10(2): 85-92.
15. Ibbs, W. and Y.-Y. Chih. Alternative methods for choosing an appropriate project delivery system (PDS). Facilities 2011; 29(13): 527-541.
16. Kleeman, W.B. Out-tasking: More Widespread than Outsourcing in the USA. Facilities 1994; 12(2): 24-26.
17. Kumaraswamy, M.M. and S.M. Dissanayaka. Developing a decision support system for building project procurement. Building and Environment 2001; 36(3): 337-349.
18. Lateef, O.A. Building maintenance management in Malaysia. Journal of Building Appraisal 2009; 4(3): 207–214.
19. Lateef, O.A. Case for alternative approach to building maintenance management of public universities. Journal of Building Appraisal 2010b; 5(3): 201–212.
20. Lateef, O.A., M.F. Khamidi, and A. Idrus. Building maintenance management in a Malaysian university campuses: a case study. Australasian Journal of Construction Economics and Building 2010a; 10(1/2): 76-89.
21. Lau, K.H. and J. Zhang. Drivers and obstacles of outsourcing practices in China. International Journal of Physical Distribution & Logistics Management 2006; 36(10): 776-792.
22. Lavy, S. and D.L. Bilbo. Facilities maintenance management practices in large public schools, Texas. Facilities 2009; 27(1): 5-20.
23. Leech, N.L., K.C. Barrett, and G.A. Morgan, IBM SPSS for Intermediate Statistics : Use and Interpretation. 4th ed. 2011, New York: Taylor & Franciz Group.
24. Love, P.E.D., Z. Irani, E. Cheng, and H. LI. A model for supporting inter-organizational relations in the supply chain. Engineering Construction and Architectural Management 2002; 9(1): 2-15.
25. Love, P.E.D., M. Skitmore, and G. Earl. Selecting an Appropriate Procurement Method for the Construction Process: An Empirical Study. Construction Management and Economics 1998; 16(2): 221-233.
26. Luu, D.T., S.T. Ng, and S.E. Chen. A case-based procurement advisory system for construction. Advances in Engineering Software 2003a; 34(7): 429-438.
27. Masterman, J.W.E., An Introduction to Building Procurement Systems. 1992, London: Spon Press.
28. Morledge, R., A. Smith, and D.T. Kashiwagi, Building Procurement. 1st ed. 2006, UK: Blackwell Publishing Ltd.
29. Musa, Z.N., Determining the Best Options for Facilities Management(FM) Service Delivery in UK Shopping Complex, in School of the Built Environment 2011; Liverpool John Moores University: Liverpool: 309.
30. Ng, S.T., D.T. Luu, and S.E. Chen. Decision Criteria and Their Subjectivity in Construction Procurement Selection. The Australian Journal of Construction Economics and Building 2002; 2(1): 70-80.
31. Pesamaa, O., P.E. Eriksson, and J.F. Hair. Validating a model of cooperative procurement in the construction industry. International Journal of Project Management 2009; 27: 552–559.
32. Piaw, C.Y., Buku 1: Kaedah Penyelidikan. 2nd ed. 2011, Malaysia: McGraw-Hill Companies.
33. Pirdashti, M., A. Ghadi, M. Mohammadi, and G. Shojatalab. Multi-Criteria Decision-Making Selection Model with Application to Chemical Engineering Management Decisions. World Academy of Science, Engineering and Technology 2009; 49: 54-59.
34. Quinn, J.B. and F.G. Hilmer. Strategic outsourcing. Sloan Management Review 1994; 35(4): 43-55.
35. Royal Institution of Chartered Surveyors (RICS), Building maintenance: strategy, planning and procurement, in RICS guidance note 2nd edition 2009; Royal Institution of Chartered Surveyors (RICS): UK.
36. Saaty, T.L., Decision making for leaders : the analytical hierarchy process for decisions in a complex world. 1982, United States of America: Lifetime Learning Pub. 286.
37. Saaty, T.L. Decision making with the analytic hierarchy process. International Journal of Services Sciences 2008; 1(1): 83-98.
38. Saaty, T.L. Highlights and critical points in the theory and application of the Analytic Hierarchy Process. European Journal of Operational Research 1994a; 74(3): 426-447.
39. Saaty, T.L. How to Make a Decision: The Analytic Hierarchy Process. Interfaces 1994b; 24(6): 19-43.
40. Saaty, T.L. How to make a decision: The Analytic Hierarchy Process. European Journal of Operational Research 1990; 48: 9-26.
41. Sheng, L.C. Overview of In-house and Outsourcing Strategies for Property Maintenance and Management Services. The Malaysian Surveyor 2012; 47(1): 54-56.
42. Steane, P.D. and D.H.T. Walker. Competitive tendering and contracting public sector services in Australia – a facilities management issue. Facilities 2000; 18(5): 245-255.

43. Straub, A. Performance-based maintenance partnering: a promising concept. Journal of Facilities Management 2007; 5(2): 129-142.
44. Weston, R. It's hard to buck outsourcing tide. PC Week;7/15/96 1996; 13(28): 1.
45. Williams, B., Facilities Management in the UK. 2003, Kent: Building Economics Bureau Ltd.
46. Wong, J., Billions wasted, in The Star 2006: Kuching, Malaysia.
47. Wordsworth, P., Lee's Building Maintenance Management. 4th ed. 2001, Britain: Blackwell Science.
48. Zawawi, E.M.A., S.N. Kamaruzzaman, A.S. Ali, and R. Sulaiman. Assessment of building maintenance management in Malaysia: Resolving using a solution diagram. Journal of Retail & Leisure Property 2010; 9(4): 349–356.

Shirley ChuaJin Lin
Azlan Shah Ali
Anuar Bin Alias
Faculty of Built Environment,
University of Malaya,
50603 Kuala Lumpur, Malaysia.
Emails: shirleychua88@um.edu.my, shirleychua01@yahoo.com

Article citation info:
FLIZIKOWSKI J, TOPOLIŃSKI T, OPIELAK M, TOMPOROWSKI A, MROZIŃSKI A. Research and analysis of operating characteristics of energetic biomass micronizer. Eksploatacja i Niezawodnosc – Maintenance and Reliability 2015; 17 (1): 19–26.

Józef FLIZIKOWSKI
Tomasz TOPOLIŃSKI
Marek OPIELAK
Andrzej TOMPOROWSKI
Adam MROZIŃSKI

RESEARCH AND ANALYSIS OF OPERATING CHARACTERISTICS OF ENERGETIC BIOMASS MICRONIZER

BADANIA I ANALIZA EKSPLOATACYJNYCH CHARAKTERYSTYK MIKRONIZATORA ENERGETYCZNEJ BIOMASY*

The analysis covers interrelations between the following factors: the machine movement, states and transformations of particles of the micronized biomass, particle shifts, mixing, grinding of energetic straw and its particles. It has been found that these relationships, among other things, depend on friction conditions, impacts, cutting, structural components of the micronizer as the dynamic movement of the machine structural components and biomass (particles) takes place under the conditions of idle movement and workload in order to accomplish an external goal. This paper aims at systematization, calculation and complementary research on micro-grinding performance characteristics (idle and operating), for constant and different rotational speeds (angular and linear).

Keywords: *operating characteristics, biomass, grinding.*

Poddano analizie wzajemne relacje: ruchu użytkowego, stany i przemiany cząstek rozdrabnianej biomasy, ich przemieszczenia, mieszanie, rozdrabnianie słomy energetycznej i jej cząstek. Wykazano, że zależą one m.in. od warunków tarcia, zderzeń, cięcia, cech konstrukcyjnych mikronizatora, przy czym dynamiczne przemieszczanie elementów (części) konstrukcji maszyny i biomasy (cząstek), następuje w warunkach ruchu jałowego i obciążenia roboczego, dynamicznej realizacji celu zewnętrznego. Celem pracy jest systematyzacja, obliczenia i badania uzupełniające charakterystyk użytkowych (jałowych i roboczych) mikro-rozdrabniania, sporządzanych przy stałej i różnej prędkości obrotowej (kątowej lub liniowej).

Słowa kluczowe: *charakterystyki eksploatacyjne, biomasa, rozdrabnianie.*

1. Introduction

Both European and home regulations impose on electricity producers strict rules concerning energy production (according to fixed dates) requiring to generate more and more energy from renewable sources. By the year 2020 the percentage share of renewable sources in total energy consumption in Poland will have to be 15% (in the European Union 20%) and according to the Ministry of Economy of in 2010 this share was 9.5% (Polish Energy Policy – PER 2030. Polish agriculture is capable of providing sufficient amount of energetic plants (biomass) which properly processed will allow to decrease dependence of the Polish economy on fossil fuels. This will also enable to reduce emission of harmful products of combustion.

One of methods to be used for reduction of fossil fuels consumption is industrial co-combustion of biomass and coal. However, it poses some problems such as for example unburnt particles that are left both in slag and fly ash. Evidently, it is a loss of energy as the fuel does not deliver its whole energy and its unused part is irreversibly lost [3, 8, 21, 31].

The investigations carried out in power plants which burn biomass have revealed significant influence of the biomass fraction dimensions on the final content of coal in ash [3, 5, 6]. In order to prevent from this to happen it is necessary to apply a repeatable process of biomass grinding to achieve possibly the tiniest solid fractions.

The experiences of the Polish power plants indicate clearly that the outlays and costs connected with the process are high, depending on:

- decrease in energy efficiency of boilers which are subjected to the process of modernization and adjustment to perform biomass combustion, due to change in the way of heat exchange, especially the growing amount of unburnt matter,
- Increase in electrical energy demand by installation of a device for preparation and combustion of biomass (transport systems, precise milling etc.),
- significant increase in residue of furnace fireboxes impairing availability of boilers,
- fast corrosion due to high temperature caused by chlorine content in biomass (mainly straw),
- instability of biomass price on the free market caused by big competition and significant dispersion of the material providers [14].

Advantages of co-combustion include:

- lower emission of harmful compounds :SO_2, NO_x, CO_2,which has a positive influence on the environment and on the price of a generated heat unit (ETS)
- flexibility of the process – when there is not enough biomass the boiler can be used only for burning coal,
- co-combustion process is stabilized by burning coal [13, 15, 19].

(*) Tekst artykułu w polskiej wersji językowej dostępny w elektronicznym wydaniu kwartalnika na stronie ***www.ein.org.pl***

This study presents a description and analysis of technical conditions necessary for preparation of high quality product of biomass grinding (micronization) with the use of a micronizer as well as an analysis of its operating characteristics which will enable to develop of a new grinding technology for appropriate preparation of energy efficient biomass to be co-burnt with coal.

In order to achieve the goal, the following aspects have been studied: the nature of co-combustion, availability of biomass for energy production, development of a new technology of micro-grinding to optimize the process.

2. The nature of co-combustion technology

Co-combustion involves simultaneous burning of coal and biomass in a furnace firebox of a boiler thus distributing the heat into the system. Boilers (eg.OP-230) were designed to burn only coal, hence after being adjusted to co-combustion of biomass they are bound to reveal some decrease in heat output due to application of fuel with lower energy value [8, 11, 12, 15, 19, 22, 23].

Apart from the biomass heating value, its moisture is important for the combustion process as well [1]. Dry biomass burns very well with stable flame, whereas moist biomass moves the flame cone up the furnace firebox which is undesirable due to NOx emission and deterioration of heat exchange in boiler [8]. In order to obtain maximum economic efficiency it is necessary to produce ash with the content of combustible parts lower than 6% which can be sold to cement plants for production of e.g. cellular concrete [8].

3. Precision milling engineering

To prevent from numerous adverse phenomena connected with co-combustion of biomass and coal it is necessary to provide repeatable operating characteristics and precision milling of biomass to obtain most possible tiny solid fractions.

Capacity of the most commonly used hammer mills strictly depends on: the purpose of grinding, the mill structure, especially the working set(tools), quality parameters of the process, biomass quality, amount of ash and friction material contained in the material to be milled [11, 16, 20, 32]. In the lines available for preparation of furnace feed biomass is most frequently transported by worm conveyors and directed to hammer mills. Hammer mills can comminute the supplied biomass into dust with granulation degree up to 1mm [2,4,5,6]. In order to provide the comminuted biomass with appropriate quality/quantity, during operation at full capacity and in case of the machine shutdown or its overhaul, the systems are equipped with numerous mills (e.g. four sets of mills).

A micronizer (Fig. 1), along with the technological line (Fig. 3) [28], was applied to the Patent Office on 24.03.2011 under the title *Method and Device for Biomass Micronization* – no. P.394325.

The heart of a micronizer is fast rotating disk (17) driven by shaft (18), whose integral part are straight or arc blades. The disk can be opened or closed. Revolutions of the disk are matched so that it is possible to provide its external diameter with very high peripheral speed in the range (300–800) m·s^{-1}.

High usable rotational speed of the disk causes generation of high sub-pressure in the zone of drying and initial grinding (24) in result of which the speed of air flowing onto the disk ranges between (250….350) m/s. Biomaterial is sucked by the flowing air which rapidly accelerates and hits the disk (17) in zone (24) undergoing initial grinding.

Under the influence of centrifugal forces the micronized material together with the air change the direction of flow from axial to perpendicular to working disk rotary axis (17).

After entering the channels between the blades it is then accelerated up to the value to match the disk diameter and its rotational speed.

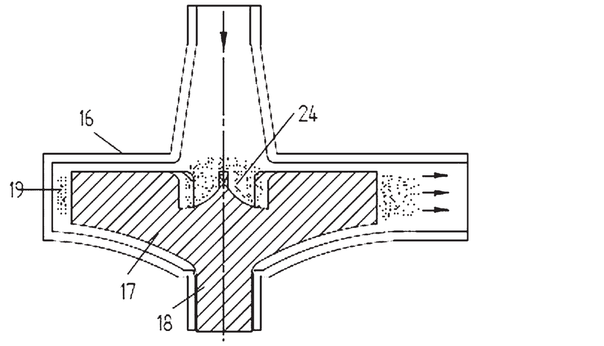

Fig. 1. Device for biomass micronization according to patent application P. 394325; 16 – casing, 17 – rotational disk, 18 – drive shaft, 19 – high turbulence zone, 24 – initial micronization zone

In effect of the physical factors impact the material is ejected to high turbulence zone (19) where it is micronized in the process made up of coexisting three processes: deagglomeration, densification and disintegration caused by cavitation and propagation of impact waves in result of radial-peripheral collisions of supersonic mass flows.

After filling the feed port (Fig. 1 and 2) the overlap of the process channel cross-sections starts to diminish. The initial assumption was that in each particle undergoes division in the micronization space (through friction, impacts, equalization of tensions). The assumption was made that the position of micronized particles in relation to the micronization plane is of random character and with uniform distribution. Thus, in effect of micronization, the particles with initial length disintegrate with similar probabilities, each into two smaller parts, each with the sum of lengths being the length (dimension) prior to division.

The very process of disintegration is caused by the state of complex loads /permanent strains and it always occurs in the material which, before being shifted, was in the preceding section of the working set (Fig. 2). Distribution of the particle length during grinding, in a material which has filled empty space of the (n+1) th segment, changes according to dependence [25, 26]:

$$\tilde{\rho}^m_{n+1}(x) = A_{n,m}\rho^m_n = \left(1-\frac{x}{y_{n+1}-\tilde{y}^m_{n+1}}\right)\rho^m_n(x) + \frac{1}{y_{n+1}-\tilde{y}^m_{n+1}}\int_x^{l_{\max}} \rho^m_n(l)\,dl, \quad (1)$$

whereas, in a material which has been left in the n-th segment:

$$\tilde{\rho}^{m+1}_n(x) = \tilde{B}_{n,m}\rho^m_n = \left(1-\frac{x}{\tilde{y}^m_n}\right)\rho^m_n(x) + \frac{1}{\tilde{y}^m_n}\int_x^{l_{\max}} \rho_n(l)\,dl, \quad (2)$$

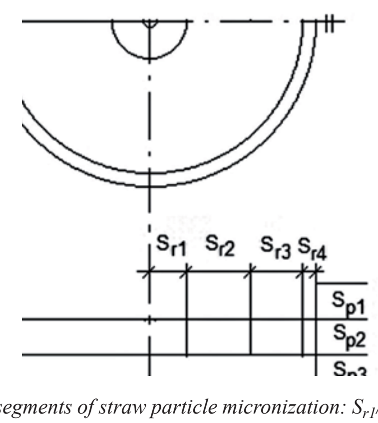

Fig. 2. Radial segments of straw particle micronization: S_{r1}/S_{P1} - initial introductory zone/level, S_{r2}/S_{P2} - zone/level of initial acceleration of particles, Sr3/SP3 - working zone/level, Sr4/SP4 - zone/level of biomass particles impact division.

The obtained functions are non-negative, being a sum of non-negative elements. By integrating, according to the product dimension, from 0 to l, it is easy to check that the functions are probability distributions:

$$\int_0^{l_{\max}} \tilde{\rho}_n^{m+1}(x)dx = 1 - \frac{\bar{x}}{\tilde{y}_n^m} + \frac{1}{\tilde{y}_n^m}\int_0^{l_{\max}}\int_x^{l_{\max}} \rho_n(l)dldx = 1 - \frac{\bar{x}}{\tilde{y}_n^m} + \frac{1}{\tilde{y}_n^m}\int_0^{l_{\max}}\int_0^x \rho_n(l)dxdl = \\ 1 - \frac{\bar{x}}{\tilde{y}_n^m} + \frac{1}{\tilde{y}_n^m}\int_0^{l_{\max}} x\rho_n(l)dx = 1 \tag{3}$$

and similarly, for distribution $\tilde{\rho}_{n+1}^m$. Thus, operators $A_{n,m}$ and $\tilde{B}_{n,m}$ are correctly determined stochastic operators.

For simplification, it was assumed that after grinding the distribution of grain length in the (n+1)th segment will be homogenous (the comminuted fraction and the one present in the segment before division will get mixed), thus being a weighted mean from z ρ_{n+1}^k i ρ_n^k :

$$\rho_{n+1}^m(x) = \frac{\tilde{y}_{n+1}^m}{y_{n+1}}\rho_{n+1}^{m-1} + \frac{y_n - \tilde{y}_{n+1}^m}{y_{n+1}}A_{n,m}\rho_n^m(x) \tag{4}$$

Removal process: After division, the layers (streams) of the micronized material move (are shifted) in relation to each other in the directions set by working channels of the revolving disk this generating centrifugal force and acceleration with a gradient of interacting speeds caused by mass differences of the biomass particular particles . The particles are removed from the preceding segment (it is affected by the component of centrifugal force induced by the shape model of working channels, a force whose direction is perpendicular to the working plane of a channel in which take place difficult to describe aerodynamic phenomena boosting the micronization process), whereas, they are not removed from the successive segment (as the component of force is perpendicular in the direction from the disk).

Thus, after division, the length distribution will be [27]:

$$\tilde{\rho}_n^{m+1}(x) = B_{n,m}\rho_{n,m} = \begin{cases} \tilde{\rho}_n^{m+1}(x)\left(\int_{l_{\min}}^{l_{\max}} \tilde{\rho}_n^{m+1}(x)\right)^{-1} & x\rangle l_{\max} \\ 0 & x\langle l_{\min} \end{cases} \tag{5}$$

The level of material after the *m-th* division (before *m*+1) in the *n*-th segment, $\tilde{y}_n^{m+1}$ is as follows:

$$\tilde{y}_n^{m+1} = \left(y_n - y_{n+1} + \tilde{y}_{n+1}^k\right)\left(1 - \frac{\int_0^{l_{\min}} \tilde{B}_{n,m}\rho_n^m(x)xdx}{\int_0^{l_{\max}} \tilde{B}_{n,m}\rho_n^m(x)xdx}\right) \tag{6}$$

In order to obtain distribution of the channel whole space before the *(m+1)-th* division (after being covered again), it is necessary to use a weighted mean:

$$\rho_n^{m+1}(x) = \frac{y_n - \tilde{y}_n^{m+1}}{y_n}A_{n-1,m}\rho_{n-1}^m + \frac{\tilde{y}_n^{m+1}}{y_n}B_{n,m}\rho_n^m \tag{7}$$

Operator $B_{n,m}$ is not linear like $A_{n,m}$, as it depends on the level of material which was left in the *n-th* segment after the first division and is a function of probability distribution in the material (which has an influence on which part of the material is to be removed from the disk and the division space). In order to be able to treat *Bn,m* as linear operators, quantities y_n^m need to be treated in each step of the procedure, as being pre assigned and iteratively adjusted to experimental tests [17, 24].

The flow of particles leaving the machine. During the m-th micronization, the flow of particles leaving the machine through a gap between the n-th and the (n+1)th segments is given by the probability distribution:

$$s_n^m(x) = \begin{cases} \int_x^{l_{\max}} \rho_n(l)dl\left(\int_0^{l_{\min}}\int_x^{l_{\max}} \rho_n(l)dldx\right)^{-1} & l\langle l_{\min} \\ 0, & l\rangle l_{\min} \end{cases} \tag{8}$$

and its volume is equal to:

$$V_n^m(x) = \left(y_n - y_{n+1} + \tilde{y}_{n+1}^k\right)\frac{\int_0^{l_{\min}} \tilde{B}_{n,m}\rho_n^m(x)xdx}{\int_0^{l_{\max}} \tilde{B}_{n,m}\rho_n^m(x)xdx} \tag{9}$$

Linear velocity of grinding in the disk adjacent segments:

$$\begin{aligned} \Delta v_{L(i+1)-j/i-k} &= v_{(i+1)-j} - v_{i-k} \\ \Delta v_{L(i+1)-j/i-k} &= \pi \cdot D_{(i+1)-j} \cdot n_{i+1} - \pi \cdot D_{i-k} \cdot n_i \\ \Delta v_{L(i+1)-j/i-k} &= \pi \cdot (D_{(i+1)-j} \cdot n_{i+1} - D_{i-k} \cdot n_i) \end{aligned} \tag{10}$$

where:

$\Delta v_{L(i+1)-j/i-k}$ – gradient of linear velocity between adjacent ra dial segments (S_{r1-4}) or peripherals of the grinding set disk $m \cdot s^{-1}$,

$v_{(i+1)-j}$ – linear velocity in the *(i+1) th* segment, on the *j-th* level (S_{p1-4}), $m \cdot s^{-1}$,

v_{i-k} – linear velocity in the *(i+1) th* segment, on the *k-th* level (S_{p1-4}), $m \cdot s^{-1}$,

$D_{(i+1)-j}$, D_{i-k} – respective guide diameters of the *(i+l)-th* segment (Sr1-4)and the *i-th* level (S_{p1-4}), *j-th* or the *k-th* row of grinding (S_{r1-4}), m,

n_{i+1} – rotational speed of a segment more distant from the feed entry (e.g. Sr3), s^{-1},

n_i – rotational speed of a segment closer to the feed entry (e.g. Sr2), s-1;

Thus, it is necessary to match the working disk rotational (angular) speed in such a way that the speed of particles micronized in its particular segments would be of (sub)optimal range:

$$\omega = f(\Delta v_{L(i+1)-j/i-k}) \tag{11}$$

Transformations of particle length distributions. The distribution of particle lengths in the *n-th* division is expressed by denotation ρ_n^m. Operators which carry out distribution ρ_n^m w ρ_{n+1}^m i w ρ_n^{m+1} are denoted respectively as $A_{n,m}$ i $B_{n,m}$.

State ρ_0^0 is given (distribution of particle lengths in the input material, e.g. the first grinding, second grinding ,…..). State ρ_n^m is obtained from an equation of the sum of A and B operator products in state ρ_0^0. The products represent all the paths which can be used to reach this state from state ρ_0^0. For example:

$$\rho_2^3 = \left(A_{1,2}A_{0,1}B_{0,0} + A_{1,2}B_{1,1}A_{0,0} + B_{2,2}A_{1,1}A_{0.0}\right)\rho_0^0 \tag{12}$$

State ρ_n^m can be reached by using operator A n times and operator B² m-times. The path is unambiguously defined by an n-element subset of steps making up the whole path { 1……m}, steps with operation of operator A. The number of such subsets, that is, products in the sum is $\binom{m}{n}$. In general, operators A and B do not commute. Calculation of such expressions is crucial for further studies. States ρ are positive elements of Banach space L^1 ([0, 1]), whereas operators *A* and *B* are endomorphisms of this space [9, 29, 30]. For practical reasons it is necessary to approximate *p* states by positive elements R^d, and operators *A* and *B* by matrixes $d\times d$. Physically, it corresponds to division of a particle of length l (e.g. the feed initial dimension) into d-number of further indivisible parts (e.g. product dimension close to 0) – corresponding to a linear measure of disintegration (degree). It can also correspond to dimensional classes: (l>1.4) mm, (0.8<l<1.4) mm, (0.4<l<0.8) mm, (l<0.4) mm.

Literature offers inconsistent data on the amount of straw to be used for energy production purposes. However, it can also be accepted that the surplus between its total production and utilization in agriculture in 2010 was 11.6 mln tons [Flizikowski 2011, Flizikowski 2013].

Fig. 3 shows a scheme of a technological system for biomass grinding. The micronized material is supplied through a dumping hopper, to basket (1) from where it is delivered by conveyor (2) to feeder (3). The feeder fills a suction pipe which feeds an axial-disk micronizer powered by an electric motor (4). The micronized biomass flows in the form of air and vapor mixture to cyclone separator (5), from where it is fed to external containers by conveyor belt (6). Humid air free from micronized material flows to a drier and next to fine filter (7), from where it is carried outside. Fractions separated from both filters are turned to a second micronization (thick fraction) or are supplied to external containers (fine fraction). Dust silos, bag filters and biomass silos are equipped with anti-explosion systems [7, 8, 23].

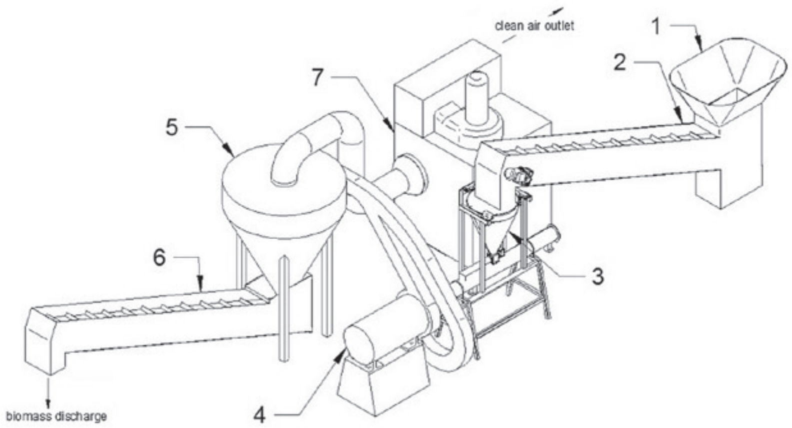

Fig. 3. Technological system for biomass micronization: 1-basket with dumping hopper, 2-coveyor belt, 3-feeder, 4-micronizer with electric motor, 5-cyclon, 6-conveyor belt,7-filtration device

4. Presentation of micronization experiments results (Statistica 10)

The tests were carried out on a test stand, being a prototype innovative technological system for biomass micronization.

A comparison of measuring elements: mass and percentage share of the investigated rye straw fractions has been presented in table1 for selected rotational speeds of the first micro-milling.

A sample of rye straw was the statistical population. The tests involved a quantitative feature, that is, the share of mass of particular fractions in the sample total mass, measured in % in relation to the value of rotational speed in two time intervals (10 and 30) s. A portion of rye straw with mass 40 g served as a statistical unit, 12 such portions were tested. Four kinds of fractions were separated: (> 1.4, 1.4–0.8, 0.8–0.4 and < 0.4)mm and eleven values of rotational speed – (from 0 to 18.000) min^{-1}.

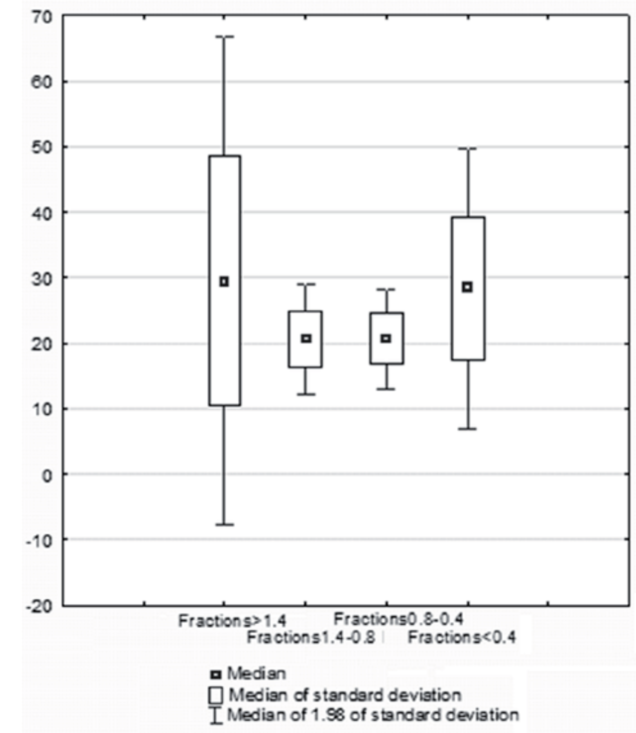

Fig. 4. Values of the mean and percentage mass content of the tested fractions for range rotational speed range (0…18.000) min^{-1} in testing time of 10s

Statistical measures are used for a description of the tested specimen structure (Tab. 1).

The mean percentage share of rye straw fraction (>1.4) mm of the micronization product was 29.52%, for all the rotational speeds, in time of 10 seconds, fraction (1.4–0.8) mm – 20.563%, fraction (0.8–0.4) mm – 20.683%, and fraction (< 0.4) mm – 28.319%. It means that the highest mean percentage was found for the extreme intervals. Half of specimens of fraction (>1,4) mm contained 27.488%, fraction (1.4–0.8) mm and (0.8-0.4) mm – nearly 21.5 %, and fraction (< 0.4) mm – 28.087% (median).

In the studied population, there occurs relation Xśr>Me between the measures of central tendency in fractions (>1.4) mm and (<0.4)mm which indicates right sided asymmetry (not dangerous) and in fractions (1.4–0.8) mm and (0.8–0.4) mm – relation Xśr< Me, (<0.4) mm – 6.203% (feed), which indicates left sided asymmetry (not dangerous, either). The lowest percentage share of rye straw fraction for all rotational speeds, during 10 seconds, was found for fraction (<0.4) mm – 6.203% (feed), and the highest for fraction (>1.4) mm – 74.240% (feed). The highest absolute difference between value of the highest and the lowest percentage share was: in fraction (<0.4) mm – 6.203% (feed), and the highest in fraction (>1.4) mm – 62.946, and in fraction (<0.4) mm – 35.726. The lowest value of range was observed in fraction (0.8–0.4) mm – 13.995. Portions of rye straw dust were characterized by diversified mass percentage share of particular fractions.

On the average it was ±18.989 % for fraction (<0.4) mm. The lowest value of standard deviation was found for fraction (0.8–0.4) mm –

Table 1. Mass and percentage share of the tested rye straw fractions for selected rotational speeds.

Rotational speed min^{-1}, t=10s	Moisture of speci-mens , %	Mass of specimen, g	fraction > 1.4		fraction 1.4-0.8		fraction 0.8-0.4		fraction < 0.4	
			mass g	share%	mass g	share %	mass g	share %	mass g	Share %
0 (wsad)	13.2	40.14	29.8	74.240	3.79	9.442	4.41	10.987	2.49	6.203
9000	13.0	40.1	16.32	40.698	7.71	19.227	7.17	17.880	8.51	21.222
10000	13.1	40.12	15.64	38.983	7.55	18.819	7.84	19.541	8.11	20.214
11000	13.2	40.04	15.93	39.785	7.41	18.506	7.73	19.306	8.5	21.229
12000	12.9	39.99	13.92	34.809	8.07	20.180	8.51	21.280	9.5	23.756
13000	13.0	40.09	11.02	27.488	8.65	21.576	8.7	21.701	11.26	28.087
14000	13.1	39.98	5.75	14.382	9.06	22.661	8.75	21.886	16.07	40.195
15000	12.9	40.02	4.52	11.294	9.28	23.188	9.16	22.889	16.78	41.929
16000	13.0	40.03	5.4	13.490	9.65	24.107	9.14	22.833	14.71	36.747
17000	13.2	40.15	6.17	15.367	9.84	24.508	9.73	24.234	14.18	35.318
18000	13.1	39.99	5.67	14.179	9,59	23.981	9.99	24.981	14.64	36.609
18000 t=30s	13.0	40.07	5.25	13.102	9.87	24.632	9.08	22.660	15.54	38.782

Table 2. Descriptive statistics of mass percentage share of the tested rye straw fractions for rotational speeds from 0 to 18.000 for testing time 10sec.

Variable	Mean	Median	Minimum	Maximum	Lower quartile	Upper quartile	Range
fraction > 1.4	29.520	27.488	11.294	74.240	14.179	39.785	62.946
fraction 1.4-0.8	20.563	21.576	9.442	24.508	18.819	23.981	15.066
fraction 0.8-0.4	20.683	21.701	10.987	24.981	19.306	22.889	13.995
fraction < 0.4	28.319	28.087	6.203	41.929	21.222	36.747	35.726
Variable	Variance	Standard deviation	Confidence limit Standard deviation – 95.00%	Confidence limit Standard deviation . +95.00%	Variabiity coefficient	Data skew	Curtosis
fraction > 1.4	360.58	18.989	13,268	33.324	64.327	1,300	1.9806
fraction 1.4-0.8	18.50	4.301	3.005	7.548	20.917	-1.870	4.3669
Fraction 0.8-0.4	14.85	3.853	2.692	6.763	18,630	-1.688	3.6968
Fraction < 0.4	119.13	10.915	7.626	19.155	38.542	-0.606	-0.0923

3.853%. This dispersion is considered to be significant as the relative measure of variability (v) is maximally 64.327 % for fraction (>1.4) mm, and minimally 18.63% for fraction (0.8–0.4) mm (Tab. 2).

The highest diversity of the fraction mass percentage share for different values of rotational speed (from 0 do 18.000) min^{-1}, in testing time 10 seconds, was characteristic of fraction (>1.4) mm (range from 10.513 do 48.509) and fraction (<0.4) mm (from 17.404 do 39.234). The lowest diversity characterizes fractions (1.4–0.8) mm and (0.8–0.4) mm (from about 16.5 to app. 24.5) (Fig. 4).

The results of Shapiro-Wilk test for rye straw dust fraction (>1.4) mm, for rotational speeds in the range (0…18.000) min^{-1} and testing time 10 seconds, indicate its distribution normality (W=0.083708, p=0.02892). For the analyzed fraction, the lower quartile is equal to 14.179%, which means that 25% of all the obtained results was below this value. The upper quartile is equal to 39,785%, hence 25% of all the results is found to be above this value.

The results of Shapiro-Wilk test for rye straw dust fraction (1.4–0.8) mm for rotational speed in the range (0...18.000)min^{-1} and testing time 10 seconds, indicate its normal distribution (W=0.80469, p=0.01084). The lower quartile for this fraction is equal to 18,819%, and the upper one is 23.918%.

The results of Shapiro-Wilk test for rye straw dust fraction (0.8-0.4) mm for rotational speed in the range (0…18.000)min^{-1} and testing time 10 seconds, indicate its normal distribution. (W=0.85496, p=0.04953). The lower quartile for this fraction is equal to 19.306%, and the upper one is 22.889%.

The results of Shapiro-Wilk test for rye straw dust fraction (<0.4) mm, for rotational speeds in the range ((0…18.000) min^{-1} and testing time 10 seconds, indicate lack of its distribution normality (W=0.92245, p=0.33961). For the analyzed fraction the lower quartile is equal to 21.222%, and the upper one is 36.747%.

The value percentage share of rye straw dust fraction (>1.4) mm is strongly negatively correlated with the rotational speed increase in the range (0…18.000)min^{-1} ($r=-0.96$) which means that the percentage share of fraction (>1.4) mm in the whole sample mass decreases along with an increase in rotational speed (Fig. 5). This dependence is described by regression equation:

$$fraction > 1.4 = 74.682 - 0.0037 \cdot \omega$$

The value percentage share of rye straw dust fraction (1.4–0.8) mm is strongly positively correlated with rotational speed increase in

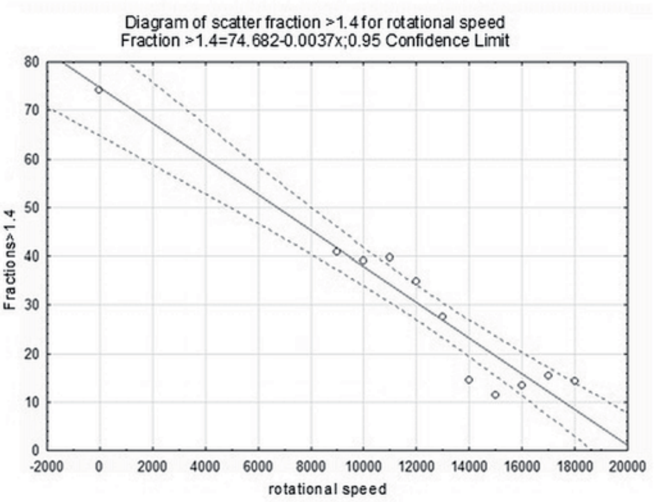

Fig. 5. Diagram of scatter for rye straw dust fraction (>1.4) mm for rotational speed of the range (0…18.000)min^{-1} and testing time 10 s.

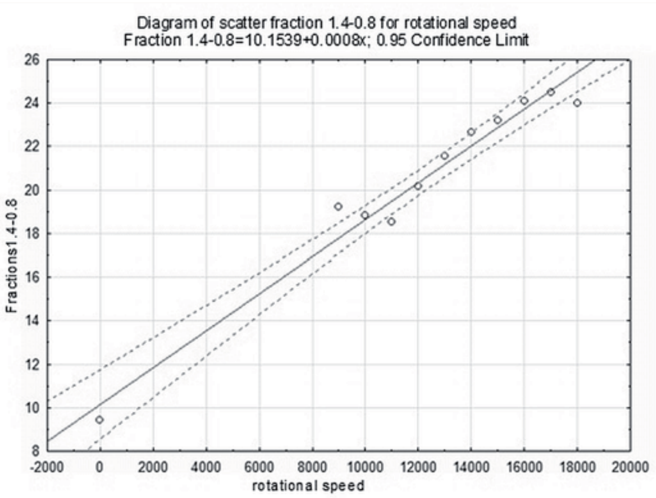

Fig. 6. Diagram of scatter for rye straw dust fraction (1.4–0.8) mm for rotational speed of the range (0…18.000)min^{-1} and testing time 10 s.

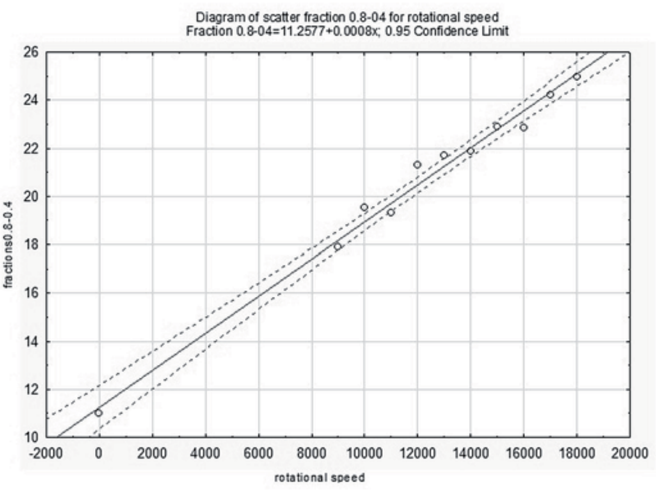

Fig. 7. Diagram of scatter for rye straw dust fraction (0.8–0.4) mm for rotational speed range (0…18.000)min^{-1} and testing time 10

the range (0…18.000)min^{-1}(r=−0.98) which means that the share of fraction (1.4–0.8) mm in the whole sample mass increases along with an increase in rotational speed (Fig. 6). This dependence is described by regression equation:

$$fraction\ 1.4\text{-}0.8 = 10.1539 + 0.0008 \cdot \omega$$

The value percentage share of rye straw dust fraction (0.8–0.4) mm is strongly positively correlated with rotational speed increase in the range (0…18.000)min^{-1} (r=−0.99) which means that the share of fraction (0.8–0.4) mm in the whole sample mass increases along with an increase in rotational speed (Fig. 7). This dependence is described by regression equation:

$$fraction\ 0.8\text{-}0.4 = 11.2577 + 0.0008 \cdot \omega$$

The value percentage share of rye straw dust fraction (<0.4)) mm is strongly positively correlated with rotational speed increase in the range (0…18.000)min^{-1} (r=−0.90) which means that the share of fraction (<0.4) mm in the whole sample mass increases along with an increase in rotational speed (Fig. 7). This dependence is described by regression equation:

$$fraction < 0.4 = 3{,}951 + 0.002 \cdot \omega$$

Also a comparative analysis of changes in mass percentage share of particular fractions has been performed through multiple grinding and for constant rotational speed 18.000min^{-1}, for different testing times (10 and 30) s (Tab. 5). The obtained data shows that the percentage share of fraction (>0.8–0.4) mm decreases along with the process duration and the percentage share of fraction (0.25–0.4) mm increases, especially dusts (<0.25) mm (Tab. 5, Fig. 8).

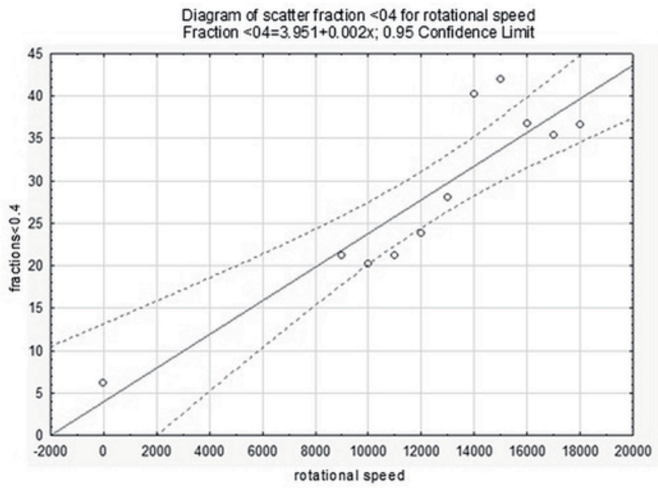

Fig. 8. Diagram of scatter for rye straw dust fraction (< 0.4) mm for rotational speed in the range (0…18.000)min^{-1} and testing time 10 seconds.

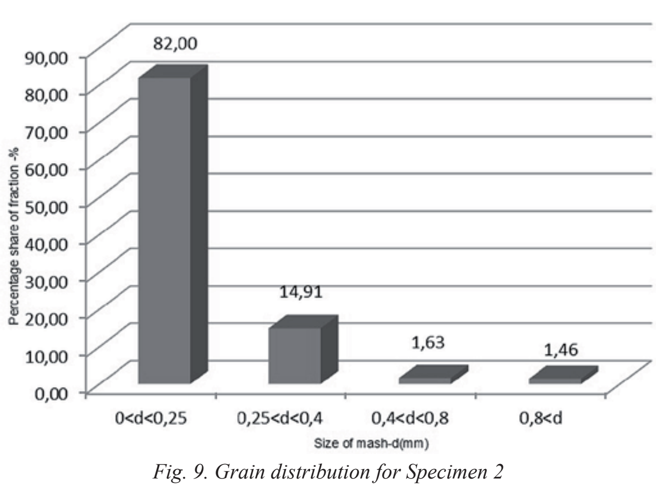

Fig. 9. Grain distribution for Specimen 2

Table 3. Mass and percentage shares of dimensional fractions from the analysis of Specimen no.2, (the second micro-milling)

Size of sieve mesh d (mm)	Mass of fraction m_1 (g)	Mass of fraction m_2 (g)	Mass of fraction m_3 (g)	Mean mass $m_{śr}$ (g)	Percent %
0<d<0,25	32.95	32.48	32.97	32.80	82.00
0,25<d<0,4	5.98	5.95	5.96	5.96	14.91
0,4<d<0,8	0.62	0.82	0.52	0.65	1.63
0,8<d	0.45	0.75	0.55	0.58	1.46

6. Conclusions

The carried out tests and analysis have proved that application of a micronizer in the process of preparation of biomass to be co-combusted with coal provides numerous benefits. Besides, thanks to the tests the influence of operating characteristics of the micronizer on the process quality improvement has been defined.

In the first micro-milling of straw particles the percentage share of rye straw dust highest fraction (>1.4) mm is strongly negatively correlated with an increase in rotational speed in the range (9.000… 18.000) min^{-1} (r=−0.96). This means that the percentage share of fraction (>1.4) mm in the product entire mass increases along with an increase in angular velocity (experimentally by 28%).

Whereas, the percentage share of rye straw dust fraction (1.4–0.8) mm is strongly positively correlated with angular velocity increase in the range (9.000…18.000)min^{-1} (r=0,98) which means that the share of fraction (1.4–0.8) mm in the entire sample mass increases along with an increase in angular velocity

The share of the smallest fraction value (<0.4) mm of rye straw dust is strongly positively correlated with rotational speed increase in the scope of (9.000…18.000)min^{-1}(r=0.90). The share of fraction (<0.4) mm in the total mass of the sample increases along with rotational speed (in experimental range even by 21%). The second micro-milling of the product provides satisfactory qualitative results: totally nearly 96% of the tiniest fraction (<0.40) mm.

Along with an increase in rotational speed the percentage share of fraction (<0.4) mm in the whole mass of the specimen increases (experimentally even by 21%). The second micro-milling of the product provides satisfactory qualitative results: totally app. 96% of the tiniest fraction (<0.40) mm.

The above mentioned advantages of biomass make it a desirable material for energy production and it seems that the Polish power generation industry is bound to develop biomass micro-grinding for energy generation. Political conditionings (both internal and European) impose strict rules on power producers involving respecting the requirements concerning the use of renewable sources for energy production according to strictly fixed dates. Agricultural character of Polish economy provides good conditions for farming energy providing plants which can limit the dependence on fossil fuels.

On the basis of the micro-grinding tests results it can be said that along with an increase in the process duration time the percentage share of fraction (>0.8–0.4) mm decreases and the percentage share of energetically desired fractions increases: (0.25–0.4) mm, especially dusts (<0.25) mm.

The research was performed in the company Hydrapress Sp. z o.o. within the project POIG 01.04.00-04-003/11-00: "Improvement of competitiveness of the company through the development of biomass shredding technology"

References

1. Armstrong P R, Lingenfelser J E, McKinney L. The Effect of Moisture Content on Determining Corn Hardness form Grinding Time, Grinding Energy, and Near – Infrared Spectroscopy. Applied Engineering in Agriculture 2007; 23(6): 793-799.
2. Bieliński K S, Flizikowski J B. Sterowanie rozgrywające i rozliczanie energomediów w obiektach. EKOMILTARIS, WAT, Zakopane 2008.
3. Błasiak W, Moberg G, Grimbrandt J. Redukcja tlenków azotu oraz optymalizacja spalania w komorach kotłów za pomocą asymetrycznego systemu podawania powietrza wtórnego. 10 Międzynarodowa Konferencja Technik Grzewczych, Göteborg, 2006.
4. Flizikowski J. Inteligentny system rozdrabniania. Inżynieria i Aparatura Chemiczna 2011; 3(50): 22-24.
5. Flizikowski J. Poziomy inteligentnego systemu rozdrabniania. Inżynieria i Aparatura Chemiczna 2011; 3(50): 24-26.
6. Flizikowski J. Micro - and Nano – energy grinding. Panstanford Publishing, Singapore, 2011.
7. Głód K, Rysiawa K. Współspalanie biomasy. Instytut Chemicznej Przeróbki Węgla. XV Wiosenne Spotkanie Ciepłowników. Zakopane 2008.
8. Golec T. Współspalanie biomasy w kotłach energetycznych. Energetyka 2004; 7(8): 437-445.
9. Hoffman P C, Ngonyamo-Majee D, Shaver R D. Technical note: Determination of can hardness in diverse corn gin diverse corn germplasm using near-infrared reflectance baseline shift as a measure of grinding resistance. Journal of Dairy Science 2010; 93(4): 1685-1689.
10. Kowalik K, Sykut B, Marczak H, Opielak M. A method of evaluating energy consumption of the cutting process based on the example of hard cheese. Eksploatacja i Niezawodnosc – Maintenance and Reliability 2013;15(3): 241-245.
11. Kruczek M, Skrzypczak G, Muraszkowski R. Spalanie i współspalanie biomasy z paliwami kopalnymi. Czysta Energia 2007; 68(6): 32-35.
12. Kryszak J. Wykorzystywanie biomasy dla pozyskiwania energii odnawialnej. Akademia Rolnicza, Poznań, 2005.
13. Kubica K. Spalanie biomasy i jej współspalanie z węglem. Instytut Chemicznej Przeróbki Węgla, Zabrze, 2004.
14. Laurow Z. Ekologiczne uwarunkowania pozyskiwania biomasy cele energetyczne w leśnictwie. Możliwości wykorzystania biomasy na cele energetyczne. Malinówka, 2003.
15. Lorenz U. Gospodarka węglem kamiennym energetycznym. IGSMiE, PAN, Kraków, 2010.
16. Macko M. Economic-energetic analysis of multi-edge comminution of polymer recyclates. Analiza ekonomiczno-energetyczna wielokrawędziowego rozdrabniania recyklatów polimerowych. Przem. Chem. 2013; 213(8): 1499-1502.
17. Mazurkiewicz D. A knowledge base of the functional properties of the conveyor belt adhesive joint for FEM simulation of its stress and strain state. Journal of Adhesion Science and Technology 2012; 26(10-11): 1429-1442.
18. Niederliński S. System i sterowanie. PWN, Warszawa, 1987.

19. Popiel P. Wpływ współspalania biomasy z pyłem węglowym na stratę niedopału. Prace Instytutu Elektrotechniki, Zeszyt 249, Politechnika Lubelska, 2011.
20. Powierża L. Zarys inżynierii systemów bioagro-technicznych. Wydawnictwo ITE, Radom, 1997.
21. Semczuk M. Ustawa o efektywności energetycznej - narzędzie w procesie budowy niskoemisyjnej i konkurencyjnej gospodarki. Rynek Energii I(V). Zeszyt tematyczny. Wydawnictwo KAPRINT, Lublin, 2010.
22. Soliński I, Jesionek J. Efekty ekologiczne współspalania biomasy z węglem kamiennym. Warsztaty; Współspalanie biomasy i termiczna utylizacja odpadów w energetyce. Kraków, 2007.
23. Ściążko M, Zuwała J, Pronobis M. Zalety i wady współspalania biomasy w kotłach energetycznych na tle doświadczeń eksploatacyjnych pierwszego roku współspalania biomasy na skalę przemysłową, Energetyka i Ekologia 2006; 3: 207-220.
24. Sharma B, Jones C L, Khanchi A. Tensile Strength and Shear Strength of Switchgrass Before and After Frost. Biological Engineering Transactions 2011; 4(1): 43-54.
25. Tomporowski A, Flizikowski J. Charakterystyki ruchowe wielotarczowego rozdrabniacza ziaren biomasy. Przem. Chem. 2013; 92(4): 498-503.
26. Tomporowski A. Stream of efficiency of rice grains multi-disc grinding. Eksploatacja i Niezawodnosc – Maintenance and Reliability 2012; 14(2): 150-153.
27. Tomporowski A, Opielak M. Structural features versus multi-hole grinding efficiency. Eksploatacja i Niezawodnosc – Maintenance and Reliability 2012; 14(3): 223-228.
28. Topoliński T. Flizikowski J. Jasiński J. Wełnowski D. Inżynieria energomechaniczna biomasy. Cz. II. Mikronizator. Inż. i Ap. Chem. 2013; 52(1): 9-10.
29. Vishwakarma R K, Shivhare U S, Nanda S K. Physical properties of guar seeds. Food Bioprocess Technology, 2012; 5: 1364-1371.
30. Walton O. Effects of interparticle friction and particle shape on dynamic angles of repose via particle - dynamics simulation. Proc. Conf. Mechanics and Statistical Physics of Particulate Materials, June 8-10, La Jolla CA, USA, 1994.
31. Węglarz A. Prawne aspekty efektywności energetycznej w Polsce w świetle Dyrektyw Unii Europejskiej. KAPE, Warszawa, 2010.
32. Zawada J, (red). Wprowadzenie do mechaniki maszynowych procesów kruszenia. ITE. Radom-Warszawa, 2005.

Józef FLIZIKOWSKI
Tomasz TOPOLIŃSKI
Andrzej TOMPOROWSKI
Adam MROZIŃSKI
Faculty of Mechanical Engineering
University of Technology and Life Sciences
ul. S. Kaliskiego 7., 85-789 Bydgoszcz, Poland
E-mails: fliz@utp.edu.pl, topol@utp.edu.pl,
a.tomporowski@utp.edu.pl, adammroz@utp.edu.pl

Marek OPIELAK
Department of Mechanical Engineering
Lublin University of Technology
Nadbystrzycka str.38, 20-816 Lublin, Poland
E-mail: m.opielak@pollub.pl

Article citation info:
CHANGYOU L, WEI W, YIMIN Z, SONG G, ZHENYUAN L, CHANGSHUAI Q. Indexing accuracy reliability sensitivity analysis of power tool turret. Eksploatacja i Niezawodnosc – Maintenance and Reliability 2015; 17 (1): 27–34.

Li CHANGYOU
Wang WEI
Zhang YIMIN
Guo SONG
Li ZHENYUAN
Qiao CHANGSHUAI

INDEXING ACCURACY RELIABILITY SENSITIVITY ANALYSIS OF POWER TOOL TURRET

ANALIZA WRAŻLIWOŚCI WSKAŹNIKA NIEZAWODNOŚCI W ZAKRESIE DOKŁADNOŚCI INDEKSOWANIA GŁOWICY NARZĘDZIOWEJ Z NAPĘDZANYMI NARZĘDZIAMI

Power tool turret (PTT) is one of the most key parts of CNC (Computer Numerical Control) turning center and CNC turning and milling machining center. Therefore, it is very important for improving these two types of machine tools' reliability to explore the indexing accuracy reliability of PTT and its sensitivity. To analyze the indexing accuracy reliability sensitivity of PTT, the angular displacement error of the rotating gear disc is discussed based on the measurement uncertainty theory. The tooth thickness wear process of the fixed gear disc, the rotating gear disc and the lock gear disc are modeled using Gamma process of which the parameters are estimated. The indexing error of PTT is formulated by employing the BP neural network and validated by the experiment data. Then, the indexing accuracy reliability equation of PTT is derived and its sensitivity to the mean and the standard deviation of random variables or wear stochastic processes is analyzed. The results show that the presented indexing accuracy reliability and its sensitivity of PTT are effective.

Keywords: *power tool turret; indexing accuracy; reliability analysis; wear; finite element.*

Głowica narzędziowa z napędzanymi narzędziami (ang. power tool turret, PTT) stanowi jedną z kluczowych części sterowanych komputerowo tokarskich i tokarsko-frezarskich centrów obróbczych CNC. Dlatego też dla poprawy niezawodności tych dwóch rodzajów obrabiarek istotne jest badanie niezawodności w zakresie dokładności indeksowania głowicy PTT oraz wrażliwości wskaźnika niezawodności. Dla celów analizy wrażliwości wskaźnika niezawodności w zakresie dokładności indeksowania głowicy PTT, omówiono błąd przesunięcia kątowego obrotowej tarczy narzędziowej w oparciu o teorię niepewności pomiaru. Proces zużycia ściernego zębów tarcz narzędziowych: stałej, obrotowej oraz uchwytowej, zamodelowano przy użyciu procesu Gamma o szacunkowych parametrach. Błąd indeksowania PTT obliczono przy zastosowaniu sieci neuronowej BP i zweryfikowano na podstawie danych doświadczalnych. Następnie wyprowadzono równanie niezawodności w zakresie dokładności indeksowania PTT oraz przeprowadzono analizę wrażliwości wskaźnika niezawodności na średnią i odchylenie standardowe zmiennych losowych lub procesów stochastycznych zużycia. Wyniki pokazały skuteczność omawianej analizy niezawodności w zakresie dokładności indeksowania PTT oraz wrażliwości wskaźnika niezawodności.

Słowa kluczowe: *głowica narzędziowa z napędzanymi narzędziami, dokładność indeksowania; analiza niezawodności; zużycie; elementy skończone.*

1. Introduction

CNC machine tool is the most key equipment in the manufacturing industry. Its output and technical level imply the advancement and competitiveness of the manufacturing industry of one country. The sale of the machine tools manufactured in China is about 31% of the world total amount in 2010 [7]. However, the most of these machine tools belong to the low-level one which own lower machining accuracy and manufacture the simpler mechanical part. For example, the ratios of the high-level, middle-level and low-level CNC machine tools manufactured in China are 2%, 18% and 80% respectively in 2009 [10]. The high-level CNC machine tools used in China are mostly from the other countries. One of seasons causing the situation is the low reliability of the high-level CNC machine tool manufactured in China. Therefore, it is very important to improve the key function unit reliability of the high-level CNC machine tool.

The CNC machine tool reliability has been investigated by a lot of researchers and many fruits have been given. The fruits might be summarized as the following fields. The first is the CNC machine tool reliability assessment based on the fault time data, such as [3, 11, 21, 22]. The main work is to identify the distribution type of the fault time data and estimate the parameters. It was reported that the time between faults of the CNC machine tool could be described by Weibull distribution or exponential distribution well [5, 19, 21]. The reliability assessment of the CNC machine tool was also investigated when the data of the time between faults was collected by the fixed or random time censoring test [2, 20]. For the small sample of the time between faults, the reliability assessment has also been investigated. For example, the neural network was trained by the existed data to generate the new data [6]. The second is to analyze the effect of the CNC machine tool fault mode or the function part on the whole reliability. There was a direct method used by Jia YZ et al [1, 17] where the fault modes were ranked according to the occurrence frequency and the key fault modes were analyzed to decrease their occurrence rate. The third is CNC machine tool reliability allocation. The new reliability allocation method should be explored because CNC machine tool could not be supposed to be a series or parallel system generally. The new method should be based on the character of the CNC machine tool. For example, the failure rate allocation method was presented by Wang YQ et al [18] to determine the reliability of fifteen subsystems of CNC lathe. Moreover, the allocation method based on the optimization theory was presented by Wang JL et al [16]. The fourth is the reliability design of the mechanical part. There were some documents where the reliability was formulated according to the fault or failure mechanism and calculated by the reliability analysis method. For example, the fatigue strength reliability analysis method was used to analyze the machine tool part [4]. The kinematic error of the machine tool or part was modeled and its reliability was analyzed when the kinematic error included the stochastic variables, such as [3]. The reliability-based optimization design of the ball screw and nut has also been investigated by Sun KZ et al [12]. Here, the goal function was to minimize the volume and the constraint conditions included the contact fatigue and stiffness reliability. The last is the acceleration reliability test and assembly reliability analysis, such as [23, 24].

Power tool turret (PTT) is one of the most key function parts of CNC turning center and CNC turning and milling machining center. It is mainly from the foreign country in the mainland of China and is being researched by some Chinese companies. But, its performance and reliability are very low. To improve the reliability of PTT manufactured in China, a Key National Science & Technology Special Project has been carried out since 2010. Its objective is to increase the mean time between failures (MTBF) from 1500 to 2250 hours. Moreover, the published document about the PTT reliability has never been found as the best knowledge of the authors. Therefore, the indexing accuracy reliability and its sensitivity will be investigated in this work.

2. Indexing accuracy reliability and its sensitivity of PTT

The considered PTT is composed of the power system, the indexing system and the tool disk. It was designed and machined by Shenyang Machine Tool (Group) Co. , Ltd of China. Its external view is shown in Fig. 1. The power of the milling is offered by the power system. The indexing system is employed to change the tool according to the machining requirement. Here, the twelve tools can be chosen based on the machined mechanical part and set up to the tool disk before the machining process. The structure of the indexing system is shown in Fig. 2. The indexing system includes gear disc system, hydraulic lock system, transmission and control system. According to the structure characteristic of the considered PTT, the indexing accuracy is determined by the gear discs system and lock force mainly. The gear discs system consists of the rotating gear disc, the fixed gear disc and the lock gear disc. Its three-dimensional drawing is shown in Fig. 3.

2.1. Distribution and parameter estimation of angular displacement error of rotating gear disc

The rotating gear disc is fastened to the output shaft of transmission shown in Fig. 3. Therefore, the angular displacement error of rotating gear disc is equal to that of the output shaft of transmission. It is composed of the one-way angular displacement error and backlash angular displacement error of transmission and its detailed effect term is shown in Table1.

The measurement uncertainty theory is employed to estimate the standard deviation of the angular displacement error of rotating gear disc. The combined measurement uncertainty of the angular displacement error of the rotating gear disc is

$$u(\delta) = \sqrt{u\left(\delta_{\phi}\right)^2 + u\left(\delta_{\varphi}\right)^2} \qquad (1)$$

$u\left(\delta_{\varphi}\right)$ and $u\left(\delta_{\phi}\right)$ are the one-way angular displacement combined measurement uncertainty and the backlash angular displacement combined measurement uncertainty of the transmission system respectively. $u\left(\delta_{\varphi}\right)$ is calculated by:

$$u\left(\delta_{\phi}\right) = \sqrt{\left[u\left(\delta_{\phi 42}\right)\right]^2 + \left[\frac{u\left(\delta_{\phi 31}\right)}{i_{34}}\right]^2 + \left[\frac{u\left(\delta_{\phi 32}\right)}{i_{34}}\right]^2 + \left[\frac{u\left(\delta_{\phi 21}\right)}{i_{34}i_{23}}\right]^2 + \left[\frac{u\left(\delta_{\phi 22}\right)}{i_{34}i_{23}}\right]^2 + \left[\frac{u\left(\delta_{\phi 11}\right)}{i_{34}i_{23}i_{12}}\right]^2} \qquad (2)$$

where $u\left(\delta_{\phi nm}\right)$ is the combined measurement uncertainty of the driving (m=1) or driven (m=2) gear on the nth shaft. The first shaft is the output end of the servo motor. The last one (n=4) is fasten to the rotating gear disc. $i_{n'n}$ ($1 \le n' \le 3$) is the transmission ratio of the n'th-stage transmission. $u\left(\delta_{\phi}\right)$ is

$$u\left(\delta_{\varphi}\right) = \sqrt{u^2\left(\delta_{\varphi 3}\right) + \frac{u^2\left(\delta_{\varphi 2}\right)}{i_{34}^2} + \frac{u^2\left(\delta_{\varphi 1}\right)}{i_{34}^2 i_{23}^2}} \qquad (3)$$

$u\left(\delta_{\phi i}\right)$ is the backlash combined measurement uncertainty of the ith-stage transmission. The calculation process of $u\left(\delta_{\phi nm}\right)$ and $u\left(\delta_{\phi i}\right)$ is described in detail in the master thesis wrote by Li ZY (This work is supervised by Zhang YM and Li CY) [9]. Here, the manufacture errors of the gear and the shaft and the shaft radial run-out in running are assumed to fellow the normal distribution and are independence mutually. Therefore, the angular displacement error of the rotating gear disc fellows the normal distribution N(0, $u(\delta)$).

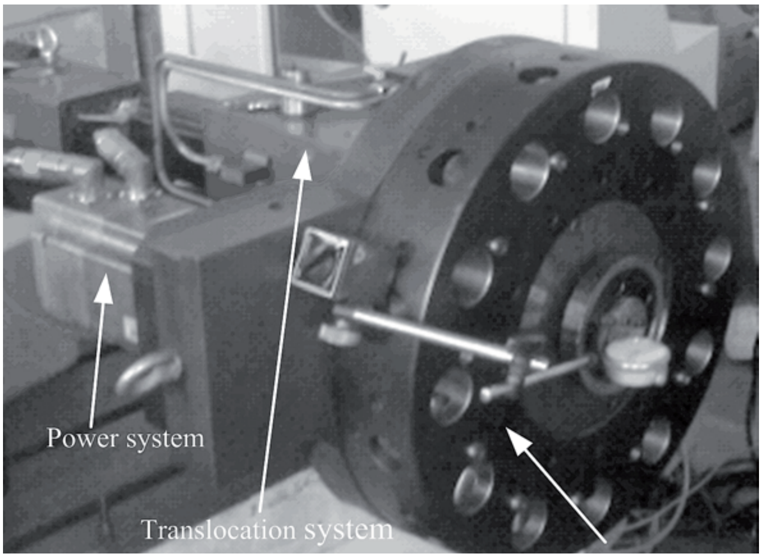

Fig. 1. External view of the considered PTT

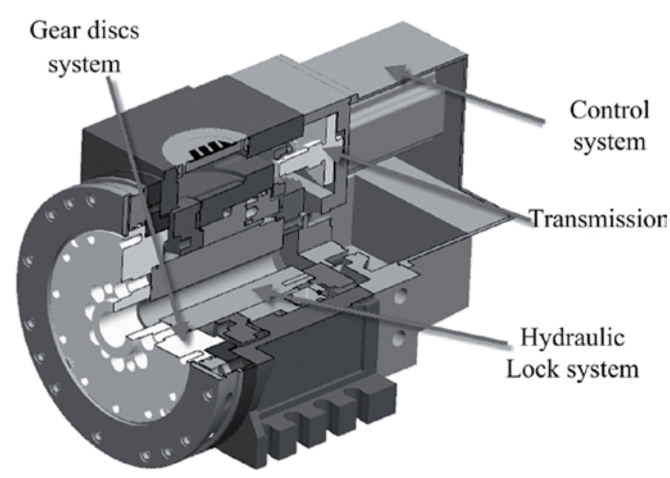

Fig. 2. Structure simplified diagram of indexing system

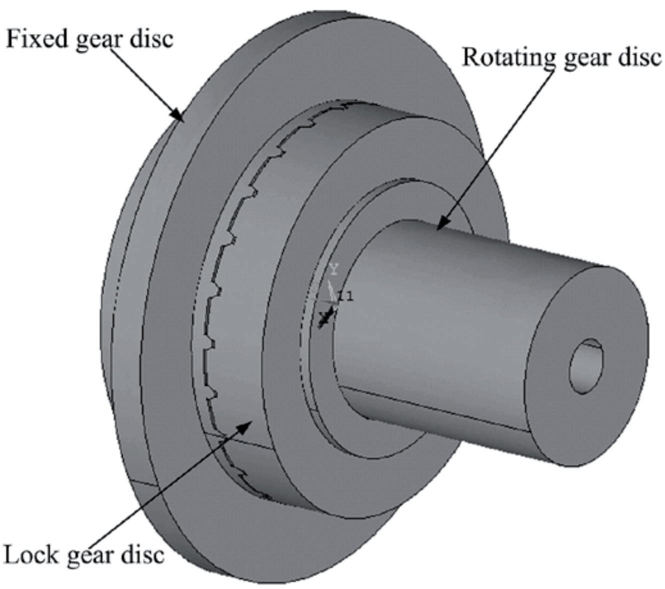

Fig. 3. Three-dimensional drawing of gear discs system

Table 1. Effect term of angular displacement error of rotating gear disc

Angular displacement error of rotating gear disc	One-way rotation error	Gear manufacture error
		Shaft manufacture error
		Gear-Shaft assembly error
	Backlash error	gear pair center distance error
		Gear manufacture error
		Gear-shaft assembly error
		Shaft radial run-out in running

2.2. Distribution and parameter estimation of other random variables

The other random variables of the indexing accuracy reliability formulation of the considered PTT are listed in Table2. The radial direction error is defined as the offset between the axis of the fixed or lock gear disc and the axis of the rotating gear disc. The verticality error describes the offset between the plane of the gear disc and the plane being vertical to the axis of the rotating gear disc. The radial direction error or the verticality error is described by a vector. The vector includes two parameters: mode and direction angle. The error is defined as the different between the designed value and the actual one. In the machining process of the parts of PTT, there are a lot of the stochastic factors, such as the manufacture and the assembly error of the machine tool parts, the environment temperature and vibration, the electric current stochastic fluctuation etc. Therefore, the direction angle of the radial direction error or the verticality error is supposed to follow the uniform distribution U(0,2π). The others are assumed to follow the normal distribution of which the mean is zero and the standard deviation is estimated by the corresponding B type measurement uncertainty.

2.3. Random variables wear of PTT

The indexing accuracy of PTT should deteriorate due to wear of some random variables listed in Table2 among the operating process. The wear process is a continuous-time and continuous-state stochastic process. It is also a monotone increasing stochastic process because it cannot be decreased by itself. For the stochastic deterioration process to be monotonic, we can best consider it as a gamma process [13,14]. Therefore, the Gamma process is employed to formulate the random variable deterioration process in this work.

A Gamma process is a stochastic process with independent, non-negative increment having a gamma distribution with an identical scale parameter. It is a continuous-time and continuous-state stochastic process. Let $\{X(t), t\geq 0\}$ be a Gamma process. It is with the following properties [8, 15]:

(1) X(0)=0 with probability one,

(2) $X(\tau)-X(t)\sim G(x\,|\,v(\tau)-v(t),u),\ \forall\,\tau>t\geq 0$,

(3) X(t) has independent increments.

where $v(t)$ is the shape function which is a non-decreasing, right-continuous, real-valued function for $t\geq 0$ with $v(0)\equiv 0$, $u>0$ is the scale parameter, and $G(\cdot)$ is the Gamma distribution.

Let $X(t)$ denote the wear of a certain random variable at time t, $t\geq 0$. In accordance with the definition of the Gamma process, its probability density function is given by:

$$f_{X(t)}(x)=\frac{u^{v(t)}x^{v(t)-1}\exp(-ux)}{\Gamma(v(t))}I_{[0,\infty)}(x) \tag{4}$$

where $\Gamma(\cdot)$ is the Gamma function, $I_A(x)=1$ for $x\in A$ and $I_A(x)=0$ for $x\notin A$. Its expectation and variance are respectively expressed as:

$$E(X(t))=\frac{v(t)}{u} \tag{5}$$

$$E((X(t)-E(X(t))^2)=\frac{v(t)}{u^2} \tag{6}$$

Empirical studies show that the expected wear at time t is often proportional to a power law [15]:

$$E(X(t))=\frac{ct^b}{u}=at^b\propto t^b \tag{7}$$

where $a>0$ (or $c>0$) and $b>0$. They are estimated by the expectation of Gamma process being equal to the theoretical calculation wear of the corresponding random variable.

Table 2. Random variables and their distribution of PTT

Part	Variable	Unit	Distribution	symbol
lock gear disc	tooth profile-half angle error	°	N(0,0.01112)	x_1
	tooth direction error	°	N(0,0.01082)	x_2
	tooth thickness error	m	N(0,0.0001412)	x_3
	radial direction error	m	N(0,0.00002442)	x_4
		rad	U(0,2π)	x_5
	verticality error	m	N(0,0.09322)	x_6
		rad	U(0,2π)	x_7
	angular displacement error	°	N(0,0.02842)	x_8
rotating gear disc	tooth profile half-angle error	°	N(0,0.01112)	x_9
	tooth direction error	°	N(0,0.01862)	x_{10}
	tooth thickness error	m	N(0,0.00012482)	x_{11}
	axial error	m	N(0,0.000004562)	x_{12}
	verticality error	m	N(0,0.004862)	x_{13}
		rad	U(0,2π)	x_{14}
	angular displacement error	°	N(0,0.03182)	x_{15}
fixed gear disc	tooth profile half-angle error	°	N(0,0.01112)	x_{16}
	tooth direction error	°	N(0,0.01932)	x_{17}
	tooth thickness error	m	N(0,0.0001412)	x_{18}
	radial direction error	m	N(0,0.000007672)	x_{19}
		rad	U(0,2π)	x_{20}
	axial error	m	N(0,0.000004172)	x_{21}
	verticality error	m	N(0,0.00132)	x_{22}
		rad	U(0,2π)	x_{23}
	angular displacement error	°	N(0,0.02082)	x_{24}
	lock pressure	MPa	N(6.61899959,0.033095002)	x_{25}

The wear of PTT is due to the relative sliding between two mechanical parts. It is belong to adhesive wear according to the wear theory. Therefore, Archard equation is used to calculate the wear mean of the random variables such as tooth thickness. It is:

$$\Delta V = K\frac{PL}{3H} \tag{8}$$

where ΔV, K, P, L and H are the total wear volume, the wear constant, the force between the friction pair, the relative sliding distance and the yield limit of the material of which the hardness is lower in the friction pair respectively. The total wear volume is proportional to the force between the friction pair from Eq. (8). Therefore, only the tooth thickness wear of the rotating gear disc, the fixed gear disc and the lock gear disc is considered in this work.

A is denoted by the contact surface area between two meshing teeth of the lock gear disc and the rotating gear disc or the fixed gear disc in the locking or loosening process. Then, the wear depth of one tooth is:

$$\Delta\overline{x} = K\frac{PL}{AH} \tag{9}$$

where the unit is meter. In the locking (loosening) process of PTT, the force P between two contact tooth surfaces changes from zero to the end force value P_1 (from P_1 to zero). The two contact tooth surfaces slide relatively and should deform due to the force P. The relationship between the stress being vertical to the contact tooth surface and the corresponding strain is:

$$\sigma = E\varepsilon \tag{10}$$

where σ, ε and E are the stress, the strain and elasticity modulus respectively. The force between two contact tooth surfaces is:

$$P = A\sigma = AE\varepsilon \tag{11}$$

The corresponding tooth thickness deformation of the lock gear disc and the rotating gear disc or the fixed gear disc are $\Delta s_{\mathrm{L}} = s_{\mathrm{L}}\varepsilon$ and $\Delta s_{\mathrm{F,R}} = s_{\mathrm{F,R}}\varepsilon$ respectively. $s_{\mathrm{F,R}} = 6.29\mathrm{mm}$ is the mean tooth thickness of the rotating gear disc or the fixed gear disc.

$$s_L = \frac{\pi\,(219+160)/2 - 6.29*24}{24} = 18.5155\mathrm{mm}$$

is the mean tooth thickness of the lock gear disc. The outside and inner circle diameters of the lock gear disc are 219mm and 160mm respectively. The total tooth number of the gear disc z is 24. The sliding friction $P_{\mathrm{F}} = \mu P$ where $\mu = 0.1$ is the sliding friction coefficient. Then, at the locking (loosening) end (start) time, the force P_1 is:

$$P_1 = \frac{F_{\mathrm{y}}}{z\left(\mu\cos\alpha + \sin\alpha\right)} \tag{12}$$

where:

$$F_{\mathrm{y}} = 4\times10^6(\mathrm{pa})\pi\left(\left(\frac{179.96}{2}\right)^2 - \left(\frac{119.96}{2}\right)^2\right)\times10^{-6}(\mathrm{m}^2)=56533.5881\ \mathrm{N}$$

is the total hydraulic lock force. 179.96 and 119.96 are the diameters of the hydraulic cylinder and the piston rod respectively. Here, the pressure angle α is 30°. In one locking or loosening process, the total tooth thickness normal deformation of the lock gear disc is:

$$\Delta s_{\mathrm{L1}} = \frac{F_{\mathrm{y}}}{z\left(\mu\cos\alpha + \sin\alpha\right)}\frac{s_{\mathrm{L}}}{AE} \tag{13}$$

and that of the rotating or fixed gear disc is:

$$\Delta s_{\mathrm{F,R1}} = \frac{F_{\mathrm{y}}}{z\left(\mu\cos\alpha + \sin\alpha\right)}\frac{s_{\mathrm{F,R}}}{AE} \tag{14}$$

Then, in one locking or loosening process, the total relative sliding distance between the lock gear disc and the fixed or rotating gear disc:

$$L_1 = \frac{\Delta s_{F,R1} + \Delta s_{L1}}{\sin(\alpha)} = \frac{F_y\left(s_{F,R} + s_L\right)}{AEz\sin(\alpha)\left(\mu\cos\alpha + \sin\alpha\right)} \tag{15}$$

dL is denoted by the relative sliding infinitesimal when the force between two contact tooth surfaces is P. According to Eq. (9), the corresponding tooth thickness wear is:

$$\mathrm{d}\Delta\overline{x} = \frac{KP}{AH}\mathrm{d}L \tag{16}$$

Eq. (16) is integrated and the total tooth thickness wear of one locking or loosening process of the gear disc is:

$$\Delta\overline{x} = \int_0^{L_1}\frac{KP}{AH}\mathrm{d}L \tag{17}$$

The relative sliding distance at any time in the locking or loosening process $L = \frac{\Delta s_{F,R} + \Delta s_L}{\sin(\alpha)} = 2\left(\Delta s_{F,R} + \Delta s_L\right)$. Then, d$L$ is:

$$\mathrm{d}L = 2\mathrm{d}\left(\Delta s_{F,R} + \Delta s_L\right) \tag{18}$$

where $\mathrm{d}\Delta s_L = \mathrm{d}\varepsilon s_L = s_L\mathrm{d}\varepsilon$ and $\mathrm{d}\Delta s_{F,R} = \mathrm{d}\varepsilon s_{F,R} = s_{F,R}\mathrm{d}\varepsilon$. Using $\mathrm{d}\varepsilon = \frac{\mathrm{d}\sigma}{E} = \frac{\mathrm{d}\left(\frac{P}{A}\right)}{E} = \frac{\mathrm{d}P}{EA}$, Eq. (18) is transformed into:

$$\mathrm{d}L = 2\left(s_{F,R} + s_L\right)\frac{\mathrm{d}P}{EA} \tag{19}$$

Then, Eq. (17) is written to:

$$\Delta\overline{x} = \int_0^{P_1}\frac{2KP\left(s_{F,R} + s_L\right)}{AH}\frac{\mathrm{d}P}{EA} = \frac{KP_1^2\left(s_{F,R} + s_L\right)}{HEA^2} \tag{20}$$

In the considered PTT, the contact surface area between two meshing teeth $A = 136.44\text{mm}^2$, elasticity modulus E=206GPa. The yield limit H=685MPa where the material of the gear disc is 20CrMo. P_1=4015.6085N by Eq. (12). The wear constant K=4.5×10^{-4}. Using Eq. (20), the total tooth thickness wear of one locking or loosening process of the gear disc is 6.8521×10^{-11}.

The time spent on one locking or loosening process is 0.3 second from the specified parameter of the considered PTT. The tooth thickness wear is directly proportional to the relative sliding distance. The relative sliding distance is directly proportional to the sliding period of time where the locking or loosening velocity is constant. Therefore, the tooth thickness cumulative wear is directly proportional to the cumulative locking and loosening time t. The relationship between the tooth thickness cumulative wear and the cumulative locking and loosening time is formulated by:

$$\overline{x}_M = 2.2840\times10^{-10}t \tag{21}$$

where the cumulative locking and loosening time t is different from the servicing time of PTT. The cumulative locking and loosening time t is the sum of the time spent in locking and loosening the gear discs system. The servicing time is the sum of the indexing time, the machining time and the downtime. The expectation of Gamma process is assumed to be equal to Eq. (21). That is:

$$\frac{ct^b}{u} = 2.2840\times10^{-10}t \tag{22}$$

Then, the parameters of Gamma process c= 2.2840×10^{-10} and u=b=1.

2.4. Indexing accuracy model of PTT

The indexing error of PTT is estimated by the finite element method. The parametric finite element model of PTT is shown in Fig. 4. It includes twenty five variables listed by Table2. It could calculate any one angular displacement error of PTT when the sample including twenty five variables is given. For example, when one sample is [−3. 2099×10^{-2}, 1. 3440×10^{-2}, −1.9920×10^{-5}, −2.5084×10^{-5}, 5.2255, −1.4060×10^{-1}, 1.1837, 6.8467×10^{-2}, −3.1164×10^{-2}, 6.5976×10^{-3}, −4.8894×10^{-5}, −5.4007×10^{-6}, −1.0811×10^{-3}, 2.3928×10^{-1}, −2.5873×10^{-2}, −2.6026×10^{-3}, −6.1497×10^{-3}, 6.8805×10^{-5}, 2.3010×10^{-5}, 5.6536, 2.6825×10^{-6}, 2.0399×10^{-3}, 1.9265, −3.4388×10^{-2}, 6.6415×10^{-6}], the absolute indexing error of PTT is equal to 1.1677×10^{-2}.

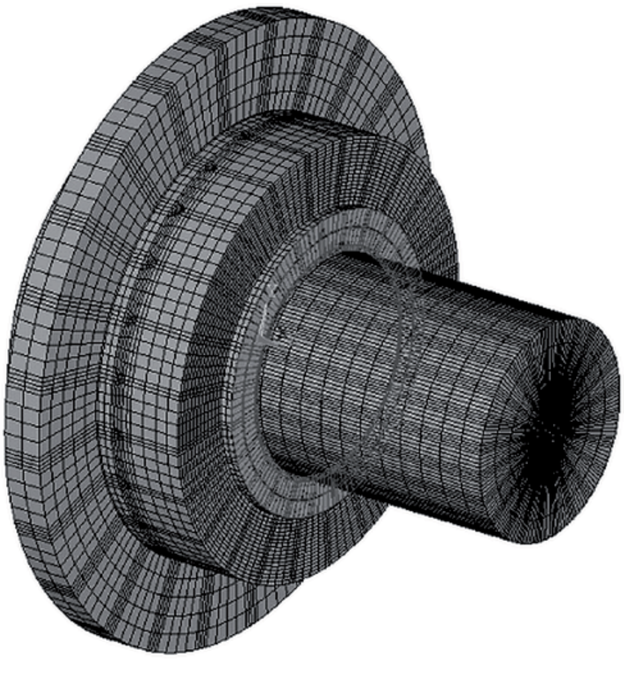

Fig. 4. Parametric finite element model of PTT

The BP neural network is employed to formulate the relationship between the absolute indexing error of PTT and twenty five random variables. The training samples are offered by the parametric finite element model of PTT. The learning result is:

$$y = b_2 + \mathbf{w}_2\frac{1}{1+\exp[-(\mathbf{w}_1\mathbf{X}+\mathbf{b}_1)]} = b_2 + \sum_{j=1}^{100}\left(\frac{\mathbf{w}_2(j)}{1+\exp\left[-\sum_{i=1}^{25}\mathbf{w}_1(j,i)\mathbf{X}(i) - \mathbf{b}_1(j)\right]}\right) \tag{23}$$

where b_1, w_1, b_2 and w_2 are the threshold and the weight between the hidden layer and the input layer, the threshold and the weight between the hidden layer and the output layer respectively. y is the output of

Table 3. Actual measurement values of the absolute indexing error of PTT

station / measurement number	1	2	3	4	5	6	7	8	9	10	11	12
clockwise 1	24.6	23.1	25.2	22.6	19.1	19.2	16.9	14.2	12.1	15.8	12.5	19.1
anticlockwise 1	23.5	22.1	19.5	22.2	15.1	18.6	15.2	13.6	11.2	15.1	17.7	11.9
clockwise 2	25.2	23.7	25.8	23.5	20.1	19.8	17	15.9	13.5	17.1	18.7	20.1
anticlockwise 2	22.9	23.4	18.9	22.9	16.3	19.8	14.7	14.8	12.8	16.4	18.4	15.8
clockwise 3	26.5	25.2	27.1	24.6	21	20.7	18.1	16.6	13.8	17.5	19.3	21.5
anticlockwise 3	25.7	24.2	21.2	23.2	16.8	20.6	16.3	15.5	13.5	17.2	19	14.1
clockwise 4	26.9	25.8	28	25.5	22.4	22	19.1	17.5	15	18.3	19.7	22.1
anticlockwise 4	24.9	24.8	20.8	24.3	16.7	20.5	15.3	14.9	13.2	17	17.4	18.9
clockwise 5	28	27	29.3	26.5	23.3	22.6	20.1	18	15.3	19.3	20.6	23.2
anticlockwise 5	24.5	26.2	20.7	23.1	17.3	21.8	17.1	17	14.7	18.3	20.5	13.5

the trained BP neural network and belongs to the set [-1,1]. The input set X is obtained by processing the input training samples from its original range to the range [-1 1]. The actual absolute indexing error (angular displacement error) of PTT is:

$$y' = \frac{y+1}{2}(y_{\text{tmax}} - y_{\text{tmin}}) + y_{\text{tmin}} \tag{24}$$

where $y_{\mathtt{tmax}}$ and $y_{\mathtt{tmin}}$ are the output maximum and the output minimum of the training sample respectively. The twenty five variables are sampled according to their distributions. The samples size is 25×1000. Then, the absolute indexing errors are calculated by Eq. (24). Their mean and standard deviation are 20.9925″ and 4.5328 respectively. The 120 actual measurement values of the absolute indexing error of PTT are shown in Table3. Their mean and standard deviation are 19.7142″ and 4.2469 respectively. Therefore, the absolute indexing error model of PTT described by Eq. (24) is acceptable.

2.5. Indexing accuracy reliability and its sensitivity of PTT

The indexing accuracy reliability of PTT is estimated by the reliability perturbation method which is proposed by Zhang YM and is described in detail in the document [25].The indexing accuracy reliability could be estimated by:

$$R\big(\beta(t)\big) = P\big[g\big(\mathbf{X}(t)\big) > 0\big] = 1 - F\big(-\beta(t)\big) \tag{25}$$

where $\beta(t)$ is the reliability index, $g\big(\mathbf{X}(t)\big)$ is the state function and the function $F(\bullet)$ is:

$$F(y) = \Phi(y) - \phi(y)\left[\frac{1}{6}\frac{\theta_g}{\sigma_g^3}H_2(y) + \frac{1}{24}\left(\frac{\eta_g}{\sigma_g^4} - 3\right)H_3(y) + \frac{1}{72}\left(\frac{\theta_g}{\sigma_g^3}\right)^2 H_5(y) + \cdots\right] \tag{26}$$

$\Phi(\bullet)$ and $\phi(\bullet)$ are the cumulative probability function and the probability density function of the standard normal distribution respectively. σ_g, θ_g and η_g the standard deviation, the third and the fourth order center moment of the state function. $H_j(\bullet)$ is the jth Hermite polynomial. If $R\big(\beta(t)\big)$ is more than 1 using Eq. (25), it is estimated by:

$$R^*\big(\beta(t)\big) = R\big(\beta(t)\big) - \frac{R\big(\beta(t)\big) - \Phi\big(\beta(t)\big)}{\big\{1 + \big[R\big(\beta(t)\big) - \Phi\big(\beta(t)\big)\big]\beta(t)\big\}^{\beta(t)}} \tag{27}$$

The indexing accuracy reliability curve of the considered PTT is shown in Fig. 5. The star is the results of Monte Carlo simulation. The solid curve is the calculated values of the reliability perturbation method. It could be seen that the different between Monte Carlo simulation and the reliability perturbation method is very small. Moreover, the reliability calculated by the reliability perturbation method is slightly less than zero among the period of time where the reliability decreases from positive number to zero in Fig. 5. It might be a numerical computation error.

The indexing accuracy reliability sensitivity of PTT to the mean and standard deviation of the random variables listed in Table2 and the wear processes could be calculated by Eq. (28) and (29) respectively:

$$\frac{\partial R(t)}{\partial \bar{\mathbf{X}}^T(t)} = \frac{\partial R\big(\beta(t)\big)}{\partial \beta(t)}\frac{\partial \beta(t)}{\partial \mu_g(t)}\frac{\partial \mu_g(t)}{\partial \bar{\mathbf{X}}^T(t)} \tag{28}$$

$$\frac{\partial R}{\partial \mathrm{Var}\big(\mathbf{X}(t)\big)} = \left[\frac{\partial R\big(\beta(t)\big)}{\partial \beta(t)}\frac{\partial \beta(t)}{\partial \sigma_g(t)} + \frac{\partial R\big(\beta(t)\big)}{\partial \sigma_g(t)}\right]\frac{\partial \sigma_g(t)}{\partial \mathrm{Var}\big(\mathbf{X}(t)\big)} \tag{29}$$

The detail description about Eq. (28) and (29) is introduced in [25]. The indexing accuracy reliability sensitivity of the considered PTT to the random variable's and the wear process's means is shown in Fig. 6. The sensitivity to the standard deviations is described in Fig. 7. Here, the subfigures (1), (2), ……, (25) are the sensitivity curves to the means or the standard deviations of x_1, x_2, ..., x_{25} respectively. The sensitivity to the means or the standard deviations of the tooth thickness wear processes of the lock gear disc, the rotating gear disc and the fixed gear disc are shown by the subfigures (26), (27) and (28) in Fig. 6 or Fig. 7 respectively.

From Fig. 6, it could be seen that (1) the sensitivity to the mean of some random variables is less than or equal to zero. These random variables include the direction angle of the radial direction error and the angular displacement error of the lock gear disc, the verticality error's mode and the angular displacement error of the rotating gear disc, the mode and the direction angle of the verticality error of the fixed gear disc and the tooth thickness wear of any one gear disc. The sensitivity of other random variables is more than or equal to zero. (2) With the increase of the cumulative locking and loosening time, the variation trend of the absolute sensitivity to the mean of all random variables increases gradually and then decreases to zero. (3) The fluctuation range of the sensitivity to the mean of the rotating gear disc of the fixed gear disc is the largest.

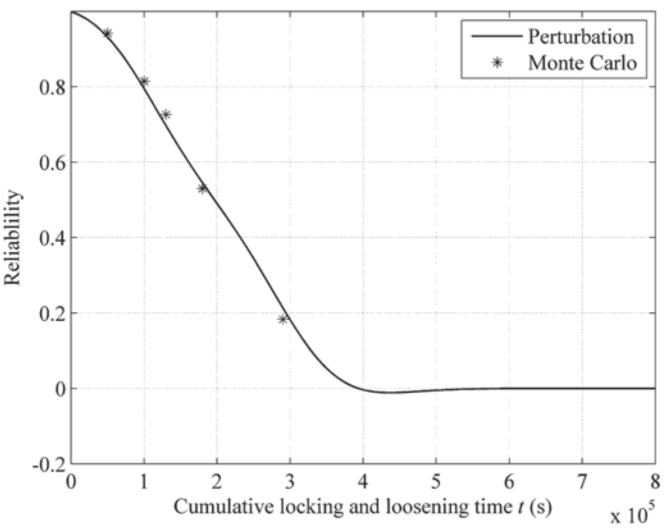

Fig. 5. Indexing accuracy reliability curve of the considered PTT

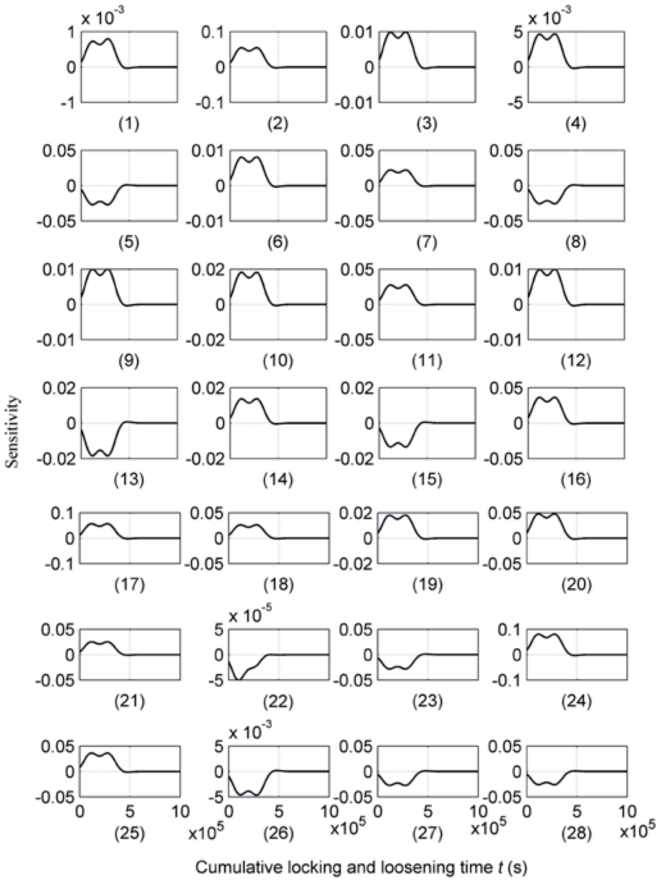

Fig. 6. Indexing accuracy reliability sensitivity of the considered PTT to the mean of the random variables and their deterioration processes

From Fig. 7, it could be seen that (1) With the increase of the cumulative locking and loosening time, the variation trend of the sensitivity to the standard deviation of all random variables decreases to the negative maximum firstly, gradually increases to the positive maximum subsequently and then decreases to zero finally. (2) The fluctuation range of the sensitivity to the standard deviation of the rotating gear disc of the fixed gear disc is the largest too.

According to the above calculated results, the indexing accuracy reliability of the considered PTT could be improved by increasing (decreasing) the mean of one of the random variables and the wear

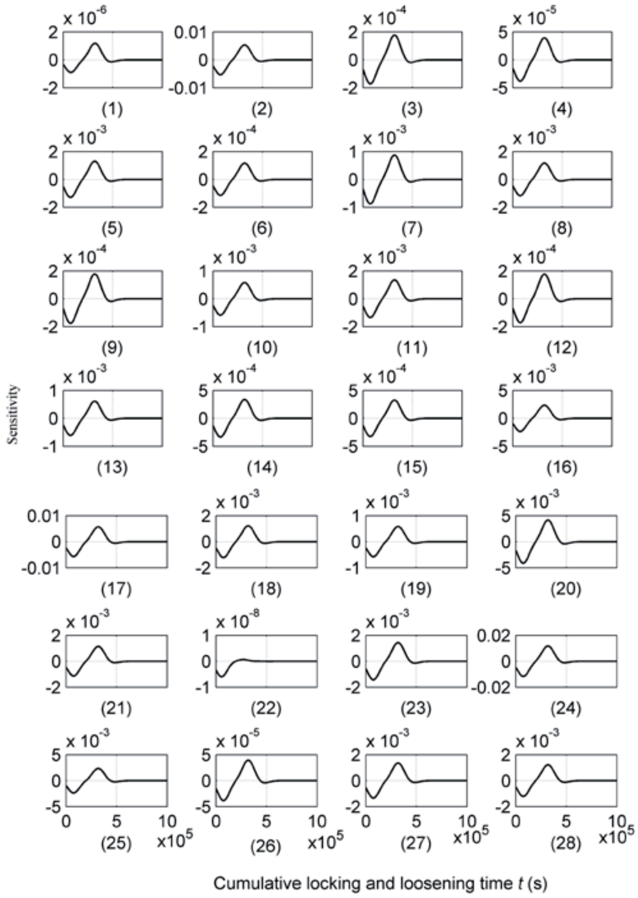

Fig. 7. Indexing accuracy reliability sensitivity of the considered PTT to the standard deviation of the random variables and their deterioration processes

stochastic processes to which the sensitivity is less (more) than or equal to zero when all parameters of other random variables are invariant. It implies that the corresponding design values, machining accuracy or wear should be decreased (increased) to improve the indexing accuracy reliability of the considered PTT. For example, the verticality of the fixed gear disc, which includes mode and direction angle, should be decreased and the tooth thickness of the gear disc should be increased.

If increase (decrease) the standard deviation of any one random variable or wear stochastic process when all parameters of other random variables are invariant, the indexing accuracy reliability of the considered PTT should be improved among the service early stage and should be reduced among the service middle stage. It means that the machining accuracy or wear should be improved (reduced) to increase (decrease) the standard deviation.

3. Conclusions

The indexing accuracy reliability and its sensitivity of PTT were presented in this work. The deterministic indexing error formulation including twenty five variables was formulated by the finite element method and BP neural network. The indexing accuracy reliability estimated by the reliability perturbation method was compared with Monte Carlo simulation and is acceptable. According to the indexing accuracy reliability sensitivity, the scheme was proposed to improve the indexing accuracy reliability of the considered PTT. A section of the scheme has been adopted and the reliability of the considered PTT has been improved observably.

Acknowledgements: *The work is supported by Chinese National Natural Science Foundation (51135003), Key National Science & Technology Special Project on "High-Grade CNC Machine Tools and Basic Manufacturing Equipment" (Grant No. 2013ZX04011-011) and China Ministry of Education new century excellent person support plan (Grant No. NCET-12-0105).*

References

1. Dai Y and Jia YZ. Reliability of a VMC and its improvement. Reliability Engineering and System Safety 2001; 72(1): 99-102.
2. Dai Y, Zhou YF and Jia YZ. Distribution of time between failures of machining center based on type I censored data. Reliability Engineering and System Safety 2003; 79(3): 377-379.
3. Hu ZQ, Xie YF and Liu JC. The research of super-heavy CNC machine accuracy reliability based on multi-body kinematics. Advanced Materials Research 2011; 211-212: 115-121.
4. Jia YZ and Jia ZX. Fatigue load and reliability design of machine-tool component. International Journal of Fatigue 1993; 15(1): 47-52.
5. Jia YZ, Wang ML and Jia ZX. Probability distribution of machining center failures. Reliability Engineering and System Safety 1995; 50(1): 12l-125.
6. Jia ZX, Zhang HB and Xi AM. Simulating and extending wire electrical discharge machining reliability data by radial basis function neural network. Chinese Journal of Mechanical Engineering 2010; 46(2): 145-149.
7. Jiao J. Analysis on the development status of CNC machine. Development & Innovation of Machinery & Electrical Products 2011; 24(3): 16-18.
8. Li CY and Zhang YM. Time-variant reliability assessment and its sensitivity analysis of cutting tool under invariant machining condition based on Gamma process. Mathematical Problems in Engineering 2012; article ID:676923.
9. Li ZY. Gradual reliability of precision and sensitivity research of power servo tool post, Master Dissertation, Shenyang, Northeastern University 2013.
10. Lin B and Shan GD. Development status and trend of CNC machine tools market in China. Oriental Enterprise Culture 2010; (9): 121.
11. Merrick JRW and Soyer R. A Bayesian semiparametric analysis of the reliability and maintenance of machine tools. Technometrics 2003; 45(1): 58-69.
12. Sun KZ, Zhou JY and Xie LY. Reliability optimum design of CNC ball screw and nut. Mechanical Science and Technology for Aerospace Engineering 2010; 29(11): 1530-1533.
13. van Noortwijk JM, Cooke RM and Kok M. A Bayesian failure model based on isotropic deterioration. European Journal of Operational Research 1995; 82(2): 270–282.
14. van Noortwijk JM, Kok M, Cooke RM. Optimal maintenance decisions for the sea-bed protection of the Eastern-Scheldt barrier, In: R. Cooke, M. Mendel, H. Vrijling (Eds.), Engineering probabilistic design and maintenance for flood protection, Kluwer Academic Publishers, Dordrecht 1997; 25–56.
15. van Noortwijk JM. A survey of the application of gamma processes in maintenance. Reliability Engineering and System Safety 2009; 94(1): 2–21.
16. Wang JL, Yang ZJ, Chen F, Li GF and Chen CH. Minimum Effort Reliability Allocation Method Considering Fuzzy Cost of Punching Machine Tools. Journal of Applied Sciences 2013; 13(20): 4107-4113.
17. Wang YQ, Jia YZ and Jiang WW. Early failure analysis of machining centers: a case study. Reliability Engineering and System Safety 2001; 72(1): 91-97.
18. Wang YQ, Yam RCM, Zuo MJ and Tse P. A comprehensive reliability allocation method for design of CNC lathes. Reliability Engineering and System Safety 2001; 72(3): 247-252.
19. Wang ZM and Yang JG. Reliability assessment of numerical control machine tools using Weibull mixture models. Advanced Materials Research 2011; 181-182: 161-165.
20. Wang ZM and Yu X. Log-linear process modeling for repairable systems with time trends and its applications in reliability assessment of numerically controlled machine tools. Proceedings of the Institution of Mechanical Engineers Part O-Journal of Risk and Reliability 2013; 227(O1): 55-65.
21. Wang ZM, Yang JG, Wang G and Zhang GB, Application of three-parameter Weibull mixture model for reliability assessment of NC machine tools: a case study. Proceedings of the Institution of Mechanical Engineers, Part C-Journal of Mechanical Engineering Science 2011; 225(C11): 2718-2726.
22. Wu J, Deng C, Shao XY and Xie SQ. A reliability assessment method based on support vector machines for CNC equipment. Science in China Series E-Technological Sciences 2009; 52(7): 1849-1857.
23. Zhang GB, Ge HY, Wang GQ and Liu J. Reliability-driven modeling approach of assembly process. Transactions of the Chinese Society for Agricultural Machinery 2011; 42(10): 192-196.
24. Zhang GB, Xu Z, He WH and Tu L, Research on reliability enhancement testing method of NC rotary table. Chinese Mechanical Engineering 2011; 22(8): 948-951.
25. Zhang YM, He XD, Liu QL, Wen BC and Zheng JX. Reliability sensitivity of automobile components with arbitrary distribution parameters. Proceedings of the Institution of Mechanical Engineers, Part D—Journal of Automobile Engineering 2005; 219(D2): 165–182.

Li CHANGYOU
Wang WEI
Zhang YIMIN
Li ZHENYUAN
Qiao CHANGSHUAI
Box NO.319, NO. 3-11, Wenhua Road, Heping District
Shenyang, P. R. China. Postal Code: 110004

Guo SONG
No.9, Hunnan East Road, Hunnan New District
Shenyang City, Liaoning, P.R.China. Postal Code: 110168

E-mails: 243465096@qq.com, ymzhang@mail.neu.edu.cn, guosong@sjzu.edu.cn, 772664104@qq.com, 727873785@qq.com

Article citation info:
CHŁOPEK Z, BIEDRZYCKI J, LASOCKI J, WÓJCIK P. Assessment of the impact of dynamic states of an internal combustion engine on its operational properties. Eksploatacja i Niezawodnosc – Maintenance and Reliability 2015; 17 (1): 35–41.

Zdzisław CHŁOPEK
Jacek BIEDRZYCKI
Jakub LASOCKI
Piotr WÓJCIK

ASSESSMENT OF THE IMPACT OF DYNAMIC STATES OF AN INTERNAL COMBUSTION ENGINE ON ITS OPERATIONAL PROPERTIES

OCENA WPŁYWU STANÓW DYNAMICZNYCH SILNIKA SPALINOWEGO NA JEGO WŁAŚCIWOŚCI UŻYTKOWE*

Internal combustion engines as systems described by non-linear models do not have any properties that would not depend on their current states. The paper presents results of testing an automotive engine in dynamic states determined by the vehicle acceleration sign in vehicle driving tests simulating the real operation of passenger cars. During the tests, pollutant emission rates and fuel flow rates averaged for specific vehicle states were examined. The processes under investigation were found to be highly sensitive both to the dynamic states and to the types of the vehicle driving tests.

Keywords: *internal combustion engines, pollutant emissions, vehicle driving tests, dynamic states.*

Silniki spalinowe jako układy opisywane modelami nieliniowymi nie mają właściwości niezależnych od stanów, w jakich się znajdują. W pracy przedstawiono wyniki badań silnika samochodowego w stanach dynamicznych zdeterminowanych znakiem przyspieszenia pojazdu w testach jezdnych symulujących rzeczywistą eksploatację samochodów osobowych. Badano uśrednione w tych stanach: natężenie emisji zanieczyszczeń i natężenie przepływu paliwa. Stwierdzono znaczną wrażliwość badanych procesów zarówno na stany dynamiczne, jak i na rodzaje testów jezdnych.

Słowa kluczowe: *silniki spalinowe, emisja zanieczyszczeń, testy jezdne, stany dynamiczne.*

1. Introduction

In general, real objects described by non-linear mathematical models considered satisfactorily consistent with the subject of modelling [9] have no properties that would be independent of the objects' states [8]. The objects of this kind include internal combustion (IC) engines. Therefore, the degree of generality of the IC engine research tasks must be limited. In particular, in the case of IC engines being in dynamic states, some constraints in the form of specific test procedures adopted, e.g. a definite class of the processes assumed as engine operation conditions or a special method of processing the test results, such as averaging within the range of process values, must be imposed on the system under investigation.

The operational properties of IC engines (for constant engine steering characteristics) are chiefly determined by the quantities that characterize the engine work intensity, described as the effective power output, and the thermal engine state defined by the temperatures of engine parts and systems [8]. The quantities characterizing the engine work intensity are usually described by engine torque output, representing the engine load, and engine crankshaft speed [8]. This description may also be supplemented with the current setting of engine steering as another engine load indicator. These three quantities, i.e. engine steering setting "s", engine torque output "M_e", and engine crankshaft speed "n", depend on each other. For static states, this interdependence is represented by an elementary function with numerical values:

$$F(s, M_e, n) = 0 \tag{1}$$

For dynamic states, it takes a form of an operational equation [2]:

$$\Im[s, M_e, n] = 0 \tag{2}$$

The load of an IC engine may also be described with the use of the resistance torque "M_o" instead of the engine torque output. For static states, the following equation obviously holds:

$$M_e = M_o \tag{3}$$

but for dynamic states, we have:

$$\frac{d}{dt}\left[J(t) \times n(t)\right] = M_e(t) - M_o(t) \tag{4}$$

where: t – time;
J – moment of inertia of the moving engine parts, reduced to the crankshaft axis.

Hence, the following functional equation with numerical values applies to static states:

$$F(s, M_o, n) = 0 \tag{5}$$

(*) Tekst artykułu w polskiej wersji językowej dostępny w elektronicznym wydaniu kwartalnika na stronie ***www.ein.org.pl***

while for dynamic states, it takes the form of an operational equation:

$$\Re\left[s, M_o, n\right] = 0 \tag{6}$$

In dynamic conditions, the operational properties of IC engines depend not only on the values of the quantities that describe the state of engine operation but also on the processes of changes in these values (time histories) [8]. For this reason, the operational properties of IC engines in static and dynamic conditions may significantly differ from each other [8].

When the thermal state of the IC engine is stable, the engine properties in its dynamic states are determined by the engine torque and crankshaft speed processes. In this connection, the operational properties of an IC engine in its dynamic states cannot be, in general, unequivocally evaluated. However, there is a possibility of considering the operational properties of an IC engine in certain dynamic states that may be assumed as elementary states. As one of the possible criteria of qualifying to the elementary dynamic states of an IC engine, the signs (positive or negative) of derivatives of the states with respect to time in the whole range of engine operation parameters may be considered. Thus, the following elementary states of engine operation are possible as combinations of engine controls setting, resistance torque, and engine crankshaft speed:

$$\frac{ds}{dt} > 0 \wedge \frac{dM_o}{dt} > 0 \;; \quad \Rightarrow \quad \frac{dn}{dt} > 0 \tag{7}$$

$$\frac{ds}{dt} > 0 \wedge \frac{dM_o}{dt} > 0 \;; \quad \Rightarrow \quad \frac{dn}{dt} < 0 \tag{8}$$

$$\frac{ds}{dt} > 0 \wedge \frac{dM_o}{dt} < 0 \;; \quad \Rightarrow \quad \frac{dn}{dt} > 0 \tag{9}$$

$$\frac{ds}{dt} < 0 \wedge \frac{dM_o}{dt} > 0 \;; \quad \Rightarrow \quad \frac{dn}{dt} < 0 \tag{10}$$

$$\frac{ds}{dt} < 0 \wedge \frac{dM_o}{dt} < 0 \;; \quad \Rightarrow \quad \frac{dn}{dt} < 0 \tag{11}$$

$$\frac{ds}{dt} < 0 \wedge \frac{dM_o}{dt} < 0 \;; \quad \Rightarrow \quad \frac{dn}{dt} > 0 \tag{12}$$

In turn, if the engine torque output is to be taken into account in the said combinations in place of the resistance torque, then the possible elementary states of engine operation may be defined as follows:

$$\frac{ds}{dt} > 0 \wedge \frac{dM_e}{dt} > 0 \;; \quad \Rightarrow \quad \frac{dn}{dt} > 0 \tag{13}$$

$$\frac{ds}{dt} > 0 \wedge \frac{dM_e}{dt} > 0 \;; \quad \Rightarrow \quad \frac{dn}{dt} < 0 \tag{14}$$

$$\frac{ds}{dt} > 0 \wedge \frac{dM_e}{dt} < 0 \;; \quad \Rightarrow \quad \frac{dn}{dt} > 0 \tag{15}$$

$$\frac{ds}{dt} < 0 \wedge \frac{dM_e}{dt} > 0 \;; \quad \Rightarrow \quad \frac{dn}{dt} < 0 \tag{16}$$

$$\frac{ds}{dt} < 0 \wedge \frac{dM_e}{dt} < 0 \;; \quad \Rightarrow \quad \frac{dn}{dt} < 0 \tag{17}$$

$$\frac{ds}{dt} < 0 \wedge \frac{dM_e}{dt} < 0 \;; \quad \Rightarrow \quad \frac{dn}{dt} > 0 \tag{18}$$

The use of descriptions (7–12) and (13–18) may also be considered with respect to the assumed ranges of values of individual processes. Moreover, there is a possibility of taking into account combinations of engine operation conditions and states defined by the ranges of values of individual processes, signs of derivatives of the processes with respect to time, and zero values of the time derivatives with tolerance ranges appropriately defined (constant-value processes), e.g.:

$$\frac{ds}{dt} > 0 \;; \qquad \frac{dM_e}{dt} \in \left[\delta_{M_e} - \frac{\varepsilon_{\delta M_e}}{2} ; \delta_{M_e} + \frac{\varepsilon_{\delta M_e}}{2}\right] \tag{19}$$

for

$$s \in \left[s_{min}; s_{max}\right] \quad n \in \left[n_{min}; n_{max}\right] \quad M_e \in \left[M_{e\,min}; M_{e\,max}\right] \tag{20}$$

In the conditions of stable thermal state of an IC engine, the state of an automotive engine in the conditions of engine operation in a moving vehicle is determined by the vehicle speed process [8]. Therefore, vehicle driving tests may be used to examine the operational properties of automotive IC engines. Such tests are commonly carried out within type-approval tests [25, 26] and special tests where special vehicle traffic conditions are simulated, e.g. those prevailing in urban traffic congestions (the "Stop-and-Go" test [5]) or in the traffic on motorways and fast roads (the "Autobahn" test [5]). Obviously, the results of examination of the operational properties of engines in the dynamic states that occur at various test procedures will differ from each other.

The need to examine the operational properties of engines in dynamic states has existed for many years. Many publications with reports of works on this subject are issued [1, 3, 4, 6–8, 10–19, 21–24] but, in principle, there are no standards so far for tests of this type; only the methods of examining the averaged properties of IC engines in dynamic states, such as those used at type-approval tests, may be considered as standards [25, 26].

Most of the works concern the controlling of IC engines with taking into account dynamic states [4, 12, 14, 17, 23]. In publication [4], a mathematical model used to simulate the injector operation in a common rail engine fuelling system has been presented. Monograph [12], prepared at ETH in Zürich, shows the present-day state of knowledge regarding the modelling of working processes in IC engines in respect of the use of such processes in engine control systems. Publication [14] is dedicated to the use of a mathematical model of the processes taking place in the IC engine to control the processes in an HCCI (Homogenous Charge Compression Ignition) engine. A multidimensional model used for developing IC engine control algorithms with the application of fuzzy logic has been shown in publication [17]. Results of examination of the parameters of controlling an automotive engine in real operation conditions have been presented in paper [23].

The properties of automotive IC engines in specific working conditions prevailing during real vehicle operation are examined as well [15, 16, 19], where e.g. mobile measurement systems PEMS (Portable Emissions Measurement System) are used. Results of the examination of pollutant emissions from non-road and automotive engines have been presented in publications [15] and [16], respectively. The impact of passenger car motion parameters on fuel consumption and pollutant emissions during real vehicle operation in urban traffic conditions has been analysed in publication [19].

Some of the works are dedicated to research on the processes of flows, air-fuel mixture formation, combustion, and formation of individual exhaust gas components in IC engines being in dynamic states [22, 24].

Most of the publications deal with motor vehicle engines; however, results of the examination of pollutant emissions from a marine IC piston engine during engine start-up and from an agricultural tractor engine have been presented in papers [13] and [15], respectively.

At this work, a decision was made to carry out tests with the use of the test procedures named as "PIMOT tests", developed by the authors during the work described in publication [7]. A unique concept of defining appropriate test procedures for the simulation of real conditions of driving a passenger car [6] was adopted. The vehicle velocity recorded in comparable traffic conditions (i.e. in the street congestion, urban, extra-urban, and high-speed traffic conditions) were treated as individual realizations of stochastic processes of vehicle velocity in the traffic conditions under consideration. Based on an analysis of the stochastic processes, several velocity processes were selected for each of the types of vehicle motion conditions, with treating individual realizations of a stochastic process as a vehicle driving test for each of the types of the traffic conditions under consideration. Individual realizations of the vehicle speed process were defined in conformity with the criterion of faithful simulation in the time domain. The vehicle driving tests were defined based on the similarity of zero-dimensional characteristics of the stochastic processes of speed in real vehicle operation and in the tests, i.e. the expected values, extreme values, and variance, taken as a criterion for comparisons.

Figs. 1–4 show the PIMOT vehicle driving tests, with each of them consisting of four realizations of the stochastic processes of vehicle velocity that characterize the vehicle motion in the following conditions:

- urban traffic congestions (denoted by "CT");
- urban traffic without congestions (denoted by "UT");
- extra-urban ("rural") traffic (denoted by "RT");
- high-speed traffic (on motorways and fast roads, denoted by "HT").

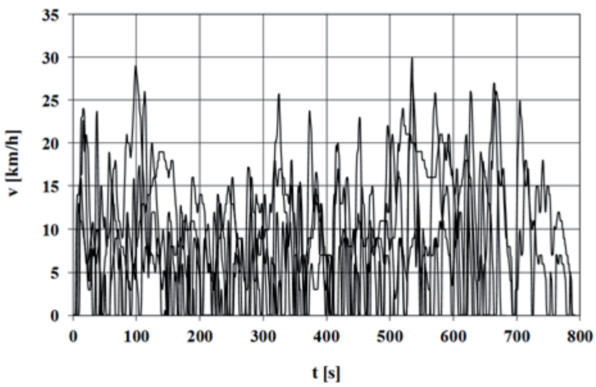

Fig. 1. The vehicle velocity – v for test drives in urban traffic congestions – the driving tests CT

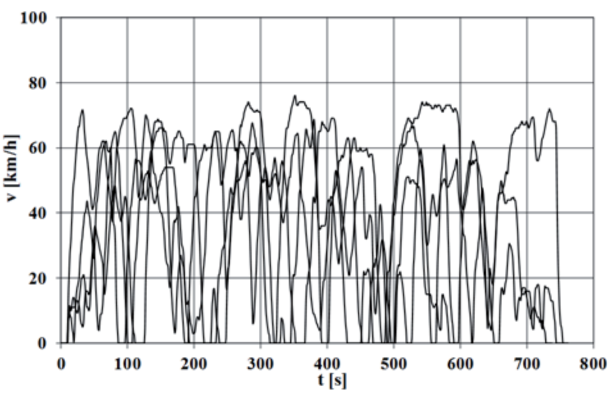

Fig. 2. The vehicle velocity – v for test drives in urban traffic – the driving tests UT

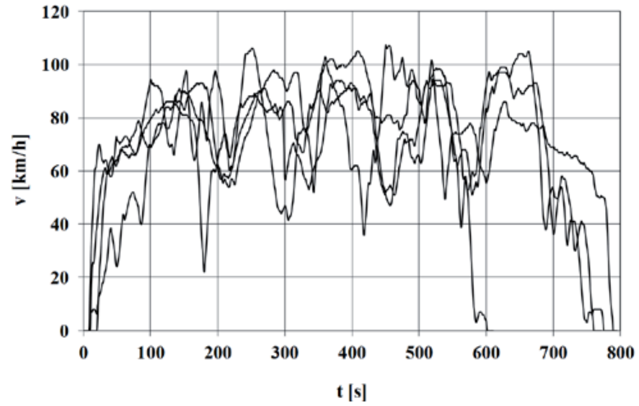

Fig. 3. The vehicle velocity – v for test drives in extra-urban traffic – the driving tests RT

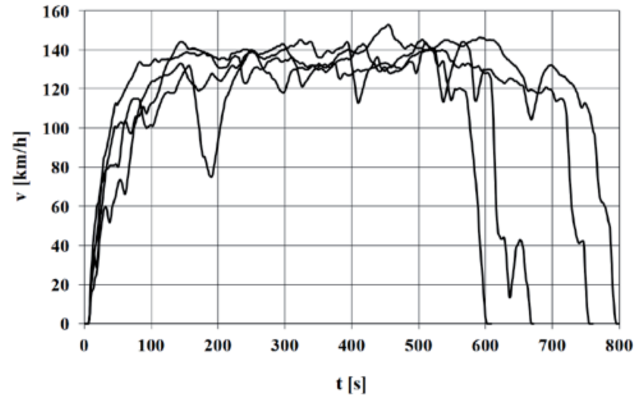

Fig. 4. The vehicle velocity – v for test drives in high-speed traffic – the driving tests HT

2. Methods, object, and results of testing

To assess the impact of dynamic states of an IC engine on its properties, a research work was done, which was based on tests carried out in conditions corresponding to negative and positive accelerations of the vehicle tested. During the tests, pollutant emissions and fuel consumption were examined. The said impact of dynamic states was assessed in the conditions of engine operation in a motor vehicle subjected to PIMOT tests.

The test specimen was a Honda Civic passenger car provided with a spark-ignition engine of 1 396 cm^3 displacement volume.

The vehicle tests were carried out on a Schenck-Komeg vehicle chassis dynamometer EMDY 48. The pollutant emissions were examined with the use of an exhaust gas analysing test stand which incorporates a Horiba Mexa 7200 system provided with the following analysers:

- AIA–721A (carbon monoxide concentration);
- AIA–722 (carbon dioxide concentration);
- MPA–720 (oxygen concentration);
- CLA–755A (nitrogen oxides concentration);
- FIA–725A (hydrocarbon concentration).

The processes subjected to investigation included the intensity of flow of the fuel consumed by the engine and the pollutant emission intensity. The signals were synchronized at the location where the exhaust gas was taken off, downstream of the multifunctional catalytic reactor; the delays in individual signals related to the exhaust gas analysis process were taken into account and the fuel flow intensity was determined from the balance of carbon mass in the signals of exhaust gas component emission intensity. The signals under investigation were pre-processed for gross errors to be eliminated and for the share of high-frequency interference to be reduced. The measurement results were sampled with a frequency of 10 Hz and then averaged for 10 subsequent samples. Thus, the sampling interval for the signals processed was equal to 1 s. The gross errors were identified by the method of analysing the current variance of measurement results. For the share of high-frequency noise in the signals to be reduced, a Golay-Savitzky low-pass filter [20] was used, where both-side approximation from two data points on each side to a polynomial of degree 2 was applied.

Let sets $\mathbf{E_{CO}}$, $\mathbf{E_{HC}}$, $\mathbf{E_{NOx}}$, $\mathbf{E_{CO2}}$ and $\mathbf{G_f}$ contain digitized values of pollutant emission intensity, fuel flow intensity, and vehicle acceleration for each of the test realizations with a sampling frequency of 1 Hz. The power of each of the sets is N. Each of the sets may be presented in the form of a sum of sets consisting of elements characterized by such a feature that the vehicle acceleration is either positive or negative:

$$\mathbf{X} = \mathbf{X_{(a<0)}} \cup \mathbf{X_{(a>0)}} \tag{21}$$

where: $\mathbf{X = E_{CO}, E_{HC}, E_{NOx}, E_{CO2}, G_f}$.

Let the power of the sets $\mathbf{X_{(a<0)}}$ be $N_{(a<0)}$ and the power of the sets $\mathbf{X_{(a>0)}}$ be $N_{(a>0)}$. The average value of elements of the sets $\mathbf{X_{(a<0)}}$ is:

$$X_{(a<0)\,AV} = \frac{1}{N_{(a<0)}} \sum_{i=1}^{N_{(a<0)}} X_{(a<0)i} \tag{22}$$

For the sets $\mathbf{X_{(a>0)}}$, this average value is:

$$X_{(a>0)\,AV} = \frac{1}{N_{(a>0)}} \sum_{i=1}^{N_{(a>0)}} X_{(a>0)i} \tag{23}$$

where: $X_{(a<0)\,AV} = E_{CO(a<0)\,j}, E_{HC(a<0)\,j}, E_{NOx(a<0)\,j}, E_{CO2(a<0)}, G_{f(a<0)\,j}$;
$X_{(a>0)\,AV} = E_{CO(a>0)\,j}, E_{HC(a>0)\,j}, E_{NOx(a>0)\,j}, E_{CO2(a>0)}, G_{f(a>0)\,j}$;
j = 1, 2, 3, 4 – item number of a realization of each of the tests.

Example test results for specific traffic types have been presented in illustrations as specified below:

- for the CT test, in Figs. 5 and 6;
- for the UT test, in Figs. 7 and 8;
- for the RT test, in Figs. 9 and 10;
- for the HT test, in Figs. 11 and 12.

The graphs shown in the said illustrations represent the average values and the relative ranges of the average fuel flow intensity and average pollutant emission intensity for the test results for negative and positive vehicle accelerations in specific test realizations.

The average value of the average pollutant emission intensity for the realizations of each of the tests is:

$$E_{x(a>0)} = \frac{1}{4} \sum_{j=1}^{4} E_{x(a>0)j} \tag{24}$$

where: x = CO, HC, NOx, CO_2.

Similarly, the average value of the average fuel flow intensity is defined as follows:

$$G_{f(a>0)} = \frac{1}{4} \sum_{j=1}^{4} G_{f(a>0)j} \tag{25}$$

The relative range is defined as the ratio of the absolute value of range R to the average value AV:

$$\delta = \frac{|R|}{AV} \tag{26}$$

where: $AV = E_{x(a<0)}, E_{x(a>0)}, G_{f(a<0)}, G_{f(a>0)}$, and

$$R = \max(y) - \min(y) \tag{27}$$

where: $y = E_{x(a<0)}, E_{x(a>0)}, G_{f(a<0)}, G_{f(a>0)}$;
max – operator of the maximum value of the elements of a set;
min – operator of the minimum value of the elements of a set.

In the graphs below, the indices (a<0) and (a>0) have been referred to in the legends.

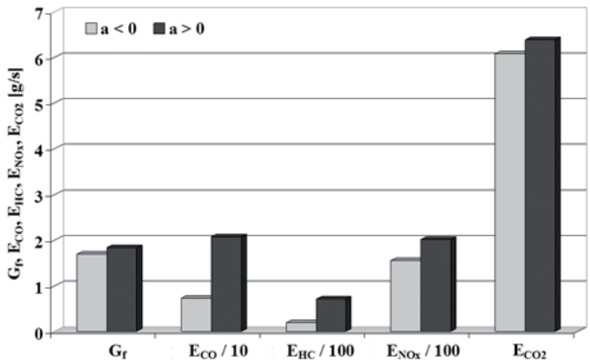

Fig. 5. Average values of the average fuel flow intensity (G_f) and of the average intensity of emission of carbon monoxide (E_{CO}), hydrocarbons (E_{HC}), nitrogen oxides (E_{NOx}), and carbon dioxide (E_{CO2}) for negative (a < 0) and positive (a > 0) vehicle accelerations in the CT test

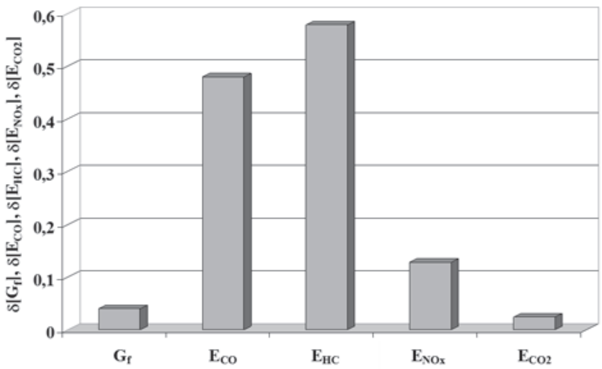

Fig. 6. Relative ranges of the average fuel flow intensity (G_f) and of the average intensity of emission of carbon monoxide (E_{CO}), hydrocarbons (E_{HC}), nitrogen oxides (E_{NOx}), and carbon dioxide (E_{CO2}) for negative and positive vehicle accelerations in the CT test

A vehicle driven in urban traffic congestions is subject to very special conditions of motion, characterized by low absolute values of vehicle acceleration. This explains the fact that the carbon dioxide emission intensity and fuel flow intensity, determined for the vehicle acceleration phase, do not significantly differ from the corresponding values measured for the deceleration phase, especially if the "averaging" properties of the exhaust gas sampling system are taken into consideration. In contrast, significant increase can be clearly seen in the intensity of emission of hydrocarbons and, in second rank, carbon monoxide.

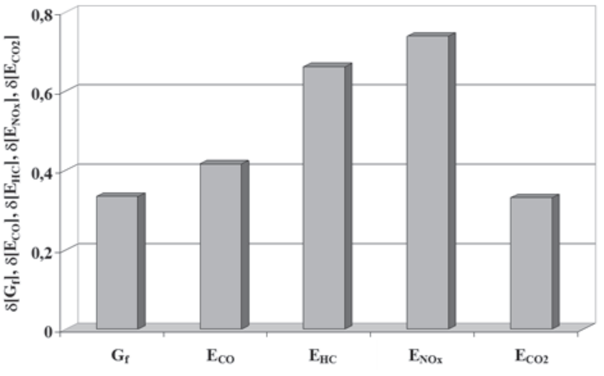

Fig. 7. Average values of the average fuel flow intensity (G_f) and of the average intensity of the emission of carbon monoxide (E_{CO}), hydrocarbons (E_{HC}), nitrogen oxides (E_{NOx}), and carbon dioxide (E_{CO2}) for negative ($a < 0$) and positive ($a > 0$) vehicle accelerations in the UT test

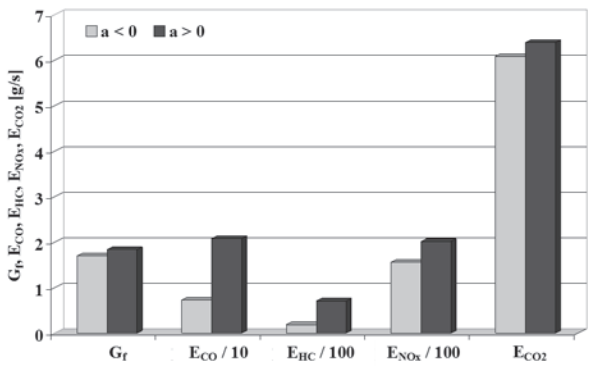

Fig. 8. Relative ranges of the average fuel flow intensity (G_f) and of the average intensity of the emission of carbon monoxide (E_{CO}), hydrocarbons (E_{HC}), nitrogen oxides (E_{NOx}), and carbon dioxide (E_{CO2}) for negative and positive vehicle accelerations in the UT test

For the vehicle driven in urban traffic conditions (exclusive of traffic congestions), the differences in pollutant emission intensity and fuel intensity rates for the phases of accelerated and decelerated vehicle motion are much bigger than those recorded for vehicle drives in urban traffic congestions. A particularly high relative range (exceeding 50%) can be noticed for the nitrogen oxides emission intensity; this is related to high engine load occurring when the vehicle is accelerating.

The relations observed in the conditions of extra-urban traffic are similar to those recorded for the urban traffic conditions, except for the fact that the impact of vehicle accelerations on the increase in pollutant emission intensity and fuel flow intensity is even more clearly visible.

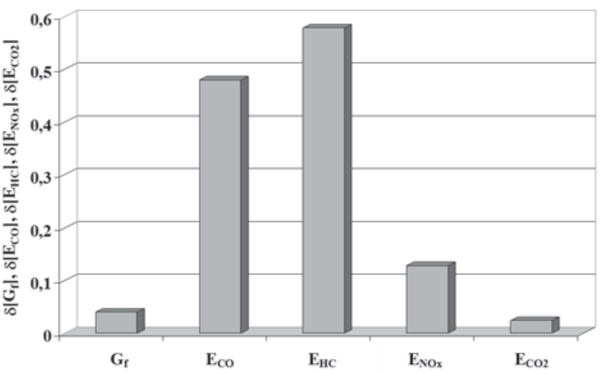

Fig. 9. Average values of the average fuel flow intensity (G_f) and of the average intensity of the emission of carbon monoxide (E_{CO}), hydrocarbons (E_{HC}), nitrogen oxides (E_{NOx}), and carbon dioxide (E_{CO2}) for negative ($a < 0$) and positive ($a > 0$) vehicle accelerations in the RT test

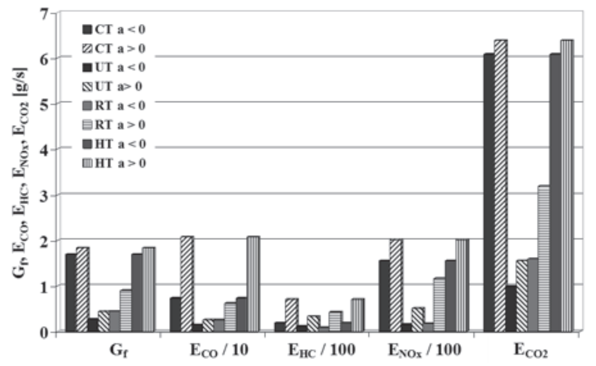

Fig. 10. Relative ranges of the average fuel flow intensity (G_f) and of the average intensity of the emission of carbon monoxide (E_{CO}), hydrocarbons (E_{HC}), nitrogen oxides (E_{NOx}), and carbon dioxide (E_{CO2}) for negative and positive vehicle accelerations in the RT test

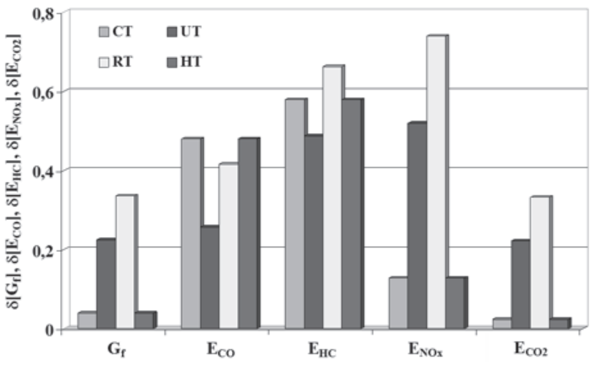

Fig. 11. Average values of the average fuel flow intensity (G_f) and of the average intensity of the emission of carbon monoxide (E_{CO}), hydrocarbons (E_{HC}), nitrogen oxides (E_{NOx}), and carbon dioxide (E_{CO2}) for negative ($a < 0$) and positive ($a > 0$) vehicle accelerations in the HT test

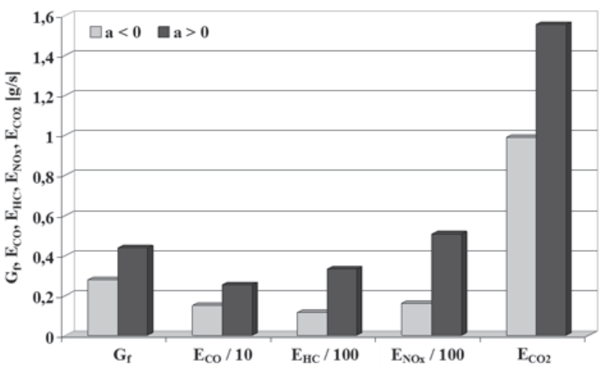

Fig. 12. Relative ranges of the average fuel flow intensity (G_f) and of the average intensity of the emission of carbon monoxide (E_{CO}), hydrocarbons (E_{HC}), nitrogen oxides (E_{NOx}), and carbon dioxide (E_{CO2}) for negative and positive vehicle accelerations in the HT test

During vehicle drives on motorways and fast roads, the absolute vehicle acceleration values are low. In this connection, no significant differences can be seen in fuel flow intensity and carbon dioxide emission intensity for the phases of vehicle acceleration and deceleration. A similar finding may be formulated for the nitrogen oxides emission intensity. Differences occur, however, for the carbon monoxide and hydrocarbons emission intensity.

An overall graph of the average fuel flow intensity and average pollutant emission intensity for the negative and positive vehicle accelerations in the PIMOT tests has been presented in Fig. 13.

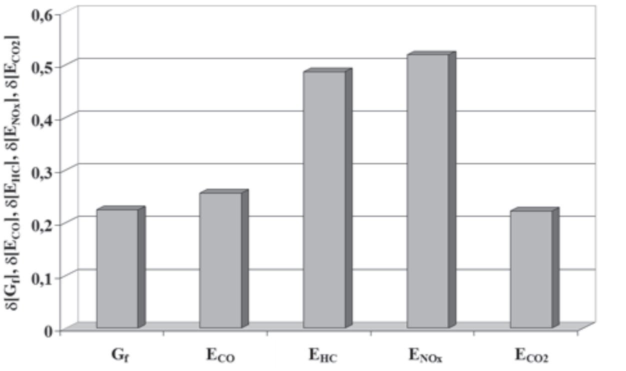

Fig. 13. Average values of the average fuel flow intensity (G_f) and of the average intensity of the emission of carbon monoxide (E_{CO}), hydrocarbons (E_{HC}), nitrogen oxides (E_{NOx}), and carbon dioxide (E_{CO2}) for negative ($a < 0$) and positive ($a > 0$) vehicle accelerations in the PIMOT tests

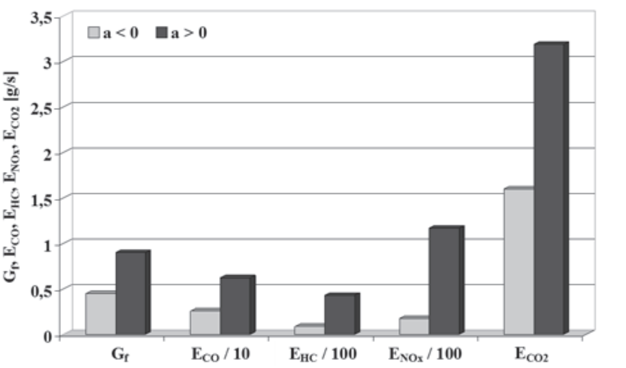

Fig. 14. Relative ranges of the average fuel flow intensity (G_f) and of the average intensity of the emission of carbon monoxide (E_{CO}), hydrocarbons (E_{HC}), nitrogen oxides (E_{NOx}), and carbon dioxide (E_{CO2}) for negative and positive vehicle accelerations in the PIMOT tests

An overall graph of the relative ranges of fuel flow intensity and pollutant emission intensity for negative and positive vehicle accelerations in the PIMOT tests has been shown in Fig. 14.

3. Conclusions

Based on the tests carried out for dynamic states of an IC engine, the following conclusions may be formulated.

1) It has been unequivocally ascertained that the values of pollutant emission intensity and fuel flow intensity in the conditions of vehicle acceleration are higher than those determined when the vehicle motion is decelerated. The values of these differences are significantly diversified depending on the quantities examined and the conditions of vehicle motion, determined by the test types adopted. The relative range of the average pollutant emission intensity and of the fuel flow intensity varies within limits from 0.024 to 0.739, where the lowest and the highest value were obtained for the carbon dioxide emission intensity in the conditions of vehicle motion in urban congestion traffic and for the nitrogen oxides emission intensity in the conditions of vehicle motion in extra-urban traffic, respectively.
2) No unequivocal interrelations have been found to exist between the increase in pollutant emission intensity and fuel flow intensity as determined for vehicle acceleration on the one hand and those determined for vehicle deceleration on the other hand, at different test types. As an example, when the vehicle was operated in the conditions of urban congestion traffic and traffic on motorways and fast roads, the quantity found to be most sensitive to the dynamic states under consideration was the hydrocarbons emission intensity; in the conditions of urban and extra-urban traffic, the highest sensitivity was observed for the nitrogen oxides emission intensity.
3) The highest values of the relative ranges of pollutant emission intensity and fuel flow intensity were recorded in the conditions of extra-urban traffic; the values of these relative ranges were on the lowest level for the conditions of urban congestion traffic.
4) The relative range of pollutant emission intensity in the vehicle acceleration phase reached the highest value for the hydrocarbons emission while the lowest values of this relative range were recorded for the carbon dioxide emission intensity and for the fuel flow intensity.

In general, a statement may be made that in the states of IC engine operation when the vehicle acceleration sign is positive, the average intensity of flow of the fuel consumed and the average pollutant emission intensity are higher than those corresponding to negative vehicle acceleration. In some cases, this difference is very big, i.e. the relative range of these quantities even exceeds 70%.

Acknowledgement: *The paper has been based on results of tests carried out within research project No. N N509 556440 entitled "Sensitivity of pollutant emission and fuel consumption to the conditions of operation of a spark-ignition engine", sponsored by the National Science Centre.*

References

1. Arregle J, Bermudez V, Serrano JR, Fuentes E. Procedure for engine transient cycle emissions testing in real time. Experimental Thermal and Fluid Science 2006; 30(5): 485–496.
2. Banach S. Théorie des opérations linéaires. Monografie Matematyczne 1. Warszawa, 1932.
3. Bermúdez V, Luján JM, Serrano JR, Pla B. Transient particle emission measurement with optical techniques. Measurement Science and Technology 2008; 19(6): 065404.
4. Bianchi GM, Falfari S, Parotto M, Osbat G. Advanced modeling of common rail injector dynamics and comparison with experiments. SAE paper 2003–01–0006.
5. Buwal, infras AG. Luftschadstoffemissionen des Strassenverkehrs 1950–2010. BUWAL–Bericht Nr. 255, 1995.
6. Chłopek Z, Biedrzycki J, Lasocki J, Wójcik P. Investigation of the motion of motor vehicles in Polish conditions. The Archives of Automotive Engineering – Archiwum Motoryzacji 2013; 60(2): 3–20.
7. Chłopek Z, Biedrzycki J, Lasocki J, Wójcik P. Sprawozdanie z pracy N N509 556440 „Wrażliwość emisji zanieczyszczeń i zużycia paliwa na warunki użytkowania trakcyjnego silnika o zapłonie iskrowym. Warszawa, 2013. (Praca nie publikowana).
8. Chłopek Z. Modelowanie procesów emisji spalin w warunkach eksploatacji trakcyjnej silników spalinowych. Prace Naukowe. Seria „Mechanika" z. 173. Warszawa: Oficyna Wydawnicza Politechniki Warszawskiej, 1999.

9. Chłopek Z, Piaseczny L. Remarks about the modelling in science researches. Eksploatacja i Niezawodnosc – Maintenance and Reliability 2001; 11(4): 47–57.
10. Chłopek Z. Some remarks on engine testing in dynamic states. Silniki Spalinowe – Combustion Engines 2010; 143(4): 60–72.
11. Daw CS, Kennel MB, Finney CEA, Connolly F T. Observing and modeling nonlinear dynamics in an internal combustion engine. Physical Review E 1998; 57(3): 2811–2819.
12. Guzzella L, Onder Ch. Introduction to modeling and control of internal combustion engine systems. Springer Verlag. 2nd ed., 2010.
13. Kniaziewicz T, Piaseczny L, Zadrąg R. Toksyczność spalin okrętowego silnika spalinowego podczas jego rozruchu. Zeszyty Naukowe Akademii Marynarki Wojennej 1999; 2: 51–63.
14. Ma H, Xu HM, Wang JH. Real-time control oriented HCCI engine cycle-to-cycle dynamic modelling. International Journal of Automation and Computing 2011; 8(3): 317–325.
15. Merkisz J, Lijewski P, Fuć P, Weymann S. Exhaust emission tests from non-road vehicles conducted with the use of PEMS analyzers. Eksploatacja i Niezawodnosc – Maintenance and Reliability 2013; 15(4): 364–368.
16. Merkisz J, Gis W. Exhaust emission from vehicles under real conditions. Proceedings of the Ninth Asia–Pacific International Symposium on Combustion and Energy Utilization. APISCEU. Beijing, 2008.
17. Piltan F, Sulaiman N, Talooki I A, Ferdosali P. Control of IC engine: design a novel MIMO fuzzy backstepping adaptive based fuzzy estimator variable structure control. International Journal of Robotics and Automation 2011; 2(5): 360–380.
18. Quintero HF, Romero CA, Vanegas Useche LV. Thermodynamic and dynamic analysis of an internal combustion engine with a noncircular-gear based modified crank-slider mechanism. 12th IFToMM World Congress, Besançon (France), June18–21, 2007: 1–6.
19. Romaniszyn K, Nowak A. Analiza wpływu parametrów ruchu pojazdu na zużycie paliwa i emisję zanieczyszczeń przy przejeździe przez Bielsko-Białą. Zeszyty Naukowe OBRSM BOSMAL 2004; 23(1): 43–49.
20. Savitzky A, Golay M J E. Smoothing and differentiation of data by simplified least squares procedures. Analytical Chemistry 1964; 36: 1627–1639.
21. Wang J, Storey J, Domingo N, Huff S, Thomas J, West B. Studies of diesel engine particle emissions during transient operations using an engine exhaust particle size. Aerosol Science and Technology 2006; 40(11): 1002–1015.
22. Wang Z-s, Liu D-g, Xu Ch-s. The dynamic modelling and simulation for air supplying mechanism of internal combustion engine based on Bond graph. Intelligent System Design and Engineering Application 2010;. 2: 647–650.
23. Wendeker M, Godula A. Research on variability in control parameters for spark ignition engines in real-life operation. Eksploatacja i Niezawodnosc – Maintenance and Reliability 2002; 16(4): 12–23.
24. Whitelaw JHW, Payri F, Desantes J M. Thermo- and fluid-dynamic processes in diesel engines. Springer 2002.
25. Worldwide emission standards. Heavy duty & off-road vehicles. Delphi. Innovation for the real world. 2013/2014.
26. Worldwide emission standards. Passenger cars and light duty vehicles. Delphi. Innovation for the real Word. 2014/2015.

Zdzisław CHŁOPEK
Institute of Vehicles, Faculty of Automotive
and Construction Machinery Engineering
Warsaw University of Technology
ul. Narbutta 84, 02-524 Warszawa, Poland
E-mail: zchlopek@simr.pw.edu.pl

Jacek BIEDRZYCKI
Department of Environmental Protection and Natural Energy Use
Automotive Industry Institute
ul. Jagiellońska 55, 03-301 Warszawa, Poland
E-mail: j.biedrzycki@pimot.eu

Jakub LASOCKI
Institute of Vehicles, Faculty of Automotive
and Construction Machinery Engineering
Warsaw University of Technology
ul. Narbutta 84, 02-524 Warszawa, Poland
E-mail: j.lasocki@simr.pw.edu.pl

Piotr WÓJCIK
Department of Environmental Protection and Natural Energy Use
Automotive Industry Institute
ul. Jagiellońska 55, 03-301 Warszawa, Poland
E-mail: p.wojcik@pimot.eu

Article citation info:
MIKULSKI M, WIERZBICKI S, PIĘTAK A. Zero-dimensional 2-phase combustion model in a dual-fuel compression ignition engine fed with gaseous fuel and a divided diesel fuel charge. Eksploatacja i Niezawodnosc – Maintenance and Reliability 2015; 17 (1): 42–48.

Maciej MIKULSKI
Sławomir WIERZBICKI
Andrzej PIĘTAK

ZERO-DIMENSIONAL 2-PHASE COMBUSTION MODEL IN A DUAL-FUEL COMPRESSION IGNITION ENGINE FED WITH GASEOUS FUEL AND A DIVIDED DIESEL FUEL CHARGE

ZERO-WYMIAROWY 2-FAZOWY MODEL SPALANIA W DWUPALIWOWYM SILNIKU O ZAPŁONIE SAMOCZYNNYM ZASILANYM PALIWEM GAZOWYM I DZIELONĄ DAWKĄ OLEJU NAPĘDOWEGO*

The problem of using alternative fueling sources for combustion engines has been growing in importance recently. This is connected not only with the dwindling oil resources, but also with the growing concern for the natural environment and the fight against global warming. This paper proposes the concept for a zero-dimensional model of a multi-fuel engine, enabling the determination of thermodynamic system parameters based on the basic geometric and material object data (complete model). The basic problems in the creation of this model and the modeling of the accompanying subprocesses have been outlined and the methodology of the numerical solution of the obtained mathematical description has been proposed. The basic characteristics of the developed model are: the application of an original model of liquid fraction injection based on normal distribution, a new Assanis correlation for computing the diesel fuel self-ignition delay period in the presence of gas, first-order chemical reaction kinetic equations for describing the course of combustion for combustible components of the gas/air mixture, the implementation of a self-consistency procedure in modeling heat exchange and the effect of exhaust recirculation, the inclusion of both a single liquid fuel injection and the possibility of performing computations for a divided charge.

Keywords: *dual-fuel engine, engine combustion process, mathematical model, computer simulation, heat exchange*

W ostatnim czasie problem wykorzystania alternatywnych źródeł zasilania silników spalinowych zyskuje szczególnie na znaczeniu. Związane jest to nie tylko z kurczącymi się zasobami ropy naftowej, ale również z coraz większą troską o środowisko naturalne oraz walką z globalnym ociepleniem. W niniejszej pracy zaproponowano koncepcję zero-wymiarowego modelu silnika wielopaliwowego, umożliwiającego, wyznaczenie parametrów termodynamicznych układu w oparciu o podstawowe dane geometryczne i materiałowe obiektu (model kompletny). Nakreślono podstawowe problemy w zagadnieniu tworzenia takiego modelu i modelowania podprocesów towarzyszących oraz zaproponowano metodykę numerycznego rozwiązywania uzyskanego opisu matematycznego. Podstawowe wyróżniki opracowanego modelu to: zastosowanie autorskiego modelu procesu wtrysku frakcji ciekłej opartego na rozkładzie normalnym, nowej korelacji Assanisa do obliczenia okresu zwłoki samozapłonu oleju napędowego w obecności gazu, jednostopniowych równań kinetyki reakcji chemicznej do opisu przebiegu spalania składników palnych mieszaniny gaz-powietrze, implementacja procedury samouzgodnienia w modelowaniu procesu wymiany ciepła i wpływu recyrkulacji spalin, uwzględnienie zarówno pojedynczego wtrysku paliwa ciekłego jak i możliwość prowadzenia obliczeń dla dawki dzielonej.

Słowa kluczowe: *silnik dwupaliwowy, proces spalania w silniku, model matematyczny, symulacja komputerowa, wymiana ciepła.*

1. Introduction

The current research on compression ignition combustion engines is primarily oriented towards the use of alternative renewable fuels, reduction of toxic air emissions and the development of new engine diagnostic methods [5, 6, 15]. One of the increasingly often-addressed problems in engine research is the possibility of dual-fueling engines with the main fuel charge fed as a gaseous fuel.

An increased interest in dual-fuel compression ignition engines in recent years has contributed to the development of both experimental and model testing on this fueling method.

One of the first valuable models simulating the combustion process in the full cycle of a dual-fuel engine was proposed by Raine in 1990 [24]. The operation of this model was limited only to the computation of the system's efficiency parameters.

Mansour et al. [14] proposed a simple, zero-dimensional model of combustion in a CNG-fueled engine with a pilot diesel fuel charge. Heat exchange with the chamber walls in this model was limited to convection and a number of other simplifying assumptions were adopted. The authors used a Wiebe function to describe energy release during diesel fuel and natural gas combustion in the first program

(*) Tekst artykułu w polskiej wersji językowej dostępny w elektronicznym wydaniu kwartalnika na stronie ***www.ein.org.pl***

step. The calculated pressure and temperature values were used as the input data for detailed kinetic computations, for which the commercial CHEMKIN package was used. The integration of complex combustion mechanisms with processes occurring in the dual-fuel engine, with the adopted simplifications, seems justified only in detailed research on exhaust toxicity, for which this model was used. In the assessment of efficiency and the power attained by the engine, the adopted simplifications in the description of individual subprocesses do not justify the need to apply very accurate combustion models, which require the use of dedicated computational environments.

Abd Alla [2] presented a model of pure methane combustion in a dual-fuel engine, calling it quasi-two zone. Leaving the nomenclature aside, the main distinguishing feature of this model was the application of detailed reaction kinetics for the description of gaseous phase combustion. A scheme of 178 elementary reactions, in which 41 chemical species participated, was used in this model, a Wiebe function was used to describe liquid phase combustion. The model description included the compression phase through combustion until the outlet valve opening. A detailed submodel of exhaust component formation was added to the basic thermochemical model. The basic advantage of this approach was the creation of connections between the progress of combustion and time and thermodynamic load parameters. This model showed quite good agreement with the experiment and a high predictive capacity over a wide range of engine operating conditions.

Stelmasiak [25] proposed a relatively simple and complete approach to the problem of modeling dual-fuel systems. The zero-dimensional model assumed the separate combustion of two phases – liquid and gaseous. It is assumed in this model that the start of combustion is the same for both fuels and is determined by the ignition delay period. The combustion end angles for diesel fuel and CNG were different and set by the modeler. The heat release rate and the concentrations of the homogeneous gas/DF/air mixture components were imposed by a Wiebe function, separately for gas and diesel fuel. The empirical formula of Prakash [23] was used to predict diesel fuel ignition lag, taking into account the presence of natural gas in the cylinder.

Papagiannakis et al. used a gradually-improved model of a dual-fuel engine burning natural gas and diesel fuel in a number of their papers [9, 10, 11, 17, 18]. The authors used the fundamental laws of conservation of mass, energy and momentum for combustion process simulation. They proposed a two-zone description of the load in the cylinder space with division into the unburnt load zone and the exhaust zone. The fuel combustion front was described as a cone surface propagating from the point of injection. The propagation occurs in the direction normal to each cone surface with the speed defined by the jet model of Hiroyasu et al. [8]. The energy released during combustion depends, according to the authors, only on the propagation speed of the front, behind which the homogeneous product zone immediately changes into the homogeneous exhaust zone. The effect of gas composition on the combustion process is neglected in this approach and the combustion rate is correlated with experimental data. The model was verified for a single-cylinder CI engine – Lister LV1 modified for dual-fuel operation. Good agreement with measurement results was demonstrated and the model was successfully used for testing the effect of the initiating charge size on engine operation parameters [19]. The basic model limitations result from its operating range. The simulation starts at the combustion start point, which must be given as an input parameter; similarly, the mean cylinder temperature and pressure during the cycle must be calculated from experimental data.

Perini et al. [21] developed a two-phase, quasi-dimensional model of a SI engine operating on LPG admixed with hydrogen and Ma et al. [13] proposed a mathematical simulation of a hydrogen engine. A dual-fuel engine operating on LPG with a hydrogen admixture was modeled using equilibrium reactions by Lata and Ashok Misra [12]. Wang [26] proposed a similar model for CNG and hydrogen mixtures based on a CFD code and chemical reaction kinetics.

Agarwal and Assanis [1] proposed a complex, multi-dimensional model of natural gas combustion under conditions typical for compression ignition engines. The model used detailed chemical reaction kinetics.

The problem of the mathematical modeling of dual-fuel systems is still innovative. Complete models are still lacking which, including all processes occurring in the cylinder, are able to predict with sufficient accuracy changes in thermodynamic working medium parameters, using only the basic object data available from its technical documentation. Among the available models, an even lower number has undergone full experimental verification, which limits their reliability. Moreover, there is a lack of research results on the effect of gas composition on the course of combustion in a dual-fuel engine. A properly constructed and verified model can significantly contribute to the filling of these deficiencies.

2. Assumptions of the model of combustion in a dual-fuel CI engine

In dual-fuel engines, a full description of the combustion process is much more difficult compared to single fuel engines. The cylinder contains gaseous fuel mixed with air, into which liquid fuel is injected near TDC. Extremely different mechanisms dominate in the combustion of these two fractions, both of a physical (mass and energy transport processes) and chemical nature, resulting from the kinetics of fuel reaction with oxygen. All processes must therefore be analyzed, taking into account not only their effect on the gaseous and liquid fuel combustion rate, but also in regard to the proportions of individual-fuels.

On the other hand, the liquid and gaseous phases are combusted at the same time, in the same space and the presence of one fraction affects the combustion of the other. The mechanisms of this influence are not yet well-known.

The examination of all these elements allowed the model assumptions to be formulated, bearing in mind both the accuracy of its results and the complexity level, affecting the autonomy (the amount of necessary experimental data) and the computational speed.

Analyzing natural gas combustion in the engine, the following assumptions were made, which characterize the postulated model. It is assumed that a homogeneous gas/air mixture is in the cylinder during compression and temperature and pressure distribution at each point of the cylinder space is constant. This assumption leads to a zero-dimensional model. At the same time, the working medium is treated at each moment as a mixture of semi-ideal gases, mixed in any proportions. The specific heat of the mixture at each computational point is the sum of functions approximating data from thermodynamic tables for each component [4]. The approximating polynomials are functions of temperature. The changes occurring in the modeled space are treated as quasi-static. In the developed model, heat exchange with the cylinder walls was based on convection between gas and the surface of the given component and a zero wall temperature gradient was adopted, assuming that it was constant. The heat removed from the system is the sum of three fluxes passing through the surface of the piston head, the cylinder head and the time-variable cylinder wall surface. Increased heat exchange as a result of flame radiation was additionally taken into account in the combustion process.

The developed model takes into account the effect of the mass of the injected pilot charge on the thermodynamic state of the system, through a simplified fuel injection submodel based on normal distribution. This original approach allows the model to operate independently of the detailed experimental data on the course of the pressure drop and the injector needle lift for the tested object. It is assumed in the built model that combustion starts at the moment of diesel fuel ignition, which initiates the gas mixture ignition. The two fuels are combusted separately and the emitted heat is the sum of heat released in the combustion of both fuels. The course of diesel fuel combustion is described by empirical equations for the ignition delay period and process rate – as represented by a Wiebe function. This is a simplified approach, but justified for dual-fuel engines because of the small pilot charge size.

Basic research on combustion processes proves that methane combustion is a very complex process and consists altogether of a system of 132 chemical reactions, whose rates are interrelated by the concentration of individual reactants. The implementation of such a complex model in a complete dual-fuel engine working cycle is unjustified due to the applied simplifications in the description of the other subprocesses (heat exchange, fuel injection etc.). A satisfactory representation of the combustion process can be obtained using even one methane combustion macroreaction [20]. In the proposed model, a system of three interrelated global reactions, including the combustion of the most important combustible components used to fuel gas engines, was implemented for the description of gaseous phase combustion.

It is assumed that the developed model with the adopted assumptions will enable precise examination of the effect of gas composition on the character of combustion in a dual-fuel engine.

3. Basic equations of the developed model of fuel combustion in a dual-fuel engine

According to the discussed assumptions, the cylinder load is a homogeneous mixture of air, natural gas, diesel fuel and exhaust at each moment of time. The proportions of individual components change with the stages of the injection and combustion of combustible components. With such assumptions, starting from the energy conservation law, the basic equations of the model can be introduced in a differential form:

$$\begin{cases} \dfrac{dQ_{in}}{d\alpha} = \dfrac{dU}{d\alpha} + p\dfrac{dV}{d\alpha} + \dfrac{dQ_{out}}{d\alpha} - h_{ON}\cdot\dfrac{dM_{ON}}{d\alpha} \\ p\cdot V = n(\alpha)\bar{R}T \end{cases} \tag{1}$$

The first equation expresses the first law of thermodynamics in a differential form for an open system, where: dU – increase in the internal energy of the system, p, V – are the pressure and volume of the working medium in the cylinder, respectively, Q_{out} represents the heat exchanged with the cylinder walls, Q_{in} – the heat fed to the system, h_{ON} – is diesel fuel enthalpy and M_{ON} – the mass of injected fuel. The second equation of the system represents an equation of state, where: R is the universal gas constant, n – medium moles in the cylinder and T its temperature. All the quantities in the system (1) are functions of the crank angle.

Heat exchange with the walls was included in the developed model as the sum of three fluxes passing through the cylinder wall and head and the piston head. Because the main part of heat is removed in CI engines as a result of convection between gas in the working space and the given surface, it can be written:

$$\frac{dQ_{out}}{d\alpha} = \frac{1}{\omega}\cdot h_c(T,p,V)\cdot\left[A_g\cdot(T-\bar{T}_g)+A_t\cdot(T-\bar{T}_t)+A_s(\alpha)\cdot(T-\bar{T}_s)\right] \tag{2}$$

A simplified model of heat exchange in a combustion chamber wall and on the side of the coolant is included in equation (2) by expressions for the mean value of cylinder piston (t), head (g) and wall (s) temperatures:

$$\bar{T}_{gts} = \frac{\bar{h}_c\bar{T} + k_{gts}T_{ch}}{\bar{h}_c + k_{gts}} \tag{3}$$

These temperatures were computed as the weighted mean from the mean temperature $\bar{T}$ of the medium in the chamber with the mean heat transfer coefficient $\overline{h_c}$ and coolant temperature T_{ch} with the coefficient of heat transmission through the respective wall $k_{g,\,t,\,s}$:

$$k_{gts} = \frac{1}{\dfrac{1}{h_{ch}} - \dfrac{\delta_{gts}}{\lambda_{gts}}}\int_{\alpha_A}^{\alpha_E} h_c d\alpha \tag{4}$$

where: λ_{gts} – heat transfer coefficient of the wall material, δ_{gts} – wall thickness.

Heat transfer occurs under a number of conditions – variable cylinder gas pressure and temperature and with locally variable rates of medium flow in the cylinder. These conditions are taken into account in the model by adopting an appropriate heat exchange coefficient h_c. Washini's formula was used for this purpose, in the form modified by Hohenberg [9]:

$$h_c = 130\cdot\frac{\left(p\cdot 10^5\right)^{0,8}}{V^{0,06}T^{0,4}}\cdot(C_{\acute{s}r}+1,40) \tag{5}$$

where: $C_{\acute{s}r}$ – mean piston speed.

The thermodynamic medium parameters change during liquid fuel injection into the engine's combustion chamber. The effect of the fuel mass flux supplied to the cylinder must therefore be taken into account. In direct ignition engines, temperature change as a result of stream evaporation can be neglected, because of a low ratio of the injected fuel volume to the working medium volume. This assumption is all the more justified for dual-fuel engines with diesel fuel charges of up to fifteen percent of the main charge. Another paper by the authors [16] discusses using complex hydraulic models to describe the diesel fuel mass flux in zero-dimensional models. It was demonstrated that a simple, complete model based on normal distribution with normalization to the total fuel charge could be used in this case without an observable loss of accuracy:

$$\dot{M}_{ON}(\alpha) = \begin{cases} 0 & \alpha_{pw} > \alpha < \alpha_{kw} \\ \dfrac{hB_{ON}}{\sqrt{\pi}}e^{-h^2(\alpha-\alpha_{\max})} & \alpha_{pw} < \alpha < \alpha_{kw} \\ 10^{-3}B_{ON} & \alpha_{pw} = \alpha = \alpha_{kw} \end{cases} \tag{6}$$

In a dual-fuel engine, the air/gas mixture ignites from the energy released from the combustion of the pilot diesel fuel charge. Test results show that even for a pilot charge lower than 1% of the total energy, the ignition energy can be by around 35 J higher in a dual-fuel engine than the electric pulse energy in a spark engine [25]. It can thus be assumed that in a dual-fuel engine the start of the combustion of both fractions (liquid and gas) is the same and the problem of ignition moment determination comes down to the accurate modeling of pilot charge ignition lag. This process, however, takes place under conditions significantly different from those in a classical compression ignition engine. Increasing the concentration of combustible gases in the cylinder causes, in most cases, a longer diesel fuel self-ignition delay. In an earlier paper [22], the authors examined the possibility of using ignition delay correlations verified for traditional CI engines. The equation proposed by Assanis [3] was used in the developed model to determine self-ignition lag:

$$\tau_{id} = 2,4\varphi^{-0,2} p^{-1,02} \exp\left(\frac{E_a}{\bar{R}T}\right) \tag{7}$$

It was demonstrated in the paper [22] that this correlation, taking into account cylinder load composition, describes self-ignition delay in dual-fuel engines better than others.

Diesel fuel combustion was represented in the developed model with a Wiebe function [7]. This allows the effect of the course of diesel fuel combustion on gaseous fraction combustion to be tested; however, this requires prior model validation for single fueling.

The natural gas combustion model was based on first-order oxidation macroreactions for the main combustible mixture components: methane (CH_4), ethane (C_2H_6) and propane (C_3H_8). This leads to a system of three global reactions of the form:

$$C_nH_{2n+2} + \left(\frac{5}{4}n + \frac{1}{2}\right)O_2 \rightarrow nCO_2 + (n+1)H_2O \tag{8}$$

for n = 1...3. The expression for the global reaction rate in this case will assume the form:

$$\frac{d[C_nH_{2n+2}]}{dt} = A_n \exp\left(-\frac{E_{a_n}}{\bar{R}T}\right) \cdot [C_nH_{2n+2}]^{a_n} [O_2]^{b_n} \tag{9}$$

The constant values present in equation (9), for individual gases, were collected in Table 1.

Table 1. Values of the constants included in equation (9). Activation energy Ea (kcal/mol).

No	Fuel	A	E_a	a	b
1	CH_4	$8{,}3\cdot10^6$	30	-0,3	1,3
2	C_2H_6	$1{,}1\cdot10^{12}$	30	0,1	1,65
3	C_3H_8	$8{,}6\cdot10^{11}$	30	0,1	1,65

The solution of each equation of the system (9) fully determines the course of heat release in the gas combustion process at any moment.

4. Methodology of the model's numerical computations

The developed mathematical model was implemented in the MathWorks MATLAB environment. The basis for creating the software program was the assumption of its modular structure. Individual submodels (e.g. of heat exchange, fuel injection, ignition delay, heat release during combustion, change in medium moles etc.) were treated as separate functional m-files called by the main program built around the basic system of differential equations for state variables (1). This approach guarantees program clarity, which facilitates its verification and optimization. The modular structure ensures, moreover, project expandability, by easy exchange of individual submodels with others – more detailed – when these are available.

The operation of the program starts with the entry of the basic input data into the global memory, i.e. engine geometry, engine material data (necessary for heat exchange computations), engine operating parameters etc. The thermodynamic load parameters (λ_o, T_o, p_o) at the start of compression are then computed, from which the computation of cylinder temperature and pressure during the entire cycle starts.

The computational cycle of the main program was divided into 3 main processes: compression, combustion and expansion. The system of equations (1) for compression can be reduced to a single, nonlinear first-order differential equation for cylinder medium temperature as a function of the crank angle. Developing the expression for the internal energy of the system and heat exchanged with the walls (2), we obtain in this case:

$$\sum n_i C_{vi} \frac{dT}{d\alpha} + \bar{R}\frac{n(\alpha)}{V(\alpha)} \cdot \frac{dV(\alpha)}{d\alpha} \cdot T + \frac{1}{\omega} \cdot \left[(130 \cdot 10^4) \frac{\bar{R}^{0,8} \cdot n^{0,8}}{V^{0,86}} \cdot (C_{fr} + 1{,}40)\right] \cdot \\ \cdot T^{0,4} \cdot [A_g \cdot (T - \bar{T}_g) + A_T \cdot (T - \bar{T}_t) + A_c(\alpha) \cdot (T - \bar{T}_c)] = 0 \tag{10}$$

Due to the complexity level of the above equation, using the dedicated MATLAB package functions for solving differential equations was dropped in favor of a solution by the iterative method. The temperature derivative can be expressed, based on its definition, as the difference quotient limit:

$$\frac{dT}{d\alpha} = \lim_{\Delta\alpha \to 0} \frac{T(\alpha + \Delta\alpha) - T(\alpha)}{\Delta\alpha} \tag{11}$$

In the numerical solution approximation, the quantity $\Delta\alpha \rightarrow 0$ can be replaced with a finite value, obtaining instead of the differential equation (10) the corresponding difference equation, in which the successive temperature values are calculated based on the values computed in the previous step. The accuracy of the computations will be higher, the lower the value of the computational step is. The parameters for the next angle $\alpha_A + \Delta\alpha$ are calculated this way starting from the values T_o, p_o, corresponding to the crank angle α_A falling on the inlet valve closure. The other quantities in the equation (10) are calculated by complementary subprograms: the moles of individual components $n_i(\alpha)$ and the total load moles $n(\alpha)$ from the solution of the kinetics equations (9). The volume $V(\alpha)$ is calculated from rod-crank system geometry etc.

The procedure continues until the angle for which liquid fuel pumping starts is reached. Starting from this point, the pilot charge injection submodel (6) is included. For the same point, the ignition angle α_p is computed based on the calculated temperature and pressure values, according to the adopted model (7). The compression procedure continues until the calculated α_p value is reached, starting from which combustion starts. In this loop, computations are performed analogously as for compression including the heat flux released during combustion, with variable instantaneous values of load moles depending on the rotation angle. The combustion end angle is defined by the moment when combustible components burn out.

Expansion proceeds according to an analogous equation as for compression with the moles of individual components determined at the combustion end point. The parameters for expansion are calculated until the angle corresponding to the outlet valve opening is reached, which ends the model operation.

It should be noted that the heat exchange equation used in the model (2) requires the mean temperature and the mean heat exchange coefficient for the cylinder load over the entire cycle for the computation of cylinder wall, head and piston head temperatures (3). It is obvious that these values are not known until the instantaneous values of these parameters are calculated. In the simplest approximation, the above mean values can be set as model operation parameters, based on the modeler's experience or the results of experimental tests on the given engine. The first solution causes high uncertainties of computation results and the second leads to considerable limitation of model autonomy. These problems were solved by running the discussed main program (Fig. 1) in a loop leading to the autocorrelation of the results. The main program is called by an external m-file with set initial values of the mean temperature T_{sr} = 600 K and the heat exchange coefficient h_{csr} = 800 W/m^2. After computations are performed by the main program (cylinder pressure and temperature changes), new mean values are calculated and the results are recalculated in the next loop. The procedure is repeated until the results become self-consistent, i.e. until the moment when the difference between the mean values from the two latest loops does not exceed the set threshold. This approach considerably lengthens computations, but ensures the required autonomy without loss of accuracy. Preliminary calculations showed that with set initial parameters, running the main program 3–4 times is sufficient for the difference not to exceed the value of 1 (K and W/m^2, respectively) for both quantities.

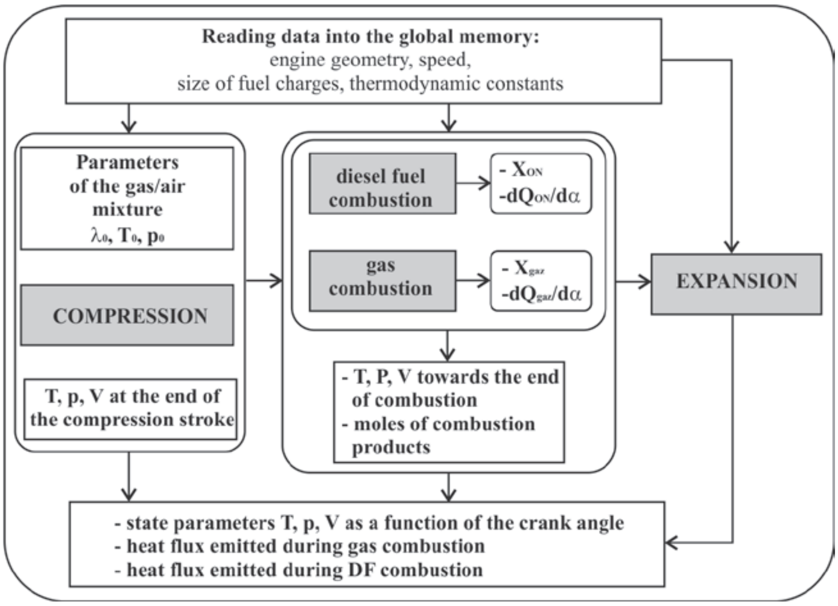

Fig. 1. Computational structure of the main program (excluding submodels)

The exhaust residue percentage in the load sucked into the cylinder is determined similarly. In the first computational step, the exhaust residue percentage is not included because the moles of individual exhaust components have not yet been calculated by the model. The calculations from the first loop are included in the next loop. The procedure of updating the computation results for the moles is repeated until the model self-consistency procedure ends.

5. Simulation capacity of the developed model

The presented model was subjected to the procedure of experimental verification by comparing the calculated pressure changes with the results of indicator tests on a dual-fueled ADCR engine. The verification tests of the model were conducted on the tested engine both for a single diesel fuel charge and for a divided charge (pilot and main charge injection). Good agreement of the computation results was obtained during model verification (Table 2). Example pressure changes recorded in the engine's combustion chamber and the changes obtained from the developed model are shown in Fig. 2.

Detailed discussion of the methodology and broader results of the verification tests will be presented in further papers by the authors.

The developed model in its present specification can be used as a research tool in two main ranges, i.e. autonomous operation and semi-autonomous operation, in the analysis of experimental changes.

In the autonomous operation range, only the basic technical data of the tested engine and the parameters characterizing the working point are used as the input data. Each input parameter can be used as an independent variable, which enables the simulation of different real processes. Moreover, it is possible in the model to insert the calculation of some parameters and their introduction into the computational program as an independent variable, e.g. the ignition delay angle. With such model applicability, the effect on the course of combustion in a dual-fuel engine can be tested for such parameters as:

- engine geometry;
- injection start angle (of both a single and a dual charge);
- temperature of the medium sucked into the cylinder;
- consumption (of air, liquid fuel, gas);
- ignition delay angle;
- gaseous fuel composition;
- diesel fuel combustion time.

In the semi-autonomous operation mode, the model can be successfully used for the analysis of real changes obtained during the performed experiments. For example, cylinder pressure changes do not have to be calculated by the model, they can be introduced there from an external file. In this case, the model can calculate all the other thermodynamic load parameters for the real cycle.

The proposed model, regardless of the mode of operation, based on available data without additional experimental tests on the data, enables the calculation of thermodynamic cylinder load parameters as a function of the crank angle (Fig. 3). The basic changes generated by the computational program are:

- cylinder pressure changes;
- cylinder temperature changes;
- cylinder volume changes;
- changes in the (total) heat flux removed through the surface of the cylinder, piston head, cylinder head, changes in DF, CH_4, C_2H_6, C_3H_8 combustion;

Table 2. Range of conditions for which the model was verified and a synthetic summary of verification results

Engine operation type	verification parameters				maximum error		
	n	M_{ob}	P_{max}	U_{on}	instantaneous		in cycle
	RPM	Nm	bar	%	bar	%	%
compression and expansion	750 3400	0	27 42	0	1,1	5	6,6
DF operation non-divided charge	2300 3400	50 200	49 92	100	6,5	8	8,4
DF operation divided charge	1500	20-200	36-87	100	3,7	6	6,8
DF+CNG operation non-divided charge	3400	50-200	35-48	80	6,5	11	6,1
DF+CNG operation divided charge	1500	50 150	40 72	16 80	8	15	6,2

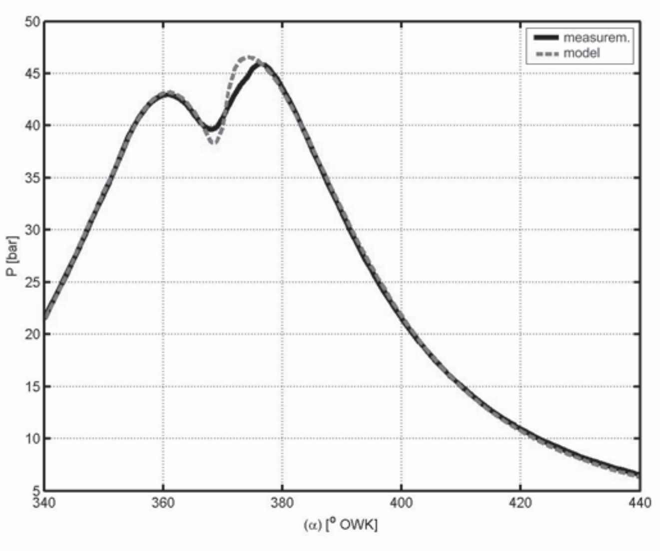

Fig. 2. Comparison of model computation results for dual-fuel operation with the mean recorded pressure changes in the combustion chamber for: n = 1500 (RPM), U_{on} = 70 (%) – divided charge

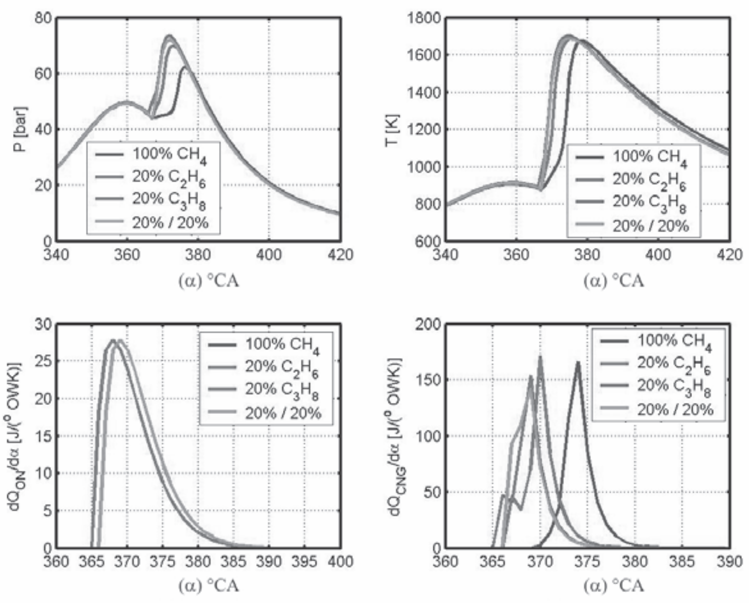

Fig. 3. Example results of simulation computations using the model, for different methane contents relative to combustible gas admixtures and a constant diesel fuel percentage U_{on} = 30%

The model uses around fifteen submodels to determine these relationships, which compute a number of additional parameters in real time. The results of these partial computations can also be used in the testing procedure in inference. The most important additional parameters computed by the program include:

- excess air coefficients for the cylinder mixture (λ_{ON}, λ_{CNG}, λ_A);
- ignition delay angle (and combustion start angle);
- mean temperatures (of the load, cylinder, piston head, cylinder head);
- specific heat changes (for CO_2, CO, N, O_2, H_2, H_2O, CH_4, C_2H_6, C_3H_8);
- changes in the moles in the cylinder (for CO_2, O_2, H_2O, CH_4, C_2H_6, C_3H_8, DF) – under the adopted combustion model.

Different parameters and synthetic characteristics can be calculated based on the generated changes, including:

- *P*/*V* characteristics;
- phase portrait of the engine;
- mean indicated pressure;
- indicated power and thermal efficiency of the engine.

6. Summary

The developed zero-dimensional simulation model of the working cycle of a dual-fuel engine fed with gaseous fuel with an initiating diesel fuel charge includes the compression, combustion and expansion phases. The main characteristics of the proposed model are:

- application of an original approach to modeling liquid fuel injection, based on normal distribution;
- application of a new Assanis correlation for describing diesel fuel self-ignition delay in the presence of gas;
- application of chemical reaction kinetics equations for describing the course of combustion for combustible components of the gas/air mixture in the zero-dimensional dual-fuel engine model;
- implementation of a self-consistency procedure in modeling heat exchange and the effect of exhaust recirculation, which allows a high degree of model completeness to be maintained;
- inclusion of both a single liquid fuel injection and the possibility of performing computations for a divided charge.

The basic advantages of this model include:

- a high degree of completeness, which permits autonomous computational program operation, using only the basic technical data of the tested engine;
- a wide spectrum of model applicability;
- relatively fast computational time, which enables model use on standard PC computers;
- a modular structure, ensuring easy modification and expandability of the model. The model can be developed by adding new submodels or changing the existing ones when more accurate correlations are available, without the need to change the main program;
- the model was subjected to thorough verification in several stages, which ensures its high reliability.

Acknowledgment: *This paper was partially financed by research grant No N N509 573039, given by Polish National Science Centre.*

References

1. Agarwal A, Assanis DN. Multidimensional modeling of natural gas ignition under compression ignition conditions using detailed chemistry. SAE Technical Paper 1998; 980136.
2. Alla GH, Soliman HA, Badr OA, Rabbo FM. Combustion Quasi-zone predictive model for dual fuel engines. Energy Conversion and Management 2001; 42: 1477-1498.
3. Assanis N, Filipi ZS, Fiveland SB, Syrimis M. A predictive ignition delay correlation under steady-state and transient operation of a direct injection diesel engine. Journal of Engineering for Gas Turbines and Power 2005; 125(2): 450-457.
4. Chase M W. NIST–JANAF thermochemical tables. Geithersburg: National Institute of Standards and Technology, 1998.

5. Czech P, Wojnar G, Burdzik R, Konieczny Ł, Warczek J. Application of the discrete wavelet transform and probabilistic neural networks in IC engine fault diagnostics. Journal of Vibroengineering 2014; 16(4): 1619 1639.
6. Ghazikhani M, Feyz ME, Mahian O, Sabazadeh A. Effects of altitude on the soot emission and fuel consumption of a light-duty diesel engine. Transport 2013; 28(2): 130-139.
7. Heywood JB. Internal combustion engines fundamentals. Singapore: McGraw-Hill International, 1988.
8. Hiroyasu H, Kadota T, Arai M. Development and use of a spray combustion model to predict diesel engine efficiency and pollutant emission. Bulletin of the JSME 1983; 26(24): 569-575.
9. Hohenberg GF. Advanced approaches for heat transfer calculations. SAE Technical Paper 1979; 790825.
10. Hountalas DT, Papagiannakis RG. Development of a simulation model for direct injection dual fuel diesel–natural gas engines. SAE Technical Paper 2000; 2000-01-0286.
11. Hountalas DT, Papagiannakis RG. A simulation model for the combustion process of natural gas engines with pilot diesel fuel as an ignition source. SAE Technical Paper 2001; 2001-01-1245.
12. Lata DB, Misra A. Theoretical and experimental investigations on the performance of dual fuel diesel engine with hydrogen and LPG as secondary fuel. International Journal of Hydrogen Energy 2010; 35: 11918-11931.
13. Ma J, Su Y, Zhou Y, Zhang Z. Simulation and prediction on the performance of a vehicle's hydrogen engine. International Journal of Hydrogen Energy 2003; 28: 77-83.
14. Mansour C, Bounif A, Aris A, Gaillard F. Gas–Diesel (dual-fuel) modeling in diesel engine environment. International Journal of Thermal Sciences 2001; 40: 409-424.
15. Makarevičienė V, Matijošius J, Pukalskas S, Vėgneris R, Kazanceva I, Kazancev K: The exploitation and environmental characteristics of diesel fuel containing rapeseed butyl esters. Transport 2013; 28(2): 158-165.
16. Mikulski M. The problems of multi-fuel engines modeling in the context of systems operational parameters estimation – Part I - fuel injection. Zeszyty Naukowe Instytutu Pojazdów 2011; 5(86): 113-124.
17. Papagiannakis RG, Hountalas DT. Theoretical and experimental investigation of a direct injection dual fuel diesel–natural gas engine. SAE Technical Paper 2002; 2002-01-0868.
18. Papagiannakis R G, Hountalas D T, Kotsiopoulos P N. Experimental and theoretical analysis of the combustion and pollutants formation mechanisms in dual fuel DI diesel engines. SAE Technical Paper 2005; 2005-01-1726.
19. Papagiannakis RG, Hountalas DT, Rakopoulos CD. Theoretical study of the effects of pilot fuel quantity and its injection timing on the performance and emissions of a dual fuel diesel engine. Energy Conversion and Management 2007; 48: 2951–2961.
20. Pawlaczyk A, Gosiewski K. Estimation of kinetic parameters for the homogenous oxidation of lean methane – air mixtures based on experimental temperature profiles. Chemical and Process Engineering 2009; 30: 139–147.
21. Perini F, Paltrinieri F, Mattarelli EA. Quasi-dimensional combustion model for performance and emissions of SI engines running on hydrogen-methane blends. International Journal of Hydrogen Energy 2010; 35(10): 687-701.
22. Piętak A, Mikulski M. On the modeling of pilot dose ignition delay in a dual-fuel, self ignition engine. Silniki Spalinowe – Combustion Engines 2011; 3(146): 94-102.
23. Prakash G, Shaik AB, Remesh A. An approach for estimation of ignition delay in a dual fuel engine. SAE Technical Paper 1999; 1999-01-0232.
24. Raine RR. A performance model of the dual fuel (diesel/natural gas) engine. SAE Technical Paper 1990; 900387.
25. Stelmasiak Z. Studium procesu spalania w dwupaliwowym silniku o zapłonie samoczynnym zasilanym gazem ziemnym i olejem napędowym. Bielsko-Biała: Wydawnictwo ATH w Bielsku Białej, 2003.
26. Wang Y, Zhang X, Li C, Wu J. Experimental and modeling study of performance and emissions of SI engine fueled by natural gas-hydrogen mixtures. International Journal of Hydrogen Energy 2010; 35(7): 2680–2683.

Maciej MIKULSKI
Sławomir WIERZBICKI
Andrzej PIĘTAK
University of Warmia and Mazury in Olsztyn
Faculty of Technical Sciences
ul. Słoneczna 46A
10-710 Olsztyn, Poland

E-mails: maciej.mikulski@uwm.edu.pl, slawekw@uwm.edu.pl, apietak@uwm.edu.pl

Article citation info:
CZECHLOWSKI M, GOLIMOWSKI W, SĘK T, SZYMANOWICZ J. Exhaust opacity in a diesel engine powered with animal fats. Eksploatacja i Niezawodnosc – Maintenance and Reliability 2015; 17 (1): 49–53.

Mirosław CZECHLOWSKI
Wojciech GOLIMOWSKI
Tadeusz SĘK
Jacek SZYMANOWICZ

EXHAUST OPACITY IN A DIESEL ENGINE POWERED WITH ANIMAL FATS

ZADYMIENIE SPALIN SILNIKA Z ZAPŁONEM SAMOCZYNNYM ZASILANEGO TŁUSZCZAMI ZWIERZĘCYMI*

The diversification of sources of energy has been recognised as one of the actions preventing the negative effects of human activity on the environment. In order to do so it is necessary to solve the problems related with the replacement of fossil fuels with biofuels, including the increase in the prices of food products caused by the dynamic development of biofuels made from plants. Therefore, the aim of the study was to make an experiment assessing the technical possibilities to replace diesel fuel with rendered animal fats. As results from the initial study, the kinematic viscosity of animal fats at a temperature of 120°C is comparable to that of diesel at 40°C. Apart from that, the diesel engine powered with animal fats emitted 70% less particulates in exhaust than the engine powered with a diesel fuel.

Keywords: *biofuels, pig fat, kinematic viscosity, exhaust opacity.*

Dywersyfikację źródeł energii uznano za jedno z działań zapobiegających negatywnemu oddziaływaniu człowieka na środowisko. W tym celu konieczne jest rozwiązanie problemów związanych z zastępowaniem paliw kopalnych biopaliwami, m. in. wzrost cen produktów spożywczych, wywołany dynamicznym rozwojem biopaliw pochodzenia roślinnego. Dlatego za cel badań przyjęto wykonanie eksperymentu, polegającego na ocenie możliwości technicznych zastąpienia oleju napędowego wytopionymi tłuszczami zwierzęcymi. Z przeprowadzonych badań wstępnych wynika, że tłuszcze w temperaturze 120°C charakteryzują się lepkością kinematyczną porównywalną do oleju napędowego w 40°C, ponadto zasilany nimi silnik ZS emitował o 70% mniej cząstek stałych w spalinach w porównaniu do silnika zasilanego olejem napędowym.

Słowa klucze: *biopaliwa, tłuszcz wieprzowy, lepkość kinematyczna, zadymienie spalin.*

1. Introduction

All over the world transportation is dependent on a continuous supply of liquid and gas fuels. Due to the increasing nuisance of vehicles emitting toxic gases to the natural environment many scientific institutions make attempts to solve the problem. One of such solutions is the introduction of fuels substituting fossil fuels, which are generally known as biofuels. They are made from different types of biomass by means of different technologies and they are processed into formed fuels.

Liquid fuels made from vegetable oils are a type of biofuels which stand the greatest chance for development in economy [13]. So far research results have proved that there are no technical barriers to the application of pure vegetable oil as a fuel for farming machinery [10, 22]. In 2006 Czechlowski et al. did not observe the negative influence of biofuels on the working parts of the injection pump in a farm tractor [7]. On the other hand, in 2001 Koniuszy noted that the penetration of biofuels into engine oil deteriorates the lubrication of the engine parts, which causes the need to change the oil in a diesel engine more frequently [16].

On the other hand, the use of biofuels made from vegetable oils is a serious social and economic problem. In 2012 Nonhebel stressed that the production of biofuels from biomass was a serious threat to food production [19]. In 2011 Mueller et al. published the results of research which prove that the prices of cereals were closely correlated with an increase in the supply of biofuels [18]. In 2013 Peri & Baldi proved a strong correlation of market prices between diesel and vegetable oil [21]. To sum up, we can say that an increase in the prices of diesel fuel strongly affects the prices of food and biomass, which biofuels are made from.

The replacement of diesel with biofuels made from plants is regarded as an environment-friendly action because the emission of CO_2 is reduced. As results from the study conducted by Dziemiszewski in 2009, as far as biofuels are concerned, the emission of CO_2 is much higher than from diesel if we consider the workload which is necessary to produce biofuels and the emission from their combustion in diesel engines [6]. This phenomenon is chiefly caused by considerable amount of work that goes into energy crops grown for specific purposes. In response to this information, in 2010 Pasyniuk stated that when diesel engines were powered with biofuels, the CO_2 balance was retained, because plants absorb the total amount of CO_2 emitted from engines powered with fuels made from plants [20]. It is also necessary to stress the fact that engines powered with biofuels emit much less toxic substances, i.e. carbon monoxide, hydrocarbons and particulates. In 2013 Shirneshan proved that these compounds were reduced by 30% when the share of biofuels reached 20% [24]. Also, in 2010 Kalam et al. found that as the share of biofuels in diesel increased, the emission of toxic compounds was considerably reduced [14]. However, in both cases the emission of nitrogen oxides increased. In 2010 Hossain & Davies proved that it was possible to reduce the emission of nitrogen oxides when diesel was partly replaced with sunflower oil

(*) Tekst artykułu w polskiej wersji językowej dostępny w elektronicznym wydaniu kwartalnika na stronie ***www.ein.org.pl***

[12]. In 2005 Senthil et al. made experiments in which they powered an engine with hot animal fats and they observed that as the temperature of that fuel increased, the emission of nitrogen oxides was limited [25]. These results point to the fact that it is justified to produce biofuels from biomass which does not come directly from plant production. This will certainly enable the limitation or even abandonment of energy crops grown for a specific purpose.

The production of biofuels from non-food fats and animal fats is an interesting solution worth consideration. In 2012 Roszkowski found that 2015–2017 was the realistic time of implementation of the technologies enabling the production of biofuels from fats derived from the secondary market in the EU [23]. As results from the research conducted so far, there are no technical barriers which would make it impossible to power older generation engines with fats of different origin. In 2012 Czaczyk et al. made an active experiment in which they investigated the energetic parameters of the engine of a farm tractor powered with post-frying fats [5]. In 2013 Wegner et al. published the results of investigations of the energetic parameters of an engine powered with a fuel containing from 15% to 50% of used soybean oil [27]. In recent years there have also been numerous studies on the parameters of operation of a diesel engine powered with animal fat esters [2, 3]. In comparison with conventional fuels the application of biofuels contributes to reduction of exhaust opacity and increases the emission of NO_x [1]. On the other hand, the use of rendered animal fats or fats in the form of emulsion with ethanol as a fuel considerably reduces both exhaust opacity and the emission of NO_x [15, 26].

The amount of raw materials, i.e. animal fats and oils from the secondary market is limited. In 2010 Marczak published the estimates concerning the amount of animal fats produced in Poland which could be used for the production of biofuels without the negative effect on the prices of food products. He found that by 2020 every year Poland would have produced about 60 thousand Mg of cow and pig fat which was not used as food, including fats from slaughterhouse waste [17]. In 2003 Ferenc & Pikoń estimated the production potential of waste fats in Poland. They found that in 2002 Poland produced a total of about 130 thousand Mg of such fats and in the following year - about 150 thousand Mg. In the authors' opinion the data are strongly understated, because there was considerable discrepancy between the results of questionnaire surveys and the data from periodical reports on waste [7].

The analysis of the state of knowledge presented above was the basis for initial research which was conducted to determine temperature-induced changes in the rheological properties of rendered animal fats and the possibilities to reduce the exhaust opacity in a diesel engine in consequence of using fat heated to a temperature above 80°C as a fuel.

2. Research methodology

The research was conducted in two stages. In the first stage the distribution of the kinematic viscosity of pig fat in the temperature function was measured. In the second stage the exhaust opacity of a diesel engine powered with pig fat at different temperatures was measured.

The assumption was that the kinematic viscosity of pig fat would be measured within the range of temperatures from 60°C to 160°C at 10°C intervals. Simultaneously, the researchers agreed that each measurement would be made three times and the arithmetic mean of the three measurements would be assumed as the result.

Viscosity was measured according to the standard PN-77/C-04014. As a result of the measurement, the kinematic viscosity was determined. The measurement of fat viscosity consisted in measuring the flow time of 200 cm^3 of the fat under study at a particular temperature and the flow time of the same volume of distilled water at a temperature of 20°C under the conditions specified in the standard (PN-77/C-04014). Next, the relative viscosities were calculated in Engler degrees °E and on the basis of the results the kinematic viscosity of the fat under study was read from tables attached to the standard. Before the measurements the constant k was calculated for the Engler viscometer used in the investigations. For that purpose the flow time of distilled water was measured at a temperature of 20°C. The arithmetic mean of the three measurements was assumed as the constant k of the device.

During the measurements the viscometer was filled with hot pig fat at a higher temperature than the assumed measurement temperature. Simultaneously, the liquid which filled the water bath of the viscometer was preheated to the temperature at which the measurement was to be made. When the viscometer was filled with a sample, it was necessary to wait until the viscometer and the sample reached the assumed measurement temperature. When this happened, the flow time of the fat under study into a volumetric flask was measured.

In order to make an active experiment assessing the exhaust opacity was used a diesel engine with a displacement of 1588 cm^3 and nominal power of 37 kW at 4800 rpm. The fuel feed system consisted of a distributor injection pump with a system of indirect injection into the swirl chamber. Because of the fact that a comparative study was conducted, the degree of the engine wear was not taken into consideration in the control sample, where the investigations were made on standardised diesel fuel.

The engine was equipped with two fuel tanks – an unheated one for diesel and an insulated one, fitted with a heating system for animal fat. In order to reduce the heat loss the fuel hoses were fitted with an electric heating system, which enabled us to keep the set temperature of the fuel injected into the cylinders.

A Junkers H0 stationary hydraulic dynamometer was used to load the engine so it could reach thermal equilibrium. The dynamometer was directly connected to the engine flywheel by means of an articulated telescopic shaft.

In order to measure the exhaust opacity an optical opacimeter Radiotechnika DO 9500 was used. The basic technical specifications of the opacimeter are shown in the table below. The opacity was measured when the engine powered with the fuel under investigation was hot.

Table 1. Optical opacimeter Radiotechnika DO 9500 – technical specifications

Values measured	Range	Resolution	Unit
Exhaust opacity: Absorption coefficient k Opacity N	 0...∞ 0...100	 0.01 1 or 0.1	 m^{-1} %
Rotational speed	60...9999	1	rpm
Oil temperature T_{ol}	0...150	1	°C

The exhaust opacity was measured according to the following procedure. After the start-up the engine was initially warmed up and then it was loaded with its nominal power until it reached thermal equilibrium. Immediately after the warmup we determined the external operating characteristics of the engine powered with diesel. Then the exhaust opacity of the engine powered with a standard diesel fuel was measured.

The absorption coefficient k was measured with the free acceleration method, which consisted in loading the engine with the inertia of the rotating parts of the engine itself and the engine brake connected to it. In order to make the measurement the rotational speed of the engine was rapidly increased from the idle speed to the maximum speed by making a decisive move shifting the fuel dosage lever from the idle position to the position of the maximum fuel dose. In order to average the results the measurements were made ten times, with 15-second periods of the engine idling before consecutive measurements.

Having finished the measurement, the engine fuel system was filled with pig fat and for 15 minutes the engine ran at its nominal power in order to guarantee that the diesel was completely removed from the fuel system. Then the measurement procedure described above was repeated three times for selected temperatures of pig fat.

3. Discussing research results

The constant k for the viscosity measurement system was 50.66, where the coefficient of variation was <1%. The arithmetic means of the fat flow times, where the coefficient of variation was <5%, had the logarithmic distribution with the coefficient of determination $R^2>0.99$ until the moment of change in the temperature.

The kinematic viscosity of fat which was measured within the assumed temperature range (60–160°C) reached the values ranging from 1.8 to 12 $mm^2 \cdot s^{-1}$ and it was negatively correlated with the temperature $r=-0.94$ (Fig. 1).

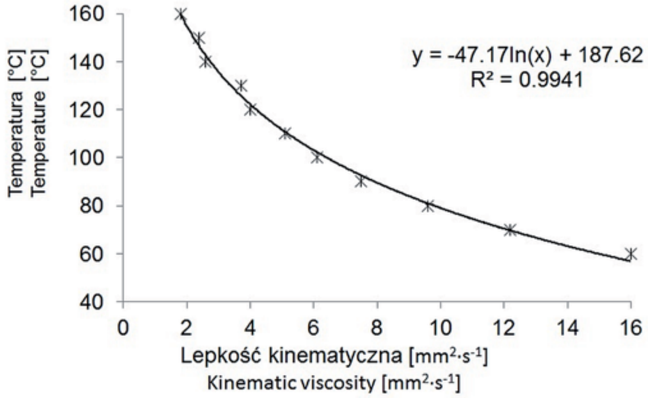

Fig. 1. The correlation between the kinematic viscosity of pig fat and heating temperature

The temperature where the kinematic viscosity of pig fat is similar to the kinematic viscosity of diesel at 40°C ranges from 120°C to 140°C. Animal fats contain about 35% of stearic acid and palmitic acid (melting point: 70°C and 64°C, respectively). Therefore, they retain the solid state of matter at ambient conditions [5]. The freezing point of such fuels can be changed chemically by the process of transesterification. As a result of the process, the freezing point of these fuels is about 10°C. According to Goodrum et al., animal fats can be used as a component of heating oil in heating installations, where the fuel is preheated and its storage conditions do not change [11].

The type of applied fuel and the temperature of pig fat did not have significant influence on the power generated by the engine. As results from the research, the engine powered with hot animal fat (fuel temperatures of 80°C, 120°C and 160°C) generated the average maximum power of 34.9 kW ± 4%, whereas the engine powered with diesel generated the power of 32.3 kW ± 8% (Fig. 2). Thus, as a result of a univariate analysis of variance with the 5% level of confidence, the type of applied fuel was not observed to have significant influence on the maximum power generated by the engine under investigation (p= 0.08).

The next stage of the research involved the measurement of exhaust opacity in the engine powered with diesel and then with rendered animal fats. The average value of exhaust opacity in the engine powered with diesel was $k=1.38\ m^{-1}$. When this value was compared with the values obtained when the engine was powered with hot animal fat, which ranged from $k=0.38\ m^{-1}$ (80°C) through $k=0.30\ m^{-1}$ (120°C) to $k=0.39\ m^{-1}$ (160°C), a considerable decrease in the exhaust opacity was observed, reaching about 70% (Fig. 3). Such a low value

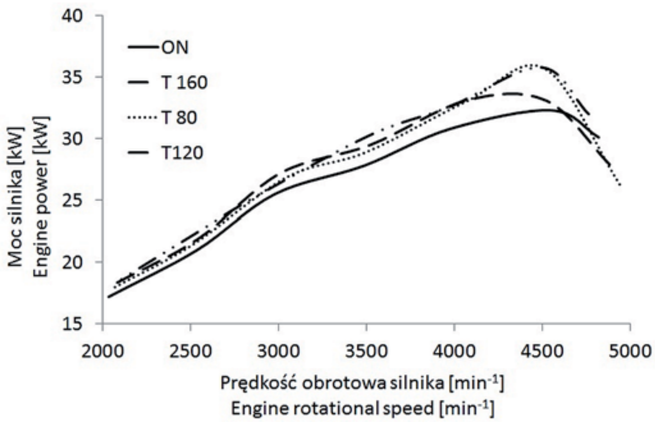

Fig. 2. The engine power at the maximum setting of the fuel injection pump; ON – diesel; T80, T120, T160 – pig fat at temperatures of 80°C, 120°C and 160°C, respectively

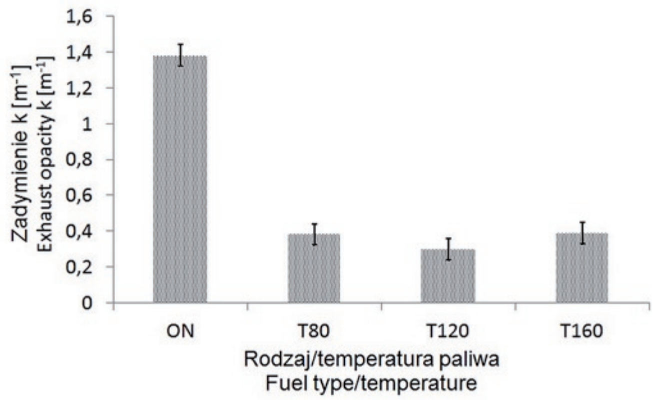

Fig. 3. A comparison of exhaust opacity in the engine powered with diesel and the engine powered with pig fat: ON – diesel; T80, T120, T160 – pig fat at temperatures of 80°C, 120°C and 160°C, respectively

of the exhaust opacity may have resulted from differences in the content of carbon and oxygen in the fuels under comparison. The content of carbon in diesel reaches 84-87% and there is almost no oxygen, whereas the content of carbon in animal fats is about 73% (m/m) and the content of oxygen is about 12.5% (m/m) [25].

4. Summary

As results from the literature, fats are a mixture of fatty acids, which are characterised by different flow temperatures, ranging from −14°C for linolenic acid to 70°C for stearic acid [8]. As results from the study by Golimowski et al., regardless of the type and origin the kinematic viscosity of fats is about 19.67 $mm^2 \cdot s^{-1} \pm 5\%$ at a temperature of 60°C (except post-frying fats) [9]. On the other hand, at lower temperatures the kinematic viscosity depends on the type of fat. Thus, in view of this fact and with reference to the findings of this research we can assume the hypothesis that the kinematic viscosity of fats made from plants will be similar to that of diesel at a temperature exceeding 120°C. In order to confirm the hypothesis it is necessary to conduct the research again according to the methodology developed by the authors.

In 2005 Senthil et al. proved that an increase in the temperature of animal fats used to power a diesel engine reduces the exhaust opacity. In comparison with the engine powered with diesel the opacity of exhaust emitted by the engine powered with fats at a temperature of 30°C was lower by about 30%. When the temperature increased to 70°C, the exhaust opacity was reduced by 60% in comparison with diesel [25]. The researchers observed that when the engine was powered with pig fat at a temperature of 80°C, the exhaust opacity was reduced by about 70% in comparison with the engine powered with diesel. Apart from that, further increase in the temperature of fat did not cause significant changes in the degree of exhaust opacity. Senthil et al. observed that the lower exhaust opacity resulted from the characteristics of heat release in the cylinders. During the first phase, when the pressure in the cylinders increased dynamically, the dynamics of heat release was lower when animal fats were applied. The situation was opposite at the second phase where the unburned fuel is completely burning [25]. This phenomenon was caused by the lower content of carbon in fat and by the presence of oxygen. The larger amount of heat at the second phase of fuel burning favours the higher temperature of exhaust emitted by the engine [2]. Barrios et al. observed that differences in the exhaust opacity of the engine powered with diesel and then with a mixture of biodiesel from animal fat and diesel (50/50) did not depend on the engine load. As the average velocity of the vehicle in motion increased, and in consequence, as the engine load increased, there were equal and directly proportional differences in the degree of exhaust opacity for all of the engine load values under investigation [3]. Another effective method of reduction of exhaust opacity is to use animal fat emulsified with ethanol [15]. Thus, it would be necessary to start research in order to make a complex assessment of the influence of fuels made from plants and animals at a temperature where the kinematic viscosity would be comparable to that of diesel at 40°C on the operation parameters and level of exhaust emission from a diesel engine.

5. Conclusions

– Rendered animal fats are characterised by the kinematic viscosity of 2.5–4 $mm^2 \cdot s^{-1}$ (diesel viscosity at 40°C) at temperatures ranging from 120°C do 140°C.
– Powering a diesel engine with hot animal fats considerably reduces exhaust opacity and increases the engine power by 10% in comparison with a diesel fuel. As results from the research, engines powered with hot animal fats at higher temperatures than 80°C emit 70% less solid pollutants into the atmosphere.
– The fuel can be preheated with the engine refrigerant and then heated to a minimum temperature of 80°C by means of the electric system. Further increase in the temperature of fats had no influence on changes in the engine parameters under investigation.

References

1. Armas O, Gracja-Contreras R, Ramos A. Emissions of light duty vehicle tested under urban and extraurban real-world driving conditions with diesel, animal fat biodiesel and GTL fuels. SAE Technical Paper 2013; 13240176.
2. Awad S, Loubar K, Tazerout M. Experimental investigation on the combustion, performance and pollutant emissions of biodiesel from animal fat residues on a direct injection diesel engine. Energy 2014; 69: 826-836.
3. Barrios CC, Dominguez-Saez A, Martin C, Alvarez P. Effects of animal fat based biodiesel on a TDI diesel engine performance, combustion characteristics and particle number and size distribution emissions. Fuel 2014; 117: 618-623.
4. Czechlowski M, Krysztofiak A, Adamski M, Antczak W. Wpływ stosowania oleju rzepakowego jako paliwa na trwałość aparatury wtryskowej silników ZS. Inżynieria Rolnicza 2006; 12(87): 85–92.
5. Czaczyk Z, Czechowski M, Golimowski W, Dereń B. Badanie parametrów fizycznych zużytych tłuszczów naturalnych i ich wpływ na parametry pracy silnika ciągnika rolniczego. Journal of Research and Applications in Agricultural Engineering 2012; 2(57): 51–57.
6. Dzieniszewski G. Wybrane aspekty ekologiczne i ekonomiczne zasilania silników Diesla paliwami roślinnymi. Inżynieria Rolnicza 2009; 6(115): 45–52.
7. Ferenc Z, Pikoń K. Przegląd rodzajów i ilości odpadów tłuszczowych i olejowych w Polsce. Archiwum Gospodarki Odpadami i Ochrony Środowiska 2005; 2: 69–80.
8. Gawęcki J. Prawda o tłuszczach. Warszawa. W: Instytut Danone FPZ 1997. ISBN 83-907366-1-6: 78.
9. Golimowski W, Golimowska R, Kliber A. Zależność temperaturowa lepkości kinematycznej tłuszczów zwierzęcych, olejów roślinnych oraz produktów reakcji transestryfikacji. Journal of Research and Applications in Agricultural Engineering 2011; 1(56): 50-55.
10. Golimowski W., Pasyniuk P., Berger A.W. 2013. Common rail diesel tractor engine performance running on pure plant oil. Fuel 2013; 103: 227–231.
11. Goodrum JW, Geller DP, Adams TT. Rheological characterization of animal fats and their mixtures with #2 fuel oil. Biomass and Bioenergy 2003; 3(24): 249–256.
12. Hossain AK, Davies PA, Plant oils as fuels for compression ignition engines: A technical review and life-cycle analysis. Renewable Energy 2010. 35: 1–13.
13. Jackowska I, Krasucki W, Piekarski W, Tys J, Zając G. Rzepak z pola do baku. PWRL Warszawa 2004, ISBN 83-09-01781-2: 134.
14. Kalam MA, Masjuki HH, Jayed MH, Liaquat AM. Emission and performance characteristics of an indirect ignition diesel engine fuelled with waste cooking oil. Energy 2011; 1(36): 397–402.
15. Kerihuel A, Santhil K.M, Belletter J, Tazerout M. Investigations on a CI Engine Using Animal Fat and Its Emulsions With Water and Methanol as Fuel. SEA Technical Paper 2005; 05011729.
16. Koniuszy A. 2001. Wpływ stosowania biopaliwa RME w silnikach wysokoprężnych pojazdów rolniczych na wybrane własności użytkowe oleju silnikowego. Inżynieria Rolnicza 2001; Nr 1(21): 135–140.
17. Marczak P. Wykorzystanie tłuszczu zwierzęcego jako biopaliwa – Wybrane zagadnienia. Opracowania tematyczne OT-589. Warszawa2010: 14.
18. Mueller SA, Anderson JA, Wallington TJ. Impact of biofuel production and other supply and demand factors on food price increases in 2008. Biomass and Bioenergy 2011; 5(35): 1623–1632.
19. Nonhebel S. Global food supply and the impacts of increased use of biofuels. Energy 2012; 1(37): 115–121.
20. Pasyniuk P. Ograniczenie emisji gazów cieplarnianych przez zastąpienie oleju napędowego olejami roślinnymi. Problemy Inżynierii Rolniczej 2010; 4: 79-89
21. Peri M, Baldi L. The effect of biofuel policies on feedstock market: Empirical evidence for rapeseed oil prices in EU. Resource and Energy Economics 2013; 1(35): 18–37.

22. Rathbauer J, Krammer K, Kriechbaum T, Prankl H, Breinesberger J. Rapsöl als Treib-stoffalternative für die Landwirtschaft BMLFUW-LE.1.3.2/0037-II/1/2006. Forschungsprojekt No. 1337: 317.
23. Roszkowski A. Biodiesel w UE i Polsce – obecne uwarunkowania i perspektywy. Problemy Inżynierii Rolniczej 2012. 3(77): 65–78.
24. Shirneshan A. HC, CO, CO2 and NOx emission evaluation of a diesel engine fueled with waste frying oil methyl ester. Procedia – Social and Behavioral Sciences 2012; 3(75): 292–297.
25. Senthil KM, Kerihuel A, Bellettre J, Tazerout M. Experimental investigations on the use of preheated animal fat as fuel in a compression ignition engine. Renewable Energy 2005; 9(30): 1443–1456.
26. Takayuki M, Takaaki M. Diesel Engine Operation and Exhaust Emissions When Fueled with Animal Fats. SEA Technical Paper 2005; 05013673.
27. Wegner EP, Lambert PD, Moyle TM, Koehle MA. Diesel vehicle performance on unaltered waste soybean oil blended with petroleum fuels. Fuel 2013; 107: 757-765.

Mirosław CZECHLOWSKI
The Institute of Biosystems Engineering
Poznań University of Life Sciences
ul. Wojska Polskiego 28, 60-637 Poznań, Poland

Wojciech GOLIMOWSKI
Department of Renewable Energy Sources
Institute of Technology and Life Sciences
ul. Biskupińska 67, 60-463 Poznań, Poland

Tadeusz SĘK
Jacek SZYMANOWICZ
The Institute of Biosystems Engineering
Poznań University of Life Sciences
ul. Wojska Polskiego 28, 60-637 Poznań, Poland

E-mails: mczech@up.poznan.pl , w.golimowski@itep.edu.pl

Article citation info:
GRĄDZKI R, LINDSTEDT P. Method of assessment of technical object aptitude in environment of exploitation and service conditions. Eksploatacja i Niezawodnosc – Maintenance and Reliability 2015; 17 (1): 54–63.

Rafał GRĄDZKI
Paweł LINDSTEDT

METHOD OF ASSESSMENT OF TECHNICAL OBJECT APTITUDE IN ENVIRONMENT OF EXPLOITATION AND SERVICE CONDITIONS

METODA OCENY STANU ZDATNOŚCI OBIEKTU TECHNICZNEGO W OTOCZENIU WARUNKÓW UŻYTKOWANIA I JAKOŚCI OBSŁUGI*

In the article, results of exploitation research of three various technical objects (public transportation bus engines) are presented. Gathered data is presented in three sets (1 – concerning object, 2 – concerning driving conditions, 3 – concerning driver, where sets 2 and 3 are object environment) in form of points (expert number assessments). Relation between point information on object and point information on environment was described using coupled state interaction equations. Such approach allowed to determine the following for each moment of exploitation: technical condition parameter a_T and operating condition parameter a_R, therefore in each moment of exploitation data regarding operating and technical condition of exploited object (bus) is available. This data allows for identification of object aptitude condition and thus optimally control processes of exploitation and service of particular objects as element of set of objects and set of objects.

Keywords: *diagnostics, regulation, aptitude.*

W artykule przedstawiono wyniki badań eksploatacyjnych trzech różnych obiektów technicznych (silników autobusów komunikacji miejskiej). Zebrana informacja została przedstawiona w 3 zbiorach (1 – dotyczy obiektu, 2 – dotyczy warunków jazdy, 3 – dotyczy kierowcy; przy czym zbiory 2 i 3 stanowią otoczenie obiektu) w postaci umownych punktów (eksperckich liczbowych ocen). Relację między punktową informacją o obiekcie i punktową informacją o otoczeniu opisano za pomocą sprzężonych równań stanu. Takie podejście pozwoliło wyznaczyć dla każdej chwili eksploatacji: parametr stanu technicznego aT i parametr stanu działania aR, Zatem w każdej chwili eksploatacji może być dostępna informacja o stanie technicznym i stanie działania każdego eksploatowanego obiektu (autobusu). Informacja ta pozwala identyfikować w każdej chwili stan zdatności obiektu, a zatem pozwala optymanie sterować procesami użytkowania i obsługi poszczególnych obiektów jako elementu zbioru obiektów i zbiorem obiektów.

Słowa kluczowe: *diagnostyka, regulacja, zdatność.*

1. Introduction

Long term exploitation of machine leads to its gradual damage caused by decrease in its material properties and mechanical wear. Technical service is therefore tasked with constant (current) assessment of object technical condition and ability of proper operation of technical objects based on measured diagnostic signals, exploitation signals and conditions in which the object is exploited. This allows to observe changes of operating and technical condition and, subsequently, changes of technical object reliability state [2, 7, 15, 19, 23].

A concept of new exploitation research method is presented based on the assumption that all data (diagnostic signals, exploitation signals, exploitation condition signals) are expressed (presented) in form of points and thus may be easily processed.

Diagnostic signals in form of points were first applied in diagnostics of SH-2G onboard-based helicopter (USA) [22]. In this method, object aptitude is analyzed only by summing all of the points. Subsequently, assessment is made whether the obtained number of points characterizing serviced object is lower than acceptable threshold specified by manufacturer (USA).

Innovative method of using exploitation data (in form of points) proposed in the article is based on fact that each change of diagnostic signals, signals concerning exploitation quality and signals concerning exploitation conditions (depending on their value and time of occurrence) is correlated with number of points determined by the experts. Subsequently, basing o the aforementioned, parameters of operating condition a_R and technical condition a_T are determined using coupled interaction equations [3, 12, 13, 15, 21] for each moment of object exploitation.

The described method may prove very useful, as global exploitation condition of the object is unequivocally presented by unequivocal values of a_R and a_T parameters (where a_R – operating condition parameter, a_T – technical condition parameter). This allows to predict how the object should be used in future and when the object should be serviced (repaired, overhauled).

2. Diagnostic research of technical object and its environment

Exploited technical object (e.g. bus engine) should be properly used and serviced in conditions according to its destination [4, 5, 8, 9, 16÷18, 24÷ 26, 29].

Particular role in exploitation system if fulfilled by expert-driver and expert-diagnostician (expert being a specialist assessing system and its environment). Experts are the main source of knowledge that should be used to increase probability of elaborating comprehensive and reliable assessment of technical object aptitude condition during the process of its service and use including exploitation costs [2, 7, 10, 11, 27, 28].

(*) Tekst artykułu w polskiej wersji językowej dostępny w elektronicznym wydaniu kwartalnika na stronie ***www.ein.org.pl***

The research was conducted on three MAN bus engines in Municipal Transport Company of the City of Białystok. The aim of the research was obtaining diagnostic signals concerning object condition D_K (data from diagnostician) and data on its environment U (expert data from driver).

Research was conducted in subsequent months of the year, therefore obtaining database for 12 months of the year.

The following was used in order to conduct exploitation analysis:

- opacimeter – measurement of exhaust fumes fogging [1/m],
- acoustimeter – noise measurement [dB],
- diagnostical stand (chassis dynamometer) – fuel consumption measurement[l/100km],
- expert knowledge from driver and diagnostician.
- Obtained data: determined (measurable), probabilistic and heuristic (expert) was divided onto two sets:
- signals concerning technical condition D_K (Tab. 1)
- signals concerning environment influence condition U (Tab. 2)

Table 1. Information on diagnostic research of MAN engine:

D_{M1}	average fuel consumption without heating [l/100km]
D_{M2}	average fuel consumption with heating [l/100km]
D_{M3}	fogging value in engine blow [1/m]
D_{M4}	fogging value during engine operation [1/m]
D_{M5}	noise peak value [dB]
D_{M6}	noise average value [dB]
D_{M7}	braking force value on front axis – left wheel [kN]
D_{M8}	braking force value on front axis – right wheel [kN]
D_{M9}	percent value of difference between braking forces of left and right wheel of front axis [%]
D_{M10}	braking force value on rear axis – left wheel [kN]
D_{M11}	braking force value on rear axis – right wheel [kN]
D_{M12}	percent value of difference between braking forces of left and right wheel of rear axis [%]
D_{E1}	clatters
D_{E2}	unattended stalls (on neutral gear)
D_{E3}	stalls (during operation)
D_{E4}	bus mileage [km]

Table 2. Information on environment research of MAN engine:

U_{K1}	job experience [years]
U_{K2}	number of hours of work in a month [h]
U_{K3}	driving smoothness (braking, accelerating)
U_{D1}	number of stops
U_{D2}	route length [km]
U_{D3}	surface and lay of the land
U_{P1}	environment temperature [^{o} C]
U_{P2}	wind speed [m/s]
U_{P3}	atmospheric pressure [hPa]
U_{P4}	rainfall [mmHg]

Data from Tab. 1 and 2 is of physical nature. Therefore in each case, data is transformed into a point value.

3. Special method of consideration of expert knowledge for "weighing" data

In order to obtain knowledge from specialists (experts) and to weigh data with points, specific questionnaires were developed with users – bus drivers. [10, 28]

Research was conducted on group of 20 experts.

Table 3. Expert weight of assessment of condition engine – diagnostic (diagnostician is the expert), driver and environment (driver is the expert)

Signal	Signal name	Group importance	Importance within group	Ep
D_{M1}	average fuel consumption without heating	5	3	15
D_{M2}	average fuel consumption with heating		3	15
D_{M3}	fogging value in engine blow		2	10
D_{M4}	fogging value during engine operation		2	10
D_{M5}	noise peak value		1	5
D_{M6}	noise average value		1	5
D_{E1}	clatters	4	2	8
D_{E2}	unattended stalls (on neutral gear)		1	4
D_{E3}	stalls		3	12
D_{E4}	bus mileage		1	4
U_{K1}	job experience	3	1	3
U_{K2}	number of hours of work in a month [h]		2	6
U_{K3}	driving smoothness (braking, accelerating)		3	9
U_{D1}	number of stops	2	2	4
U_{D2}	route length		1	2
U_{D3}	surface and lay of the land		3	6
U_{P1}	environment temperature	1	3	3
U_{P2}	wind speed		1	1
U_{P3}	atmospheric pressure		2	2
U_{P4}	rainfall		3	3

Ep – expert weight points (importance of matter)

Data (signals) connected to object $\{D_{Mi}\}$, $\{D_{Ei}\}$ and its environment $\{U_{Ki}\}$, $\{U_{Di}\}$, $\{U_{Pi}\}$ were subjected to expert processing. Experts (Tab. 3) determined importance of signal groups and importance of signal within that group and number of Ep for transforming exploitation fact into point description. The respondents answered the questions by putting points (from range 1–5) in proper section of questionnaire, where 1 was least important data.

Importance of data D_i and U_i expressed by proper point weights including knowledge of expert diagnostician is presented in Tab. 4.

Basing on Tab. 4, every situation, phenomenon and exploitation fact may be expressed in form of proper number of points.

Table 4. Expert point weights for assessment of condition of engine, diagnostician and driver (Tab. 3)

Signal	Diagnostic signal name	Ep	N	N + 5%	N + 10%	N + 15%	N + 20%
D_{M1}	average fuel consumption without heating [l/100km]	15	1	16	31	46	61
D_{M2}	average fuel consumption with heating [l/100km]	15	1	16	31	46	61
D_{M3}	fogging value in engine blow [1/m]	10	1	11	21	31	41
D_{M4}	fogging value during engine operation [1/m]	10	1	11	21	31	41
D_{M5}	noise peak value [dB]	5	1	6	11	16	21
D_{M6}	noise average value [dB]	5	1	6	11	16	21

Signal	Diagnostic signal name	Ep	<1%	1-10%	10-20%	20-30%	>30%
D_{M7}	braking force value on front axis – left wheel [kN]	-	-	-	-	-	-
D_{M8}	braking force value on front axis – right wheel [kN]	-	-	-	-	-	-
D_{M9}	percentage difference between DM7 and DM8 [%]	15	1	16	31	46	61
D_{M10}	braking force value on rear axis – left wheel [kN]	-	-	-	-	-	-
D_{M11}	braking force value on rear axis – right wheel [kN]	-	-	-	-	-	-
D_{M12}	percentage difference between DM10 and DM11 [%]	15	1	16	31	46	61
D_{M13}	braking force value on middle axis – left wheel [kN]	-	-	-	-	-	-
D_{M14}	braking force value on middle axis – right wheel [kN]	-	-	-	-	-	-
D_{M15}	percentage difference between DM13 and DM14 [%]	10	1	11	21	31	41

Signal	Diagnostic signal name	Ep	0-2	2-5	>5
D_{E1}	clatters	8	1	9	17
D_{E2}	unattended stalls (on neutral gear)	4	1	5	9
D_{E3}	stalls (during operation)	12	1	13	25

Signal	Diagnostic signal name	Ep	< 500 k	500 k – 1 mln	>1 mln
D_{E4}	bus mileage	4	1	5	9

Signal	Environment signal name	Ep	< 5 years	5-12 years	>12 years
U_{K1}	job experience [years]	3	1	4	7

Signal	Environment signal name	Ep	< 140 h	140-180 h	>180 h
U_{K2}	number of hours of work in a month [h]	6	1	7	13

Signal	Environment signal name	Ep	<10	10-15	>15
U_{K3}	driving smoothness (braking, accelerating)	9	1	10	19

Table 4. (continued) Expert point weights for assessment of condition of engine, diagnostician and driver (Tab. 3)

Signal	Environment signal name	Ep	<15	15-30	>30
U_{D1}	number of stops	4	1	5	9

Signal	Environment signal name	Ep	<10 km	10-15 km	> 15km
U_{D2}	route length	2	1	3	5

Signal	Environment signal name	Ep	good surface	mediocre surface	poor surface
U_{D3}	surface and lay of the land	6	1	7	13

Signal	Environment signal name	Ep	< −10°C	−10–10°C	10–20°C	20–30°C	>30°C
U_{P1}	environment temperature	3	7	4	1	4	7

Signal	Environment signal name	Ep	<28,4 km/h	28,4–61,56 km/h	>61,56 km/h
U_{P2}	wind speed	1	1	2	3

Signal	Environment signal name	Ep	<994,66 hPa	996,66–1020 hPa	>1020 hPa
U_{P3}	atmospheric pressure	2	1	3	5

Signal	Environment signal name	Ep	no rainfall	no significant rainfall	small rainfall	rainfall	small snowfall	snowfall
U_{P3}	rainfall	3	1	4	7	10	13	16

Table 5. Compilation of diagnostic signals in physical form

	Diagnostic signals															
Month	D_{M1}	D_{M2}	D_{M3}	D_{M4}	D_{M5}	D_{M6}	D_{M7}	D_{M8}	D_{M9}	D_{M10}	D_{M11}	D_{M12}	D_{E1}	D_{E2}	D_{E3}	D_{E4}
1	35,7	35,7	0,37	0,02	95	92	12	13,2	9	15,8	14,7	6	0	0	0	215582
2	35,7	35,7	0,37	0,02	95	92	12	13,2	9	15,8	14,7	6	0	1	0	217982
3	35,7	35,7	0,37	0,02	95	92	12	13,2	9	15,8	14,7	6	0	0	0	220102
4	35,7	35,7	0,37	0,02	95	92	12	13,2	9	15,8	14,7	6	0	0	2	222669
5	35,7	35,7	0,37	0,02	95	92	12	13,2	9	15,8	14,7	6	1	0	0	225125
6	35,7	35,7	0,37	0,02	95	92	12	13,2	9	15,8	14,7	6	0	3	0	227358
7	33,7	33,7	0,45	0,03	94	90	11,4	12	5	12,5	12,3	1	0	0	0	229758
8	33,7	33,7	0,45	0,03	94	90	11,4	12	5	12,5	12,3	1	0	0	0	232273
9	33,7	33,7	0,45	0,03	94	90	11,4	12	5	12,5	12,3	1	0	0	0	234571
10	35,1	35,1	0,42	0,03	91,9	91	8,8	12,6	29	11,9	13,3	10	3	3	0	236699
11	35,1	35,1	0,42	0,03	91,9	91	8,8	12,6	29	11,9	14,7	10	0	0	0	239047
12	35,1	35,1	0,42	0,03	91,9	91	8,8	12,6	29	11,9	14,7	10	0	0	0	241392

Table 6. Compilation of environment signals in physical form

Environment signals										
Month	U_{K1}	U_{K2}	U_{K3}	U_{D1}	U_{D2}	U_{D3}	U_{P1}	U_{P2}	U_{P3}	U_{P4}
1	4	125	5	33	15	2	−0,8	15,2	995,7	no significant rainfall
2	24	164	5	21	9,4	1	−5,8	16,2	1002,2	small rainfall
3	24	160	5	21	9,4	1	7,7	19,4	999,3	no significant rainfall
4	10	179	5	21	9,4	1	14,9	16,3	987,2	no significant rainfall
5	10	146	5	40	16,9	2	20,9	14,9	997,0	no significant rainfall
6	16	187	6	40	16,9	2	22,1	16,4	992,2	small rainfall
7	16	110	6	40	16,9	2	26,6	13,7	995,8	no significant rainfall
8	16	144	4	40	16,9	2	23,8	14,6	996,7	no significant rainfall
9	16	170	4	40	16,9	2	20,2	16,4	995,7	no rainfall
10	4	144	4	29	14,6	2	11,8	16,0	994,0	no significant rainfall
11	4	154	7	29	14,6	2	6,9	15,8	995,7	no rainfall
12	4	185	7	29	14,6	2	−2,3	16,3	994,5	no significant rainfall

Table 7. Compilation of diagnostic signals in point form

Month	D_{M1P}	D_{M2P}	D_{M3P}	D_{M4P}	D_{M5P}	D_{M6P}	D_{M9P}	D_{M12P}	D_{E1P}	D_{E2P}	D_{E3P}	D_{E4P}
1	15	15	10	10	5	5	30	30	0	0	0	4
2	15	15	10	10	5	5	30	30	0	4	0	4
3	15	15	10	10	5	5	30	30	0	0	0	4
4	15	15	10	10	5	5	30	30	0	0	12	4
5	15	15	10	10	5	5	30	30	8	0	0	4
6	15	15	10	10	5	5	30	30	0	8	0	4
7	15	15	10	10	5	5	30	15	0	0	0	4
8	15	15	10	10	5	5	30	15	0	0	0	4
9	15	15	10	10	5	5	30	15	0	0	0	4
10	15	15	10	10	5	5	60	30	16	8	0	4
11	15	15	10	10	5	5	60	30	0	0	0	4
12	15	15	10	10	5	5	60	30	0	0	0	4

Table 8. Compilation of environment signals in point form

Month	U_{K1P}	U_{K2P}	U_{K3P}	U_{D1P}	U_{D2P}	U_{D3P}	U_{P1P}	U_{P2P}	U_{P3P}	U_{P4P}
1	3,00	6,00	9,00	12,00	4,00	12,00	2,03	1,00	1,55	2,32
2	9,00	12,00	9,00	12,00	2,00	6,00	2,25	1,07	1,61	2,89
3	9,00	12,00	9,00	12,00	2,00	6,00	1,58	1,13	1,77	2,06
4	6,00	12,00	9,00	12,00	2,00	6,00	1,43	1,03	1,17	2,10
5	6,00	12,00	9,00	12,00	6,00	12,00	1,65	1,00	1,71	2,26
6	9,00	18,00	9,00	12,00	6,00	12,00	1,80	1,00	1,33	2,73
7	9,00	6,00	9,00	12,00	6,00	12,00	2,35	1,00	1,52	1,94
8	9,00	12,00	9,00	12,00	6,00	12,00	1,97	1,03	1,65	1,97
9	9,00	12,00	9,00	12,00	6,00	12,00	1,47	1,03	1,70	1,40
10	3,00	12,00	9,00	12,00	4,00	12,00	1,29	1,06	1,45	1,55
11	3,00	12,00	9,00	12,00	4,00	12,00	1,77	1,00	1,57	1,33
12	3,00	18,00	9,00	12,00	4,00	12,00	2,03	1,06	1,55	2,03

Values of signals $U_{P1}\div U_{P3}$ in Tab. 6 are average values form the whole month, whereas U_{P4} signal value is the most frequently occurring in given month. In Tab. 8 a summed number of points was created through transforming observed signals into point values on daily basis and subsequently summing them in the end of the month and dividing them by number of days in a month.

Basing on data in Tab. 5 and 6 and including expert weights (Tab. 3 and 4), point form of signals were obtained – Tab. 7 and 8 (data for other two buses was filled analogously).

4. Algorithm of determination parameters of technical condition and operating condition of technical object

Driver, through his influence on the bus, alters its environment (accelerating, braking, turning). Influence is only effective is bus technical condition is sufficient. Bus performing its daily duties is subjected to wear (increase in noise, fogging, fuel consumption). Intensity of wear depends on varying environment in which the bus operates. Therefore exploitation is an environment for technical condition and technical condition is environment for exploitation. These facts may be expressed by coupled interaction equations [3, 13]:

$$\frac{dD_K}{dt} = a_T D_K + b_T U \tag{1}$$

$$\frac{dU}{dt} = a_R U + b_R D_K \tag{2}$$

where: U – variable of operating condition (exploitation signal), D_K – signal of bus technical condition, a_R – operating condition parameter, depending mostly on object operation and influence of object technical condition, b_R – parameter of influence of technical condition on operating condition, a_T – technical condition parameter, depending mostly on diagnostic signals and signals resulting from environment, b_T – parameter of influence of regulation condition on bus technical condition.

According to rules of static and dynamic identification [20], the following is obtained from equation (1):

$$\hat{a}_T = \frac{\sum \Delta D_K \Delta U}{\sum \Delta U^2} \tag{3}$$

$$a_T = \frac{\Delta D_K}{\frac{\Delta\Theta}{resurs}(D_K + \hat{a}_T U)} \tag{4}$$

Parameter a_T characterizes technical condition of the system and depends on diagnostic signals as well as signals resulting from actions of driver and environment.

According to rules of static and dynamic identification [20], from equation (2) the following is obtained:

$$\hat{a}_R = \frac{\sum \Delta D_K \Delta U}{\sum \Delta D_K{}^2} \tag{5}$$

$$a_R = \frac{\Delta U}{\frac{\Delta\Theta}{resurs}(U + \hat{a}_R D_K)} \tag{6}$$

Signals D_K and U in homogeneous point form (Tab. 6) were transformed into resultant diagnostic signal (D_K) and environment signal (U).

$$D_K = \sqrt{\begin{aligned}&D^2_{M1P} + D^2_{M2P} + D^2_{M3P} + D^2_{M4P} + D^2_{M5P} + + D^2_{M6P} + \\ &+ D^2_{M9P} + D^2_{M12P} + D^2_{15P} + D^2_{1EP} + D^2_{2EP} + D^2_{3EP} + D^2_{4EP}\end{aligned}} \tag{7}$$

$$U = \sqrt{\begin{aligned}&U^2_{K1P} + U^2_{K2P} + U^2_{K3P} + U^2_{D1P} + U^2_{D2P} + U^2_{D3P} + U^2_{P1P} + \\ &+ U^2_{P2P} + U^2_{P3P} + U^2_{P4P}\end{aligned}} \tag{8}$$

Table 9. Procedure of calculating of parameters of technical and regulation condition for bus no. 301

Determination of technical a_T and regulation a_R potentials															
Month	Time of work θ	D_K	U	Δθ	$ΔD_K$	ΔU	D_K*U	ΣD_K*U	U²	ΣU²	$D_K{}^2$	Σ$D_K{}^2$	$\hat{a}_T$	$\hat{a}_R$	a_T	a_R
1	215582	50,16	21,05	2346	50,16	21,05	1055,65	1055,65	442,92	442,92	2516	2516	-2,3834	-0,4196	0	0
2	217982	50,32	22,52	4746	100,48	43,57	1133,20	2188,84	507,16	950,08	2532	5048	-2,3038	-0,4336	-0,01354	0,01308
3	220102	50,16	22,39	6866	150,64	65,95	1122,93	3311,78	501,18	1451,27	2516	7564	-2,2820	-0,4378	-0,02366	0,02258
4	222669	51,58	21,30	9433	202,21	87,26	1098,80	4410,57	453,89	1905,16	2660	10224	-2,3151	-0,4314	0,00951	-0,00979
5	225125	50,79	24,43	11889	253,01	111,69	1240,79	5651,36	596,73	2501,89	2580	12804	-2,2588	-0,4414	-0,00485	0,00468
6	227358	50,79	28,70	14122	303,80	140,38	1457,60	7108,96	823,49	3325,38	2580	15384	-2,1378	-0,4621	-0,00204	0,00190
7	229758	42,91	23,12	16522	346,71	163,50	992,06	8101,02	534,59	3859,97	1841	17225	-2,0987	-0,4703	-0,00374	0,00336
8	232273	42,91	25,33	19037	389,61	188,83	1086,75	9187,78	641,52	4501,48	1841	19066	-2,0411	-0,4819	-0,00233	0,00213
9	234571	42,91	25,26	21335	432,52	214,09	1083,83	10271,60	638,07	5139,55	1841	20907	-1,9985	-0,4913	-0,00268	0,00240
10	236699	74,40	23,35	23463	506,93	237,44	1737,47	12009,07	545,30	5684,86	5536	26443	-2,1125	-0,4541	0,00086	-0,00097
11	239047	72,22	23,37	25811	579,15	260,82	1688,13	13697,20	546,35	6231,21	5216	31659	-2,1982	-0,4326	0,00108	-0,00128
12	241392	72,22	27,01	28156	651,37	287,83	1951,05	15648,25	729,79	6961,00	5216	36875	-2,2480	-0,4244	0,00201	-0,00281

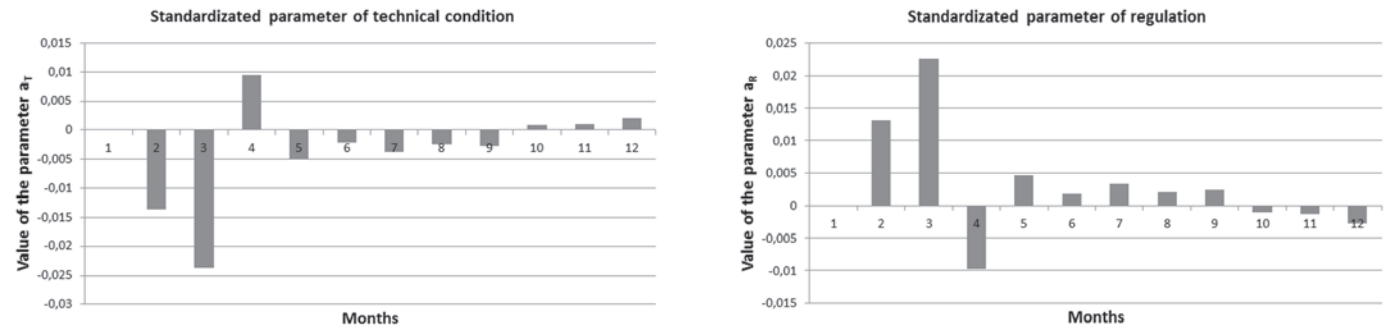

Fig. 1. Changes of normalized parameter of technical and regulation condition of bus no. 301

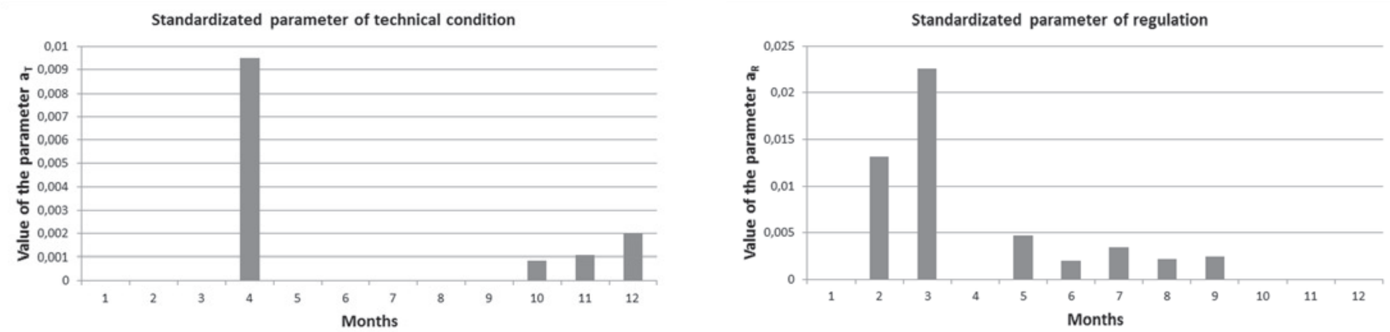

Fig. 2. Changes of normalized parameter of technical and regulation condition of bus no. 301 after eliminating negative values

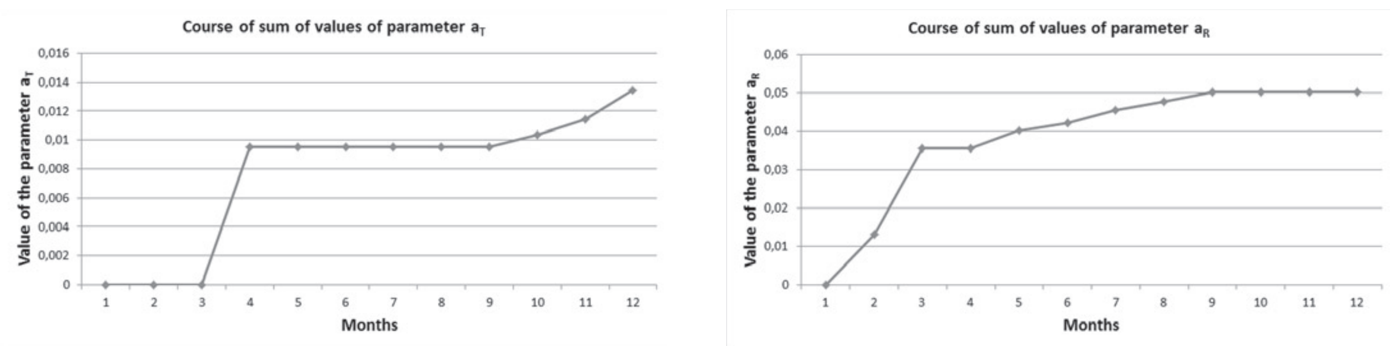

Fig. 3. Course of the sum of values of normalized parameter of technical and regulation condition of bus no. 301

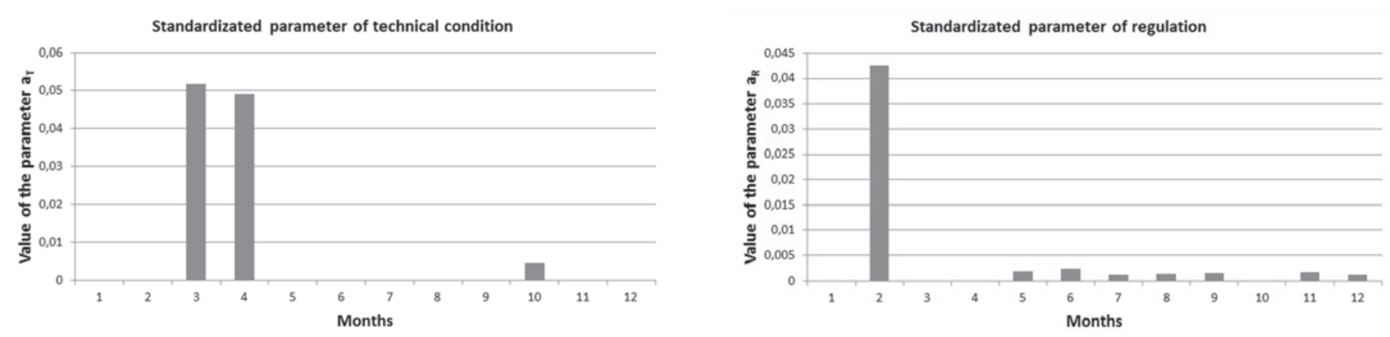

Fig. 4. Changes of normalized parameter of technical and regulation condition of bus no. 303 after eliminating negative values

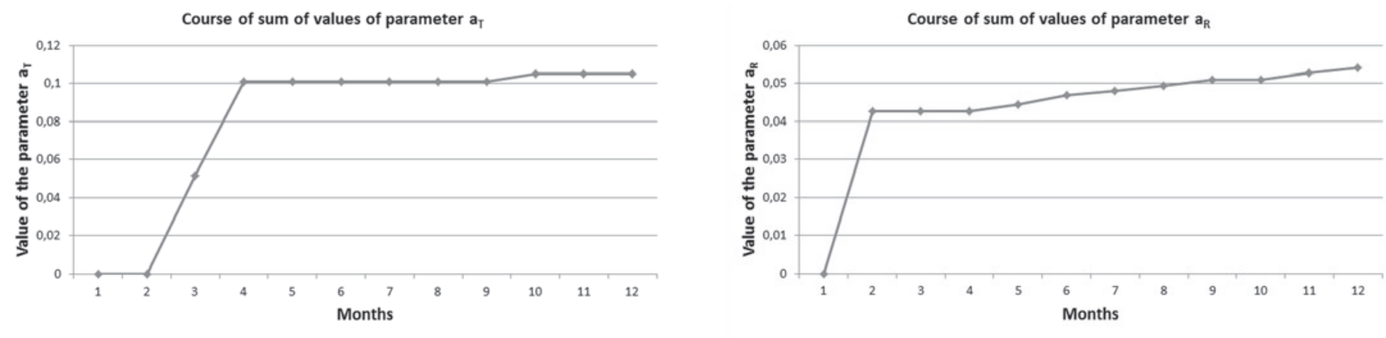

Fig. 5. Course of the sum of values of normalized parameter of technical and regulation condition of bus no. 303

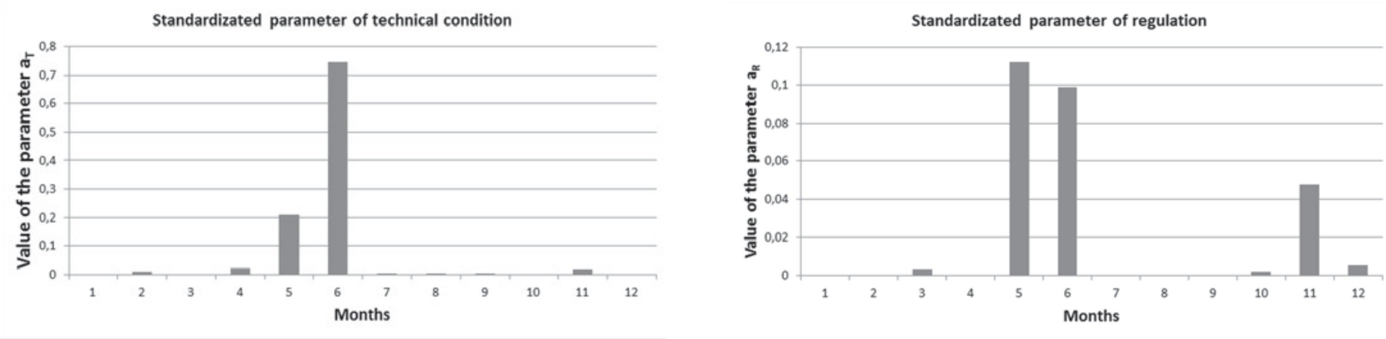

Fig. 6. Changes of normalized parameter of technical and regulation condition of bus no. 304 after eliminating negative values

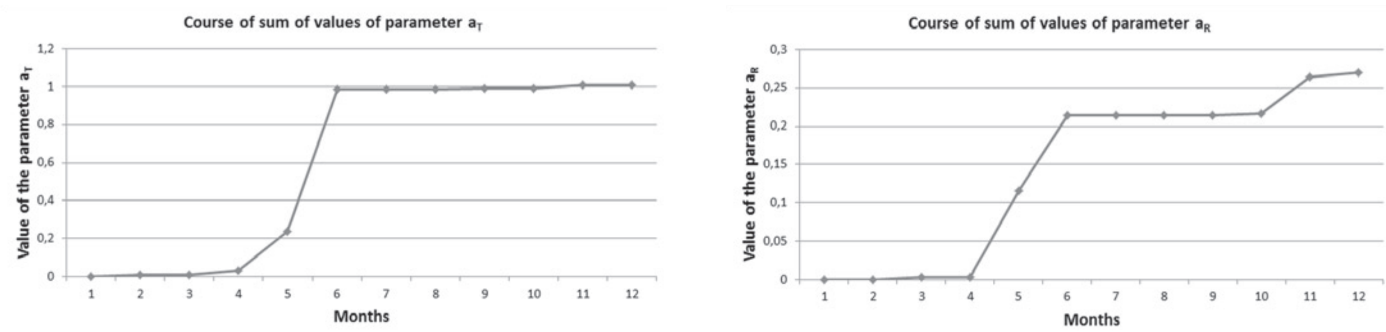

Fig. 7. Course of the sum of values of normalized parameter of technical and regulation condition of bus no. 304

Table 10. Procedure of calculating technical and regulation condition parameters

	bus no. 301	bus no. 303	bus no. 304
a_T average	0,0027	0,0263	0,1120
a_T sum	0,0134	0,1053	1,0081
a_R average	0,0063	0,0060	0,0385
a_R sum	0,0501	0,0541	0,2698

Using data from Tab. 7 and 8 and equations 1–6, increases of technical condition described by parameter a_T and operating (regulation) condition described by parameter a_R were calculated.

Algorithm of calculating a_T (based on equation 4) and a_R (based on equation 6) are presented in Tab. 9

Subsequently, Σa_T expressing degree of object wear as well as Σa_R expressing degree of proper operation ability loss are determined.

Results of course of changes of normalized parameters a_R and a_T for bus no. 301 are presented on Fig. 1 and 2, for bus no. 303 and Fig. 4 and for bus no. 304 on Fig. 6. Courses of sums of these parameters are presented on Fig. 3, 5 and 7 respectively. Charts do not contain first month, as a_R and a_T parameters are impossible to determine (initial value of D_K and U signals is unknown).

The buses have mileage of – bus no. 1 – 241 392 km, bus no. 2 – 239 829 km, bus no. 3 – 244 003 km. Expert may therefore assume that the buses are already run in. Hence, no possibility exist to improve technical condition of analyzed buses (in case where bus would be in running in process, negative values of a_T and a_R should also be considered). Therefore assumption is made that a_T and a_R parameters may not be negative (Fig. 1). Hence the negative values are considered 0. The above chart assumes the following form (Fig. 2).

Basing on data from Tab. 10, expert obtains complex information on operating (a_R) and technical (a_T) condition of the object. Sum of a_T is information on object wear and sum of a_R is information on change of regulation susceptibility. Therefore assumption can be made that best technical condition (i.e. the least worn) is that of bus no. 301. The greatest potential of operating (regulation) condition is also that of bus no. 301. The above conclusion was verified by 20 experts (Tab. 3).

Such approach allows for simple qualification of objects to further exploitation or to service.

5. Summary

Exploitation research activity is conducted in the process of object exploitation in order to determine its current and future operating and technical condition. In advanced and complex technical objects, multiple research methods are applied simultaneously, each based on data in different form (determined signals, probabilistic, heuristic). [4, 5, 8, 9, 12, 13, 16, 18, 21, 25, 26, 29]

Assumption of innovatory method of using diagnostic data (presented in form of points) was presented in the article. For each change of signal (depending on its value and moment of occurrence) proper amount of points set by the experts is assigned. In previous diagnostic method, points are summed and, subsequently, range to which the object belong is determined as well as its condition and extent of its exploitation [22].

This method is versatile and may be applied to any technical object (bus, helicopter, aircraft). The method requires itemization of signals connected to analyzed object and signals connected to its environment and, subsequently, expressing these signals in form of points using proper weights. This activity is performed by expert or team of experts. Subsequently, signals in form of points are used to determine technical and operating condition parameters (equation 4, 6) [3, 6, 7, 12, 13, 14, 15, 19] from coupled interaction equations [1, 2, 3, 6, 12, 13]. This allows for constant control of technical and operating condition of the object during its exploitation. The described method might prove very useful, as global exploitation condition is unequivocally presented using a_R and a_T parameters and thus allows to predict how the object should be exploited and when should it be serviced (repaired, overhauled).

The article was created during realization of young PhDs scholarship, granted from project "Podniesienie potencjału uczelni wyższych jako czynnik rozwoju gospodarki opartej na wiedzy" implemented by Białystok Technical University as a part of Operational Programme Human Capital 2007-2013, financed by European Social Fund and National Budget.

References

1. Ashby R. W. Wstęp do cybernetyki. Warszawa: PWN, 1963.
2. Bukowski L. Prognozowanie niezawodności i bezpieczeństwa systemów zautomatyzowanych, Materiały XXXI Szkoły Niezawodności, Szczyrk 2003.
3. Cempel C. Teoria i inżynieria. Poznań: Wydawnictwo Naukowe Instytutu Technologii Eksploatacyjnej PIB, 2006.
4. Cempel C, Natke H G. Damage Evolution and Diagnosis in Operating Systems. Safety Evaluation Based on Identification Approaches Related to Time-Variant and Nonlinear Structures. Springer 1993: 44-61.
5. Filipczyk J. Faults of duty vehicles in the aspects of securing safety. Transport Problems 2011, Vol. 6; 1: 105-110.
6. Grądzki R, Lindstedt P. Determination of parameters of a technical and control states of the bus engine by using its discretized operation information. Journal of KONBIN 2013; Z.2: 97-108.
7. Günther H. Diagnozowanie silników wysokoprężnych. Warszawa: Wydawnictwo Komunikacji i Łączności, 2006.
8. Jardine A K S, Lin D, Banjevic D. A review on machinery diagnostics and prognostics implementing condition-based maintenance. Mechanical Systems and Signal Processing 2006, Vol 20; 7: 1483–1510.
9. Jaźwiński J, Klimaszewski S, Żurek J. Metoda prognozowania stanu obiektu w oparciu o badania kontrolne. Zagadnienia Eksploatacji Maszyn 2003, Vol. 38; 2: 33-44.
10. Jaźwiński J, Szpytko J. Zasady wyznaczania zespołu ekspertów w badaniach niezawodności i bezpieczeństwa urządzeń technicznych. XXXIV Zimowa Szkoła Niezawodności PAN „Niekonwencjonalne metody oceny trwałości i niezawodności". Szczyrk 2006: 157–167.
11. Jaźwiński J, Żurek J. Modelowanie i identyfikacja systemu „Człowiek−obiekt techniczny−otoczenie" w aspekcie jego niezawodności i gotowości. XIV Zimowa Szkoła Niezawodności PAN „Człowiek–obiekt techniczny–otoczenie. Problemy niezawodności i utrzymania ruchu". Szczyrk 1986.
12. Lindstedt P. Reliability and its relation to regulation and diagnostics in the machinery exploitation systems. Journal of KONBiN 2006, Vol. 1; 2: 317-330.
13. Lindstedt P. The Method of complex worthness assessment of an engineering object in the process of its use and service. Solid State Phenomena 2009; 144: 45-52.
14. Lindstedt P. The effect of pilot's work quality on technical condition of propeller engine bearing. Journal of Vibroenginering 2006, 8(2): 6-10.
15. Lindstedt P, Sudakowski T. The Method of Assessment of Suitability of the Bearing System Based on Parameters of Technical and Adjustment State. Solid State Phenomena Mechatronic systems and materials V 2013; 73-78.
16. Madej H, Filipczyk J. The methods of assessment of car technical condition regarding ennironmental protection. Journal of KONES 2009; 16(2): 103-108.
17. Nowakowski T. Reliability Model of Combined Transportation System. Probabilistic Safety Assessment and Management. Springer 2004: 2012-2017.
18. Sarangaa H, Knezevicb J. Reliability prediction for condition-based maintained systems. Reliability Engineering & System Safety. Elsevier 2001; 71(2): 219–224.
19. Smalko Z. Podstawy eksploatacji technicznej pojazdów. Warszawa: Oficyna Wydawnicza PW, 1998.
20. Söderström T, Stoica P. Identyfikacja systemów. Warszawa: PWN, 1997.
21. Sudakowski T. Premises of operational method of calculation of reliability of machines on the base of parametric and momentary symptoms of damage. Acta mechanica et automatica 2009; 3(4): 73-79.
22. Szawłowski S. Przegląd kontrolny ASPA w systemie obsługiwania śmigłowca pokładowego SH-2G, 8 Międzynarodowa konferencja AIRDIAG Warszawa 27-28.10.2005.

23. Szczepaniak C. Podstawy modelowania sytemu człowiek – pojazd – otoczenie. Warszawa: PWN, 1999.
24. Szpytko J, Kocerba A. Metodyka kształtowania niezawodności eksploatacyjnej środka transportu. Methodology of exploitation reliability shaping of transport device. XXXV Zimowa Szkoła Niezawodności PAN „Problemy niezawodności systemów”. Szczyrk 2007:483–492.
25. Szpytko J, Kocerba A. Przyczynowo-skutkowa metodyka oceny stanu technicznego środków transportu. XXXIII Zimowa Szkoła Niezawodności PAN „Metody badań przyczyn i skutków uszkodzeń”. Szczyrk 2005.
26. Tylicki H, Żółtowski B. Zmiana stanu maszyny w procesie eksploatacji. XXXIII Zimowa Szkoła Niezawodności PAN „Metody badań przyczyn i skutków uszkodzeń”. Szczyrk 2005.
27. Woropay M, Muślewski Ł, Ślęzak M, Szubartowski M. Assessment of the impact of human on safety of transportation system operation. Journal of KONBiN 2013; (1)25: 97-106.
28. Zając M. Wykorzystanie badań ankietowych do oszacowania niezawodności systemu transportu intermodalnego. XXXIV Zimowa Szkoła Niezawodności PAN „Niekonwencjonalne metody oceny trwałości i niezawodności”. Szczyrk 2006.
29. Żółtowski B. Metody diagnostyki technicznej w ocenie destrukcji maszyn. XXXV Zimowa Szkoła Niezawodności PAN „Problemy niezawodności systemów”. Szczyrk 2007.

Rafał GRĄDZKI
Bialystok University of Technology
Faculty of Mechanical Engineering
ul. Wiejska 45C, 15-351 Bialystok, Poland

Paweł LINDSTEDT
Air Force Institute of Technology
ul. Księcia Bolesława 6A, 01–494 Warsaw, Poland

E-mails: r.gradzki@pb.edu.pl, sekretariat.naukowy@itwl.pl

Article citation info:
GLOWACZ A, GLOWACZ W, GLOWACZ Z. Recognition of armature current of DC generator depending on rotor speed using FFT, MSAF-1 and LDA. Eksploatacja i Niezawodnosc – Maintenance and Reliability 2015; 17 (1): 64–69.

Adam GLOWACZ
Witold GLOWACZ
Zygfryd GLOWACZ

RECOGNITION OF ARMATURE CURRENT OF DC GENERATOR DEPENDING ON ROTOR SPEED USING FFT, MSAF-1 AND LDA

ROZPOZNAWANIE SYGNAŁÓW PRĄDU TWORNIKA GENERATORA PRĄDU STAŁEGO W ZALEŻNOŚCI OD PRĘDKOŚCI OBROTOWEJ WIRNIKA Z ZASTOSOWANIEM FFT, MSAF-1 I LDA*

Recognition of states of electrical systems is very important in industrial plants. Article describes a recognition method of early fault detection of DC generator. The proposed approach is based on an analysis of the patterns. These patterns are the armature currents of selected electrical machine. Information contained in signals of armature current is depending on generator state. Researches were carried out for four states of generator with the use of Fast Fourier Transform (FFT), method of selection of amplitudes of frequencies (MSAF-1) and Linear Discriminant Analysis (LDA). The results of analysis show that the method is efficient and can be used to protect DC generators. This method was verified with the aid of acoustic signals recognition method.

***Keywords**: fault detection, pattern recognition, armature current, DC generator.*

Rozpoznawanie stanów układów elektrycznych jest bardzo ważne w zakładach przemysłowych. W artykule opisano metodę rozpoznawania stanów przedawaryjnych generatora prądu stałego. Proponowane podejście jest oparte na badaniu wzorców. Wzorce te są prądami twornika wybranej maszyny elektrycznej. Informacja zawarta w sygnałach prądu twornika jest zależna od stanu generatora. Przeprowadzono badania dla czterech stanów generatora z zastosowaniem FFT, metody wyboru amplitud częstotliwości (MSAF-1) i liniowej analizy dyskryminacyjnej (LDA). Wyniki analizy pokazują, że metoda jest skuteczna i metoda może być stosowana do ochrony generatorów prądu stałego. Metoda została zweryfikowana za pomocą metody rozpoznawania sygnałów akustycznych.

***Słowa kluczowe**: detekcja uszkodzenia, rozpoznawanie wzorców, prąd twornika, generator prądu stałego.*

1. Introduction

Nowadays rotating machines are more complex than 20 years ago. Electrical generators deteriorate over time gradually. Condition of machines can be recovered through appropriate maintenance activities. In recent years, many signal processing methods were applied for diagnostics of electrical devices and machines [6, 7, 10, 11, 41]. Most of them were based on patterns recognition. Development of diagnostic systems is important to guarantee quality of machines and materials [2, 8, 11-14, 27, 29, 30, 33, 35, 36, 40, 44]. Diagnostic of electric machines can be based on various signals such as: electric, acoustic, thermal, magnetic or vibroacoustic [6, 8-11, 15, 16, 42, 43]. An armature current is a diagnostic signal. It can be measured by measuring card and LEM current sensor. Armature current can be used to diagnose type of fault. The analysis of armature current of Direct Current generator can decrease the costs of maintenance of these types of generators in the industrial plant and wind plants. It can also lead to the more modern diagnostic systems.

In this paper authors propose early fault detection technique. This technique uses method of selection of amplitudes of frequencies (MSAF-1) and Linear Discriminant Analysis to classify feature vector.

2. Recognition of armature current of Direct Current generator

Recognition of armature current is not an easy problem. The database of patterns is needed to solve this problem. This database is used in a pattern creation process. Second database of test samples is needed in an identification process. These databases should be prepared properly.

The process of recognition of armature current can be defined as two processes: pattern creation process and identification process. First of them starts with registering of armature current. Signal of armature current is converted to the TXT file with data. After that TXT file is split into small samples of current. The next step is selection of amplitudes of frequencies. In this purpose authors propose new method described in chapter 2.2. The method gives us 1 feature vector from 1 sample. At the end of the pattern creation process Linear Discriminant Analysis is used to create patterns (Fig. 1).

The identification process is based on the same methods as previous process. Feature vectors are calculated by the same processing methods. After that feature vectors are compared by Linear Discriminant Analysis.

(*) Tekst artykułu w polskiej wersji językowej dostępny w elektronicznym wydaniu kwartalnika na stronie ***www.ein.org.pl***

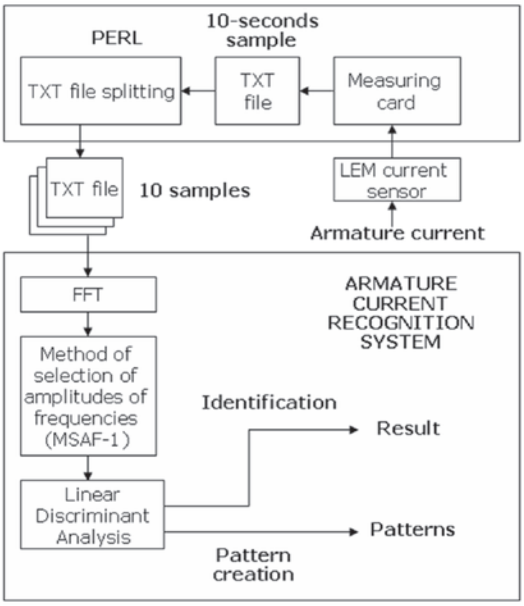

Fig. 1. Process of recognition of armature current of DC generator with the use of method of selection of amplitudes of frequencies and Linear Discriminant Analysis

2.1. Measurement of armature current

Direct current generator has been loaded by an external resistance. This armature current was measured by LEM current sensor and measuring card. Then signal of armature current was converted to the text file. After that TXT file was split into small samples of current. Each sample had duration time of 1 second. Sampling frequency of measuring card was 20000 Hz, so sample contained 20000 values. Spectrum of frequency of armature current was presented in Figure 2.

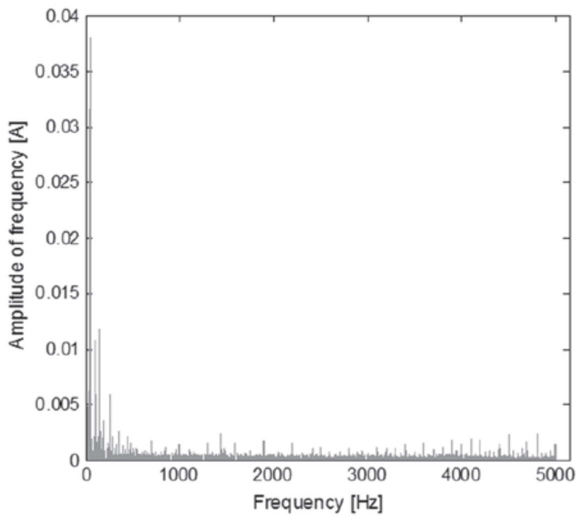

Fig. 2. Amplitudes of frequencies of armature current depending on frequency for faultless DC generator with rotor speed 600 rpm

2.2. Method of selection of amplitudes of frequencies

Proposed method of selection of amplitudes of frequencies (MSAF-1) was based on differences between amplitudes of various states of DC generator. The armature current was dependent on the state, rotor speed and construction of generator.
Steps of MSAF-1 are following:

1) Calculate spectrum of frequency for each state of DC generator.
2) Calculate differences between states of DC generator: **a-b**, **a-c**, **a-d**, **b-c**, **b-d**, **c-d**, where **a** denoted the spectrum of armature current of faultless DC generator, **b** denoted the spectrum of armature current of DC generator with 3 shorted rotor coils, **c** denoted the spectrum of armature current of DC generator with 6 shorted rotor coils, **d** denoted the spectrum of armature current of DC generator with broken rotor coil.
3) Calculate absolute values of differences between states of DC generator: |**a-b**|, |**a-c**|, |**a-d**|, |**b-c**|, |**b-d**|, |**c-d**|.
4) Select 8 maximal amplitudes of the frequencies for each difference between states of DC generator: $\max_1|\mathbf{a-b}|$, ..., $\max_8|\mathbf{a-b}|$, ..., $\max_1|\mathbf{c-d}|$,..., $\max_8|\mathbf{c-d}|$ and determine corresponding frequencies.
5) Find common frequencies (1-8) and then determine for these frequencies the amplitudes of spectrum for each state of DC generator.

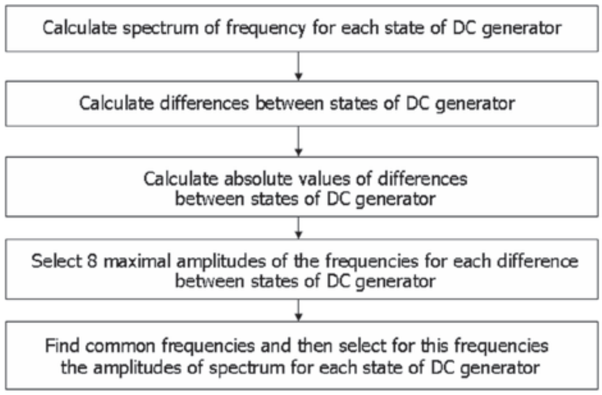

Fig. 3. Block scheme of MSAF-1

The method of selection of amplitudes of frequencies of DC generator in form of block scheme has been presented in Fig. 3.

Differences between spectra for 4 states of DC generator with rotor speed 600 rpm were presented in Figures 4–6. Selection of common amplitudes of frequencies for 4 states of DC generator with rotor speed 600 rpm was presented in Figure 7.

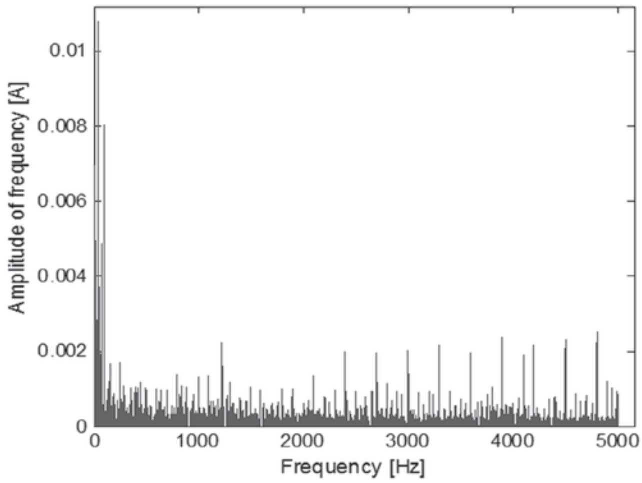

Fig. 4. Difference between frequency spectrum of armature current of faultless DC generator and DC generator with 3 shorted rotor coils (|a-b|) with rotor speed 600 rpm

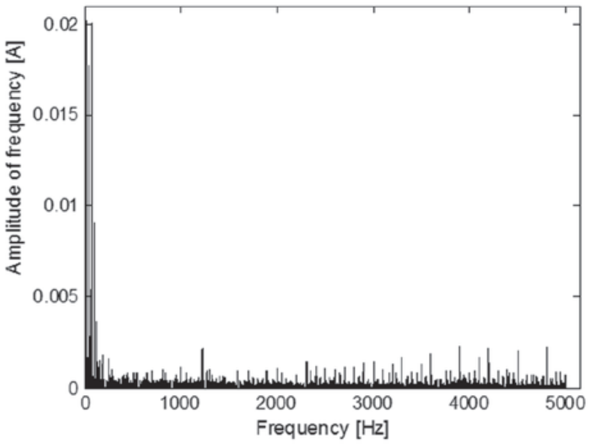

Fig. 5. Difference between frequency spectrum of armature current of faultless DC generator and DC generator with 6 shorted rotor coils (|a-c|) with rotor speed 600 rpm

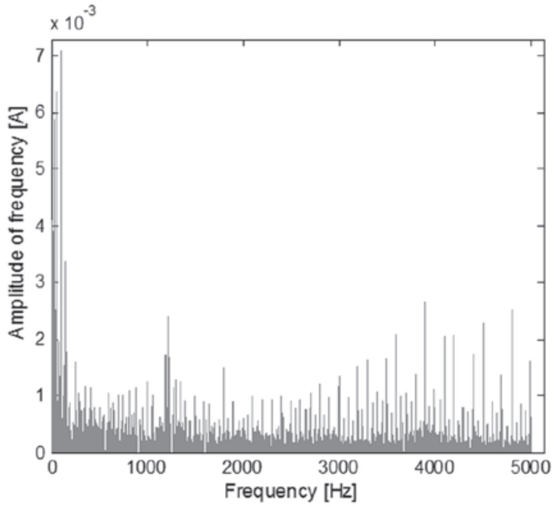

Fig. 6. Difference between frequency spectrum of armature current of faultless DC generator and DC generator with broken coil (|a-d|) with rotor speed 600 rpm

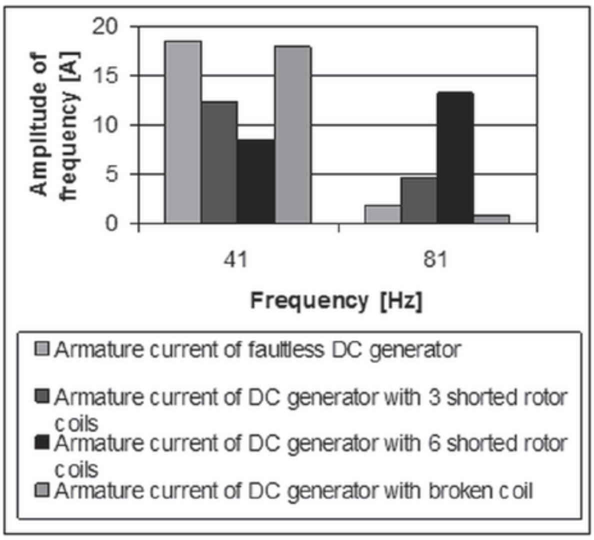

Fig. 7. Selection of common amplitudes of frequencies for 4 states of DC generator with rotor speed 600 rpm (41 and 81 Hz)

Selected amplitudes of frequencies formed the feature vector used by Linear Discriminant Analysis.

2.3. Linear Discriminant Analysis

There are many methods for data processing and feature vectors classification [3–5, 17–26, 28, 31, 32, 34, 37–39, 41, 45–48]. The feature vectors are processed by Linear Discriminant Analysis (LDA). LDA maximizes the ratio (quotient) of between-class variance to the within-class variance. Maximal ratio guarantees separability between the classes. Data sets and the test sets should be formulated appropriately at the beginning of classification. Training sets are defined as $set_1,\ldots, set_k$. Next the mean for each training set and mean of all training sets are computed.

The means of sets $set_1,\ldots, set_k$ are defined as $\mu_1,\ldots, \mu_k$. Whereas the mean of all training sets is called μ. This mean is given by equation 1:

$$\mu = p_1 \times \mu_1 + \ldots + p_k \times \mu_k \tag{1}$$

where $p_1,\ldots,p_k$ are the a priori probabilities of the classes.

Next a linear combination of features is created by Linear Discriminant Analysis. This method uses within-class scatter matrix and between-class scatter matrix [1, 32]. Both matrices are used to formulate criteria for separability of the classes. Within-class scatter matrix is defined as follows:

$$W = \sum_{k=1}^{c} \sum_{i=1}^{N_k} (x_i^k - \mu_k)(x_i^k - \mu_k)^T \tag{2}$$

where μ_k denotes the mean of class k, x_i^k is the sample with the index i of class k, c denotes the number of classes of training sets, and N_k is the number of samples of class k [1, 31].

Between-class scatter matrix is expressed by formula:

$$B = \sum_{k=1}^{c} (\mu_k - \mu)(\mu_k - \mu)^T \tag{3}$$

where μ denotes the mean of all training sets, $\mathbf{x}$, $\boldsymbol{\mu}$ vectors of dimensions equal to the selected number of common frequencies.

The ratio of between-class scatter matrix determinant to the within-class scatter matrix determinant is the criterion of Linear Discriminant Analysis. In this method it is essential to maximize the ratio ($Det|B|$ / $Det|W|$) [31]. The axes of the transformed space are defined by the solution obtained by maximizing the ratio ($Det|B|$ / $Det|W|$).

3. The results of recognition of armature current

Measuring card and LEM current sensor were used to record armature current signals. Parameters of current signal were: sampling frequency - 20000 Hz, format - TXT. Operation parameters of DC generator with rotor speed 600 rpm were following:

- faultless DC generator: U_a =51 V, I_a = 70 A, U_e = 159.1 V, I_e = 2.5 A,
- DC generator with 3 shorted rotor coils: U_a =50.5 V, I_a = 71.5 A, U_e = 160.8 V, I_e = 2.5 A, I_{sc} = 58 A,
- DC generator with 6 shorted rotor coils: U_a =50 V, I_a = 70.5 A, U_e = 161,2 V, I_e = 2.5 A, I_{sc} = 138 A,

– DC generator with broken coil: U_a =50.5 V, I_a = 70 A, U_e = 163.3 V, I_e = 2.5 A,

where U_a - armature voltage of DC generator, I_a - armature current of DC generator, U_e - excitation voltage of DC generator, I_e - excitation current of DC generator, I_{sc} - current of the short-circuit.

Groups of three and six loops rotor coils were shorted with the use of resistance R_{sc} = 0.085 mΩ. This resistance was connected with DC generator to protect the rotor windings. Investigations were carried out for four current signals: armature current of faultless DC generator, armature current of generator with 3 shorted rotor coils, armature current of generator with 6 shorted rotor coils (Fig. 8), armature current of generator with broken coil. 32 training samples with a duration of one second were used in the pattern creation process. 128 test samples with a duration of one second were used in the identification process.

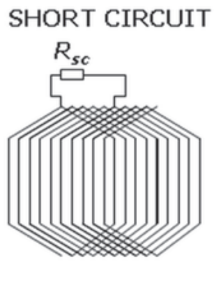

Fig. 8. Scheme of rotor windings of DC generator with 6 shorted coils

Armature current recognition efficiency determines the relationship:

$$ACRE = \frac{NoWRTS}{NoATS}100\% \quad (4)$$

where: $ACRE$ – armature current recognition efficiency, $NoWRTS$ – number of well recognized test samples, $NoATS$ – number of all test samples.

Researches were carried out for DC generator with rotor speed 700 rpm, 600 rpm, 500 rpm, 400 rpm. Armature current recognition efficiency depending on the rotations of rotor is presented in Figures 9 and 10.

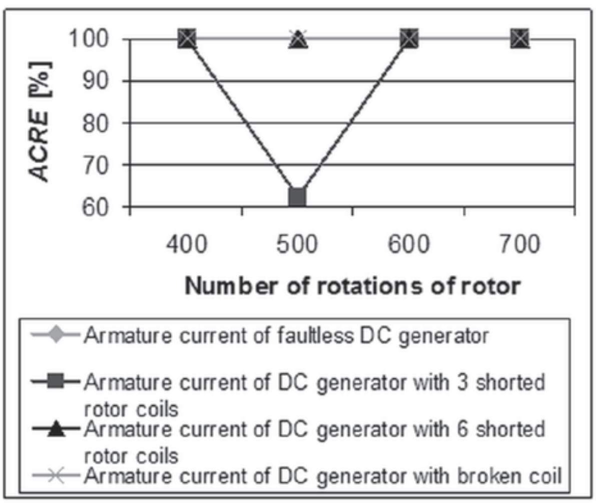

Fig. 9. Armature current recognition efficiency depending on the rotor speed of DC generator

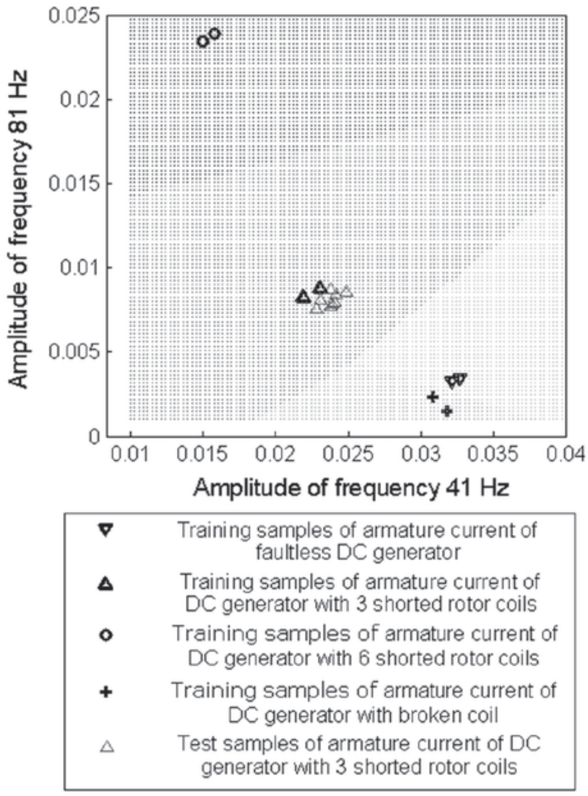

Fig. 10. Recognition of test samples of armature current of DC generator with 3 shorted rotor coils with rotor speed 600 rpm

Armature current recognition efficiency of faultless generator was 100%. 8 of 8 test samples were classified as faultless generator. The samples were prepared on the basis of measurements and authors knew that these 8 test samples were generated by faultless generator. Armature current recognition efficiency of generator with 3 shorted rotor coils was 62.5-100%. Armature current recognition efficiency of generator with 6 shorted rotor coils was 100%. Armature current recognition efficiency of generator with broken coil was 100%. Results for the two-element vectors were good. If the system selects the number of common amplitudes of frequency equal 1-8, then LDA will process 1-8 element vectors.

4. Conclusion

In this paper authors proposed technique and a system of recognition of armature current of DC generator. Researches involving the application of signal processing methods to armature current recognition has been carried out for faultless DC generator and faulty DC generator.

The experiments proved that the methods such as MSAF-1, FFT, and LDA were sufficient enough for diagnostics of DC generator. Armature current recognition efficiency of DC generator was 100% for rotor speed 400 rpm, 600 rpm, 700 rpm. When the rotor speed was equal 500, then armature current recognition efficiency of DC generator was 62.5–100%.

Advantage of this method over acoustic signal recognition is that the armature current is easier to process. Further researches will focus on implementations of new processing methods and cooperation of various diagnostic signals.

Acknowledgments:
This work has been partly supported by AGH University of Science and Technology, grant nr 11.11.120.612 (Adam Glowacz).
This work has been partly supported by AGH University of Science and Technology, grant nr 11.11.120.815 (Witold Glowacz).
This work has been partly supported by AGH University of Science and Technology, grant nr 11.11.120.354 (Zygfryd Glowacz).

References

1. Balakrishnama S, Ganapathiraju A. Linear Discriminant Analysis - A brief tutorial. Presentation, Institute for Signal and Information Processing Department of Electrical and Computer Engineering Mississippi State University.
2. Krolczyk G, Legutko S, Stoic A. Influence of cutting parameters and conditions onto surface hardness of Duplex Stainless Steel after turning process. Tehnicki Vjesnik-Technical Gazette 2013; 20 (6): 1077-1080.
3. Glowacz A. Diagnostics of Synchronous Motor Based on Analysis of Acoustic Signals with the use of Line Spectral Frequencies and K-nearest Neighbor Classifier. Archives of Acoustics 2014; 39 (2): 189-194.
4. Czopek K. Cardiac Activity Based on Acoustic Signal Properties. Acta physica polonica A 2012; 121 (1A): A42-A45.
5. Dudek-Dyduch E, Tadeusiewicz R, Horzyk A. Neural network adaptation process effectiveness dependent of constant training data availability. Neurocomputing 2009; 72 (13-15): 3138-3149.
6. Dudzikowski I, Ciurys M. Analysis of operation of a car starter with BLDC motor. Przeglad Elektrotechniczny 2010; 86 (4): 166-169.
7. Florkowski M, Furgal J, Kuniewski M. Impact of transformers from overvoltages transferred through windings. Przeglad Elektrotechniczny 2012; 88 (5A): 104-107.
8. Glowacz A, Glowacz W. Dc machine diagnostics based on sound recognition with application of FFT and fuzzy logic. Przeglad Elektrotechniczny 2008; 84 (12): 43-46.
9. Glowacz A, Glowacz A, Korohoda P. Recognition of Monochrome Thermal Images of Synchronous Motor with the Application of Binarization and Nearest Mean Classifier. Archives of Metallurgy and Materials 2014; 59 (1): 31-34.
10. Glowacz A, Glowacz A, Glowacz Z. Diagnostics of Direct Current generator based on analysis of monochrome infrared images with the application of cross-sectional image and nearest neighbor classifier with Euclidean distance. Przeglad Elektrotechniczny 2012; 88 (6): 154-157.
11. Glowacz W. Diagnostics of Induction motor based on Spectral Analysis of Stator Current with Application of Backpropagation Neural Network. Archives of Metallurgy and Materials 2013; 58 (2): 559-562.
12. Stepien K. Research on a surface texture analysis by digital signal processing methods. Tehnicki Vjesnik-Technical Gazette 2014; 21 (3): 485-493.
13. Gogola D, Krafcík A, Strbak O, Frollo I. Magnetic Resonance Imaging of Surgical Implants Made from Weak Magnetic Materials. Measurement Science Review 2013; 13 (4): 165-168.
14. Smolnicki T, Stanco M, Pietrusiak D. Distribution of loads in the large size bearing – problems of identification. Tehnicki Vjesnik-Technical Gazette 2013; 20 (5): 831-836.
15. Golebiowski L, Golebiowski M, Mazur D. Unscented kalman filter in rotor diagnostic testing of the asynchronous motor. Przeglad Elektrotechniczny 2011; 87 (8): 48-52.
16. Golebiowski L, Golebiowski M, Mazur D. Controlling of the 1-and 3-phase power factor correction (PFC) rectifiers, Przeglad Elektrotechniczny 2011; 87 (8): 53-58.
17. Gorski P, Morzynski L. Active Noise Reduction Algorithm Based on NOTCH Filter and Genetic Algorithm. Archives of Acoustics 2013; 38 (2): 185-190.
18. Hachaj T, Ogiela MR. Application of neural networks in detection of abnormal brain perfusion regions. Neurocomputing 2013; 122 (Special Issue): 33-42.
19. Hachaj T, Ogiela MR. A system for detecting and describing pathological changes using dynamic perfusion computer tomography brain maps. Computers in Biology and Medicine 2011; 41 (6): 402-410.
20. Valis D, Zak L, Walek A, Pietrucha-Urbanik K. Selected mathematical functions used for operation data information. 22nd Annual Conference on European Safety and Reliability (ESREL), Amsterdam, Netherlands, Sep 29-Oct 02, Safety, Reliability and Risk Analysis: Beyond the Horizon 2014, 1303-1308.
21. Jaworek J, Augustyniak P. A cardiac telerehabilitation application for mobile devices. IEEE Conference on Computing in Cardiology 2011; Hangzhou, China: 241-244.
22. Glowacz A. Diagnostics of DC and Induction Motors Based on the Analysis of Acoustic Signals. Measurement Science Review 2014; 14 (5): 257-262.
23. Kantoch E, Smolen M, Augustyniak P, Kowalski P. Wireless Body Area Network System based on ECG and Accelerometer Pattern. IEEE Conference on Computing in Cardiology 2011; Hangzhou; China: 245-248.
24. Kmiec M, Glowacz A, Dziech A. Towards robust visual knife detection in images: active appearance models initialised with shape-specific interest points. Multimedia communications, services and security, MCSS, Book Series: Communications in Computer and Information Science 2012, 287, 148–158.
25. Zajdel M, Filipowicz B. Exit selection process during crowd evacuation, modelled on the cockroach emergent behaviour. Bulletin of the Polish Academy of Sciences-Technical Sciences 2014; 62 (3): 557-563.
26. Korohoda P, Dabrowski A. Wavelet-like decomposition stage with windowed filters defined for the Discrete Trigonometric Transforms (DTTs). Przeglad Elektrotechniczny 2012; 88 (6): 30-35.
27. Kulesza G, Panek P, Zieba P. Silicon Solar Cells Efficiency Improvement by the Wet Chemical Texturization in the HF/HNO3/diluent solution. Archives of Metallurgy and Materials 2013; 58 (1): 291-295.
28. Lin DF, Chen PH, Williams M. Measurement and Analysis of Current Signals for Gearbox Fault Recognition of Wind Turbine. Measurement Science Review 2013; 13 (2): 89-93.
29. Kozlowski M, Choromanski W. Dynamics simulation studies on the electric city car with an electromechanical differential and the rear wheels drive. Bulletin of the Polish Academy of Sciences-Technical Sciences 2013; 61 (3): 661-673.

30. Koscielny JM, Syfert M. Application properties of methods for fault detection and isolation in the diagnosis of complex large-scale processes. Bulletin of the Polish Academy of Sciences-Technical Sciences 2014; 62 (3): 571-582.
31. Martinez AM, Kak AC. PCA versus LDA IEEE Transactions on Pattern Analysis and Machine Intelligence 2001; 23 (2): 228-233.
32. MathWorks – MATLAB and SimuLink for Technical Computing 2014; www.mathworks.com.
33. Mazurkiewicz D. Problems of identification of strength properties of rubber materials for purposes of numerical analysis: a review. Archives of Civil and Mechanical Engineering 2010; 10 (1): 69-84.
34. Pleban D, Piochowicz J, Kosala K. The Inversion Method in Measuring Noise Emitted by Machines in Opencast Mines of Rock Material. International Journal of Occupational Safety and Ergonomics 2013; 19 (2): 321-331.
35. Pietrzak K, Olesinska W, Kalinski D, Strojny-Nedza A. The relationship between microstructure and mechanical properties of directly bonded copper-alumina ceramics joints. Bulletin of the Polish Academy of Sciences-Technical Sciences 2014; 62 (1): 23-32.
36. Kulka Z. Advances in Digitization of Microphones and Loudspeakers. Archives of Acoustics 2011; 36 (2): 419-436.
37. Orzechowski T, Izworski A, Tadeusiewicz R, Chmurzynska K, Radkowski P, Gatkowska I. Processing of pathological changes in speech caused by dysarthria. Proceedings of ISPACS 2005, IEEE International Symposium on Intelligent Signal Processing and Communication Systems ISPACS 2005: 49-52.
38. Roj J. Neural Network Based Real-time Correction of Transducer Dynamic Errors. Measurement Science Review 2013, 13 (6), 286-291.
39. Skrodzka EB, Linde BBJ, Krupa A. Effect of Bass Bar Tension on Modal Parameters of a Violin's Top Plate. Archives of Acoustics 2014; 39 (1): 145-149.
40. Barglik J, Smalcerz A, Przylucki R, Dolezel I. 3D modeling of induction hardening of gear wheels. Journal of Computational and Applied Mathematics 2014; Vol. 270: 231-240.
41. Smolen M, Kantoch E, Augustyniak P, Kowalski P. Wearable Patient Home Monitoring Based on ECG and ACC Sensors. 5th European Conference of the International Federation for Medical and Biological Engineering, IFMBE Proceedings 2012; 37: 941-944.
42. Sulowicz M, Borkowski D, Wegiel T, Weinreb K. Specialized diagnostic system for induction motors. Przeglad Elektrotechniczny 2010; 86 (4): 285-291.
43. Szymanski Z. Application of the Magnetic Field Distribution in Diagnostic Method of Special Construction Wheel Traction Motors. Advanced Computer Techniques in Applied Electromagnetics, Book Series: Studies in Applied Electromagnetics and Mechanics, 2008; 30: 449-456.
44. Tokarski T, Wzorek L, Dybiec H. Microstructure and Plasticity of Hot Deformed 5083 Aluminum Alloy Produced by Rapid Solidification and Hot Extrusion. Archives of Metallurgy and Materials 2012; 57 (4): 1253-1259.
45. Trzupek M, Ogiela MR, Tadeusiewicz R. Intelligent image content semantic description for cardiac 3D visualisations. Engineering Applications of Artificial Intelligence 2011; 24 (8): 1410-1418.
46. Tu YQ, Yang HY, Zhang HT, Liu XY. CMF Signal Processing Method Based on Feedback Corrected ANF and Hilbert Transformation. Measurement Science Review 2014; 14 (1): 41-47.
47. Pleban D. Definition and Measure of the Sound Quality of the Machine. Archives of Acoustics 2014; 39 (1): 17-23.
48. Ziolko M, Galka J, Ziolko B, Drwiega T. Perceptual Wavelet Decomposition for Speech Segmentation. 11th Annual Conference of the International Speech Communication Association 2010 (INTERSPEECH 2010), Vols 3 and 4; 2234-2237.

Adam GLOWACZ
Witold GLOWACZ
AGH University of Science and Technology,
Faculty of Electrical Engineering, Automatics, Computer Science and Biomedical Engineering
Department of Automatics and Biomedical Engineering
al. A. Mickiewicza 30, 30-059 Krakow, Poland

Zygfryd GLOWACZ
AGH University of Science and Technology
Faculty of Electrical Engineering, Automatics, Computer Science and Biomedical Engineering
Department of Power Electronics and Energy Control Systems
al. A. Mickiewicza 30, 30-059 Krakow, Poland

E-mails: adglow@agh.edu.pl, wglowacz@agh.edu.pl, glowacz@agh.edu.pl

Article citation info:
CHEN X, XIAO L, ZHANG X, XIAO W, LI J. An integrated model of production scheduling and maintenance planning under imperfect preventive maintenance. Eksploatacja i Niezawodnosc – Maintenance and Reliability 2015; 17 (1): 70–79.

Xiaohui CHEN
Lei XIAO
Xinghui ZHANG
Weixiao XIAO
Junxing LI

AN INTEGRATED MODEL OF PRODUCTION SCHEDULING AND MAINTENANCE PLANNING UNDER IMPERFECT PREVENTIVE MAINTENANCE

MODEL ZINTEGROWANY HARMONOGRAMOWANIA PRODUKCJI I PLANOWANIA OBSŁUGI TECHNICZNEJ W RAMACH NIEPEŁNEJ KONSERWACJI ZAPOBIEGAWCZEJ

For a successful company, machines are always required to work continuously to make more profit in a certain period. However, machines can be unavailable due to the scheduled maintenance activities or unexpected failures. Hence, a model connected production scheduling with maintenance planning for a production line which is composed of multiple machines is developed. Suppose preventive maintenance is imperfect and cannot renew all the machines. Age reduction factor and hazard rate increase factor are introduced to illustrate the imperfect character. Aperiodic preventive maintenance policy is adopted. Replacement as perfect maintenance could restore the machine "as good as new". When and whether to perform replacement is based on a cost-time rate function which is defined to judge whether or not the preventive maintenance is economical. The objective of the joint model is to maximize the total profit which is composed of production value, production cost, maintenance cost (including the preventive maintenance cost and replacement cost), and tardiness cost (which is related to the job sequence and maintenance activities). To optimize the objective, immune clonal selection algorithm is utilized. The proposed model is validated by a numerical example.

Keywords: *aperiodic imperfect preventive maintenance; production scheduling; maintenance planning; immune clonal selection algorithm; total profit.*

Aby firma mogła działać z powodzeniem i przynosić większe zyski w danym okresie czasu, zainstalowane w niej maszyny muszą pracować w sposób nieprzerwany. Niestety, z powodu planowych działań obsługowych lub nieoczekiwanych awarii, maszyny są czasami wyłączane z produkcji. Dlatego też w niniejszym artykule opracowano model łączący harmonogramowanie produkcji z planowaniem obsługi technicznej dla linii produkcyjnej złożonej z wielu maszyn. W pracy założono, że konserwacja zapobiegawcza jest niepełna i nie prowadzi do odnowy wszystkich maszyn. Aby zilustrować jej niepełny charakter, wprowadzono pojęcia czynnika redukcji wieku oraz czynnika wzrostu wskaźnika zagrożenia. Przyjęto politykę nieokresowej konserwacji zapobiegawczej. Wymiana jako forma pełnej konserwacji pozwala na przywrócenie maszyny do stanu "fabrycznej nowości". Kiedy i czy należy przeprowadzić wymianę zależy od funkcji wskaźnika kosztu w stosunku do czasu, który pozwala ocenić, czy konserwacja zapobiegawcza jest opłacalna. Model zintegrowany ma na celu maksymalizację całkowitego zysku, który jest wypadkową wartości produkcji, kosztów produkcji, kosztów obsługi (w tym kosztów konserwacji zapobiegawczej oraz kosztów wymiany) i kosztów nieterminowego zakończenia zadania (ang. lateness, związanych z kolejnością wykonywanych zadań i czynności obsługowych). Aby zoptymalizować opisany cel, wykorzystano algorytm odpornościowej selekcji klonalnej Proponowany model zweryfikowano na przykładzie liczbowym.

Słowa kluczowe: *nieokresowa niepełna konserwacja zapobiegawcza; harmonogramowanie produkcji; planowanie konserwacji; algorytm odpornościowej selekcji klonalnej; całkowity zysk.*

1. Introduction

In manufacturing industry, machines' high availability and reliability is the key factor to make companies competitive in fierce business competition. With the increased machine's usage and age, the machine's reliability and performance could decline and result in failure. The unexpected failures could result in not only catastrophic losses but also security event. Preventive maintenance is an effective way to avoid unexpected failures and keep machine in good condition. It is a bridge connected machine's degradation with production process. The machine's degradation can be described and predicted [26]. But in some cases, a machine may become unavailable because of scheduled maintenance activities or unexpected failures [13]. A good production scheduling makes the company complete more order forms in a certain period. This is critical for company to obtain high profit. In addition, high reliability and short breakdown is the goal for managers.So there is a time-conflict problem between production scheduling and maintenance planning. In addition, in some real manufacturing context, the two activities are employed separately [15]. So how to optimize the two activities simultaneously is a problem.

The integrated problem has aroused researchers' interest for many decades. And many works have been published on this issue. Among the existing works, most of them focus on a single machine [24, 4, 8]. Because the single machine problems could be interpreted as fundamental basis for more complex problems [10, 23]. While in practise, many products should be processed on different machines, so, it is more difficult to build the integrated model of production scheduling and maintenance planning for multi-machine system. Hence, this study develops the jointed model in a multi-machine context.

According to the condition of a machine after maintenance in a repairable system, maintenance can be classified into three types [19, 12]. (1) Perfect maintenance. It can renew the machine. (2) Minimal maintenance. It just restores the machine to its prior state before failure. (3) Imperfect maintenance. It just makes the machine less deteriorated. Most of the current models based on the assumption that the preventive maintenance is perfect [9, 18, 5]. Pham and Wang [19] pointed out not all the machines or systems can be restored to "as good as new" status after maintenance, some actions just make them younger. Moreover, not all the damage is thoroughly recovered [1,16]. Therefore, imperfect preventive maintenance should be considered. Wong et al. [25] stressed preventive maintenance tasks included lubrication, cleaning, inspection, adjustment, alignment and/or replacement. In this study, we redefine replacement and preventive maintenance as two different activities. Replacement is replacing the failed system by a brand new one. It makes the machine "as good as new". Preventive maintenance is imperfect and just undertaken to the key components in a system.

Although many papers optimized preventive maintenance and replacement simultaneously [6, 14, 3], few works considered preventive maintenance, production scheduling and replacement together. Roux et al. [21] considered bloc replacement policy when optimizing preventive maintenance and production scheduling. Ruiz et al. [22] mentioned replacement should be undertaken for longer maintenance, but they didn't illustrate when to implement concretely. Different with the aforementioned works, in this study, we defined a cost-time function which is used to illustrate when to perform replacement. Meanwhile, the function could evaluate whether or not the preventive maintenance is economical.

The objective of the integrated problem is to maximize the total profit. To construct the objective, production value and production cost of each job, tardiness cost which is impacted by job sequence and maintenance cost including preventive maintenance cost and replacement cost, all the factors should be considered. As proved by Qi et al. [20] the joint optimization of production scheduling and preventive maintenance planning is a NP-hard problem. So one issue appears that how to optimize the objective. Traditionally, enumeration method is used to solve the joint problem [2]. However, when the number of jobs is large, it takes much time and space to calculate and get the optima. Therefore, artificial intelligent research algorithm should be utilized. Hence, in this study, immune clonal selection algorithm is used to optimize the integrated problem.

Overall the analysis above, we focus on the joint problem of production scheduling and maintenance planning in a production line composed of multiple machines. We suppose the preventive maintenance is imperfect and the degradation is accelerated after each preventive maintenance. While replacement can renew the machine. When to implement replacement is based on a cost-time rate function which is also used to evaluate the economy of preventive maintenance. The objective of the integrated model is to maximize the total profit which is impacted by job sequence, production cost, production value, tardiness cost and the cost for preventive maintenance and replacement. To solve the complex problem and obtain the optimal, immune clonal selection algorithm is used.

The rest of the paper is organized as follows: Section 2 describes the development of the integrated model. In Section 3, the optimization methodology based on immune clonal selection algorithm is illustrated. Section 4 reports the validation of a numerical example and the results. Finally, Section 5 concludes the paper and proposes the future research.

2. Development of the integrated model

2.1. Assumption, acronyms and notations

A1: Suppose there are many jobs to be processed on different machines. All jobs are predetermined at the beginning of the production horizon and pre-empting one job for another is not allowed.

A2: Suppose, all the machines are new at the beginning of production horizon. For each machine, there is a key system, if the key system failed, the machine cannot work. If the system is renewed, the machine is renewed. If the system is not "as good as new", the machine is not "as good as new". Namely, the machine's degradation is exactly equal to the corresponding key system's degradation.

A3: Even though each system's failure is stochastic, the system's failure rate function can be described. And after preventive maintenance, the machine begins a new degradation process.

A4: Minimal repair is undertaken upon failure and restores the system "as bad as old". The time and cost for minimal repair is negligible. Preventive maintenance is imperfect and just makes the system less deteriorated. Replacement is perfect maintenance.

A5: The unplanned failure can be inspected once it occurs.

A6: Time for the machine's setup and transition is negligible.

A7: The continuum between two sequential preventive maintenance activities is called preventive maintenance cycle.

PM: preventive maintenance	cr: cost-time rate
PMC: the preventive maintenance cost	RC: replacement cost
T_i: the i^{th} preventive maintenance cycle	PMT: the preventive maintenance time
R_f: reliability threshold	λ_i: failure rate in T_i
t: time variable in each T_i	a_i: age reduction factor in T_i
b_i: failure rate increase factor in T_i	RT: replacement time
AIS: artificial immune system	CS: clonal selection
GA: genetic algorithm	ICSA: immune clonal selection algorithm
ST: start time of each job	ET: end time of each job
MTs: the times of maintenance	

2.2. Problem description

Suppose there will be many jobs to be processed on a production line which contains multiple different machines. Usually, once the machine's reliability is lower than the predetermined reliability threshold, then periodic preventive maintenance (PM) is implemented.One issue is how to determine the periodic interval. Traditionally, the periodic interval is determined according to experts' experience. While this kind of periodic PM is irrational especially under imperfect maintenance system. Because "over maintenance" or "less maintenance" would happen and it is uneconomic and high hazardous.

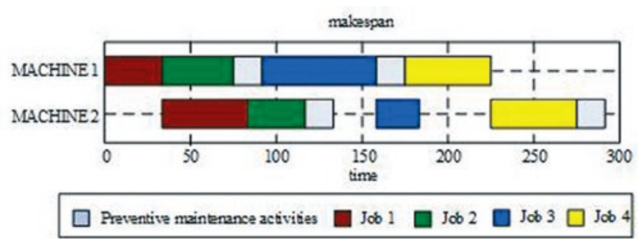

Fig. 1. Information of machine's service and maintenance with considering production and PM simultaneously

Under the imperfect PM policy, machine's reliability could be restored to a better status, but not to the new status. To illustrate the imperfect character, age reduction factor (Malik [11]) and failure rate increase factor (Nakagawa [17]) is introduced. Hence, machine's failure rate is bigger than the former PM cycle. Figure 2 describes the machine's reliability during the production horizon.

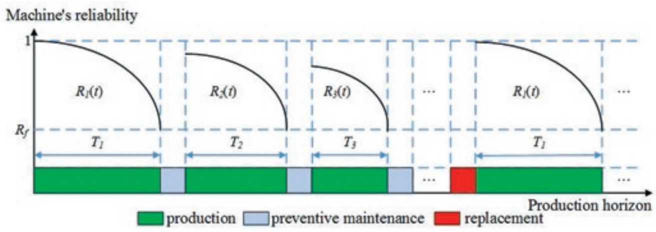

Fig. 2. The illustration of the system's reliability during the production horizon

Suppose preventive maintenance is just undertaken to key components of the key system. Due to the introduction of age reduction factor and failure rate increase factor, the system's failure rate is bigger than in the former PM cycle. So, with the increased machine's usage and maintenance times, the maintenance cost becomes rather high, and the machine's operational time is much less than before preventive maintenance cycle. Thus, when involved in this situation, replacing the key system by a brand new one will be reasonable and economical after certain number of preventive maintenance. However, a new problem is raised that is how to determine the number of preventive maintenance. Namely, how to determine the upper bound of preventive maintenance, because after the certain number of preventive maintenance, it is uneconomical to perform preventive maintenance. This study defines a cost-time rate (*cr*) function to evaluate the economy of preventive maintenance for a new machine.

$$cr = \frac{N \times PMC + RC}{\sum_{i=1}^{N} T_i + N \times PMT} \tag{1}$$

The cost-time rate (*cr*) means maintenance cost per unit time.With the increased number of preventive maintenance, *cr* decreases. After certain number of preventive maintenance, *cr* will increase. The inflection point of *cr* is the most economical number of preventive maintenance. It means in the same unit time, the maintenance cost is lowest at the inflection point. Hence, the inflection point is chosen to regard as the best time to implement replacement. The variation of *cr* with the increased number of preventive maintenance is shown in Figure 3.

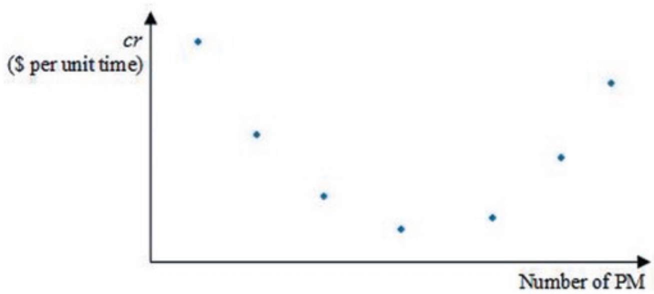

Fig. 3. The variation of cr with the increased number of preventive maintenance

Therefore, the machine's usage with considering preventive maintenance and replacement is described in Figure 4.

Step 1. Making a job sequence and organizing production.

Step 2. Predicting the machine's reliability.

Step 3. Comparing the current reliability $R_i(t)$ and reliability threshold R_f. If $R_i(t)$ is bigger than R_f, go to Step 4, otherwise, go to Step 1.

Step 4. Calculating *cr* and judging whether or not the preventive maintenance is economical. If the preventive maintenance is uneconomical, go to Step 5. Otherwise, go to Step 6.

Step 5. Replacement. Replacing the system by a new brand one. After replacement, the machine's status is "as good as new". Then go to Step 1 until the all the jobs are finished.

Step 6. Preventive maintenance. Preventive maintenance is just undertaken to the key components of the key system. After preventive maintenance, go to Step 1 until the all the jobs are finished.

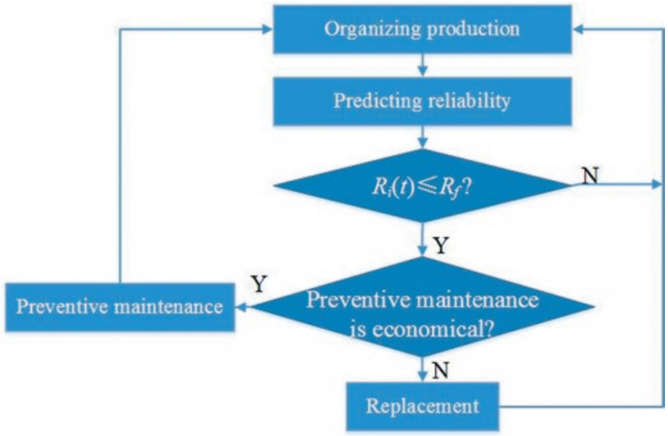

Fig. 4. Usage of a machine

2.3. Model for implementing aperiodic imperfect preventive maintenance

It is obvious that the machine's failure rate will increase with increased usage and age. Age reduction factor and failure rate increase factor is introduced to describe the imperfect character. The age reduction factor is used to illustrate the machine cannot be renewal. Failure rate increase factor is used to represent the failure rate is increased. Therefore, the failure rate function is defined as follows:

$$\lambda_{i+1}(t) = b_i \lambda_i (t + a_i T_i) \tag{2}$$

Where, a_i is the age reduction factor and b_i is the failure rate increase factor in T_i respectively. $0<a_i<1<b_i$ and $1<b_1<b_2<\cdots<b_i$.

According to the theoretical relationship between the failure rate function and reliability, the machine's reliability is shown as Equation 3:

$$R_{i+1}(t) = \exp\left[-\int_0^t b_i \lambda_i (t' + a_i T_i) dt'\right] \tag{3}$$

It is supposed that machine's reliability reaches the reliability threshold (R_f), so the machine's reliability at the end of the current preventive maintenance cycle can be inferred as:

$$R_f = \exp\left[-\int_0^{T_{i+1}} b_i \times \lambda_i \left(t' + a_i \times T_i\right) dt'\right] \tag{4}$$

Rewritten as:

$$\ln R_f = -\int_0^{T_{i+1}} b_i \times \lambda_i\left(t' + a_i \times T_i\right)dt' \quad (5)$$

So, the preventive maintenance cycle (T_{i+1}) can be calculated according to the reliability threshold (R_f), age reduction factor (a_i), failure rate increase factor (b_i) and the failure rate function of the machine ($\lambda_i(t)$) in the current preventive maintenance cycle (T_i).

The current processing job is can be interrupted due to scheduled maintenance even though it is unfinished. Therefore, the machine's service time is related to the status of Job m in the current maintenance cycle.

$$wt_j = \begin{cases} \overline{wt}_{j-1} + it_m \\ \overline{wt}_{j-1} + \overline{it_m} \end{cases} \quad (6)$$

Where, $\overline{wt}_{j-1}$ is the service time before the jth processing, wt_j is the service time after the jth processing. it_m means Job m could be just finished in this maintenance cycle. $\overline{it_m}$ is the finished part of Job m in this maintenance cycle if the machine is disrupted due to the maintenance. Suppose that the machine is maintained for k times (including PM and replacement) before completing Job m. The calculated completion time of Job m in calendar (t_{cm}) could be got by Equation (7):

$$t_{cm} = \sum_{k'=0}^{k} t_{r,k'} + \sum_{m'=1}^{m} it_{m'} \quad (7)$$

Where, $t_{r,k'}$ is the maintenance time including preventive maintenance time (PMT) and replacement time (RT). $it_{m'}$ is the processing time of Job m. Therefore tardiness of Job m (θ_m) is as follows:

$$\theta_m = \max\left(0, t_{cm} - dt_m\right) \quad (8)$$

Where, dt_m denotes the delivery time of Job m. Suppose the machine is maintained for K times (including PM and replacement) before completing all jobs, so the total profit I_{total} of the task should consist four parts: (1) production value of all the jobs, (2) production cost of all the jobs, (3) maintenance cost (including PMC and RC) and (4) total tardiness cost:

$$I_{total} = \sum_{m=1}^{n} it_m \times \left(pv_m - pc_m\right) - \sum_{k=0}^{K} cp_k - \sum_{m=1}^{n} \theta_m \times dc_m \quad (9)$$

Where, pv_m, pc_m and dc_m are production value, production cost and tardiness cost of Job m respectively. cp_k denotes the cost of the kth maintenance activity including PMC or RC. From Equation (9), maintenance planning and production scheduling is jointed and could be optimized simultaneously.

2.4. Model for implementing periodic perfect preventive maintenance

In other current works, periodic PM activities are generally considered. And another basic assumption is that preventive maintenance could renew the machines. Suppose a machine is always implemented periodic PM without replacement, therefore the calculated completion time of Job m in calendar (t^p_{cm}) is Equation (10):

$$t^p_{cm} = \sum_{k'=0}^{k_p} t_{p,k'} + \sum_{m'=1}^{m} it_{m'} \quad (10)$$

Where, $t_{p,k'}$ represents the time for each periodic PM. Thereby, the tardiness of Job m is Equation (11):

$$\theta^p_m = \max\left(0, t^p_{cm} - dt_m\right) \quad (11)$$

Subsequently, the total profit is as follows:

$$I^p_{total} = \sum_{m=1}^{n} it_m \times \left(pv_m - pc_m\right) - \sum_{k=0}^{K_p} cp_k - \sum_{m=1}^{n} \theta^p_m \times dc_m \quad (12)$$

Noting that, different from Equation (9), the third monomial in the Equation (12) just includes preventive maintenance cost without replacement cost.

3. Optimization methodology

The joint optimization of production scheduling and preventive maintenance planning has been proved as a NP-hard problem [20]. Artificial immune system (AIS) as a kind of random researching algorithm is usually used to solve optimization problem. Compared with deterministic optimization methods, there are two main characteristics and advantages for AIS. (1) The optimum is searched from a series of points simultaneously in the solution sets rather than from one single point. (2) The objective is used in the iteration process rather than the derivative or other additional information. Clonal selection (CS) is one of the most important theory in AIS. Different from genetic algorithm (GA), CS performs selection based on the rate of affinity between antibodies and antigens. Besides, CS constructs memory cells which contain a group of optima. Moreover, CS could diversify the population by replacing the old antibodies. The basic steps of the immune clonal selection algorithm (ICSA) are illustrated in Figure 5.

Step 1: Problem recognition. The fitness function for ICSA is the objective which is to maximize the total profit. Each chromosome is encoded to represent one job sequence and each gene presents one unique job. For example, chromosome{1, 5,6,9,4,3,7,2,8,10} represents the sequence of all the jobs processed on one certain machine.

Step 2: Initializing parameters. The parameters contain the number of population (*popsize*), the number of antibodies for replacement (*Ar*), the number of iteration (*iteration*), the clonal selection probability (*Ps*), the initial clone number (*Cn*), the clonal inhibited radius (*Cir*), the inspiration parameter (*Ip*), the clonal recombination probability (*Pre*), the gene change probability (*Pc*), the gene shift probability (*Psh*), the inverse probability (*Pi*), and density selection probability (*Pd*).

Step 3: Calculating initial solution sets. Each chromosome's value is calculated based on the objective.

Step 4: Judging whether the terminal condition is met. Here, the terminal condition is the optimum beyond certain value. If met, go to Step 11, otherwise, go to Step 5.

Step 5: Sorting the solution set in descending order.

Step 6: Immune clone. This step contains clonal selection and immune clone. First, the affinity should be calculated, which is as follows:

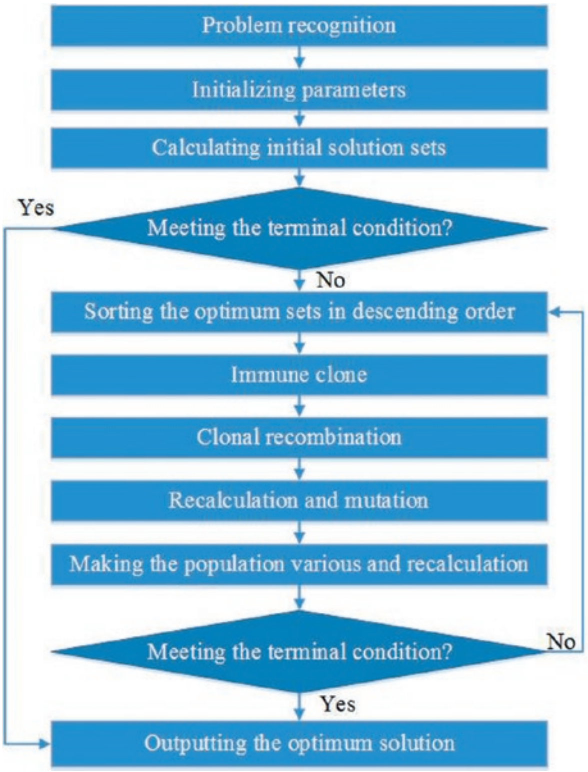

Fig. 5. Process of immune clonal selection algorithm

$$aff = \frac{p - \min p}{\max p - \min p} \tag{13}$$

Where, p is the total profit of each chromosome, $\min p$ is the minimum among p, and $\max p$ is the maximum. In this way, aff is in the interval (0,1) which is convenient to be compared. Before calculating similarity of every two chromosomes, a whole zero matrix is set, if the genes from two chromosomes represent the same meaning, the corresponding value is changed into 2, if the selected genes are different, then the value in the zero matrix should be transformed into 1, the unselected genes are still 0. Then the matrix is divided by 2 and named it hk. If the value in the matrix is bigger than 0, the calculation should follow Equation (14), otherwise, it is still 0:

$$HK = -hk \times \ln(hk) \tag{14}$$

Then the similarity and antibodies density is calculated respectively:

$$ayy = \frac{1}{1 + HK} \tag{15}$$

$$density = \frac{cumsum}{popsize} \tag{16}$$

Where, *cumsum* means the cumulative sum of all the genes from each chromosome which similarity is bigger than the given *Cir*.

Chromosomes with higher affinity can be regarded as Cell B. To determine the number of clone for each Cell B (*Cnt*), Equation (17) is developed:

$$Cnt = round\left(Cn \times \frac{aff_t}{aff_n}\right) \tag{17}$$

Where, the aff_t and aff_n is the affinity of each Cell B and the cumulative sum affinity of each Cell B respectively.

Step 7: Clonal recombination. Before clonal recombination, all the clones are separated into two parts, the ahead-ranked part and the latter-ranked part. The ahead-ranked part contains the first half of all the clones, and the latter-ranked part includes the rest clones. Recombinants are from the two parts named the first chromosome and the second chromosome respectively. Firstly, the initial cross position is determined according to two random numbers which are between two adjacent jobs. Then cross operation is followed. For the first chromosome, all genes are compared with genes from the second chromosome which are locates the initial cross position. If they are different, the gene from the first chromosome replaces the gene next to the initial cross position from the second chromosome. Next time, the next position is replaced.

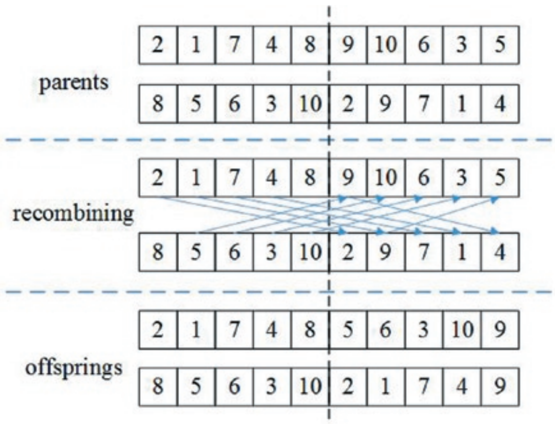

Fig. 6. Illustration of clonal recombination

Step 8: Recalculation and mutation. After clonal recombination, the affinity and the objective should be recalculated. If the affinity of the offspring is smaller than the parents', the offspring are replaced by the parents. Then mutation operation is followed including genetic exchange, genetic inverse and genetic shift. After each operation of mutation operation, the objective and affinity should be recalculated.

Step 9: Population diversification and recalculation. According to *Pd*, the clones with high similarity should be wiped out. The remaining chromosomes and the initial population are combined to form a new matrix named matrix *E*. The formula for inspiration of matrix *E* is Equation (18):

$$act = aff\_E \times e^{\frac{-density\_E}{lp}} \tag{18}$$

Where, *aff_E* and *density_E* is the affinity and density of matrix *E* respectively.

The chromosomes with high incentive degree are selected to construct a new matrix named *F*. Matrix *F* is sorted according to affinity by descend. To vary samples, *Ar* chromosomes are generated to replace the chromosomes with small inspiration in matrix *F*. Then the new matrix is named matrix *P* and calculated the objective, the affinity, the similarity and density.

Step 10: Judging whether the terminal condition is met. Here the terminal condition is whether the iteration reaches the maximum step. If met, go to Step 11, otherwise, go to Step 5.

Step 11: Outputting the optimum solution.

4. A Numerical example

In this section, a numerical example is designed to validate the integrated model which is proposed in Section 2. Suppose there are 10 jobs to be processed on a production line which is composed of 5 different machines. The jobs' processing time on each machine and the maintenance information for each machine is listed in Table 1.

Table 1. The jobs' processing time and maintenance information on each machine

Machines	Operation Time										PMT	PMC	RT	RC
	J1	J2	J3	J4	J5	J6	J7	J8	J9	J10				
M1	25	17	41	74	37	72	11	31	32	27	2	180	4	2000
M2	15	41	155	12	95	34	77	39	92	114	5	230	8	4000
M3	12	22	83	24	72	62	31	141	42	21	4	170	6	3600
M4	40	36	121	48	52	32	26	56	74	90	3	200	5	2700
M5	60	58	160	78	153	162	32	79	102	52	5	500	7	2000

J1 represents the first job, M1 is the first machine, by such analogy. For each machine, its failure is subject to Weibull distribution. Because, Weibull distribution has been widely used to illustrate system's failure rate, and also usually adopted to study the problem of maintenance policy and production scheduling. The corresponding parameters are listed in Table 2.

Each machine's reliability threshold according to expertise and total operation time (*TOT*) is calculated according Table 1.

Besides, the factors which are important to influence the objective are given including each job's delivery time in calendar (*dt*), production cost (*pc*), production value (*pv*) and tardiness cost (*dc*) in Table 4.

4.1. Validation and results

As analysed, age reduction factor and failure rate increase factor

Table 2. Shape parameter and scale parameter of each machine

	M1	M2	M3	M4	M5
Shape Parameter	2	2.2	1.8	1.8	1.2
Scale Parameter	175	225	184	236	318

Table 3. Machines' reliability threshold and total operation time

	M1	M2	M3	M4	M5
R_f	0.6	0.6.	0.7	0.7	0.75
TOT	367	674	510	575	936

Table 4. The basic information about each job

Jobs	*dt*	*pc*	*pv*	*dc*
J1	322	27	98	121
J2	286	40	133	184
J3	1050	39	143	193
J4	645	23	89	127
J5	821	21	90	127
J6	577	34	115	128
J7	446	49	148	190
J8	788	29	118	168
J9	515	37	129	138
J10	751	25	98	152

is used to illustrate PM is imperfect and degradation is increased. In order to simplify the calculation, age reduction factor is assumed as a constant, a_i=0.1. Failure rate increase factor b_i is variant according to number of preventive maintenance (i):

$$\begin{cases} b_0 = 1 \\ b_i = b_0 + 0.1 \times (i-1) \end{cases} \tag{19}$$

Meantime, to simplify the calculation, the calculated T_i is processed by Equation (20):

$$T_i = fix(T_i) \tag{20}$$

Some essential parameters for ICSA are set, which is used to optimize the joint problem.

Table 5. Parameters for ICSA

Popsize	*Ar*	*iteration*	*Ps*	*Cn*	*Cir*	*Ip*	*Pre*	*Pc*	*Psh*	*Pi*	*Pd*
50	30	150	0.7	80	0.7	100	0.6	0.3	0.3	0.3	0.7

Table 6. MTs and revised Ti for aperiodic imperfect PM

Machines	MTs					Ti						
M1	3	125	113	108	103							
M2	4	165	149	144	138	133						
M3	5	103	94	89	85	81	78					
M4	4	133	120	115	109	105						
M5	10	112	107	98	92	86	80	76	72	68	112	107

Table 7. ST and ET under aperiodic imperfect PM

(a) Job sequence is {1,2,6,7,9,4,10,8,5,3}

	J1		J2		J6		J7		J9		J4		J10		J8		J5		J3	
	ST	ET	ST	ET	ST	ET	ST	ET	ST	ET	ST	ET	ST	ET	ST	ET	ST	ET	ST	ET
M1	0	25	25	42	42	114	114	125	127	159	159	233	233	262	262	293	293	330	330	373
M2	25	40	42	83	114	148	148	230	230	322	322	334	334	453	453	492	492	592	592	752
M3	40	52	83	105	148	210	230	265	322	364	364	388	453	478	492	637	637	713	752	839
M4	52	92	105	141	210	242	265	294	364	438	438	489	489	579	637	696	713	765	839	963
M5	92	152	152	215	242	409	409	441	441	553	553	631	631	688	696	780	780	943	963	1135

(b) Job sequence is {2,1,6,7,9,4,10,8,5,3}

	J2		J1		J6		J7		J9		J4		J10		J8		J5		J3	
	ST	ET	ST	ET	ST	ET	ST	ET	ST	ET	ST	ET	ST	ET	ST	ET	ST	ET	ST	ET
M1	0	17	17	42	42	114	114	125	127	159	159	233	233	262	262	293	293	330	330	373
M2	17	58	58	73	114	148	148	230	230	322	322	334	334	453	453	492	492	592	592	752
M3	58	80	80	92	148	210	230	265	322	364	364	388	453	478	492	637	637	713	752	839
M4	80	116	116	156	210	242	265	294	364	438	438	489	489	579	637	696	713	765	839	963
M5	116	174	174	239	242	409	409	441	441	553	553	631	631	688	696	780	780	943	963	1135

Table 8(a)The tardiness for the job sequence {1,2,6,7,9,4,10,8,5,3}

	J1	J2	J6	J7	J9	J4	J10	J8	J5	J3
Tardiness	0	0	0	0	38	0	0	0	122	85

Table 8(b)The tardiness for the job sequence {2,1,6,7,9,4,10,8,5,3}

	J2	J1	J6	J7	J9	J4	J10	J8	J5	J3
Tardiness	0	0	0	0	38	0	0	0	122	85

Table 9. Reliability at the end of each maintenance cycleunder aperiodic PM

Machines	Reliability (at the end of each maintenance cycle)										
M1	0.6004	0.6010	0.6025								
M2	0.6032	0.6031	0.6011	0.6026							
M3	0.7033	0.7016	0.7037	0.7030	0.7046						
M4	0.7003	0.7033	0.7009	0.7028							
M5	0.7514	0.7506	0.7523	0.7502	0.7503	0.7530	0.7516	0.7517	0.7533	0.7514	0.7506

Table 11. ST and ET of job sequence {2,1,7.6,9,4,10,8,5,3} under periodic perfect PM.

	J2		J1		J7		J6		J9		J4		J10		J8		J5		J3	
	ST	ET	ST	ET	ST	ET	ST	ET	ST	ET	ST	ET	ST	ET	ST	ET	ST	ET	ST	ET
M1	0	17	17	42	42	53	53	125	127	159	159	233	233	262	262	293	293	330	330	371
M2	17	58	58	73	73	150	150	189	189	281	281	293	293	412	412	451	451	551	551	711
M3	58	80	80	92	150	181	189	255	281	323	323	347	412	437	451	596	596	672	711	794
M4	80	116	116	156	181	207	255	290	323	397	397	445	445	538	596	655	672	724	794	918
M5	116	174	174	239	239	271	290	457	457	564	564	647	647	699	699	783	783	941	941	1111

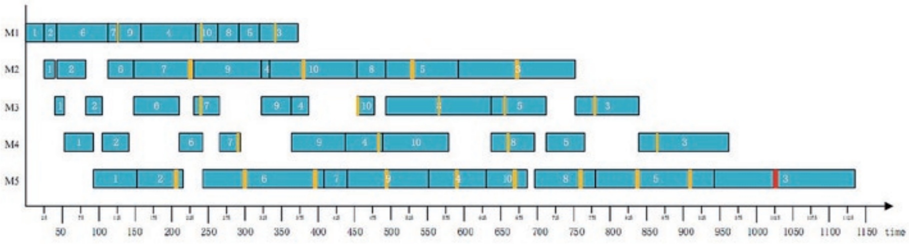

(a) {1,2,6,7,9,4,10,8,5,3}

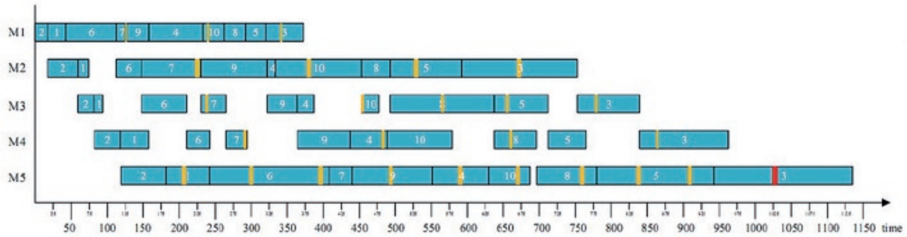

(b) {2,1,6,7,9,4,10,8,5,3}

Fig. 7. The machine's service time and maintenance information under aperiodic imperfect PM

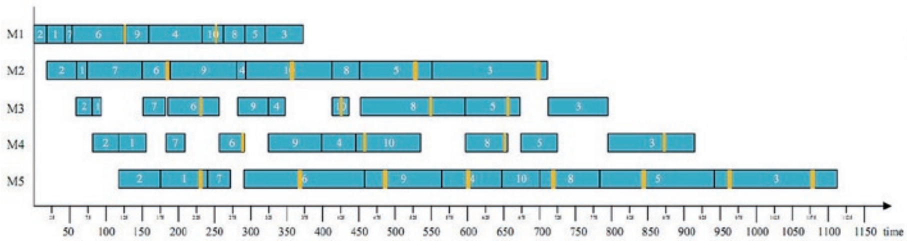

Fig. 8. The machine's service time and maintenance information of job sequence {2,1,6,7,9,4,10,8,5,3} under periodic perfect PM

4.1.1. Scenario 1: Aperiodic imperfect preventive maintenance

For the imperfect preventive maintenance system, the number of maintenance (*MTs*) and PM cycle of each machine is listed in Table 6.

Noting that in Table 6, there is a replacement on M5. Using ICSA, the optimized total profit is 213553 with total tardiness 245. The best job sequences are {1,2,6,7,9,4,10,8,5,3} and {2,1,6,7,9,4,10,8,5,3}. The start time (ST) and end time (ET) is given as follows.

In Figure 7, some jobs are separated into 2 parts by yellow or red lines. The yellow lines mean PM and the red line is replacement. The corresponding tardiness of the two job sequences for each job is listed in Table 8.

At the end of each maintenance cycle, the machines' reliability is listed in Table 9.

To show the better performance of the proposed aperiodic imperfect PM, the periodic perfect *PM* is implemented. Because the age reduction factor and failure rate increase factor is unintroduced, the failure rate in each preventive maintenance is same [7]. Therefore, each preventive maintenance cycle is same. The number of preventive maintenance and PM cycle is listed in Table 10.

By calculating, the total profit is 219517 and the corresponding total tardiness is 232. The proper job sequence is {2,1,7,6,9,4,10,8,5,3}.

The tardiness for each job of best job sequence is given in Table 12.

The machines' reliability at the end of each PM cycle is listed in Table 13.

4.2. Results from ICSA and GA.

To validate the algorithm proposed in Section 3, the traditional GA is used to compare. The compared GA just contains selection operation, crossover operation, and mutation operation. Selection probability is decided by roulette, crossover probability and mutation probability is set as 0.6 and 0.05 respectively. The number of population (*popsize*) and the number of iteration (*iteration*) is same with ICSA's. Considering the random of the initial solution, we test 5 times for each algorithm, the results are listed in Table 14.

Table 10. MTs and revised T_i for periodic perfect PM

Machines	*MTs*	T_i								
M1	2	125	125	125						
M2	4	165	165	165	165	165				
M3	4	103	103	103	103	103				
M4	4	133	133	133	133	133				
M5	8	112	112	112	112	112	112	112	112	112

Table 12. The tardiness for each job under the periodic perfect PM

	J2	J1	J7	J6	J9	J4	J10	J8	J5	J3
Tardiness	0	0	0	0	49	2	0	0	120	61

Table 13. Reliability at the end of each PM cyclefor periodic perfect PM.

Machines	Reliability (at the end of each PM cycle)							
M1	0.6004	0.5421						
M2	0.6032	0.5379	0.5055	0.4751				
M3	0.7033	0.6622	0.6355	0.6098				
M4	0.7003	0.6589	0.6320	0.6061				
M5	0.7514	0.7390	0.7170	0.6956	0.6749	0.6548	0.6353	0.6164

4.3. Results discussion

This study tries to optimize production scheduling and preventive maintenance simultaneously. By comparing with the two scenarios and the results from ICSA and GA, the better performance of the proposed model is validated by comparing with periodic perfect PM. In addition, some conclusions can be gotten:

(1) The proper job sequences with consideration of periodic perfect PM and aperiodic imperfect PM may be the same.However, the correspondingtotal profit is different. Although the aperiodic

Table 14. Results compared ICSA and GA

(a) Results from aperiodic imperfect PM

	Aperiodic imperfect PM			
	No.	The first step to get the optima	Total profit	Total tardiness
ICSA	1	42	213553	245
	2	77	213553	245
	3	75	213553	245
	4	57	213553	245
	5	18	213553	245
	Overall	53.8	213553	245
GA	1	**150**	**204257**	**313**
	2	**150**	**204257**	**313**
	3	23	213553	245
	4	96	213553	245
	5	49	213553	245
	Overall	93.6	209830	272.2

(b) Results from periodic perfect PM

	Periodic perfect PM			
	No.	The first step to get the optima	Total profit	Total tardiness
ICSA	1	41	219517	232
	2	61	219517	232
	3	64	219517	232
	4	32	219517	232
	5	55	219517	232
	Overall	50.6	219517	232
GA	1	86	219517	232
	2	90	219517	232
	3	39	219517	232
	4	**150**	**218886**	**229**
	5	40	219517	232
	Overall	81	219398	231.4

imperfect PM can get less profit and more tardiness, the machine's reliability at each end of the maintenance cycle is always higher than the machine's reliability under periodic perfect PM. (Compared Table 9 and Table 13). More important, the machine's reliability which is under aperiodic imperfect PM policy is always higher than the reliability threshold. While, the assumed periodic perfect PM policy cannot guarantee the machine's reliability is always higher than the reliability threshold.

(2) The best job sequence may not be unique. For some jobs, when the tardiness is sufficient, the job's sequence can be interchanged before the deadline of these jobs which has sufficient tardiness.

(3) Compared with GA, ICSA could get the solution in less iterations for both the aperiodic imperfect PM and periodic perfect PM. ICSA could get more profit with less average iteration steps (compared the overalls in Table 14). Even though, sometimes the optima could be gotten from GA which is in less iteration than from ICSA, the results from GA are not stable. For example, sometimes the iteration has met the terminal condition (for example the terminal condition is maximum step), GA still cannot get the optima. (Table 14).

(4) More factors which impact the objective (to maximize the total profit) are helpful to get the optimum job sequence. Because the more influence of each job is taken into consideration, the difference of jobs is concerned. Some jobs may stress the delivery time and the tardiness cost is high. And some jobs may not be needed in urgent time, therefore, it could be processed later. Therefore, more information about each job should be considered when optimizing the joint scheduling problem.

5. Conclusions and future work

Production scheduling is usually considered to meet certain demands, such as, to minimize total tardiness, the total cost or to maximize total profit etc. Preventive maintenance is an effective way to keep the machine in high availability and reliability. But when maintenance operation is implemented, the machine is disrupted. Moreover, in practice, production scheduling and maintenance planning are optimized and performed separately. Based on this scheme, this study proposed an integrated model to joint production scheduling and maintenance planning in a multi-machine system. In this model, the PM is imperfect. Furthermore, at each end of PM cycle, the cost-time rate function is used to judge the economy of PM. The jointed model aims at maximizing the total profit with considering the factors which could impact the total profit. The proposed model is validated by a numerical example through comparing two scenarios, the results show that the aperiodic imperfect preventive maintenance could ensure the machines in good operational condition in each PM cycle. Meanwhile, the reliability is guaranteed.

In the future, we will focus on more practical situation and take advantages of advanced technology. For example, sensors are used to monitor machine's condition and develop real-time health evaluation model jointed with the production scheduling. To avoid sudden breakdown, the finite preventive maintenance, replacement, inventory and purchasing should be taken into consideration simultaneously.

***Acknowledgements**:*

The authors would like to thank anonymous referees for their remarkable comments and great support by Key Project supported by National Science Foundation of China(51035008); Natural Science Foundation project of Chongqing (CSTC, 2009BB3365), and the Fundamental Research Funds for the State Key Laboratory Of Mechanical Transmission, Chongqing University(SKLMT-ZZKT-2012 MS 02).

References

1. Brown M PF. imperfect repair. Journal of Applied Probability 1983; 20(4): 851-859.
2. Cassady CR, Kutanoglu E. Integrating Preventive Maintenance Planning and Production Scheduling for a Single Machine. IEEE Transactions on Reliability 2005; 54(2): 304-309.

3. Dehayem Nodem FI, Kenné JP, Gharbi A. Simultaneous control of production, repair/replacement and preventive maintenance of deteriorating manufacturing systems. International Journal of Production Economics 2011; 134(1): 271-282.
4. Fitouhi M, Nourelfath M. Integrating noncyclical preventive maintenance scheduling and production planning for a single machine. International Journal of Production Economics 2012; 136(2): 344-351.
5. Jin X, Li L, Ni J. Option model for joint production and preventive maintenance system. International Journal of Production Economics 2009; 119(2): 347-353.
6. Liao W, Pan E, Xi L. Preventive maintenance scheduling for repairable system with deterioration. Journal of Intelligent Manufacturing 2010; 21(6): 875-884.
7. Liao W, Wang Y, Pan E. Single-machine-based predictive maintenance model considering intelligent machinery prognostics. The International Journal of Advanced Manufacturing Technology 2012; 63(1-4): 51-63.
8. Ma Y, Chu C, Zuo C. A survey of scheduling with deterministic machine availability constraints. Computers & Industrial Engineering 2010; 58(2): 199-211.
9. Malik MAK. Reliable Preventive Maintenance Scheduling. A I I E Transactions 1979; 11(3): 221-228.
10. Ming Tan C, Raghavan N. A framework to practical predictive maintenance modeling for multi-state systems. Reliability Engineering & System Safety 2008; 93(8): 1138-1150.
11. Moghaddam KS. Multi-objective preventive maintenance and replacement scheduling in a manufacturing system using goal programming. International Journal of Production Economics 2013; 146(2): 704-716.
12. Moghaddam KS, Usher JS. Preventive maintenance and replacement scheduling for repairable and maintainable systems using dynamic programming. Computers & Industrial Engineering 2011; 60(4): 654-665.
13. Moradi E, Fatemi Ghomi SMT, Zandieh M. Bi-objective optimization research on integrated fixed time interval preventive maintenance and production for scheduling flexible job-shop problem. Expert Systems With Applications 2011; 38(6): 7169-7178.
14. Nakagawa T. Optimum Policies When Preventive Maintenance is Imperfect. IEEE Transactions on Reliability 1979; R-28(4): 331-332.
15. Nakagawa T. Sequential imperfect preventive maintenance policies. IEEE Transactions on Reliability 1988; 37(3): 295-298.
16. Pan E, Liao W, Xi L. Single-machine-based production scheduling model integrated preventive maintenance planning. The International Journal of Advanced Manufacturing Technology 2010; 50(1): 365-375.
17. Pham H, Wang H. Imperfect maintenance. European Journal of Operational Research 1996; 94(3): 425-438.
18. Qi X, Chen T, Tu F. Scheduling the Maintenance on a Single Machine. The Journal of the Operational Research Society 1999; 50(10): 1071.
19. Roux O, Duvivier D, Quesnel G, Ramat E. Optimization of preventive maintenance through a combined maintenance-production simulation model. International journal of production economics 2013; 143(1): 3-12.
20. Ruiz R, Carlos García-Díaz J, Maroto C. Considering scheduling and preventive maintenance in the flowshop sequencing problem. Computers and Operations Research 2007; 34(11): 3314-3330.
21. Wang H. A survey of maintenance policies of deteriorating systems. European Journal of Operational Research 2002; 139(469-489.
22. Wang S, Liu M. A branch and bound algorithm for single-machine production scheduling integrated with preventive maintenance planning. International Journal of Production Research 2012; 51(3): 847-868.
23. Wong CS, Chan FTS, Chung SH. A joint production scheduling approach considering multiple resources and preventive maintenance tasks. International Journal of Production Research 2013; 51(3): 883-896.
24. Zhang X, Kang J, Jin T. Degradation Modeling and Maintenance Decisions Based on Bayesian Belief Networks. Reliability, IEEE Transactions on 2014; 63(2): 620-633.

Xiaohui CHEN
Lei XIAO
Weixiao XIAO
Junxing LI
The State Key Lab of Mechanical Transmission
Chongqing University
Chongqing, 400030, China

Xinghui ZHANG
Mechanical Engineering College
Shijiazhuang, 050003, China

Emails: chenxiaohui@cqu.edu.cn, leixiao211@163.com,
xiaoweixiao@126.com, lijun-xing2008@163.com
dynamicbnt@gmail.com

Article citation info:
LOTKO M, LOTKO A. Cluster analysis of knowledge workers assessment of occupational threats and attitudes to character of work. Eksploatacja i Niezawodnosc – Maintenance and Reliability 2015; 17 (1): 80–89.

Małgorzata LOTKO
Aleksander LOTKO

CLUSTER ANALYSIS OF KNOWLEDGE WORKERS ASSESSMENT OF OCCUPATIONAL THREATS AND ATTITUDES TO CHARACTER OF WORK

ZASTOSOWANIE ANALIZY SKUPIEŃ DO OCENY ZAGROŻEŃ ZAWODOWYCH PRACOWNIKÓW WIEDZY I ICH POSTAW WOBEC CHARAKTERU PRACY*

The goal of the paper was to discover, if knowledge workers' occupational threats can be linked to some logical constructs and if knowledge workers can be grouped into some logical items concerning their assessment of these threats and attitudes to character of work. On a basis of literature studies peculiarity of knowledge-based work and specific occupational threats were identified. They were examined as observable variables with the use of a questionnaire method on a sample of 500 knowledge workers. Then, variables were classified using multidimensional exploratory technique - cluster analysis. As a research implication, the structure of perception of knowledge workers' occupational threats and their attitudes to character of work were revealed. As a practical implication, a proposed classification of variables allows to measure perception of occupational threats and use the results e. g. when designing trainings on occupational health and safety and to better fit them to this specific group of employees. Thus, job safety can be effectively improved by raising awareness of certain threats. The paper's contribution is a novel way of measuring and classifying knowledge workers' occupational threats and attitudes to character of work.

***Keywords**: knowledge workers, occupational threats, character of work, assessment, cluster analysis.*

Celem artykułu było zbadanie, czy zagrożenia zawodowe pracowników wiedzy mogą być pogrupowane w logiczne konstrukty i czy pracownicy wiedzy mogą być logicznie pogrupowani biorąc pod uwagę ich ocenę zagrożeń i postawy wobec pracy. Na podstawie studiów literaturowych zdefiniowano szczególny charakter pracy opartej na wiedzy i zagrożeń związanych z jej wykonywaniem. Zbadano je empirycznie jako zmienne obserwowalne z wykorzystaniem metody ankietowej na próbie 500 pracowników wiedzy. Następnie przeprowadzono klasyfikację zmiennych z wykorzystaniem wielowymiarowej techniki eksploracyjnej – analizy skupień. Jako wniosek badawczy odkryto strukturę postrzeganych przez pracowników wiedzy zagrożeń zawodowych. Jako wniosek praktyczny, proponowana klasyfikacja zmiennych pozwala mierzyć postrzeganie zagrożeń zawodowych przez pracowników wiedzy i wykorzystać wyniki np. podczas projektowania szkoleń z zakresu bezpieczeństwa i higieny pracy, aby lepiej dopasować je do tej szczególnej grupy pracowników. Dlatego bezpieczeństwo pracy może być wyraźnie poprawione poprzez podniesienie świadomości określonych zagrożeń. Wkładem artykułu jest nowatorski sposób pomiaru i klasyfikacji zagrożeń zawodowych przez pracowników wiedzy i ich postaw wobec pracy.

***Słowa kluczowe**: pracownicy wiedzy, zagrożenia zawodowe, charakter pracy, ocena, analiza skupień.*

1. Introduction

Knowledge is the source of competences, improvement of efficiency and effectiveness of management and productivity [10, 21, 54]. Knowledge workers deal with creating, processing, applying and disseminating knowledge and information. They constitute a group educated in a formal way, however they understand the wide context of work, creative thinking, creativity, openness to changes and challenges as well as exercise treatment of work. They are responsible for creation and implementation of new ideas thanks to which organizations can better adapt to the rapid changes taking place in the surrounding environment. In contemporary economy, this particular group is becoming even more numerous. Still, specification of work based on knowledge triggers new occupational threats. Advantage of psycho-sociological threats over physical threats is a characteristic phenomenon [35].

Proper relations in the human-technique-environment system constitute a necessary condition to provide safety and well-being of a worker in the working process. Performance of every work is strictly connected with the occurrence of various type of threats. Occupational threats constitute potential events which by virtue of their appearance, i.e. occurrence in practice, exert a negative impact on the working environment or psychophysical condition of the workers. Such events may cause accidents at work or occupational diseases. Every factor and/or situation which may cause such accident or disease constitutes a threat in the working environment.

The goal of the paper was to discover, if knowledge workers can be grouped into some logical items concerning their assessment of occupational threats and character of work.

From such defined a goal, the following research hypotheses were drawn:

- H1: occupational threats posed to knowledge workers can be grouped into few logical items.
- H2: knowledge workers can be grouped into clusters according to their perception of occupational threats.
- H3: there are between cluster differences according to demographical variables.
- H4: there are between cluster differences according to the department and role in organization.
- H5: there are between cluster differences according to the assessment of the character of knowledge-based work.

(*) Tekst artykułu w polskiej wersji językowej dostępny w elektronicznym wydaniu kwartalnika na stronie ***www.ein.org.pl***

The aim was reached and the hypotheses were verified on the basis of the results of empirical research with the use of multidimensional exploratory techniques.

2. Professions and knowledge workers – the state of the art

Issues concerning knowledge workers are mainly discussed by the following foreign authors: T. Davenport [8], P. Drucker [11], W. Cortada [4], D. Jemielniak [27], J. Patalas-Maliszewska [48], J. Evetts [13], M. Roell [51], M. Granitzer and S. Linsteadt [18], D. Kleinmann and S. Vallas [30], and in Poland: E. Skrzypek [54, 53], M. Morawski [44, 42], G. Filipowicz [15], T. Kawka [28], D. Makowski [38], D. Jemielniak [26], M. Staniewski [57] and K. Łysik [37]. Authors conducting research in this topic define the term of knowledge workers (W. Cortada, D. Jemielniak, D. Makowski, T. Kawka), they also present the results of research concerning their creativity (E. Skrzypek), productivity (M. Granitzer and S. Linsteadt; E. Matson and L. Prusak [39]) and effectiveness (G. Filipowicz), as well as group work (K. Lewis [33]), motivation [27], communicating (D. Straub and E. Karahanna [60]) acquisition (B. Mikuła [41]) and sharing knowledge (M. Roell, K. Czop and D. Mietlicka [6]), specification of work based on knowledge (D. Jemielniak [26]) as well as methods of managing knowledge workers (T. Davenport, J. Patalas-Maliszewska, M. Morawski, M. Staniewski), management models (J. Patalas-Maliszewska) and challenges (K. Łysik) in this area. However there are no analyses available concerning self-awareness and self-assessment of work's character conducted by particular knowledge workers. Consequently we can observe a research gap which we tried to eliminate at least partly by means of this study.

Complexity of the management of knowledge in organizations and the lack of applicable definition of the knowledge worker result in the establishment of a number of various classification schedules connected with the processing of knowledge. Thus Ch. Handy divides workers into three categories [21]:

- routine workers – employed in order to operate shop cash desks or to enter data on floppy disks,
- suppliers of external services,
- analytics who work with numbers, ideas and words – journalists, financial analytics, consultants, architects, managers, etc.

M. Morawski claims that a knowledge worker is perceived in the context of formal education often exceeding the average level, he combines knowledge with different disciplines and at the same time he possesses deepened specialist knowledge and particular solid and practical skills based on the specialist knowledge, which are very often beyond the access of others [43]. Whereas T. Davenport acknowledges that knowledge workers are distinct from office workers as they not only process data by means of process of thinking but they also analyse them, understand them and create new knowledge in terms of its quality [8]. At the same time "they do not like to receive instructions, the mode of their work is difficult to be organized and foreseen, the best results are achieved when working with others in the contact nets".

A good example of knowledge workers constitute representatives of independent professions such as: doctors, attorneys, chartered accountants or architects [37]. E. Skrzypek maintains that knowledge workers are professionals processing symbols, paid for the effectiveness [53]. They have professional skills, interpersonal competences and unique competences the use of which creates an added value included in modern products and technologies"; they create, keep, apply and disseminate knowledge. According to C. Sikorski [52] the most important workers existing in modern economy, are psychologically ready for frequent changes at work, are not afraid of these changes, are flexible and they eagerly take risk, are not focused on a long-lasting career in one organization and are oriented towards the result – they have a strong need for achievements supported by a pursuit of continuous learning and a will to exert impact on the environment being subject to a minimalized control.

An interesting and wide review of definitions and features of knowledge workers are among other discussed by: T. Davenport [8], P. Drucker [10], A. Kidd [29], D. Kleinmann and S. Vallas [30], M. Strojny [61], T. Kowalski [31], A Fazlagić [14] or J. Szaban [62].

3. Threats to knowledge workers – the state of the art

Contemporary environmental and professional threats require a wider and deeper study [19, 16, 1]. The World Health Organization (WHO) promotes the strategy of health and safety at work [64], and the International Labour Organization (ILO) promotes the safety of work in the „green economy" of sustained development, which brings new and unknown threats to the workers [25]. Attention is also paid to the specific nature of occupational threats in the information society [34]. A threat is a potential source of a damage i.e. of an injury or other kind of deterioration of health [49]. A dangerous situation is a situation in which a given person is exposed to at least one danger. Such exposure may cause damage immediately or after some time.

The interest of the empirical part of this study is the assessment of occupational threats of the knowledge workers. The author discussed this issue in her previous works [36, 35, 34]. The awareness within the scope of occupational threats is particularly significant as the most frequent cause of accidents at work constitute the consequences of improper conduct of a worker [3]. On the other hand studies in the way the workers perceive their organization, concentrate on three different aspects of its functioning and culture: as the environment to solve problems and as the environment of self-development [5]. Within the first of the aspects mentioned above, one of the stress-causing factors constitutes the role served by a worker in a given organization. This threat mainly relates to the problems connected with the conflict of the roles in organization and responsibility for other people as well as to the possibility to receive support from the management and co-workers [32]. Uncertainty connected with the development of the professional career of a knowledge worker and uncertainty regarding the employment are both perceived as a serious threat. Threats resulting from the work itself include working environment, project of the task, pace of work and work schedule. Monotonous repeatability of tasks, insufficient use of worker's skills, incompatibility of duties and capabilities of a worker and a high level of uncertainty, these are the kind of stress-causing threats connected with a particular type of work performed by a knowledge worker. Significant threats resulting from the work itself include work schedule and pace of work leading to overwork [24, 9]. Threats listed above have a psychological background.

Another group of threats are threats resulting from improper organization of work. Factors limiting occupational threats of organizational character include breaks during work, possibility to perform various tasks, freedom of decisions concerning the manner of performance of the entrusted work, attainable deadlines for the performance of duties [3].

When considering technical threats we should take into account the peculiarity of a given workplace. Workers perform the majority of their duties using office electronic equipment. Work stations should have an access to the day light and electric light. Work with a computer monitor, minimisation of personal computers including the monitors results in sight disorders. Moderate temperature and quietness are important elements for conceptual work. On the other hand non-ergonomic position at work results in disorders of musculoskeletal system and spine injuries. Seemingly not dangerous, but the effect of such disorders and injuries is cumulating for years what causes chronic illnesses which very often require a long-term treatment [36].

The last group of threats to the working environment of knowledge workers includes safety threats concerning the „material" of which the knowledge is made of, i.e. data and information processed in an organization, especially in the environment of computer networks. Basic attributes defining safety of information are confidentiality, integrity and accessibility [50]. Threats to these attributes are of psycho-sociological and stress-causing character.

4. Research methodology

Sampling was purposive – among working students of the University of Technology and Humanities in Radom 500 persons were selected, who specified the nature of their work as a "knowledge worker". The adopted methodology provided the veracity of one of the qualification criteria of the knowledge workers concerning the possession of formally documented specialist knowledge – they had at least a bachelor or engineer title.

A questionnaire method was applied to collect statistical material whereas the author designed a special tool, i.e. a questionnaire form. Examined knowledge workers filled in the questionnaire composed of 28 questions. The first five questions were in the form of a certificate, the next 7 questions evaluated the self-awareness of the knowledge workers and the last 16 concerned the assessment of occupational threats (placed in table no. 3). Observable variables concerning the self-assessment of worker's knowledge and the assessment of occupational threats was described on the five-point Likert scales which measure the compatibility degree of a given respondent with a particular statement. For the purpose of the study of statistical material, a questionnaire method was used, whereas the author designed a special tool in the form of a questionnaire. Because of the assumed scales, where each item is described by a positive statement, low value of a variable means perceiving threat as a weak one, as high value of a variable means perceiving threat as a strong one. Such an approach allowed to treat occupational threats as "hidden" ones, not expressed in an explicit manner, hence not dictated to the surveyed employees.

Cluster analysis was used during this study. The term cluster analysis was introduced by R. Tryon [63] and then developed by R. Cattell [2]. The use of cluster methods has increased dramatically in the last 30 years [17]. Cluster analysis encompasses a number of different algorithms and methods for grouping objects of similar kind into respective categories. A general question facing researchers in many areas of inquiry is how to organize observed data into meaningful structures, that is, to develop taxonomies. In other words cluster analysis is an exploratory data analysis tool which aims at sorting different objects into groups in a way that the degree of association between two objects is maximal if they belong to the same group and minimal otherwise [58]. Cluster analysis is a term used to describe a family of statistical procedures specifically designed to discover classifications within complex data sets. The objective of cluster analysis is to group objects into clusters such that objects within one cluster share more in common with one another than they do with the objects of other clusters. Thus, the purpose of the analysis is to arrange objects into relatively homogeneous groups based on multivariate observations. cluster methods are used to group people (or other objects) together based on their scores across a set of variables [17].

Cluster analysis can be used to discover structures in data without providing an explanation and interpretation. In other words, cluster analysis simply discovers structures in data without explaining why they exist [58]. This method is unsupervised, which means that all the relationships are found only on a basis of input variables. It should be added, that cluster analysis is not as much a typical statistical test as it is a collection of different algorithms that put objects into clusters according to well defined similarity rules. The point here is that, unlike many other statistical procedures, cluster analysis methods are mostly used when we do not have any a priori hypotheses, but are still in the exploratory phase of our research.

Cluster methods lend themselves to use by investigators considering a wide range of empirical questions. Investigators in the life sciences, for example, are often interested in creating classifications for life forms, chemicals, or cells. They may be interested in developing complete taxonomies or in delimiting classifications based on their particular research interests. Medical scientists rely on clinical diagnoses and may use cluster methods to identify groups of people who share common symptoms or disease processes. The use of cluster methods in the behavioral sciences is as varied as the fields that constitute this branch of inquiry. A psychologist might be interested in exploring the possible relations among types of counseling interventions. In contrast, the economist may be charged with identifying economic similarities among developing countries. Clustering methods are useful whenever the researcher is interested in grouping together objects based on multivariate similarity [17].

D. Speece [56] encourages researchers to consider the purpose for their classification during this stage of the study. Cluster analysis may be used to develop a typology or classification system, as a test of existing classification systems, or simply to explore possible undiscovered patterns and similarities among objects. This author notes that classification systems may be used either to promote communication with practitioners or to enhance prediction.

Clustering techniques have been applied to a wide variety of research problems. Whenever it is needed to classify a large amount of information into manageable meaningful piles, cluster analysis is of great utility. The methods used in cluster analysis encompass [58]:

- joining (tree clustering),
- k-means clustering,
- two-way joining,
- expectation maximization clustering.

Two types of clustering algorithms can be distinguished: hierarchical and non-hierarchical. Hierarchical methods lead to creating a hierarchical tree-like structure of the elements of the analyzed set, which in its horizontal version is called a tree plot, and in its vertical version - an icicle plot. So, the effects of the algorithm can be presented as a tree, which shows the next steps of the performed analyses [40]. This way a final segmentation can be obtained, which means an orderly combination of a breakdown into segments. Different methods can be used here. Owing to the efficiency of reproducing the real data structure, the Ward method is recommendable. It uses the rule of minimizing variation [40]. These methods do not require an earlier assumption on the number of clusters – a plot can be "cut off" on a proper height in the end of an analysis and then interpreted. As a criterion for specifying an optimal number of segments, the first distinct growth of the distance, implying from the analyses of the distance graph for the next stages of bonding can be acknowledged. However, for the large data sets they require high computing power. The most popular method here is joining (tree clustering). In turn, non-hierarchical methods are quick to calculate, but they require to declare the assumed number of clusters in advance, which strongly influences the quality of obtained segmentation. Here, a method of k-means is very popular.

The joining or tree clustering method uses the dissimilarities (similarities) or distances between objects when forming the clusters. Similarities are a set of rules that serve as criteria for grouping or separating items. The most straightforward way of computing distances between objects in a multi-dimensional space is to compute Euclidean distances. This is probably the most commonly chosen type of distance. It simply is the geometric distance in the multidimensional space [58].

Summing up, a concise and relevant review of the development, applications, methods and problems of cluster analysis is provided by P. Gore [17]. Interesting and classical examples of cluster analysis applications are discussed by T. Hastie, R. Tibshirani and J. Friedman [23] as well as P. Guidici and S. Figini [20]. Also, an excellent summary of the many published studies reporting the results of cluster analyses is provided by J. Hartigan [22].

It the paper, the clustering methods were used twice:

1. Firstly, to check if the latent variables can be grouped into some clusters describing knowledge workers occupational threats posed to knowledge workers. The analysis was performed by clustering variables (by columns).
2. Secondly, to check if knowledge workers can be grouped into clusters according to their assessment of occupational threats. The analysis was performed by clustering cases (by rows), firstly using Ward method to identify the number of clusters, then using a k-means method to group cases and interpret them on a basis of a mean value of each variable in each cluster.

5. Discussion on the results of the study

Firstly, grouping variables by columns was performed. The aim was to examine the research hypothesis H1 stating that occupational threats posed to knowledge workers can be grouped into few logical items. A vertical tree graph (icicle plot) drawn in Figure 1 shows clusters for occupational threats obtained in another steps, while graph in Figure 2 shows the growth of linkage distance in another steps (iterations).

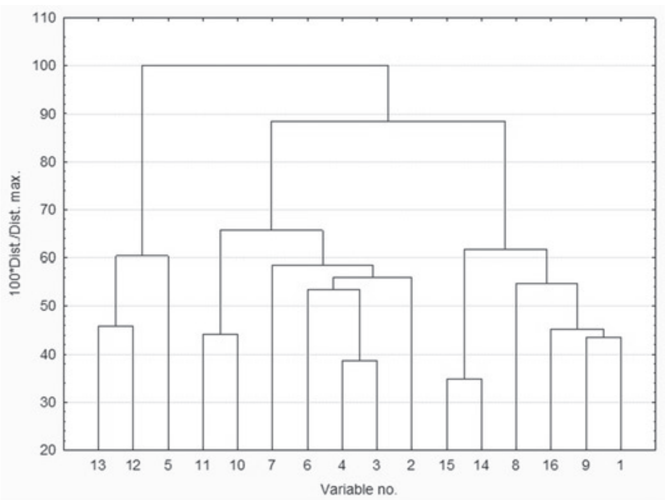

Fig. 1. Icicle plot for occupational threats cluster analysis. Source: authors' own study

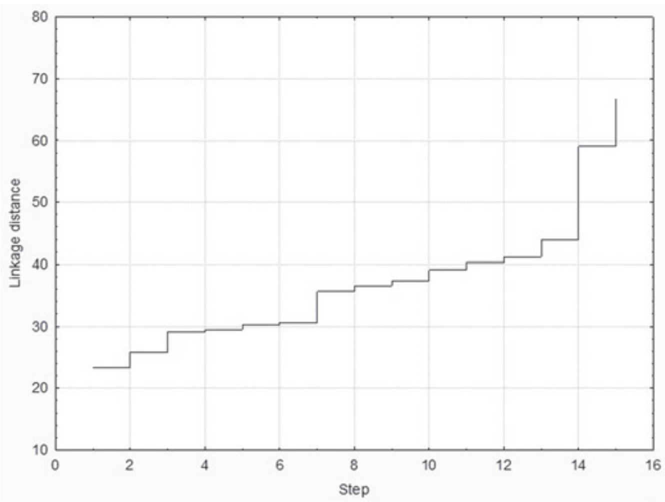

Fig. 2. Linkage distance in another steps for occupational threats cluster analysis. Source: authors' own study

From Figure 1 it can be seen that cutting a plot off at a standardized linkage distance e. g. 62, 4 clusters are obtained. Then, Figure 2 shows that the distinct increase in linkage distance appear in 7th and 14th of 15 steps of analysis. Interpretation of the obtained clusters is as follows (the order of linking variables was preserved, hence they are not sorted):

1. Cluster 1 - "physiology" (P), links variables 13, 12, 5, linking mainly physiological threats (threats to sight and musculoskeletal system) and the pressure of time.
2. Cluster 2 – "physical conditions" (F), links variables 11, 10, linking physical conditions at a workplace (temperature, noise, ability to concentrate).
3. Cluster 3 – "psycho-sociology" (S), links variables 7, 6, 4, 3, 2, linking psycho-sociological threats – ability to decide about the way of performing work, ability to relax, proper use of worker's abilities, estimation of the future and salary satisfaction.
4. Cluster 4 – "data and autonomy" (D), links 15, 14, 8, 16, 9, 1, linking threats posed to data security (confidentiality, integrity, availability), illumination of a workplace, diversity of tasks at work and support in performing them.

Analysis shows, that it is hard to logically interpret joining variables to clusters in 2 cases: variable 5 (pressure of time) to the cluster 1 and variable 9 (illumination of a workplace) to the cluster 4. Mapping variables describing occupational threats to clusters is given in Table 1.

Table 1. Mapping observable variables to clusters

Var.	Statement	Mapping to a cluster
1	I can count for the support in solving problems encountered at work.	D1
2	I am satisfied with the remuneration that I receive.	S1
3	I perceive the future of my career optimistically.	S2
4	My skills are properly used in organization.	S3
5	I work under time pressure.	P1
6	Breaks at work allow me to relax.	S4
7	I make the decisions concerning the manner in which I perform the work by myself.	S5
8	Performed tasks are diversified.	D2
9	My work station has appropriate lighting.	D3
10	At my work station, the temperature is at a comfortable level.	F1
11	Surrounding of my work station allows for concentration.	F2
12	During the work my eyesight can rest.	P2
13	During the work I have comfortable and ergonomic position.	P3
14	Data and information used at work are at the disposal of authorised persons only.	D4
15	Data and information used at work are protected from unauthorised modification.	D5
16	Data and information used at work are available when necessary.	D6

Source: authors' own study

Although this is a bit different classification than the one obtained with the use of factor analysis, where 5 factors (dimensions) were discovered [34], the hypothesis H1 was verified.

Because of the assumed scales, where each item is described by a positive statement, low value of a variable means perceiving threat as a weak one, as high value of a variable means perceiving threat as a strong one. Such an approach allowed to treat occupational threats as "hidden" ones, not expressed in an explicit manner, hence not dictated to the surveyed employees. Having the clusters linking occupational threats defined, it is now possible to measure the value of each of the groups of threats. The profile of occupational threats assessment is shown in Figure 3.

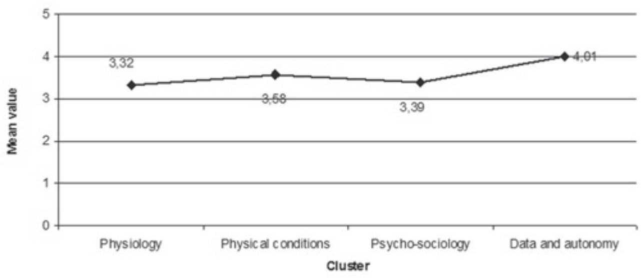

Fig. 3. Assessment of occupational threats clusters (mean values), Source: authors' own study

From Figure 3 it can be read that knowledge workers' perception covers mostly threats coming from physiology and psycho-sociology (there are low values of positive statements). Threats concerning physical conditions and threats to data security and lack of autonomy are perceived as relatively weak.

Then, grouping variables by rows (cases) was performed. The aim was to examine the research hypothesis H2 stating that knowledge workers can be grouped into clusters according to their perception of occupational threats. A vertical tree graph (icicle plot) in Figure 4 shows clusters for cases obtained in another steps, and graph in Figure 5 shows the growth of linkage distance in another steps (iterations).

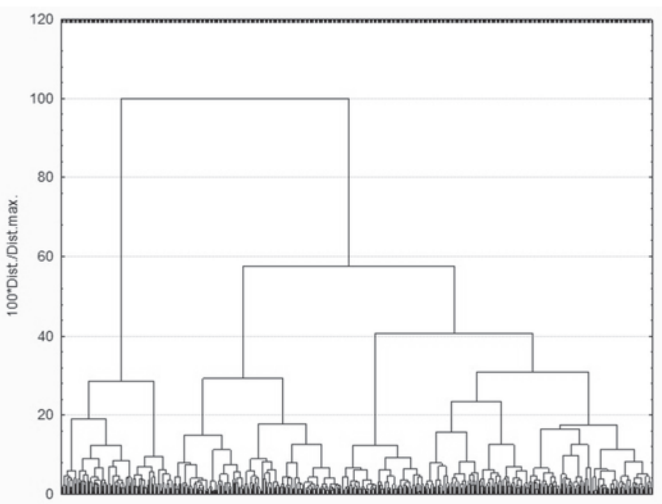

Fig. 4. Icicle plot for cases cluster analysis. Source: authors' own study

Table 2. Distances between clusters

Distance	Cluster 1	Cluster 2	Cluster 3	Cluster 4	Cluster 5
Cluster 1	0,000000				
Cluster 2	0,785190	0,000000			
Cluster 3	0,931778	0,957400	0,000000		
Cluster 4	1,623008	1,220837	1,071241	0,000000	
Cluster 5	1,005950	0,907696	1,246267	1,289286	0,000000

Source: authors' own study

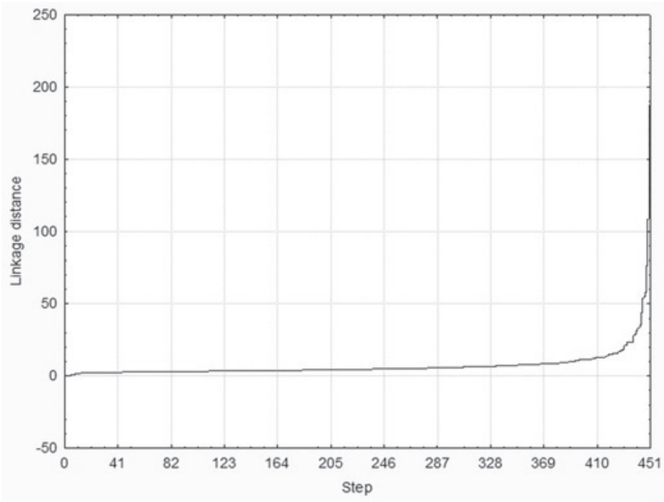

Fig. 5. Linkage distance in another steps cases cluster analysis. Source: authors' own study

From Figure 4 it can be concluded, that cutting the plot off at a standardized distance e. g. 30 allowed to identify 5 clusters. Then, Figure 5 shows that a substantial increase in a standardized linkage distance indeed took place in the last few iterations.

From Table 2 it can seen that there are considerable between cluster Euclidean distances – all of them are above 0,78. So it can be taken for granted that the clusters really reflect different groups of workers.

In Table 3 mean values of variables measuring assessment of occupational threats are given broken down into clusters and overall. These values are shown in Figure 6.

Table 3. Mean values of variables measuring assessment of occupational threats: in clusters and overall

Variable	Cluster 1	Cluster 2	Cluster 3	Cluster 4	Cluster 5	Overall
1	4,43	4,36	4,35	3,20	4,25	4,19
2	3,88	2,09	3,35	1,95	2,52	2,93
3	4,20	3,31	3,68	2,26	3,09	3,46
4	4,29	3,57	4,00	2,71	3,83	3,80
5	3,01	3,10	2,91	3,68	3,99	3,32
6	4,24	3,68	3,83	2,59	2,41	3,46
7	4,16	2,16	3,28	2,14	3,66	3,29
8	4,24	3,48	3,95	3,00	4,24	3,89
9	4,62	4,61	3,95	2,68	4,09	4,13
10	4,30	4,23	3,66	2,09	3,07	3,61
11	4,29	3,71	3,92	2,26	2,84	3,54
12	3,12	3,12	2,77	2,82	4,52	3,32
13	3,02	2,81	3,03	3,15	4,56	3,33
14	4,48	4,30	2,35	2,65	4,64	3,91
15	4,39	4,35	2,12	2,39	4,69	3,83
16	4,45	4,47	3,25	3,17	4,51	4,10

Source: authors' own study

From Table 3 and Figure 6 it can be seen that the analysis of classifying cases into each of the 5 clusters, done with the use of a k-means method, allows to generalize the following conclusions regarding characteristic of each of the clusters according to the perception of occupational threats (because of the assumed scales, where each item is described by a positive statement, low value of a variable means perceiving threat as a weak one, as high value of a variable means perceiving threat as a strong one):

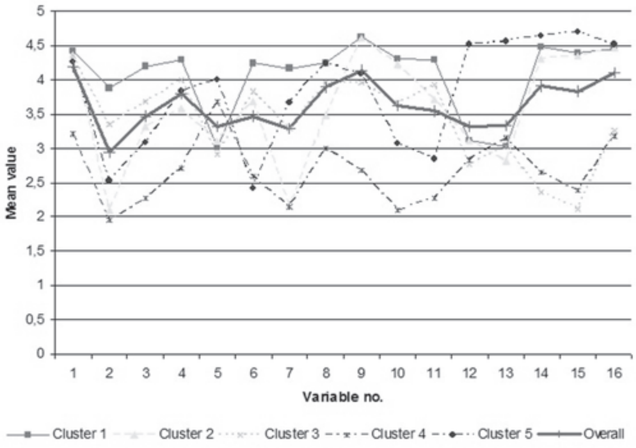

Fig. 6. Mean values of variables measuring assessment of occupational threats: in clusters and overall

1. Cluster 1 (linking 146 cases) „perceiving physiological threats" – most of variables are assessed rather highly, so this group of workers rather does not perceive occupational threats. Within this cluster variables 5, 12 and 13 have low values, what means that these workers are aware mainly of threats to an eyesight and implying from an uncomfortable position at work. These threats are of physiological character.
2. Cluster 2 (linking 77 cases) „perceiving psycho-sociological threats" – the assessment of threats is rather average for most of variables, highly assessed values are 1, 9 and 16, still the lowly assessed ones are 7, 8 and 11. Hence this group of workers perceives occupational threats mostly in psycho-sociological categories: lack of autonomy in choosing a way of realizing tasks, low diversity of tasks and difficulties with concentration at work.
3. Cluster 3 (linking 66 cases) „perceiving threats to information" – most of variables are have values near to average, low assessment accords to variables 14 and 15, so this group of workers perceives mostly threats posed to information, exactly to data confidentiality and integrity.
4. Cluster 4 (linking 67 cases) „lacking motivation, under esteemed and perceiving physical threats" – here many variables are of low values, especially 2, 3, 4, 8, 9, 10, 11, 12. These workers lack motivation and feels psycho-sociologically threaten. The main threats observed here are dissatisfaction from salary, pessimistic estimation of the future, improper use of a worker's skills and competencies, low diversity of tasks, but also the ones of a physical character: improper lighting, temperature and inability to concentrate (noise).
5. Cluster 5 (linking 95 cases) „perceiving bad organization of work process and physical conditions at work" – many variables are highly esteemed, nevertheless variables number 6, 10 and 11 have low values, so this group of workers perceives mainly threats implying from an organization of work process and physical conditions at a workplace (difficulties with relax, temperature, difficulties with concentration).

   This way hypothesis H2 was verified.

Then, the research hypotheses H3 and H4 were examined, stating that there are between cluster differences according to demographical variables and that there are between cluster differences according to the department and role in organization accordingly. Table 4 includes the percentage of knowledge workers' sex broken down into clusters and overall.

Table 5 includes the percentage of knowledge workers' age grouped into ranges and broken down into clusters and overall.

Table 4. Percentage of sex: in clusters and overall

Sex	Cluster 1	Cluster 2	Cluster 3	Cluster 4	Cluster 5	Overall
Man	48,98	64,00	36,92	45,45	71,13	53,88
Woman	51,02	36,00	63,08	54,55	28,87	46,12

Source: authors' own study

Table 5. Percentage of age: in clusters and overall

Age	Cluster 1	Cluster 2	Cluster 3	Cluster 4	Cluster 5	Overall
<=27	42,18	56,00	56,92	40,91	38,14	45,45
28-37	29,93	24,00	10,77	21,21	21,65	23,06
38-47	12,24	10,67	9,23	21,21	17,53	14,19
48-57	8,16	4,00	18,46	15,15	17,53	11,97
>=58	7,48	5,33	4,62	1,52	5,15	5,32

Source: authors' own study

Table 6 includes the percentage of employees working in certain organizational divisions broken down into clusters and overall.

Table 6. Percentage of organizational divisions: in clusters and overall

Division	Cluster 1	Cluster 2	Cluster 3	Cluster 4	Cluster 5	Overall
Office	44,90	46,67	21,54	21,21	48,45	38,14
Produc-tion	11,56	18,67	30,77	37,88	10,31	19,07
Market-ing	6,12	6,67	4,62	7,58	4,12	5,76
Finance	10,88	2,67	3,08	7,58	8,25	7,32
Cus-tomer service	19,73	17,33	21,54	15,15	22,68	19,73
R&D	4,76	4,00	15,38	4,55	4,12	5,99
IT	2,04	4,00	3,08	6,06	2,06	3,99

Source: authors' own study

The classification of roles of knowledge workers was based on the one proposed by I. Nonaka and H. Takeuchi [47] and covers:

1. Knowledge practitioners: ordinary employees or lower management:
   a) Knowledge operators (operational management, employees interacting with customers, direct control employees).
   b) Knowledge specialists (R&D employees, planners, market researchers).
2. Knowledge constructors (tactical management, designers, programmers, engineers, marketers).
3. Knowledge leaders – higher management.

Table 7 includes the percentage of roles in organization broken down into clusters and overall.

Table 7. Percentage of roles in organization: in clusters and overall

Role	Cluster 1	Cluster 2	Cluster 3	Cluster 4	Cluster 5	Overall
Knowledge operator	60,54	69,33	70,77	65,15	76,29	67,63
Knowledge specialist	19,05	16,00	15,38	15,15	10,31	15,52
Knowledge constructor	10,88	12,00	6,15	13,64	9,28	10,44
Knowledge leader	6,80	1,33	7,69	4,55	4,12	5,11

Source: authors' own study

In Tables 4–7 it is visible that each of the cluster is characterized by four features: two demographic (sex and age, shown in Tables 4 and Table 5 accordingly) and two organizational (division and role, shown in Table 6 and Table 7 accordingly). The results are given below:

1. Cluster 1 – the split between men and women is nearly equal. The highest percentage of employees in the age range 28-37 years belongs here. High percentage of office and financial division workers belongs here, still the percentage of production workers is small. These employees describe their role in organization mot often as knowledge specialists and knowledge leaders. So, according to discussed variables, cluster 1 can be named "young office leaders".
2. Cluster 2 – nearly 2/3 of these employees are men. Very high percentage of the young employees (27 or younger) belongs here. These are mostly office workers, the smallest percentage of financial division employees qualified to this cluster. Very few of this group are knowledge leaders, and proportion between knowledge operators, specialists and constructors is very similar to overall average. So, according to discussed variables, cluster 2 can be named "young not managing gentlemen".
3. Cluster 3 – this group is visibly "feminized". The structure of age is rather towards young personnel, still there is the highest percentage of employees aged 48-57 among all clusters. Only a few office workers are joined here, with a huge advantage of production and research & development workers. These employees define themselves as knowledge operators, but also knowledge leaders more than overall average. So, according to discussed variables, cluster 3 can be named "R&D ladies".
4. Cluster 4 – within this group a proportion of sex is close to equal. The structure of age is moved towards middle-aged employees. Very few office workers are joined to this cluster and the organizational divisions appearing meaningfully more often than overall average are production and IT. As to a role in organization, there is a highest percentage employees of all clusters defining it as "knowledge leader". So, according to discussed variables, cluster 4 can be named "middle-aged IT or production leaders".
5. Cluster 5 – this cluster is the most "masculine" of all, as nearly 3/4 of employees in this group are men. Also, there is a visible advantage of middle-aged and older employees, aged in the range 38–57. Nearly half of them are office workers and this is the highest percentage of all clusters. In this cluster there is the highest percentage of employees working in customer service as well. These workers clearly identify themselves mostly (over 3/4 of them) as knowledge operators (the highest percentage of all clusters). So, according to discussed variables, cluster 5 can be named "middle-aged office or customer service operators".

This way each of the clusters is characterized in terms of demography and organizational roles. So the research hypotheses H3 and H4 were verified.

At last, the research hypothesis H5 stating that there are between cluster differences according to the assessment of the character of knowledge-based work was examined. Variables describing a knowledge-based work character, also measured on a 5-point Likert scales, were as follows:

1. My work requires proper education.
2. In my work intellectual capital (experiences, thoughts, intellectual effectiveness) is of substantial meaning.
3. In my work I make use of unique specific and general competencies.
4. In my work I freely use telecommunication and information technologies.
5. In my work I am self-reliant, I solve tasks and problems by myself.
6. My work is results in creating innovations – new products or services.
7. My work requires permanent education, gathering new knowledge.

Table 8 includes mean values for variables measuring assessment of knowledge-based work character broken down into clusters and overall. These results are also shown in Figure 7.

Table 8. Mean values of variables measuring assessment of knowledge-based work character: in clusters and overall

Variable	Cluster 1	Cluster 2	Cluster 3	Cluster 4	Cluster 5	Overall
1	4,20	3,96	3,77	3,28	4,20	3,96
2	4,50	4,16	4,23	3,64	4,62	4,30
3	3,97	3,69	3,40	3,14	3,58	3,63
4	4,35	4,27	3,83	3,61	4,56	4,20
5	4,29	3,69	3,82	3,44	4,30	4,00
6	2,65	2,55	2,88	2,36	2,42	2,58
7	4,03	3,92	3,74	3,35	4,00	3,86

Source: authors' own study

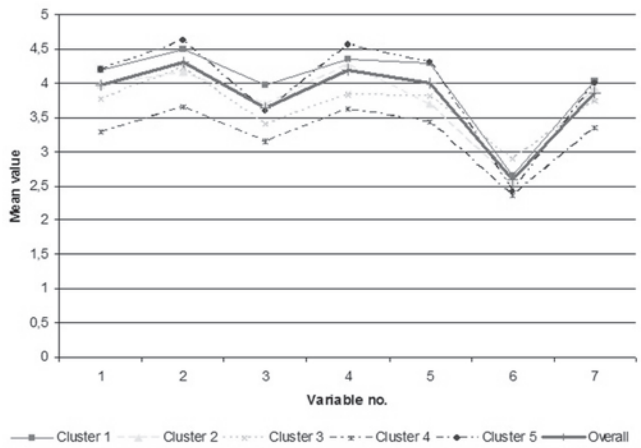

Fig. 7. Mean values of variables measuring assessment of knowledge-based work character: in clusters and overall

From the data in Table 8 and graph in Figure 7 it implies that in overall knowledge workers describe the character of their work as demanding high input of an intellectual capital (experiences, thoughts, intellectual effectiveness) (variable 2), requiring free usage of advanced telecommunication and information technologies (variable 4) and independency, autonomy, solving tasks and problems on one's own hand. These three variables have the highest mean value overall. What is interesting, the variable describing creating innovations – new products or services (variable 6) was assessed visibly on a lowest level. This means that knowledge workers perceive this feature rather as not a proper attribute for describing the character of their work.
Further, from breaking the analysis down into clusters, the following facts imply:

1. Knowledge workers joined to cluster 1 highly assess all of the variables, especially the ones concerning having proper education (variable 1), using unique general and specific competencies (variable 3), self-reliance (variable 5) and permanent education together with gathering knowledge (variable 7). So employees linked to this cluster can be called "education seeking and self-reliant".

2. Knowledge workers joined to cluster 2 assess the examined variables the average for most variables, still highly assessing the need of using unique general and specific competencies (variable 3) and a free use of information and telecommunication technologies. Hence they can be named “intensive IT-users”.
3. Knowledge workers joined to cluster 3 estimate most of the determinants of the knowledge-based work character below the overall mean value, with one exception for the fact that their work results in creating innovations – new products or services (variable 6). So this cluster can be called “innovators”.
4. Knowledge workers joined to cluster 4 assessed all of the variables well below the overall mean value. Hence this group can be named “noticing no special features of work” they do.
5. At last, knowledge workers joined to cluster 5 ascribed high values to most of the examined variables. Especially high values are given to variables describing the role of intellectual capital (experiences, thoughts, intellectual effectiveness) in the knowledge-based work (variable 2), a use telecommunication and information technologies (variable 4) and permanent education, gathering new knowledge (variable 7). So employees linked to this cluster can be called “intellectualists”.
   So the research hypothesis H5 was verified.

6. Putting together the results of the so far study

Putting together demographical and organizational characteristics of the identified clusters of knowledge workers and the perception of character of work within each cluster the statements shown in Table 9 can be generated.

The results in table 9 seem sensible and easy to interpret. Each of the 5 statements in this table reflects the character of work defined by each cluster of knowledge workers.

Finally, putting together demographical and organizational characteristics of the identified clusters of knowledge workers and the perception of occupational threats within each cluster, the statements shown in Table 10 can be generated.

Again, each of the 5 statements shown in this table reflects the perception of occupational threats by each cluster of knowledge workers.

Table 9. Knowledge workers clusters in terms of demography and organization versus perception of character of work

Cluster No.	Cluster in terms of demography and organization	Verb	Cluster in terms of perceiving character of work
1	Young office leaders	are	education seeking and self-reliant
2	Young not managing gentlemen		intensive IT-users
3	R&D ladies		innovators
4	Middle-aged IT or production leaders		noticing no special features of work
5	Middle-aged office or customer service operators		intellectualists

Source: authors' own study

Table 10. Knowledge workers clusters in terms of demography and organization versus perception of occupational threats

Cluster No.	Cluster in terms of demography and organization	Cluster in terms of perceiving occupational threats
1	Young office leaders	perceive physiological threats
2	Young not managing gentlemen	perceive psycho-sociological threats
3	R&D ladies	perceive threats to information
4	Middle-aged IT or production leaders	lack motivation, are under esteemed and perceive physical threats
5	Middle-aged office or customer service operators	perceive bad organization of work process and physical conditions at work

Source: authors' own study

7. Conclusion

Conduct of empirical studies of the self-assessment of occupational threats and the character of work by the knowledge workers by means of observable variables and application of one of the multidimensional exploratory techniques, cluster analysis, allowed to establish the following:

1. Occupational threats posed to knowledge workers were grouped into 4 logical items (clusters): “physiology” (P), “physical conditions” (F), “psycho-sociology” (S) and “data and autonomy” (D). Knowledge workers’ perception covers mostly threats coming from physiology and psycho-sociology. Threats concerning physical conditions and threats to data security and lack of autonomy are perceived as relatively weak.
2. Knowledge workers were grouped into 5 clusters according to their perception of occupational threats. Cluster 1 covers employees „perceiving physiological threats”, cluster 2 - „perceiving psycho-sociological threats”, cluster 3 - „perceiving threats to information”, cluster 4 - „lacking motivation, under esteemed and perceiving physical threats” and cluster 5 „perceiving bad organization of work process and physical conditions at work”.
3. There are between cluster differences according to demographical variables and to the department and role in organization. Taking these characteristics into consideration cluster 1 can be defined as “young office leaders”, cluster 2 – “young not managing gentlemen”, cluster 3 - “R&D ladies”, cluster 4 – “middle-aged IT or production leaders” and cluster 5 – “middle-aged office or customer service operators”.
4. There are between cluster differences according to the assessment of the character of knowledge-based work. Taking this criterion into consideration, cluster 1 covers employees “education seeking and self-reliant”, cluster 2 - “intensive IT-users”, cluster 3 – “innovators”, cluster 4 - “noticing no special features of work” they do and cluster 5 – “intellectualists”.
5. Putting together results of study covering all of the research hypothesis and according to the clusters built to classify variables within the presented universe of discourse, it can be stated that:

a) According to the demographical and organizational variables versus the perception of the character of the knowledge based work: (1) young office leaders are education seeking and self-reliant, (2) young not managing gentlemen are intensive IT-users, (3) R&D ladies are innovators, (4) middle-aged IT or production leaders are noticing no special features of work and (5) middle-aged office or customer service operators are intellectualists.

b) According to the demographical and organizational variables versus the perception of occupational threats: (1) young office leaders perceive physiological threats, (2) young not managing gentlemen perceive psycho-sociological threats, (3) R&D ladies perceive threats to information, (4) middle-aged IT or production leaders lack motivation, are under esteemed and perceive physical threats and (5) middle-aged office or customer service operators perceive bad organization of work process and physical conditions at work.

The conclusions are of both cognitive and utilitarian character. In first case – the analysis revealed and explained the structure of perception of knowledge workers' occupational threats and the character of knowledge-based work, in second – the classification of variables allows to measure perception of occupational threats and use the results e. g. when designing trainings on occupational health and safety and to better fit them to this group of employees.

In the future research, a comparison of classification of variables with the use of different multidimensional exploratory techniques could bring interesting results.

References

1. Brown G. The Global Threats to Workers' Health and Safety on the Job. Social Justice 2002; 29 (3): 12-25.
2. Cattell R. A note on correlation clusters and cluster search methods. Psychometrica 1944; 9: 169-184.
3. CIOP. Materiały informacyjne CIOP. Poradnik do oceny ryzyka zawodowego. Nurnberg: CIOP, 2007.
4. Cortada W. Rise of the Knowledge Worker. Boston: Heinemann, 1998.
5. Cox T, Howarth I. Organizational Health, Culture and Helping. Work & Stress, 1990.
6. Czop K, Mietlicka D. Dzielenie się wiedzą w przedsiębiorstwie. Ekonomika i Organizacja Przedsiębiorstwa 2011; 6: 51-59.
7. Czubała A et al. Marketing usług. Kraków: Wolters Kluwer, 2006.
8. Davenport T. Zarządzanie pracownikami wiedzy. Kraków: Wolters Kluwer, 2007.
9. Dembe A, Erickson J, Delbos R, Banks S. The impact of overtime and long work hours on occupational injuries and illnesses. Occupational and Environmental Medicine 2005; 62 (9): 588-597.
10. Drucker P. Management Challenges for 21st Century. New York: Butterworth-Heinemann, 2007.
11. Drucker P. Zarządzanie w czasach burzliwych. Warszawa: Nowoczesność, 1995.
12. Europejska Fundacja na Rzecz Poprawy Warunków Życia i Pracy: Czwarte europejskie badanie warunków pracy. Dublin: Eurofound, 2005.
13. Evetts J. The construction of professionalism in new and existing occupational contexts: promoting and facilitating occupational change. International Journal of Sociology and Social Policy 2003; 23 (4/5): 22-35.
14. Fazlagić A. Budowanie strategii przedsiębiorstwa opartego o wiedzę. [In:] Wawrzyniak B. (ed.) Zarządzanie wiedzą w organizacji. Warszawa: PFPK, 2001.
15. Filipowicz G. Rozwój organizacji przez rozwój efektywności pracowników. Kraków: Wolters Kluwer, 2008.
16. Frumkin H. Across the water and down the ladder: Occupational health in the global economy. Occupational Medicine: State of the Art Review 1999; 14 (3): 637-663.
17. Gore P. Cluster Analysis. [In:] Tinsley H, Brown S. Handbook of Applied Multivariate Statistics and Mathematical Modelling. San Diego: Academic Press 2000.
18. Granitzer M, Lindstaedt S. Knowledge Work: Knowledge Worker Productivity, Collaboration and User Support. Journal of Universal Computer Science 2010; 17 (10): 1365-1366.
19. Greenberg M. Contemporary Environmental and Occupational Health Issues: More Breadth and Depth. American Journal of Public Health 2007; 97 (3): 395-397.
20. Guidici P, Figini S. Applied Data Mining – Statistical Methods for Business and Industry. New York: Wiley and Sons, 2009.
21. Handy Ch. Wiek paradoksu. Warszawa: Dom Wydawniczy ABC, 1996.
22. Hartigan J. Clustering Algorithms. New York: Wiley and Sons, 1975.
23. Hastie T, Tibshirani R, Friedman J. The Elements of Statistical Learning – Data Mining, Inference and Prediction. New York: Springer, 2009.
24. Hiyama T, Yoshikara M. New Occupational Threats to Japanese Physicians. Occupational and Environmental Medicine 2008; 65 (6): 428-429.
25. Promoting Safety and Health in a Green Economy. Geneva: International Labour Organization, 2012.
26. Jemielniak D. Praca oparta na wiedzy. Warszawa: WAiP, 2008.
27. Jemielniak D. The New Knowledge Workers. Cheltenham: Edward Elgar Publishing, 2012.
28. Kawka T. Pracownik w czasach nowej gospodarki. [In:] Potocki A (ed.) Globalizacja a społeczne aspekty przeobrażeń i zmian organizacyjnych. Warszawa: Difin, 2009.
29. Kidd A. The Marks on the Knowledge Workers. [In:] Proceedings of the SIGCHI Conference on Human Factors in Computing Systems, New York: ACM, 1994.
30. Kleinmann D, Vallas S. Science, capitalism, and the rise of the knowledge worker. Theory and Society 2001; 30 (4): 451-492.
31. Kowalski T. Pojęcie i cechy pracownika wiedzy. Studia Lubuskie 2011; VII: 309-323.
32. Landy F. Work Design Stress. [In:] Keita G, Sauter S. (ed.) Work and Well Being: an Agenda for the 1990s. Washington: American Psychological Association, 1992.
33. Lewis K. Knowledge and Performance in Knowledge Worker Teams. Management Science 2004; 50 (11): 1519-1533.
34. Lotko M, Żuchowski J. Occupational Threats in the Information Society. Radom: ITeE, 2014.
35. Lotko M. Ocena zagrożeń pracowników wiedzy w procesie pracy. Problemy Jakości 2012; 9: 12-16.
36. Lotko M. Zarządzanie bezpieczeństwem pracy pracowników wiedzy. Radom, Wyd. Politechniki Radomskiej, 2011.
37. Łysik K. Zarządzanie pracownikami wiedzy. Kwartalnik Nauk o Przedsiębiorstwie 2011; 3 (20): 57-62.
38. Makowski D. Pracownicy intelektualni. Profesjonalizacja wiedzy. [In:] Koźmiński A, Jemielniak D (ed.) Zarządzanie wiedzą. Warszawa: WAiP, 2008.
39. Matson E, Prusak L. Boosting the Productivity of Knowledge Workers. McKinsey Quarterly 2010; September: 1-4.
40. Migut G. Zastosowanie technik analizy skupień i drzew decyzyjnych do segmentacji rynku. Kraków: StatSoft, 2009.
41. Mikuła B. Strategie pozyskiwania i rozwoju wiedzy w organizacji. Ekonomika i Organizacja Przedsiębiorstwa 2004; 1: 28-33.
42. Morawski M. Zarządzanie profesjonalistami. Warszawa: PWE, 2009.
43. Morawski M. Metody zarządzania pracownikami wiedzy – założenia wstępne. [In:] Skrzypek E (ed.) Future 2002 – Zarządzanie przyszłością przedsiębiorstwa. Lublin: Wyd. UMCS, 2002.

44. Morawski M. Problematyka zarządzania pracownikami wiedzy. Przegląd Organizacji 2003; 1: 17-20.
45. Morawski M. Zarządzanie wiedzą – ujęcie systemowe. Organizacja i Kierowanie 2006; 4: 53-68.
46. Morawski M. Zarządzanie wiedzą. Prace Naukowe Akademii Ekonomicznej we Wrocławiu 2006; 1134: 41-46.
47. Nonaka I, Takeuchi H. The Knowledge-creating Company. New York: Oxford University Press, 1995.
48. Patalas-Maliszewska J. Managing Knowledge Workers. Berlin Heidelberg: Springer-Verlag, 2013.
49. PN-EN-ISO 12100-1:2005 Bezpieczeństwo maszyn. Pojęcia podstawowe, ogólne zasady projektowania. Część 1: Podstawowa terminologia, metodyka. Warszawa: PKN, 2005.
50. PN-ISO/IEC 27001:2007 Technika informatyczna. Techniki bezpieczeństwa. Systemy zarządzania bezpieczeństwem informacji. Wymagania. Warszawa: PKN, 2007.
51. Roell M. Distributed KM - Improving Knowledge Workers' Productivity and Organisational Knowledge Sharing with Weblog-based Personal Publishing. Vienna: BlogTalk 2.0, 2004.
52. Sikorski C. Profesjonalizm. Filozofia zarządzania nowoczesnym przedsiębiorstwem. Warszawa: PWN, 1997.
53. Skrzypek E. Kreatywność pracowników wiedzy i ich wpływ na konkurencyjność przedsiębiorstw. [In:] Materiały V Konferencji „Wiedza i innowacje". Kraków: Wydawnictwo UJ, 2009.
54. Skrzypek E. Miejsce zarządzania informacją i wiedzą w strategii przedsiębiorstwa. [In:] Stabryła E (ed.) Zarządzanie firmą w społeczeństwie informacyjnym. Kraków: Wydawnictwo EJB, 2002.
55. Sokołowski A. Empiryczne testy istotności w taksonomii. Kraków: Wyd. Akademii Ekonomicznej w Krakowie, 1992.
56. Speece D. Cluster analysis in perspective. Exceptionality 1995; 5: 31-44.
57. Staniewski M. Zarządzanie zasobami ludzkimi a zarządzanie wiedzą w przedsiębiorstwie. Warszawa: Vizja Press&it, 2008.
58. STATISTICA PL. Tom III: Statystyki II. Kraków: StatSoft, 1997.
59. Stevens J. Applied Multivariate Statistics for the Social Sciences. New York: Routledge, 2009.
60. Straub D, Karahanna E. Knowledge Worker Communications and Recipient Availability. Organization Science 1998; 9 (2): 160-176.
61. Strojny M. Pracownicy wiedzy – przegląd badań. Zarządzanie Zasobami Ludzkimi 2004; 6: 75-81.
62. Szaban J. Inteligentna firma i jej pracownicy. [In:] Wawrzyniak B (ed.) Zarządzanie wiedzą w organizacji. Warszawa: Wyd. PFPK, 2001.
63. Tryon R. Cluster Analysis. New York: McGraw-Hill, 1939.
64. Global strategy on occupational health for all: The way to health at work. Beijing: WHO, 1994.

Małgorzata LOTKO
Aleksander LOTKO
Department of Economics
Kasimir Pulaski University of Humanities and Technology
ul. Chrobrego 31, 26-600 Radom, Poland
E-mails: m.lotko@uthrad.pl, aleksander.lotko@uthrad.pl

Article citation info:
BEER-LECH K, SUROWSKA B. Research on resistance to corrosive wear of dental CoCrMo alloy containing post-production scrap. Eksploatacja i Niezawodnosc – Maintenance and Reliability 2015; 17 (1): 90–94.

Karolina BEER-LECH
Barbara SUROWSKA

RESEARCH ON RESISTANCE TO CORROSIVE WEAR OF DENTAL CoCrMo ALLOY CONTAINING POST-PRODUCTION SCRAP

BADANIE ODPORNOŚCI NA ZUŻYCIE KOROZYJNE STOMATOLOGICZNEGO STOPU CoCrMo ZAWIERAJĄCEGO ZŁOM POPRODUKCYJNY*

Use of metal base dental prostheses is accompanied by not only wear due to biomechanical loads that occur during the process of chewing, but also by corrosive wear occurring in aggressive oral environment. Corrosive wear of metal elements of prosthesis may result in excluding it from further use by the occurrence of allergic or even carcinogenic reactions in patient, resulting from the release of toxic metal ions into the body. A common practice in prosthetic laboratories used in order to reduce production costs of dental prostheses is using so-called post-production scrap to subsequent castings. This scrap constitute the elements of casting channels, defectively made skeletons of prostheses or metal residues after prosthetic treatment. Use of post-production scrap to manufacture components to fulfill such high performance criteria (presence of complex biomechanical loads), and in particular taking into account the evaluation of biocompatibility, is the subject of discussion not only in the environment of scientists, but also the producers of dental alloys.The aim of the study was to investigate resistance to corrosive wear of dental cobalt alloy containing post-production scrap. The commercial dental alloy Wironit extra-hard with cobalt matrix has been used in this research. The study was based on a conducted polarity by means of potentiodynamic method in a solution of artificial saliva. Tested alloy samples, containing different percentage intake of post-production scrap, were cast by two casting methods - centrifugal and vacuum-pressure. Average values of parameters of Wironit extra – hard alloy resistance to corrosive wear: corrosion potential – E_{cor} , corrosion current Icor, polarisation resistance R_{pol} and pitting potential – E_{pit} were determined. In order to assess alloy surface after corrosion microscopic observation was made. The results of research confirm high resistance of alloy to corrosive wear in environment of artificial saliva. Castings made using centrifugal methods provide lower current density in the passive state than those carried out by vacuum – pressure method, which suggests greater durability of passive layer confirmed by analysis of microstructure of samples after corrosion. Determination of correlation between content of post-production scrap and resistance to corrosion is ambiguous.

Keywords: *corrosive wear, cobalt alloys, post-production scrap.*

Eksploatacji stomatologicznych protez na podbudowie metalowej towarzyszy nie tylko zużycie wskutek obciążeń biomechanicznych, występujących podczas procesu żucia, ale również zużycie korozyjne mające miejsce w agresywnym środowisku jamy ustnej. Zużycie korozyjne metalowych elementów protezy skutkować może wyłączeniem jej z dalszego użytkowania wskutek wystąpienia u pacjenta reakcji alergicznych lub nawet kancerogennych, będących rezultatem uwalniania do organizmu toksycznych jonów metali. Częstą praktyką w laboratoriach protetycznych stosowaną w celu obniżania kosztów produkcji protez jest stosowanie tzw. złomu poprodukcyjnego do kolejnych odlewów. Złom ten stanowią elementy kanałów odlewniczych, wadliwie wykonane szkielety protez bądź metalowe pozostałości po obróbce protetycznej. Zastosowanie złomu poprodukcyjnego do wytwarzania elementów mających spełniać tak wysokie kryteria eksploatacyjne (występowanie złożonego stanu obciążeń biomechanicznych), a zwłaszcza biorąc pod uwagę ocenę biokompatybilności otrzymanych wyrobów, jest tematem dyskusyjnym nie tylko w środowisku naukowców, ale również i samych producentów stopów stomatologicznych. Celem pracy było zbadanie odporności na zużycie korozyjne stomatologicznego stopu kobaltu zawierającego złom poprodukcyjny. Do badań zastosowano komercyjny stop stomatologiczny Wironit extra – hard na osnowie kobaltu. Badanie polegało na przeprowadzeniu polaryzacji metodą potencjodynamiczną w środowisku roztworu sztucznej śliny. Próbki stopu poddane badaniu, zawierające różny udział procentowy złomu poprodukcyjnego, odlane zostały dwiema metodami odlewniczymi - odśrodkową i próżniowo-ciśnieniową. Wyznaczono średnie parametrów określających odporność stopu Wironit extra – hard na zużycie korozyjne: potencjał korozji – E_{kor}, prąd korozji I_{kor}, opór polaryzacyjny R_{pol} i potencjał przebicia – E_{pit}. W celu oceny powierzchni stopu po korozji dokonano obserwacji mikroskopowych. Wyniki badań potwierdzają dużą odporność stopu na zużycie korozyjne w środowisku sztucznej śliny. Odlewy wykonane za pomocą metody odśrodkowej cechują się niższą gęstością prądu w stanie pasywnym niż te wykonane metodą próżniowo – ciśnieniową, co sugeruje większą trwałość warstwy pasywnej potwierdzoną analizą mikrostruktury próbek po korozji. Wyznaczenie zależności pomiędzy zawartością złomu poprodukcyjnego a odpornością na korozję jest niejednoznaczne.

Słowa kluczowe: *zużycie korozyjne, stopy kobaltu, złom poprodukcyjny.*

(*) Tekst artykułu w polskiej wersji językowej dostępny w elektronicznym wydaniu kwartalnika na stronie ***www.ein.org.pl***

1. Introduction

CoCrMo alloys are some of the most popular alloys used in medical implants [8], and skeletal dentures but due to a combination of good mechanical properties, corrosion resistance and biocompatibility and favorable price and easy-to-treatment [3, 19].

Metal base skeletal dentures properties and their design would have a significant impact on their durability during their maintenance in the oral cavity [2]. Use of metal skeletons of dentures is accompanied not only by wear of fixing elements of prosthesis due to biomechanical loads that occur during the process of chewing, but also corrosive wear occurring in aggressive oral environment. Corrosive wear of prosthesis may result in excluding it from further use by the occurrence of allergic or even carcinogenic reactions in patient, resulting from the release of toxic metal ions into the body.

A common practice in prosthetic laboratories, allowing for a substantial reduction in the manufacturing cost of dentures, is the use of metals or their alloys, which has already been used in casting process [20, 21]. In the production process of metal skeletons of prostheses is produced a significant amount of post-production scrap constituting very often badly made castings, casting channels or which is residues after dental treatment. Use of post-production scrap to manufacture components to fulfill such high performance criteria of mechanical resistance (presence of state of complex biomechanical loads), and in particular taking into account the evaluation of biocompatibility, is the subject of discussion not only in the environment of scientists, but also the producers of dental alloys. Literature data indicate that performance characteristics of alloys containing post-production scrap may vary from factory alloys [1, 4, 6, 7, 11, 18]. Authors of research sometimes observe a change in chemical composition of alloy [4, 6] after use of secondary casting. These changes may affect connection strength of alloy with dental porcelain [11, 18], as well as affecting the growth of cytotoxicity of alloys [1] and affect the corrosion resistance [7].

Many manufacturers of dental alloys permit implementation of recasting, but with not less than 50% of intake of new material, provided that all the material must be from the same batch. Also, there is a manufacturer group, who does not allow recasting materials, or gives no information on the use of such dental alloys.

Corrosive wear of cobalt alloys as biomaterials was already the subject of many scientific studies, but mostly in the context of alloys intended for knee and hip joints implants, e.g. [5, 8, 17]. There is also a considerable group of research dealing with corrosive resistance of dental cobalt alloys, e.g. [12, 16].

Negligible number of research concerns the impact of addition of post-production scrap or secondary casting of metal on the resistance to corrosive wear [7, 9]. Furthermore, the views of authors of research on the prevalence of potential changes in resistance to corrosion, after applying in castings recasted materials, are contradictory.

The aim of the study was to investigate resistance to corrosive wear of dental cobalt alloy containing post-production scrap and identifying the impact of casting method on this type of wear.

2. Materials and methods

For research was applied commercial dental alloy – Wironit extra – hard from Bego Co. with the following chemical composition (by mass) – specified by the manufacturer: Co – 63 %, Cr – 30,01 %, Mo – 5.0 %, Si – 1.1 %, Mn, C<1.

From the alloy were cast samples in form of cylinders with a diameter of 5 mm. Precision casting technique by method of melt models was implemented. The silicone wax model primed with acrylic resin was placed in metal ring and primed with refractory ceramic material (the so-called covering) with trade name Wirovest by Bego. After drying wax was melt in an oven at temperature of 523 K, then a form was heated to a temperature of 1223 K to sinter the form, to burn rests of wax and remove gases. The inductively melt inserts were cast by two methods: vacuum - pressure in Nautilius Bego device (samples marked with PC) and centrifugal in Rotocast casting machine by Roco Dental Equipment (samples marked with W). Ceramic crucibles were used. The casting temperature was in line with the alloy manufacturer's recommendations. For both methods it was 1693 K. Made casts contained respectively 0, 50 and 100% of factory alloy, supplemented with a sufficient amount of post-production scrap. The marking of samples is given in Table 1.

Table 1. The marking of samples for testing

No.	Casting method - vacuum -pressure	Casting method - centrifugal	Sample determination / the content of factory alloy
1.	0_PC	0_W	A sample containing 100% of post-production scrap
2.	50_PC	50_W	A sample containing 50% of factory alloy and 50% of post-production scrap
3.	100_PC	100_W	A sample containing 100% of factory alloy

The surface of the samples before the test has been subjected to a treatment consisting of grinding with abrasive papers of gradation equal to 220–1200 on rotary grinders and then mechanical polishing on diamond discs by Buehler with use of dedicated diamond suspensions MetaDi one by one (9 µm and 3 µm) and colloidal silica ~ 0.05-mm MasterMet), cleaning in ultrasonic washer in ethanol and dried with compressed air.

An assessment of resistance to corrosive wear was conducted by electrochemical method supported with quality observations of surface. For corrosive measurements was used electrochemical test-kit ATLAS 0531, consisted of potentiostat – galvanostat controlled by a computer and trielectrode electrochemical vessel placed in a Faraday cage. Trielectrode electrochemical vessel consisted of the tested electrode, which was consecutive samples of Wironit extra – hard alloy, a platinum auxiliary electrode and saturated calomel reference electrode with electrolytic bridged finished with a Ługgin's capillary. In addition, this kit was equipped with a heater with thermostat and electromagnetic stirrer allowing to maintain temperature of measuring environment at a constant level of 310K (37°C) with a measuring accuracy of ±0,5 °C.

Measurement was taken in a solution environment of artificial saliva [14], the composition of which is given in Table 2.

During the tests current-voltage characteristics were recorded. Polarization was carried out with a speed change of potential equal to1 mV/s in respect of the value of potential from −1000 to +1200mV. To determine characteristic values of E_{cor}, I_{cor}, R_{pol} and E_{pit} was used Atlas Lab software. It can be used to calculate the polarisation resistance from a sector of a curve along with corrosion potential, Tafel constants b_a and b_c, corrosion potential E_{cor} and corrosion current I_{cor}

Table 2. The composition of artificial saliva solution per 1 dm³ of solution

The composition of artificial saliva solution:	The amount in the solution [g]:
NaCl	0,4
KCl	0,4
NaH_2PO_4 x H_20	1,35
NaH_2P	0,78
Na_2S x 9 H_2O	0,005

and plotting Tafel curves. In addition, from polarisation curves, using „extrapolation" option was determined pitting potential E_{pit}. The average values for series of measurements were calculated using a modulus for mathematical analysis.

In addition, in order to compare the state of surface of the samples before and after corrosive was conducted microscopic observation using metallographic optical microscope Nikon MA100.

3. The results of research and discussion

The results of research (Figure 1 and 2, Table 3) show that Wironit extra-hard alloy has a very good ability to passivation expressed by broad passive area and low density of passivation current. In Figures 1 and 2 are presented the representative polarisation curves of Wironit extra – hard alloy samples carried out without the addition of post-production scrap. A similar shape of curves was also registered for samples containing post-production scrap.

Table 3 shows the results of the tests containing average values of the corrosion potential E_{cor} , corrosion current $I_{cor,}$ polarisation resistance R_{pol} and potential, above which were formed corrosion pits (of pitting potential) E_{pit}.

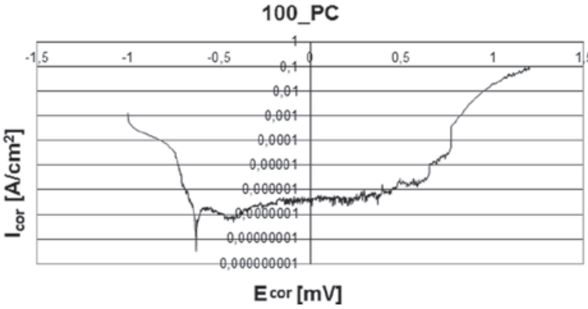

Fig. 1. The example of polarisation curve for sample 100_PC

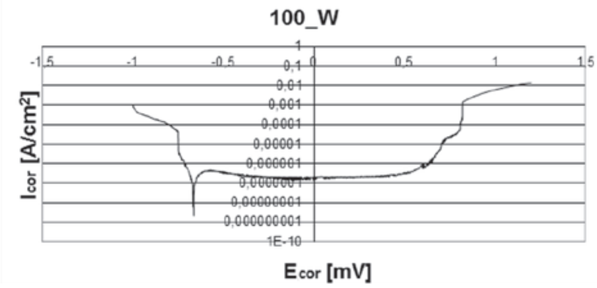

Fig. 2. The example of polarisation curve for sample 100_W

Table 3. The results of the tests of electrochemical corrosion of Wironit extra - hard alloy

The content of manufacturing alloy [%]	$\overline{E}_{cor}$ [mV]	$\overline{I}_{cor}$ [A/cm²]	$\overline{R}_{pol}$ [Ω*cm²]	$\overline{E}_{pit}$ [mV]
0_PC	-673	$6,29*10^{-7}$	57 667	442
50_PC	-486	$13,8*10^{-7}$	152 850	593
100_PC	-561	$8,38*10^{-7}$	90 125	603
0_W	-674	$14,4*10^{-7}$	56 000	623
50_W	-406	$6,19*10^{-7}$	196 000	620
100_W	-583	$5,92*10^{-7}$	141 000	600

Data in Table 3 and in Figures 3 and 4 indicate the existence of differences in corrosive resistant of Wironit extra – hard alloy samples cast using two methods: vacuum-pressure and centrifugal, containing varying amounts of post-production scrap. Castings made by centrifugal method are characterized with greater durability of passive layer expressed by the lower current density in the passive state. These results do not confirm observation [13, 15], that the marginal impact on dental alloys corrosion resistance has the casting method used, and only chemical composition of these alloys decide on their resistance to corrosive wear. Comprehensive research of macro- and microstructure of castings described by the author in earlier publications [3, 20] indicate, however, the observed dependence of corrosion liability from a macro- and microstructure of alloys.

However, determining the best resistance of Wironit extra - hard alloy to corrosive wear due to the content of manufacturing alloy and post-production alloy is not clear.

Due to the corrosion potential the best parameters (the highest value of E_{cor}) show castings containing 50% of factory alloy with corrosion potential E_{cor} equal to −486 mV for 50_PC and −406 mV for 50_W. The next in order are castings made of factory alloys, the smallest values of the corrosion potential has been reported for samples from both methods performed fully from post-production scrap. However, taking into account the value of the corrosion current I_{cor} most favourable properties indicate successively castings 100_W, where I_{cor} is $5.92 * 10^{-7}$ A/cm ^{2} , 50_W ($I_{cor} = 6{,}19 * 10^{-7}$A/cm ^{2}) and 0_PC ($6{,}29 * 10^{-7}$A/cm^2). Polarization resistance of vacuum-pressure and centrifugal method showed the highest value for samples containing 50% of factory alloy, while average the greatest pitting potential E_{pit} for vacuum-pressure method for samples 100_PC – 603 mV, and for centrifugal method for samples 0_W – 623mV.

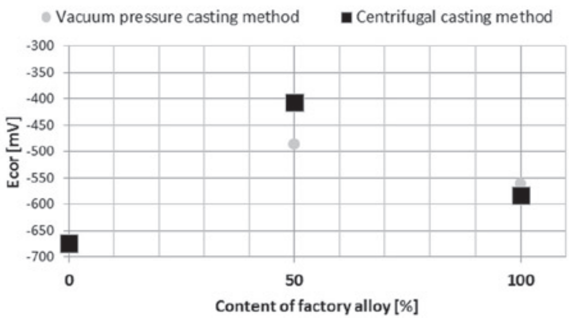

Fig. 3. The value of mean corrosion potential for samples with different content of factory alloy made by vacuum – pressure and centrifugal method

Figure 5 shows dendritic microstructure of samples without addition of post-production scrap cast by vacuum – pressure and centrifugal method. In the structure have been found casting defects (5a and b) in form of porosity. Microstructures of the same casts after corrosive research are shown in Figure 6. The dendritic structure of samples after the test has been more highlighted. Present passive layer, particularly clearly visible in Figure 6a, is not continuous.

The casting defects occurring in the structure contribute to the development of surface, ingression of aggressive environment and make difficult uniform deposition of passive layer being a cause of increased corrosion, what is known from the literature [10]. Also interdendritic segregations in block form are described in greater detail in [20], not covered with oxide layer due to difference of potentials, may initiate the occurrence of corrosion pits.

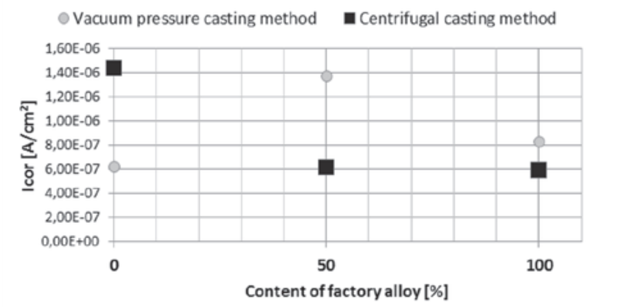

Fig. 4. The value of mean corrosion current for samples with different content of factory alloy made by vacuum – pressure and centrifugal method

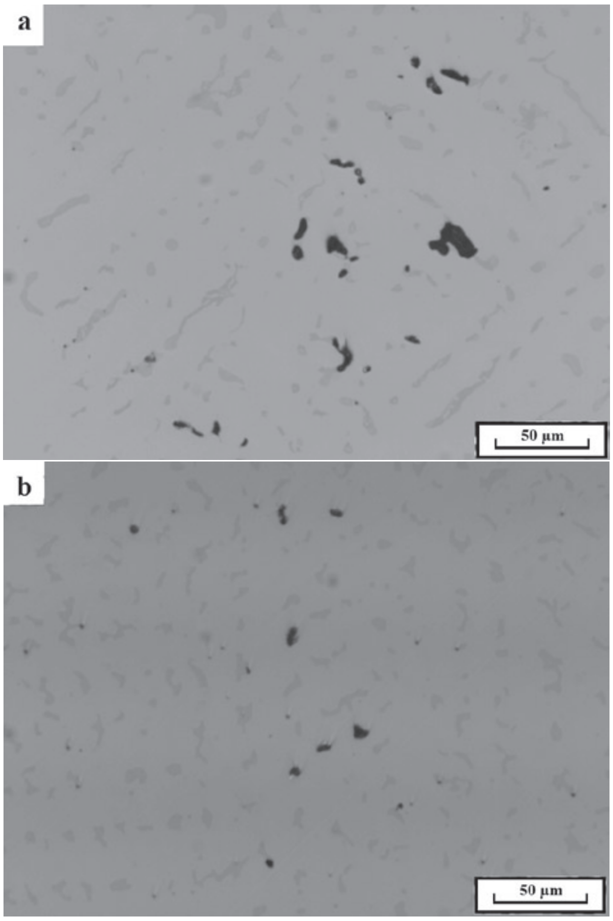

Fig. 5. The microstructure of Wironit extra – hard alloy before the test: a) the sample 100_PC; b) the sample 100_W

Observations of samples indicate the occurrence of corrosion pits and damage to the surface in form of intergranular corrosion (the darkest areas in the figures). These pits, created after a pitting of passive layer, occur on the borders of block precipitates (Figure 6a and b), in these precipitates (6b) and in the interdendritic areas along continuous precipitates (Figure 6b). This is most likely related to chromium zone segregation in the samples. This element, responsible for corrosion resistance in Co-Cr -Mo alloys, in accordance with the results [12], dominates in the block precipitates, as shown by previous research of the authors [20], while the boundaries between precipitates and matrix are depleted in this element. Greater number of pits was observed for vacuum-pressure method, which is consistent with the results of electrochemical measurements.

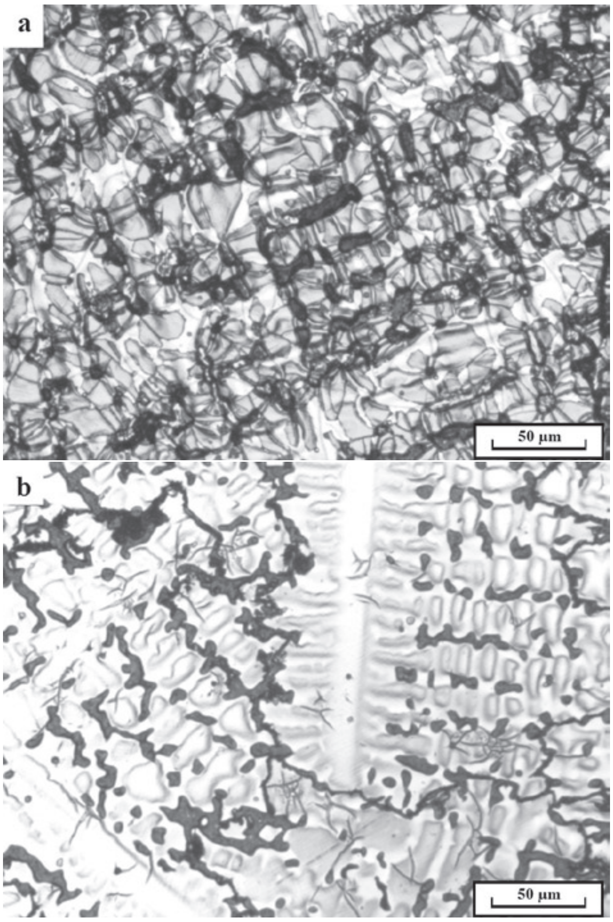

Fig. 6. The microstructure of Wironit extra-hard alloy after the test on electrochemical corrosion: a) the sample 100_PC; b) the sample 100_W

The presented results confirm that problem of resistance changes to corrosive wear of dental CoCrMo alloys after applying of post-production scrap is a complex issue and worth further research in order to obtain convincing proof whether implementation of recastings has actually a significant effect on dental alloys corrosion resistance, as pointed out [7] or rather marginal [9].

4. Conclusions:

Research on resistance to corrosive wear of Wironit extra - hard alloy showed high resistance of alloy to electrochemical corrosion in artificial saliva solution. This alloy has a very good passivation ability, and broad passive area, and low current density in the passive state. Castings made using the centrifugal method demonstrate higher durability of passive layer expressed by lower passivation current than castings made by vacuum pressure method. However, determination of dependence of resistance of Wironit extra - hard alloy to corrosive wear from manufacturing alloy content and post-production scrap is not possible without taking into account other factors (changes of chemical composition, microstructure, macrostructure).

Acknowledgements:

The paper was created in the course of the project of National Science Center „Preludium" No. 2011/01/N/ST8/07774.
Authors are grateful for Professor Janusz Borowicz, MD, Ph.D. for assistance in preparation of samples for testing.

References

1. Al-Hiyasat AS, Darmani H. The effects of recasting on the cytotoxicity of base metal alloys. The Journal of Prosthetic Dentistry 2005; 93: 158-163.
2. Beer K, Pałka K, Surowska B, Walczak M, A Quality assessment of casting dental prosthesis elements. Eksploatacja i Niezawodnosc - Maintenance and Reliability 2013; 3(15): 230-236.
3. Büscher R, Täger G, Dudziński W, Gleising B, Wimmer MA, Fischer A. Subsurface microstructure of metal-on-metal hip joints and its relationship to wear particle generation. Journal of Biomedical Materials Research 2004; 72B(1): 206-214.
4. Harcout HJ. The remelting of cobalt-chromium alloys. British Dental Journal. 1962; 6: 198-204.
5. Hodgson AWE, Kurz S, Virtanen S, Fervel V, Olsson COA, Mischler S. Passive and transpassive behavior of CoCrMo in simulated biological solutions. Electrochemica Acta 2004; 49: 2167-2178.
6. Hong J, Razoog ME, Lang BR. The effect of recasting on the oxidation layer of palladium-silver porcelain alloy. The Journal of Prosthetic Dentistry 1986; 55: 420-425.
7. Horosawa N, Marek M. The effect of recasting on corrosion of a silver–palladium alloy. Dental Materials, 2004; 4(20): 352–357.
8. Julian LC, Munoz A.I. Influence of microstructure of HC CoCrMo biomedical alloys on the corosion and wear behaviour in simulated body flulids. Tribology International 2011; 44: 318-329.
9. Khamis E, Seddik M. Corrosion evaluation of recasting non-precious dental alloys. International Dental Journal 1995; 45: 209-217.
10. Kim SJ, Ko Y-M, Choe H-C. Pitting corrosion of TiN coated dental cast alloy with casting methods. Advanced Materials Research. 2007 17(15): 164-168.
11. Lopes MB, Consani S, Sinhoreti MAC, Correr-Sobrinho L. Influence of recasting palladium-silver alloy on the fit of crowns with different marginal configurations. The Journal of Prosthetic Dentistry 2005; 5(94): 430–434.
12. Mareci D, Nemtoi Gh, Aelenei N, Bocanu C. The electrochemical behavior of various non-precious Ni and Co based alloys in artificial saliva, European Cells and Materials 2005; 10: 1-7.
13. Mülders C. Darwisch M. and Holze R. The influence of alloy composition and casting procedure upon the corrosion behavior of dental alloys: An in vitro study. Journal of Oral Rehabilitation 1996; 23: 825-831.
14. PN-EN ISO 10271:2012. Stomatologia – Metody badania korozji materiałów metalowych.
15. Saji VS, Choe H-Ch. Electrochemical behavior of Co-Cr and Ni-Cr dental alloys. Transactions of Nonferrous Metals Society of China 2009; 19: 785-790.
16. Schmalz G, Garhammer P. Biological interactions of dental cast alloys with oral tissues [J], Dental Materials 2002; 18: 396-406.
17. Sinnett – Jones PE, Wharton JA, Wood RJK. Micro-abrasion-corrosion of a CoCrMo alloy in simulated artificial hip joint environments. Wear 2005; 259: 898-909.
18. Ucar Y, Aksahin Z, Kurtoglu C. Metal Ceramic Bond After Multiple Castings of Base Metal Alloy. Journal of Prosthetic Dentistry 2009; 3(102): 165-171.
19. Vidal VC, Munoz IA. Electrochemical characterization of biomedical alloys for surgical implants in simulated body fluids. Corrosion Science 2008; 50:1954-1961.
20. Walczak M. Beer K. Surowska B. Borowicz J. The issue of ussing remelted CoCrMo alloys in dental prosthetics. Archives of Civil and Mechanical Engineering 2012; 12: 171-177.
21. Walczak M. Pieniak D. Niewczas AM. Effect of recasting on the useful properties CoCrMoW alloy. Eksploatacja i Niezawodnosc – Maintenance and Reliability 2014; 2(16): 330-336.

Karolina BEER-LECH
Barbara SUROWSKA
Department of Materials Engineering
Faculty of Mechanical Engineering
Lublin University of Technology
ul. Nadbystrzycka 36, 20-618 Lublin, Poland
E-mails: k.beer@pollub.pl, b.surowska@pollub.pl

Article citation info:
AMBROZIK A, AMBROZIK T, ŁAGOWSKI P. Fuel impact on emissions of harmful components of the exhaust gas from the ci engine during cold start-up. Eksploatacja i Niezawodnosc – Maintenance and Reliability 2015; 17 (1): 95–99.

Andrzej AMBROZIK
Tomasz AMBROZIK
Piotr ŁAGOWSKI

FUEL IMPACT ON EMISSIONS OF HARMFUL COMPONENTS OF THE EXHAUST GAS FROM THE CI ENGINE DURING COLD START-UP

WPŁYW PALIWA NA EMISJĘ SZKODLIWYCH SKŁADNIKÓW SPALIN SILNIKA O ZAPŁONIE SAMOCZYNNYM PODCZAS ZIMNEGO ROZRUCHU*

The paper presents the results of tests on the compression ignition PEUGEOT 2.0 HDI engine. It was fuelled by commercial diesel oil, B50 blend (50 % diesel oil and 50 % rapeseed oil fatty acid methyl esters), and blend of diesel oil and 5% EKO-V fuel additive manufactured by the INWEX company. The tests were conducted for cold and hot engine. When the engine started up from cold, the temperature of the coolant and lubricating oil was equal to the ambient temperature. In hot engine start-up, the temperature of the engine oil and the coolant was 90 ºC. The values of concentrations of the exhaust gas harmful components were measured before the catalytic converter.

Keywords*: diesel engine, engine start-up, biofuel, exhaust emission.*

W artykule przedstawiono wyniki badań silnika o zapłonie samoczynnym PEUGEOT 2.0 HDI zasilanego handlowym olejem napędowym, mieszaniną B50 (50 % oleju napędowego i 50 % estrów metylowych kwasów tłuszczowych oleju rzepakowego) i oleju napędowego z dodatkiem 5% preparatu EKO-V firmy INWEX. Badania wykonano dla zimnego i rozgrzanego silnika. Podczas rozruchu zimnego silnika temperatura cieczy chłodzącej i oleju smarnego była równa temperaturze otoczenia, natomiast podczas rozruchu silnika ciepłego temperatura oleju silnikowego i cieczy chłodzącej wynosiła 90ºC. Wartości stężeń szkodliwych składników spalin zmierzono przed katalizatorem utleniającym zainstalowanym w układzie wydechowym silnika.

Słowa kluczowe*: silnik o zapłonie samoczynnym, rozruch silnika, biopaliwo, emisja spalin.*

1. Introduction

Rapid development of the motor industry, observed in recent years, has led to search for new fuels to power internal combustion piston engines. Many national research centres have conducted tests on engines running on biofuels derived from different plants [1, 2, 3, 12, 13, 14, 17, 26, 27]. Engine fuelling by biofuels has many advantages. Biofuels are completely biodegradable, they allow reduction in the exhaust emissions of carbon monoxide, hydrocarbons and particulate matter [12, 25]. The research has also concerned the effect produced by adding plant oil fatty acid methyl and ethyl esters to diesel oils on the emissions of the exhaust gas harmful components during the CI engine cold start-up [8, 16, 19, 23, 28, 29]. In papers [4, 5, 7, 9, 15, 20, 21], it is stated that in the first stage of the cold engine start-up, the emissions of carbon monoxide, hydrocarbons and particulate matter are higher than those for the warm engine start-up. In addition to increased emissions of the exhaust gas harmful components, other negative phenomena may occur in the cold start-up. Those will be related to a higher level of vibration, noise, and the engine uneven running [9, 10]. The phenomena can be attributed to unfavourable conditions in the cylinder during the ignition of air-fuel mixture, e.g. worse fuel spray and vaporization of the injected fuel droplets. Auto-ignition delay period is affected by many factors, including, among others, the working medium temperature, fuel physical and chemical properties, fuel injection and cylinder air-filling profiles. In the regular engine operation, combustion is more complete when compared with cold engine.

The paper presents problems related to the cold start-up of internal combustion piston engine with compression ignition. The engine was fuelled by commercial diesel oil, diesel oil/ rapeseed oil fatty acid methyl esters blend B50 (50% of commercial diesel oil and 50% of rapeseed oil fatty acid methyl esters), and also by commercial diesel oil with EKO-V additive developed by the INVEX company (95% of commercial diesel oil + 5% of EKO-V additive). The tests were intended to assess the impact of the fuels listed above on the emissions of the exhaust gas toxic components. In the compression ignition engine, the combustion is preceded by auto-ignition delay period. It is a very important time interval, in which fuel injection occurs and fuel undergoes physical and chemical changes that constitute the so-called pre-flame reactions.

The properties of the fuel injected into the cylinder considerably affect the start-up duration and reliability, and also the engine reaching thermal balance. Fuel surface tension is of major importance as it influences the quality of the fuel spray. Other physical and chemical fuel properties also affect the fuel spray quality. The ignition delay period also depends on the temperature of the working medium in the cylinder. For a cold start-up, auto-ignition delay is longer, which results primarily from a longer time of fuel vaporisation, leading to an extension of the physical part of auto-ignition delay. Chemical part of ignition delay also has a significant effect on auto-ignition delay. According to [18, 22], at a lower temperature of the working medium, the chemical part of ignition delay is prolonged because the speed of chemical reactions decreases much faster than the speed of physical transformations occurring during that time. At high temperatures in

(*) Tekst artykułu w polskiej wersji językowej dostępny w elektronicznym wydaniu kwartalnika na stronie ***www.ein.org.pl***

the cylinder, the speed of chemical reactions is high. Consequently, the auto-ignition delay period is determined by physical processes, such as speed of injection, fuel vaporization and air/fuel vapour mixing. Fuels with higher cetane number have better auto-ignition properties and are characterised by shorter auto-ignition delay periods.

Cold engine start-up and emissions of the exhaust gas toxic components depend on physical and chemical properties of fuels. Those include the following: cetene number, distillation point of a specified fuel portion, viscosity, density, surface tension, cold filter plugging point and freezing temperature. Fuel for compression ignition engines should have high vaporization capacity. Fuels characterised by lower distillation point of a fuel fraction allow easier engine start-up, especially at low ambient temperatures. Fuels with a higher cetane number provide for easier engine start-up.

When the engine starts from cold, the exhaust gas contains more unburnt hydrocarbons, fuel vapours and incomplete combustion products [5, 6]. One of interesting solutions aimed at lowering the concentrations of the exhaust gas toxic components during the start of the cold engine is a short start-up without delivering fuel to the engine, which causes the pre-heating of the combustion chamber due to compression. As a result, lower concentrations of carbon monoxide, hydrocarbons and particulates are obtained [15]. During the cold start-up of the engine equipped with the exhaust gas recirculation system, some of the gas returns to the engine and can shorten the auto-ignition delay period [11]. Due to stricter standards on concentrations in the exhaust gas from internal combustion piston engines, it is necessary to use alternative fuels that produce lower negative environmental impact. Following those trends, the paper investigated the effect of using FAME and eco-friendly EKO-V additive, manufactured by the INVEX company, in diesel oil blends. The tests were aimed at measuring concentrations of the exhaust gas basic components during the start-up of cold and warm engine.

2. The test object and the measurement stand

The test object was four-cylinder High Pressure Direct Injection (HDI) engine with the Common Rail system and the exhaust gas recirculation system. The specifications of the engine developed by PSA Peugeot Citroën are presented in Table 1.

Table 1. The engine specifications

PEUGEOT compression ignition engine, engine code: DW10TD		
Parameter	Unit	Value
Cylinder arrangement	-	in-line
Number of cylinders	-	4
Injection type	-	direct
Compression ratio	-	17.6
Cylinder bore	mm	85
Piston travel	mm	88
Engine cubic capacity	dm^3	1997
Maximum engine power	kW	66
Rotational speed at maximum power	rpm	4000
Maximum engine torque	Nm	209
Rotational speed at maximum torque	rpm	1900
Engine idling speed	rpm	800

The test stand was equipped with the KTS 540 diagnostic tester, the fuel flow meter made by the AUTOMEX company and the AVL exhaust gas analyser which allows measurements of nitrogen oxide, hydrocarbon, carbon monoxide and carbon dioxide concentrations. After the cold and warm start-up, the engine operated at idle speed for 120 s. In accordance with [30], the cold engine start-up was assumed to occur when the engine temperature was equal to the ambient temperature, i.e. 15°C. The warm engine start-up was assumed to be that when the temperature of the lubricating oil was 90°C. In the tests, the engine ran on commercial diesel oil, B50 blend and diesel oil with 5% eco-friendly, multi-purpose EKO-V additive developed by the INVEX company. The additive characteristics were given in study [24]. According to the manufacturer's info, the additive facilitates the engine start-up and reduces the fuel consumption.

Investigations into physical and chemical properties of fuels on which the engine ran were performed using used the ERASPEC-FTIR oil analyser by Eeralytics company. The results of investigations are presented in Table 2.

Table 2. Physico-chemical properties of the examined fuels

Parameter	Ekodiesel Ultra D diesel oil	B50 fuel	Diesel oil with 5% EKO-V content
Cetane number	52.4	50.8	55,5
Cetane index	52.8	51.4	58.2
Density at 15ºC, kg/m3	0.832	0.8535	0.8341
Amount of aromatic hydrocarbons, % (V/V)	24.2	23.0	20.7
FAME content, % (V/V)	7.28	53.4	6.02
Distillation point, T10, °C	214.3	246.5	221.4
Distillation point, T50, °C	280.4	336.2	286.2
Distillation point, T90, °C	342.7	369.7	336.3
Distillation point, T95, °C	355.1	371.3	346.2
Final boiling point, °C	372.2	384.9	392.0

Taking into account a significant effect of fractional composition of the fuel on its vaporization capacity, thus on its start-up properties, the measurements of 10, 50, 90 and 95% (V/V) distillation points of the fuels were taken. The results presented in Table 2 indicate that 50% content of rapeseed oil fatty acid methyl esters in diesel oil/ FAME blends produces an unfavourable effect the fuel start-up properties as T10, T50, T90 and T95 distillation points are higher when compared with those for neat diesel oil. It should be noted that the lowest T10 distillation point, equal to 214.3°C, was obtained for diesel oil. The lowest values of T90 and T95 distillation points were found for diesel oil with 5% EKO-V additive.

3. Experimental results

The experimental investigations into the PEUGEOT 2.0 HDI engine involved measurements of crankshaft rotational speed during cold and warm engine start-up. The measurements also included concentrations of: nitrogen oxides (NO_X), hydrocarbons (HC), carbon monoxide (CO) and carbon dioxide (CO_2). In the tests, the engine operated at the factory settings and was fuelled by the following: commercial diesel oil, B50 rapeseed oil fatty acid methyl esters (50%) / diesel oil (50%) blend, and diesel oil with 5% EKO-V fuel additive developed by the INWEX company.

The graph shown in Fig. 1 indicates that during the first stage of the start-up, the crankshaft rotational speed increased rapidly to approx. 870 rpm, which was followed by a decrease to approx. 730 rpm. Then after about 10 s, the crankshaft rotational speed stabilised at roughly 800 rpm, which corresponds to the engine idling speed.

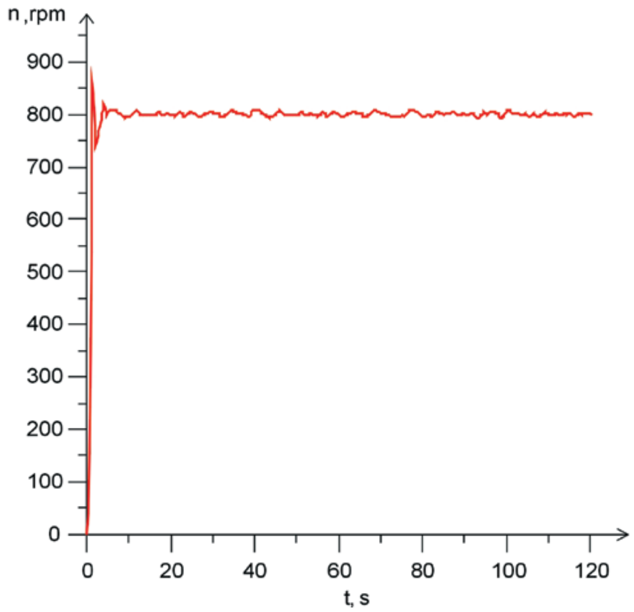

Fig. 1. Profile of crankshaft rotational speed during the cold start-up for Peugeot 2.0 HDI engine fuelled by diesel oil

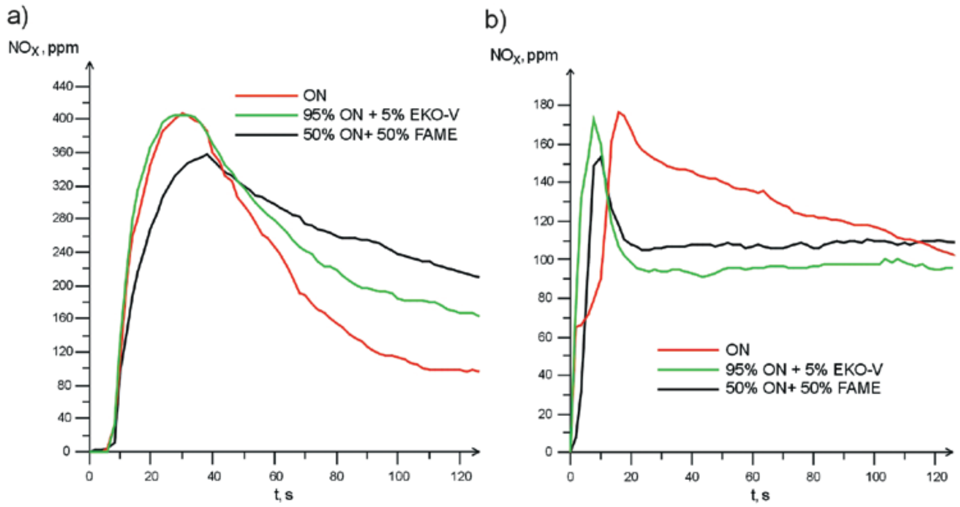

Fig. 2. Profile of nitrogen oxide concentrations in the exhaust gas from the Peugeot 2.0 HDI engine running on three fuels during: a) cold engine start-up; b) warm engine start-up

In Fig. 2, one can see graphs of nitrogen oxides concentrations during the cold and warm engine start-up for the engine running on three different fuels mentioned above.

The graphs presented in Fig. 2 indicate that during the initial stage of both the cold and warm engine start-ups, concentrations of nitrogen oxides increased rapidly. During the cold engine start-up, the maximum concentrations of nitrogen oxides were almost twice as high as those during the warm engine start-up. For cold and warm start-ups of the engine fuelled by B50 blend, the maximum values of nitrogen oxide concentrations were found to be lower. During the cold start-up of the engine fuelled by B50 blend, nitrogen oxide concentrations decreased more slowly when compared with two other fuels. During the warm start-up of the engine fuelled by B50 blend and by diesel oil with 5% eco-friendly EKO-V additive, after approx. 30 s from the start-up, values of nitrogen oxide concentrations stabilised at the level of 90÷110 ppm.

The analysis of the exhaust nitrogen oxide concentrations during the cold start-up, within the first operation stage of approx. 60 s following the start-up, demonstrates that for the engine fuelled by commercial diesel oil and by diesel oil with 5% EKO-V additive, concentrations of nitrogen oxides are twice higher when compared with the values measured 100 s after the engine start-up. Higher concentrations of nitrogen oxides during the cold start-up of the engine fuelled by B50 and by diesel oil with 5% EKO-V additive in comparison with neat diesel oil fuelling are found. That is caused by greater intensity of the combustion process, thus by higher in-cylinder temperature, resulting in a higher rate of nitrogen oxide formation. Greater intensity of the combustion process in the engine fuelled by B50 and by diesel oil with 5% EKO-V additive facilitates the engine reaching thermal balance, at which the emissions of nitrogen oxides stabilise. This stabilisation is primarily linked to the rate of the combustion of fuels on which the engine runs.

Fig. 3 shows the graphs of hydrocarbon concentrations during the cold and warm engine start-up for the Peugeot 2.0 HDI engine running on three different fuels mentioned above.

The analysis of graphs in Fig. 3 shows that during the initial stage of the cold engine start-up, hydrocarbon concentrations are lower than during the warm engine start-up. The reason may be a lower temperature of the combustion chamber walls, resulting in reduced vaporization intensity and vapour diffusion into air during the combustible mixture formation. Therefore, a greater amount of fuel mixes with the lubricating oil in the near-wall layer and flows to the engine crankcase. During the cold engine start-up, the lowest hydrocarbon concentrations were found when the engine was fuelled by B50. For the warm engine start-up, the highest hydrocarbon concentrations were observed for the engine fuelled by diesel oil with 5% EKO-V additive. A small increase in hydrocarbon concentrations during the warm start-up of the engine fuelled by commercial diesel oil with 5%

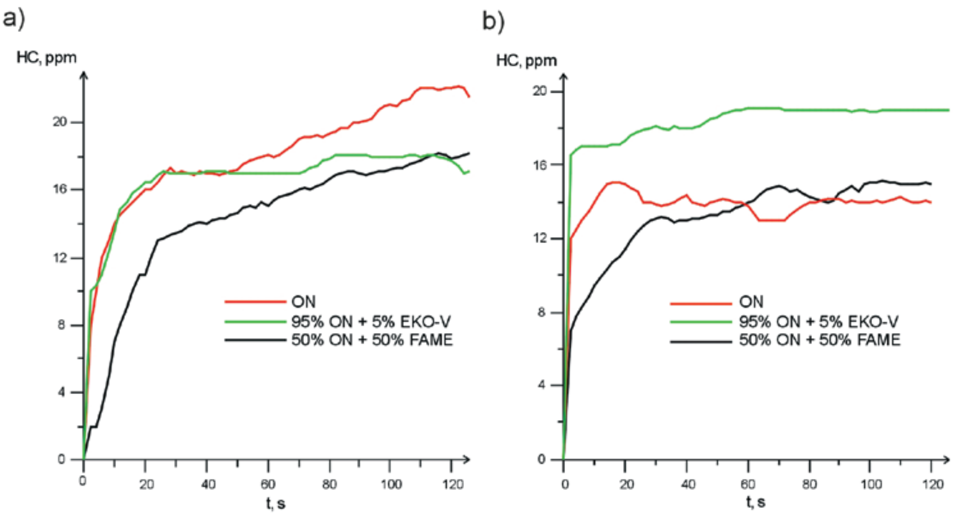

Fig. 3. Profile of hydrocarbon concentrations in the exhaust gas from the Peugeot 2.0 HDI engine running on three fuels during: a) cold engine start-up; b) warm engine start-up

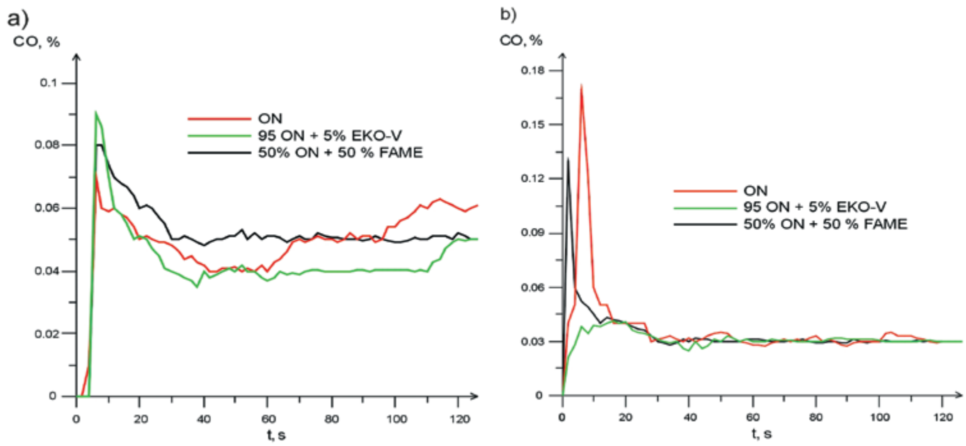

Fig. 4. Profile of carbon monoxide concentrations in the exhaust gas from the Peugeot 2.0 HDI engine running on three fuels during a) cold engine start-up; b) warm engine start-up

EKO-V additive and by B50 may be caused by the lowering of the temperature of the engine operating at idle speed. Increase in hydrocarbon concentrations during the cold engine start-up may be related to the incomplete combustion of the fuel injected into the cylinder. During the combustion process, the fuel-air mixture is not homogeneous and the mixture zones with different values of excess air coefficient are found.

The graphs illustrating carbon monoxide concentrations in the exhaust gas from the Peugeot 2.0 HDI engine running on the fuels selected for the tests can be seen in Fig. 4.

Carbon monoxide concentrations grew rapidly at the initial stage of the engine start-up. That referred both to the cold and warm engine start-ups for the engine fuelled by diesel oil and by B50 blend. For all fuels of concern, during the cold engine start-up, carbon monoxide concentrations stabilised after approx. 30 s. For the engine fuelled by commercial diesel oil with the EKO-V additive, during the cold start-up, the lowest carbon monoxide concentrations were observed after approx. 30 s of the engine operation. During the warm start-up of the engine running on diesel oil with the EKO-V additive, at the first stage of the start-up (up to approx. 15 s), the lowest carbon monoxide concentrations were found. The graphs shown in Fig. 4b indicate that during the warm start-up of the engine fuelled by diesel oil and by B50 blend, combustion was incomplete at the first stage of the engine operation (up to approx. 10 s), which led to increased emissions of carbon monoxide.

Fig. 5 presents carbon dioxide concentrations during cold and warm start-ups when the Peugeot 2.0 HDI engine was fuelled by the three fuels of concern.

Carbon dioxide concentrations stabilised within approx. 10 s after the cold and warm engine start-ups. Higher concentrations of carbon dioxide, which ranged 5.0÷5.6 %, were noted during the cold engine start-up.

During the warm engine start-up, carbon dioxide concentrations ranged 3.8÷4.6 % after 10 s. For the cold start-up of the engine fuelled by commercial diesel oil, higher concentrations of carbon dioxide resulted from the combustion of a larger fuel charge delivered to the cylinder during the start-up.

4. Conclusions

On the basis of the analysis of the experimental results, the following conclusions can be drawn:

- the period of the cold engine start-up is characterised by high concentrations of nitrogen oxides,
- the use of rapeseed oil fatty acid methyl esters in blends with diesel oil results in lower concentrations of nitrogen oxides and hydrocarbons in the exhaust gas at the first stage of the cold engine start-up (up to 40 s after the start),
- concentrations of carbon monoxide and carbon dioxide during the cold engine start-up are higher when compared with the engine that is heated at the start-up,
- during the cold engine start-up, at the initial stage of the engine operation, a rapid increase in carbon monoxide and carbon dioxide concentrations in the exhaust gas is found,
- carbon monoxide and carbon dioxide concentrations in the exhaust gas during the engine start-up were comparable for the three fuels of concern,
- during the warm engine start-up, after approx. 20 s, the lowest concentrations of nitrogen oxides were noted for the engine fuelled by diesel oil with 5% eco-friendly EKO-V additive,
- during the warm engine start-up, the highest concentrations of hydrocarbons were observed for the engine fuelled by diesel oil with 5% eco-friendly EKO-V additive.

Summing up, it can be stated that the amounts of the exhaust gas toxic components during the cold engine start-up are much higher in comparison with those during the start-up of the pre-heated engine.

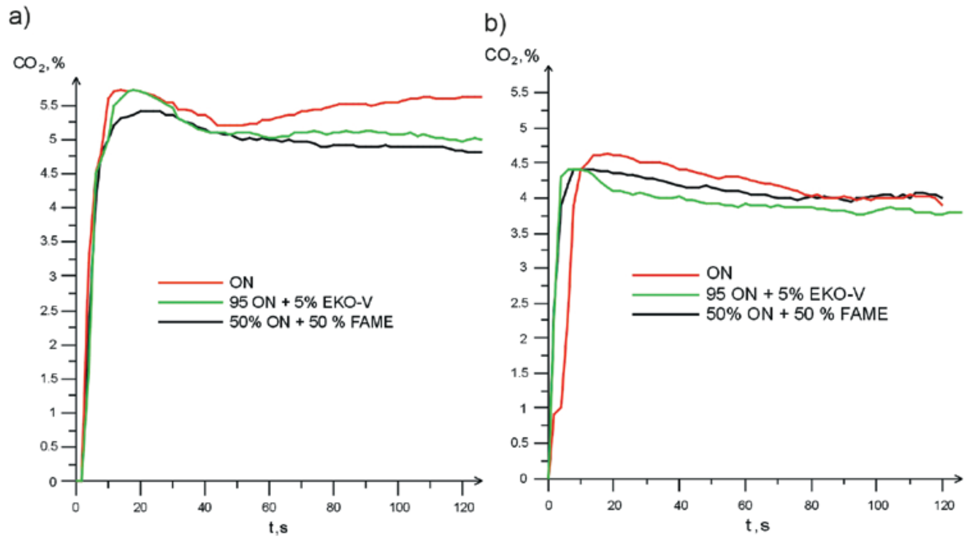

Fig. 5. Profile of carbon dioxide concentrations in the exhaust gas from the Peugeot 2.0 HDI engine running on three fuels during: a) cold engine start-up; b) warm engine start-up

References

1. Ambrozik A., Ambrozik T., Jakóbiec J., Łagowski P. Relationship between fuel spray parameters and heat release characteristics in self-ignition engine. Monografia Zespołu Systemów Eksploatacji PAN „Problems of maintenance of sustainable Technological Systems", Wydawnictwo Polskie Naukowo-Techniczne Towarzystwo Eksploatacyjne 2010; 1: 7-17.
2. Ambrozik A., Ambrozik T., Łagowski P. The influence of hydrocarbon fuels and biofuels on self-ignition delay period. Teka Komisji Motoryzacji i Energetyki Rolnictwa 2007, 7: 15-23.
3. Ambrozik A., Ambrozik T., Orliński P., Orliński S. Wpływ zasilania silnika Perkins 1104C bioetanolem na ekonomiczne i energetyczne wskaźniki jego pracy. Logistyka 2011; 3: 29-36.
4. Bielaczyc P, Merkisz J, Pielecha J. A method of reducing the exhaust emissions from DI diesel engines by the introduction of a fuel cut off system during cold start. SAE Technical Papers 2001; 2001-01-3283.
5. Bielaczyc P, Merkisz J, Pielecha J. Investigation of exhaust emissions from DI diesel engine during cold and warm start. SAE Technical Papers 2001; 2001-01-1260.
6. Bielaczyc P., Merkisz J., Pielecha J. Stan cieplny silnika spalinowego a emisja związków szkodliwych, Poznań: Wydawnictwo Politechniki Poznańskiej, 2001.
7. Broatch A., Lujan J. M., Ruiz S., Olmeda P. Measurement of hydrocarbon and carbon monoxide emissions during the starting of automotive DI diesel engines, International Journal of Automotive Technology 2008, 9(2): 129-140.
8. Brzozowski K., Wojciech S. Wyznaczanie natężenia emisji po zimnym rozruchu silnika z zastosowaniem sztucznych sieci neuronowych, Archiwum Motoryzacji 2007; 2: 119-134.
9. Droździel P. Badania wybranych parametrów rozruchu samochodowego silnika spalinowego o zapłonie samoczynnym. Zeszyt nr 13. Rozruch silników spalinowych. Komisja Motoryzacji i Energetyki Rolnictwa Polska Akademia Nauk Oddział w Lublinie, Politechnika Szczecińska 2005; 53-60.
10. Droździel P. Start-up of a diesel engine, Eksploatacja i Niezawodnosc – Maintenance and Realiability 2007, 2: 51-59.
11. Haiyong Peng, Yi Cui, Lei Shi, Kangyao Deng. Effects of exhaust gas recirculation (EGR) on combustion and emissions during cold start of direct injection (DI) diesel engine, Energy 2008; 33: 471–479.
12. Jakóbiec J. Efektywność i aspekt ekologiczny zasilania silników spalinowych paliwami odnawialnymi, Polskie Towarzystwo Inżynierii Rolniczej 2010; 156–160.
13. Kruczyński S., Orliński P., Biernat K. Olej lniankowy jako biopaliwo dla silników o zapłonie samoczynnym. Przemysł Chemiczny 2012; 1: 111-114.
14. Kruczyński S. Performance and emission of CI engine fuelled with camelina sativa oil, Energy Conversion and Management 2013; 65: 1–6.
15. Kuranc A. The ecological aspect of a cold and hot starting of a spark ignition combustion engine, Eksploatacja i Niezawodnosc – Maintenance and Realiability, 2008; 2: 40-44.
16. Mario Luciano Randazzo, Jose Ricardo Sodre. Cold start and fuel consumption of a vehicle fuelled with blends of diesel oil–soybean biodiesel–ethanol, Fuel 2011; 90: 3291–3294.
17. Merkisz J., Pielecha J., Radzimirski S. Emisja zanieczyszczeń motoryzacyjnych w świetle nowych przepisów Unii Europejskiej, Warszawa: Wydawnictwo Komunikacji i Łączności, 2012.
18. Mysłowski J. Rozruch silników samochodowych z zapłonem samoczynnym, Warszawa: Wydawnictwo Nauk Technicznych, 1996.
19. Myung C.L, Park S. Exhaust nanoparticle emissions from internal combustion engines: a review, International Journal of Automotive Technology 2012; 13(1): 9‒22.
20. Octavio Armas, Reyes García-Contreras, Ángel Ramos. Pollutant emissions from engine starting with ethanol and butanol diesel blends, Fuel Processing Technology 2012; 100: 63–72.
21. Payri F., Broatch A., Salavert J.M., Martín J. Investigation of Diesel combustion using multiple injection strategies for idling after cold start of passenger-car engines, Experimental Thermal and Fluid Science 2010; 34: 857–865.
22. Pszczółkowski J. Charakterystyki rozruchowe silników o zapłonie samoczynnym, Warszawa: Wydawnictwo Stowarzyszenie Edukacyjne Pedagogów Praktyków „Cogito", 2004.
23. Serdecki W. Badania silników spalinowych, Poznań: Wydawnictwo Politechniki Poznańskiej, 2012.
24. Szczepaniak S., Szczepaniak R. Ekologiczne dodatki do paliw motorowych, Przemysł Chemiczny 2004; 1: 3-4.
25. Szlachta Z. Zasilanie silników wysokoprężnych paliwami rzepakowymi, Warszawa: Wydawnictwo Komunikacji i Łączności, 2005.
26. Wcisło G. Applicationof the cold stamping method for rapeseed oil extraction, Teka Komisji Motoryzacyjnej i Energetyki Rolnictwa 2006; 6: 175–181.
27. Węgrzyn A., Zając G. Analysis of work parameters changes of diesel engine powered with diesel fuel and FAEE blends, Eksploatacja i Niezawodnosc – Maintenance and Realiability 2008; 2: 17-24.
28. Zając G., Piekarski W. Ocena poziomu zużycia paliwa przez silnik o zapłonie samoczynnym przy zasilaniu FAME i FAEE. Inżynieria Rolnicza 2009; 8(117): 281-288.
29. Zając G., Piekarski W., Krzaczek P. Ocena zużycia paliwa przez silnik o zapłonie samoczynnym przy zasilaniu wybranymi paliwami. Inżynieria Rolnicza 2008; 2(100): 323-330.
30. BN-82/1374-10. Określanie właściwości rozruchowych w niskich temperaturach.

Andrzej AMBROZIK
Tomasz AMBROZIK
Piotr ŁAGOWSKI
Department of Automotive Engineering and Transport
Faculty of Mechatronics and Mechanical Engineering, Kielce University of Technology
Al. 1000-lecia Państwa Polskiego 7, 25-314 Kielce, Poland
E-mail: silspal@tu.kielce.pl

Article citation info:
YANG D, REN Y, WANG Z, LIU L, SUN B. A novel logic-based approach for Failure Modes Mitigation Control and Quantitative System Reliability Analyses. Eksploatacja i Niezawodnosc – Maintenance and Reliability 2015; 17 (1): 100–106.

Dezhen YANG
Yi REN
Zili WANG
Linlin LIU
Bo SUN

A NOVEL LOGIC-BASED APPROACH FOR FAILURE MODES MITIGATION CONTROL AND QUANTITATIVE SYSTEM RELIABILITY ANALYSES

ORYGINALNA, OPARTA NA LOGICE METODA KONTROLI OGRANICZANIA PRZYCZYN USZKODZEŃ I ILOŚCIOWEJ ANALIZY NIEZAWODNOŚCI SYSTEMU

The core idea of reliability design is to mitigate the product's failure modes. However, for the cross-links among potential failure modes of a complex product, it is very difficult to establish the mapping relationship between failure modes mitigation and quantitative values of reliability, and the decision of failure modes mitigation have to be performed by virtue of experience, which always increase design period. In order to solve these problems, a novel logic-based approach for failure modes mitigation control and quantitative system reliability analyses is provided. Firstly, a hybrid of active and passive control process of reliability design is proposed. Secondly, a novel concept of failure modes correlation set (FMCS) and a determination approach based on deductive theory are presented. According to the changes in failure modes probabilities of occurrence, the reliability formulas of the components and assemblies are provided to depict the effects of failure mode mitigation on reliability of components and assemblies. And then the FMCS mitigation sequence is decided to determine reliability design activities. Thirdly, a closed control process of FMCS mitigation is provided integrated with logic decision method. By exposing the design of a helicopter fuel system, the present study demonstrates that all approaches are feasible, and the relationship between reliability parameters and qualitative design exists. Hence the failure modes mitigation could be controlled for the achievement of quantitative reliability requirements.

Keywords: *failure, reliability, failure mitigation control, quantitative reliability analyses.*

Podstawowym problemem w procesie projektowania niezawodności jest ograniczenie przyczyn uszkodzeń produktu. Jednakże, w przypadku sieci połączeń pomiędzy możliwymi przyczynami uszkodzeń złożonego produktu, trudno jest ustalić mapę zależności pomiędzy ograniczaniem przyczyn uszkodzeń i ilościowymi wartościami niezawodności, a decyzje względem ograniczania przyczyn uszkodzeń muszą bazować na własnym doświadczeniu, co znacznie wydłuża okres projektowania. W celu rozwiązania powyższych problemów, zaproponowano oryginalną, opartą na logice, metodę kontroli ograniczania przyczyn uszkodzeń i ilościowej analizy niezawodności systemu. Na wstępie, zaproponowano mieszany proces aktywnej i pasywnej kontroli niezawodności projektu. Następnie, zaprezentowano oryginalną koncepcję zbioru korelacji przyczyn uszkodzeń (FMCS) i metodę oznaczania opartą o teorię dedukcji. Na podstawie zmian dotyczących prawdopodobieństwa występowania przyczyn uszkodzeń, określono wzory niezawodności części i układów w celu pokazania wpływu ograniczania przyczyn uszkodzeń na niezawodność części i układów. Określono następnie ograniczającą sekwencję FMCS, ażeby ustalić założenia dla projektowania niezawodności. Na koniec zaprezentowano zamknięty proces kontroli ograniczania FMCS w powiązaniu z logiczną metodą podejmowania decyzji. Analizując pod tym kątem projekt systemu paliwowego helikoptera, wykazano w niniejszej pracy przydatność wszystkich powyższych metod, jak również związek pomiędzy parametrami niezawodności a projektowaniem jakościowym. Dlatego też ograniczanie przyczyn uszkodzeń powinno być kontrolowane w celu osiągnięcia wymaganej niezawodności ilościowej.

Słowa kluczowe: *uszkodzenie, niezawodność, kontrola ograniczania uszkodzeń, ilościowe analizy niezawodności.*

1. Introduction

Reliability plays an essential role as a major driver of life-cycle costs and has considerable influence on product performance, but its achievement is gradually, a well-defined program for the process is very important. In traditional reliability design process, the design activities are not parameter achieving oriented, they are mainly performed by virtue of experience. By using cybernetics, its process can be expressed as Fig. 1. In such way, the quantitative reliability were obtained, and the deviation could be determined by comparing them with reliability requirements by sensor unit, and then the failures could be pinpointed by execution unit. Simultaneously, designers give the improvements and apply them on product. Reliability engineers evaluate product's reliability after completing the functional design through reliability analysis [6, 12, 19], simulation [9, 18], test [2, 4] etc. The achievement of the requirements would be ensured according to the process. However, this process put the designers in a passive position as in order to meet the requirements. The development cycle is difficult to control, and designers may have to go through several iterations which may lead to enormous waste of time and money.

The newest reliability program standard GEIA-STD-0009 [8] proposes a new systematic process to include reliability in product design. The core idea is to progressively understand the loads and stresses of products at each level, to gradually recognize the failure

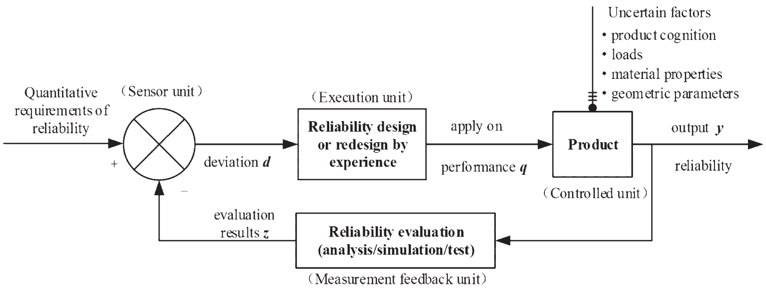

Fig. 1. The traditional reliability design process

modes and mechanism, and to actively mitigate the exposed failure modes. Therefore, mitigating the potential failure modes is the central task of reliability design. For a product with simple structure, designers should mitigate all the failure modes identified as possible. For a complex product, there are thousandths of potential failure modes. It is unrealistic to mitigate all the identified failure modes. Furthermore, cross-links exist among potential failure modes, the mitigation of a failure mode may cause occurrence of other failure modes, which make it very difficult to decide the sequence of mitigation, and have high risk to repeat the design cycle for many times. In order to control the failure modes mitigation to achieve reliability requirements quickly, it is necessary to construct a reliability design process.

In the literature about failure mode mitigation, current research mainly focused on the improvements for specific failure modes, such as run-time error mitigation in software [10], structural damage mitigation [3, 13], signal jamming [1, 14], sensor bias, drift, scaling, and dropout [5, 7]. Although these literatures show the idea of failure modes mitigation, they did not provide the control approach for failure modes mitigation on the basis of cybernetics. Furthermore, the cross-links among failure modes were often neglected when mitigating failure modes, which is unfavourable for optimized design [17].

The main purpose of this paper is to present a novel logic-based approach for failure modes mitigation control and quantitative system reliability analyses. This paper is organized as follows. Section 2 introduces the hybrid of active and passive control process based on the traditional passive reliability design process. In Section 3, an approach to determine the cross-links among failure modes and the mapping relationship between failure modes mitigation and quantitative requirements of reliability is presented in detail. The proposed approach is illustrated with the help of a fuel system example. Section 4 provides the control process of failure mode mitigation. Concluding remarks and future work are given in Section 5.

2. The hybrid of active and passive control process of reliability design

Aiming to shorten the development cycle and reduce the cost, reliability design should be carried out actively in the early stage of design. And then reliability and performance requirements could be achieved simultaneously.

2.1. The Active Process of Reliability Design

The active process of reliability design can be characterized as failure modes mitigation.

Definition 1: Failure modes mitigation [8] should be an active process, shown in Fig. 2. In this process, designers are active to identify potential failure modes of the product systematically. And then the improvements, operational compensatory provisions, diagnosis means are employed to eliminate the failure modes or reduce the failure modes' probabilities of occurrence according to their causes and severity. Furthermore, efficiency of the improvements applied should be validated.

This process is applicable to the product with sufficient prior knowledge. From the perspective of the achievement of quantitative reliability requirements, it is a problem to determine which failure modes to be mitigated. And then it is also a problem to control the achievement process of quantitative reliability requirements.

2.2. The Hybrid Control Process of Reliability Design

Integrating with the traditional process (shown in Fig. 1) and the active process (shown in Fig. 2), the paper proposes a new control process with the hybrid of active and passive one, shown in Fig. 3.

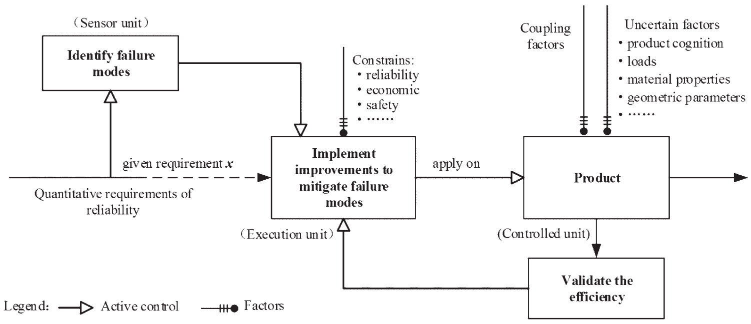

Fig. 2. The active process of reliability design

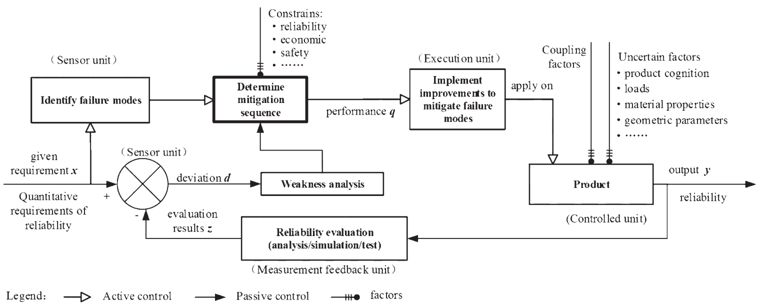

Fig. 3. The hybrid of active and passive control process of reliability design

Due to the complexity of products, failure modes would be unavoidably introduced with the design development. Therefore, designers should identify all possible failure modes through methods such as failure modes and effects analysis (FMEA), reliability simulation test. However, while designers recognize a specific failure mode, they should not take improvements to mitigate it immediately. Because different failure modes are not mutually independent - the mitigation of a failure mode may cause some others to be mitigated too, or/and may introduce some new failure modes simultaneously. And the effects of failure modes mitigation on reliability are also different. Therefore, designers must analyse the cross-links among different failure modes and determine the mitigation sequence at the outset.

Designers should be sure that the improvements are reasonable through simulation, principle analysis etc. before applying the improvements on product. After that, designers could implement the improvements on product in the order given by mitigation sequence, to eliminate the critical failure modes or reduce their probabilities of occurrence and severity.

Designers should further evaluate the product through reliability analyses, simulation, and tests. The purpose of those evaluations or revaluations is to determine the deviation between reliability achievements and its requirements under the current product configuration. If the deviation is positive (i.e., the evaluation result is greater than the required one), designers maintain the configuration, otherwise designers need to do further analysis to find out weaknesses, determine improvements and apply them on the product. In addition, there may be other disturbance factors, such as the uncertainty of product recognition, loads, material properties and geometric parameters. These factors may lead to the instability of the product. Therefore, designers should monitor the development, evaluate the product and feedback the results to the "sensor unit" in real-time.

For the hybrid process, the active process guarantees that critical failure modes will be identified timely, and the passive process can improve the product scheme exactly. Therefore, the design objective can be achieved with minimal resources and the design period would be shortened. The approaches for reliability design on the basis of the passive process have been presented. Restricted to the length, we do not give the details. The paper will focus on the active control process orienting to quantify achievement of reliability requirements.

3. Failure Modes Mitigation Sequence Decision

The determination procedure of failure modes mitigation sequence for the quick achievement of quantitative reliability requirements is as follows.

1. Identify the failure modes of the component and consider the new failure modes introduced by system integration, and the interrelationship among different failure modes, namely, to determine the failure modes correlation sets (FMCS).
2. Construct quantitative effect models of failure modes mitigation on reliability and calculate the effect of FMCS mitigation on reliability.
3. Determine the mitigating sequence of the failure modes according to the importance of reliability effect.

3.1. Determine FMCS based on Deductive Theory

To definite FMCS of f_i (the failure mode has been mitigated) proposed, we take the follows into consideration only.

1. The failure modes which are eliminated with f_i simultaneously
2. The failure modes that their probabilities of occurrence are reduced with f_i simultaneously
3. The failure modes which are introduced while f_i is mitigated

On the basis of constrains given above, the definition of FMCS can be achieved.

Definition 2: Hypothesize that there is a failure mode set $\mathbf{f}=\{f_1,f_2,\cdots,f_n\}$ for a product. Given one of the failure modes $f_i\in\mathbf{f}\left(i\in\{1,\cdots,n\}\right)$ has been mitigated by some improvements, such that $f_i\notin\mathbf{f}'$ (where $\mathbf{f}'$ is the new failure modes set for the product after failure modes mitigation) or its probability of occurrence is reduced. If $\exists\left\{f_{i_1},f_{i_2},\cdots,f_{i_m}\right\}\subset\mathbf{f}$ (m is the number of failure modes which are mitigated simultaneously with f_i), $\exists\left\{f_{j_1},f_{j_2},\cdots,f_{j_b}\right\}\subset\mathbf{f}'$ (b is the number of failure modes which are introduced with mitigation of f_i), and they satisfy following conditions:

1. $i_t\neq i\left(t=1,\cdots,m\right)$
2. $f_{i_t}\notin\mathbf{f}'$ or their probabilities of occurrence are reduced for $\forall t\in\{1,\cdots,m\}$
3. $f_{j_h}\notin\mathbf{f}\left(h=1,\cdots,b\right)$

Then the coupling set $\left\{f_i,f_{i_1},f_{i_2},\cdots,f_{i_m},f_{j_1},f_{j_2},\cdots,f_{j_b}\right\}$ is referred to as failure modes correlation set corresponding to f_i , denoted as $FMCS_{fi}$. Unambiguously, it can be referred to as failure modes correlation set abbreviation, denoted as FMCS.

3.1.1. The types of failure modes interrelationship

Assume that all the failure modes mitigation actions are reasonable and effective, the condition that one eliminated failure mode increasing some other failure modes' probabilities of occurrence are not under consideration. Based on this assumption, the interrelationship among different failure modes could be divided into the following types:

1. Type I (a failure mode is eliminated with another introduced): Although the failure mode f_1 is eliminated, some new failure modes $f_1^{eN},f_2^{eN},\cdots,f_{te}^{eN}$ are introduced, and the corresponding probabilities of occurrence are denoted by $\bar{\beta}_1^{eN},\bar{\beta}_2^{eN},\cdots,\bar{\beta}_{te}^{eN}$. Let type I FMCS be denoted as $\mathrm{FMCS_I}=\left\{f_1,f_1^{eN},f_2^{eN},\cdots,f_{te}^{eN}\right\}$.
2. Type II (concurrently eliminated): The failure mode f_1 is eliminated, and the failure modes $f_1^{ee},f_2^{ee},\cdots,f_E^{ee}$ are eliminated simultaneously. Denote type II FMCS as $\mathrm{FMCS_{II}}=\left\{f_1,f_1^{ee},f_2^{ee},\cdots,f_E^{ee}\right\}$, and the corresponding probabilities of occurrence are denoted by $\beta_1^{ee},\beta_2^{ee},\cdots,\beta_E^{ee}$. Note that the failure modes mitigated not necessarily belong to the same product (hereinafter the same, will not go into details).
3. Type III (one eliminated with another reduced): The failure mode f_1 is eliminated, and the failure modes probabilities of occurrence $f_1^{ed},f_2^{ed},\cdots,f_{De}^{ed}$ are reduced from the original $\beta_1^{ed},\beta_2^{ed},\cdots,\beta_{De}^{ed}$ to $\bar{\beta}_1^{ed},\bar{\beta}_2^{ed},\cdots,\bar{\beta}_{De}^{ed}$ respectively. Let type III FMCS be denoted as $\mathrm{FMCS_{III}}=\left\{f_1,f_1^{ed},f_2^{ed},\cdots,f_{De}^{ed}\right\}$.
4. Type IV (one reduced with another introduced): Although the failure mode probability of occurrence f_1 is reduced, some new failure modes $f_1^{dN},f_2^{dN},\cdots,f_{td}^{dN}$ are introduced, and the corresponding probabilities of occurrence are denoted by $\bar{\beta}_1^{dN},\bar{\beta}_2^{dN},\cdots,\bar{\beta}_{td}^{dN}$. Let type IV FMCS be denoted as $\mathrm{FMCS_{IV}}=\left\{f_1,f_1^{dN},f_2^{dN},\cdots,f_{td}^{dN}\right\}$.
5. Type V (concurrently reduced): The failure mode probability of occurrence f_1 is reduced, and meantime one of failure modes $f_1^{dd},f_2^{dd},\cdots,f_{Dd}^{dd}$ is also reduced from the original $\beta_1^{dd},\beta_2^{dd},\cdots,\beta_{Dd}^{dd}$ to $\bar{\beta}_1^{dd},\bar{\beta}_2^{dd},\cdots,\bar{\beta}_{Dd}^{dd}$ respectively. Let type V FMCS be denoted as $\mathrm{FMCS_V}=\left\{f_1,f_1^{dd},f_2^{dd},\cdots,f_{Dd}^{dd}\right\}$.
6. Type VI (one integrated with another introduced): Considering the interface failure modes, and the failure modes with high severity rank introduced by system integration, the corresponding probabilities of occurrence are denoted by $\bar{\beta}_1^{IN},\bar{\beta}_2^{IN},\cdots,\bar{\beta}_{tI}^{IN}$. Let type VI FMCS be denoted as $\mathrm{FMCS_{VI}}=\left\{f_1^{IN},f_2^{IN},\cdots,f_{tI}^{IN}\right\}$.

Since the interrelationships among failure modes are not identical, the FMCS is the union of Type I, II and III FMCS, namely $\mathrm{FMCS}=\mathrm{FMCS_I}\cup\mathrm{FMCS_{II}}\cup\mathrm{FMCS_{III}}$, denoted by $\mathrm{FMCS^E}$, or the union of Type IV and Type V FMCS, namely

$\mathrm{FMCS} = \mathrm{FMCS}_{\mathrm{IV}} \bigcup \mathrm{FMCS}_{\mathrm{V}}$, denoted by $\mathrm{FMCS}^{\mathrm{D}}$. The Type VI FMCS is introduced by system integration, denoted by $\mathrm{FMCS}^{\mathrm{I}}$, which is independent of Type I and Type V. It should be noted that designers should deeply analyze the mitigation of $\mathrm{FMCS}^{\mathrm{I}}$. Therefore it could be further divided into two subsets: $\mathrm{FMCS}^{\mathrm{E}}$ and $\mathrm{FMCS}^{\mathrm{D}}$.

3.1.2. The determination of FMCS

In practical projects, it is very difficult to determine FMCS. The determination should be made according to the products working principles and fault propagation etc. The paper proposes an approach based on deductive theory [16] to determine the FMCS. It consists of two steps:

Step 1: Construct a logic tree of failure mode mitigation to determine the FMCS of a specific failure mode. In this step, a logic tree of the specific failure mode mitigation will be achieved. An example is shown in Fig. 4. It contains four layers, as follows:

1. Layer 1 (the mitigation object layer): specify mitigation object, namely choose the specific failure mode for mitigation.
2. Layer 2 (the mitigation procedures layer): according to Definition 1, classify the procedure of failure modes mitigation into two categories: the eliminated failure mode; and the reduced failure mode. Therefore, construct the layer by the logic "OR" between elimination of the failure mode and reduction of its occurrence probability.
3. Layer 3 (the improvements layer): according to the detailed failure mitigation procedures, including the reasons that lead to the occurrence of failure mode, determine the procedures and methods to construct the third layer. Namely, this layer is the relationship of AND, OR, CONDITION et al.
4. Layer 4 (failure modes correlation layer): according to the procedures and methods to improve the product, integrating product's functional principle and interrelationship, analyze all possible associated failure modes at the forth layer. In the logic tree, the paper adds a logic gate "failure modes correlation gate", denoted by "$\boxed{\geqslant}$". It not only denotes the AND logical relationship, but also shows the mitigation sequence of failure modes, namely from left to right.

Step 2: Determine FMCS. Identify the FMCS through descending method or ascending method according to the logic relationship implicated in the figure:

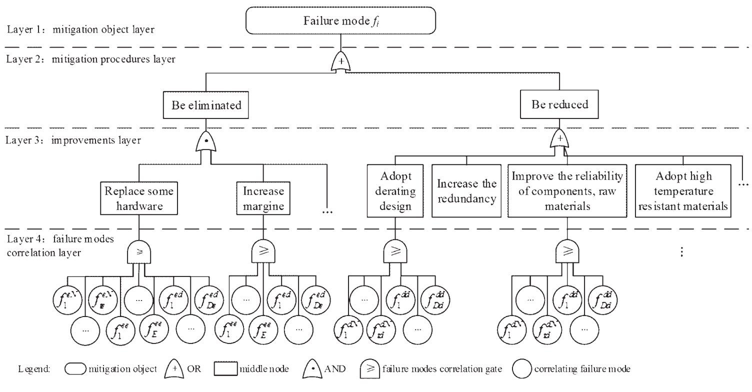

Fig. 4. An example of logic tree

3.2. Construct quantitative impact models of failure modes mitigation on reliability

The impact model shows the mapping relationship between failure modes mitigation and reliability parameter. It indicates the product's reliability after mitigation of a specific failure mode. According to the characteristic of Type II and Type III FMCS, they will be considered as the same type when constructing the impact models.

The common reliability parameters for complex products can be summarized as shown in Table 1.

Table 1. The common reliability parameters for complex products

Name	Applicable scope	
	assembly	component
failure rate	√	√
mean time between failures (MTBF)	√	√
mean time to failure (MTTF)		√
mean time between critical failures (MTBCF)	√	
mission reliability	√	

Notation: √ represents "applicable".

Considering the interrelationship types of failure modes, the impact models can be divided into two categories:

1. The impact models of the component-level reliability
2. The impact models of assembly-level reliability

3.2.1. The impact models of the component-level reliability

Let t denote a component. Assume its life is subjected to exponential distribution, namely its failure rate is a constant, and the failure mode probability of occurrence f_i is β_i. If f_i was mitigated, let $\bar{\beta}_i I_i \left(I_i = \begin{cases} 1 & f_i \text{ probability of occurrence was reduced} \\ 0 & f_i \text{ was eliminated} \end{cases} \right)$ denote the probability of occurrence. Then the failure rate of product t is given by:

$$\begin{aligned} \bar{\lambda}_t &= \lambda_t - \left(\beta_i - \bar{\beta}_i I_i \right) \\ &+ \left(1 - I_i\right) \left(\sum_{j=1}^{te} \bar{\beta}_j^{eN} - \sum_{j=1}^{E} \beta_j^{ee} - \sum_{j=1}^{De} \left(\beta_j^{ed} - \bar{\beta}_j^{ed} \right) \right) \\ &+ I_i \left(\sum_{j=1}^{td} \bar{\beta}_j^{dN} - \sum_{j=1}^{Dd} \left(\beta_j^{dd} - \bar{\beta}_j^{dd} \right) \right) \end{aligned} \quad (1)$$

If there are some failure modes contributing to other products, it should be calculated in accordance with the products respectively. The same is to the following equations.

MTBF of the product t is given by:

$$\mathrm{MTBF}_t = 1 / \bar{\lambda}_t \quad (2)$$

3.2.2. The impact models of the assembly-level reliability

Suppose that the product P is comprised of H devices and does not take failure modes introduced by system integration into consideration, then the model of the assembly-level reliability influenced by component-level failure modes mitigation should be established first.

Then, combined with reliability theory, the expression of the P's failure rate is as follows:

$$\lambda_s = \sum_{t=1}^{H} \bar{\lambda}_t + \sum_{j=1}^{tI} \bar{\beta}_j^{IN} \quad (3)$$

In general, the assembly-level products are repairable. Correspondingly, the MTBF is given by:

$$\mathrm{MTBF}_s = 1 / \lambda_s \quad (4)$$

The MTBCF is given by:

$$\text{MTBCF}_s = \frac{\lambda_s}{\sum_{i=1}^{k} \beta_{CFi}} \times \text{MTBF}_s \quad (5)$$

where $\frac{\lambda_s}{\sum_{i=1}^{k} \beta_{CFi}}$ denotes critical failure factor. β_{CFi} denotes the occurrence probability of the critical failure mode i after mitigation. k denotes the total number of critical failure modes.

If the lifetime of the complex product follows an exponential distribution, then its mission reliability is given by

$$R_s = e^{-T/\text{MTBCF}_s} \quad (6)$$

where T denotes the mission duration.

In fact, new failure modes will be introduced by system integration, which could be mitigated by the designers. The impact models of reliability could be established according to the approach applied in components.

3.3. Order the FMCS mitigation sequence

Combining the impact models established above, designers can calculate the impact on reliability of different FMCS. According to the principle of maximization, designers can determine the failure modes mitigation sequence.

Theoretically, we should take all relevant reliability parameters into consideration. However, it can be seen from the equation (1) to (6) that reliability parameters are mutually dependent on each other. All other reliability parameters could be directly obtained from failure rate. Based on the attribution simplification rule [11], the mitigation sequence could be directly determined by failure rate. It is given by:

$$\left\{f_1, f_1^{eN}, f_1^{ee}, f_2^{ee}\right\} \succ \left\{f_2, f_1^{ed}, f_2^{ed}\right\} \succ \cdots \quad (7)$$

where $\succ$ denotes order relation, namely $\left\{f_1, f_1^{eN}, f_1^{ee}, f_2^{ee}\right\}$ should be mitigated prior to $\left\{f_2, f_1^{ed}, f_2^{ed}\right\}$.

3.4. Illustrative example

Here, a fuel system of a native helicopter was taken as an example to verify the feasibility of the approaches and models. The failure rate of the fuel system is 0.00000224(10^{-6}/h), and the failure rates of its components under current configuration are shown in Table 2.

Table 2. The failure rates of components of fuel system (section)

Components	Failure rate (10^{-6}/h)	Components	Failure rate (10^{-6}/h)
1 fuel tank	0.22	5 fuel supply hose assemblies	0.18
2 fuel boost pump	0.45	6 one-way valve	0.45
3 suction port assembly	0.25	7 drain valve	0.24
4 fireproof fuel supply hose assemblies	0.45		

Table 3. The results of fuel system's FMEA (section)

Components	Failure modes	S	β (10^{-6}/h)	After mitigation β (10^{-6}/h)	…
fuel tank	f_{11}: fuel tank wall leakage	IV	0.15	0.08	…
	f_{12}: fuel leakage after crash	II	0.07	0.04	…
fuel boost pump	f_{21}: fuel booster pump not working	II	0.12	0.08	…
	f_{22}: no flow	II	0.15	0	…
	f_{23}: pressure pulsation	II	0.18	0	…
suction port components	f_{31}: blocking	II	0.12	0	…
	f_{32}: leakage	II	0.13	0	…
fireproof fuel supply hose components	f_{41}: fuel leakage at inter faces	I	0.45	0	…
fuel supply hose components	f_{51}: fuel leakage at inter faces	II	0.18	0	…
one-way valve	f_{61}: blocking	II	0.15	0	…
	f_{62}: leakage	III	0.18	0.18	…
	f_{63}: seepage	II	0.12	0	…
drain valve	f_{71}: cannot open	III	0.12	0.08	…
	f_{72}: cannot turned off	IV	0.12	0.08	…

Notation: S denotes severity rank. β denotes a failure mode probability of occurrence.

By using FMEA, all possible failure modes can be identified, some of which are shown in Table 3. If a failure mode was mitigated, then its probability of occurrence (shown in column 5) could be predicted on the basis of NPRD 2011 [15] and experiment data.

1. Determine FMCS based on the deductive method

Since the severity rank of "f_{23}: fuel boost pump pressure pulsation" is II as in Table 3, and the correctness "optimization of inlet filter pore diameter" is feasible in technology and economy, so take it to be eliminated. According to the functional model of fuel system, failure modes "f_{22}: the fuel boost pump no flow", "f_{31}: suction port components blocking" and "f_{61}: one-way valve blocking" were eliminated simultaneously. According to the steps in section 3.1.2, the mitigation logic tree was achieved, as shown in Fig. 5. Furthermore, FMCS of f_{23} was then deduced. It was $\{f_{23}, f_{22}, f_{31}, f_{61}\}$. Similarly, other FMCSs were $\{f_{32}, f_{41}, f_{51}, f_{63}\}$, $\{f_{11}, f_{12}\}$, $\{f_{21}, f_{71}, f_{72}\}$.

2. Calculate the fuel system's failure rate after mitigation

After mitigation of FMCS, the failure rate of the fuel system was arrived according to Equation (1) and the data shown in Table 2 and 3, shown as follows:

1) $\{f_{23}, f_{22}, f_{31}, f_{61}\}$: 0.00000164
2) $\{f_{32}, f_{41}, f_{51}, f_{63}\}$: 0.0000013
3) $\{f_{11}, f_{12}\}$: 0.00000202
4) $\{f_{21}, f_{71}, f_{72}\}$: 0.00000212

According to the failure rates above, the failure modes mitigation sequence was determined as follows:

$$\{f_{32}, f_{41}, f_{51}, f_{63}\} \succ \{f_{23}, f_{22}, f_{31}, f_{61}\} \succ \{f_{11}, f_{12}\} \succ \{f_{21}, f_{71}, f_{72}\}$$

By adopting the proposed process to control the failure modes mitigation of the fuel system, the reliability objective was achieved through iterations, and the development cycle was greatly shortened.

4. The control process of failure modes mitigation

In line with the mitigation sequence, designers can mitigate the failure modes. A specific logic-based control process is proposed to guide the mitigation of FMCS, as shown in Fig. 6.

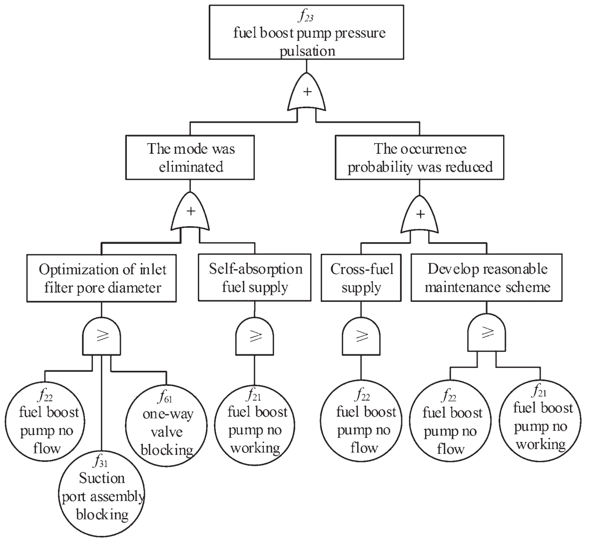

Fig. 5. The logic tree of fuel boost pump pressure pulsation mitigation

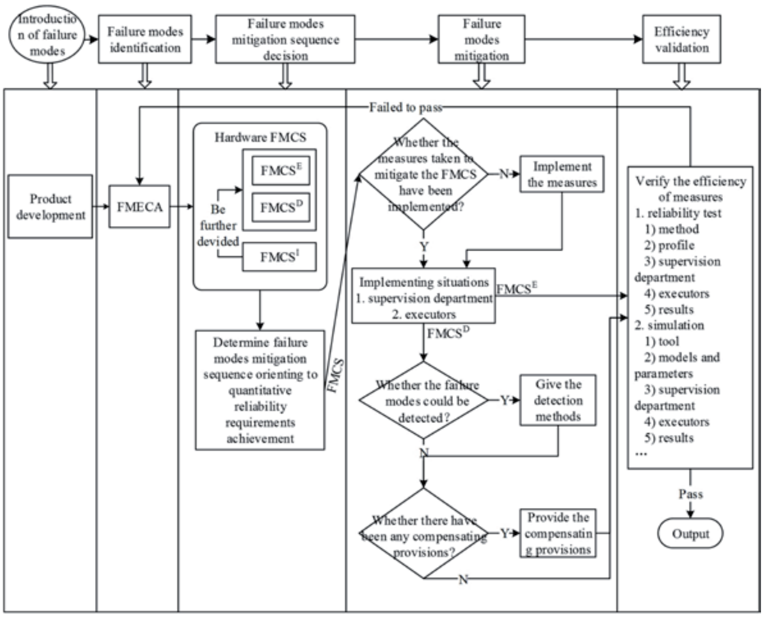

Fig. 6. The hardware FMCS mitigation process based on logic decision

For the FMCS, designers determine whether the improvements taken to mitigate the failure modes have been implemented. If the answer is "Yes", designers should record the implementing situations including supervision department and executors. If the answer is "No", designers should take the mitigating improvements, and track the process to make sure the failure modes are mitigated.

For the $FMCS^D$, designers should further determine whether the failure modes can be detected. If the answer is "Yes", designers should give the detection methods. Then, designers should determine whether there have been any compensating provisions. If the answer is "Yes", designers should also provide the compensating provisions.

Furthermore, designers should verify the efficiency of the mitigation improvements, detection methods and compensating provisions through reliability tests, simulation etc. Certainly, designers should also verify their final efficiency during operation stage, and make it guidance of the similar products design.

5. Conclusions

Failure modes mitigation is the core of reliability design process and should be well programmed. The pilot study had proposed a novel logic-based approach for failure modes mitigation control, the failure modes correlation sets (FMCS) had been defined and the links between qualitative and quantitative realization of reliability had been established. The approach takes the cross-links among failure modes into consideration and makes the novel hybrid control process, which constructs a bridge between the quantitative reliability parameters and the design and redesign activities, and would shorten the development cycle time. Hence, the provided approach is efficient for solving the decision problem of failure modes mitigation sequence.

The failure modes mitigation was illustrated for a fuel boost pump pressure pulsation, focusing on its typical failure modes. The study revealed that the proposed approach is efficient in this typical condition. In the future, more examples should be considered. Also, it is reasonable to develop correlation sets of coupled failure modes and impact model of its mitigation. And it is necessary for the authors to apply the approach repeatedly in more practical projects to provide sufficient evidence. The assumption that life of product is subjected to exponential distribution makes it easy to calculate the effect of failure mitigation on reliability. Nevertheless, the assumption may not reasonable, and the failure rates of the components of fuel system are not constant in fact. More work will be done to optimize the approach in the future.

References

1. Bhuiyan M Z H, Zhang J, Lohan E S, Wang W, Sand S. Analysis of multipath mitigation techniques with land mobile satellite channel model. Radioengineering 2012; 21(4): 1067-1077.
2. Chen Y X, Zeng Z G, Kang R. Validation methodology for distribution-based degradation model. J Syst Eng Electron 2012; 23(4): 553-559.
3. Chimpalthradi R A, Dattaguru B, Iyengar N G R. Adaptive control for structural damage mitigation. Global journal of researches in engineering: D aerospace engineering 2011; 11(5): 13-19.
4. Cotroneo D, Pietrantuono R, Russo S. Combining operational and debug testing for improving reliability. IEEE T Reliab 2013; 62(2): 408-423.
5. da Silva J C, Saxena A, Balaban E, Goebel K. A knowledge-based system approach for sensor fault modeling, detection and mitigation. Expert Syst Appl 2012; 39(12): 10977-10989.
6. Dui H Y, Si S B, Cai Z Q, Sun S D, Zhang Y F. Importance measure of system reliability upgrade for multi-state consecutive k-out-of-n systems. J Syst Eng Electron 2012; 23(6): 936-942.
7. Fong X Y, Kim Y S, Choday S H, Roy K. Failure mitigation techniques for 1T-1MTJ spin-transfer torque MRAM bit-cells. IEEE T VLSI Syst 2014; 22(2): 384-395.
8. GEIA-STD-0009, Reliability program standard for systems design, development, and manufacturing. ITAA 2008.

9. Johansson J, Hassel H, Zio E. Reliability and vulnerability analyses of critical infrastructures: comparing two approaches in the context of power systems. Reliab Eng Syst Saf 2013; 120: 27-38.
10. Jozef H, Teun H. Models in Software Engineering. Lecture Notes in Computer Science 2008; 5002: 225-236.
11. Komorowski J, Polkowski L, Skowron A. Rough sets: a tutorial. rough-fuzzy hybridization: a new method for decision making, Singapore: Springer-Verlag 1998; pp. 36-45.
12. Michael P. Product Reliability, Maintainability, and Supportability Handbook. 2nd ed. New York: Taylor & Francis Group, LLC, 2009.
13. Nayfeh A H, Hammad B K, Hajj M R. Discretization effects on flutter aspects and control of wing/store configurations. J Vib Control 2012; 18(7): 1043-1055.
14. Park D B, Shin D H, Oh S H, Kim H S. Velocity aiding-based anti-jamming method for GPS adaptor kits. T JPN Soc Aeronaut S 2011; 54(184): 130-136.
15. Reliability Information Analysis Center (RIAC). Nonelectronic Parts Reliability Data (NPRD-2011), 2011.
16. Tarski A. Introduction to logic and to the methodology of deductive sciences, 4th ed. NY: Oxford University Press, pp. 24-45, 1994.
17. Wang J W. Mitigation strategies on scale-free networks against cascading failures. Physica A 2013; 392(9): 2257-2264.
18. Xu S W, Wu X Y. Simulation method for reliability of TT&C mission with high redundancy and small time horizon. J Syst Eng Electron 2012; 23: 943-948.
19. Yang Q Y, Zhang N L, Hong Y L. Reliability analysis of repairable systems with dependent component failures under partially perfect repair. IEEE T Reliab 2013; 62(2): 490-498.

Dezhen YANG
Yi REN
Zili WANG
Linlin LIU
Bo SUN
School of Reliability and Systems Engineering
Beihang University
Xueyuan Rd., 100191 Beijing, China
E-mail: muyidz@126.com, renyi@buaa.edu.cn, wzl@buaa.edu.cn, liullcn@163.com, sunbo@buaa.edu.cn

Article citation info:
ANTOSZ K, STADNICKA D. Evaluation measures of machine operation effectiveness in large enterprises: study results. Eksploatacja i Niezawodnosc – Maintenance and Reliability 2015; 17 (1): 107–117.

Katarzyna ANTOSZ
Dorota STADNICKA

EVALUATION MEASURES OF MACHINE OPERATION EFFECTIVENESS IN LARGE ENTERPRISES: STUDY RESULTS

MIERNIKI OCENY EFEKTYWNOŚCI FUNKCJONOWANIA MASZYN W DUŻYCH PRZEDSIĘBIORSTWACH: WYNIKI BADAŃ*

Maintaining a proper productivity and efficiency level of a technical infrastructure of an enterprise requires, above all, the use of appropriate managing methods and tools as well as an appropriate organization of services responsible for their management. Using a variety of measures is indispensable to evaluate the effectiveness of these practices as well as of the machine performance in any enterprise. The data obtained from measuring particular indicators are a primary source of information on the necessity of taking particular actions. Large companies are particularly willing to implement appropriate indicators of effectiveness evaluation because of a large number of machines and a vast range of their technical maintenance. Different indicators presented in the references are said to be efficient and willingly used by enterprises. The aim of the study, of which the results are presented in this article, was to identify the real actions taken by the surveyed enterprises concerning the use of the machine effectiveness evaluation metrics. Apart from that, the study also intended to obtain the information on which indicators are actually applied by enterprises. The study was carried out in large production enterprises of different industries on a specified area.

Keywords: *technical infrastructure, machine effectiveness, evaluation indicators, maintenance.*

Utrzymanie infrastruktury technicznej przedsiębiorstwa na odpowiednim poziomie produktywności i wydajności wymaga przede wszystkim stosowania właściwych metod i narzędzi zarządzania oraz właściwej organizacji służb odpowiedzialnych za jego realizację. Nieodłącznym elementem oceny efektywności tych działań oraz funkcjonowania maszyn w przedsiębiorstwie jest stosowanie różnorodnych mierników. Dane uzyskiwane z pomiarów określonych wskaźników są podstawowym źródłem informacji o konieczności podejmowania działań określonego rodzaju. Szczególnie duże firmy są chętne, aby wdrożyć odpowiednie wskaźniki oceny efektywności maszyn ze względu na dużą liczbę maszyn i duży zakres prac związanych z ich obsługą techniczną. W literaturze przedmiotu prezentowane są różne wskaźniki wskazywane, jako skuteczne i chętnie stosowane przez przedsiębiorstwa. Celem badań, których wyniki przedstawiono w niniejszej pracy, było zidentyfikowanie rzeczywistych działań realizowanych przez badane przedsiębiorstwa w zakresie stosowania mierników oceny skuteczności maszyn oraz pozyskanie informacji o tym, jakie wskaźniki są przez firmy stosowane w praktyce. Badania przeprowadzono w dużych przedsiębiorstwach produkcyjnych funkcjonujących w różnych branżach przemysłu na określonym obszarze.

Słowa kluczowe: *infrastruktura techniczna, efektywność maszyn, wskaźniki oceny, utrzy-manie maszyn.*

Introduction

One of the main components of the properly organized process of the machine and equipment supervision in any enterprise is the choice and the use of a proper management strategy. The literature widely describes kinds of management strategies and the actions within them [5, 9, 10, 14, 17, 40]. The implementation of the particular methods of machine and equipment supervision in an enterprise requires, however, periodic evaluation of the action effectiveness as well as of the state of the owned technical infrastructure. The degree of reliability of the information obtained is a basic condition for receiving positive final reports, and it facilitates taking proper decisions concerning preventive actions. There are many ways of obtaining information on the operation of particular machines and technological equipment. However, establishing what will be measured is the most important.

Thus, the choice of the appropriate evaluation measures is crucial. These measuring metrics help to evaluate the key actions realized within machines maintenance and they indicate the efficiency of the actions taken in relation to the goals of an organization [6, 10].

The references define different measures of the machine supervision evaluation [22], among them e.g. OEE [8, 18] or MTTR [7, 11, 21]. The references have also been reviewed for the measures used for the machine effectiveness evaluation in an industrial sector [24, 33]. The correlation of the selected indicators with other evaluation methods was assessed as well [2, 24].

Moreover, the analysis of the references showed that there were also studies conducted concerning maintenance activities based on the MTTF values obtained [22]. The study, that was carried out, also regarded the evaluation of the OEE measure values obtained [2, 18], the possibilities of its improvement [31, 39] as well as its computer based (automated) calculation [30]. Different models of optimization of the machine maintenance were also presented [32].

According to the authors, the analysed references lack a comprehensive comparative analysis of the machine evaluation measures practically applied that would take into account e.g. enterprise's size, industry, capital type, or production type. Additionally, in the articles analyzed, it is difficult to find any information on the problems of the enterprises regarding the application of the machine evaluation measures.

(*) Tekst artykułu w polskiej wersji językowej dostępny w elektronicznym wydaniu kwartalnika na stronie ***www.ein.org.pl***

This article indicates the basic measures of machine operation, and the ways of their calculating. Next, it was checked if these measures were being actually applied.

1. Measures of the machine operation effectiveness evaluation

Effectiveness is one of the characteristics determining the properties in a set of items or systems. It is commonly understood as a property of an item (or system) which conditions the achievement level of the goals of an item or a system in the specified conditions of use and in the specified time period [14].Exploitation effectiveness can be defined as the quotient of the results obtained in a given period of the duration of a certain state concerning the operation object to the expenditures incurred to achieve these effects. System effectiveness is conditioned by both pre-exploitation factors such as the required activities and initial inputs related to the required system features and the features of the system environment, as well as by exploitation factors identified in the exploitation process (external factors e.g. cooperating systems or exploitation properties of a system such as reliability, durability, reparability) [40]. However, in case of an item exploitation (a machine, an appliance) we can talk about technical effectiveness of an item defined as a relation between its unreliability and its potential task capability in a system. In its classical approach, in order to describe machine operation, the literature e.g. [12, 20, 26] distinguishes two reliability states, which are fault and up states. Nevertheless, in some other articles e.g. [13, 35], the authors introduce multi-state classifications what results from the complexity and multitasking of some machines.

The machine up state requires defining two basic notions: task operability and functional operability [5].

Task operability is the ability to accomplish the task t in a chosen period of time Δt or any other figure.

Functional operability is the ability to accomplish a task in a chosen moment of time t for each task out of the set of tasks which are possible to accomplish by a machine.

Modelling the two states of operability may take place at every stage of a machine operation in a production system or at every stage of the running technological machines system (of the technological machines park). These stages are: organizing the system, its use and liquidation or reorganisation with a particular maintenance strategy. To evaluate the system effectiveness different evaluation criteria may be used. In the articles [15, 16, 19, 23, 27, 29, 34, 36, 37, 42, 43] the authors propose the criteria of a system evaluation. Different indicators are used for each of the particular criterion. Table 1 presents the examples of indicators of the system according to the four criteria. The table shows their characteristics and sample types.

Most of these indicators can also be used at different levels in order to measure the quality of the production area, the selected line or used equipment or technological machines. PN-EN 15341: 2007 also classifies KPIs service by three main criteria: economic, organizational and technical. In addition, this standard defines the indicators according to the specified criteria on three levels. What is more, this standard [28] specifies the proper selection of indicators for assessing effectiveness. The selection of indicators for the assessment should take into account some relevant criteria such as: the efficiency of maintenance of machines and equipment reliability. When searching for the appropriate indicators, the standard recommends two approaches: – First, the selection of indicators from these available that meet the requirements of the analysis; Second, begin with a method that starts evaluating different machine maintenance processes chosen through the functional analysis. In practice, two approaches may be used. Among the indicators recommended by the standard there are MTBF (Mean Time Between Failure) and MTTR (Mean Time To Repair) indicators. MTBF (Mean Time Between Failure) shows from a static point of view how often the technical object is damaged. In enterprises this indicator is used to determine the preventive maintenance schedule. MTTR (Mean Time To Repair) defines the average time required to repair at the moment of failure. It is used to evaluate the effectiveness of staff maintenance services, as well as for the assessment the repair tasks they carried out [11]. The ways of calculating these indicators are as follows:

- MTBF (Mean Time Between Failures) – denotes the average time between failures or the failure rate. The indicator is understood as the average time of operation between failures in the specified time. It is calculated according to the formula (1).

Table 1. Criteria of the system evaluation. Source: own study based on [15, 16, 19, 23, 27, 29, 34, 36, 37, 42, 43]

No.	Criterion	Characteristics	Exemplary indicators
1.	Informational and operational	Related to the organisation and course of maintenance processes, as well as those concerning the achievement of goals or certain needs, and the impact of the control system on its operation.	Indicator of technological advancement Indicator of machine average age Indicator of repair service rate Indicator of repair requirements accomplishment Indicator of maintenance staff employment Indicator of timeliness of executing major, medium, current repairs and overhauls, Indicator of maintainability
2.	Economic	Related to plus (benefits) and minus (inputs) value effects as well as to profitableness of investment and finance activities in a system.	Indicator of profitability Fixed and variable costs of machines maintenance Indicator of the costs of major and medium repairs, and current maintenance Spare parts maintenance costs
3.	Technical and maintenance	Related to the system elements operability, particularly to technical means, and expressing the impact of technology on their operation; related to the operation of the elements and means for the system continuity, they also express the influence on the system capability to remain in an up state in the specified time.	Indicator of performance Indicator of machine idle time Indicator of machines damage and failures Indicator of technical availability Indicator of machine use Indicator of a shift system
4.	Safety	Related to the risk of losses (human – loss of life or damage to health, ecological, material), which commonly relate fault states of the system elements to the probability of loss caused by them; the extent of the potential losses.	A number of accidents at machine operation and use A number of hazards arisen during machine operation and use

$$MTBF = operating\ time/\ number\ of\ failures\ in\ this\ time \quad (1)$$

– MTTR (Mean Time To Repair) – the average time to complete-of repair. It is understood as the average time of the actual repair from the point of its being reported until the point it is finished. It is calculated according to the formula (2).

$$MTTR = repair\ time\ /\ number\ of\ failures \quad (2)$$

Another indicator, which importance in the production process improvement has been emphasized in articles [1, 30, 31, 38], is OEE indicator. OEE describes the three basic areas of business activity: the availability, efficiency and quality of products. Calculating OEE enables to define the improvement actions implemented in the field of production processes, it allows to measure their effect on the implementation and the elimination of existing problems. It allows to identify bottlenecks and main problems of a company.

– OEE – Overall Equipment Effectiveness. It is calculated as a multiplier of other measuring metrics: availability, performance and quality, which are its constituent elements. The OEE indicator is calculated according to the formula (3). Its individual parameters are calculated according to the formulae (4–7).

$$OEE = Availability \times Performance \times Quality\ x\ 100\% \quad (3)$$

Availability is calculated according to the formula:

$$A = production\ time – downtime/\ production\ time \quad (4)$$

where:

$$downtime = maintenance + setups + failures + other \quad (5)$$

Performance is calculated according to the formula:

$$P = parts\ produced\ (good\ and\ bad\ quality)/\ production\ time \times rated\ performance \quad (6)$$

Quality is calculated according to the formula:

$$Q = parts\ produced – losses/\ parts\ produced \quad (7)$$

OEE considers a process. That means that it takes into account not only the availability time but also performance (actual performance / nominal performance) and a quality factor (good parts/ parts produced). In fact, it compares the machine use to its ideal use, which takes place when the production and its preparation follow the plan [25, 39, 41].

2. The scope and methodology of the study

This paper shows the results of the study conducted in the selected large enterprises located on a limited geographical area (Poland, podkarpackie voivodeship). The study regards the identification of real activities performed by the surveyed enterprises within the application of the machine effectiveness evaluation, as well as the indication of which indicators are actually used by the companies.

The study was carried out in two stages. The first stage was carried out in the following areas:

1. Analysis of the current state of knowledge.
2. Defining the scope and the area of research.
3. Developing a research sheet.
4. Selection of the study.
5. Conducting the research and the analysis of results.

The second stage of the research was carried out as follows: testing, analysis of the results, the proposal of changes in the use of machines assessment indicators. A detailed analysis of the results is presented in this work afterward.

3. Study results

3.1. The first stage of the study

3.1.1. Area and carrying out of research

The first stage of the study concerned identification of the measures for the evaluation of technological machines operation effectiveness. The study involved production enterprises of different industries on the area of podkarpackie voivodeship (Poland). As a detailed subject of the study the following areas were analyzed:

– the information gathered on the machine supervision,
– kinds of downtimes recorded in enterprises,
– the way of recording the information on machine failures,
– the average failure time,
– measuring parameters of quality, performance and availability,
– OEE indicator.

150 enterprises were invited to take part in the studies. Any enterprise, plant or its department that had its own strategy and accounted of its accomplishments could be the object of the study. 46 questionnaires were obtained as a feedback.

The study took the form of interviews. The subjects of the study were the representatives of a medium and top management as well as the employees directly responsible for the process of the technological machines and appliances supervision in a company, as well as the chosen machine operators. The study was conducted in a conjunctive multiple choice format, and included a list of prepared, provided in advance options presented to a respondent with a multiple response item in which more than one answer might be chosen. Additionally, a respondent could give other answers if they were not among the provided options.

3.1.2. The structure of the studied enterprises

During the study, the enterprises were classified according to the following criteria: industry type, production type, ownership (type of capital) and technical infrastructure organization. Table 2 shows the structure of the studied enterprises.

Most companies, because as many as 42%, were aviation companies and 34% were automotive companies. The remaining industries included, among others, metal processing, chemical, wood and paper, and food industry. Among the studied enterprises most were the organizations with a big-batch production as a dominant type of production – 27%. In the 6% of the studied companies, there are a few types of production combined at the same time.

Most of the studied companies (91%) are privately owned, the rest (9%) are state-owned. 68% of them possess foreign majority capital, 15% domestic majority capital, whereas 17% possess entirely Polish capital. In most of the companies, CNC machines are mainly used. In the majority of the studied enterprises, numerically controlled machines prevailed (74%). Among other technical machines, i.a. automatic machines, were mentioned. Most of the studied enterprises, because 72%, describe their situation as developing, and 28% as stable. None of the companies described their situation as difficult.

3.1.3. Study results

The effectiveness of the technical infrastructure management depends largely on the kind and amount of information on machines.

Table 2. The structure of the studied enterprises

Criterion	The structure of the studied enterprises					
Industry	Aviation	Automotive	Metal processing	Wood and paper	Food	Chemical
	42%	34%	13%	5%	3%	3%
Production type	Piece	Small-batch	Medium-batch	Big-batch	Mass	A few types
	20%	22%	18%	27%	12%	6%
Ownership type	Private			State		
	91%			9%		
Capital type	Entirely Polish capital	Polish majority capital		Foreign majority capital		
	17%	15%		68%		
Type of possessed machines	Mainly manually-controlled machines		Mainly numerically-controlled machines		Other	
	24%		74%		12%	

If we are not aware of the problems and of where they occur, we can neither eliminate nor prevent them.

Collecting the needed information, taking the right decisions in the right time as well as providing intended actions and accurate reactions are a continuous challenge for the information system of an organization.

One of the groups of information which should be recorded in companies concerns the information on downtimes. The study shows that the most commonly recorded types of downtimes are machine failures, what was indicated by 93% of the surveyed enterprises (Fig. 1). 71% of the companies record downtimes caused by setups.

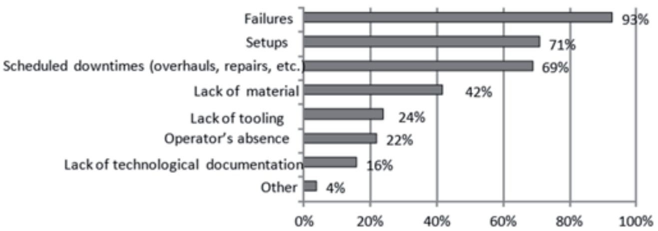

Fig. 1. Types of downtimes recorded in enterprises

Different types of information concerning machines are gathered in the enterprises. They consider both single workstations as well as production lines or departments. They concern machine uptimes, the waiting time for service or machine spare parts, as well as machine performance and load. The conducted study shows that the information, which is the most commonly gathered in the companies in order to facilitate machine-related actions, concerns a number of failures of particular machines (72%). Figure 2 also shows other information gathered as well as the percentage of enterprises which record such information.

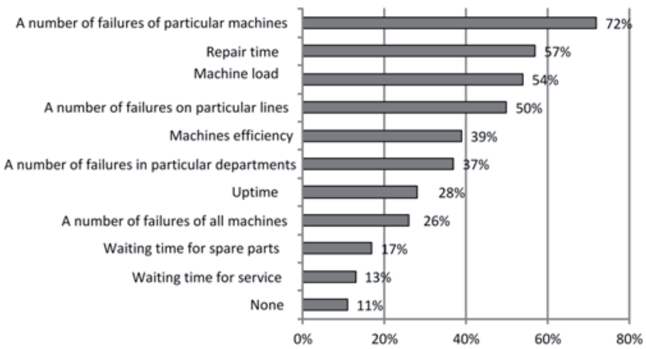

Fig. 2. Types of machine-related information gathered in enterprises

An important element of the completeness and credibility of the obtained data is to determine an appropriate and effective way of the data collecting and recording. In most of the companies (81%) a maintenance worker is responsible for collecting information on machines. At the same time, it is worth mentioning that in 52% of the companies, a few people collect and record information. A question may arise if the same kinds of information are recorded by different people and if the data overlap in such a case. However, it wasn't verified in the conducted study. Among other people engaged in collecting information, a continuous improvement specialist and a technologist were also mentioned.

In 65% of the cases, the place of recording the information regarding machines is the maintenance department. In 42% of the companies the information is directly entered into IT system e.g. via an information kiosk located in a production hall.

The main aim of the study was to gather the information concerning the types of measures used for the machine effectiveness evaluation. The survey involved the questions on determining if the machine quality, performance and availability were measured. The quality metric was defined as a number of conformity products out of the total products produced on the machine. The machine performance was defined as a number of total parts produced on the machine to the production rate of a machine. The machine availability was defined as the actual amount of production time the machine is operating to the production time the machine is available. The detailed results of these studies are shown in the work [3].

The results are presented in Fig. 3. The study shows that 53% of the enterprises do not analyze the quality metric of their machines. This fact impedes the analysis and the possibilities of identifying the

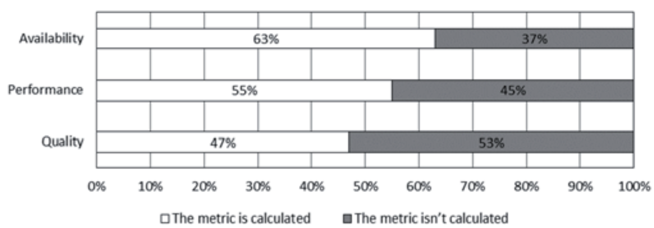

Fig. 3. Percentage of the enterprises which calculate quality, performance and availability parameters

potential causes of nonconformities occurrence in the production.

In case of the performance metric, as many as 55% of the enterprises calculate and analyze it. Collecting such information considerably facilitates the process of production planning which allows on-time processing of customers' orders. It helps to identify machines

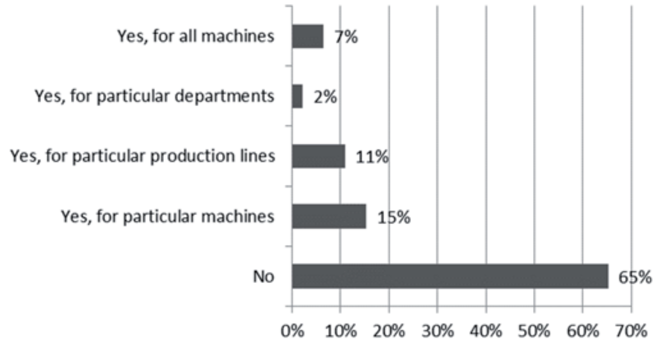

Fig. 4. Percentage of the companies calculating OEE indicator

of bigger or smaller production capacity and thus, indirectly, evaluate the technical condition of the machines owned.

The availability metric is recorded and analyzed in 63% of the enterprises. The value of this metric indicates the actual operating time of the production process. It helps to identify the production stations at which machines often fail or their setup time is too long. Due to this information the enterprise may take actions which result in minimizing the risk of unplanned downtimes and failures. These actions include TPM (Total Productive Maintenance) implementation or the implementation of the methods which allow to reduce the setup times such as SMED (Single Minute Exchange of Die).

One of the measures recommended in the references is OEE indicator. While evaluating the effectiveness of the owned machines and of TPM implementation this parameter is very important. The study shows that it is not always used [4]. This indicator was also analyzed in the conducted study. The obtained information proved that as many as 65% of the enterprises did not use it, and only 15% of the companies calculate OEE for the chosen machines (Fig. 4). Merely 7% of the analyzed companies calculate it for all the machines owned.

Analyzing closely the companies on the production type (Fig. 5)

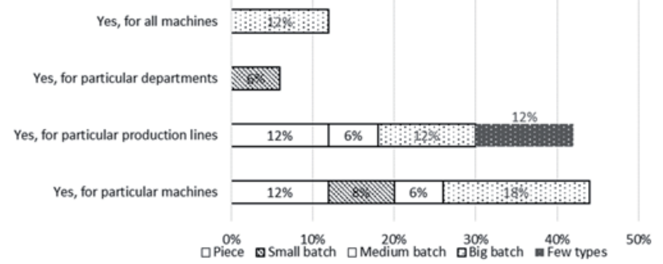

Fig. 5. Percentage of the companies calculating the OEE indicator on the basis of the production type

and industry (Fig. 6), it occurs that OEE is calculated in case of a big-batch production. It mainly concerns the electric, metal processing and automotive industries. For the particular departments, the indicator is calculated only in case of a small batch production, in aviation and automotive sectors. The analyzed enterprises predominantly calculate OEE for the particular, chosen machines in most of the production types and industries.

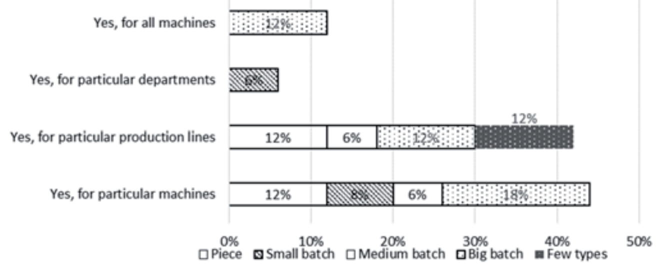

Fig. 6. Percentage of the companies calculating the OEE indicator on the basis of the industry

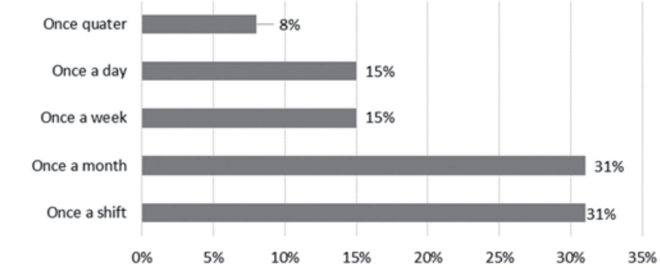

Fig. 7. The OEE calculation rate

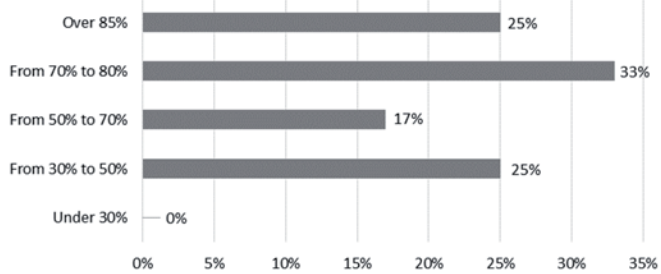

Fig. 8. The average value of the OEE indicator in the enterprises

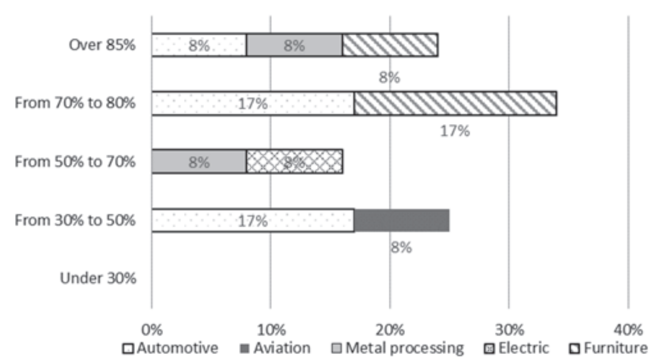

Fig. 9. The values of the OEE indicator for particular industries

Another significant issue was to obtain information which concerned the OEE calculation rate. The rate of obtaining such information is substantial because the values of OEE keep us informed about the productivity of the machines owned. If the information is gathered too sporadically we won't be able to react promptly when there is any decline in the machines use. The study showed that in 31%, the analyzed enterprises calculate shift and daily indicators (Fig.7). Only 8% of the companies calculate the OEE indicator quarterly (Fig.8).

It was significant during the study to gather the information concerning OEE values. Its value is important because it initially helps to make a general analysis of the effectiveness of the machines owned. World class standard for this indicator is over 85%. In the enterprises such a standard is reached only by 25% of the analyzed enterprises whereas 33% of the companies range between 70–80% of the OEE value (Fig. 8).

Figure 9 presents the OEE values obtained in the particular industries. The highest value of the indicator is obtained in the automotive industry for the metal processing machines, and in the furniture industry. The lowest value of the indicator was reported in the aviation and automotive industries.

3.1.4. Discussion and data analysis after the first stage of the study

The study conducted in the first stage shows that many companies collect many information concerning effectiveness of the technical infrastructure owned. The information on failures, unplanned downtimes as well as the data related to efficiency and quality of all and particular machines are also collected. The study proves that almost half of the surveyed companies do not evaluate the effectiveness of the machines owned and do not use metrics for their evaluation. The results show that this issue is worth studying and making the companies aware of the fact that monitoring the performance, quality and availability of the technological machines park owned is important for the timely production.

In the further analyses, the authors searched for the relations between:
- the capital type and the indicators of the machine effectiveness evaluation indicators used,
- the industry type of the company and the indicators used,
- the production volume and the indicators used.

For the data presented, *Chi²* analyses were conducted to evaluate if there is a statistically justified influence of the industry type, type of the possessed capital, or the production volume on the actions undertaken within the process of data collection as well asthe evaluation of the value of the analyzed indicators in an enterprise. The results of the analyses are presented in Table 3.

Table 3. Hypotheses made and P-values obtained

It.no.	Hypothesis	*P-value*
1.	There is no difference betweenthe kinds of indicators calculated by the enterprises with Polish capital or Polish majority capital and the enterprises with foreign capital	0,000
2.	There is no difference between the kinds of indicators calculated by the enterprises of different industries	0,995
3.	There is no difference between the kinds of indicators calculated by the enterprises with different production volumes	0,981

The analyses conducted show that both the collection and evaluation of the value of the analyzed indicators are not conditioned by the industry type, nor by the production volume of large enterprises. However, they are dependent on the type of capital, what is confirmed by P-value of 0,000 (<0,005).

Figure 10 shows the types of measuring metrics based on the capital type possessed by the enterprises.

As the figure 10 shows, the machine quality, performance as well as availability metrics are predominantly calculated in the companies with the foreign capital. The quality metric is calculated by 28%, performance metric by 37% and availability metric by 43% of the analyzed companies with the foreign capital.

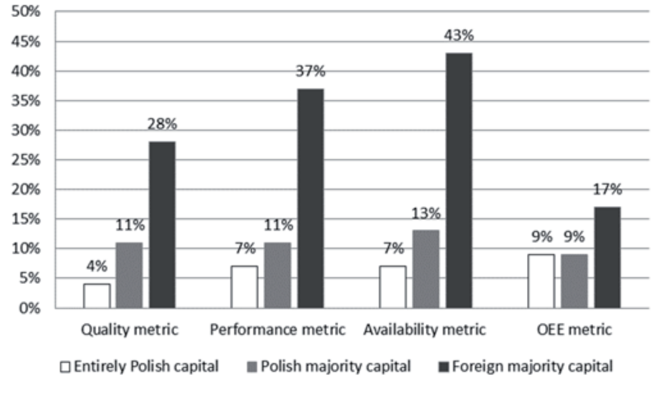

Fig. 10. Types of the metrics collected based on the capital possessed by a company

3.2. The second stage of the study

3.2.1. Study area and methodology

The second stage of the study concerned a detailed analysis of the indicators of the technological machines effectiveness evaluation on the basis of a randomly chosen enterprise. As a detailed subject the following areas were analyzed:
- kinds of machine maintenance actions,
- kinds of the metrics of effectiveness evaluation used in the enterprise,
- the values of the metrics used,
- the manner of recording the information on machines
- the use of OEE and the values obtained.

The results of the analyses conducted at the first stage of the study show that collecting and evaluating the values of the analyzed indicators depend on the capital type. That is why, that was a main criterion in choosing an enterprise. For the further study, out of the studied group, one enterprise with the foreign majority capital was chosen.

This production enterprise operates in the aviation industry in podkarpackie voivodeship. The data obtained during the own study as well as the data from the article [44] were used for the analysis.

The analyzed enterprise operates in production, repair and maintenance, service as well as in design and research. The company business is particularly involved in the production of aircraft components and drive units.

3.2.2. Machine maintenance

The actions related to the machine maintenance in an enterprise are performed by the maintenance services (MS) which are present centrally as well as in particular departments. Preventive maintenance is mainly used in the enterprise. The enterprise uses a modern strategy of the technological machines management that is TPM. The size of the technological machine park owned is about 2500 machines. These machines are mainly numerically controlled machines.

Over 300 workers of different professions and at different posts are employed in MS. Figure 11 presents the workers of the central and departmental levels of maintenance.

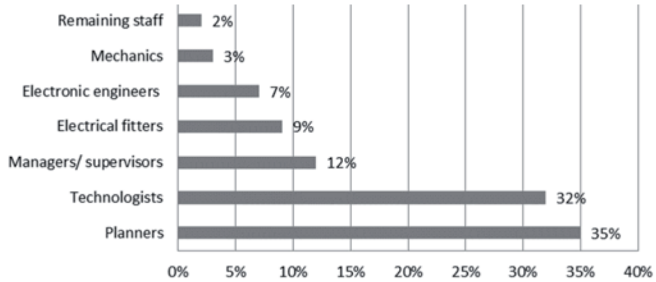

Fig. 11. Workers of the Maintenance Services

The largest number of workers are mechanics. The category of ‘remaining staff’ includes auxiliary service workers such as the workers of OSH, distribution and sharpening departments which function within MS. They constitute 35% of the MS employees, and their duties and the scope of their work are not related to this unit in any way.

The fundamental actions realized by MS of the analyzed enterprise include the actions realized in five basic areas. Table 4 presents the areas and their characteristics.

Based on the working time, the percentage of maintenance services in particular actions was identified (Fig.12).

The largest share of the MS tasks (74%) is constituted by the area related to the current maintenance of the machines and equipment. The remaining actions cover merely 26% of the available time.

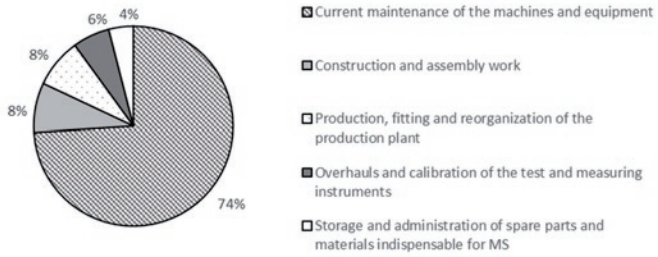

Fig. 12. Percentage of MS in particular areas

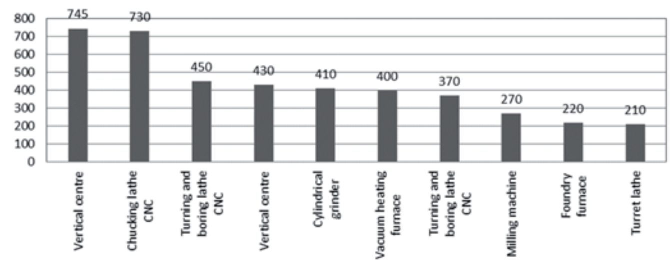

Fig. 13. The most damageable machines in a chosen period of time

Table 4. Areas of MS operating in the analyzed enterprise.

It. No.	Area	Characteristics
1.	Current machine and appliances maintenance	Failure removal, periodical overhauls of machines and equipment, actions related to TPM implementation, preventive maintenance, machine repairs and modernization.
2.	Construction and assembly work	Actions related to maintaining the technical condition of buildings and building structures, removing defects of the equipment in production halls, construction of steel structures and sanitary systems.
3.	Production, fitting and reorganization of the production hall	Repair and regeneration of tooling, service and supervision of pressure instruments, machine tool setups, production hall reorganization – relocation of machines and equipment.
4.	Overhauls and calibration of the test and measuring instruments	Actions related to calibration and overhauls of the equipment such as manometers, thermocouples, dispersed systems, electrical measures, etc.
5.	Storage and administration of spare parts and materials indispensable for MS	Identification of the spare parts needed, resupplying the stock, management of the materials indispensable for MS operation.

3.2.3. Measures of machine effectiveness evaluation

To evaluate the effectiveness of the machine system operation, the enterprise applies a few measures of machine effectiveness evaluation. Table 5 shows their characteristics.

Table 5. Measures of the machine system effectiveness evaluation in the studied enterprise.

It. no.	Measure name	Characteristics
1.	Machine downtime	Downtime is a total equipment stoppage time that is counted since reporting the failure till it is repaired and the machine is restarted, for different kinds of downtimes, e.g. a breakdown, modernization, overhaul, etc.
2.	Timeliness of the overhauls performed	The comparison between the actual time of an overhaul and a period of time determined for the service, i.e. the time is counted according to the scheduled date based on the service schedule ±14 days (Note: it is possible to consider a different period of time).
3.	Failure rate graph – Top 10	The graph of the 10 most prone to failure machines in a specified analyzed time.
4.	Percentage measure of preventive actions to failures ratio	Percentage of the time devoted to maintenance actions to the failure time (according to 80:20 rule)

Figures 13–16 present the way of the representation of some measures and their values in a chosen time. Figure 13 presents the graph of the most damageable machines – TOP 10 in a chosen period of time. Such a graph is developed for both particular production lines as well as for particular departments. It is prepared weekly and monthly. This measure allows to monitor on ongoing basis the most damageable machines in a given production area. It results in the increase of preventive actions on such machines. A trend graph in figure 14 shows the data concerning machine downtimes in a chosen period of time.

The compiled data, as shown in figure 14, allow to monitor machine downtimes as well as their types in a given period of time. Downtimes are classified as follows: failure, certification, defect, overhaul, actions targeted at TPM implementation and other. Such compilation allows a detailed analysis of the most frequent downtime and its duration. Completing the further periods with e.g. the data concerning scheduled overhauls, TPM related actions or modernization, additionally enables a more effective production planning process. The measure allows to optimize the actions related to machine maintenance, both in particular production areas as well as in the entire enterprise.

Figure 15 presents the percentage of preventive actions and failures in a chosen period of time. The maintenance services of the enterprise use the 80:20 rule to analyze this measure, where 80% of the MS working time devoted to preventive maintenance is supposed to result in reducing the failure duration to the level of 20% of the total available working time. The presented data show that during twelve months the failure indicator decreased considerably from the highest value of 77,8% to 51,9%. The change of the value of this indicator was caused by the significant increase and improvement of preventive maintenance performed in the enterprise. The indicator's value increased from 22,2% to 58,1%. To improve the preventive maintenance in the enterprise, the company applied chosen methods and tools of Lean Manufacturing such as a process approach, Value Stream Mapping (VSM), TPM implementation for the most of machines. In addition, the company entirely changed the organization of maintenance services work.

The evaluation of the overhauls timeliness is significant in machine maintenance effectiveness evaluation (table 6). The record allows current monitoring of the scheduled overhauls progress. It allows to analyze the timeliness of overhauls in particular departments what makes it possible to send more workers to the areas where machine overhauls need speeding up. The available data are used for different analyses which help to identify machines awaiting for an overhaul, those after overhauls or the ones with delayed overhauls in a quick and easy manner. Table 6 shows on-time overhauls marked red and the delayed overhauls grey. Electronic reporting and ordering of overhauls help to eliminate laborious manual records, and they facilitate the data analysis.

Unfortunately, the studied company doesn't use the OEE indicator for the effectiveness analysis. The company has tried to apply this indicator, however with no effect. As the explanation of the failure, the company gives the following reasons:

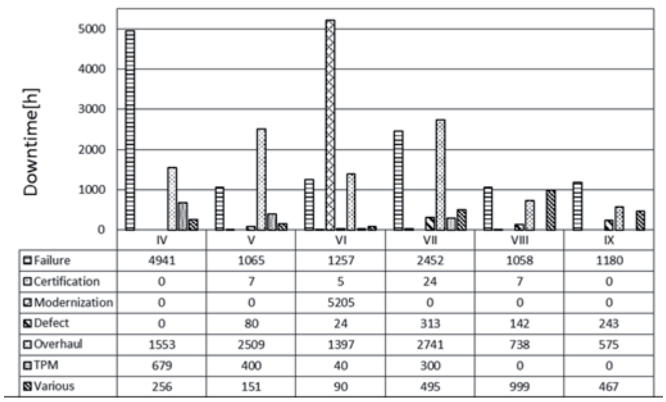

Fig. 14. Machine downtimes in a chosen period of time

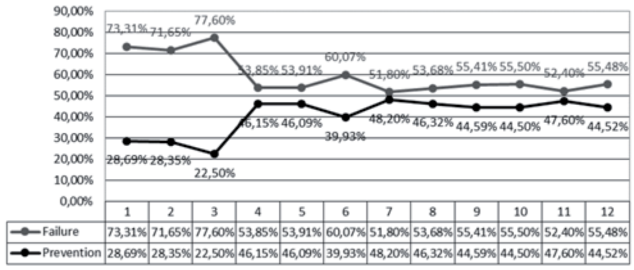

Fig. 15. Percentage of the prevention and failure rate in a chosen period of time

- too much information needed what requires engaging many people from several organizational units to collect it,
- too much effort at the manual system of its calculation, in particular because it is a large enterprise with lots of machines and equipment,
- automated data collection should be introduced as the data collected manually are often encumbered with a big measuring error,
- emerging problems with the regular collection of data in different areas,
- electronic and automatic system of data collection is also indispensable to analyze the data systematically because only that could help to implement the OEE indicator effectively, however it occurred to be too expensive to implement,
- the implementation of the OEE indicator requires the standardization of procedures and of the type of the information gathered in all departments of the enterprise, what unfortunately turned out to be too difficult and time-consuming.

The company has plans for another attempt to implement the OEE indicator. The first step to achieve this is the standardization of the machine supervision processes as well as of the collection of the information on their performance in a production process in particular departments.

3.2.4. Discussion after the second stage of the study

The study conducted in a chosen enterprise showed that not only the proper organization of the services responsible for the machine performance but, above all, the right choice of the measures applied are important for the machine effectiveness evaluation. The analyzed enterprise uses very simple measures of the machine effectiveness evaluation. However, they are, according to the enterprise, sufficient and they provide a lot of information helpful for the effective process of technological machine and equipment supervision. The study shows that some of the elements of the appropriate process of the machine effectiveness monitoring are completeness, availability and reliability of the obtained information. Unfortunately, obtaining the above requires electronic and automatic system of support.

4. Conclusions and suggestions on indicators to use in enterprises

An effective process of machine and equipment supervision in an enterprise requires not only the choice of the right strategy for the technical infrastructure management but, above all, reliable indicators of its performance evaluation. The conducted study determined that almost the half of the studied companies don't evaluate the effectiveness of the owned machines or they use only some indicators for its evaluation.

The study shows that only 35% of the enterprises apply the recommended OEE indicator. In the second stage of the study, the machine evaluation indicators used in a chosen enterprise were analyzed in detail. The analysis proved that the enterprise do not use most of the indicators recommended by the references such as OEE, MTTR or MTBF, despite the fact that it is a large enterprise with the foreign majority capital. The company has developed and used its own simple measures which don't require the workers to be involved in an excessive and additional task of collecting the needed data.

The enterprise, while evaluating the effectiveness of its machines, requires simple, concise and useful information on the machines and their effectiveness. Additionally, it also needs the information on support services responsible for the machines supervision. Based on the information obtained from the conducted study, the authors suggested a set of indicators which the enterprises may use for the evaluation of

Table 6. The database of the timeliness of machine and equipment overhauls in a chosen period of time

Position	Scheduled date	Date of completion	Location	Difference	Timeliness/ status
Universal lathe 1	2010-01-01	2010-01-08	Prod. Dep.	7	On-time
Universal lathe 2	2010-01-01	2010-01-19	Prod. Dep.	18	Overdue time
Universal lathe 3	2010-01-02	2010-02-08	Prod. Dep.	27	Overdue time
Universal lathe 4	2010-01-02	2010-01-02	Prod. Dep.	0	On-time
Universal lathe 5	2010-01-02	2010-01-19	Prod. Dep.	17	Overdue time
Universal lathe 6	2010-01-02	2009-12-28	Prod. Dep.	-5	On-time
Universal lathe 7	2010-01-02	2010-01-12	Prod. Dep.	10	On-time
Universal lathe 8	2010-01-02	2010-02-01	Prod. Dep.	31	Overdue time
Universal lathe 9	2010-01-03	2010-03-01	Prod. Dep.	58	Overdue time
Universal lathe 10	2010-01-03	2010-01-11	Prod. Dep.	8	On-time
Universal lathe 11	2010-01-03	2010-01-08	Prod. Dep.	5	On-time
Universal lathe 12	2010-01-03	2010-01-19	Prod. Dep.	16	Overdue time

Table 7. The indicators suggested for the evaluation of machines and support services.

It. no.	Criterion	The indicator suggested	Information necessary for the indicator's evaluation	Manner of its calculation
	Informational and operational	percentage of preventive maintenance	• type of tasks done by support services • tasks duration	$DP = \frac{\sum_1^m T_{DPm}}{\sum_1^n T_{Dn}} * 100\%$ where: DP – Preventive maintenance T_{DPm} – actual time devoted to preventive maintenance (h) T_{Dn} – available operating time (h)
		indicator of timeliness of work completion – mainly of scheduled overhauls and repairs	• work due dates • schedule of works	$T_P = T_{rz} \pm 7 day.$ where: T_P– scheduled due date of overhaul T_{rz}– actual due date of overhaul (**Note**: Instead of $\pm 7 days$ other period is possible)
		mean time to repair (MTTR)	• repair duration • a number of failures	$MTTR = \frac{\sum_1^n T_{WP_n}}{K_A}$ where: T_{WPn} – repair time (h) K_A – number of failures
2.	Economic	indicator of task completion costsrelated to machine maintenance	• particular tasks costs • type of particular tasks	$K_{RP} = \sum_1^n K_{Pn}$ where: Krp – implementation costs K_{Pn} – particular tasks completion costs
		Total and unit cost of maintaining and exchanging spare parts	• costs related to the maintenance and exchange of spare parts	$K_{CZ} = \sum_1^n K_{Wn} + \sum_1^m K_{Um}$ where: Kcz – costs of spare parts K_{Wn}– Total cost of spare parts exchange K_{Um} – totalcost of spare parts maintenance
3.	Technical and maintenance	indicator of machine performance	• types of machine downtimes • information concerning the number and duration of both planned as well as unplanned downtimes • machine operating time in a production process **Note**: Information can be collected and analyzed for individual workstations or a group of machines	$W = \frac{\sum_1^n P_{Wn}}{T_P \times W_Z}$ where: W – performance P_{Wn} – parts produced (good +bad) (parts) T_P – available run time (h) W_Z – nominalperformance(u/h)
		indicator of machine availability		$D = \frac{T_P - T_{PRZ}}{T_P}$ where: D – availability; T_P – available run time (h) $T_{PRZ} = T_K + T_A + T_S + \ldots + N$ T_{PRZ} – downtime duration (h) T_K – maintenance duration (h) T_A – failure duration (h) T_S – setup duration (h); N - other
4.	Safety	number of accidents at machine operation and use	• information concerning the level of safety in the process of machine operation and use	K_W – number of accidents K_Z – number of hazards (**Note**: values of these indicators may be analyzed on a daily, quarterly or monthly basis)
		number of hazards emerged at machine operation and use		

the machine performance and support services, and which usage is not related to excessive workload (Table 7). Table 7 presents a set of indicators, the criteria of their choice, the sort of information needed for setting the value of each of the indicators and the manner of their determining. The authors propose to use both the indicators which were most frequently used by the studied enterprises as well as the indicators which according to the authors' assessment are useful and should be used.

The indicators which have been suggested will allow to obtain the information that will be the basis for taking actions aiming at the improvement of technological machine park operation in a company. What is more, it will result in the quality of machine performance improvement, costs reduction as well as in the work safety improvement.

5. The need for further studies

It is worth to extend such studies to small and medium enterprises which, as a rule, possess smaller financial means that could be spent on the technical infrastructure improvement as well as on the process of the machine effectiveness monitoring.

It would also be advisable to examine the relation of the technical infrastructure management strategy to the measures of the machine park effectiveness evaluation used in an enterprise, taking into consideration both the type of capital as well as the type of production.

The obtained results could indicate the course of action that should be taken in order to motivate companies to improve the methods of supervision and to make them aware of the benefits and the impact of the proper machine supervision on rising the competitiveness of enterprises on an increasingly harder global market.

References:

1. Ahire ChP, Relkar AS. Correlating Failure Mode Effect Analyses (FMEA) with Overall Equipment Effectiveness (OEE). Procedia Engineering 2012; 38: 3482–3486.
2. Ahlmann H. From traditional practice to the new understanding: The significance of life cycle profit concept in the management of industrial enterprises. Maintenance Management & Modelling conference Växjö, 2002.
3. Antosz K, Stadnicka D. The results of the study concerning the identification of the activities realized in the management of the technical infrastructure in large enterprises. Eksploatacja i Niezawodnosc – Maintenance and Reliability 2014; 16 (1): 112–119.
4. Antosz K, Stadnicka D. TPM in large enterprises: study results. World Academy of Science, Engineering and Technology. International Journal of Industrial Science and Engineering, October 2013; Issue 82, Barcelona, 3, str. 320-327. ICIESM 2013: International Conference on Industrial Engineering and Systems Management. Barcelona, Spain October 14-15, 2013.
5. Będkowski L. Elementy diagnostyki technicznej, Warszawa: WAT, 1992.
6. Bergman B, Klefsjö B. Quality: from customer needs to customer satisfaction. Lund: Studentlitteratur, 2010.
7. Chand G, Shirvani B. Implementation of TPM in cellular manufacture. Journal of Materials Processing Technology 2000; 103: 149-154.
8. Dal B, Tugwell P, Greatbanks R. Overall equipment effectiveness as a measure of operational improvement, a practical analysis. International Journal of Operations and Production Management 2000; 12: 1488–1502.
9. Downarowicz O. Systemy eksploatacji. Zarządzanie zasobami techniki. Radom: ITE, 2000.
10. Fredriksson G, Larsson H. An analysis of maintenance strategies and development of a model for strategy formulation - A case study. Göteborg: Chalmers University of Technology, 2012.
11. Gulati R, Smith R. Maintenance and Reliability Best Practices. [Electronic] New York: Industrial Press, 2009.
12. Haviland R. Niezawodność systemów technicznych, Warszawa: WNT, 1968.
13. Hebda M, Mazur T. Teoria eksploatacji pojazdów, Warszawa: WKiŁ, 1980.
14. Kaźmerczak. J. Eksploatacja systemów technicznych. Gliwice: Wydawnictwo Politechniki Śląskiej, 2000.
15. Kwiotkowska A. Zagadnienia działalności remontowej w przedsiębiorstwie produkcyjnym w ujęciu logistycznym. Gliwice: Wydawnictwo Politechniki Śląskiej, 2006.
16. Legutko S. Eksploatacja maszyn. Poznań: Wydawnictwo Politechniki Poznańskiej, 2007.
17. Legutko S. Trendy rozwoju utrzymania ruchu urządzeń i maszyn. Eksploatacja i Niezawodnosc – Maintenance and Reliability 2009; 42 (2): 13-16.
18. Ljungberg, Ö. Measurement of Overall Equipment Effectiveness as a Base for TPM Activities. International Journal of Operations & Production Management 1998; 2(18): 495-507.
19. Loska A. Eksploatacyjna ocean obiektów technicznych z zastosowaniem metod taksonomicznych. Eksploatacja i Niezawodnosc – Maintenance and Reliability 2013; 15 (1): 1-8.
20. Madera D. Gospodarka remontowa jako kluczowa część procesu technologicznego, Komputerowe zintegrowane zarządzanie. Warszawa: WNT, 2005.
21. McKone K. E, Schroeder R. G, Cua K. O. Total productive maintenance: a contextual view. Journal of Operations Management 1999; 17: 123-144.
22. Mobley R. K. An Introduction to Predictive Maintenance. New York: Van Nostrand Reinhold, 1990.
23. Muchiria P, Pintelona L, Geldersa L, Martinb H. Development of maintenance function performance measurement framework and indicators. International Journal of Production Economics 2011; 1(131): 295-302.
24. Muchiria P. N, Pintelona L, Martinb H, De Meyerc A. M. Empirical analysis of maintenance performance measurement in Belgian industries. International Journal of Production Research 2010; 20 (48): 5905-5924.
25. Oechsner R, Pfeffer M, Pfitzner L, Binder H, Muller E, Vonderstrass T. From overall equipment efficiency(OEE) to overall Fab effectiveness (OFE). Materials Science in Semiconductor Processing 2003; 5: 333–339.
26. Oprzędkiewicz J. Niezawodność maszyn. Kielce: Mała Poligrafia Politechniki Świętokrzyskiej, 1981.
27. Piasecki S. Optymalizacja systemów obsługi technicznej. Warszawa WNT, 1972.
28. PN-EN 15341:2007. Obsługa – Kluczowe wskaźniki efektywności obsługi. Warszawa: PKN, 2007.
29. Praca zbiorowa pod redakcją Migdalskiego J. Poradnik niezawodności. Podstawy matematyczne. Warszawa: Wydawnictwo Przemysłu Maszynowego WEMA, 1982.

30. Rathenshwar S, Dhaval D. S, Ashish M. Milesh H. S. Overall equipment efficiency(OEE) Calculation – Automation through Hardware & Software Development. Procedia Engineering 51 (2013) 579 – 584.
31. Relkar A.S, Nandurkar K.N. Optimizing & Analysing Overall equipment efficiency(OEE) through Design of Experiments. Procedia Engineering 2012; 38: 2973-2980.
32. Sharma A, Yadava G.S, Deshmukh S.G. A literature review and future perspectives on maintenance optimization. Journal of Quality in Maintenance Engineering 2011; 1(17): 5-25.
33. Simões J.M, Gomes C.F, Yasin M.M. A literature review of maintenance performance measurement: A conceptual framework and directions for future research. Journal of Quality in Maintenance Engineering 2011; 2(17): 116-137.
34. Słotwiński B. Podstawy badań i oceny niezawodności obiektów technicznych. Koszalin: WU WSI, 1992.
35. Smalko Z. Podstawy eksploatacji technicznej pojazdów. Warszawa: Wydawnictwo Politechniki Warszawskiej, 1987.
36. Stadnicka D, Antosz K, Ratnayake R.M.C. Development of an empirical formula for machine classification: Prioritization of maintenance tasks. Safety Science 2014, 63: 34–41.
37. Stadnicka D, Antosz K. Lean in Large Enterprises: Study Results. World Academy of Science, Engineering and Technology 2013; Paris: 82: 31-37.
38. The Productivity Press Development Team, OEE dla Operators: Overall Equipment Effectiveness. Wrocław: ProdPress, 2009.
39. Wang T. Y, Pan H. Ch. Improving the OEE and UPH data quality by Automated Data Collection for the semiconductor assembly industry. Expert Systems with Applications 2011; 38: 5764-5773.
40. Ważyńska – Fiok K, Jaźwiński J. Niezawodność systemów technicznych. Warszawa: PWN, 1990.
41. Wilczarska J. Efektywność i bezpieczeństwo użytkowania maszyn. Inż. i Ap. Chem. 2012; 2: 41-43.
42. Woropay M, Knopik L, Landowski B. Modelowanie procesów eksploatacji w systemie transportowym. Bydgoszcz-Radom: Biblioteka Problemów Eksploatacji. Instytut Technologii Eksploatacji, 2001.
43. Woropay M, Landowski B, Jaskulski Z. Wybrane problemy eksploatacji i zarządzania systemami technicznymi. Bydgoszcz: ATR Bydgoszcz, 2004.
44. Wróbel P. Analiza funkcjonowania maszyn na przykładzie wybranego przedsiębiorstwa, praca zrealizowana pod opieką K. Antosz, Rzeszów: Politechnika Rzeszowska, 2010.

Katarzyna ANTOSZ
Dorota STADNICKA
Faculty of Mechanical Engineering and Aeronautics
Rzeszow University of Technology
Al. Powstańców Warszawy 12, 35-959 Rzeszów, Poland
E-mails: katarzyna.antosz@prz.edu.pl, dorota.stadnicka@prz.edu.pl

Article citation info:
PROCHOWSKI L, WACH W, JACKOWSKI J, PIENIĄŻEK W. Experimental and model studies on the influence of the run flat tire damage on braking dynamics of the multi-axial special purpose vehicle. Eksploatacja i Niezawodnosc – Maintenance and Reliability 2015; 17 (1): 118–128.

Leon PROCHOWSKI
Wojciech WACH
Jerzy JACKOWSKI
Wiesław PIENIĄŻEK

EXPERIMENTAL AND MODEL STUDIES ON THE INFLUENCE OF THE RUN FLAT TIRE DAMAGE ON BRAKING DYNAMICS OF THE MULTI-AXIAL SPECIAL PURPOSE VEHICLE

EKSPERYMENTALNE I MODELOWE BADANIA WPŁYWU USZKODZENIA OPON RUN FLAT NA DYNAMIKĘ HAMOWANIA WIELOOSIOWEGO POJAZDU SPECJALNEGO*

Tire damage, that occurs quite often during operation of special purpose vehicles (building, forest, military, agricultural heavy-duty vehicles), affects a vehicle motion also during sudden braking. Motion of a four-axial vehicle has been analysed in order to evaluate the influence of tire damage (cracking, tearing) on its behaviour during sudden braking and based on that to evaluate the possibilities of driver's reactions to motion disorders resulting from that emergency condition. Using the PC-Crash software, a vehicle model was designed allowing for simulation of special-purpose vehicle motion. The vehicle model includes a possibility of occurring of sudden tire damage when in motion. In such situation a model of cooperation of a tire and a surface is of crucial significance. A semi-empirical, non-linear TMeasy tire model was used. Its parameters were obtained on the basis of the results of the tests performed on 14.00R20 tires with run flat inserts. A vehicle model parameterization was based on the results of the vehicle measurements, however the validation was based on the results of experimental road tests of braking with damaged tires. Performed calculations and simulations indicated that when braking is started a process of vehicle deviation and related motion track modification is initialized. The motion track deviation increases as the initial braking speed is increased.

Keywords: *tire use, special purpose vehicle operation, active safety, tire damage, run flat tires, driver training.*

Uszkodzenie opony, które dość często pojawia się podczas eksploatacji pojazdów specjalnych (budowlane, leśne, militarne, rolnicze), wpływa na ruch pojazdu, również podczas gwałtownego hamowania. Analizie poddano ruch czteroosiowego pojazdu w celu dokonania oceny wpływu uszkodzenia opon (pęknięcie, rozerwanie) na jego zachowanie się podczas gwałtownego hamowania, a na tej podstawie oceny możliwości reakcji kierowcy na zaburzenia ruchu wynikające z takiego stanu awaryjnego. Korzystając z programu PC-Crash opracowano model pojazdu umożliwiający symulację ruchu pojazdu specjalnego. Model pojazdu uwzględnia możliwość powstania nagłego uszkodzenia opony w czasie jazdy. W takiej sytuacji decydujące znaczenie ma model współpracy opon z nawierzchnią. Zastosowano nieliniowy semi-empiryczny model opony TMeasy, którego parametry uzyskano na podstawie wyników badań opon 14.00R20 z wkładkami run flat. Parametryzacja modelu pojazdu została oparta na wynikach pomiarów pojazdu, natomiast walidacja na wynikach eksperymentalnych badań drogowych hamowania z uszkodzonym ogumieniem. Przeprowadzone obliczenia i symulacje pokazały, że po rozpoczęciu hamowania następuje proces odchylania pojazdu i związana z tym zmiana toru jazdy. Odchylenie toru jazdy rośnie wraz ze wzrostem prędkości początkowej hamowania.

Słowa kluczowe: *eksploatacja opon, eksploatacja pojazdów specjalnych, bezpieczeństwo czynne, uszkodzenia opon, opony run flat, szkolenie kierowców.*

1. Introduction

Difficult conditions of special purpose vehicle operation result in high tire damage risk. The nature of damage varies but it always affects the vehicle traction properties and causes increased driver's effort and driving safety threat. A vehicle with damaged tires (if it is still able to continue a drive, even a short-distance one) has increased motion resistance and it is hard to keep an intended track of motion.

The analyses being carried out further on refer to the braking process of a vehicle equipped with run flat tires. The wheels with that type of equipment can be driven for a short distance after tire damage.

The goal of this paper is to analyse the behaviour of a special purpose vehicle after tire damage (cracking, tearing resulting in complete loss of internal pressure) when driving. A process of sudden braking after tire damage as a basis for evaluation of driver's abilities to react to that type of motion disorders is being considered. The purpose of performed calculations is a detailed evaluation of the influence of location (position) of damaged tires on the behaviour of a vehicle during sudden braking and most of all on a vehicle motion track and a course of variations of parameters that characterize that motion. Braking from the initial speed of 40 and 80 km/h is considered. The essential attention was paid to a process of validation of a multi-axial vehicle with damaged run flat type tires. There are few available papers including that type of a problem [1, 4, 7, 15, 17]. There are papers concerning the influence of a tire pressure on a vehicle driving properties [2, 10], however there are no works that discuss the influence of tire damage on a process of sudden braking of a multi-axial vehicle.

(*) Tekst artykułu w polskiej wersji językowej dostępny w elektronicznym wydaniu kwartalnika na stronie ***www.ein.org.pl***

Identification of the influence of tire damage on the safety of further vehicle motion can be a source of many indications for vehicle structure improvement and for practical driver training.

2. A model of dynamics of the braking process with damaged tires

Using the PC-Crash software [11], a model of a special purpose vehicle and a driver model were built. The vehicle model includes possibility of simulation of sudden tire damage when driving. The driver model allows for reaction to such situation.

The vehicle model includes a rigid body and 8 wheels with independent suspension and it has 14 degrees of freedom:

$$q=\left[x,y,z,\varphi,\theta,\psi,\Omega_1,\Omega_2,\Omega_3,\Omega_4,\Omega_5,\Omega_6,\Omega_7,\Omega_8\right]^T, \tag{1}$$

where: x, y, z – the coordinates of the vector r describing the position of the centre of gravity (CG) of the vehicle body C and the origin of local system of coordinates at the same time in the global system {O}; the local system {C} of coordinates is related to a vehicle and fixed to the vehicle's CG,

φ, θ, ψ − quasi-Euler's angles of system orientation $\{C\}$ in relation to the system $\{O\}$, that is:

φ – roll angle (angle of the body rotation around longitudinal axis x' of the system $\{C\}$),

θ – pitch angle (angle of the body rotation around the transverse axis y' of the system {C}),

ψ – yaw angle, i.e. angle of body rotation around the vertical axis parallel to the axis z' of the system{O},

Ω_k, $k = 1,.., 8$ – the k-th wheel rotation angle.

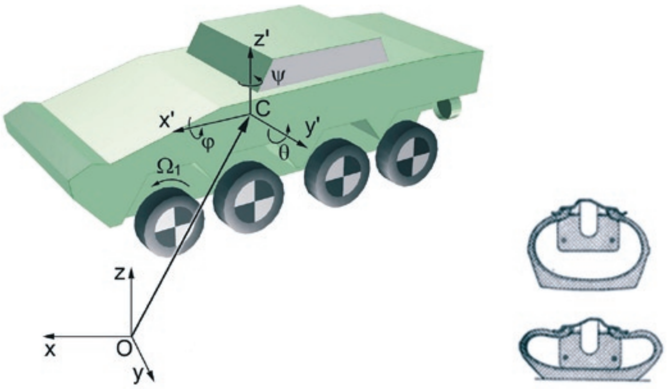

Fig. 1. Vehicle and systems of coordinates, section of a tire with a run flat insert

Vehicle motion equations are expressed with vector dependencies, respectively:

$$m\left(\dot{\mathbf{v}}+\boldsymbol{\omega}\times\mathbf{v}\right)=\sum_{i=1}^{n}\mathbf{F}_i, \tag{2}$$

$$\mathbf{T}\dot{\boldsymbol{\omega}}+\boldsymbol{\omega}\times\mathbf{T}\boldsymbol{\omega}=\sum_{i=1}^{n}\mathbf{M}_j \tag{3}$$

where: m − vehicle mass,

$\mathbf{v}=\dot{\mathbf{r}}$ – velocity of the CG expressed in the global system {O},

$\dot{\mathbf{v}}=\ddot{\mathbf{r}}$ – change of the CG velocity in {O},

$\mathbf{r}$ − vector from the origin of the inertial system {O} to the vehicle's CG in {O},

$\mathbf{F}_i$ and $\mathbf{M}_j$ − respective external forces and moments acting on the vehicle body in $\{C\}$,

$\mathbf{T}$ − tensor of inertia of the vehicle in relation to the centre of mass $\{C\}$,

$\boldsymbol{\omega}$ − angular body velocity vector in $\{C\}$.

Mass deviation moments were neglected so tensor **T** looks as follows:

$$\mathbf{T}=\begin{bmatrix} I_{x'} & 0 & 0 \\ 0 & I_{y'} & 0 \\ 0 & 0 & I_{z'} \end{bmatrix}, \tag{4}$$

where: $I_{x'}, I_{y'}, I_{z'}$ −main central moments of inertia of the vehicle.

Interaction between a wheel and a road was described by means of non-linear TMeasy tire model [14, 16]. It allows for determination of forces and moments generated by a tire (affecting the suspension and the vehicle) on the basis of the results of experimental tests. The results of the tests performed on 14.00R20 tires with *run flat* inserts [12] were used, as the analysed vehicle is equipped with that type of tires. The TMeasy model needs to include on each wheel the longitudinal and lateral force depending on the longitudinal and lateral slip respectively:

$$F_X(s_X,t)=\mu\cdot\mu_X(s_X)\cdot F_z(t) \tag{5}$$

$$F_Y(s_Y,t)=\mu\cdot\mu_Y(s_Y)\cdot F_z(t) \tag{6}$$

where: μ – coefficient of friction;

$F_z(t)$ – current value of the vertical reaction of the road on the wheel;

Normalized longitudinal and lateral forces depending on longitudinal and lateral slip respectively

$$\mu_X\left(s_X\right)=\frac{X_K(s_X)}{Z_K} \tag{7}$$

$$\mu_Y\left(s_Y\right)=\frac{X_K(s_Y)}{Z_K} \tag{8}$$

are determined during the tire tests, while Z_K means vertical reaction during the study. Examples of characteristics $X_K(s_X)$ and $Y_K(s_Y)$ and notation applied are shown in figure 2.

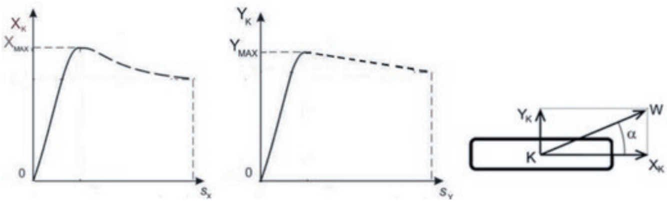

Fig. 2. Tangential reactions of the road on the wheel [13], K – centre of the tire-road contact

Braking force F_H, applied by a driver, is used for calculation of longitudinal force F_X considering the properties of applied tire model. At the same time, the resultant tangential force W (compare fig. 2) cannot exceed the following value:

$$W \leq \mu F_Z(t) \tag{9}$$

During simulation of the vehicle motion, the values, required at each moment of the time, of longitudinal force F_X and lateral force F_Y of the k-th wheel are calculated considering the local coefficient of friction and current reaction of the road on the whe F_Z. It allows for considering variation of traction at the moment of tire damage. In the modelling process it is assumed that damage of a tire with a run flat insert results in:

- decrease of radial tire stiffness;
- change in the cornering stiffness characteristics and most of all decrease of resistance to the side slip;
- rolling resistance increase.

Properties of a tire after damage were modelled by modifications of its characteristic – an example is shown in figures 3 and 4.

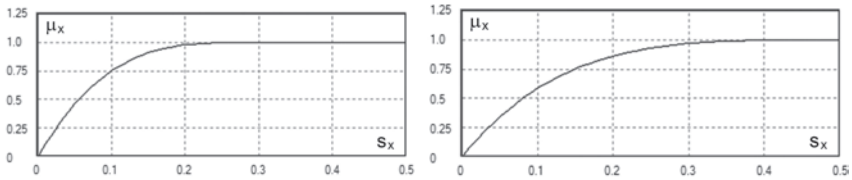

Fig. 3. Normalized longitudinal force as a function of longitudinal slip $\mu_X = f(s_X)$: a) good tire, b) damaged tire

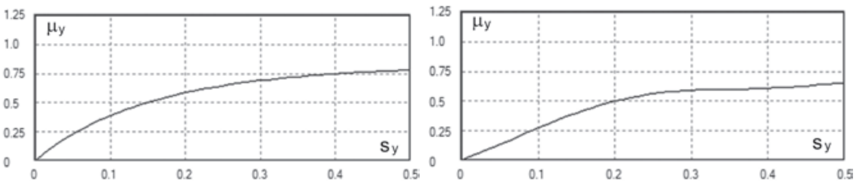

Fig. 3. Normalized lateral force as a function of lateral slip $\mu_Y = f(s_Y)$: a) good tire, b) damaged tire

3. Determining vehicle model parameters and characteristics

A model of vehicle dynamics and driver's actions was developed by using PC-Crash 9.2 software. It was assumed that the mass is evenly distributed around the axis *x'* of the vehicle body. The vehicle model has 4 steering wheels turning around vertical axes, going through their centres and parallel to axis *z'*.

When the suspension deflects the wheels are moving parallel to the vertical vehicle axis *z'*. Tire characteristics are non-linear. A moment of wheel inertia in relations to the rotation axis was included. The wheels are suspended independently by means of springing and damping elements of characteristics reduced to the wheel centres. The force in the suspension is a sum of the springing and damping forces and it is described by the sectional linear characteristic.

Braking is executed by individual force values of each wheel (in order to simulate the damages) and considering the tire model and a braking force limiter. The characteristic of the braking force limiter has a significant influence on the course of braking. A limiter with characteristic presented in figure 5, was installed on the vehicle model axes 3 and 4. Its influence on the longitudinal rear axles forces values during braking F_{Xt} results from the following dependency:

$$q_t = \frac{F_{Xt}}{Q} \leq q_{t0} \tag{10}$$

where: Q – vehicle weight,
$z = a_H/g$, a_H – braking deceleration,

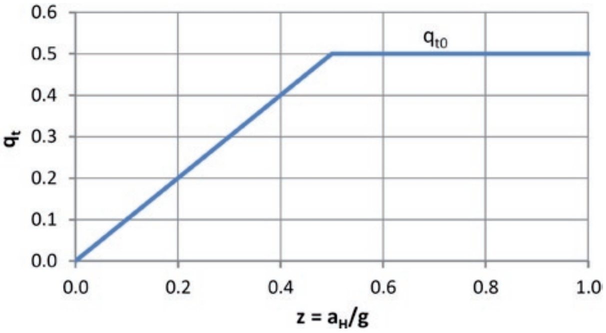

Fig. 5. Braking force limiter characteristics

q_{t0} – characteristic of the braking force limiter according to fig. 5.

The main determination of model parameters and characteristics was made on the basis of vehicle measurements described in [8, 12]. Then the vehicle was used for the braking tests with damaged tires. Some input data was supplemented on the basis of values generated in PC-Crash for that vehicle category. Collected data made an exit point in the model parameterization process. Figure 6 shows adopted vehicle wheel numbering.

The driver model executes a set function of the steering angle of steered wheels as an input affecting the vehicle model. A PID (Proportional- Integral- Derivative) regulator was used for that purpose.

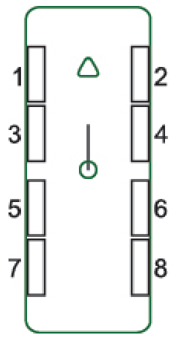

Fig. 6. Wheel numbering

4. Validation process

4.1. Initial calculations and their results

The validation process is an action performed in order to evaluate in what degree a developed calculation software and applied models have properties in accordance with a tested vehicle in the aspect of a course of sudden braking process with damaged tires. A described process leads to obtaining simulation results that successfully reflect behaviour of a tested vehicle including the results of tire damage. Three stages of the validation process were carried out. The first stage includes initial calculations where the process of vehicle braking with good tires was analysed. The second stage includes braking with one damaged tire and in the third stage analysed was the braking with two damaged tires. Corrections of values of some model parameters were made at the next stage in order to decrease the difference between the model response and the object. The tuning of model parameter values was limited to its uncertainty ranges.

The initial calculations analysed the process of braking from the initial speed of 80 km/h. Figure 7 shows time history of three components of the vector of acceleration of the vehicle's CG in the local system {C}. The effect of the body pitch during braking, resulting in tire and suspension deflection, confirm the values of the vertical body acceleration, presented in figure 7. Typical longitudinal vehicle body vibrations are visible at the moment of stopping the vehicle.

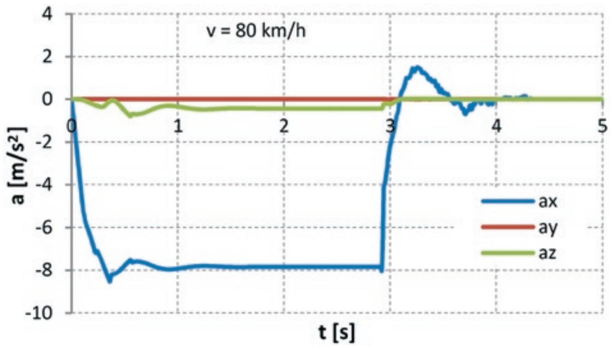

Fig. 7. Time history of three components of vehicle's CG acceleration

a)

b)

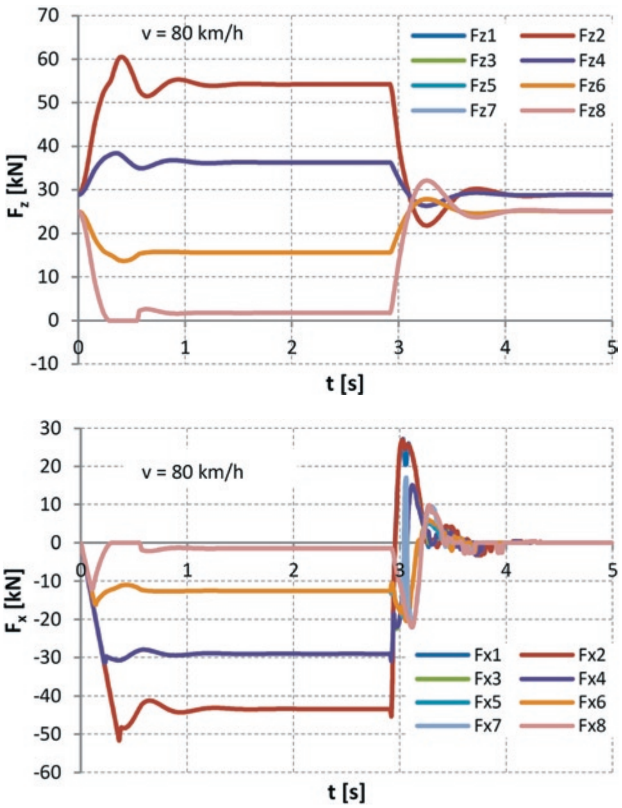

Fig. 8. Time histories of vertical reaction of the road on the tires $F_{Zi}(t)$ (a) and longitudinal tire forces F_{Xi} (b); wheel numbering according to Figure 6

Figure 8 shows a time history of the tire vertical $F_{Zi}(t)$ and longitudinal forces $F_{Xi}(t)$. Because of the symmetry of longitudinal forces on the right side and left side wheels of the vehicle (roadworthy vehicle), time histories of vertical forces of both wheels of each axle are the same, i.e. they overlap. When braking, a significant body pitch occurs and as a result the wheels 7 and 8 lost the contact with the road. Due to that tilt, braking forces of further wheels are more and more lower. The loss of contact between the wheels and the road, shown in fig. 8, results in decrease of the value F_X (fig. 8b) to zero on the wheels 7 and 8.

The results of the roadworthy vehicle braking simulation correctly reflect the properties of the vehicle braking process.

4.2. Model validation on the basis of braking simulation for a vehicle with one damaged tire

The braking tests of a vehicle with damaged tire were carried out in a *fixed control* mode. However, small modifications of the steering wheel angle, which could have been caused by the driver unwillingly at asymmetrical braking, were found in recorded time histories. It was used as a kinematic input in the simulation process, while the measured history of braking deceleration made a basis for braking force generation in the model.

In figures from 9 to 11, a dotted line shows the measurement results obtained during braking from v = 62 km/h of the vehicle with a damaged tire no. 2. Accelerations were digitally filtrated by the CFC 100 filter. It is a low-pass Butterworth's filter made according to the SAE J211 standard. The analysed figures also show the results of simulations, marked with a bold continuous line. Bold lines in fig. 9 can be treated as an input affecting the vehicle model.

It was stated that the model properly reacts to the tire damage. Observed differences (vehicle – model) of the pitch angle values θ(t) can result from the variability of wheel suspension characteristics (hydropneumatic suspension) and presence of dry friction. Obtained results of simulation calculations properly reflect the measurements that were obtained during the vehicle tests. Results of transverse displacement of the vehicle's CG during braking (y(t) in fig. 11) are the significant factor of the quality evaluation for assumed tire model. After driving for over 40 m on the road and in the presence of various wheel steer angles, the difference between the values of transverse displacement of the model and the vehicle is lower than 0.2 m.

4.3. Model validation on the basis of braking of the vehicle with two damaged wheels (wheels no. 2 and 4)

At this stage of calculations the measurement results obtained during vehicle braking with two damaged tires were used. They are compared with respective model calculation results in figures 12–14.

During braking test from 61 km/h a modification of the steering wheel angle by over 18° was observed, which is related to the previously described reasons. So the responses of the vehicle model to the same input (presented in fig. 12) are compared in figures 13 and 14 with responses of the real object.

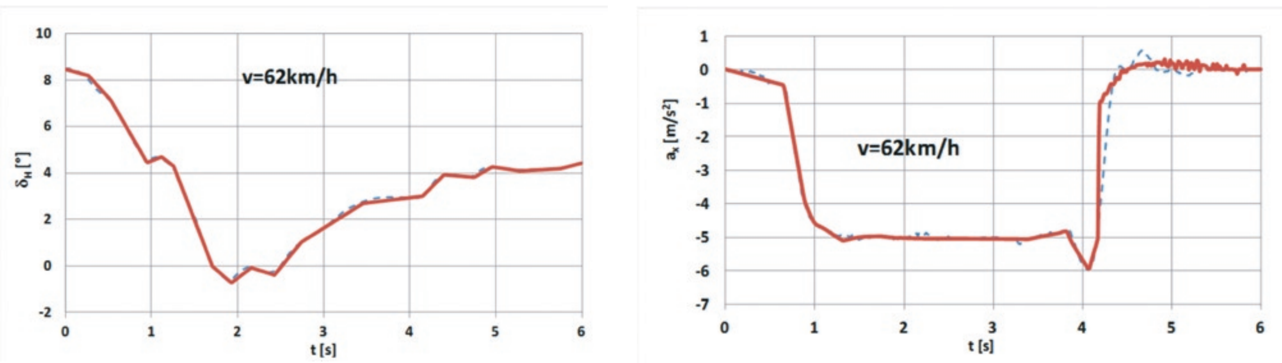

Fig. 9. Steering wheel rotation angle $\delta_H=f(t)$ and longitudinal acceleration $a_X(t)$; dotted line – vehicle, bold line – model

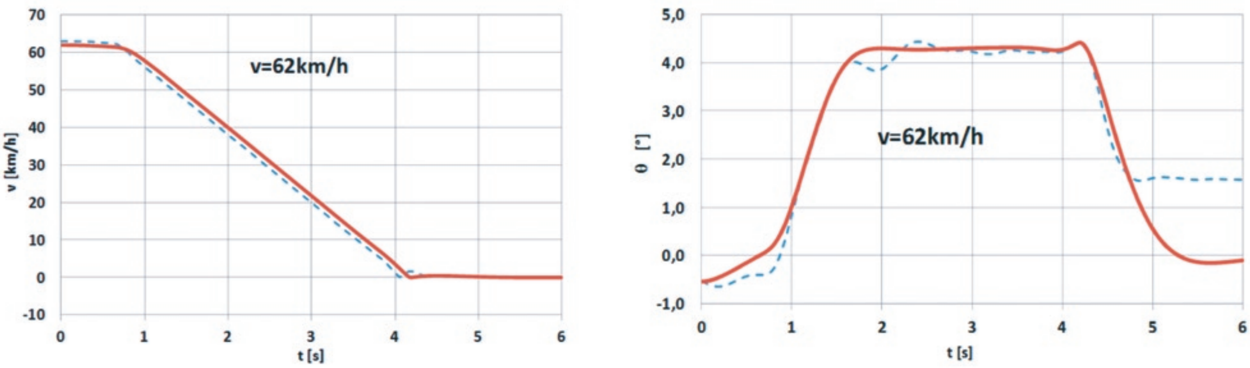

Fig. 10. Velocity of the vehicle's CG v(t) and the body pitch angle θ(t); line description as under figure 9

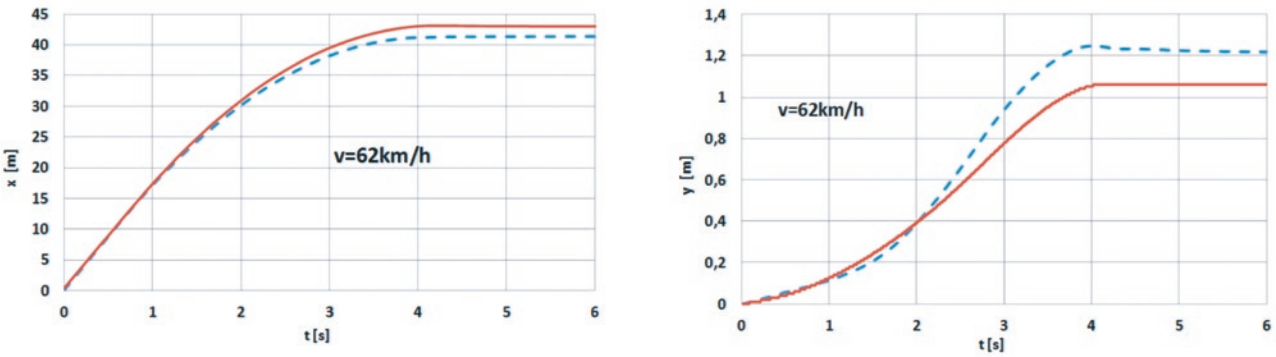

Fig. 11. Longitudinal x(t) and lateral y(t) displacement of the CG (braking path); line description as under fig. 9

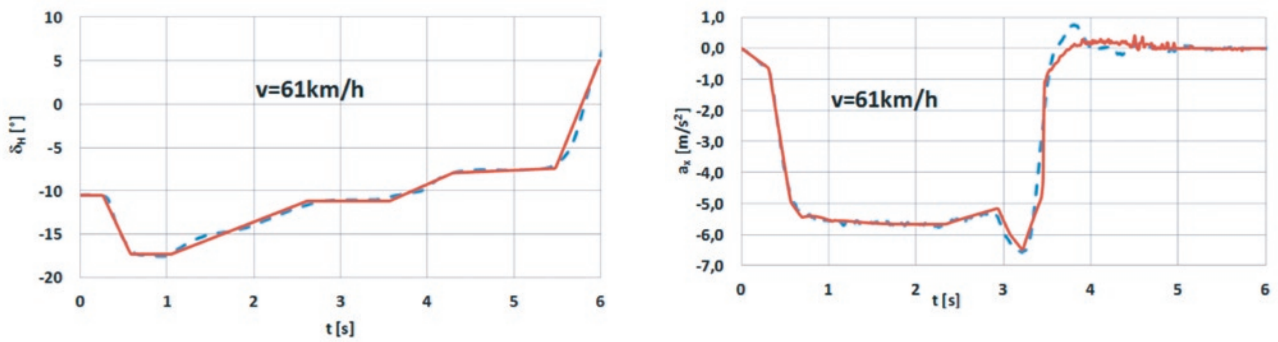

Fig. 12. Steering wheel angle $\delta_H(t)$ and longitudinal acceleration $a_X(t)$; dotted line – vehicle, bold line – model

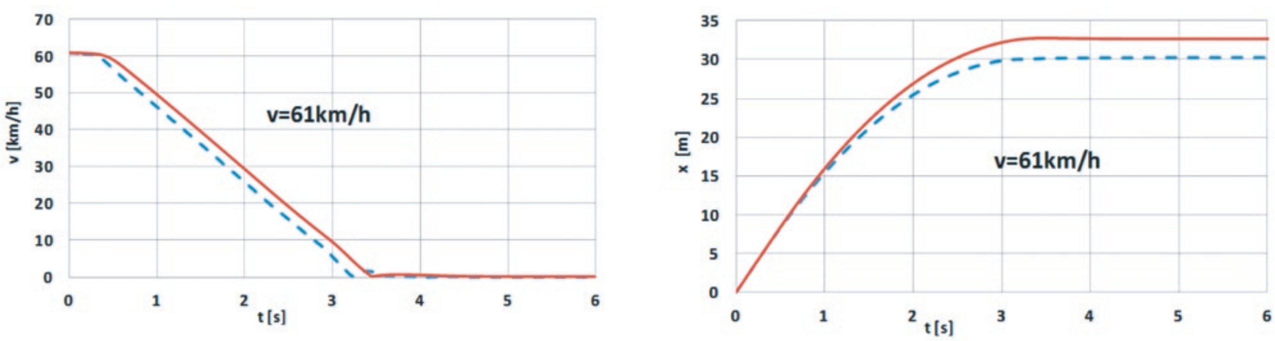

Fig. 13. Velocity of the vehicle's CG v(t) and longitudinal displacement x(t); line description as under fig. 12

Previously described effects (unintended driver's reactions) and effects caused by damaged tires result in low values of yaw rate (below 0.05 rad/s, compare fig. 14) and lateral acceleration, which does not exceed 0.6 m/s^2. Obviously at such low lateral interactions, the presence of freeplay and friction in the steering system and suspension have a significant influence on the vehicle trajectory. Despite the model does not include these factors, its reaction to the defined inputs is very similar to the real behaviour of the vehicle with dam-

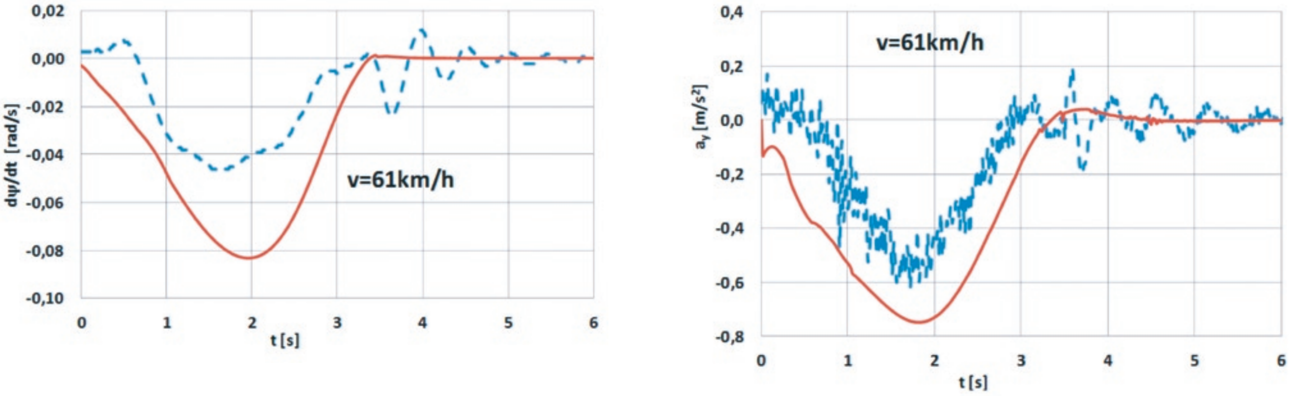

Fig. 14. Yaw rate of the vehicle $\dot{\psi}(t)$ and lateral acceleration;line description as under fig. 12

aged tires. In both simulations (p. 4.2 and 4.3) a low deviation of the vehicle trajectory from the rectilinear track was found, which results not only from the presence of damaged tires but also from the action of the driver who made a correcting turn of the steering wheel. Values of lateral displacement of the vehicle's CG notably depend on a time history of the steering wheel angle.

In the applied results of both braking tests, the time history of that angle was definitely different. Due to a fast tire destroying and wear process, the braking tests with damaged tires were not repeated (high tire cost).

Validation calculations confirm a proper model reaction to tire damage and vehicle braking. So it can be assumed that the model properly reflects the vehicle properties in the area significant for the purpose of this paper.

5. Essential calculations

5.1. Preparation of calculations

16 braking tests were prepared for the execution of the calculation goal, where the location of the wheels with damaged tires was changed. Braking in the first seven tests was started from the speed of 40 km/h, and in the following seven ones it was started from 80 km/h. In the next two test calculations (T0/40 and T0/80) a simulation of the model braking with roadworthy tires was carried out. Arrangement of wheels with damaged tires is shown in figure 15.

Selection of speed values for test calculations was based on the following reasons:

– at v ≅ 60 km/h braking process disruptions are small (compare the vehicle test results in p. 4.2 and 4.3);
– maximum speed with damaged tires should not exceed 80km/h.

Considering the initial calculation results and the above reasons, the following plan of the test calculation execution has been prepared:

1. The initial drive at constant speed of 40 or 80 km/h for 0.5 s. Tires are fully operational at that stage of the test. The driving torque on the wheels balances the motion resistance.

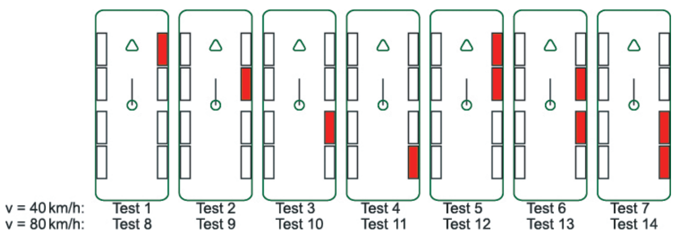

Fig. 15. Arrangement of wheels with damaged tires (darken wheels) and designation of individual tests

2. There is a sudden damage of tire(s) in 0.5 s and for a short period of time surprised driver is preparing a reaction, and at the same time the model motion parameters are stabilized, and rolling resistance of a damaged wheel(s) increases from f_j=0.01 to 0.05. On the basis of [6, 9] it was assumed that the length of time when a driver works out a reaction to analysed incident related to tire damage amounts to 1.5 s.
3. After t = 0.5 + 1.5 = 2.0 s the driver models begins sudden braking that would last until the vehicle is stopped. Deceleration increases linearly for t_n = 0.4 s, until reaching a value of a_x=5–6 m/s². All wheels were not blocked in order to avoid vehicle drifting but trends resulting from the operation of damaged wheels appeared.
4. The example of the time history of braking is shown in figure 16.

All calculation tests were conducted out at fixed steering wheel (*fixed control*). It made the result analysis easier in the aspect of the influence of damaged tires on the motion trajectory.

5.2. Results of calculations for braking with one damaged wheel no. 2 or 4, 6, 8

Figures 16 and 17 show time histories of the CG acceleration and vehicle body pitch angle during rectilinear braking from the speed of 40 km/h and 80 km/h with all roadworthy tires (T0/40 and T0/80).

Time histories in these figures are in accordance with a generally known histories of braking process of a roadworthy vehicle. While the majority of values analysed further on has zero values (side slip angle, yaw angle , yaw rate) and therefore they are not shown in figures 16 – 17.

Results of simulations of the braking process of the vehicle with one damaged tire is shown in table 1. In the consecutive tests T1-T4 and T8-T11 practically the same time history of longitudinal acceleration $a_X = a_H = f(t)$ was obtained as during braking of the model with roadwothy tires (fig. 16). Therefore these figures are not included in Table 1.

Due to a presence of a damaged tire (compare calculation plan, t > 0.5s) the CG trajectory deflection from the rectilinear one occurs already when driving without breaking. Table 1 shows the increase of side slip angle α_{CG} and body yaw angle ψ at constant yaw rate 0.1–0.2 °/s in time t = 0.5–2.0 s. After the beginning of breaking, the process of body yawing and related change of the motion trajectory (deflection to the right side, towards the position of a damaged tire) becomes intensified.

During braking from the speed of 40 km/h observed motion trajectory deflection from the straight track (transverse displacement $y(t)$ and yaw angle $\psi(t)$) are low (compare table 1 and 3). A driver can correct the track of motion without any problem, irrespectively of a location of a damaged wheel. The situation is different when braking

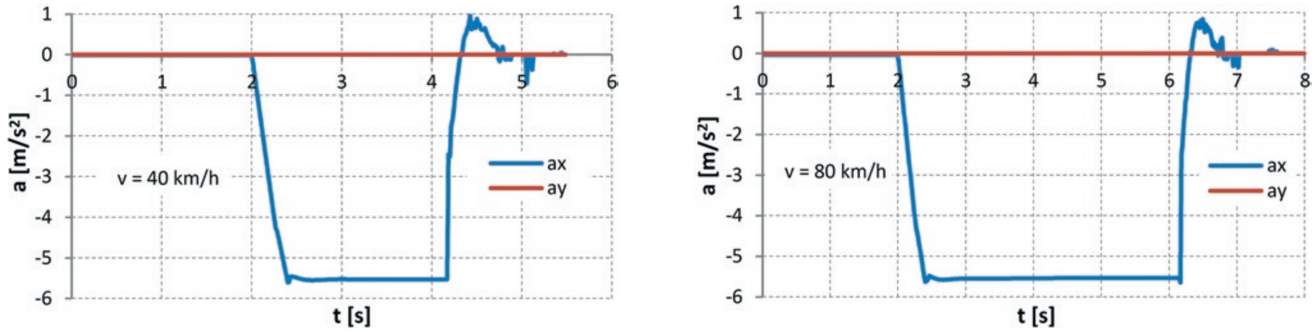

Fig. 16. Components of CG acceleration $a_X(t)$ and $a_Y(t)$ in the local system {C}: a) v = 40 km/h, b) v = 80 km/h

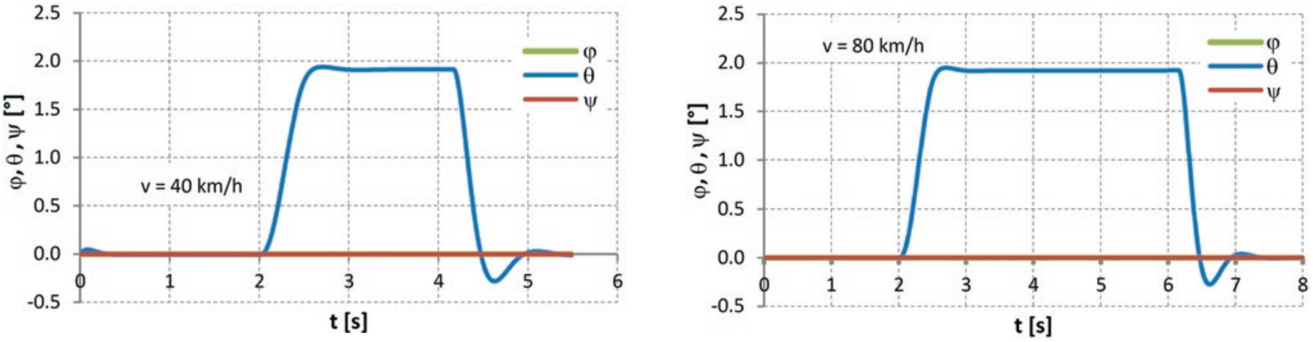

Fig. 17. Roll φ, pitch θ and yaw ψ; a) v = 40 km/h, b) v = 80 km/h

from the speed of 80 km/h. Values of deflection from the straight line of motion in fact depend on the location of a damaged wheel and resultant wheel load. The lowest deflection occurs in case of damaged wheel no. 6, and the highest in case of a damaged wheel no. 8. Then $\psi(t)$ it reaches 17.6° at the end of braking T11, and the extreme value of the yaw rate amounts to about 10°/s (Table 4). These are significant values and clearly visible. Presence of one underinflated tire has a small influence on the braking distance compared to the roadworthy vehicle braking (table 3 and 4).

5.3. Results of braking calculations for two damaged wheels no. 2-4, 4-6, 6-8

Table 2 shows results of simulation calculations of the braking process of the model with two damaged wheels located in three different places at the right side of the vehicle. The values, previously presented in table 1, were compared.

A time history of longitudinal acceleration $a_X(t)$ was added, because during braking from v = 80 km/h significantly differs from the one presented in figure 16b. These differences result from high values of the vehicle yaw angle and tire lateral slip drifting that caused transverse position of the vehicle (compare fig. 18) and thereby reduction of its longitudinal displacement.

Tables 3 and 4 compare the values of longitudinal displacement $x(t)$ of the vehicle's CG in individual tests, from the moment of stepping on the brake pedal until stopping the vehicle. The specification also includes results of calculations for the roadworthy vehicle. Presence of damaged tires has a small influence on the braking distance at the speed of 40 km/h. While the influence of two damaged tires on a braking time history at the speed of 80 km/h is high and results in a significant vehicle yaw from a rectilinear motion track. Reduction of longitudinal displacement $x(t)$ in the tests no. T12-T14 compared to T8-T11 results from drifting of the rear part of the vehicle at the final stage of motion and thereby the use of the lateral components of the tire reaction which was higher than the longitudinal components in that situation.

Values of the vehicle yaw angle during braking at v = 40 km/h are low, while at braking from v = 80 km/h (the vehicle with two damaged wheels) the vehicle rotates and drifts. So taking into account that braking variant, the most dangerous location of damaged wheels is respectively: 6 and 8 (test 14), 4 and 6 (test 13) as well as 2 and 4 (test 12).

Yaw rates in the braking tests from the speed of 40 km/h (T5 to T7) do not exceed 0.02 rad/s, while at the speed of 80 km/h (T11, 12 and 13) they are significant and almost 70 times higher than at the speed of 40 km/h. Yaw rate increase results in high lateral acceleration values. During braking at the speed of 40 km/h they do not exceed 0.13 m/s^2, while at the speed of 80 km/h lateral acceleration exceeds 7 m/s^2 (table 4), i.e. it reaches the values that often result in the vehicle rollover. It results from decrease in wheel loads of the axle 3 and 4 during braking and therefore also from the reduced potential of high lateral reactions on these axes. Moreover, a potential of lateral reactions decreases when damaged tires appear (compare fig. 4).

In the braking tests at the speed of v = 80 km/h with two damaged wheels, i.e. T12–14 there is a temporary loss of contact between the wheels 6 and 8 and the road during drifting of the rear part of the vehicle as indicated calculations of wheel vertical forces.

6. Summary and conclusions

Built models, performed process of their validation and obtained results of simulations, allowed for identification of the influence of damaged tires and their location in a vehicle on the safety of the sudden braking process of a special purpose vehicle with *run flat* tires. Calculations for 16 braking tests were carried out, changing the location of the wheels with damaged tires. The analysis of calculation results in the aspect of evaluation of a driver's reaction abilities allows for making the following statements:

- tire damage affects the movement of a special purpose vehicle;
- after damage of one tire a vehicle still has an ability to brake effectively and its trajectory can be corrected by a driver;
- damage of one wheel practically does not affect the braking distance;

Table 1. The results of braking calculations for a vehicle with one damaged wheel from the speed of 40 km/h (tests T1- T4) and from the speed of 80km/h (tests T8-T11): dψ/dt – yaw rate, ψ – yaw angle, α_{CG} – side slip angle of the CG

Tests T1–T4; v = 40 km/h	Tests T8–T11; v = 80 km/h
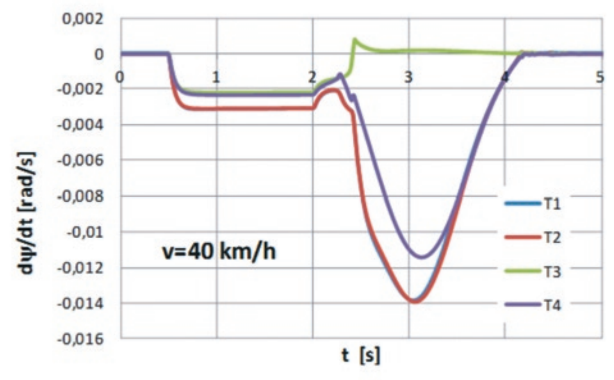	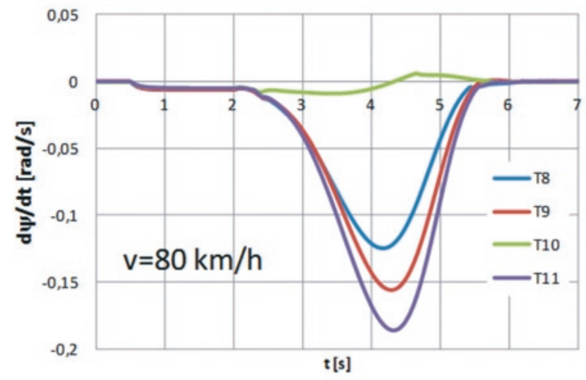
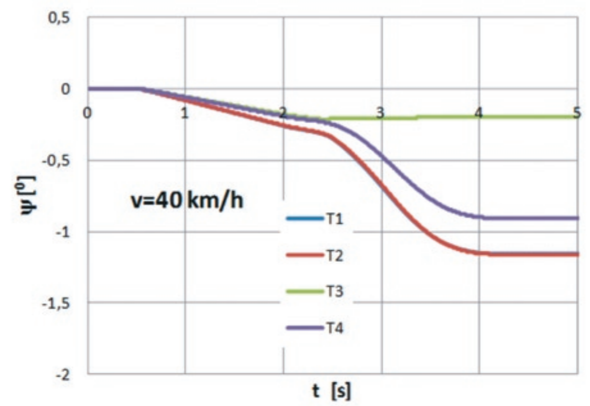	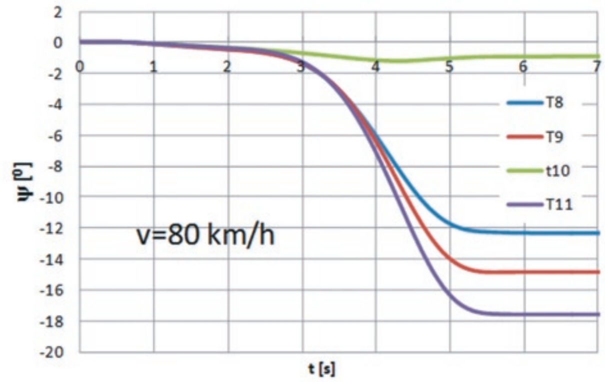
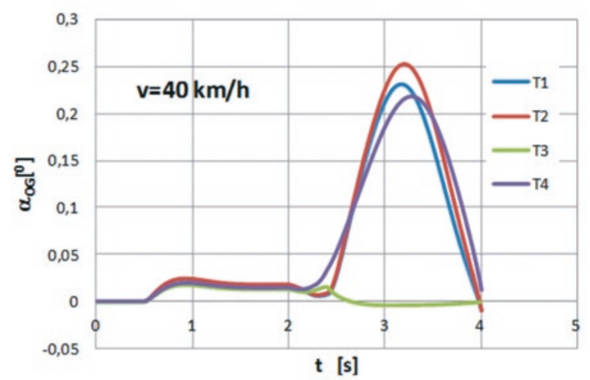	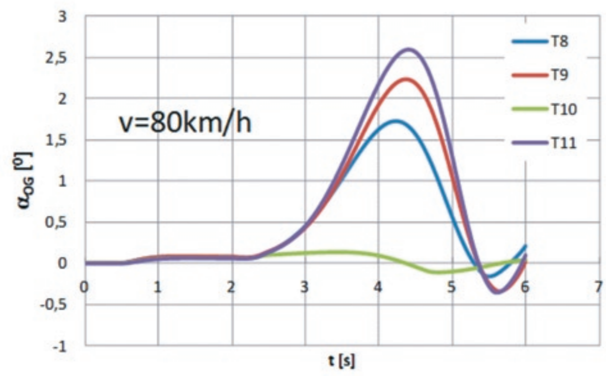

- braking with one damaged wheel from the speed of 40 km/h does not create a serious danger, but this danger gets higher as the initial braking speed increases and the vehicle yaw from a set track of motion towards a damaged tire increases;
- during braking with one damaged wheel, the strongest influence on the vehicle motion occurs in the tests T8 and T9, that is when wheels 2 or 4 are damaged (steered wheels on the right side of the vehicle);
- damage of two wheels significantly affects the vehicle braking process; observed reduction of the braking distance at high driving speed (tests T12 – T14) is related with dangerous drifting of the rear part of the vehicle;
- a significant factor of the movement safety threat includes a vehicle yaw from the set track of motion; this yaw angle does not exceed 2° (test T5) with two damaged wheels and low driving speed, but it increases rapidly as the initial braking speed increases and at v = 80 km/h the yaw angle exceeds 90° (test T13 and T14), and yaw rate amounts to 100°/s;
- when braking with two damaged wheels and v = 80 km/h there are high lateral acceleration values 5.0–7.7 m/s^2; these are values that can result in vehicle rollover.

When braking from the speed of 40 km/h, a properly trained driver can correct the motion trajectory, irrespective of the location of a damaged wheel. Extreme yaw rate values at v = 40 km/h occur in 1.1–1.2 s from the beginning of braking with one and two damaged wheels.

The tests indicate [3, 5] that a driver can identify and feel horizontal accelerations exceeding 0.02 m/s^2 and yaw rate of over 0.001 rad/s. So already when a vehicle with one damaged wheel brakes from v = 40 km/h, the physical interactions on a driver (compare table 3) amounts to the values that can "signal" him undergoing changes of the

Table 2. The results of braking calculations for a vehicle with two damaged wheels from the speed of 40 km/h (tests T5- T7) and from the speed of 80km/h (tests T12-T14): a_x – longitudinal acceleration, $d\psi/dt$ – yaw rate, ψ – yaw angle, α_{CG} – side slip angle of the CG

<table>
<tr><th>Tests T5–T7; v = 40 km/h</th><th>Tests T12–T14; v = 80 km/h</th></tr>
<tr><td>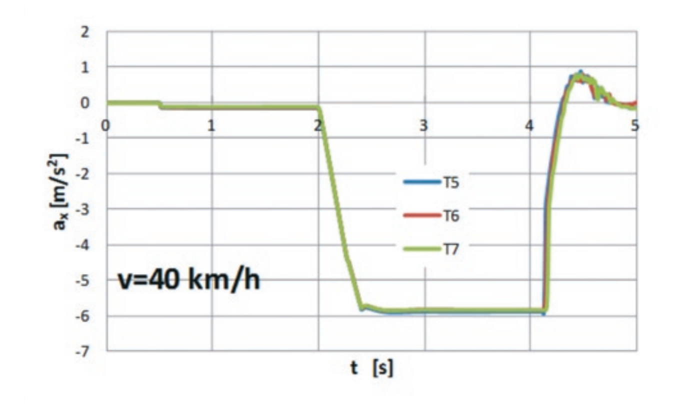
</td><td>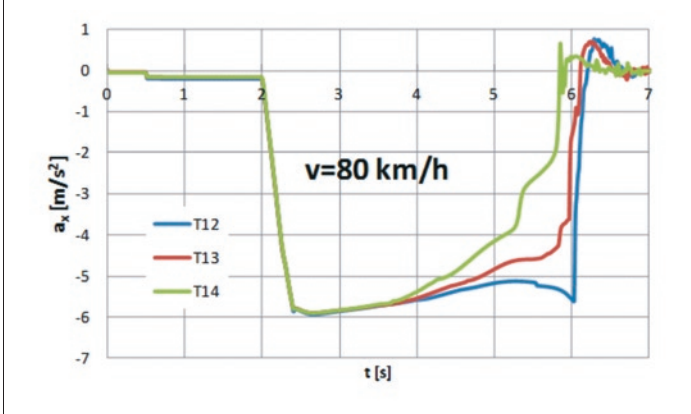
</td></tr>
<tr><td>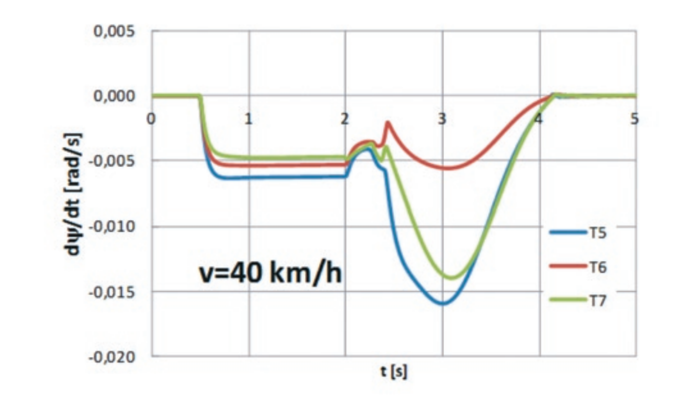
</td><td>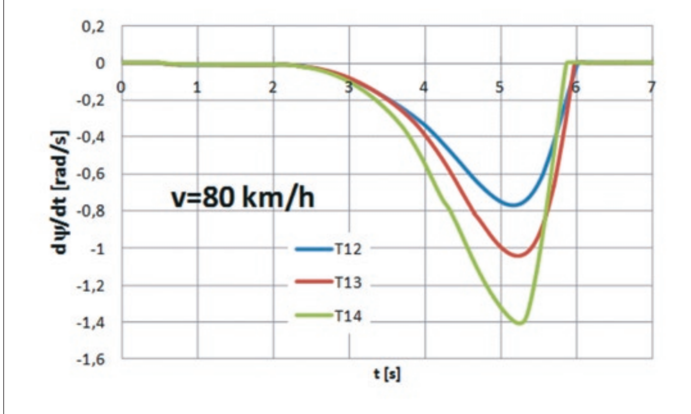
</td></tr>
<tr><td>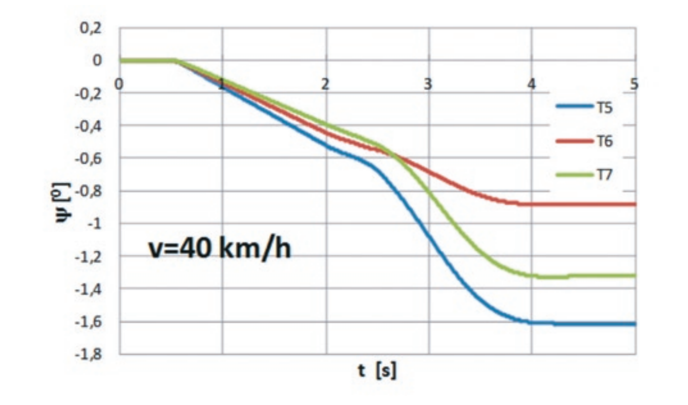
</td><td>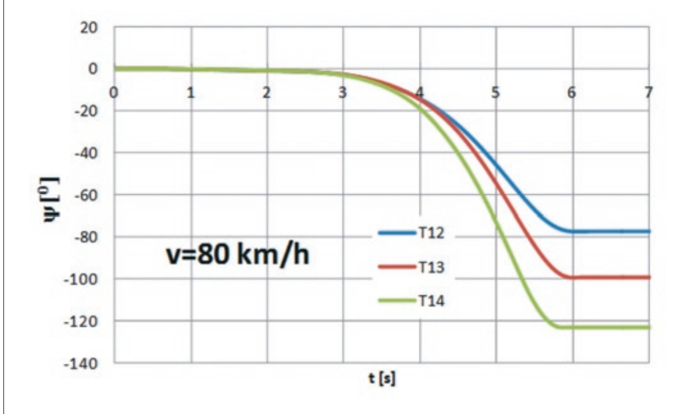
</td></tr>
<tr><td>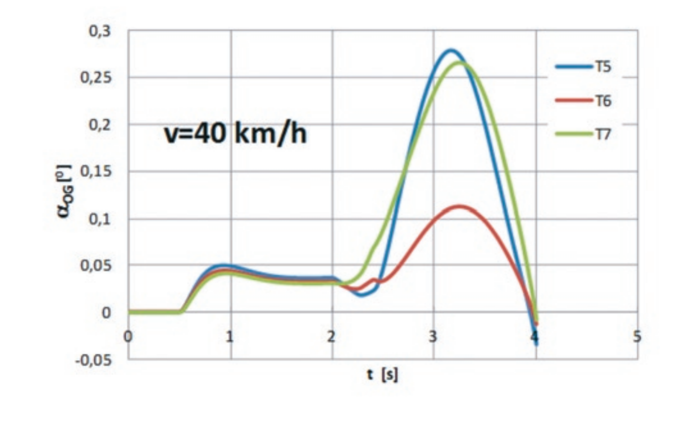
</td><td>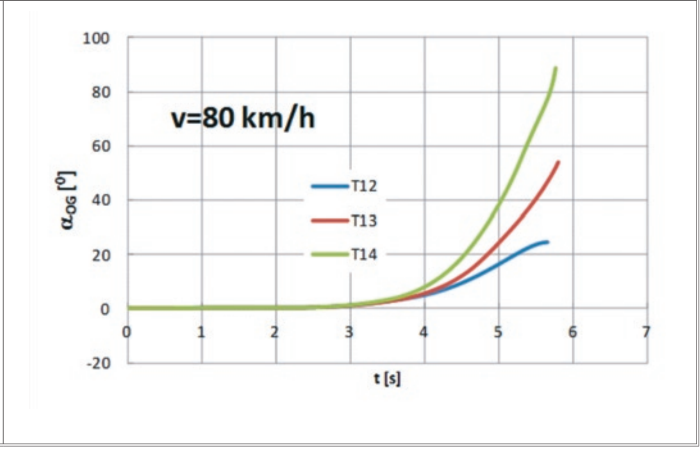
</td></tr>
</table>

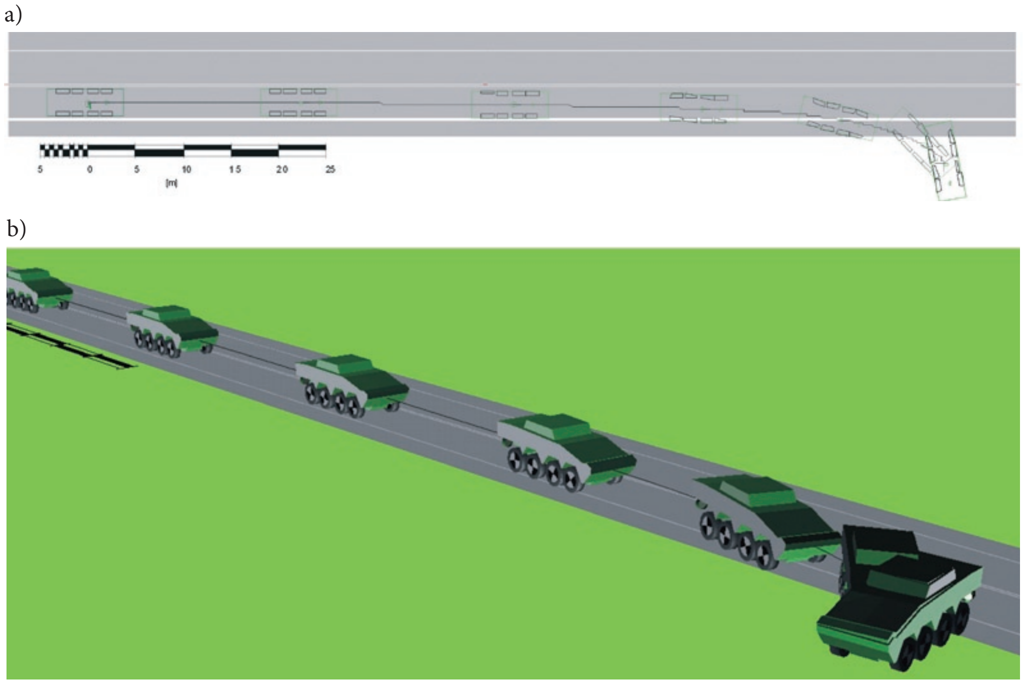

Fig. 18. Road lane and consecutive vehicle positions at 1.0 s time interval, test T12; a) plan view, b) spatial view

Table 3. Extreme values (WE) and final values (WK) of the vehicle body motion parameters depending on a location of damaged tires; braking from v = 40km/h

Specification	T0/40	T1	T2	T3	T4	T5	T6	T7
Longitudinal displacement of the vehicle's CG, [m]	12.85	12.71	12.71	12.85	12.87	12.45	12.58	12.68
Transverse acceleration, WE; [m/s^2]	0	0.06	0.06	0.01	0.10	0.10	0.04	0.13
Yaw rate, WE; [rad/s]	0	–0.014	–0.014	–0.002	–0.01	–0.02	–0.005	–0.01
Yaw, WK; [°]	0	–1.16	–1.16	–0.21	–0.91	–1.62	–0.88	–1.32
Side slip, WE; [°]	0	0.02	0.03	0.01	0.22	0.28	0.11	0.27
Lateral displacement, WK ; [m]	0	–0.10	–0.09	–0.05	–0.07	–0.16	–0.12	–0.13

Table 4. Extreme values (WE) and final values (WK) of the vehicle body motion parameters depending on a location of damaged tires; braking from v = 80km/h

Specification	T0/80	T8	T9	T10	T11	T12	T13	T14
Longitudinal displacement of the vehicles' CG. [m]	47.58	47.43	47.34	47.49	47.61	45.63	45.50	44.95
Transverse acceleration, WE; [m/s^2]	0	1.8	2.0	0.3	2.4	5.2	6.3	7.7
Yaw rate, WE; [rad/s]	0	–0.12	–0.15	–0.01	–0.18	–0.77	–1.04	–1.41
Yaw, WK; [°]	0	–12.3	–14.9	–1.23	–17.6	–77.6	–98.9	–123.3
Side slip, WE; [°]	0	1.71	2.24	0.13	2.54	24.2	53.7	88.9
Lateral displacement, WK ; [m]	0	–2.71	–2.96	–0.62	–3.33	–6.15	–5.99	–6.32

motion trajectory. It is important as in critical situations a driver reacts not only to observed motion track deflection from a set track but also to perceived physical signals.

The situation is different in case of braking at the speed of 80 km/h with two damaged tires. Then the vehicle yaw rate amounts to 100°/s, and lateral acceleration even to 7 m/s^2. At the speed of v = 80 km/h the extreme values of yaw rate occur in 2.2–2.3 s from the beginning of braking with one damaged tire and in 3.2–3.3 s in a vehicle with two damaged wheels. The wheels on one side of the vehicle detach from the road. So the critical situation in the vehicle behaviour occurs.

The results of the tests and analyses indicate that driver's operation after sudden tire damage is of crucial significance to the vehicle motion safety [1, 17]. Practical driver training within that scope is expensive and dangerous. Therefore there is a need to obtain knowledge on the basis of reliable models of simulation of vehicle motion during braking. The results of this article can be also used in the process of programming of driving simulators for training the special purpose vehicle drivers. A key role of tire inserts, that allowed for a limited time vehicle motion in analysed situations, deserves a separate emphasis.

A part of this paper was prepared according to the Project OR 00008312, financed by the Ministry of Science and Higher Education.

References:

1. Blythe W., Day T. D., Grimes W. D., 3-Dimentional Simulation of Vehicle Response to Tire Blow-outs, SAE Technical Paper 980221; Warrendale PA 1998.
2. Ejsmont J., Jackowski J., Luty W., Motrycz G., Stryjek P., Świeczko-Żurek B., Analysis of rolling resistance of tires with Run Flat insert, Key Engineering Materials 2014; 597: 165-170.
3. Fard M., A., Ishihara T., Inooka H., Dynamics of the head-neck complex in response to the trunk horizontal vibration: modeling and identification, Journal of Biomechanical Engineering 2003; 125(4): 533-539.
4. Grover C., Lambourn R. F., Smith T. L., Walter L., Braking and manoeuvring characteristics of oncorrectly inflated low-profile and run-flat tyres, [in:] Proceedings of the 16th Annual Congress of the European Association for Accident Research and Analysis (EVU), Institute of Forensic Research Publishers, Kraków 2007; 181-213.
5. Jex H., R., Roll Tracking Effects of G-vector Tilt and Various Types of Motion Washout , Proceedings of 14 Annual Conference on Manual Control, University of Southern California 1978.
6. Jurecki R., S., Stańczyk T., L., Jaśkiewicz M., J., Driver's reaction time in a simulated, complex road incident, Transport, 2014 http://dx.doi.org/10.3846 /16484142.2014.913535.
7. Lozia Z., Simulation Tests of Biaxial Vehicle Motion after a Tire Blow-out, SAE Technical Paper 2005-01-0410; Warrendale PA 2005.
8. Lozia Z., Guzek M., Pieniążek W., Zdanowicz P., Methodology and examples of results of simulation tests on a motion of a multi-axial special vehicle in explosive tire damage conditions, Zeszyty Naukowe Instytutu Pojazdów – Proceedings of the Institute of Vehicles 2012; 4(90): 19-42.
9. Olson P. L., Forensic aspects of driver perception and response, Lawyers & Judge Publishing Co, Tuscon 1996.
10. Parczewski K., Effect of tyre inflation pressure on the vehicle dynamics during braking manouvre. Eksploatacja i Niezawodnosc – Maintenance and Reliability 2013; 15(2): 134-139.
11. PC-Crash, A simulation program for vehicle accidents. Operating and technical manual, Version 10.0, Dr. Steffan Datentechnik, Linz, Austria 2010.
12. Collective paper, Experimental and simulation tests on multi-axial vehicle dynamics in tire damage conditions, Publishing of the Cracow University of Technology, Cracow 2012.
13. Prochowski L., Motor Vehicles. Mechanics of Movement, WKŁ, 2nd Edition, Warsaw 2009.
14. Rill G., Simulation von Kraftfahrzeugen, Vieweg & Sohn Verlag GmbH, Braunschweig/Wiesbaden 1994.
15. Robinette R., Deering D., Fay R. J., Drag and Steering Effects of Under Inflated and Deflated Tires, SAE Technical Paper 970954; Warrendale PA 1997.
16. Wach W. Simulation of vehicle accidents using PC-Crash, Institute of Forensic Research Publishers, Cracow 2011.
17. Zębala J., Wach W., Ciępka P., Janczur R., Bypassing manoeuvre driving a car with reduced and no tire pressure, [in:] Proceedings of the 22th Annual Congress of the European Association for Accident Research and Analysis (EVU), Published by EVU, Firenze 2013, 145–155.

Leon PROCHOWSKI
Faculty of Mechanical Engineering
Military University of Technology
ul. Gen. Sylwestra Kaliskiego 2, 00-908 Warsaw, Poland

Wojciech WACH
Institute of Forensic Research
ul. Westerplatte 9, 31-033 Cracow, Poland

Jerzy JACKOWSKI
Faculty of Mechanical Engineering
Military University of Technology
ul. Gen. Sylwestra Kaliskiego 2, 00-908 Warsaw, Poland

Wiesław PIENIĄŻEK
Faculty of Mechanical Engineering
Cracow University of Technology
al. Jana Pawła II 37, 31-864 Cracow, Poland

E-mails: lprochowski@wat.edu.pl, wwach@ies.krakow.pl,
jjackowski@wat.edu.pl, wupe44@gmail.com

Article citation info:
KURANC A. Exhaust emission test performance with the use of the signal from air flow meter. Eksploatacja i Niezawodnosc – Maintenance and Reliability 2015; 17 (1): 129–134.

Andrzej KURANC

EXHAUST EMISSION TEST PERFORMANCE WITH THE USE OF THE SIGNAL FROM AIR FLOW METER

EKSPLOATACYJNE BADANIA EMISJI SPALIN Z WYKORZYSTANIEM SYGNAŁU Z PRZEPŁYWOMIERZA POWIETRZA*

The paper presents selected technical solutions in the area of exhaust emissions research conducted in real operational conditions of a vehicle. The author describes his own road emissions research methodology with the use of information about the air flow supplying an engine (OBD II) and the measured volumetric shares of particular fumes components (exhaust gas analyser). Test results confirm the possibility of applying this measurement method, and their analysis shows the inadequacy of the type-approval tests compared to the real operation of the vehicle.

Keywords: *exhaust emission test, mobile systems, emissions of CO_2, driving tests.*

W pracy omawiane są wybrane rozwiązania techniczne w zakresie badań emisji spalin w warunkach rzeczywistej eksploatacji pojazdu. Autor opisuje własną metodykę drogowych badań emisji spalin z wykorzystaniem informacji o wydatku powietrza zasilającego silnik (OBD II) i zmierzonych udziałów objętościowych poszczególnych składników (analizator spalin). Wyniki badań potwierdzają możliwość stosowania opisanej metody pomiarowej, a ich analiza wskazuje ponadto na nieadekwatność testów homologacyjnych w odniesieniu do realnej eksploatacji pojazdu.

Słowa kluczowe: *badania emisji spalin, mobilne systemy pomiarowe, emisja CO_2, testy jezdne.*

1. Introduction

The high pace of the development of motorization, apart from its many advantages, creates ecological organic threats. The literature reports emphasize the significance of the negative impact of motorization on the environment, especially with regard to noise emission, the risk of heavy metals, as well as the ambient air quality which is treated as a priority [5, 22, 23]. In the general European profile ca. 20% of the anthropogenic emission of CO_2 come from transport sources. The adverse effect of internal combustion engines on the environment is determined, among others, by the estimation of harmful pollutants emission levels in relation to the limits set in the applicable legal acts [21]. For example, by 2012 the JRC (Joint Research Centre) had carried out tests in real road traffic conditions for 16 new vehicles from group of LDV (Light Duty Vehicle). The test results confirmed the fulfilment of the Euro 5 and Euro 6 requirements in almost all cases. The exception was the emission of NO_X from vehicles equipped with CI engines, which significantly exceeded the limits [21, 26]. Among others, it is due to the problem of controlling the engine in a vehicle. Indeed, it is difficult to achieve low fuel consumption and high power output with low emissions of NO_X and PM (Particle Matter).

New engines are initially tested at laboratory engine's dynamometer test-stands for exhaust emissions. Then the results are being analysed and then corrective control algorithm changes are introduced. After that further trials and adjustments are conducted, and then the following ones. So far such a procedure was satisfactory but the complexity of modern combustion engines controlling systems makes the optimization of engines more complicated [7, 12]. The examples of such systems with a high reduction potential in the area of NO_X and PM emissions and fuel consumption are engines based on compression ignition of homogeneous mixtures – HCCI (Homogeneous Charge Compression Ignition). They require precise controlling of the variable valve timing, variable compression ratio, and especially, exhaust gas recirculation and direct fuel injection [7]. The interrelationship between the variable parameters makes it difficult to develop a coherent strategy.

The next step after the tests at an engine dynamometer is testing of the vehicle mounted engine at a chassis dynamometer, and finally testing it in real road traffic conditions. The latter tests provide a lot of information about the true impact of the vehicle on the environment the real emissions and fuel consumption. They, in fact, reflect the real conditions of the vehicles use [15–17, 24–26].

Vehicle manufacturers, ensuring compliance with emission standards, base mainly on the official driving cycles. Necessarily, they apply conditions for the measurements which inherently were to provide the base for vehicles evaluation. Unfortunately they differ from the conditions of the vehicles later real operation. That can lead to a distortion of the market image of the product, particularly from the point of view of its user.

An example of a very problematic research are tests of hybrid propulsion systems, whose parameters can be objectively verified only in traffic conditions [15].

The review of the literature on the subject of emissions testing in natural operation of vehicles [1, 12, 15–17] indicates that there are highly specialized measuring instruments, generally referred to PEMS (Portable Emission Measurement System), although they are very expensive. Road tests with the use of PEMS have shown that in the case of certain fumes ingredients their emissions are about a couple of hundred percent greater than the values encountered in the type-approval tests [13, 17].

The presented thesis led the author to conduct exhaust emissions tests under the conditions of vehicle real operation, but with the use of a simplified measuring method and commonly available equipment instead of the type-approval tests. The methodology of the research

(*) Tekst artykułu w polskiej wersji językowej dostępny w elektronicznym wydaniu kwartalnika na stronie ***www.ein.org.pl***

and the preparation of a set of results is quite laborious but it allows to obtain information on emissions or fuel consumption. Additionally, it points out the possibility of constructing simplified systems or separate measuring devices that can be used in comparative studies.

2. Exploitation exhaust emission tests

Exhaust fumes tests with the use of a diagnostic gas analyser have been for years the basic type of emission tests which are done during the periodic technical inspection of a vehicle at a vehicle inspection station or at a workshop installing gas supplying systems (LPG or CNG). The so called four-compounds gas analysers are used for the measurements. They enable the user to determine the content of the exhaust gases: carbon monoxide (CO), carbon dioxide CO_2, oxygen O_2, hydrocarbons HC (sometimes an additional option is the measurement of nitric oxides NO_X) [10]. The devices of this type are also used in scientific research, examples of which are described in the literature [8, 9, 18, 19].

The homologation approval tests are much more complicated. They are conducted in laboratory chassis dynamometers and are based on special driving cycles, forming the basis for vehicles comparisons, as well as their assessment in relation to the adopted emission limits [1, 3, 13, 20]. In this case, the measuring apparatus is more complicated. Dilution tunnels are used for the exhaust gas sampling system maintaining a constant volume of samples – CVS (Constant Volume Sample), and heated measuring lines are applied to prevent the formation of condensate, while the detectors of gaseous components are adapted to their physical-chemical properties [1, 20].

The tests carried out in conditions of road traffic are the most desirable when we analyse the research for the information about the real fumes emission to the environment.

The author's own studies carried out during road trips, as well as presented in the literature [4, 11, 28] have shown that the registration of selected engine operating parameters via interface DLC (Data Link Connector) can be very useful for the evaluation of an engine operating conditions, and, in the case described by the author, also to calculate the quantity of emitted fumes and their harmful ingredients.

3. Research methodology

Due to the fact that the gas analyser measures the volumetric shares of selected exhaust components without the possibility of determining their rates of flow, there is a need to complete the system under construction with an element enabling the definition of the flow. Accordingly, DLC can be used to register the airflow passing through the intake manifold.

To determine the mass flow of a particular exhaust component, one must specify the volumetric shares of the major exhaust components, designate the relationship between volumetric and mass shares of the components, and make an assumption that the mass of the fumes is the sum of the mass of air and the mass of combusted fuel. In fact, the mass of the fumes is reduced by the mass of the (possible) condensate.

The information on volumetric shares of some components has been obtained as a result of the gas analyser measurement. However, the shares of N_2, H_2O and Ar were needed, too. To obtain that purpose the combustion reaction was examined (1).

$$C_\beta H_\alpha O_\varepsilon + \lambda \cdot \left[\left(\beta + \frac{\alpha}{4}\right) - \frac{\varepsilon}{2}\right] \cdot O_2 + \lambda \cdot \left[\left(\beta + \frac{\alpha}{4}\right) - \frac{\varepsilon}{2}\right] \cdot \frac{78}{21} N_2 + \lambda \cdot \left[\left(\beta + \frac{\alpha}{4}\right) - \frac{\varepsilon}{2}\right] \cdot \frac{1}{21} Ar \rightarrow$$
$$\rightarrow \beta \cdot CO_2 + \frac{\alpha}{2} H_2O + \lambda \cdot \left[\left(\beta + \frac{\alpha}{4}\right) - \frac{\varepsilon}{2}\right] \cdot \frac{78}{21} N_2 + \lambda \cdot \left[\left(\beta + \frac{\alpha}{4}\right) - \frac{\varepsilon}{2}\right] \cdot \frac{1}{21} Ar + (\lambda - 1) \cdot \left[\left(\beta + \frac{\alpha}{4}\right) - \frac{\varepsilon}{2}\right] \cdot O_2 \quad (1)$$

where:

$C_\beta H_\alpha O_\varepsilon$ – fuel,

β, α, ε – molar ratio of carbon, hydrogen, oxygen to carbon in the hypothetical fuel molecule $C_\beta H_\alpha O_\varepsilon$,

λ – air excess coefficient,

O_2, N_2, Ar – selected air components,

CO_2, H_2O, O_2, N_2, Ar – selected exhaust components.

Literature data differ in indicating molecular composition of gasoline [7, 10, 20]. The substitute formula $C_1H_{1,89}O_{0,016}$ has been finally accepted for the calculations [20]. It has been initially assumed that the spark-ignition engine combustion is stoichiometric (λ = 1), overall and total. Basing on the calculated coefficients at the combustion process products (2) their volumetric shares were determined.

$$C_1H_{1,89}O_{0,016} + 1,4645 \cdot O_2 + 5,4396 \cdot N_2 + 0,0697 \cdot Ar \rightarrow$$
$$\rightarrow 1 \cdot CO_2 + 0,945 \cdot H_2O + 5,4396 \cdot N_2 + 0,0697 \cdot Ar \quad (2)$$

This way we obtained: 12,68% – H_2O, 13,42% – CO_2, 72,97% – N_2 and 0,94% – Ar. These are the major components of the fumes of the gasoline engine working on the stoichiometric mixture. Unfortunately, there is no information about the emissions of other gases arising from the defects of the real combustion process. Simplifying, it can be assumed that their shares are relatively small and do not affect the next calculations significantly.

For further analysis calculated values of the volumetric shares of N_2 and Ar (2) were used, (a) and in the case of the other ingredients the measured values were utilized. The share of H_2O was treated as consequential.

It should be noticed that for the stoichiometric mixture the mass of emitted fumes is greater than the mass of utilized air by the mass of the fuel which is 1/14.28 of the mass of air. Finally, also minor changes of the air excess coefficient λ were included with the use of Brettschneider's formula (3) [10,20] and the measured volumetric shares of CO, CO_2, HC, O_2 and NO_X.

$$\lambda = \frac{c_{CO_2} + \frac{c_{CO}}{2} + c_{O_2} + \frac{c_{NO}}{2} + \left[\frac{\alpha}{4} \cdot \frac{3,5}{3,5 + \frac{c_{CO}}{c_{CO_2}}} - \frac{\varepsilon}{2}\right] \cdot \left(c_{CO_2} + c_{CO}\right)}{\left[1 + \frac{\alpha}{4} - \frac{\varepsilon}{2}\right] \cdot \left(c_{CO_2} + c_{CO} + K1 \cdot c_{HC}\right)} \quad (3)$$

where:

λ – air excess coefficient,

C_{CO}, C_{CO2}, C_{HC}, C_{O2}, C_{NOx} – volumetric exhaust components shares [%],

For the calculation it has been assumed:

$\alpha = 1,89$ – molar ratio of hydrogen/carbon for the fuel,

ε = 0,016 – molar ratio of oxygen/carbon for the fuel

$K1 = 6$ – a conversion factor for the HC calculations from FID method (Flame Ionisation Detector) to NDIR (Non-Dispersive Infrared) [20].

Next, the formula determining the relationship between the fumes outlay and the outlays of given components has been set (4).

$$q_i = q_{air} \cdot \left(1 + \frac{1}{\lambda \cdot AFR}\right) \cdot x_{mi} \quad (4)$$

q_i – mass outlay of the i-th component [g·s^{-1}],

q_{air} – mass outlay of the air [g·s^{-1}],

x_{mi} – mass share of the i-th component [-].

To complement the formula (5), the relationship between the volumetric and mass shares of particular components was specified with the use of their molar masses:

$$x_{mi} = \frac{c_i \cdot \mu_i}{\sum_{j=n}^{j=1} c_j \cdot \mu_j} \qquad (5)$$

where:

c_i – volumetric share of the i-th component [-]

μ_i – molar mass of the i-th component [g·mol^{-1}]

$$\sum_{j=n}^{j=1} c_j \cdot \mu_j = \mu_{CO} \cdot c_{CO} + \mu_{HC} \cdot c_{HC} + \mu_{CO_2} \cdot c_{CO_2} + \mu_{O_2} \cdot c_{O_2} + \mu_{NO_X} \cdot c_{NO_X} + \mu_{N_2} \cdot c_{N_2} + \mu_{Ar} \cdot c_{Ar} +$$
$$+ \mu_{H_2O} \cdot \left(1 - (c_{CO} + c_{HC} + c_{CO_2} + c_{O_2} + c_{NO_X} + c_{N_2} + c_{Ar})\right) \qquad (6)$$

Table 1. Molar mass of selected fumes components expressed in [g·mol^{-1}]

μ_{CO}= 28,01	μ_{CO2}= 44,009	μ_{O2}= 31,999	μ_{H2O}= 18,015
μ_{HC}= 86,202 (1)	μ_{NOx}= 38,006 (2)	μ_{N2}= 28,013	μ_{Ar}= 39,948

1 – data for hexane C_6H_{14}, 2 – data for NO_X in composition (NO –50% NO_2 –50%)

The presented dependences were used for further calculations and, thanks to that, the emissions of selected fumes components were obtained for urban driving conditions.

Table 2. Toyota Verso MPV Facelift 1.8 Valvematic 147 HP [29]

Fuel consumption	EU Directive 80/1268 to 1999/100 EC
- average - combined	6,8 l/100km
- on the road (highway)	5,7 l/100km
- town	8,7 l/100km
CO2 emission	158 g/km
emission standard	Euro 5
fuel	petrol fuel 95
curb weight	1430-1525kg (1500kg)
engine	2ZR-FAE
number and cylinders arrangement	4, rzedowy
valves	16 v, DOHC, Valvematic
fuel injection system	MPI
displacement	1798 cm^3
maximum engine power	108 kW (147 HP) by 6400 rpm
maximum torque	180 Nm, by 4000 rpm
year model	2013
drive type, transmission axle	front axle drive, 6 gear, manual
maximum speed	190 km/h
acceleration (0 do 100km/h)	10,4 s

Table 3. Toxic exhaust gas components emission limits for the tested vehicle [21]

Curb weight kg	Engine type	Fuel	Emission limits mg/km				Validity
			CO	NMHC	HC	NO_x	
below 2620	PI, MPI	petrol, natural gas, liquefied petroleum gas	1000	68	100	60	type approval from 01.09.2009.

3.1. Object of research

The object used in tests was the new vehicle of Toyota make, model Corolla Verso 2013 with a mileage of 16500 km, equipped with a multipoint fuel injected gasoline engine 2ZR-FAE with a variable valve timing system Valvematic [29] and a system EOBD (European On Board Diagnosis) and DLC enabling the connection of an engine's performance data recorder.

Before the vehicle was introduced to the market it had been subjected to the type-approval tests, as a result of which, the conformity with the requirements of the emission standard Euro 5 had been proven. The limits for this vehicle are presented in table 3.

Tab. 3. Toxic exhaust gas components emission limits for the tested vehicle [21]

3.2. Measurement instruments

The main devices used in the research were: MGT5 exhaust gas analyser of MAHA make classified in class 0 according to OIML (Organisation Internationale de Métrologie Légale), an engine data recorder and a phone with a GPS receiver to record the data of the route travelled.

Fig. 1. View of MGT5 analyser prepared for tests

Table 4. Selected technical data of MGT5 analyser [10]

Measured parameter	Measurement method	Range	Resolution indications
carbon monoxide CO	NDIR	0-15% vol.	0,001%
carbon dioxide CO_2	NDIR	0-20 % vol.	0,01%
hydrocarbons HC	NDIR	1). 0 - 4000 ppm	0,1 ppm
hydrocarbons HC	NDIR	2). 0 - 20000 ppm	1 ppm
oxygen O2	electrochemical	0-15 % vol.	0,01%
	electrochemical	4-25 % vol.	0,01%
nitric oxides NO_x	electrochemical	0-5000 ppm	1 ppm
λ	computing	0,5-9,99	0,01

Table 5. Selected technical parameters of the recorder OBD Log [28]

Vehicle interface	EOBD, 16 pin socket
Supported protocols EOBD	J1850-41.6, J1850-10.4, ISO9141-2 K/L, ISO 11898
Power	DLC connector OBD, USB from PC
Sampling frequency	1 second
Working time	up to 90 hours
Operating temperature	-40°/+85°C

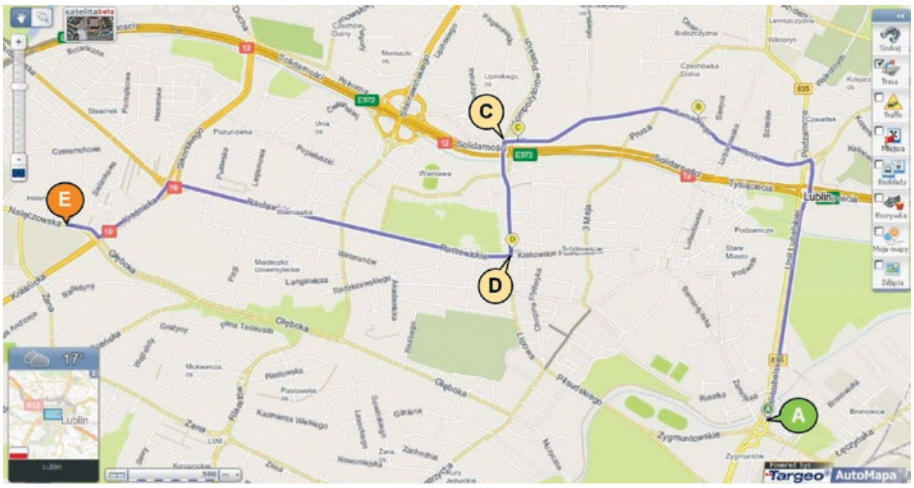

Fig. 2. The route plan for the urban driving measurement [27]

To read and record the selected parameters of the engine the device called OBD Log of Texa make was used whose basic data are listed in Table 5.

3.3. Measurements in road conditions

Driving was carried out in a manner adapted to other road users while driving in Lublin on a route of 6.95 km length with the average speed of $v = 25.8$ km/h. The starting route point (A) (Fig. 2) is located at an altitude of about 168 meters above sea level, and its end point (E) is about 50 meters higher. The greatest gradient of altitude changes is located in the middle part of the route, between points C and D (approx. 30 m). Temperature, atmospheric pressure and relative humidity average levels were 18°C, 981 hPa and 67% respectively. The vehicle was loaded with its own mass, the mass of the measurement equipment, a driver and a passenger. Before the drive, the test object had been weighed on a car scales and the total mass of 1726 kg had been noted. At the beginning of the drive the engine of the vehicle was warmed up.

Similar tests have been also carried out for suburban driving. However, due to their more stable nature only the urban test bas been presented.

4. Results of research

Knowing the changes of the mass expenditure of the individual components of exhaust fumes as functions of time, as well as the route length and the travel time, emissions can be expressed in g/km, just like for the type-approval tests (Table 3). However, to make it possible, it is necessary to measure and record the air flow and volumetric shares of the fumes components.

Due to the length of the gas analyser measuring pipe, its current indications concern the previous status of the engine from a few seconds before. For the accuracy of the emission calculations it is therefore significant to properly adjust the results recorded by the analyser and the air flow data. After the synchronization of the data it can be assumed, due to the accuracy of the measurement equipment and sensors, that the error of this method will not exceed a few percent and its value will be decreasing as the speed of driving will stabilize.

Figure 3 illustrates the values of fumes shares against the running speed and the mass air flow. The relationship of the air flow and the running speed is connected with the engine load and its rotational speed. Changes in volumetric shares also correlate with engine load. However, they are not so strong as air flow changes which have a significant impact on the emissions scale.

The effects of calculations based on the methodology described in chapter 3 are presented in Figure 4. In this case, the increase of exhausted gaseous amounts accompanying the increase of engine load, for example during acceleration, it is clearly visible. It is especially clear in the case of CO emission analysis, which is observed just during acceleration. It is near zero while driving without acceleration, which is represented by the flat nature of the CO emission curve (Fig. 4) observed in those periods.

The mass of the exhaust gases emitted in the test is presented in another bar chart (Fig. 5). The results of the calculations show that during the test, the car's engine emitted nearly 7,5 kg exhausts, in which 1,48 kg was carbon dio-

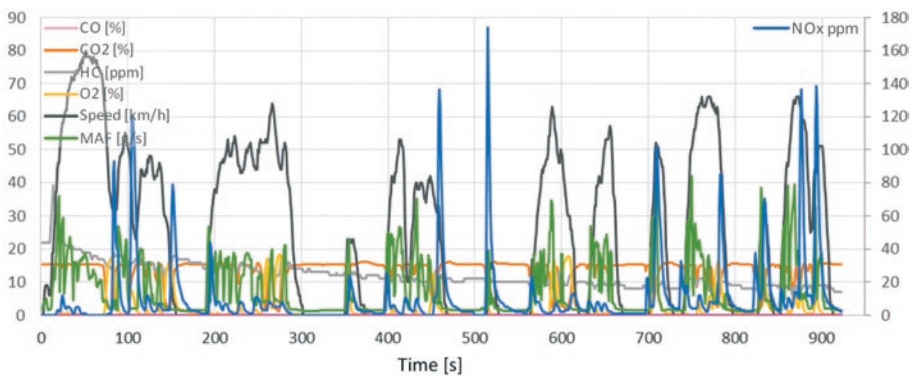

Fig. 3. The volumetric shares of selected fumes components registered during the urban drive against the running speed

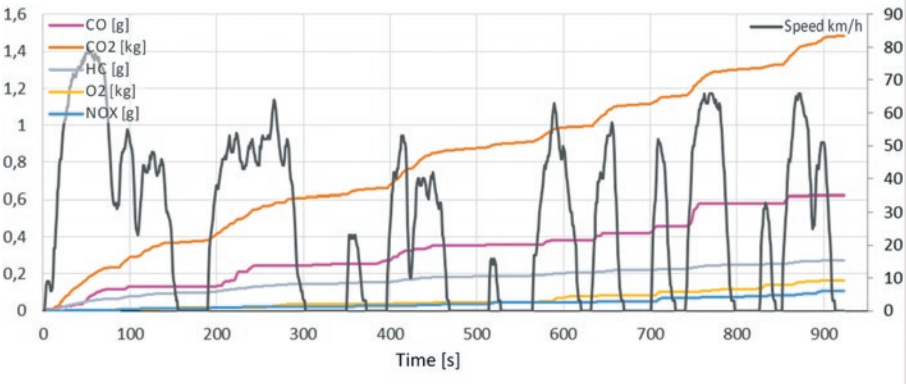

Fig. 4. The chart of cumulative emissions of selected fumes components obtained on the basis of the registered fumes composition

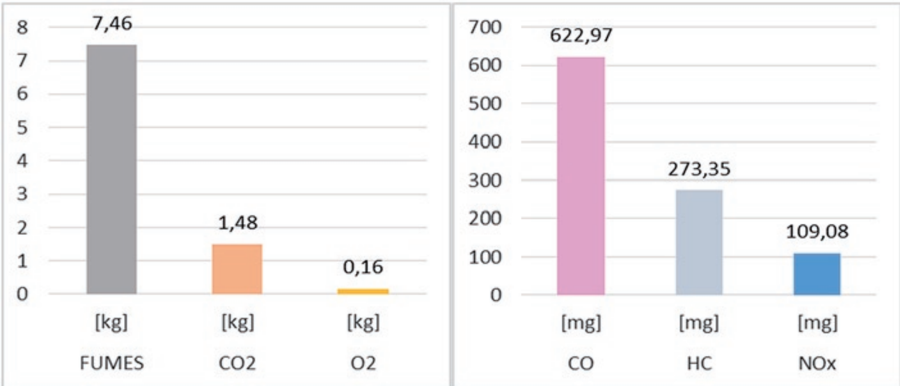

Fig. 5. Mass emissions of selected components of exhaust gases during the test

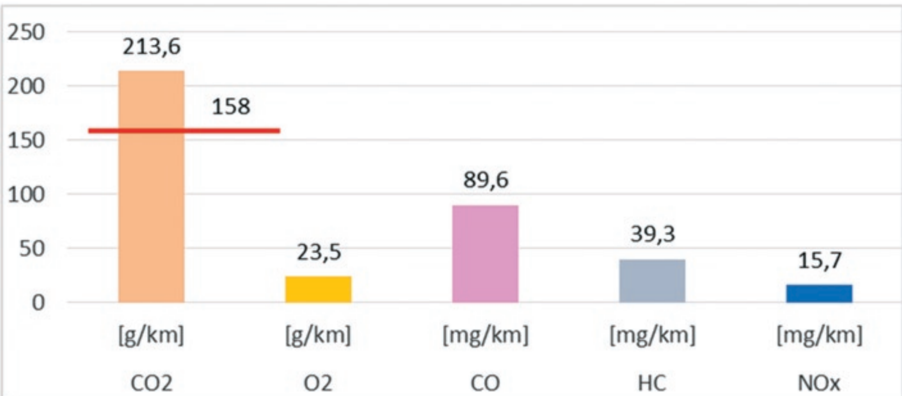

Fig. 6. The emissions of the selected components of exhausts during the test per kilometre

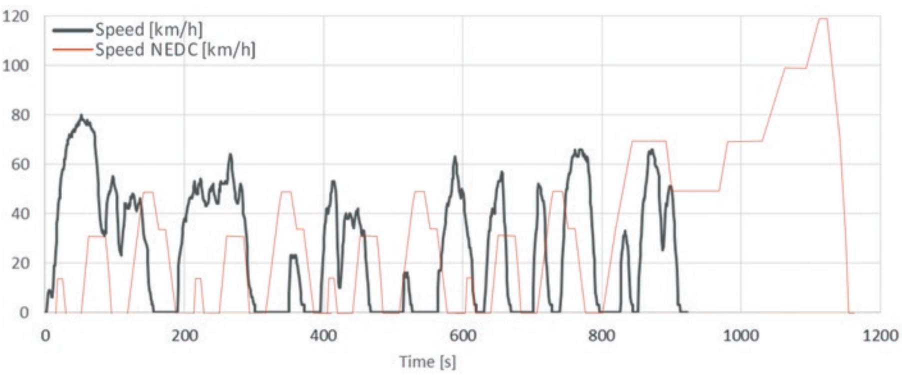

Fig. 7. The speed runs in the performed test and in NEDC

xide. Carbon monoxide emission was 623 mg, hydrocarbons ca 273 mg and nitric oxides ca 109 mg. This information is not clear without the reference to the distance travelled. Figure 6 is the supplement which allows the reader further evaluation. Therefore, it can be concluded that 213.6 g/km of carbon dioxide were issued in the test and the value (Fig. 6) is 35% bigger than the one obtained in the approval-test (Table. 2), while the emissions of toxic exhaust substances do not exceed the allowable standard values [21].

CO_2 emission, higher by more than 35%, is the result of a different than NEDC driving test. The test has been executed in conditions differing from the NEDC conditions due to the character of driving in a given agglomeration.

In the described case there are different vehicle properties and different moving resistances associated with them. Larger values of speed and its local fluctuations (Fig. 7) as well as higher vehicle weight (1726 kg) and hill route (average w = 0.7%) contribute to an increase of the engine's load and CO_2 emission. On the other hand, it should be noted that the test was implemented at the hot engine without the cold phase which would certainly additionally increase the emissions of CO_2 and CO and HC.

5. Summary and conclusions

The research and its results described in the paper confirm the possibility of the use of simplified method to exam the emission in a normal exploitation of a vehicle. However, the obtained data show that the real operation of the vehicle in an urban environment differs significantly from the specific nature of the NEDC test. (Fig. 7).

Comparing vehicles on the basis of such a test also seems to be an imperfect approach because it does not include full loads of an engine. The driver who controls a dynamic engine will surely try to use its power when fighting for a better position at the lights.

Hence there is a need for tests which also include situations where there occurs an acceleration with a maximum intensity, accompanied by random disturbances and operating states of an engine difficult to represent in a laboratory. Therefore, it should be emphasized that the road tests show the most accurately the real nature of the work of an engine work and its impact on the environment. The literature data confirm the need for changes in that area and indicate their tendencies [2, 6, 24].

Based on the analysis of the subject and the presented results of the research, the following conclusions can be made:

– the study described in the paper confirm that the emission measurements are possible with the use of a diagnostic gas analyser and signals available from EOBD via DLC,
– exhaust emissions measured in actual road conditions can significantly vary from the limits specified for the type-approval test performed in a laboratory (213 g/km vs 158 g/km),

- the presented research methodology and the results preparation are quite laborious but they show the possibility of constructing similar measurement systems that enable the user an automatic calculation and results registration for the quantitative exhaust emissions,
- the approval-tests such as NEDC can contribute misunderstandings, because vehicle users will nearly never reach the fuel consumption (CO_2 emission) at such a low level that is stated for the approval-test.

References

1. Bielaczyc P, Szczotka A, Pajdowski P, Woodburn J. Development of automotive emissions testing equipment and test methods in response to legislative, technical and commercial requirements. Combustion Engines. 2013; (1):28-41.
2. Bonnel P, Kubelt J. Heavy-duty engines conformity testing based on PEMS – Lessons learned from the European pilot program. EUR Draft report. EC-JRC. Ispra, Italy. 2010.
3. Chłopek Z, Biedrzycki J, Lasocki J, Wójcik P. Emisja zanieczyszczeń z silnika samochodu w testach jezdnych symulujących rzeczywiste użytkowanie trakcyjne. Zeszyty Naukowe Instytutu Pojazdów 2013; (92)1:67-76.
4. Cieślikowski B. Monitorowanie układu odprowadzania par paliwa. AUTOBUSY. 2011; (10):106-113.
5. Exceedance of air quality limit values in urban areas (CSI 004) - Assessment published Oct 2013. EEA – European Environmental Agency. Source: http://www.eea.europa.eu. Accessed: 31 June 2014.
6. Gautam M. In-Use, On-Road Emissions Testing of Heavy-Duty Diesel Vehicles: Challenges and Opportunities. Source: http://epa.gov/air/caaac/mstrs/gautam.pdf. Accessed: 11 July 2014.
7. Hunicz J. An experimental study of negative valve overlap injection effects and their impact on combustion in a gasoline HCCI engine. FUEL 2014, Part A; (117):236-250.
8. Kuranc A, Tarasińska J. The analysis of significance level of relation between ambient temperature and exhaust emission in the initial term of SI engine work. Teka Komisji Motoryzacji i Energetyki Rolnictwa. 2009; (9): 145-154.
9. Kuranc A. A continuous measurement of CO, CO_2, HC and NO_X at the work of a combustion engine fed with petrol in unstable thermal conditions. Teka Komisji Motoryzacji i Energetyki Rolnictwa. 2005; (5): 107-115.
10. MAHA Maschinenbau Haldenwang GmbH & Co. KG. Technical Handbook Motor Gas Tester MGT 5 Five-Gas Tester. 1999.
11. Mamala J, Brol S, Jantos J. Parametry pracy silnika spalinowego w teście drogowym. Silniki Spalinowe. 2011; (3):45-52.
12. Martini E, Coghlan N. Emissions calibration yesterday, today, tomorrow. 3rd International Exhaust Emission Symposium. Current and Future trends in automotive emissions, fuels, lubricants and test methods – 2012, BOSMAL, 24-25 May 2012, Bielsko-Biała, Poland, ISBN 978-83-931383-2-6.
13. Mazanek A. Badania porównawcze emisji toksycznych składników gazów wylotowych z silnika o zapłonie samoczynnym zasilanego ON i B10. Nafta - Gaz 2010; 66 (9): 835-840.
14. Merkisz J, Lijewski P, Fuć P, Weymann S. Exhaust emission tests from non-road vehicles conducted with the use of PEMS analyzers. Eksploatacja i Niezawodnosc - Maintenance and Reliability 2013; 15 (4): 364-368.
15. Merkisz J, Pielecha I, Pielecha J, Brudnicki K. Ekologiczność pojazdów z systemem Start/Stop w rzeczywistych warunkach ruchu miejskiego. Logistyka 2010; (6), CD-ROM
16. Merkisz J, Pielecha J, Gis W. Gasoline and LPG Vehicle Emission Factors in a Road Test, SAE Technical Paper Series, 2009-01-10937, 2009.
17. Merkisz J. Real Road Tests – Exhaust Emission Results from Passenger Cars. Journal of KONES Powertrain and Transport. 2011;18 (3): 253-260.
18. Niewczas A, Antol M. Automotive environmental pollution - investigation of toxic emissions from the vehicles operated in the city of Lublin. Part 2. Eksploatacja i Niezawodnosc – Maintenance and Reliability 2002; 13 (1): 13-24.
19. Niewczas A, Potapczuk P. Gas fumes environmental contamination - testing the emission of exhaust gas toxic components of the vehicles used in the site of Lublin. Part 1. Eksploatacja i Niezawodnosc – Maintenance and Reliability 1999; 1 (1): 15-24.
20. Regulamin nr 83 EKG ONZ – Jednolite przepisy dotyczące homologacji pojazdów w zakresie emisji zanieczyszczeń w zależności od paliwa zasilającego silnik. Dz. U. UE L42, Tom 55, 15 lutego 2012.
21. Regulation (EC) No. 715/2007 of the European Parliament and of the Council of 20 June 2007 on type approval of motor vehicles with respect to emissions from light passenger and commercial vehicles (Euro 5 and Euro 6) and on access to vehicle repair and maintenance information. Official Journal of the EU L 171:1-16.
22. Szyszlak-Bargłowicz J, Słowik T, Zając G, Piekarski W. Inline Plantation of Virginia Mallow (Sida hermaphrodita R.) as Biological Acoustic Screen. Annual Set The Environment Protection. 2013; (1): 538-550.
23. Szyszlak-Bargłowicz J, Słowik T, Zając G, Piekarski W. Metale ciężkie w rowach odwadniających ciągów komunikacyjnych. Annual Set The Environment Protection. 2013; (3): 2309–2323.
24. Vlachos T, Bonnel P, Perujo A, Weiss M. et al. In-Use Emissions Testing with Portable Emissions Measurement Systems (PEMS) in the Current and Future European Vehicle Emissions Legislation: Overview, Underlying Principles and Expected Benefits. SAE Int. J. Commer. Veh.; 2014; 7(1):199-215.
25. Vojtisek-Lom M, Fenkl M, Dufek M, Mareš J. Off-cycle, real-world emissions of modern light duty diesel vehicles. 2009: SAE 2009-24-0148.
26. Weiss M, Bonnel P, Hummel R, Manfredi U, Colombo R, Lanappe G, Le Lijour P, Sculati M. Analyzing on-road emissions of light-duty vehicles with Portable Emission Measurement Systems (PEMS). JRS scientific and Technical Reports JRC62639, EUR 24697 EN – 2011.
27. www.targeo.pl
28. www.texapoland.pl
29. www.toyota.pl

Andrzej KURANC
Department of Power Engineering and Vehicles
University of Life Sciences in Lublin
ul. Głęboka 28, 20-612 Lublin, Poland; e-mail: andrzej.kuranc@up.lublin.pl

Article citation info:
KOLAKOWSKI Z, MANIA RJ, GRUDZIECKI J. Local nonsymmetrical postbuckling equilibrium path of the thin FGM plate. Eksploatacja i Niezawodnosc – Maintenance and Reliability 2015; 17 (1): 135–142.

Zbigniew KOLAKOWSKI
Radosław J. MANIA
Jan GRUDZIECKI

LOCAL NONSYMMETRICAL POSTBUCKLING EQUILIBRIUM PATH OF THE THIN FGM PLATE

NIESYMETRYCZNA LOKALNA ŚCIEŻKA RÓWNOWAGI POKRYTYCZNEJ CIENKIEJ PŁYTY Z MATERIAŁU FUNKCJONALNIE GRADIENTOWEGO

The influence of the imperfection sign (sense) on local postbuckling equilibrium path of plates made of functionally graded materials (FGMs) has been analyzed. Koiter's theory has been used to explain this phenomenon. In the case of local buckling, a nonsymmetrical stable equilibrium path has been obtained. The investigations focus on a comparison of the semi-analytical method (SAM) and the finite element method (FEM) applied to the postbuckling nonlinear analysis of thin-walled complex FG plated structures.

Keywords: *FGM, FEM, Koiter's theory, semi-analytical method, postbuckling path.*

W pracy przedstawiono analizę wpływu znaku imperfekcji wstępnej na charakterystykę lokalnej pokrytycznej ścieżki równowagi płyty wykonanej z materiału gradientowego. Do wyjaśnienia tego efektu zastosowano teorię Koitera. W przypadku lokalnej utraty stateczności uzyskano niesymetryczne stateczne ścieżki równowagi. Prezentowane badania były skoncentrowane na porównaniu wyników uzyskanych na podstawie własnej metody pół-analitycznej z wynikami uzyskanymi przy zastosowaniu metody elementów skończonych w nieliniowej analizie cienkościennych konstrukcji płytowych wykonanych z materiałów gradientowych.

Słowa kluczowe: *materiały funkcjonalnie gradientowe, MES, teoria Koitera, metoda pól-analityczna, ścieżka pokrytyczna.*

1. Introduction

Since the mid 1980's Functionally Graded Materials (FGMs) have been a relatively new class of composite materials, which have become a very popular research field and have been used in numerous engineering applications. A standard functionally gradient material is an inhomogeneous composite made up of two constituents – typically of metallic and ceramic phases. Within FGMs, different microstructural phases have different functions, and the overall FGMs attain the multistructural status from their property gradation. In most cases, these phases content changes gradually along the thickness of the plate or shell. This eliminates adverse effects between the layers (e.g., shear stress concentrations and/or thermal stress concentrations), typical for layered composites what generally improves material utility properties. The combination of ceramic with a metal component improves the characteristics of FGM structures i.e. a better resistance to high temperature (ceramic) and good mechanical features (metal), reducing further a fracture possibility of the whole gradient structure. These features make high temperature environments the leading application area of FGM structures.

The nonlinear analysis of plates and shells devoted to basic types of loads is covered in the monograph by Hui-Shen [4]. Author considers static bending and thermal bending as an introduction to buckling and postbuckling behaviour of FGM plates and shells. The shear deformation effect is employed in the framework of Reddy's higher order shear deformation theory (HSDT) [20].

In [19], alongside the HSDT for FGM plates, Reddy compares the application of the first order shear deformation theory (FSDT) and the classical laminated plate theory (CLPT) to functionally graded plate analysis. According to the presented results for thin-walled plates, it is obvious that an application of the FSDT gives practically the same results as the HSDT. The discrepancy between both theories is of 2% in the calculated deflections of the plates under analysis.

The buckling problem of functionally graded plates is discussed in the frame of different approaches and for different loads: in [21] - biaxial in-plane compression; thermal loads (constant temperature) with axial compression in [24]; biaxial in-plane compression in [2] and [16], and through the thickness temperature gradient in [23].

Birman and Byrd [1] give a wide review of theories employed for a description of grading material properties and focus on the principal developments in functionally graded materials (FGMs) with an emphasis on the recent works published since 2000 (up to 300 works cited).

In some papers (e.g.,[14, 27]), the concept of 'physical neutral surface' that allows one to uncouple the in-plane and out-of-plane deformations is introduced.

Due to the complexity of buckling problems of FG plates under compound mechanical and thermal loads, the finite element method (FEM) seams to be the only possible solution in many cases. Therefore, in the literature one can find many papers which present results of a solution to different problems of FG plate buckling, obtained with an application of the FEM, for example [15, 17, 22].

In current paper in the finite element method solution, FG plates were modelled as multilayered composite structures whose graded material properties in the range of 10–40 isotropic layers were defined. After the convergence analysis the model with twenty layers was accepted. For meshing, a shell element with four nodes and six degrees of freedom in each node was employed. The rotational DOF in the plane of the element was constrained via the penalty function.

Conducting with the FEM the nonlinear buckling analysis of a rectangular FGM plate, subjected to one-directional compression in its plane, the authors of the present paper have observed some intriguing influence of the imperfection sign (i.e., its direction) on postbuckling equilibrium paths of investigated FGM plates. Therefore, this work is aimed at an explanation of this phenomenon. The general asymptotic Koiter's theory of stability has been assumed as the basis of investigation. Among all versions of the general nonlinear theory, Koiter's theory [6, 7, 25, 26] of conservative systems is the most popular one, owing to its general character and development. Even more, so after Byskov and Hutchinson [3] formulated it in a convenient way. The theory is based on asymptotic expansions of the postbuckling path for potential energy of the system.

The nonlinear stability of thin-walled multilayer structures in the first order approximation of Koiter's theory is solved with the modified analytical-numerical method (ANM) presented in [8]. The analytical-numerical method (ANM) should also consider the second order approximation in the postbuckling analysis of elastic composite structures. The second order postbuckling coefficients were estimated with the semi-analytical method (SAM) [12], modified by the solution method given in [11]. The investigation of stability of equilibrium states requires an application of a nonlinear theory that enables us to estimate an influence of different factors on the structure behaviour. The analysis of postbuckling behaviour of thin-walled composite plate structures using the SAM will be by far faster and more thorough than the FEM.

The initial imperfections were introduced by updating the finite element mesh with the first mode shape of the eigen-buckling solution, with a given magnitude corresponding to the plate thickness and assumed sign (direction). The eigen-buckling analysis, where the critical load was determined despite the eigen-mode, preceded the nonlinear buckling analysis.

2. Formulation of the problem

The square plate is supported at all their edges. It is assumed that the FG plate obeys Hooke's law. The material properties are assumed to be temperature independent.

In strain-displacement relations - in order to enable the consideration of both out-of-plane and in-plane bending of the plate, all nonlinear terms are present [8, 9, 11]:

$$\begin{aligned} \varepsilon_x &= u_{,x} + \tfrac{1}{2}\ (w_{,x}^2 + v_{,x}^2 + u_{,x}^2) \\ \varepsilon_y &= v_{,y} + \tfrac{1}{2}\ (w_{,y}^2 + u_{,y}^2 + v_{,y}^2) \\ 2\varepsilon_{xy} &= \gamma_{xy} = u_{,y} + v_{,x} + w_{,x}w_{,y} + u_{,x}u_{,y} + v_{,x}v_{,y} \end{aligned} \tag{1}$$

and

$$\kappa_x = -w_{,xx} \qquad \kappa_y = -w_{,yy} \qquad \kappa_{xy} = -2w_{,xy} \tag{2}$$

where: u, v, w – are components of the displacement vector of the plate in the x, y, z axis direction, respectively, and the plane $x-y$ overlaps the midplane before its buckling.

It should be highlighted that in the majority of publications devoted to stability of structures, the terms $(v_{,x}^2 + u_{,x}^2)$, $(u_{,y}^2 + v_{,y}^2)$ and $(u_{,x}u_{,y} + v_{,x}v_{,y})$ in strain tensor components (1) are neglected. However, the main limitation of the assumed theory lies in an assumption of linear relationships between curvatures (2) and second derivatives of the displacement w. In such an approach, finite displacements and small or moderate rotations are considered [11].

In thin-walled FG structures - plates or shells, usually the ceramic volume fraction V_c and metal fraction V_m distribution throughout the structure thickness t are described by a simple power law of:

$$V_c(z) = \left(\frac{z}{t} + \frac{1}{2}\right)^q \qquad V_m(z) = 1 - V_c(z) \tag{3}$$

where: $-t/2 \le z \le t/2$ and $q \ge 0$ is the volume fraction exponent (i.e., for $q = 0$ – plate is full ceramic and for $q = \infty$ – plate is metallic – see Fig. 1).

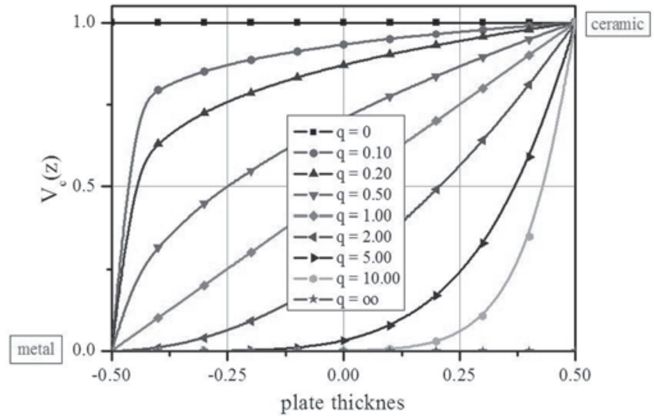

Fig. 1. Volume fraction of ceramic along the FGM plate thickness

According to the rule of mixture, the properties of the functionally graded material (E – Young's modulus, ν – Poisson's ratio etc.) can be expressed as follows:

$$E(z) = E_m + (E_c - E_m)\left(\frac{z}{t} + \frac{1}{2}\right)^q$$

$$\nu(z) = \nu_m + (\nu_c - \nu_m)\left(\frac{z}{t} + \frac{1}{2}\right)^q \tag{4}$$

In the present study, the classical plate theory is employed to obtain the governing equations of the thin FG plate equilibrium. Using the classical laminated plate theory (CLPT), the stress and moment resultants (N , M) are defined as [5, 8, 9]:

$$\begin{Bmatrix} N \\ M \end{Bmatrix} = \begin{bmatrix} A & B \\ B & D \end{bmatrix} \begin{Bmatrix} \varepsilon \\ \kappa \end{Bmatrix} \tag{5}$$

where: A, B, D – are extensional, coupling and bending stiffness matrices, respectively. For the FG plate their components are listed below:

$$A_{11} = A_{22} = \int_{-t/2}^{t/2} \frac{E(z)}{1-\nu^2(z)}\, dz$$

$$A_{12} = A_{21} = \int_{-t/2}^{t/2} \frac{E(z)\nu(z)}{1-\nu^2(z)}\, dz \tag{6a}$$

$$A_{66} = \int_{-t/2}^{t/2} \frac{E(z)}{2[1+\nu(z)]}\, dz$$

$$A_{16} = A_{61} = 0$$

$$B_{11} = B_{22} = \int_{-t/2}^{t/2} \frac{E(z)}{1-\nu^2(z)}\, zdz$$

$$B_{12} = B_{21} = \int_{-t/2}^{t/2} \frac{E(z)\nu(z)}{1-\nu^2(z)}\, zdz \tag{6b}$$

$$B_{66} = \int_{-t/2}^{t/2} \frac{E(z)}{2[1+\nu(z)]}\, zdz$$

$$B_{16} = B_{61} = 0$$

$$D_{11} = D_{22} = \int_{-t/2}^{t/2} \frac{E(z)}{1-\nu^2(z)}\, z^2dz$$

$$D_{12} = D_{21} = \int_{-t/2}^{t/2} \frac{E(z)\nu(z)}{1-\nu^2(z)}\, z^2dz \tag{6c}$$

$$D_{66} = \int_{-t/2}^{t/2} \frac{E(z)}{2[1+\nu(z)]}\, z^2dz$$

$$D_{16} = D_{61} = 0$$

and

$$\{\varepsilon\} = \begin{Bmatrix} \varepsilon_x \\ \varepsilon_y \\ 2\varepsilon_{xy} \end{Bmatrix} \quad \{\kappa\} = \begin{Bmatrix} \kappa_x \\ \kappa_y \\ \kappa_{xy} \end{Bmatrix} \tag{7}$$

Due to the presence of the nontrivial submatrix B, the coupling between extensional and bending deformations exists as it is in the case of unsymmetrical laminated plates [5, 8, 9]. An extensional force results not only in extensional deformations, but also bending of the FG plate. Moreover, such a plate cannot be subjected to the moment without suffering simultaneously from extension of the middle surface. Coupling between extension and bending is a result of a combination of the geometry and FGM properties in the structures. The stretching-bending coupling affects strongly the constitutive equations and the boundary conditions that have a complex form and the solution procedures become difficult.

The equations of stability of thin-walled structures have been derived using a variational method [8, 9, 11]. After expanding the fields of displacements $\bar{U}$ and the fields of sectional forces $\bar{N}$ into a power series with respect to the mode amplitudes ζ_1 (the dimensionless amplitude of the buckling mode), Koiter's asymptotic theory has been employed [3, 6, 7, 8, 9, 10, 13, 18, 25, 26]:

$$\begin{aligned} \bar{U} &= \lambda \bar{U}^{(0)} + \zeta_1 \bar{U}^{(1)} + \zeta_1^2 \bar{U}^{(2)} + \dots \\ \bar{N} &= \lambda \bar{N}^{(0)} + \zeta_1 \bar{N}^{(1)} + \zeta_1^2 \bar{N}^{(2)} + \dots \end{aligned} \tag{8}$$

where: λ – load parameter, $\bar{U}^{(0)}$, $\bar{N}^{(0)}$ – prebuckling state fields (the zero approximation), $\bar{U}^{(1)}$, $\bar{N}^{(1)}$ – buckling mode fields (the first order approximation), and $\bar{U}^{(2)}$, $\bar{N}^{(2)}$ – postbuckling fields (the second order approximation) for the structure.

The postbuckling equilibrium path within an imperfect structure with the amplitude ζ_1^* for the single mode (i.e., an uncoupled mode), buckling mode has the following form [3, 8, 9, 13, 26]:

$$a_1\left(1-\frac{\sigma}{\sigma_{cr}}\right)\zeta_1 + a_{111}\zeta_1^2 + a_{1111}\zeta_1^3 + \dots = a_1\frac{\sigma}{\sigma_{cr}}\zeta_1^* \tag{9}$$

where: σ_{cr} – critical (bifurcational) value of σ (instead of λ). The coefficients in equilibrium equation (9) are given in papers [3, 8, 9, 13, 26]. It can be easily seen that the amplitude ζ_1^* is a small quantity (i.e., only linear terms with respect to ζ_1^* have been accounted for) and the linear pre-buckling state is assumed.

The corresponding expression for the total elastic potential energy of the structure has the following form:

$$\Pi = -a_0\frac{\sigma^2}{2} + a_1\left(1-\frac{\sigma}{\sigma_{cr}}\right)\frac{\zeta_1^2}{2} + a_{111}\frac{\zeta_1^3}{3} + a_{1111}\frac{\zeta_1^4}{4} - a_1\frac{\sigma}{\sigma_{cr}}\zeta_1\zeta_1^* \tag{10}$$

where: $\Pi_0 = a_0\frac{\sigma^2}{2}$ is energy of the prebuckling linear state.

In the semi-analytical method (SAM), one postulates to determine approximated values of the a_{1111} coefficients on the basis of the linear buckling problem. This approach allows the values of the a_{111} coefficients - according to the applied nonlinear Byskov and Hutchinson theory [3, 8, 9, 13, 26] – to be precisely determined.

The considerations performed in [12] and the results of [11] allow for concluding that the approximated values of the a_{1111} coefficients correspond to an application of the following simple supported boundary conditions of the plate at both edges (i.e. $x = 0; \ell$)

$$\begin{aligned} &\int_0^b N_x(x=0,y)dy = \int_0^b N_x(x=\ell,y)dy = bN_x^{(0)} \\ &v(x=0,y) = v(x=\ell,y) = 0 \\ &w(x=0,y) = w(x=\ell,y) = 0 \\ &M_x(x=0,y) = M_x(x=\ell,y) = 0 \end{aligned} \tag{11}$$

The first condition in (11) means that the external loading is not subjected to any additional increment.

At the critical point, the dependence describing the relationship for the ideal structure (i.e., without the imperfection $\zeta_1^* = 0$) is subject to bifurcation between the external loading and the displacement amplitude ζ_1 . Equilibrium path equation (9) can be treated as the first variation of the system potential energy, that is to say, as the condition necessary for the system equilibrium. For the case when the postbuckling coefficients $\bar{a}_{111} = a_{111}/a_1 \neq 0$ and $\bar{a}_{1111} = a_{1111}/a_1 > 0$ (which corresponds to the case of the FGM plate), in order to determine the equilibrium state, the second variation of energy was calculated Then the intersection points of the equilibrium path and the structure stability limit of the ideal structure were determined. Finally, the coordinates of two points $p1, p2$ were arrived at:

$$\zeta_{p1} = 0 \quad \left(\frac{\sigma}{\sigma_{cr}}\right)_{p1} = 1 \tag{12}$$

$$\zeta_{p2} = -\frac{\bar{a}_{111}}{2\bar{a}_{1111}} \quad \left(\frac{\sigma}{\sigma_{cr}}\right)_{p1} = 1 - \frac{\bar{a}_{111}^2}{4\bar{a}_{1111}} \tag{13}$$

A sample equilibrium path for the ideal square FGM plate is presented in Fig. 2. There it is visible that in the case of the FG plate, an nonsymmetrical stable equilibrium path exists. The unstable configuration corresponds to the postbifurcational equilibrium path of the plate without imperfection in the range $<\zeta_{p1}, \zeta_{p2}>$.

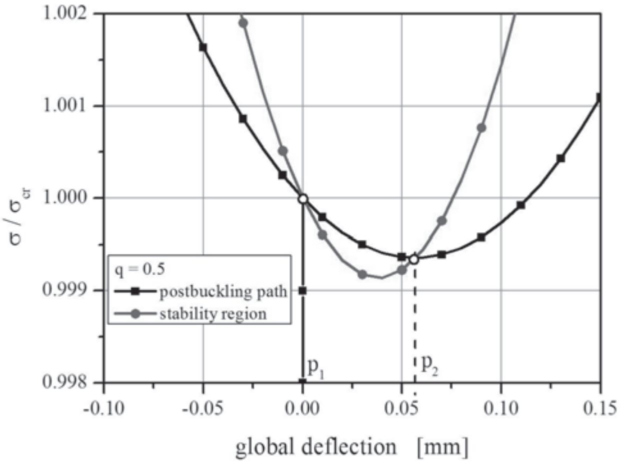

Fig. 2. Postbuckling path of FGM plate

In the linear problem, the critical stress σ_{cr} is the characteristic quantity, whereas in the nonlinear first order problem, the magnitude of the coefficient $\bar{a}_{111}$ determining the sensitivity to imperfections should be accounted for.

3. Analysis of the results

Detailed numerical computations were conducted only for a square FGM plate. The plate is subjected to uniform compression in the direction of *x* axis. All plate edges are assumed to be simply supported. Although, in the subsection devoted to determination of critical stress, some other boundary conditions along the unloaded edges are considered as well.

The following geometrical dimensions of the square plate (Fig. 3) and the material constants for Al-TiC are assumed:

$\ell = b = 100$ mm; $t = 1$ mm; $E_m = 69$ GPa; $\nu_m = 0.33$; $E_c = 480$ GPa; $\nu_c = 0.2$.

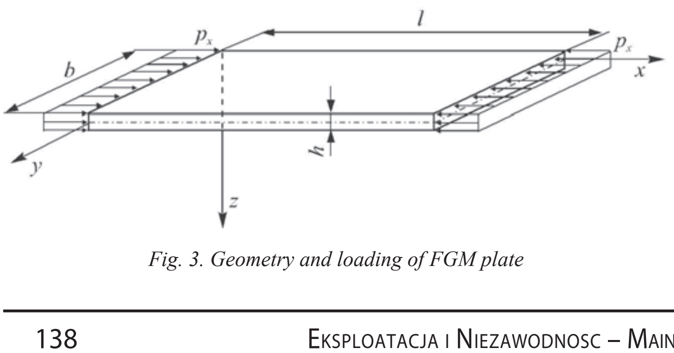

Fig. 3. Geometry and loading of FGM plate

where: indices *m* and *c* refer to the metal (Al) and ceramic material (TiC), respectively.

In [8], an unbending, prebuckling state, i.e., a distribution field of the zero state according to (A1) has been assumed. According to assumed (A1) and (8) displacements, for the zero state (i.e., prebuckling) the force and moment dependence (5) takes the form:

$$\begin{Bmatrix} N^{(0)} \\ M^{(0)} \end{Bmatrix} = \begin{bmatrix} A & B \\ B & D \end{bmatrix} \begin{Bmatrix} \varepsilon^{(0)} \\ 0 \end{Bmatrix} \tag{14}$$

Then for the zero state, it results in an occurrence of nonzero inner sectional forces (A2) $N_x^{(0)}$, $M_x^{(0)}$, $M_y^{(0)}$ in the FG plate. Special attention should be drawn to the fact that nonzero magnitudes of the sectional moments $M_x^{(0)}$ and $M_y^{(0)}$ appear as the effect of the middle surface deformations (i.e., membrane deformations) and the nontrivial coupling submatrix B but not due to an appearance of the middle surface curvatures. These moments affect the values of critical loads and the values of postbuckling coefficients.

In the subsequent three figures (Figs. 4 - 6), an effect of the volume fraction exponent q in Eq. (3), on the values of critical stresses and the postbuckling coefficients $\bar{a}_{111}$ and $\bar{a}_{1111}$ for various constrain cases of unloaded longitudinal edges, i.e., $y = 0; b$, is presented. In legends to these figures the descriptions mean:

- F – free edges, for which the following has been assumed: $N_y = N_{xy} = M_y = Q_y = 0$;
- S1 – simply supported edges - $N_y = N_{xy} = w = M_y = 0$;
- S2 – simply supported edges - $v = N_{xy} = w = M_y = 0$;
- C – clamped edges - $N_y = N_{xy} = w = \partial w / \partial y = 0$.

In the case of clamped longitudinal edges $(y = 0; b)$, the same results have been obtained as for two other possible conditions of the edge support, i.e., when:

- $v = N_{xy} = w = \partial w / \partial y = 0$
- $u = v = w = \partial w / \partial y = 0$

The values of critical loads (Fig. 4) for the boundary conditions under consideration increase with a decrease in the values of volume fractions q – as can be expected. Differences in the values of critical loads for cases S1 and S2 become visible for $q > 0.5$. They are relatively inconsiderable (below 10%) and larger for case S2.

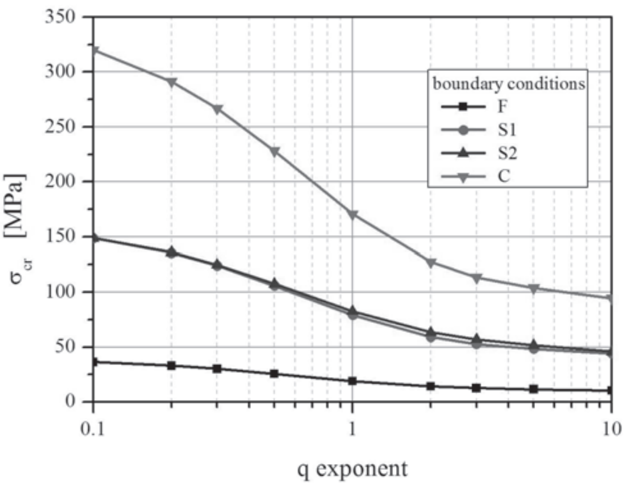

Fig. 4. Dependence of critical stress on boundary conditions and q factor

In the range $0.1 \le q \le 10$, the values of postbuckling coefficients $\overline{a}_{111}$ (Fig. 5) are negative for all considered cases of boundary conditions. The lowest values occur for case F, whereas for clamped conditions C, they are located between values for S1 and S2. The highest values have been found for boundary conditions S2. The maximal values of $\overline{a}_{111}$ for the analyzed support conditions are reached for $2 \le q \le 3$.

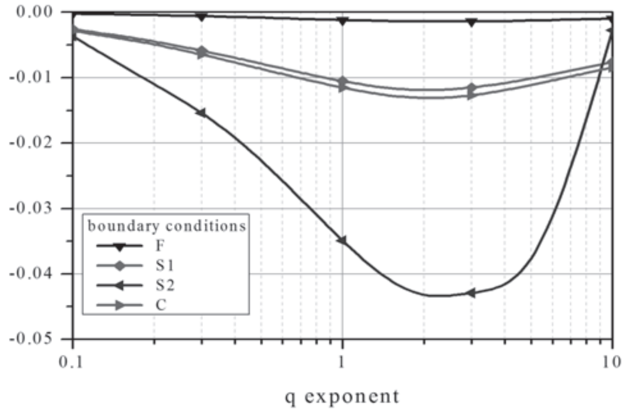

Fig. 5. Coefficient $\bar{a}_{111}$ value as a function of q and boundary conditions

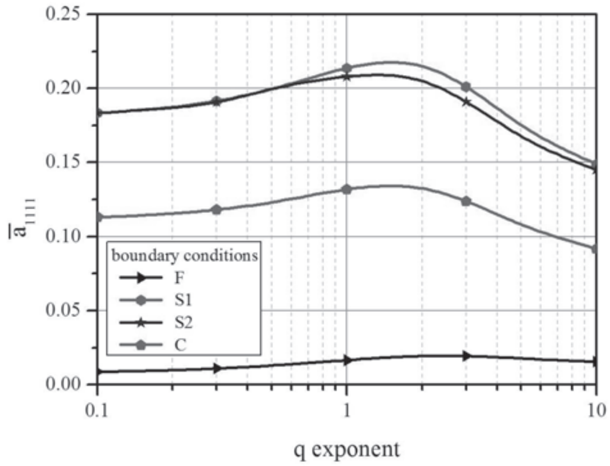

Fig. 6. Coefficient $\bar{a}_{1111}$ value as a function of q and boundary conditions

On the other hand, the values of postbuckling coefficients $\overline{a}_{1111}$ (determined according to the SAM [11, 12]), shown in Fig. 6, are positive for the assumed boundary conditions F, S1, S2, C for $0.1 \le q \le 10$. The lowest values of $\overline{a}_{1111}$ have been obtained, as expected, for case F. The values of $\overline{a}_{1111}$ for case C are by approximately 60% lower than for conditions S1 and S2. For condition S2, the values of $\overline{a}_{1111}$ are higher than for S1, and these differences become visible for $q > 0.5$. However, they do not exceed 5% for the range of variability $0.1 \le q \le 10$ under consideration.

As it has been discussed in detail in [8], sectional moments of the zero state $M_x^{(0)}$ and $M_y^{(0)}$ do not enter the first order equations of equilibrium and boundary conditions. The nonzero values of postbuckling three-index coefficients $\overline{a}_{111}$ result from an occurrence of the nonzero coupling submatrix B. The coefficient $\overline{a}_{111}$ characterizing the initial postbuckling behaviour belongs to surface integrals of the type $\sigma^{(1)} \cdot l_2(U^{(1)})$ (according to the notation introduced by Byskov and Hutchinson [3, 26]). An appearance of first order internal forces (i.e., related to the forces $N_x^{(1)}, N_y^{(1)}, N_{xy}^{(1)}$) causes that the coefficients $\overline{a}_{111}$ reach values other than zero. It should be noted yet that the values of $\overline{a}_{111}$, in principle, are relatively small. Due to the above-mentioned reasons, in the analysis of postbuckling equilibrium paths of the FG plate they have been usually neglected. However, when we take into account the nonzero values of $\overline{a}_{111}$, a phenomenon of occurrence various postbuckling equilibrium paths for different signs of imperfection (i.e., $\left|\zeta_1^*\right|$) can be explained. Due to the boundary conditions (11) assumed along the loaded edges ($x = O;\ell$) and unloaded edges ($y = O;b$) - respectively for cases F, S1, S2, and C; one obtains different distributions of inner forces of the first order, i.e., $N_x^{(1)}, N_y^{(1)}, N_{xy}^{(1)}, M_x^{(1)}, M_y^{(1)}, M_{xy}^{(1)}$. These inner forces values are determined with accuracy up to a constant, as it takes place for eigenproblems. The conditions on loaded edges (11a) enforce a generation of a self-balancing system of forces $N_x^{(1)}$. Below, few exemplary diagrams for S2 boundary conditions on longitudinal edges, for $q = 0.5$ are shown.

In Fig.7, distributions of first-order inner membrane forces $N_x^{(1)}, N_y^{(1)}, N_{xy}^{(1)}$ are shown, whereas the corresponding distributions of bending moments $M_x^{(1)}, M_y^{(1)}, M_{xy}^{(1)}$ along the plate width are additionally presented in Fig. 8. As it can be easily noticed, the values of inner forces are of the same order of magnitude. According to the assumption, the distributions of inner forces $N_x^{(1)}, N_y^{(1)}, M_x^{(1)}, M_y^{(1)}$ are symmetrical with respect to the plate axis of symmetry (i.e., for $y = O.5b$), whereas the distribution of $N_{xy}^{(1)}, M_{xy}^{(1)}$ forces is antisymmetrical. The boundary conditions of unloaded edges cause a self-resetting of $N_{xy}^{(1)}, M_y^{(1)}$. For edges $y = O;b$ the value of moment $M_x^{(1)}$ is other than zero and results from the first-order nonzero membrane deformations $\varepsilon_x^{(1)}, \varepsilon_y^{(1)}$ and the nontrivial coupling matrix B. The nonzero values of all first-order inner forces for the FGM plate cause that nonzero values of the coefficients $\overline{a}_{111}$ appear. These values are relatively low but exert a significant effect on the sensitivity of the system to values and signs of the imperfection ζ_1^*.

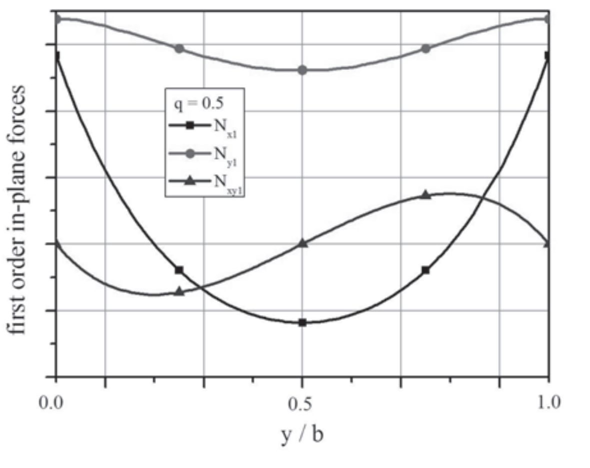

Fig. 7. First order in-plane force resultants distribution along the plate width

To verify the proposed SAM solution, finite element computations were performed for the FG plate under axial loading. The commercial ANSYS software was applied for the numerical calculations.

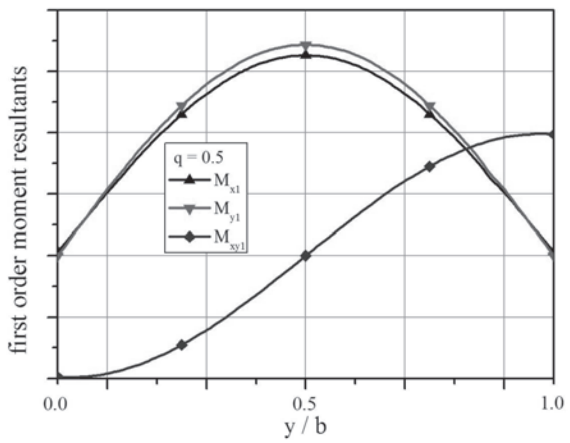

Fig. 8. First order moment resultants distribution along the plate width

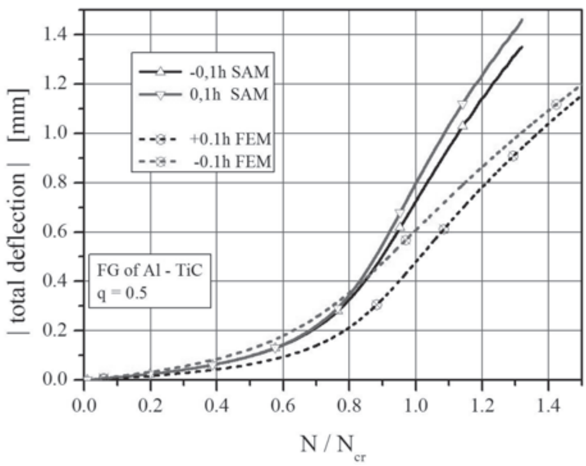

Fig. 9. Sign of imperfection influence on the buckling and postbuckling path

The numerical model was created with an application of a shell finite element. It was a multi-layered four-node element with six degrees of freedom at each node (three translations in the directions of local coordinate axes and three rotations around these axes). The rotational DOF around the normal to the plate midplane was constrained via the penalty function to relate this independent rotation with the in-plane components of displacements. This element is dedicated for modelling multi-layered structures and is equipped with the section option which allows for easy tailoring the lay-ups of the modelled plate. The sensitivity to shear strains in this element is governed by the first-order shear deformation theory, whereas the element formulation is based on the logarithmic strain measure. According to the current analysis requirements, the applied finite element was associated with linear elastic material properties. To discretize the model, a uniform mesh of elements was generated. The boundary conditions on loaded plate edges, which followed from S1 type analytical simple support, were introduced by displacement constrains in appropriate directions as well as coupling of edge node displacements to keep the edges straight.

The initial imperfection was introduced by updating the finite element mesh with the local mode shape of the eigen-buckling solution, with a given magnitude corresponding to the plate thickness. The eigen-buckling analysis, where the critical load was determined despite the eigen-mode, preceded the nonlinear analysis. Therefore, the numerical model employed large displacement formulation. The load was applied to the plate edges in the form of uniformly distributed node forces.

For the square plate under analysis and for $q = 0.5$, the results of calculations obtained from the SAM and the FEM were compared. A comparison of the results is presented in Fig. 9. For an easier comparison of an influence of the imperfection ζ_1^* sign, a change in the absolute values of total deflections $|w_t| = |w_0 + w| = |\zeta_{1t}|\ t = |\zeta_1^* + \zeta_1|\ t$ as a function of the load ratio $N / N_{cr} = \sigma / \sigma_{cr}$ has been shown. The negative value of imperfection corresponds to a initial deflection along the direction of metal, whereas the positive one - along the direction of ceramic.

The results obtained with the FEM are achieved for a full geometrically nonlinear analysis. On the other hand, in the SAM, nonlinear terms related to the imperfection ζ_1^* were neglected, whereas the values of the postbuckling coefficient $\overline{a}_{1111}$ were determined approximately. It is followed by visible differences in the results obtained with both the methods (SAM and FEM) for the same value of imperfection. It can be seen that the sign of imperfection exerts an influence on the postbuckling equilibrium path. The initial deflection ζ_1^* along ceramic yields higher values of total deflections for the given value of load N / N_{cr} than the initial deflection along the direction of metal. In both cases the assumed absolute value of imperfection $|\zeta_1^*|$ was equal.

Thus, as it was discussed above, the application of Koiter's theory through the semi-analytical method enables an explanation of the phenomenon of various postbuckling equilibrium paths for the functionally graded plate for different signs of imperfection with the same absolute magnitude $|\zeta_1^*|$. In particular, it can be seen for $N / N_{cr} = \sigma / \sigma_{cr} < 1.3$.

4. Conclusions

The analytical and numerical investigations on FGM – a relatively novel material, applications in plate and shell structures are presented. The effect of gradually varying volume fraction of constituent materials leads to continuous change from one surface to another eliminating interface problems and gives smooth material properties of final composite which is especially import in thermal environment applications.

An influence of imperfection values on various postbuckling equilibrium paths of the FG plate has been analyzed. The basis to explain the discussed behaviour is the nonlinear Koiter's theory of conservative systems. In the case of the FG plate, nonzero first-order sectional inner forces that cause an occurrence of nonzero postbuckling coefficients are responsible for the system sensitivity to imperfection. It results in the fact that postbuckling equilibrium paths of plate structures made of FGMs are unsymmetrically stable. This explains the observed differences in plate response dependence on imperfections sign (sense).

References

1. Birman V, Byrd LW. Modeling and analysis of functionally materials and structures. Applied Mechanics Review, 60, 2007, 195-216.
2. Bodaghi M, Saidi AR. Levy-type solution for buckling analysis of thick functionally graded rectangular plates based on the higher-order shear deformation plate theory. Applied Mathematical Modeling 2010; 34:3659-73.
3. Byskov E, Hutchinson JW. Mode interaction in axially stiffened cylindrical shells. AIAA J 1977;15(7):941-48.
4. Hui-Shen S. Functionally graded materials - Nonlinear analysis of plates and shells. CRC Press, Taylor & Francis, London; 2009.

5. Jones RM. Mechanics of Composite Materials. 1999; 2nd ed. Taylor & Francis, London.
6. Koiter WT. General theory of mode interaction in stiffened plate and shell structures. WTHD Report 590, Delft; 1976 p.41.
7. Koiter WT, Pignataro M. An alternative approach to the interaction between local and overall buckling in stiffened panels. In: Buckling of Structures Proc. of IUTAM Symposium, Cambridge; 1974 p.133-48.
8. Kolakowski Z, Krolak M. Modal coupled instabilities of thin-walled composite plate and shell structures. Composite Structures 2006. 76:303-13.
9. Kolakowski Z, Kowal-Michalska K. (Eds.) Selected problems of instabilities in composite structures. A Series of Monographs, Technical University of Lodz, Poland. 1999.
10. Kolakowski Z, Kubiak T. Load-carrying capacity of thin-walled composite structures. Composite Structures 2005; 67:417-26.
11. Kolakowski Z, Mania JR. Semi-analytical method versus the FEM for analysis of the local post-buckling. Composite Structures 2013; 97:99-106.
12. Kolakowski Z. A semi-analytical method for the analysis of the interactive buckling of thin-walled elastic structures in the second order approximation. Int. J. Solids Structures 1996. Vol.33, No.25, p. 3779-90.
13. Kolakowski Z, Krolak M, Kowal-Michalska K. Modal interactive buckling of thin-walled composite beam–columns regarding distortional deformations. Int. J. Eng. Sci, 1999; 37: 1577–96.
14. Kowal-Michalska K, Mania RJ. Static and dynamic buckling of FGM plates under compressive loading. Proceedings ICCES'11 Conference, Nanjing. 2011.
15. Kyung-Su Na, Ji-Hwan Kim. Volume fraction optimization of functionally graded composite panels for stress reduction and critical temperature. Finite Elements in Analysis and Design 2009; 45: 845-51.
16. Naderi A, Saidi AR. On pre-buckling configuration of functionally graded Mindlin rectangular plates. Mechanics Research Com. 2010; 37: 535-8.
17. Panda Satyajit, Ray MC. Nonlinear finite element analysis of functionally graded plates integrated with patches of piezoelectric fiber reinforced composite. Finite Elements in Analysis and Design. 2008; 44: 493-504.
18. Casciaro R. An introduction to the computational asymptotic post-buckling analysis of slender elastic structures. University of Calabria, Italy. Department of Mechanical Engineering - Laboratory for Mechanics of Materials Graduate Course. 2001.
19. Reddy JN. Analysis of functionally graded plates. Int. J. Numer. Meth. Eng 2000; 47: 663-84.
20. Reddy JN. Mechanics of laminated composite plates and shells. CRC Press, London, 2004.
21. Samsam Shariata BA, Javaherib R BA, Eslami BA. Buckling of imperfect functionally graded plates under in-plane compressive loading. Thin-Walled Structures 2005; 43:1020-36.
22. Singha MK, Prakash T, Ganapathi M. Finite element analysis of functionally graded plates under transverse load. Finite Elements in Analysis and Design 2011; 47: 453-60.
23. Sohn K-J, Kim J-H. Structural stability of functionally graded panels subjected to aero-thermal loads, Composite Structures, 82, 2008, 317-325.
24. Tsung-Lin Wu, Shukla KK, Jin H Huang. Post-buckling analysis of functionally graded rectangular plates. Composite Structures 2007; 81: 1-10.
25. van der Heijden AMA. WT Koiter's Elastic Stability of Solids and Structures. (Proceedings of the Internation.) Cambridge University Press 1st edition. 2008.
26. Zagari G. Koiter's asymptotic numerical methods for shell structures using a corotational formulation. PhD Thesis Universitua della Calabria 2009. Dottorato di Ricerca in Meccanica Computazionale, XXII ciclo, Settore scientifico disciplinare ICAR-08.
27. Zhou D-G, Zhou Y-H. A theoretical analysis of FGM thin plate based on physical neutral surface. Computational Material Science 2008; 44: 716-20.

Zbigniew KOLAKOWSKI
Radosław J. MANIA
Jan GRUDZIECKI
Lodz University of Technology TUL
Department of Strength of Materials (K12)
PL - 90-924 Lodz, ul. Stefanowskiego 1/15, Poland
E-mail: zbigniew.kolakowski@p.lodz.pl

Appendix

The prebuckling solution to the FG plate consisting of homogenous fields is assumed as (see Eq. (17) in [8]):

$$\begin{aligned} u^{(0)} &= (\ell / 2 - x)\Delta \\ v^{(0)} &= y\Delta A_{12} / A_{22} \\ w^{(0)} &= 0 \end{aligned} \tag{A1}$$

where Δ is the actual loading. This loading of the zero state is specified as a product of the unit loading and the scalar load factor.

Taking into account relationship (5), inner sectional forces of the prebuckling (i.e., unbending) state for the assumed homogeneous field of displacements (A1) are expressed by the following relationships before the redistribution of forces in the plate due to plate deformations:

$$\begin{aligned} N_x^{(0)} &= -(A_{11} - A_{12}^2 / A_{22})\Delta \\ N_y^{(0)} &= 0 \\ N_{xy}^{(0)} &= 0 \\ M_x^{(0)} &= -(B_{11} - B_{12}A_{12} / A_{22})\Delta \\ M_y^{(0)} &= -(B_{12} - B_{22}A_{12} / A_{22})\Delta \\ M_{xy}^{(0)} &= 0 \end{aligned} \tag{A.2}$$

The assumed displacement field and the field of inner forces, corresponding to it for the prebuckling state, fulfil equilibrium equations for the zero state as an identity.

The omission of the displacements of the fundamental state implies that we ignore the difference between the configuration of the non-deformed state and the fundamental state and we may consequently regard the previously defined displacements $u^{(0)}, v^{(0)}$ as the additional ones from the fundamental state to the adjacent state.

The first order approximation, being the linear problem of stability, allows for determination of values of critical loads, buckling modes, and initial postbuckling equilibrium paths.

This publication is a result of the research works carried out within the project subsidized over the years 2011-2014 by the state funds designated for the National Science Centre (NCN UMO-2011/01/B/ ST8/07441).

Article citation info:
CAI L, ZHANG Z, CHENG Q, LIU Z, GU P. A geometric accuracy design method of multi-axis NC machine tool for improving machining accuracy reliability. Eksploatacja i Niezawodnosc – Maintenance and Reliability 2015; 17 (1): 143–155.

Ligang CAI
Ziling ZHANG
Qiang CHENG
Zhifeng LIU
Peihua GU

A GEOMETRIC ACCURACY DESIGN METHOD OF MULTI-AXIS NC MACHINE TOOL FOR IMPROVING MACHINING ACCURACY RELIABILITY

METODA PROJEKTOWANIA I POPRAWY NIEZAWODNOŚCI DOKŁADNOŚCI OBRÓBCZEJ WIELOOSIOWEJ OBRABIARKI NC WYKORZYSTUJĄCA POJĘCIE DOKŁADNOŚCI GEOMETRYCZNEJ

The reliability of machining accuracy is of great significance to performance evaluation and optimization design of the machine tools. Different geometric errors have various influences on the machining accuracy of the machine tools. The main emphasis of this paper is to propose a generalized method to distribute geometric accuracy of component for improving machining accuracy reliability under certain design requirements. By applying MBS theory, a comprehensive volumetric model explaining how individual errors in the components of a machine affect its volumetric accuracy (the coupling relationship) was established. In order to reflect the ability to reach the required machining accuracy, the concept of machining accuracy reliability is proposed in this paper. Based on advanced first order and second moment (AFOSM) theory, reliability and sensitivity with single failure modes were obtained and the model of machining accuracy reliability and the model of machining accuracy sensitivity with multiple failure modes were developed. By taking machining accuracy reliability as a measure of the ability of machine tool and taking machining accuracy sensitivity as a reference of optimizing the basic parameters of machine tools to design a machine tool, an accuracy distribution method of machine tools for improving machining accuracy reliability with multiple failure modes was developed and a case study example for a five-axis NC machine tool was used to demonstrate the effectiveness of this method. It is identified that each improvement of the geometric errors leads to a decrease in the maximum values and mean values of possibility of failure, and the gaps among reliability sensitivity of geometric parameter errors improved also decreased. This study suggests that it is possible to obtain the relationships between geometric errors and specify the accuracy grades of main feeding components of mechanical assemblies for improving machining accuracy reliability.

Keywords: *Machine tool; Geometric error; Accuracy distribution; Machining accuracy reliability; Multi-body system theory.*

Niezawodność w zakresie dokładności obróbki ma wielkie znaczenie dla oceny funkcjonowania oraz projektowania optymalizacyjnego obrabiarek. Różne błędy geometryczne mają różny wpływ na dokładność obrabiarek. Głównym celem niniejszej pracy jest zaproponowanie uogólnionej metody rozkładu dokładności geometrycznej elementów składowych obrabiarki, pozwalającej na poprawę niezawodności w zakresie dokładności obróbczej przy spełnieniu pewnych wymagań projektowych. Dzięki zastosowaniu teorii układów wielomasowych MBS, opracowano kompleksowy model wolumetryczny, który wyjaśnia, w jaki sposób pojedyncze błędy występujące w elementach składowych obrabiarki wpływają na jej dokładność wolumetryczną (relacja sprzężeń). Zaproponowane w prezentowanym artykule pojęcie niezawodności dokładności obróbki odnosi się do możliwości uzyskania przez urządzenie wymaganej dokładności obróbki W oparciu o zaawansowaną teorię estymacji momentów AFOSM (Advanced First Order and Second Moment therory), obliczono niezawodność i czułość dla przypadku wystąpienia pojedynczej przyczyny uszkodzenia oraz opracowano model niezawodności dokładności obróbki oraz model czułości dokładności obróbki dla przypadku wystąpienia wielu przyczyn uszkodzeń. Przyjmując niezawodność dokładności obróbki za miarę poprawnego działania obrabiarki oraz przyjmując czułość dokładności obróbki za punkt odniesienia dla optymalizacji projektowej podstawowych parametrów obrabiarek, opracowano metodę, opartą na rozkładzie dokładności obrabiarki, mającą na celu poprawę niezawodności dokładności obróbki dla przypadku wystąpienia wielu przyczyn uszkodzeń. Skuteczność metody wykazano na przykładzie pięcio-osiowej obrabiarki NC. Stwierdzono, że każda korekta błędu geometrycznego prowadzi do spadku maksymalnych i średnich wartości możliwości wystąpienia uszkodzenia oraz zmniejsza rozstęp między poszczególnymi czułościami niezawodnościowymi skorygowanych błędów parametrów geometrycznych. Przedstawione badania wskazują, że możliwe jest ustalenie związku pomiędzy błędami geometrycznymi oraz określenie stopni dokładności głównych elementów składowych zespołów mechanicznych odpowiedzialnych za ruch posuwowy obrabiarki w celu poprawy niezawodności dokładności obróbki.

Słowa kluczowe: *Obrabiarka; Błąd geometryczny; Rozkład dokładności; niezawodność dokładności obróbki; Teoria układów wielomasowych.*

1. Introduction

Machining accuracy is critical for the quality and performance of a mechanical product and is an important consideration for any manufacturer. It is influenced by machining errors belonging to several categories, e.g. geometric errors caused by mechanical-geometric imperfections, misalignments, wear of the linkages and elements of the machine tool structure, by the non-uniform thermal expansion of the machine structure, and static/dynamic load induced errors [8]. Geometric errors include pitch errors of the lead screws, straightness errors of the guide ways, angular errors of machine slides, and orthogonal error among machine axis [3]. Because its contribution to 30% of the total error so it is given special consideration through the configuration and allocation of appropriate dimensional errors in the design of machine tools with satisfactory machining accuracy [19]. Machine tools are usually made by several assembling parts, and the dimensional and geometric variations of each part have to be specified by tolerances which guarantee a certain level of quality in terms of satisfying functional requirements [20]. A as a result, the distribution of accuracy of machine tools is a problem of distribution of tolerances of these geometric errors. However, this practice of allocation has not been developed and applied in any systematic manner to the design of machine tools.

To enhance the machining accuracy of CNC machine tools, there are two steps included in the accuracy design. The first is accuracy prediction, which refers to forecasting volumetric errors of machine tools based upon the known accuracy for updated and maintained parts, and then predict the machining accuracy of work piece. The other is accuracy allocation, which is to obtain the accuracy of updated and maintained parts from the preset total accuracy of machine tools, and let the accuracy of parts reach optimal scheme [15]. Before accuracy distribution, a error modeling is crucial to maximize the performance of machine tools, and robust and accurate volumetric error modeling is also the first step to correct and compensate these errors [5], therefore, a model explaining how individual error of the components of a machine affect its volumetric accuracy is crucial to the accuracy distribution approach and it is one aspect of importance of this paper.

Geometric errors for each of the assembled parts and components are random variables; the machining errors caused by such errors are also random [40]. As a result, the dimensional and geometric variations for each error source are random and have to be specified by variance (or standard deviation) and the probabilistic nature of the errors produced on the dimensions of a manufactured part is taken into consideration in this paper. Uncertainty in parameters such as material, loading, geometry and the model exist in the process of structural design and optimization, and it results from data shortage, model simplification and human error [18]. Some of these errors can be reduced by collecting more data, with a better understanding of the problem and by implementing strict quality control; however, others such as deviations due to random events cannot be reduced by the above means [6]. To solve this problem, two main philosophies dealing with the uncertain deviations exist: 'Deterministic Structural Optimization' (DSO) uses safety-factors to accomplish the safety, while 'Reliability-Based Structural Optimization' (RBSO) takes the random character of the variables into consideration [27]. Reliability-based design optimization simulates all the uncertain variables to the random variables or random process and minimizes an objective function under probabilistic constraints. The reliability of machine tool reflects the ability to perform its specified functions under the stated conditions for a given period of time and it is often studied by possibility of failure [26], so accuracy distribution based on the reliability theory can maintain and improve the level of quality in terms of satisfying functional requirements while keeping the maximum tolerances of these geometric errors. As a result, the development of a systematic method to realize accuracy distribution of machine tool based on reliability theory according to failure modes for improving machining accuracy reliability is the second very important aspect of this paper.

The rest of this study is organized as follows: In Section 2, the review of accuracy design of machine tool is given. Section 3 explains the process of modeling machining tool geometric errors. Section 4 presents the proposed method to realize accuracy distribution of machine tool. A case study is accomplished as an example in Section 5. The conclusions are presented in the last Section.

2. Accuracy Design of NC Machine Tool

2.1. Accuracy prediction

Up to present, there are many researches on the error modeling technique to show the difference between the actual response of a machine to a command issued according to the accepted protocol of that machine's operation and the response to that command anticipated by that protocol [9]. The development of modeling methods has been experienced many years and it turns out to be various kinds such as matrix translation method, error matrix method, rigid body kinematic, D-H method, model methods based on the multi-body system kinematics theory and so on. In 1973 Love and Scarr obtained the combined effects of the elemental errors in the machine tool and then developed the volumetric errors of a multi-axis machine by using the trigonometric technique [25]. In 1977 a matrix translation method was reported and a calibration technique using three-dimensional metrology on a coordinate measuring machine (CMM) was presented by Hocken et al. [13]. In 1981 Dufour and Groppetti reported the "error matrix" method to obtain error predictions by interpolation between the stored values [10]. In 1982 Portman used rigid body kinematics to evolve an expression for the geometric error of a mechanism [30]. In 1991, Kiriden developed a general model to understand the effects of component geometric errors on the kinematic chain of a machine and the volumetric errors in the work space [21]. In 1993, they used the D–H convention to develop kinematic models for three types of machine. In 1995 a method based on direct consideration of the shape and joint transformations was put forward by Srivastava et al. [33]. In 2007 Bohez et al. presented a new method to identify and compensate the systematic errors in a multi-axis machine tool [1]. In recent years, multi-body system (MBS) theory is used to generalize and provide a unique systematic approach for its advantages such as stylization, normalization, versatility, and ease for computer modeling [36]. There are many investigators have carried out error modeling research for complicated machinery system using MBS [41, 23, 44, 39], mainly focus on designing and constructing a model to determine geometric error of machine tool and developing the key technique for compensation-identifying geometric error parameters.[43, 17, 4, 7, 22, 2, 11] introduce the methods of geometric error compensation, thermal error modeling, position error compensation, position-independent geometric errors modeling, volumetric error modeling and sensitivity analysis and establishing a product of exponential(POE) model for geometric error integration.

2.2. Accuracy allocation

In earlier years, many researches focused their attention to obtain the tolerance allocation on structural design. In 2005 Prabhaharan et al. introduced a kind of metaheuristic approach as an optimization tool for minimizing the critical dimension deviation and allocating the cost-based optimal tolerances [29]. In 2006 Huang and Shiau obtained the optimized tolerance allocation of a sliding vane rotary compressor's components for the required reliability with the minimum cost and quality loss [16]. In 2007 Huang and Zhong established the sequential linear optimization models based on the process capabilities to release the working tolerances, reduce manufacturing costs [14]. Siva Kumar and Stalin [31] used Lagrange multiplier method to simultaneously allocate both design and manufacturing tolerances based on minimum total manufacturing cost. Isabel González et al. [12] developed a methodology to allow an automatic tolerance allocation capable of minimizing manufacturing costs based on statistical approach. Muthu et al. [28] used metaheuristic method to balance the manufacturing cost and quality loss to achieve near optimal design and process tolerances simultaneously for minimum combined manufacturing cost and quality loss over the life of the product. In 2010 K. Sivakumar, et al proposed a novel multi-objective optimization method to enhance the operations of the non-traditional algorithms and Multi-Objective Particle Swarm Optimization and systematically distribute the tolerances among various the components of mechanical assemblies [32]. From the above literature, the previous researches on tolerance allocation mainly focus on structural design taking manufacturing cost or manufacturing process into consideration, besides, there are many of accuracy allocation in the field of hull construction, robotics, military application, and instruments [35, 24, 37, 42, 34]. However, works on accuracy allocation of multi-axis machine tools are few. Reliability is a specification to measure the ability of machine tool to overcome a certain functions and reliability sensitivity reflects the influence of basic parameters to the possibility of failure, so reliability theory plays an important role in accuracy allocation of NC machine tools by determining the levels for these geometric parameter errors, what's more, multi-axis NC machine tools composed of various parts are complex structures and so they have multiple failure modes. In 1994 Dorndorf U proposed an error allocation approach to optimize allocation of manufacturing and assembly tolerances along with specifying the operating conditions to determine the optimal level for these errors so that the cost is minimized [9], it is regardless of reliability sensitivity and the model is a two-axis machine. In 2013 Yu proposed a geometric error propagation model and reliability approximately model to by response surface method with error samples and improved the functions of machine tools by optimization of the sensitivity [40] with single failure model. As a result, the continuous effort lies on accuracy allocation of NC machine tools taking machining accuracy reliability and sensitivity with multiple failure modes into consideration.

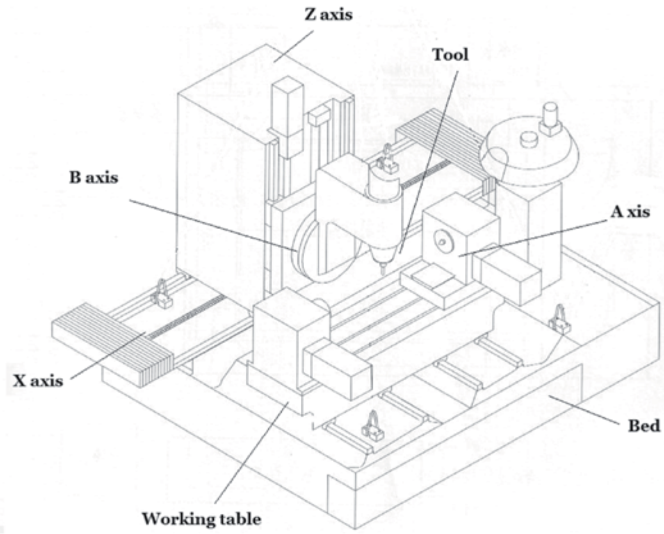

Fig. 1. The 3-dimension digital structure model of the NC machine tool

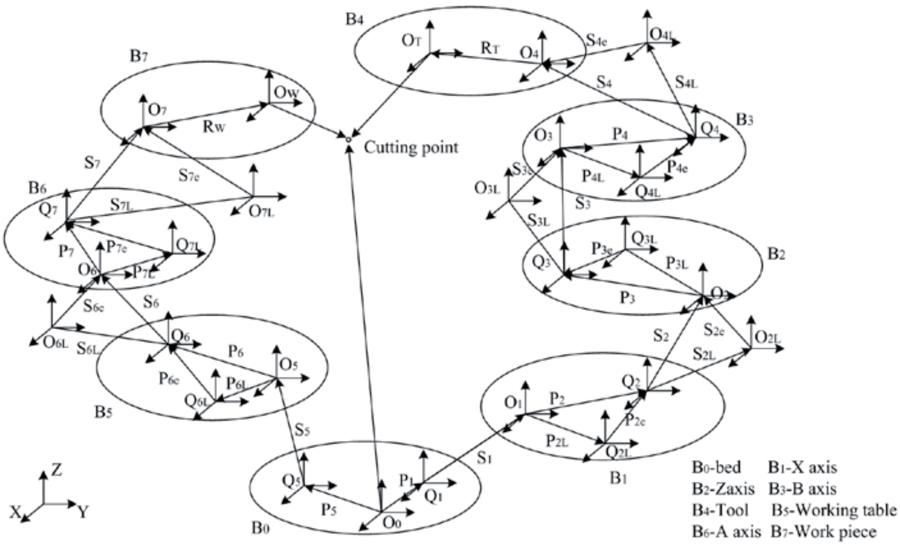

Fig. 2. The coordinate system structure diagram

Table 1 Lower body array of five-axis NC machine tool

Topic body j	1	2	3	4	5	6	7
$L^0(j)$	1	2	3	4	5	6	7
$L^1(j)$	0	1	2	3	0	5	6
$L^2(j)$	0	0	1	2	0	0	0
$L^3(j)$	0	0	0	1	0	0	0
$L^4(j)$	0	0	0	0	0	0	0
$L^5(j)$	0	0	0	0	0	0	0
$L^6(j)$	0	0	0	0	0	0	0

3. Error modeling of NC machine tool

There are two important aspects in this study: the first is the development of a systematic approach to obtain geometric/kinematic errors on the kinematic chain of a machine tool. Another aspect, considered more important, is the proposing of the concept of machining accuracy reliability and the addressing a reliability and sensitivity analysis method in the multiple failure modes to realize the distribution of the standard deviation for the geometric errors.

A method called MBS is used to establish a machine tool geometric/kinematic error model showing the relation between the individual error of the components of a machine, and its volumetric accuracy is crucial to the allocation of standard deviation for the geometric parameter errors. In this paper, a 5-axis machine tool is used to analyze geometric errors and the geometric/kinematic error model is developed. This XKH1600 five-axis machining center is designed for leaf blade machining, configured as three linear axes X, Y, Z axes and two rotary axes A, B axis. The 3-dimension digital structure model of the machine tool is shown in Figure 1.

Taking the error factors and coupling relations of the various parts into consideration, based on the MBS theory, the five-axis machine tool can be abstracted into a multi-body system. The coordinate system structure diagram is shown in Figure 2. The error model between B_K and B_j revealed, when the displacement and the displacement error are zero, O_k and Q_k coincide, q_k refers to the initial position vector between O_j (B_j 's origin) and O_k (B_K 's origin), and q_{ke} is the position error vector, including load error and thermal error. S_k is the displacement vector between B_K and B_j , and S_{ke} is the displacement error vector, including geometric error and dynamic error. When there is a displacement in one part or component of a machine tool, this displacement is the position increment. The lower body array is listed in Table 1.

$$\mathbf{P}_t = \begin{bmatrix} P_{tx} & P_{ty} & P_{tz} & 1 \end{bmatrix}^T \tag{1}$$

The work-piece forming point in the work-piece coordinate system coordinate is:

$$\mathbf{P}_w = \begin{bmatrix} P_{wx} & P_{wy} & P_{wz} & 1 \end{bmatrix}^T \tag{2}$$

When the machine tool moves in ideal form, that means the machine tool is without error, the ideal forming function of tool forming point in work-piece coordinate system is:

$$\left(\prod_{k=n,L^n(t)=0}^{k=1} \boldsymbol{T}^P_{L^k(t)L^{k-1}(t)} T^S_{L^k(t)L^{k-1}(t)} \right) \boldsymbol{P}_t = \left(\prod_{u=n,L^n(w)=0}^{u=1} \boldsymbol{T}^P_{L^u(w)L^{u-1}(w)} \boldsymbol{T}^S_{L^u(w)L^{u-1}(w)} \right) \boldsymbol{P}_w \tag{3}$$

In this paper, the ideal forming function of tool forming point of this five-axis machine tool is:

$$\begin{aligned} \boldsymbol{P}_t &= \left(\prod_{k=n,L^n(t)=0}^{k=1} \boldsymbol{T}^P_{L^k(t)L^{k-1}(t)} T^S_{L^k(t)L^{k-1}(t)} \right)^{-1} \left(\prod_{u=n,L^n(w)=0}^{u=1} \boldsymbol{T}^P_{L^u(w)L^{u-1}(w)} \boldsymbol{T}^S_{L^u(w)L^{u-1}(w)} \right) \boldsymbol{P}_w \\ &= \begin{pmatrix} 1 & 0 & 0 & -x_t \\ 0 & 1 & 0 & -y_t \\ 0 & 0 & 1 & -z_t \\ 0 & 0 & 0 & 1 \end{pmatrix} \begin{pmatrix} -\cos\varphi & \sin\varphi & 0 & 0 \\ -\sin\varphi & -\cos\varphi & 0 & 0 \\ 0 & 0 & 1 & 0 \\ 0 & 0 & 0 & 1 \end{pmatrix} \begin{pmatrix} 1 & 0 & 0 & 0 \\ 0 & -\cos A & \sin A & 0 \\ 0 & -\sin A & -\cos A & 0 \\ 0 & 0 & 0 & 1 \end{pmatrix} \\ &\quad \begin{pmatrix} 1 & 0 & 0 & 0 \\ 0 & 1 & 0 & 0 \\ 0 & 0 & 1 & -z \\ 0 & 0 & 0 & 1 \end{pmatrix} \begin{pmatrix} 1 & 0 & 0 & 0 \\ 0 & 1 & 0 & -y \\ 0 & 0 & 1 & 0 \\ 0 & 0 & 0 & 1 \end{pmatrix} \begin{pmatrix} 1 & 0 & 0 & x \\ 0 & 1 & 0 & 0 \\ 0 & 0 & 1 & 0 \\ 0 & 0 & 0 & 1 \end{pmatrix} \\ &\quad \begin{pmatrix} -\cos B & 0 & -\sin B & 0 \\ 0 & 1 & 0 & 0 \\ \sin B & 0 & -\cos B & 0 \\ 0 & 0 & 0 & 1 \end{pmatrix} \begin{pmatrix} 1 & 0 & 0 & x_{wd} \\ 0 & 1 & 0 & y_{wd} \\ 0 & 0 & 1 & z_{wd} \\ 0 & 0 & 0 & 1 \end{pmatrix} \boldsymbol{P}_w \end{aligned} \tag{4}$$

Machining accuracy is determined by relative displacement error between the tool forming point of machine and work-piece. During the actual machining process, the actual position of cutting tool point will inevitably deviate from the ideal location, which results in volumetric error. Table 2 lists the characteristic matrices of this 5-axis CNC machining center, including body ideal static, motion characteristic matrix ($\boldsymbol{T}^P_{L^k(t)L^{k-1}(t)}, T^S_{L^k(t)L^{k-1}(t)}$) and body static, kinematic error characteristic matrix ($\Delta\boldsymbol{T}^P_{L^k(t)L^{k-1}(t)}, \Delta T^S_{L^k(t)L^{k-1}(t)}$).As a result, the comprehensive volumetric error caused by the gap between actual point and ideal point in this paper can be written as:

$$\begin{aligned} E &= \left[\prod_{u=n,L^n(7)=0}^{u=5} T^P_{L^u(7)L^{u-1}(7)} \Delta T^P_{L^u(7)L^{u-1}(7)} T^S_{L^u(7)L^{u-1}(7)} \Delta T^S_{L^u(7)L^{u-1}(7)} \right] P_w - \left[\prod_{u=n,L^n(4)=0}^{u=1} T^P_{L^u(4)L^{u-1}(4)} \Delta T^P_{L^u(4)L^{u-1}(4)} T^S_{L^u(4)L^{u-1}(4)} \Delta T^S_{L^u(4)L^{u-1}(4)} \right] p_t \\ &= T^P_{05}\Delta T^P_{05} T^S_{05} \Delta T^S_{05} T^P_{56} T^S_{56} \Delta T^S_{56} T^P_{67} \Delta T^P_{67} T^S_{67} P_w - T^P_{01} T^S_{01} \Delta T^S_{01} T^P_{12} \Delta T^P_{12} T^S_{12} \Delta T^S_{12} T^S_{23} \Delta T^P_{23} \Delta T^S_{23} T^P_{34} \Delta T^P_{34} p_t \end{aligned} \tag{5}$$

In the above equation, the values and means of the expressions such as T^P_{05} , ΔT^P_{05} , T^S_{05} , ΔT^S_{05} and so on can be obtained from Table 2.

4. Accuracy allocation based on Reliability Theory

In Section 3, the development of a systematic approach to obtain geometric/kinematic errors on the kinematic chain of a machine tool has been finished. As a result, the concept of machining accuracy reliability should be proposed, besides, a reliability and sensitivity analysis method with multiple failure modes for improving machining accuracy reliability to realize the geometric errors allocation should be addressed.

4.1. The concept of Machining Accuracy Reliability and AFOSM Theory

The reliability of structure reflects the ability to perform its specified functions under the stated conditions for a given period of time and it is often studied by possibility of failure. In order to reflect the ability of machine tools to reach the required machining accuracy, machining accuracy reliability is proposed in this paper and can be defined as possibility of fulfilling the specified machining accuracy, expressed by the possibility of failure of machine accuracy. Besides, the probabilistic nature of the errors produced on the dimensions of a manufactured part is taken into consideration in this paper. In order to develop an approach to obtain the machining accuracy reliability and sensitivity of this five-axis machine tool, there is an assumption that the errors produced on a dimension are drawn from a Gaussian distribution. Our task of error allocation is therefore to determine the optimal levels for these geometric parameter errors according to the machining accuracy reliability. In order to overcome this task, Advanced First Order and Second Moment (AFOSM) theory is introduced at first.

Supposing that there is a performance function $Z = g(x_1, x_2, \ldots, x_n)$, with some uncorrelated parameters $x_i \sim N(\mu_{x_i}, \sigma_{x_i})$, which are subject to random variation about their nominal values, let the functional requirements be of the form Z=0 (limit state equation) which divides the parameter space into two regions, one a failure domain can be expressed as $F = \{T : g(x) \le 0\}$ and the other is the safe domain.

Supposing that there is a design point (the most possibility failure point) $\boldsymbol{P}^*(x_1^*, x_2^*, ..., x_n^*)$ in the failure domain, then $g(x_1^*, x_2^*, ..., x_n^*) = 0$ is obtained and $G_i = g(x_1^*, x_2^*, ..., x_n^*) + \sum_{i=1}^{n} (\frac{\partial g}{\partial x_i})_{\mathrm{p}^*} (x_i - x_i^*)$ can be developed to represent the linear part as to $Z = g(x_1, x_2, \ldots, x_n)$ by Taylor, so the performance equation is $\sum_{i=1}^{n} (\frac{\partial g}{\partial x_i})_{\mathrm{p}^*} (x_i - x_i^*)$ =0.

Suppose $\mu_z = \sum_{i=1}^{n} (\mu_{x_i} - x_i^*)(\frac{\partial g}{\partial x_i})_{\mathrm{p}^*}$, $\sigma_z^2 \approx \sum_{i=1}^{n} [(\frac{\partial g}{\partial x_i})_{\mathrm{p}^*} \sigma_{x_i}]^2$,

$\alpha_i = \dfrac{(\frac{\partial g}{\partial x_i})_{\mathrm{p}^*} \sigma_{x_i}}{\{\sum_{i=1}^{n} [(\frac{\partial g}{\partial x_i})_{\mathrm{p}^*} \sigma_{x_i}]^2\}^{1/2}}$, $(i = 1, 2, ..., n)$ which refers to the Sensi-

Table 2. Characteristic matrices of the 5-axis NC machining center

adjacent body	Body ideal static, motion characteristic matrix ($T^P_{L^k(t)L^{k-1}(t)}$, $T^S_{L^k(t)L^{k-1}(t)}$)	Body static, kinematic error characteristic matrix ($\Delta T^P_{L^k(t)L^{k-1}(t)}$, $\Delta T^S_{L^k(t)L^{k-1}(t)}$)
0-1 X axis	$T_{01P}=I_{4\times4}$ $T_{01s}=T_{01s(x)}=\begin{pmatrix}1&0&0&x\\0&1&0&0\\0&0&1&0\\0&0&0&1\end{pmatrix}$	$\Delta T_{01s}=\begin{pmatrix}1&-\Delta\gamma_x&\Delta\beta_x&\Delta x_x\\\Delta\gamma_x&1&-\Delta\alpha_x&\Delta y_x\\-\Delta\beta_x&\Delta\alpha_x&1&\Delta z_x\\0&0&0&1\end{pmatrix}$
1-2 Z axis	$T_{12P}=I_{4\times4}$ $T_{12s}=T_{12s(z)}=\begin{pmatrix}1&0&0&0\\0&1&0&0\\0&0&1&z\\0&0&0&1\end{pmatrix}$	$\Delta T_{12p}=\begin{pmatrix}1&0&\Delta\beta_{xz}&0\\0&1&-\Delta\alpha_{yz}&0\\-\Delta\beta_{xz}&\Delta\alpha_{yz}&1&0\\0&0&0&1\end{pmatrix}$ $\Delta T_{12s}=\begin{pmatrix}1&-\Delta\gamma_z&\Delta\beta_z&\Delta x_z\\\Delta\gamma_z&1&-\Delta\alpha_z&\Delta y_z\\-\Delta\beta_z&\Delta\alpha_z&1&\Delta z_z\\0&0&0&1\end{pmatrix}$
2-3 B axis	$T_{23P}=I_{4\times4}$ $T_{23s}=\begin{pmatrix}\cos B&0&\sin B&0\\0&1&0&0\\-\sin B&0&\cos B&0\\0&0&0&1\end{pmatrix}$	$\Delta T_{23p}=\begin{pmatrix}1&-\Delta\gamma_{yb}&0&0\\\Delta\gamma_{yb}&1&-\Delta\alpha_{yb}&0\\0&\Delta\alpha_{yb}&1&0\\0&0&0&1\end{pmatrix}$ $\Delta T_{23s}=\begin{pmatrix}1&-\Delta\gamma_B&\Delta\beta_B&\Delta x_B\\\Delta\gamma_B&1&-\Delta\alpha_B&\Delta y_B\\-\Delta\beta_B&\Delta\alpha_B&1&\Delta z_B\\0&0&0&1\end{pmatrix}$
3-4 Tool	$T_{34p}=\begin{pmatrix}1&0&0&x_{td}\\0&1&0&y_{td}\\0&0&1&z_{td}\\0&0&0&1\end{pmatrix}$ $T_{34S}=I_{4\times4}$	$\Delta T_{34p}=\begin{pmatrix}1&-\Delta\gamma_{td}&\Delta\beta_{td}&\Delta x_{td}\\\Delta\gamma_{td}&1&-\Delta\alpha_{td}&\Delta y_{td}\\-\Delta\beta_{td}&\Delta\alpha_{td}&1&\Delta z_{td}\\0&0&0&1\end{pmatrix}$ $T_{34P}=I_{4\times4}$
0-5 Y axis	$T_{05P}=I_{4\times4}$ $T_{05s}=\begin{pmatrix}1&0&0&0\\0&1&0&y\\0&0&1&0\\0&0&0&1\end{pmatrix}$	$\Delta T_{05p}=\begin{pmatrix}1&-\Delta\gamma_{xy}&0&0\\\Delta\gamma_{xy}&1&0&0\\0&0&1&0\\0&0&0&1\end{pmatrix}$ $\Delta T_{05s}=\begin{pmatrix}1&-\Delta\gamma_y&\Delta\beta_y&\Delta x_y\\\Delta\gamma_y&1&-\Delta\alpha_y&\Delta y_y\\-\Delta\beta_y&\Delta\alpha_y&1&\Delta z_y\\0&0&0&1\end{pmatrix}$
5-6 A axis	$T_{56P}=I_{4\times4}$ $\mathrm{T}_{56s}=\begin{bmatrix}1&0&0&0\\0&\cos A&-\sin A&0\\0&\sin A&\cos A&0\\0&0&0&1\end{bmatrix}$	$\Delta T_{56\mathrm{p}}=\begin{bmatrix}1&-\Delta\gamma_{ya}&\Delta\beta_{xa}&0\\\Delta\gamma_{ya}&1&0&0\\-\Delta\beta_{xa}&0&1&0\\0&0&0&1\end{bmatrix}$ $\Delta T_{56\mathrm{s}}=\begin{bmatrix}1&-\Delta\gamma_a&\Delta\beta_a&\Delta x_a\\\Delta\gamma_a&1&-\Delta\alpha_a&\Delta y_a\\-\Delta\beta_a&\Delta\alpha_a&1&\Delta z_a\\0&0&0&1\end{bmatrix}$
6-7 Work piece	$T_{67p}=\begin{pmatrix}1&0&0&x_{wd}\\0&1&0&y_{wd}\\0&0&1&z_{wd}\\0&0&0&1\end{pmatrix}$ $T_{67P}=I_{4\times4}$	$\Delta T_{67p}=\begin{pmatrix}1&-\Delta\gamma_{wd}&\Delta\beta_{wd}&\Delta x_{wd}\\\Delta\gamma_{wd}&1&-\Delta\alpha_{wd}&\Delta y_{wd}\\-\Delta\beta_{wd}&\Delta\alpha_{wd}&1&\Delta z_{wd}\\0&0&0&1\end{pmatrix}$

tivity coefficient, reflecting the influence of the random parameter x_i acting on the σ_z, so $\sigma_z = (\frac{\partial g}{\partial x_i})_{p^*} \sigma_{x_i}\alpha_i$, and then the reliability index and the possibility of failure are obtained as follows[26]:

$$\beta = \frac{\mu_z}{\sigma_z} = \frac{\sum_{i=1}^{n}(\mu_{x_i} - x_i^*)(\frac{\partial g}{\partial x_i})_{p^*}}{(\frac{\partial g}{\partial x_i})_{p^*} \sigma_{x_i}\alpha_i} \tag{6}$$

$$P_f = \Phi(-\beta) \tag{7}$$

Compare with machining accuracy reliability as a specification to measure the ability of machine tool to overcome a certain functions, machining accuracy sensitivity reflects the influence of basic parameters to the possibility of failure, which can be used for improving and optimizing the basic parameters of machine tool. As a result, machining accuracy sensitivity plays an important role in determining the levels for these geometric parameter errors. Based on the AFOSM theory, the performance function $Z = g(x_1, x_2, \dots, x_n)$ can be changed: into the following equation at the design point $\boldsymbol{P}^*(x_1^*, x_2^*, ..., x_n^*)$,

$$g \approx g(x_1^*, x_2^*, ..., x_n^*) + \sum_{i=1}^{n}(\frac{\partial g}{\partial x_i})_{p^*}(x_i - x_i^*)$$

Suppose $c_0 = g(x_1^*, x_2^*, ..., x_n^*) - \sum_{i=1}^{n}(\frac{\partial g}{\partial x_i})_{p^*} x_i^*$, $c_i = (\frac{\partial g}{\partial x_i})_{p^*}$,

Then,

$$g(x) \approx G(x) = c_0 + \sum_{i=1}^{n} c_i x_i$$

In this way, $\beta = \frac{\mu_G}{\sigma_G} = \frac{c_0 + \sum_{i=1}^{n} c_i \mu_{x_i}}{\sqrt{\sum_{i=1}^{n} c_i^2 \sigma_{x_i}^2}}$ and $P_f = \Phi(-\beta)$ are obtained.

From the following equations, the reliability sensitivity can be obtained as follows:

$$\frac{\partial P_f}{\partial \sigma_{x_i}} = \frac{\partial P_f}{\partial \beta}\frac{\partial \beta}{\partial \sigma_{x_i}} = -\frac{c_i^2 \sigma_{x_i}^2 \mu_G}{\sqrt{2\pi}\sigma_G^3}\exp[-\frac{1}{2}(\frac{\mu_G}{\sigma_G})^2] \tag{8}$$

4.2. An AFOSM Reliability and Sensitivity Analysis Method with Multiple Failure Modes

Failure mode is critical to the reliability of any structure. The number of limit state equations divides failure mode into two parts: single failure mode and multiple failure modes. Single failure mode which means that there is only one limit state equation in the whole system or structure, in contract, multiple failure modes refers to multiple limit state equations in the system and its complexes lies in the logical relationship, correlation coefficient and joint probability density of a system or a structure with multiple failure modes[38]. According to the logical relationship with the failure modes of a machine tool, this machine tool has multiple failure modes and so it is a serial system. As a result, this paper aims to the reliability and sensitivity analysis of such serial system.

4.2.1. The Narrow Bounds Method

The narrow bounds is the main method used for the reliability and sensitivity analysis of a serial system though it fails to obtain the certain valves of reliability and sensitivity, as a result, it is used for verification of the method introduced in this paper.

Supposing that there are "m" failure modes, the reliability P {F} and the reliability sensitivity $\frac{\partial P\{F\}}{\partial \sigma_{x_i}}$ based on AFOSM Theory are expressed as follows [9]:

$$P\{F\} \subseteq [P\{F_1\} + \sum_{2}^{m}\max[P\{F_i\} - \sum_{j=1}^{i-1}P\{F_i \cap F_j\};0], \sum_{i=1}^{m}P\{F_i\} - \sum_{i=2}^{m}\max(j<i)P\{F_i \cap F_j\}] \tag{9}$$

$$\frac{\partial P\{F\}}{\partial \sigma_{x_i}} = \sum_{j=1}^{n}[f(\beta_j)\frac{\partial(\beta_j)}{\partial \sigma_{x_i}}(-1)] + \sum_{j=2}^{n}\sum_{k=1}^{j-1}[{}^{(3)}\tau_{jk}[{}^{(1)}\tau_{jk}({}^{(4)}\tau_{jk}\cdot{}^{(4)}\zeta_{\sigma_{x_i}} + {}^{(5)}\tau_{jk}\cdot{}^{(5)}\zeta_{\sigma_{x_i}}) + {}^{(2)}\tau_{jk}\cdot{}^{(2)}\zeta_{\sigma_{x_i}}]] \tag{10}$$

In the above expressions, F_i and F_j are the events of failing with respect to the Z_i and Z_j condition respectively.

$P(F_i) = \Phi(-\beta_i)\Phi(-\frac{\beta_j - \rho_{ij}\beta_i}{\sqrt{1-\rho_{ij}^2}})$, $P(F_j) = \Phi(-\beta_j)\Phi(-\frac{\beta_i - \rho_{ij}\beta_j}{\sqrt{1-\rho_{ij}^2}})$,

$\rho_{ij} = \frac{q_i q_j Cov(g_i, g_j)}{\sqrt{Var[g_i]}\sqrt{Var[g_j]}}$, β_i and β_j are the reliability indices with respect to the ith and jth failure conditions respectively, and ρ_{ij} is the correlation between the two failure conditions, q_i is positive when Z>0 and is negative when Z≤0.

$${}^{(2)}\zeta_{\sigma_{x_i}} = {}^{(4)}\zeta_{\sigma_{x_i}} + {}^{(5)}\zeta_{\sigma_{x_i}},$$

$${}^{(4)}\zeta_{\sigma_{x_i}} = \phi(-\beta_j)\frac{\partial}{\partial \sigma_{x_i}}(-\beta_j)\Phi(-u_{jk}) + \phi(-u_{jk})\frac{\partial}{\partial \sigma_{x_i}}(-u_{jk})\Phi(-\beta_j)$$

$${}^{(5)}\zeta_{\sigma_{x_i}} = \phi(-\beta_k)\frac{\partial}{\partial \sigma_{x_i}}(-\beta_k)\Phi(-v_{jk}) + \phi(-v_{jk})\frac{\partial}{\partial \sigma_{x_i}}(-v_{jk})\Phi(-\beta_k),$$

$$\phi(t) = \frac{1}{\sqrt{2\pi}}e^{-\frac{1}{2}t^2},$$

$$\frac{\partial \beta_j}{\partial \sigma_{x_i}} = \frac{\left(c_0 + \sum_{i=1}^{n} c_i \mu_{x_i}\right) c_i^2 \sigma_{x_i}}{[\sum_{i=1}^{n} c_i^2 \sigma_{x_i}^2]^{3/2}}, \quad u_{ij} = \frac{\beta_j - \beta_i \rho_{ij}}{\sqrt{1-\rho_{ij}^2}}, \quad v_{ij} = \frac{\beta_i - \beta_j \rho_{ij}}{\sqrt{1-\rho_{ij}^2}},$$

$${}^{(1)}\tau_{jk} = \begin{cases} 1 & \tau_{jk} \ge 0 \\ 0 & \tau_{jk} < 0 \end{cases},$$

$${}^{(2)}\tau_{jk} = \begin{cases} 0 & \tau_{jk} \ge 0 \\ 1 & \tau_{jk} < 0 \end{cases},$$

$${}^{(1)}\tau_{jk} + {}^{(2)}\tau_{jk} = 1$$

$${}^{(3)}\tau_{jk} = \begin{cases} 1 & if\ P_{fjk} = \max(k<j) P_{fjk} \\ 0 & otherwise \end{cases}$$

$${}^{(4)}\tau_{jk} = \begin{cases} 1 & if\ \Phi(-\beta_j)\Phi(-u_{jk}) \ge \Phi(-\beta_k)\Phi(-v_{jk}) \\ 0 & otherwise \end{cases}$$

$${}^{(5)}\tau_{jk} = \begin{cases} 1 & if\ \ \Phi(-\beta_k)\Phi(-v_{jk}) > \Phi(-\beta_j)\Phi(-u_{jk}) \\ 0 & otherwise \end{cases}$$

$${}^{(4)}\tau_{jk} + {}^{(5)}\tau_{jk} = 1$$

4.2.2. A Method for Reliability and Sensitivity Analysis with Multiple Failure Modes

For the failure to obtain the certain valves of the reliability and sensitivity by the narrow bounds, a method used for reliability and sensitivity analysis with multiple failure modes was introduced in this paper and the solution procedure roughly follows the approach developed by[38].

Given that there are "m" multiple failure modes in a system, the calculation of its possibility of failure is to obtain the integration of a multidimensional normal joint distribution. As a result, the possibility of failure of a serial structure with multiple failure modes is given by:

$$P\{F\}=P(\bigcup_{i=1}^{m} F_i < 0)=1\text{-}\Phi(\beta;\rho)=1\text{-}\int_{-\infty}^{\beta_1}\int_{-\infty}^{\beta_2}\ldots\int_{-\infty}^{\beta_m} \varphi_m(m;\rho)dm_1 dm_2 \ldots dm_m \tag{11}$$

As to a general serial system, the possibility of failure can be expressed as follows:

$$P\{F\} = P\{(F_1 \le 0) \bigcup (F_2 \le 0) \bigcup \ldots \bigcup (F_m \le 0)\} \tag{12}$$

In order to calculate the equation (12), the correlation coefficient is proposed to show the correlation with multiple failure modes. If there are two failure modes, the possibility of failure can be expressed as follows:

$$P\{F_{12}\} = (F_1 \bigcup F_2) = P(F_1) + P(F_2) - P(F_1 \bigcap F_2) = P(F_1) + P(F_2) - P(F_1 F_2) \tag{13}$$

Supposing $P(F_1 F_2) = \alpha_{12} P(F_2)$, α_{12} is the correlation coefficient of these two failure modes. As a result, $P\{F_{12}\} = P(F_1) + P(F_2) - \alpha_{12} P(F_2) = P(F_1) + (1-\alpha_{12}) P(F_2)$ and the possibility of failure with three failure modes can be given by:

$$\begin{aligned} P(F_{123}) &= P(F_1 \bigcup F_2 \bigcup F_3) = P(F_{12} \bigcup F_3) \\ &= P(F_{12}) + P(F_3) - \alpha_{123} P(F_3) = P(F_{12}) + (1-\alpha_{123}) P(F_3) \end{aligned} \tag{14}$$

In a similar way, the possibility of failure with "m" multiple failure modes in a serial system can be obtained by:

$$\begin{aligned} P(F) &= P(F_{12\ldots m-1}) + (1-\alpha_{12\ldots m}) P(F_m) \\ &= P(F_1) + (1-\alpha_{12}) P(F_2) + (1-\alpha_{123}) P(F_3) + \ldots + (1-\alpha_{12\ldots m}) P(F_m) \end{aligned} \tag{15}$$

In the equation (15), $\alpha_{ij} \approx \Phi(\frac{-\beta_i + \rho_{ij}\Upsilon_j}{\sqrt{1-\rho_{ij}^2 \Upsilon_j(-\beta_j + \Upsilon_j)}})$, $\Upsilon_j = \frac{\varphi(-\beta_j)}{\Phi(-\beta_j)}$.

Up to now, the possibility of failure with "m" multiple failure modes is obtained and the next work is to focus attention on the calculation of reliability sensitivity. For lack of space, a description of the complete theoretical analysis is avoided and only a conceptual description and important results are given.

$$\begin{aligned} \frac{\partial P(F)}{\partial \sigma_{x_i}} &= \frac{\partial P(F_1)}{\partial \sigma_{x_i}} + (1-\alpha_{12}) \frac{\partial P(F_2)}{\partial \sigma_{x_i}} + (-P(F_2)) \frac{\partial \alpha_{12}}{\partial \sigma_{x_i}} + (1-\alpha_{123}) \frac{\partial P(F_3)}{\partial \sigma_{x_i}} \\ &+ (-P(F_3)) \frac{\partial \alpha_{123}}{\partial \sigma_{x_i}} + \ldots + (1-\alpha_{12\ldots m}) \frac{\partial P(F_m)}{\partial \sigma_{x_i}} + (-P(F_m)) \frac{\partial \alpha_{12\ldots m}}{\partial \sigma_{x_i}} \end{aligned} \tag{16}$$

In the equation (16), $\frac{\partial P(F_i)}{\partial \sigma_{x_i}}$ can be obtain by equation(8) and $\frac{\partial \alpha_{ij}}{\partial \sigma_{x_i}} = \phi(\beta_{ij}) \frac{\partial \beta_{ij}}{\partial \sigma_{x_i}}$, $\Xi_j = \Upsilon_j(-\beta_j + \Upsilon_j)$,

$$\frac{\partial \beta_{ij}}{\partial \sigma_{x_i}} = \frac{1}{\sqrt{1-\rho_{ij}^2 \Xi_j}} (\frac{\partial \beta_i}{\partial \sigma_{x_i}} + \rho_{ij} \frac{\partial \Upsilon_j}{\partial \sigma_{x_i}}) + \frac{-\beta_i + \rho_{ij}\Upsilon_j}{2(1-\rho_{ij}^2 \Xi_j)^{\frac{3}{2}}} \rho_{ij}^2 \frac{\partial \Xi_j}{\partial \sigma_{x_i}},$$

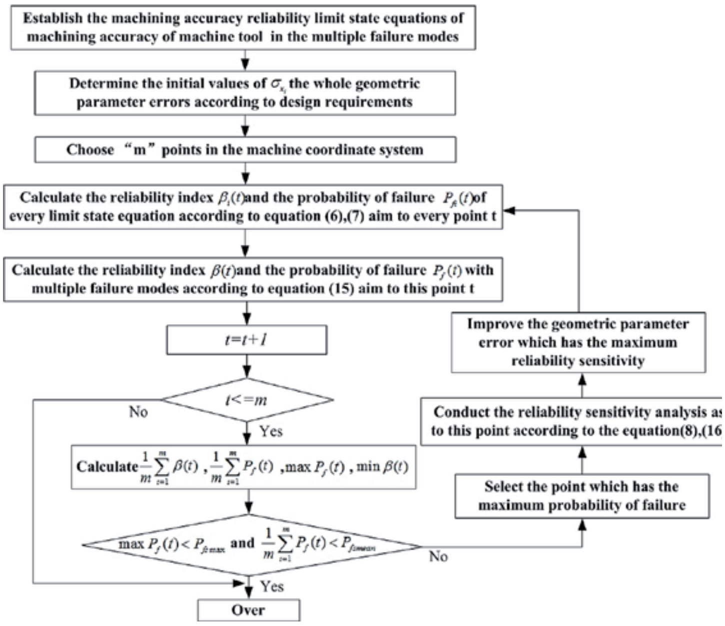

Fig. 3. The flowchart of method for geometric accuracy allocation of multi-axis machine tool for improving machining accuracy reliability

$$\frac{\partial \Upsilon_j}{\partial \sigma_{x_i}} = \frac{-\Phi(-\beta_j)\beta_j \phi(-\beta_j) + \phi^2(-\beta_j)}{\Phi^2(-\beta_j)}\left(-\frac{\partial \beta_j}{\partial \sigma_{x_i}}\right),$$

$$\frac{\partial \Xi_j}{\partial \sigma_{x_i}} = (2\Upsilon_j - \beta_j)\frac{\partial \Upsilon_j}{\partial \sigma_{x_i}} - \Upsilon_j \frac{\partial \beta_2}{\partial \sigma_{x_i}}$$

In order to develop an approach to distribute this five-axis machine tool on machining accuracy, the method used for the machining accuracy reliability and sensitivity with multiple failure modes is introduced in this paper and the calculation of the reliability and reliability sensitivity is developed in MatLab software. Besides, the process of this accuracy distribution method in this paper can be shown in Figure 3.

5. Case Study

In the preceding section, a method of geometric accuracy design of multi-axis machine tool for improving machining accuracy reliability was introduced and a machining accuracy reliability model and a sensitivity model with multiple failure modes based on AFOSM theory were established. Previous to it, a method for relating the volumetric accuracy of a machine to the errors on individual links and joints in its kinematic chain was described and the error model can be expressed by the form:

$$\boldsymbol{E} = \left[E_X, E_Y, E_Z\right]^T \tag{17}$$

In this paper, the machining accuracy reliability limit state equations of the machine tool are subject to the expression as follows:

$$\begin{gathered} l_{11} \le E_x \le l_{12} \\ l_{21} \le E_Y \le l_{22} \\ l_{31} \le E_Z \le l_{32} \end{gathered} \tag{18}$$

From the equation (18), it is not difficult to notice that this machine tool has 26 failure modes in total, including 6 single failure modes, 12 double failure modes and 8 triple failure modes.

One of important aspect of the design requirements of such machine tool is that the probability of failure of position error less than 0.03mm should be no more than 5%. According to "Test code for machine tools- Part 1: Geometric accuracy of machines operating under no-load or finishing conditions" and "Test code for machine tools-Part 2: Determination of accuracy and repeatability of positioning numerically controlled axes", the values of geometric parameter errors of five-axis NC machine tool were set initially and were shown in Table 3.

Table 3. Initial values of geometric parameter errors of five-axis NC machine tool (mm)

Number i	1	2	3	4	5	6	7	8
Parameter	Δx_x	Δy_x	Δz_x	$\Delta\alpha_x$	$\Delta\beta_x$	$\Delta\gamma_x$	Δx_y	Δy_y
Value	0.0065	0.0065	0.0065	0.0037/ 1000	0.0037/ 1000	0.0037/ 1000	0.007	0.007
Number i	9	10	11	12	13	14	15	16
Parameter	Δz_y	$\Delta\alpha_y$	$\Delta\beta_y$	$\Delta\gamma_y$	Δx_z	Δy_z	Δx_z	Δx_z
Value	0.007	0.0028/ 1000	0.0028/ 1000	0.0028/ 1000	0.007	0.007	0.007	0.0028/ 1000
Number i	17	18	19	20	21	22	23	24
Parameter	$\Delta\beta_z$	$\Delta\gamma_z$	Δx_A	Δy_A	Δz_A	$\Delta\alpha_A$	$\Delta\beta_A$	$\Delta\gamma_A$
Value	0.0028/ 1000	0.0028/ 1000	0.0058	0.0058	0.0058	0.0061/ 1000	0.0061/ 1000	0.0061/ 1000
Number i	25	26	27	28	29	30	31	32
Parameter	Δx_B	Δy_B	Δz_B	$\Delta\alpha_B$	$\Delta\beta_B$	$\Delta\gamma_B$	$\Delta\gamma_{xy}$	$\Delta\beta_{xz}$
Value	0.0068	0.0068	0.0068	0.0049/ 1000	0.0049/ 1000	0.0049/ 1000	0.0037/ 500	0.0037/ 500
Number i	33	34	35	36	37			
Parameter	$\Delta\alpha_{yz}$	$\Delta\gamma_{xa}$	$\Delta\beta_{xa}$	$\Delta\gamma_{yb}$	$\Delta\alpha_{yb}$			
Value	0.0037/ 500	0.011/ 300	0.011/ 300	0.011/ 300	0.011/ 300			

In order to improve the machining accuracy reliability of this five-axis NC machine tool, the models based on AFOSM theory addressed in section 4 was used. The process was divided into two steps: one was to determine some points by orthogonal sampling method in the X-, Y- plane of this machine tool to obtain the reliability, and the other was to realize accuracy allocation of all the geometric parameter errors of this machine tool. Five points 50, 225, 275, 325, 500 were chosen in X-axis and −225, −50, 0, 50, 225 were selected in Y-axis, as a result, there were 25 points in X-,Y- plane. The machining accuracy reliability model for accuracy allocation of machine tool addressed in this paper used to optimize errors was given by the expression (15), and its process of calculation was operated in the MatLab environment. According to the constraint conditions, if $\max P_f(t) > 5\%$ or $\frac{1}{m}\sum_{t=1}^{m} P_f(t) > 3\%$, $\max P_f(t)$ was obtained and chosen to calculate $\frac{\partial \max P_f(t)}{\partial \sigma_{x_i}}$ to determine the geometric parameter error to be improved. This process was over until $\max P_f(t) < P_{fs\max}$ and $\frac{1}{m}\sum_{t=1}^{m} P_f(t) < P_{fsmean}$. In this expression, $l_{11}, l_{12}, l_{13}, l_{21}, l_{22}, l_{23}$ were obtained though putting the vector of each point into the equation (5) and σ_{x_i} should be no more than the initial valves shown in Table 3. In order to verify the effectiveness of the method introduced in this paper, the possibility of failure of this machine tool based on the narrow bounds method was also calculated. The values of the possibility of failure of machining accuracy before improvement were acquired and shown in Table 4.

$$
\begin{aligned}
&M && : \max P_f(t), \max \frac{\partial \max P_f(t)}{\partial \sigma_{x_i}} \\
&\text{S. t.} && : l_{11} \le E_X \le l_{12} \\
& && \quad l_{21} \le E_Y \le l_{22} \\
& && \quad l_{31} \le E_Z \le l_{32} \\
& && \quad 0 < \sigma_{x_i} \le \textit{initial values} \\
& && \quad \frac{1}{m}\sum_{t=1}^{m} P_f(t) \le 3\% \\
& && \quad \max P_f(t) \le 5\%
\end{aligned}
$$

It is not difficult to notice that there are two important points in Table 4: one is that the method developed in this paper is verified because the values of possibility of failure calculated by such method are in the intervals obtained according to the narrow bounds method, and the other is that the initial values of the reliability of this machine tool failed to satisfy the design requirement (no more than 5% and 3% respectively). As a result, it is necessary to reallocate the initial values of geometric parameter errors in Table 3 according to the sensitivities of such errors shown in Figure 4. In order to satisfy the design requirement five times improvements have been developed. From the Figure 4 to Figure 8 we can learn that geometric parameter errors $\Delta\beta_{xz}$, $\Delta\alpha_{yz}$, $\Delta\alpha_y$, $\Delta\gamma_x$, $\Delta\beta_x$ have the largest values of reliability sensitivity and have been improved as the changing objects in turn as a result, besides, the machine accuracy reliability (expressed by possibility of failure) with these five improvements have been calculated as shown in Table 5. It suggests that the whole process of accuracy distribution have been finished after the forth improvements.

Figure 9 illustrates the relation between the probability of failure and each improvement, it is clear that each improvement leads to a decrease in the maximum values and mean values of possibility of failure and such decrease becomes very tight after a certain improvement. Figure 10 illustrates the relation between the reliability sensitivity of geometric parameter errors improved and each improve-

Table 4. Values of the possibility of failure of machining accuracy before improvement

Vector of point i	Narrow bounds method	The method in this paper	
		Reliability index	Possibility of failure
(50, 225)	[0.0961,0.1132]	1.236	0.1079
(50,50)	[0.0689,0.0821]	1.427	0.0766
(50.0)	[0.0531,0.0598]	1.578	0.0572
(50,-50)	[0.0689,0.0821]	1.427	0.0766
(50, -225)	[0.0961,0.1132]	1.236	0.1079
(225, 225)	[0.0997,0.1124]	1.234	0.1083
(225,50)	[0.0689,0.0821]	1.426	0.0766
(225,0)	[0.0531,0.0598]	1.578	0.0572
(225,-50)	[0.0689,0.0821]	1.426	0.0766
(225, -225)	[0.0997,0.1124]	1.234	0.1083
(275, 225)	[0.0997,0.1124]	1.233	0.1083
(275,50)	[0.0689,0.0821]	1.426	0.0766
(275,0)	[0.0556,0.0606]	1.576	0.0575
(275,-50)	[0.0689,0.0821]	1.426	0.0766
(275, -225)	[0.0997,0.1124]	1.233	0.1083
(325, 225)	[0.1042,0.1134]	1.231	0.1088
(325,50)	[0.0689,0.0821]	1.421	0.0772
(325,0)	[0.0556,0.0606]	1.576	0.0575
(325,-50)	[0.0689,0.0821]	1.421	0.0772
(325, -225)	[0.1042,0.1134]	1.231	0.1088
(500, 225)	[0.1042,0.1134]	1.231	0.1088
(500,50)	[0.0668,0.0792]	1.421	0.0772
(500,0)	[0.0567,0.0605]	1.564	0.0584
(500,-50)	[0.0668,0.0792]	1.421	0.0772
(500, -225)	[0.1042,0.1134]	1.231	0.1088
Mean value		1.378	0.0856

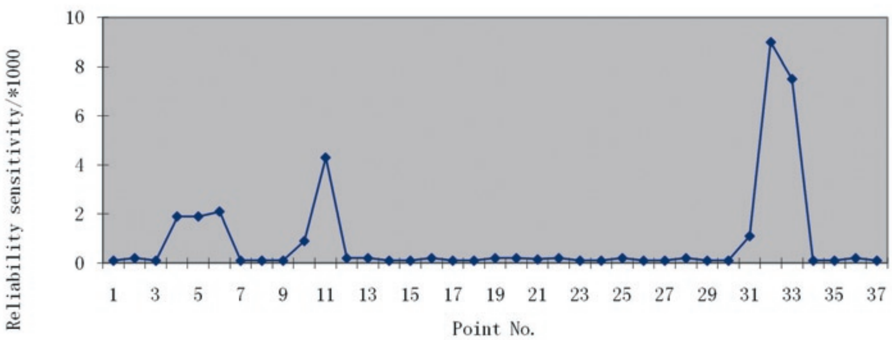

Fig. 4. Initial values of the reliability sensitivity of geometric parameter errors

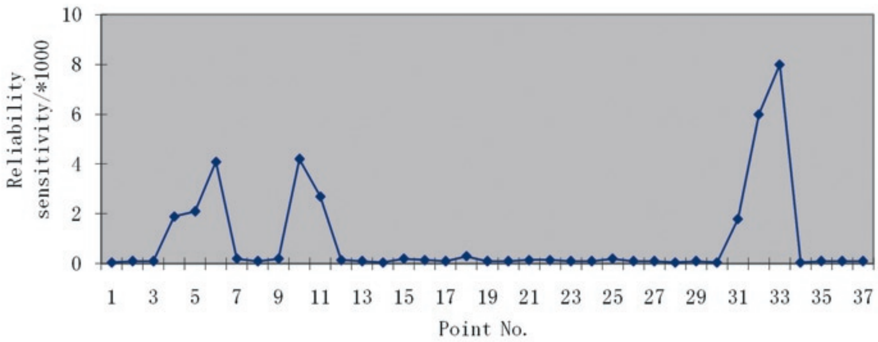

Fig. 5. Reliability sensitivity of geometric parameter errors after the first improvement

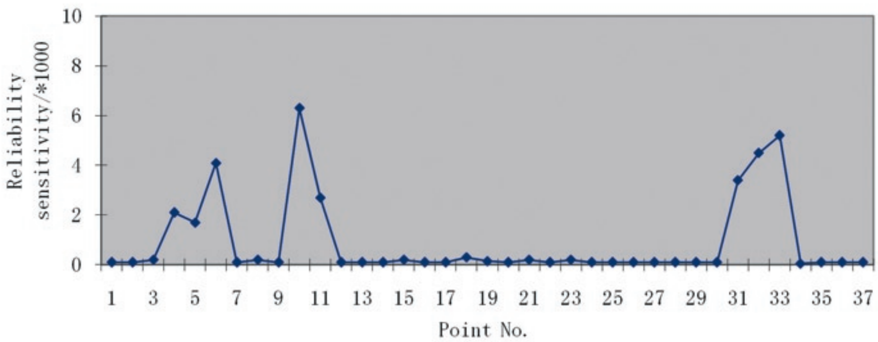

Fig. 6. Reliability sensitivity of geometric parameter errors after the second improvement

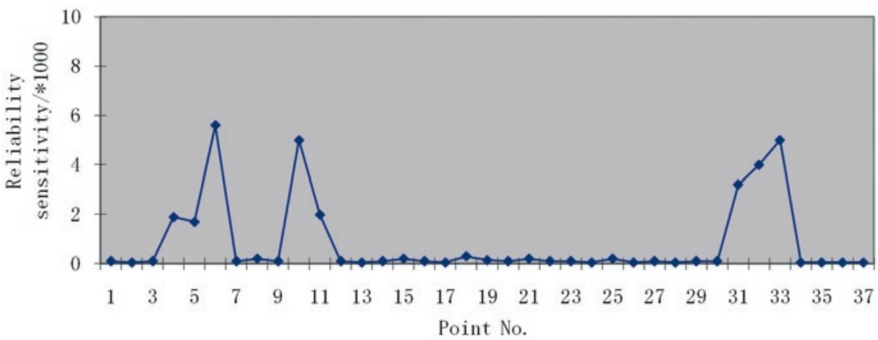

Fig. 7. Reliability sensitivity of geometric parameter errors after the third improvement

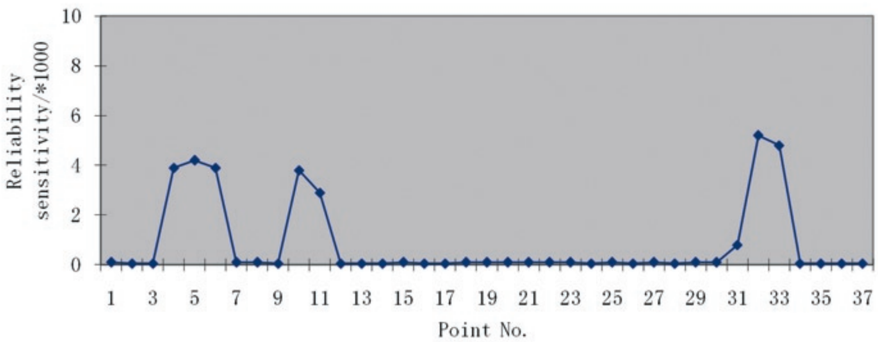

Fig. 8. Reliability sensitivity of geometric parameter errors after the fourth improvement

ment. As expected, with each improvement, the gaps among reliability sensitivity of geometric parameter errors improved decreased because the aim of each improvement is to reduce or eliminate the largest reliability sensitivity of geometric parameter errors. Figure 11 illustrates that the values of reliability sensitivity of geometric parameter errors unimproved change in a small scope, which means that these errors have smaller sensitivity to the reliability of machine tool in this machining case.

Conclusions

Different geometric errors have varying influence on accuracy of the machine tools. The main emphasis of this research is to develop a generalized method to obtain an optimal σ_i of each geometric error under certain machine accuracy design requirements. For machine accuracy reliability can be as a specification to measure the ability of machine tools to overcome a certain functions and reliability sensitivity can reflect the influence of basic parameters to the possibility of failure, which can be used for improving and optimizing the basic parameters of machine tools, the accuracy distribution of machine tools for improving the machine accuracy reliability was a process of optimizing or reallocating σ_i of each geometric error by taking reliability as a measure of the ability of machine tool and taking reliability sensitivity as a reference of optimizing the basic parameters of machine tools to design a machine tool.

In order to realize the distribution of σ_i of each geometric error, a generalized machine accuracy reliability model and a sensitivity model for accuracy distribution of machine tools with multiple failure modes are developed here. Based on such models, the optimal σ_i of each geometric error can be obtained for improving accuracy of machine tools. This study contains:

(1) A comprehensive volumetric model explains how individual errors in the components of a machine affect its volumetric accuracy (the coupling relationship). This was established by MBS theory, which shows the geometric structure, the change of comparative position and orientation, and the geometric errors.

(2) The definition of machine accuracy reliability of machine tool was given .Because it can reflect the ability to perform its specified functions and machine accuracy sensitivity can be used for optimizing the basic parameters of machine tools, accuracy distribution based on the reliability theory can improve the level of machining accuracy in terms of satisfying design requirements such as machining accuracy reliability while keeping the maximum tolerances of these geometric errors. As a result, the development of a systematic method to realize accuracy distribution of machine tool based on reliability theory according to failure modes is the second very important aspect of this paper.

(3) In order to use the systematic method to realize accuracy distribution of machine tool, a reliability theory called advanced first order and second moment (AFOSM) theory was introduced to obtain the reli-

Table 5. Improved values of errors and possibility of failure in different improvements

		The first improvement	The second improvement	The third improvement	The forth improvement	The fifth improvement
Improved object		$\Delta\beta_{xz}$	$\Delta\alpha_{yz}$	$\Delta\alpha_{y}$	$\Delta\gamma_{x}$	$\Delta\beta_{x}$
Parameter errors	Initial value	0.0037/500	0.0037/500	0.0037/1000	0.0028/1000	0.0037/1000
	Improved value	0.003/500	0.003/500	0.003/1000	0.002/1000	0.003/1000
Possibility of failure	maximum value	8.96%	7.32%	5.89%	4.57%	3.95%
	Mean value	7.36%	5.53%	4.25%	2.79%	2.43%

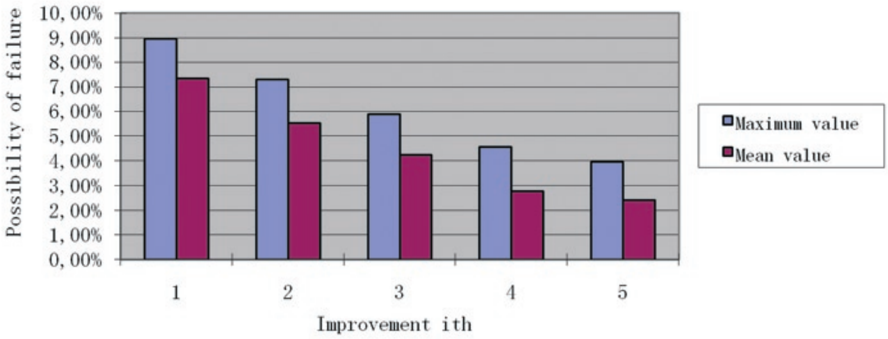

Fig. 9. Tendency of the maximum values and mean values of possibility of failure with different improvements

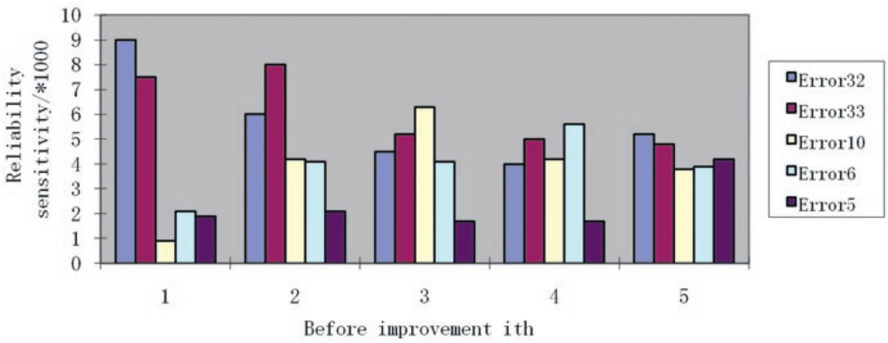

Fig. 10. Tendency of the reliability sensitivity of geometric parameter errors improved

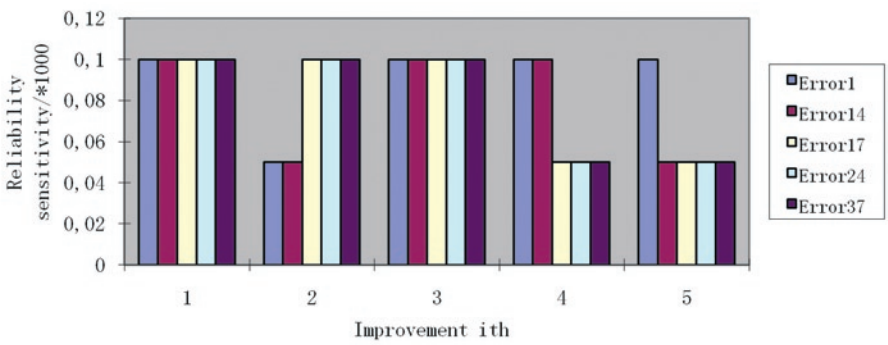

Fig. 11. Tendency of the reliability sensitivity of geometric parameter errors unimproved

ability and sensitivity with single failure mode. Besides, the multiple failure modes based on AFOSM theory were studied and the model of reliability and the model of sensitivity of a serial system with multiple failure modes were established.

(4) Based on the previous theoretical research, a case study example for a five-axis machine tool was used to demonstrate the effectiveness of this method. Each geometric error under certain accuracy design requirements was optimized. Accuracy grades of main feeding components of mechanical assemblies were also specified.

Despite the progress, a number of issues need to be further investigated to improve the method proposed here: the proposed method is developed on the premise that the volumetric machining accuracy is influenced only geometric errors, however, thermal errors and dynamic errors as other main errors can arise as a result of joint interface deformation between machine tool structural components and contribute to volumetric machining accuracy. As a result, the development of a method of accuracy allocation of machine tool for improving machining accuracy reliability while considering such errors would be a focus of future research.

Acknowledgment

The authors are most grateful to the National Natural Science Foundation of China (No.51005003), the Leading Talent Project of Guangdong Province, Rixin Talent Project of Beijing University of Technology, Beijing Education Committee Scientific Research Project and Basic Research Foundation of Beijing University of Technology for supporting the research presented in this paper.

References

1. Bohez EL, Ariyajunya B, Sinlapeecheewa C, et al. Systematic geometric rigid body error identification of 5-axis milling machines . International Journal of Comp. Aided Des. 2007; V 39(4): 229-244.
2. Chen GD, Liang YC, Sun YZ. Volumetric error modeling and sensitivity analysis for designing a five-axis ultra-precision machine tool. International Journal of Advanced Manufacturing Technology 2013; (68):2525-2534.
3. Chen JS. Computer-aided accuracy enhancement for multi-axis CNC machine tool. International Journal of Machine Tools and Manufacture 1995; 35(4):593–605.
4. Chen JX, Lin SW, He BW, et al. Geometric error compensation for multi-axis CNC machines based on differential transformation. International Journal of Advanced Manufacturing Technology 2014; (71):635-642.
5. Cheng Q, Wu C, Gu PH. An Analysis Methodology for Stochastic Characteristic of Volumetric Error in Multi-axis CNC Machine Tool. Journal of Mathematical Problems in Engineering 2013; (2013):1-12.
6. Chu QB, Ma L, Chang LM. Deterministic design, reliability design and robust design. Machinery Industry Standardization and Quality 2012; 8(471):16-20.
7. Deng C, Xie SQ, Wu J, et al. Position error compensation of semi-closed loop servo system using support vector regression and fuzzy PID control. International Journal of Advanced Manufacturing Technology 2014; (71):887-898.
8. Diplaris SC, Sfantsikopoulos MM. Cost–Tolerance Function. A New Approach for Cost Optimum Machining Accuracy. International Journal of Advanced Manufacturing Technology 2000; (16):32-38.
9. Dorndorf U, Kiridena VSB, Ferreira PM. Optimal budgeting of quasistatic machine tool errors. Journal of Engineering for Industry 1994; 116(1): 42-53.
10. Dufour P, Groppetti R. Computer Aided Accuracy Improvement in Large NC Machine-Tools. In Proceedings of the 2006 International Conference on the MTDR 1981; 22: 611-618.
11. Fu GQ, Fu JZ, Xu YT. Product of exponential model for geometric error integration of multi-axis machine tools. International Journal of Advanced Manufacturing Technology 2014; (71):1653-1667.
12. González I, Sánchez I Statistical tolerance synthesis with correlated variables. International Journal of Mech Mach Theory 2009; 44(6):1097-1107.
13. Hocken R, Simpson JA, Borchardt B, et al. Three Dimensional Metrology. Journal of Ann. CIRP 1977; 26(2): 403-408.
14. Huang MF, Zhong YR. Optimized sequential design of two-dimensional tolerances. International Journal of Advanced Manufacturing Technology 2007; (33):579-593.
15. Huang X, Ding W, Hong R. Research on accuracy design for remanufactured machine tools. In Proceedings of the 2006 International Conference on Technology and Innovation 2006; 1403-1410.
16. Huang YM, Shi CS. Optimal tolerance allocation for a sliding vane compressor. Journal of Mechanical Design 2006; 128(1):98-107.
17. Huang YQ, Zhang J, Li X. Thermal error modeling by integrating GA and BP algorithms for the high-speed spindle. International Journal of Advanced Manufacturing Technology 2014; (71):1669-1675.
18. Karadeniz H, Toğan V, Vrouwenvelder T. An integrated reliability-based design optimization of offshore towers. Reliability Engineering and System Safety 2009; 94(10): 1510-1516.
19. Khan AW, Chen WY. A methodology for systematic geometric error compensation in five-axis machine tools. International Journal of Advanced Manufacturing Technology 2011; (53):615-628.
20. Khodaygan S, Movahhedy MR. Fuzzy-small degrees of freedom representation of linear and angular variations in mechanical assemblies for tolerance analysis and allocation. Mechanism and Machine Theory 2011; (46):558-573.
21. Kiridena VSB, Ferreira PM. Kinematic modeling of quasistatic errors of three-axis machining centers. International Journal of Machine Tools and Manufacture 1994; 34(1): 85-100.
22. Lee K, Yang SH. Measurement and verification of position-independent geometric errors of a five-axis machine tool using a double ball-bar. International Journal of Machine Tools and Manufacture 2013; (70):45-52.
23. Liu HL, Li B, Wang XZ, et al. Characteristics of and measurement methods for geometric errors in CNC machine tools. International Journal of Advanced Manufacturing Technology 2011; (54):195-201.
24. Liu Y, Li Y. Dimension chain calculation precision in control of hull construction. Chinese Journal of Shipbuilding of China 2004; 45(2): 81-87.
25. Love WJ, Scarr. AJ. The determination of the volumetric accuracy of multi-axis machines. In Proceedings of the 2006 International Conference on the 14th MTDR 1973: 307-315.
26. Lu ZY, Song SF, Li HS, et al. Structural reliability and reliability sensitivity analysis organization. China: Sciences Press 2009.
27. Mínguez R, Castillo E. Reliability-based optimization in engineering using decomposition techniques and forms. Structural Safety 2009; 31(3): 214-223.
28. Muthu P, Dhanalakshmi V, Sankaranarayanasamy K. Optimal tolerance design of assembly for minimum quality loss and manufacturing cost using metaheuristic algorithms. International Journal of Advanced Manufacturing Technology 2009; (44):1154-1164.
29. Prabhaharan G, Asokan P, Rajendran S. Sensitivity-based conceptual design and tolerance allocation using the continuous ants colony algorithm (CACO). International Journal of Advanced Manufacturing Technology 2005; (25):516-526.
30. Portman VT. A Universal Method for Calculating the Accuracy of Mechanical Devices. Journal of Soviet Engineering Research 1982; V1 (7): 11-15.
31. Siva KM, Stalin B. Optimum tolerance synthesis for complex assembly with alternative process selection using Lagrange multiplier method. International Journal of Advanced Manufacturing Technology 2009; (44):405-411.
32. Sivakumar K, Balamurugan C, Ramabalan S. Concurrent multi-objective tolerance allocation of mechanical assemblies considering alternative manufacturing process selection. International Journal of Advanced Manufacturing Technology 2011; (53):711-732.
33. Srivastava A, Veldhuis S, Elbestawi MA. Modeling geometric and thermal errors in a five-axis CNC machine tool. International Journal of Machine Tools and Manufacture 1995; V35(9): 1321-1337.

34. Wang C, Fei Y, Hu P, et al. Accuracy distribution and determination of the flexible three-coordinate measuring machine. The Third International Symposium on Precision Mechanical Measurements, International Society for Optics and Photonics 2006; 62800U-7.
35. Wang E. An investigation in cyclic optimum method of accuracy allocation for instruments. Chinese Journal of Scientific instrument 1985; 6(2):140-146.
36. Wang SX, Yun JT, Zhang ZF. Modeling and compensation technique for the geometric errors of five-axis CNC Machine Tools. Chinese Journal of Mechanical Engineering 2003; 16(2):197-201.
37. Yang H, Fei Y, Chen X. Uncertainty Analysis and Accuracy Design of Nano-CMM. Journal of Chongqing University 2006; 29 (8):82-86.
38. Yang J. Research on structure reliability calculation method and sensitivity analysis. China: Dalian University of Technology, 2012.
39. Ye B, Salustri FA. Simultaneous tolerance synthesis for manufacturing and quality. Res Eng Des. 2003; 14(2):98-106.
40. Yu ZM, Liu ZJ, Ai YD, Xiong M. Geometric error model and precision distribution based on reliability theory for large CNC gantry guideway grinder. Chinese Journal of Mechanical Engineering 2013; 49(17):142-151.
41. Zhang GJ, Cheng Q, Shao XY, et al. Accuracy analysis for planar linkage with multiple clearances at turning pairs. Chinese Journal of Mechanical Engineering 2008; 21(2): 36-41.
42. Zhang X, Chang W, Tan Y. Accuracy Allocation of anti-tank missile weapon system. Journal of Projectiles Rockets Missiles and Guidance 2003; 23(2):17-19.
43. Zhu PH, Chen LH. A novel method of dynamic characteristics analysis of machine tool based on unit structure. Science China Technological Sciences 2014; 57 (5): 1052-1062.
44. Zhu SW, Ding GF, Qin SF, et al. Integrated geometric error modeling, identification and compensation of CNC machine tools, International Journal of Machine Tools and Manufacture 2012; (52): 24-29.

Appendix Nomenclature

Δx_x = Positioning error
Δy_x = Y direction of straightness error
Δz_x = Z direction of straightness error
$\Delta \alpha_x$ = Rolling error
$\Delta \beta_x$ = Britain swing error
$\Delta \gamma_x$ = Yaw error
Δx_y = X direction of straightness error
Δy_y = Positioning error
Δz_y = Z direction of straightness error
$\Delta \alpha_y$ = Rolling error
$\Delta \beta_y$ = Britain swing error
$\Delta \gamma_y$ = Yaw error
Δx_z = X direction of straightness error
Δy_z = Y direction of straightness error
Δz_z = Positioning error
$\Delta \alpha_z$ = Rolling error
$\Delta \beta_z$ = Britain swing error
$\Delta \gamma_z$ = Yaw error
Δx_B = X direction run-out error
Δy_B = Y direction run-out error
Δz_B = Z direction run-out error
$\Delta \alpha_B$ = Around the X axis turning error
$\Delta \beta_B$ = Turning error
$\Delta \gamma_B$ = Around the Z axis turning error
Δx_A = X direction run-out error
Δy_A = Y direction run-out error
Δz_A = Z direction run-out error
$\Delta \alpha_A$ = Turning error
$\Delta \beta_A$ = Around the Y axis turning error
$\Delta \gamma_A$ = Around the Z axis turning error
$\Delta \gamma_{xy}$ = X, Y -axis perpendicularity error
$\Delta \beta_{xz}$ = X, Z -axis perpendicularity error
$\Delta \alpha_{yz}$ = Y, Z -axis perpendicularity error
$\Delta \gamma_{yb}$ = B, X- axis parallelism error in XY plane
$\Delta \alpha_{yb}$ = B, Z- axis parallelism error in ZY plane
$\Delta \gamma_{xa}$ = A, Y-axis perpendicularity error
$\Delta \beta_{xa}$ = A, Z-axis perpendicularity error

Ligang CAI
Ziling ZHANG
Qiang CHENG
Zhifeng LIU
College of Mechanical Engineering and Applied Electronics Technology Beijing University of Technology, Beijing 100124, China

Peihua Gu
Department of Mechatronics Engineering
Shantou University, Shantou, Guangdong, China 515063

E-mails: hlaaok@163.com, zhangziling1119@126.com; chengqiang@bjud.edu.cn, 45080936@qq.com; gupeihua@aliyun.com

Article citation info:
TU J, CHENG R, TAO Q. Reliability Analysis Method of safety-critical avionics system based on Dynamic Fault Tree under Fuzzy Uncertainty. Eksploatacja i Niezawodnosc – Maintenance and Reliability 2015; 17 (1): 156–163.

Jiliang TU
Ruofa CHENG
Qiuxiang TAO

RELIABILITY ANALYSIS METHOD OF SAFETY-CRITICAL AVIONICS SYSTEM BASED ON DYNAMIC FAULT TREE UNDER FUZZY UNCERTAINTY

SPOSÓB ANALIZY NIEZAWODNOŚCI KRYTYCZNYCH DLA BEZPIECZEŃSTWA SYSTEMÓW ELEKTRONIKI LOTNICZEJ OPARTY NA METODZIE DYNAMICZNEGO DRZEWA BŁĘDÓW W WARUNKACH ROZMYTEJ NIEPEWNOŚCI

A safety-critical avionics system has to qualify the performance related requirements and the safety-related requirements simultaneously. This paper presents a comprehensive study on the reliability analysis method for safety-critical avionics system by using dynamic fault tree approach based on Markov chain. The reliability models were constructed applying dynamic fault tree (DFT) modeling method according to deeply analysis of the typical failure modes, causes and influence of the safety-critical avionics system by considering the aspect of repairable feature and redundancy. Taking into account the both failure phenomenon of safety-critical avionics system and many uncertainties exist in the fault status and fault reasons, fuzzy sets theory is introduced into dynamic fault tree method. Specifically, it adopts expert elicitation and fuzzy set theory to evaluate the failure rates of the basic events for safety-critical avionics system. Furthermore, the fuzzy dynamic fault tree analysis method for safety-critical avionics system based on the consecutive parameter Markov chain is proposed. The modularization design was utilized to divide the dynamic fault trees into static and dynamic sub-trees. The static tree was solved by binary decision diagram (BDD) and the dynamic tree was solved by Markov chain method. The results show that the proposed method is more flexible and adaptive than conventional fault tree analysis for fault diagnosis and reliability estimation of safety-critical avionics system.

Keywords: *safety-critical avionics system, dynamic fault tree, Markov chain, Fuzzy Uncertainty.*

Krytyczne dla bezpieczeństwa układy elektroniki lotniczej (awioniki) muszą jednocześnie spełniać zarówno wymogi eksploatacyjne jak i wymagania związane z bezpieczeństwem. W niniejszej pracy przedstawiono kompleksowe opracowanie dotyczące metody analizy niezawodności krytycznych dla bezpieczeństwa systemów awioniki wykorzystującej opartą na łańcuchu Markowa metodę dynamicznego drzewa błędów. Modele niezawodności konstruowano z zastosowaniem metody dynamicznego drzewa błędów zgodnie z przeprowadzoną dokładną analizą typowych przyczyn uszkodzeń oraz czynników wpływających na systemy elektroniki lotniczej, z uwzględnieniem aspektu naprawialności i nadmiarowości. Biorąc pod uwagę, że zarówno ze zjawiskiem uszkodzenia krytycznego dla bezpieczeństwa systemu awioniki jak i ze stanem awarii i przyczynami błędów wiąże się wiele niepewności, metodę dynamicznego drzewa błędów poszerzono o teorię zbiorów rozmytych. W szczególności, zaproponowana metoda wykorzystuje ocenę ekspercką oraz teorię zbiorów rozmytych do oceny intensywności uszkodzeń dla podstawowych zdarzeń zachodzących w krytycznych dla bezpieczeństwa systemach elektroniki lotniczej. Ponadto zaproponowano metodę analizy krytycznych dla bezpieczeństwa systemów awioniki wykorzystującą teorię rozmytych dynamicznych drzew błędów opartą na markowowskim łańcuchu następujących po sobie parametrów. Budowę modułową wykorzystano do podziału dynamicznych drzew błędów na poddrzewa statyczne i dynamiczne. Drzewa statyczne rozwiązywano za pomocą binarnego schematu decyzyjnego (BDD) a drzewa dynamiczne – metodą łańcuchów Markowa. Wyniki pokazują, że proponowana metoda diagnozowania błędów i oceny niezawodności krytycznych dla bezpieczeństwa systemów elektroniki lotniczej jest bardziej elastyczna i łatwiejsza do adaptacji niż konwencjonalna analiza drzewa błędów.

Słowa kluczowe: *krytyczne dla bezpieczeństwa układy elektroniki lotniczej, dynamiczne drzewo błędów, łańcuch Markowa, niepewność rozmyta.*

1. Introduction

Over the past several decades, reliability has been a critical issue in many embedded applications in aerospace, aircraft, road vehicles, railways, nuclear systems, and implanted devices because the failure of a safety-critical system may cause catastrophic damage or loss of life [19].With the increased concerns on reliability in safety-critical system, the requirements to improve system efficiency and reliability have become even more stringent. Modern safety-critical systems for avionics(SCAS) utilize not only an increasing amount of sophisticated software but also a software embedded hardware to process the large amount of data needed to control avionic systems and monitor their current status [4, 15]. Avionics safety is considered at the system level and has no important implications when considered separately with regard to software and hardware [14]. For fast technology innovation, the performance of key equipment in the safety-critical systems for avionics has been greatly improved with the wide application of high technology on one hand, but, on the other hand, its complexity of technology and structure increasing significantly raise challenges in system reliability analysis and evaluation. These challenges are displayed as follows [6, 16, 22]. (1) Lack of sufficient fault data: Obtaining enough failure data is time-consuming, and may be impossible for highly reliable systems. Some component state of safety-critical systems for avionics is get worsening rather than instantaneous failure in the early life cycle, so it is very difficult to obtain mass original parameters (such as the failure rate, repair rate) of the equipment which need lots of case studies in practice due to some reasons. One reason is the imprecise knowledge in an early stage of new product design. The other factor is the changes of the environmental conditions which may cause that the historical fault data can not represent the future failure behaviors. (2) Failure dependency of components: safety-critical systems for avionics adopts many redundancy units and fault tolerance techniques to improve its reliability, the failure or malfunction of software can be due to interactions with hardware. Additionally, software and hardware domains have mutual influence on each other during aviation system development and the system equipment can not carry out the necessary maintenance during operation. So, the behaviors of components in the system and their interactions, such as failure priority, sequentially dependent failures, functional dependent failures, and dynamic redundancy management, should be taken into consideration. (3) High levels of fuzzy uncertainty: it is usually operated in the harsh environment for a long-term and is greatly affected by the measurement error, human, and operational malfunctions that may lead to hazardous incidents of safety-critical systems for avionics. It is difficult to give a precise estimation of reliability characteristic values, especially for the system with very low failure rates or new parts, For example, it is common for experts to say that 'there is a low possibility that the component A fails' rather than the probability of failure of the component A is '1.2E−5'.These terms can be quantified with the use of membership functions of the corresponding fuzzy sets.

Fault tree analysis (FTA) is a systematic approach to estimate safety and reliability of a complex system, qualitatively as well as quantitatively. It is a logical and diagrammatic method for evaluating the possibility of an accident resulting from combinations of failure events. However, in traditional FTA, the failure probabilities of the basic events (BEs) are expressed by exact values, has been found to be inadequate to deal with these challenges mentioned above. And this makes quantitative analysis of a fault tree of a system questionable by conventional methods [3]. In order to handle subjective factors and nonlinear characteristics, inherent in the importance identification for a fault tree in the reliability analysis, many conscientious researchers have taken the fuzzy uncertain situations into consideration. Fuzzy set theory has been proven to be effective on solving problems where there are no sharp boundaries and precise values, while it is also efficient. The pioneering work on fuzzy fault tree analysis (fuzzy FTA) belongs to Tanaka et al. [4–5], who treated imprecise probabilities of basic events as trapezoidal fuzzy numbers and defined an index function analogous to the importance measure for ranking the effectiveness of each basic event. Since then, there have been a number of approaches where the technology of fuzzy sets was used to evaluate system reliability. For example, Ding et al. proposed a membership function of fuzzy numbers to represent a sub-system state to assess the reliability of multi-state weighted k-out-of-n systems [22].In Gargama and Chaturvedi, the membership functions of fuzzy numbers are used to represent linguistic variables and a defuzzification technique has been used to generate a crisp score for prioritize failure modes to overcome the limitation of the traditional FMEA[5,15].However, these approaches use the static fault tree to model the system fault behaviors and cannot cope with challenge (2). Dynamic fault tree analysis has been introduced [1, 6, 7, 13], which takes into account not only the combination of failure events but also the order in which they occur. Rongxing Duan [17] analysed the dependability of data communication systems with on-demand and active failure modes using dynamic fault tree and solved it to get some reliability results by equivalent Bayesian network (BN) model. However, this is an approximate solution and requires huge memory resources to obtain the joint probability distribution accurately. Furthermore, the reliability parameters by dynamic fault tree are mapped into equivalent BN calculation is complex. Some innovative algorithm has been introduced to reduce the dimension of conditional probability tables by an order of magnitude. However, this method cannot perform probability updating. Montaniet et al. proposed a translation of the dynamic fault tree into a dynamic Bayesian network (DBN) [16]. The DBN model is essentially applicable to Markov processes and the result of the calculation gives the approximated probabilities, but the method can not solve the differential equation. In order to solve a larger dynamic fault tree, a Markov state transition method was proposed for the reliability analysis of dynamic fault tree in [18]. They converted dynamic logic gates to Markov chain and calculated the reliability results by a standard formula of DFT based on the consecutive parameter Markov chain [21]. Markov state transition method can clearly describe the dynamic characteristics of system reliability and describe each state change process in reliability analysis under fault condition [2].

On the basis of the discussed notions, we attempted to conceptualize and articulate the design process of safety-Critical avionics system for achieving both performance-and reliability-related requirements by utilizing the fuzzy set and dynamic fault tree. A reliability analysis method is proposed in this paper, it pays special attention to meet the above three challenges. We adopt expert elicitation and fuzzy set theory to deal with insufficient fault data and uncertainty problem by treating the failure rates as fuzzy numbers without the need to engage basic event failure probability distribution. The reliability models were constructed applying dynamic fault tree (DFT) modeling method according to deeply analysis the typical failure modes, causes and influence of the safety-Critical avionics system. In addition, the modularization design was utilized to divide the dynamic fault trees into static and dynamic sub-trees. The dynamic fault tree model can capture the dynamic behaviors of safety-Critical avionics system failure mechanisms. The static tree was solved with binary decision diagram (BDD) and the dynamic tree was solved with Markov chain method in order to avoid the aforementioned problems.

The purpose of this study is to involve dynamic analysis into the traditional static methods using fuzzy set and dynamic fault tree for the SCAS reliability analysis, as well make Markov models more efficient for the users. After the introduction, the rest of the paper is organized as follows. Section 2 provides a brief introduction on SCAS and its dynamic fault tree model. Section 3 describes estimation of failure rates for the basic events. Section 4 presents a novel dynamic fault tree solution in which the modularization design was utilized to divide the dynamic fault trees into static and dynamic sub-trees. The outcomes of the research and future research recommendations are presented in the final section.

2. Construction of SCAS Dynamic fault tree

SCAS is a complex system consists of many key components, such as Vehicle Management system (VMS), Crew Station (CS), Mission&System Management (MSM), Local Path Generation (LPG), Scene & Obstacle Following (SOF), Among them VMS are responsible for the aircraft fuselage control. In addition, it also performs the most important task such as common System management& control. CS can provide necessary flight information for pilot, MSM implements resource sharing by the users of a real-time computer system. In order to improve the reliability of SCAS, it adopts redundancy technique to ensure higher reliability. For example, the hardware redundancy technique is adopted in designing VMS, CS, MSM, LPG and SOF. High coupling degree together with complicated logic relationships exists between these modules. So, the behaviors of components in these modules and their interactions, such as failure priority, sequentially dependent failures, functional-dependent failures, and dynamic

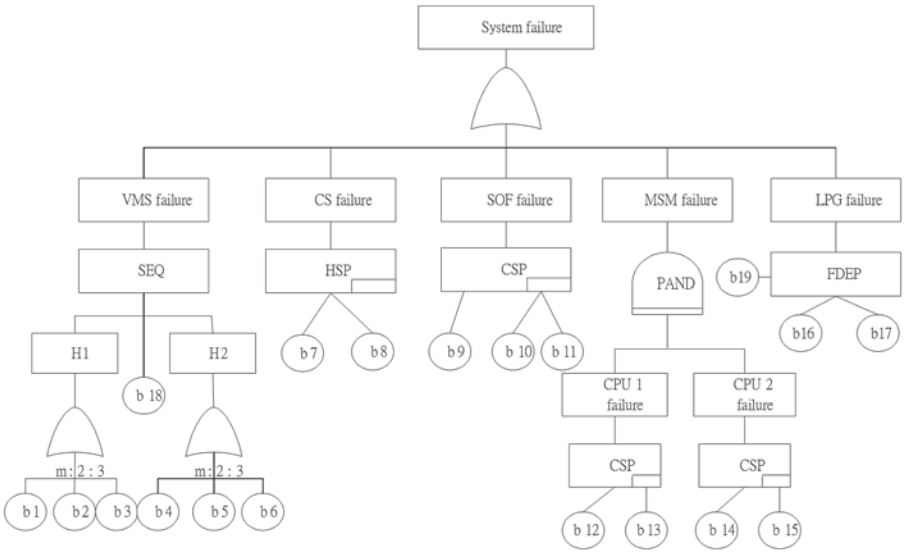

Fig. 1. DFT of SCAS

redundancy management, should be taken into consideration. Obviously, traditional static fault tree is unsuitable to model these dynamic fault behaviors. So, we use the dynamic fault tree model to capture the dynamic behavior of system failure mechanisms such as sequence-dependent events, spares and dynamic redundancy management, and priorities of failure events. A DFT is a stochastic technique for the reliability analysis, suitable to model systems characterized by time-dependent logics. By adding new gates to static (regular) Fault Trees, Dynamic Fault Trees aim to take into account dependencies among events (which typically exist in systems with spare components).

By analysis on the structure and principle of avionics system, we can found that (1) SCAS consists of five function modules, shown as "or" gate, for each module, when a hardware failure or a main software and backup software fault, then the system fault is announced. (2) There are two processing unit in the VMS and MSM subsystem, especially , in the VMS , H1 is a master component, another group of H2 as a spare unit, each set of equipment containing 3 monomer, if 3 channel main system components in the 2 failure, the main system fault is announced; in MSM subsystem, It simply detects the failure order and fails just in one case (failure occurs if CPU1 fails before CPU2,but CPU2 may fail before CPU1 without producing a failure). (3)The CS is 2:1 Parallel structure subsystem and SOF is 3:1 cold spare module, Only after all the equipment failure, then announced the subsystem fault;(4) in the LPG module, b19 is the path interface unit, b16 and b17 delegate 2 channel in path generation subsystem, only b19 or b16,b17 all failure, the LPG subsystem become failure. Based on the above analysis, the control failure of avionic system is adopt as the top event, then the DFT of SCAS is established in Figure 1.

3. A Basic event failure possibility evaluation

The motivation of this section is how to obtain basic event failure probabilities of SCAS when basic events do not have probability distributions of their lifetime to failures. Therefore, we develop a fuzzy reliability algorithm to assess basic event failure probabilities through qualitative linguistic value processing without the need to engage basic event failure probability distribution.

3.1. Linguistic value and membership function

A basic event failure possibility distribution is a set of qualitative linguistic terms used to scale the failure likelihood of the basic events of fault trees of SCAS. Based on the range of the component failure data collected from avionic system operating experiences. In this paper, the component failure rate is defined by seven linguistic values, that is, very high(VH), high(H), reasonably high(RH),moderate(M), reasonably low(RL), low(L), and very low(VL).For example, very low failure possibility can be used to represent components which are rigid and very unlikely to be failure even once. This set of qualitative linguistic values(UH) can be expressed as[8]:

$$UH = \{h_i \mid i = 1, 2, ..., 7\} = \{VL, L, RL, M, RH, H, VH\}$$

The fuzzy sets represent qualitative basic event failure possibilities defined in the [0, 1] universe of discourse. Seven membership functions of triangular fuzzy numbers have been developed in Purba et al. [9] to represent those seven basic event failure possibilities, the shapes of the membership functions to mathematically represent linguistic variables are shown in Figure 2. These membership functions are mathematically given in follows:

$$\mu_{VL}(x) = (0.00, 0.04, 0.08), \mu_L(x) = (0.07, 0.13, 0.19), \mu_{RL}(x) = (0.17, 0.27, 0.37),$$
$$\mu_M(x) = (0.35, 0.50, 0.65), \mu_{RH}(x) = (0.63, 0.73, 0.83), \mu_H(x) = (0.81, 0.87, 0.93),$$
$$\mu_{VH}(x) = (0.92, 0.96, 1.00)$$

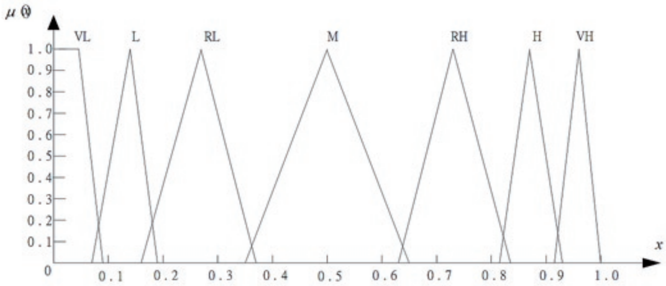

Fig. 2. The event membership functions

3.2. Fuzzification module and defuzzification module

In real-world applications, the avionic experts may have different levels of expertise, background and working experience. Hence, they may demonstrate different perceptions about the same events and subjectively provide different assessment. To eliminate bias coming from an expert and reflect their differences of assessment, different justification weights from 0 to 1 may be assigned to every expert. So, it is necessary to combine or aggregate these opinions into a single one. There are many methods to aggregate fuzzy numbers. In this paper, we adopt simple linear weighting as formula (1), which consider the weight of individual value, can be implemented in this method as well [9].

$$M_B = \begin{bmatrix} \mu_{b1}(x) \\ \mu_{b2}(x) \\ ... \\ \mu_{bl}(x) \end{bmatrix} = \begin{bmatrix} \mu_{UH}(x)^{(e_1b_1)}, \mu_{UH}(x)^{(e_2b_1)}, ..., \mu_{UH}(x)^{(e_nb_1)} \\ \mu_{UH}(x)^{(e_1b_2)}, \mu_{UH}(x)^{(e_2b_2)}, ..., \mu_{UH}(x)^{(e_nb_n)} \\ ...... \\ \mu_{UH}(x)^{(e_1b_l)}, \mu_{UH}(x)^{(e_2b_l)}, ..., \mu_{UH}(x)^{(e_nb_l)} \end{bmatrix} \bullet \begin{bmatrix} w_1 \\ w_2 \\ ... \\ w_n \end{bmatrix} \quad (1)$$

where $\mu_{bl}(x)$ is the final membership function for basic event b_l, $\mu_{UH}(x)^{(e_ib_j)}$ is the ith membership function given by expert e_i to basic event b_j, w_i is the weight given to expert e_i, n is the number of experts, and l is the number of basic events.

A failure possibility score (FPS) is a single numerical value, which is decoded from a membership function, to represent the experts' belief of the most likely score indicating that an event may occur. This step is usually called defuzzification. There are several defuzzification techniques [10]: area defuzzification technique, the left and right fuzzy ranking defuzzification technique, the centroid defuzzification technique, the area between the centroid point and the original point defuzzification technique, and the centroid based Euclidean distance defuzzification technique. Among the diversity of the methods, an area defuzzification technique(ADT) is used to map the fuzzy numbers into FPS because it has the lowest relative errors and has the closest match with the real data. More specifically, the method returns a numeric value computed as follows [10]:

$$FPS = d(\mu_{bi}(x)) = x_1 y_0 + \int_{x_2}^{d} \mu_{bi}^{R}(x) \tag{2}$$

where y_0 is the centroid point of the real fuzzy number $\mu_{bl}(x)$ on the vertical axis, x1 is the intersection point between the line y_0 and the left membership function $\mu_{bl}^{L}(x)$ on the horizontal axis, and x2 is the intersection point between the line y_0 and the right membership function $\mu_{bl}^{R}(x)$ on the horizontal axis. If it is a triangular fuzzy number $\mu_{bi}(x) = (a,b,c)$, then its FPS is calculated using formula (3):

$$FPS = \frac{1}{18}(4a + b + c) \tag{3}$$

3.3. Basic event failure probability generation

The event fuzzy possibility score is then converted into the corresponding fuzzy failure rate, which is similar to the failure rate. Based on the logarithmic function proposed by Onisawa [19], which utilizes the concept of error possibility and likely fault rate, the fuzzy failure rate(FFR) can be obtained by (4):

$$FFR = \begin{cases} \dfrac{1}{10^{2.301*[(1-FPS)/FPS]^{1/3}}}, FPS \neq 0 \\ 0, \qquad FPS = 0 \end{cases} \tag{4}$$

Table 1 shows the fuzzy failure rates of the basic events for the SCAS.

Table 1. Basic events' FPS and FFR

Basic events	Final membership functions	FPS	FFR
b1	(0.43, 0.57, 0.70)	0.165952	1.14E−4
b2	(0.43, 0.57, 0.70)	0.165952	1.14E−4
b3	(0.47, 0.60, 0.73)	0.178095	1.48E−4
b4	(0.43, 0.57, 0.70)	0.165952	1.14E−4
b5	(0.43, 0.57, 0.70)	0.165952	1.14E−4
b6	(0.43, 0.57, 0.70)	0.165952	1.14E−4
b7	(0.92, 0.96, 1.00)	0.313333	1.03E−03
b8	(0.92, 0.96, 1.00)	0.313333	1.03E−03
b9	(0.94,0.97,1.00)	0.318333	1.24 E−03
b10	(0.94,0.97,1.00)	0.318333	1.24 E−03
b11	(0.92, 0.96, 1.00)	0.313333	1.03E−03
b12	(0.55, 0.66, 0.78)	0.20238	2.32E−4
b13	(0.58,0.68,0.79)	0.2106	2.6E−4
b14	(0.43, 0.57, 0.70)	0.165952	1.14E−4
b15	(0.47, 0.60, 0.73)	0.178095	1.48E−4
b16	(0.22, 0.34, 0.45)	0.092857	1.21E−5
b17	(0.18, 0.28, 0.38)	0.077381	5.54E−6
b18	(0.32, 0.47, 0.61)	0.131905	4.87E−5
b19	(0.14, 0.23, 0.32)	0.061905	2.02E−6

4. Reliability analysis method for SCAS

With the help of dynamic gates, sequence-dependent failure behavior of SCAS can be specified using dynamic FTs that are compact and easily understood. With the increase in the number of basic elements, there is problem state space explosion [12]. To reduce state space and minimize the computational time, an improved modularization method was utilized to divide the dynamic fault trees into static and dynamic sub-trees in this paper [11]. The static tree was solved with binary decision diagram (BDD) and the dynamic tree was solved with Markov chain method, the reliability parameters of the global integrated system is calculated at last.

4.1. Analysis of static fault tree based on BDD

In the Figure 1, SCAS is comprised of five components. It is obviously that the relation five subsystem is OR gates which also combine input events, but any one is sufficient to cause the output, so we can calculate the reliability degree by use the BDD (binary decision diagram) method. BDD is a kind of simplified Boolean expression method in which has two types of endpoints, respectively is 0 and 1. In BDD, 0 represented no failure state, 1 representative failure state. Figure 3 shows the conversion of Static fault tree of SCAS into BDD, among them, S1 denote VMS subsystem, S2 denote CS subsystem, S3 denote SOF subsystem, S4 denote MSM, S5 denote LPG subsystem.

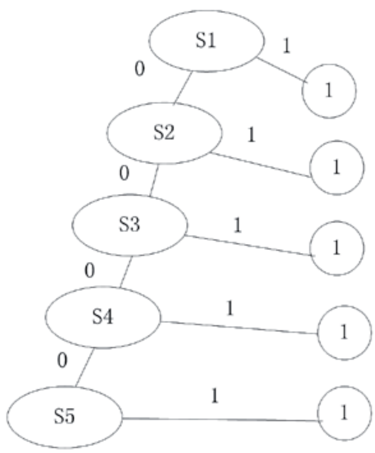

Fig. 3. BDD decomposition process of SCAS

So the structure function of fault tree for the SCAS failure accident can be obtained as follows:

$$\Phi(S) = S_1 \cup S_2\overline{S_1} \cup S_3\overline{S_2 S_1} \cup S_4\overline{S_3 S_2 S_1} \cup S_5\overline{S_4 S_3 S_2 S_1} = S_1 \cup S_2 \cup S_3 \cup S_4 \cup S_5 \tag{5}$$

When $\Phi(S) = 1$, it is denote the system failed , when $\Phi(S) = 0$ that the system failure did not occur. The system product of structure function is disjoint after BDD decomposition, so the FTA probability calculation is very simple. The probability of system failure is:

$$P(X_s) = P(\Phi(S=1)) = P(S_1) + P(S_2\overline{S_1}) + P(S_3\overline{S_2 S_1}) + P(S_4\overline{S_3 S_2 S_1}) + P(S_5\overline{S_4 S_3 S_2 S_1}) \tag{6}$$

4.2. Analysis of dynamic fault tree based on Markov chain

Dynamic fault tree (DFT) of SCAS main introduces four basic (dynamic) gates: the priority AND (PAND), the sequence enforcing (SEQ), the standby or spare (SPARE), and the functional dependency (FDEP). SPARE gates are dynamic gates modeling one or more principal components that can be substituted by one or more backups (spares) varing with the state of spare gate, it can divide into cool spare gate, hot spare gate, warm spare gate. The following example illustrates how the five functions of this system subsystem is transformed into a Markov chain, the detailed algorithm of converting a fault tree into a Markov model was proposed in [2].

4.2.1. Mapping Dynamic Fault Tree into Markov chain

In subsystem of VMS, A SEQ gate forces its inputs to fail in a particular order: when a SEQ gate is found, it never happens that the failure sequence takes place in different orders. While the SEQ gate allows the events to occur only by pre-assigned order and states that a different failure sequence can never take place. Suppose the failure rate of H1 is λ_1, H2 is λ_2, b18 is λ_{b18}, the Markov state transfer chain of VMS subsystem is shown in Figure 4. It is assumed that each device failure events is independent in this paper, the failure probability of VMS subsystem is $P(VMS) = P(H_1)P(b_{18})P(H_2)$.

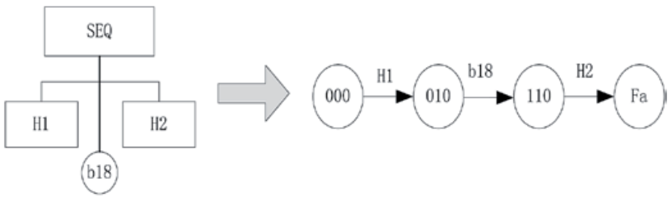

Fig. 4. The Markov chain of SEQ gate

In subsystem of CS, spare gate will have one active component (say b7) and remaining spare components (say b8). When there is no demand, it will be in standby state or may be in failed state due to on-shelf failure. It can also be unavailable due to test or maintenance state as per the scheduled activity when there is a demand for it. On the princple of hot spare gate, we can get the Markov chain of CS subsystem in Figure 5. The Failure probability of VMS subsystem is: $P(CS) = 2P(b_7)P(b_8)$.

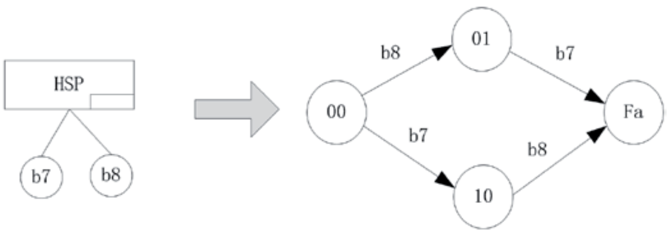

Fig. 5. The Markov chain of HSP gate

In subsystem of SOF, the process of analysis is similar to subsystem VSM. In Figure 6,but because of the failure rate of cold spare gate is 0, and each section of chain transfer in Markov state points on the self transition probability is different. The failure probability of SOF subsystem is $P(SOF) = P(b_9)P(b_{10})P(b_{11})$.

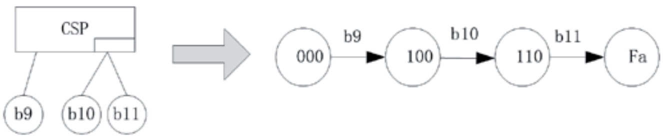

Fig. 6. The Markov chain of CSP gate

In subsystem of MSM, consider PAND gate having two active components, CPU1and CPU2. Active component is the one which is in working condition during normal operation of the system. Active components can be either in success state or failure state. The PAND gate reaches a failure state if all of its input components have failed in a pre-assigned order (usually from left to right).When the first component failed followed by the second component, it is identified as failure and simultaneous downtime is taken into account. Especially, both the components have failed simultaneously but second component has failed first hence it is not considered as failure. The Markov chain of MSM As shown in Figure 7.The failure probability of SOF subsystem is:

$$P(MSM) = 3P(b_{12})P(b_{13})P(b_{14})P(b_{15}).$$

In subsystem of LPG, The FDEP gate's output is a 'dummy' output as it is not taken into account during the calculation of the system's failure probability. When the trigger event (b19) occurs, it will lead to the occurrence of the dependent event (say b16 and b17) associated with the gate. During the down time of the trigger event, the dependent events will be virtually in failed state though they are functioning. we can get the markov chain of LPG subsystem in Figure 8. The failure probability of VMS subsystem can be derived as:

$$P(LPG) = P(b_{19}) + 2P(b_{16})P(b_{17}) + P(b_{16})P(b_{19}) + P(b_{17})P(b_{19})$$

In the above diagram, 0 represents the bottom events is normal, and 1 represents the bottom event failure. Fa represent the system failure state, the circles represent the state of a system.

4.2.2. Reliability calculation of *n* order Markov chain

For the complicated system state more, can imagine will transfer graph is decomposed into a plurality of state transfer chain state, according to the different chain length, respectively, deduces the formula. In the application of these formulas only apply, and then integrated for each chain results, we can get the reliability index of the whole system. The nth order Markov chain transfer process is illustrated as Figure 9.

The core of Markov method is to decide the state transferring probability matrix. Suppose each equipment state transfer rate obeys exponential distribution. If the process is a random continuous state space, then state i and state j fixed on arbitrary, so the transfer rate from state i to state j as follows:

$$q_{ij} = p'_{ij}(0) = \lim_{\Delta t \to 0} \frac{p_{ij}(\Delta t) - p_{ij}(0)}{\Delta t} = \lim_{\Delta t \to 0} \frac{p_{ij}(\Delta t) - \delta_{ij}}{\Delta t}, \delta_{ij} = \lim_{t \to 0} p_{ij}(t) = \begin{cases} 1, i = j \\ 0, i \neq j \end{cases} \tag{7}$$

Then the transfer rate matrix A which the chain length with N with respect to the state transfer process as follows:

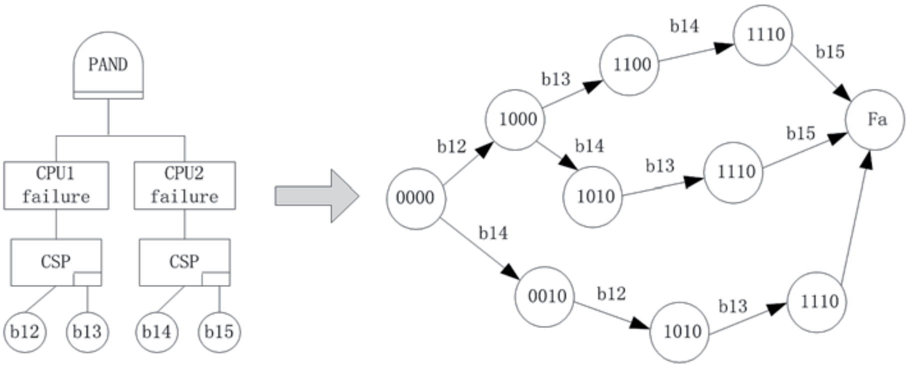

Fig. 7. The Markov chain of PAND gate

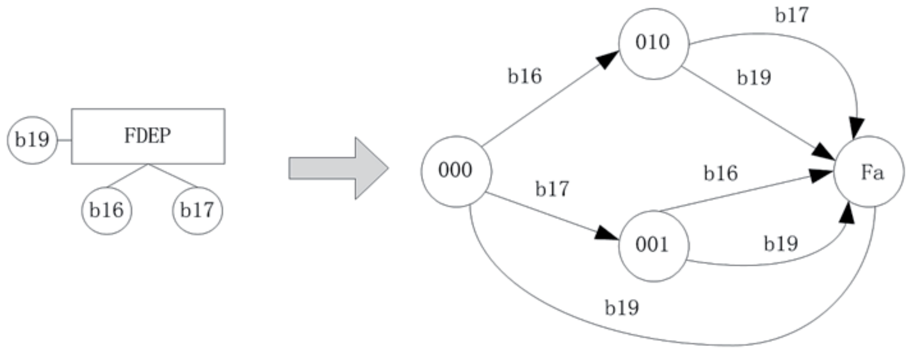

Fig. 8. The Markov chain of FDEP gate

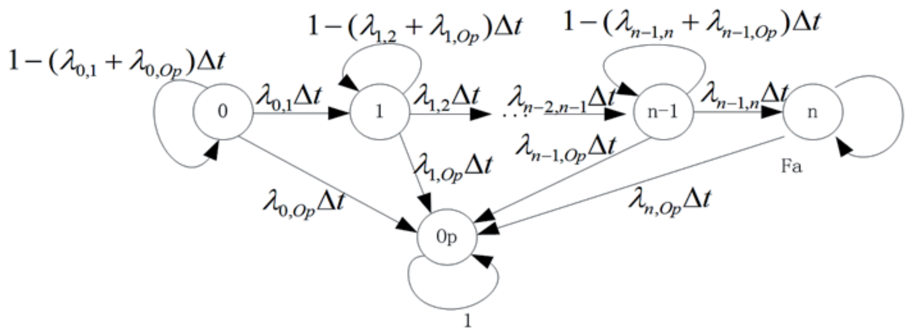

Fig. 9. The nth order Markov chain of transfer process

$$A=\begin{pmatrix} -\lambda_{0,1}-\lambda_{0,Op} & \lambda_{0,1} & 0 & 0 & \dots & 0 & 0 & \lambda_{0,Op} \\ 0 & -\lambda_{1,2}-\lambda_{1,Op} & \lambda_{1,2} & 0 & \dots & & 0 & \lambda_{1,Op} \\ \dots & \dots & \dots & \dots & \dots & \dots & \dots & \dots \\ 0 & 0 & 0 & 0 & \dots & -\lambda_{n-1,n}-\lambda_{n-1,Op} & \lambda_{n-1,n} & \lambda_{n-1,Op} \\ 0 & 0 & 0 & 0 & \dots & 0 & 0 & 0 \\ 0 & 0 & 0 & 0 & \dots & 0 & 0 & 0 \end{pmatrix}$$

According to theory of Markov processes, the state transition probability matrix equation is defined as:

$$\begin{cases} P' = AP \\ P(0) = E \end{cases},$$

P is the Column vector of each state probability, P' is the Derivatives of the Column vector P.

For solving the matrix equation, Laplace solution is be used in this paper. Suppose $L[P'(t)] = L[P(t)A]$,then $sP(s) - P(0) = P(s)A$, $P(s) = P(0)[sE - A]^{-1} = [sE - A]^{-1}$. Both sides of equation to take the inverse transform and according to the Heaviside expansion, then the failure probability P(t) of the chain can derived as:

$$P(t)=\prod_{i=1}^{n}\lambda_{i-1,i}\left(\prod_{i=1}^{n}\frac{1}{\lambda_{i-1,i}}-\sum_{i=1}^{n}\frac{e^{-\lambda_{i-1,i}t}}{\lambda_{i-1,i}\prod_{\substack{j=1\\ j\neq i}}^{n}(\lambda_{j-1,j}-\lambda_{i-1,i})}\right) \tag{8}$$

According to the dynamic fault tree shown in Figure 1 and the basic failure data shown in Table 1, we can map the dynamic fault tree into a Markov chain with different chain length using the proposed method in this paper. Once the structure of DFT is known and all the probability tables are filled, it is straight forward to compute the failure probability of each subsystem in SCAS using the formula 8 during the work time. Then the dynamic fault tree failure probability can be obtained by adding each chain probability. Table 2 shows the unreliability of each subsystem for SCAS in the 1000 hours time using proposed methods for the dynamic fault tree solution.

According to Table 2, the LPG subsystem has the maximum Failure probability, which means that they are the most unreliable components. So, when SCAS fails, we should diagnose them firstly to locate the failure of SCAS Furthermore, proper measures should be allocated for these components to improve their reliability at the stage of product design in order to decrease the failure probability of SCAS. For example, high reliability components or redundancy structure could be adopted.

Table 2. Failure probability of different subsystem and the whole system

Subsystem name	Failure probability
VMS	8.7482E-10
CS	3.743e-8
SOF	9.4364e-13
MSM	7.5324E-5
LPG	0.1229
SCAS	0.12298

5. Conclusions

This paper introduces a method for reliability assessment of complex avionics system. In order to simplify the complex reliability problems, conventional approaches make many assumptions to make it to a simple mathematical model. In real-world applications, when quantitative historical failure data are scarce or are not available at all, linguistic values are often used by decision makers to assess system reliability. This study has proposed a fuzzy reliability algorithm to handle qualitative data in order to assess basic events of fault trees through qualitative data processing. Those data are described in terms of failure possibilities and represented by fuzzy numbers, to characterize basic event failure likelihood. In terms of the challenge of failure dependency, we use a dynamic fault tree to describe the dynamical behavior of avionic wireless communication system failure mechanisms. Furthermore, the modularization design was utilized to divide the dynamic fault trees into static and dynamic sub-tree in order to avoid the state space explosion problem and huge memory resources. In this work all the basic dynamic gates (PAND, SEQ, SPARE, and FDEP) have been implemented with Markov chain approach. By using the formula of dynamic reliability of fault tree is given in this paper, the process can avoid directly solving differential equations, the convenience brought to the engineering application of dynamic fault tree.

As it can be seen from the result, the LPG sub-system has the most contribution to the top event probability. So, we should improve their reliability at the stage of product design in order to decrease the failure probability of SCAS by several approaches. The proposed method makes use of the advantages of the dynamic fault tree for model, fuzzy set theory for handling uncertainty, and Markov chain for state clearly ability, which is especially suitable for reliability evaluation and fault diagnosis of the Safety-Critical avionics System.

In the future work, we will focus on the common cause failures to optimize the dynamic fault tree model, more experimentation using various uncertainly data sets coming from other fault tree analysis would be advantageous to gain a better assessment of the performance of the model and the linguistic analysis. Furthermore, the underlying model can be further refined and enriched by admitting various classes of fuzzy sets (membership functions).

Acknowledgments

Authors gratefully acknowledge the financial support provided by the National Natural Science Foundation of China (Grant No. 51167013) and research fund for the doctoral program of higher education of NCHU, Jiang Xi, China (Project No.EA201304348). At the same time, the authors sincerely thank the reviewers for their insightful comments.

References

1. Antoine B. Rauzy, Sequence Algebra. Sequence decision diagrams and dynamic fault trees. Reliability Engineering and System Safety 2011; 96(2): 785–792.
2. Christopher C. Drovandi, Anthony N. Pettitt, Robert D. Henderson. Marginal reversible jump Markov chain Monte Carlo with application to motor unit number estimation. Computational Statistics & Data Analysis 2014; 72(3): 128-146.
3. Daqing Wang, Peng Zhang, Liqiong Chen. Fuzzy fault tree analysis for fire and explosion of crude oil tanks. Journal of Loss Prevention in the Process Industries 2013; 26(1): 1390-1398.
4. Jafarian E, Rezvani MA. Application of fuzzy fault tree analysis for evaluation of railway safety risks: an evaluation of root causes for passenger train derailment. Proceedings of the Institution of Mechanical Engineers F: Journal of Rail and Rapid Transit 2012; 226(1): 14-25.
5. Gargama, H. Chaturvedi, S.K.Criticality Assessment models for failure mode effects and criticality analysis using fuzzy logic. IEEE Transactions on Reliability 2011; 60(1): 102-110.
6. HUANG Hongzhong, TONG Xin, ZUO Mingjian. Posbist fault tree analysis of coherent systems. Reliability Engineering and System Safety 2004; 84(2): 141-148.
7. J. B. Dugan, S. J. Bavuso, and M. A. Boyd. Dynamic fault-tree models for fault-tolerant computer systems. IEEE Transactions on Reliability 1992; 41(3): 363-377.
8. Julwan Hendry Purba. A fuzzy-based reliability approach to evaluate basic events of fault tree analysis for nuclear power plant probabilistic safety assessment. Annals of Nuclear Energy 2014; 70(2): 28-30.
9. Julwan Hendry Purba, Jie Lu, Guangquan Zhang. A fuzzy reliability assessment of basic events of fault trees through qualitative data processing. Fuzzy Sets and Systems 2014; 243(1): 50–69.
10. J.H. Purba, J. Lu, G. Zhang, and D. Ruan. An area defuzzification technique to assess nuclear event reliability data from failure possibilities. International Journal of Computational Intelligence and Applications 2012; 11(4): 1-16.
11. K.DurgaRao, V.Gopika, V.V.S.SanyasiRao. Dynamic fault tree analysis using Monte Carlo simulation in probabilistic safety assessment. Reliability Engineering and System Safety 2009; 94(1): 872-883.
12. L. Meshkat, J. B. Dugan, and J. D. Andrews. Dependability analysis of systems with on-demand and active failure modes using dynamic fault trees. IEEE Transactions on Reliability 2002; 51(2): 240-251, 2002.
13. LI Yanfeng, HUANG Hongzhong, LIU Yu. A new fault tree analysis method: Fuzzy dynamic fault tree analysis. Eksploatacja i Niezawodnosc – Maintenance and Reliability 2012; 14(3): 208-214.
14. Mohsen Naderpour, Jie Lu, Guangquan Zhang. An abnormal situation modeling method to assist operators in safety-critical systems. Reliability Engineering and System Safety 2014; 119(2): 67-89.
15. Ningcong Xiao, Hong-Zhong Huang, Yanfeng Li. Multiple failure modes analysis and weighted risk priority number evaluation in FMEA. Engineering Failure Analysis 2011; 18(1): 1162-1170.
16. Peter Popov. Bayesian reliability assessment of legacy safety-critical systems upgraded with fault-tolerant off-the-shelf software. Reliability Engineering and System Safety 2013; 117(5): 98-113.
17. Rongxing Duan, Jinghui Fan. Reliability Evaluation of Data Communication System based on Dynamic Fault Tree under Epistemic Uncertainty. Mathematical Problems in Engineering 2014; 35(2): 134-142
18. S. Montani, L. Portinale, A. Bobbio, and D. Codetta-Raiteri. A tool for reliability analysis of dynamic fault trees through conversion into dynamic Bayesian networks. Reliability Engineering and System Safety 2008; 93(7): 922-932.
19. T. Onisawa. An approach to human reliability in man-machine systems using error possibility. Fuzzy Sets and Systems 1988; 27(2): 87-103.
20. Wonkeun Youn, Baeck-jun Yi. Software and hardware certification of safety-critical avionic systems: A comparison study. Computer Standards & Interfaces 2014; 36(3): 889-898.

21. Xinglong Wang, Weixiang Liu. Research on air traffic control automatic system software reliability based on Markov chain.Physics Procedia, 2012; 24(3): 1601-1606.
22. YANG Jianping, HUANG Hongzhong, LIU Yu. Evidential networks for fault tree analysis with imprecise knowledge. International Journal of Turbo & Jet Engines 2012; 29(2): 111-122.
23. Yi Ding, Zuo M.J. Lisnianski A,Wei Li. A Framework for Reliability Approximation of Multi-State Weighted -out-of- Systems. IEEE Transactions on Reliability 2010; 59(3): 297-308.

Jiliang TU
Ruofa CHENG
Qiuxiang TAO
School of Information Engineering, Nanchang Hangkong University
Nanchang Jiangxi, 330063, China
Email: tjl1980@nchu.edu.cn or 395229630@qq.com

INFORMATION FOR AUTHORS

Terms and Conditions of Publication:

- The quarterly „Maintenance and Reliability" publishes original papers written in Polish with an English translation.
- Translation into English is done by the Authors after they have received information from the Editorial Office about the outcome of the review process and have introduced the necessary modifications in accordance with the suggestions of the referees!
- Acceptance of papers for publication is based on two independent reviews commissioned by the Editor.

Fees:

- Pursuant to a resolution of the Board of PNTTE, as of 2009 the publication fee for one text is 600 zloty + VAT.
- Coloured graphical elements in the submitted text require agreement from the Editor and are charged extra.

Technical requirements:

- After receiving positive reviews and after acceptance of the paper for publication, the text must be submitted in a Microsoft Word document format.
- Drawings and photos should be additionally submitted in the form of graphical files in the *.tif, *.jpg or *.cdr (v. X3) formats.
- A manuscript should include (in accordance with the enclosed correct manuscript format: *.pdf, *.doc):
- names of authors, title, abstract, and key words that should complement the title and abstract (in Polish and in English)
- the text in Polish and in English with a clear division into sections (please, do not divide words in the text);
- tables, drawings, graphs, and photos included in the text should have descriptive two-language captions,
- if this can be avoided, no formulae and symbols should be inserted into text paragraphs by means of a formula editor
- references (written in accordance with the required reference format)
- author data – first names and surnames along with scientific titles, affiliation, address, phone number, fax, and e-mail address
- The Editor reserves the right to abridge and adjust the manuscripts.
- All submissions should be accompanied by a submission form.

Editor contact info: (Submissions should be sent to the Editor's address)

Editorial Office of „Eksploatacja i Niezawodność - Maintenance and Reliability"
Nadbystrzycka 36, 20-618 Lublin, Poland
e-mail: office@ein.org.pl

INFORMATION FOR SUBSCRIBERS

Fees

Yearly subscription fee (four issues) is 100 zloty and includes delivery costs.
Subscribers receive any additional special issues published during their year of subscription free of charge.

Orders

Subscription orders along with authorization to issue a VAT invoice without receiver's signature should be sent to the Editor's address.

Note

In accordance with the requirements of citation databases, proper citation of publications appearing in our Quarterly should include the full name of the journal in Polish and English without Polish diacritical marks, i.e.,

Eksploatacja i Niezawodnosc – Maintenance and Reliability.

Wydawca:
Polskie Naukowo Techniczne
Towarzystwo Eksploatacyjne
Warszawa

Publisher:
Polish Maintenance Society
Warsaw

Członek:
Europejskiej Federacji
Narodowych Towarzystw
Eksploatacyjnych

Member of:
European Federation of National
Maintenance Societies

Patronat naukowy:
Polska Akademia Nauk
Oddział Lublin

Scientific Supervision:
Polish Academy of Sciences
Branch in Lublin